REPORT DOCUMENTATION PAGE

READ INSTRUCTIONS BEFORE COMPLETING FORM

1. REPORT NUMBER: TR-85-01 — NAVENVPREDRSCHFAC Technical Report 85-01
2. GOVT ACCESSION NO.:
3. RECIPIENT'S CATALOG NUMBER:

4. TITLE *(and Subtitle)*:
Navy Tactical Applications Guide. Volume 5. Part 2
Indian Ocean (Arabian Sea/Bay of Bengal)
Weather Analysis and Forecast Applications

5. TYPE OF REPORT & PERIOD COVERED:

6. PERFORMING ORG. REPORT NUMBER:

7. AUTHOR(s):
Robert W. Fett
Walter A. Bohan
Ronald E. Englebretson

8. CONTRACT OR GRANT NUMBER(s):
The Walter A. Bohan Company
N00228-84-C-3207

9. PERFORMING ORGANIZATION NAME AND ADDRESS:
The Walter A. Bohan Company
2026 Oakton Street
Park Ridge, IL 60068

10. PROGRAM ELEMENT, PROJECT, TASK AREA & WORK UNIT NUMBERS:
62759N. WF 59-553.
NEPRF WU: 6.2-9

11. CONTROLLING OFFICE NAME AND ADDRESS:
Naval Air Systems Command
Department of the Navy
Washington, D.C. 20361

12. REPORT DATE:
February 1985

13. NUMBER OF PAGES:
202

14. MONITORING AGENCY NAME & ADDRESS *(if different from Controlling Office)*:
Naval Environmental Prediction Research Facility
Monterey, California 93943

15. SECURITY CLASS. *(of this report)*:
Unclassified

15a. DECLASSIFICATION/DOWNGRADING SCHEDULE:

16. DISTRIBUTION STATEMENT *(of this Report)*:
Approved for Public Release
Distribution Unlimited

17. DISTRIBUTION STATEMENT *(of the abstract entered in Block 20, if different from Report)*:

18. SUPPLEMENTARY NOTES:

19. KEY WORDS *(Continue on reverse side if necessary and identify by block number)*:
Arabian Sea
Bay of Bengal
Meteorological Satellite Systems
Analysis and Forecast Applications
Indian Ocean
Northeast Monsoon
Southwest Monsoon
Coastal Zone Phenomena
Ocean-Atmosphere Interaction

20. ABSTRACT *(Continue on reverse side if necessary and identify by block number)*:

Case studies describing regional environmental analysis and forecast applications based on satellite data and conventional meteorological observations for the Indian Ocean area are presented. Topics include Northeast Monsoon, Southwest Monsoon, coastal zone phenomena, and ocean-atmosphere interaction. The studies provide insights into identifiable patterns of weather development that occur frequently, so that once the basic pattern is recognized at an early stage this information can be used for improved weather analysis and forecasting.

ROUTINE REPLY, ENDORSEMENT, TRANSMITTAL OR INFORMATION SHEET

OPNAV 5216/158 (Rev. 7-78)
SN 0107-LF-052-1691

A WINDOW ENVELOPE MAY BE USED
Formerly NAVEXOS 3789

CLASSIFICATION (*UNCLASSIFIED when detached from enclosures, unless otherwise indicated*)
UNCLASSIFIED

FROM (*Show telephone number in addition to address*)
Commanding Officer, Naval Environmental Prediction Research Facility, Monterey, CA 93943-5006 AV 878-2837

DATE
7 October 1985

SUBJECT
FORWARDING OF NAVENVPREDRSCHFAC TECHNICAL PUBLICATION

SERIAL OR FILE NO.
5600 NEPRF/SBB:sb
Ser 293

TO:
Distribution

REFERENCE

ENCLOSURE
(1) NAVENVPREDRSCHFAC Technical Report TR 85-01: NTAG Vol. 5, Part 2, Indian Ocean, Arabian Sea/Bay of Bengal, Weather Analysis and Forecast Applications, Meteorological Satellite Systems

VIA:

ENDORSEMENT ON
_____

XX FORWARDED ☐ RETURNED ☐ FOLLOW-UP, OR TRACER ☐ REQUEST ☐ SUBMIT ☐ CERTIFY ☐ MAIL ☐ FILE

	GENERAL ADMINISTRATION
	FOR APPROPRIATE ACTION
	UNDER YOUR COGNIZANCE
XX	INFORMATION & retention
	APPROVAL RECOMMENDED ☐ YES ☐ NO
	☐ APPROVED ☐ DISAPPROVED
	COMMENT AND/OR CONCURRENCE
	CONCUR
	LOANED, RETURN BY:
	SIGN RECEIPT & RETURN
	REPLY TO THE ABOVE BY:
	REFERENCE NOT RECEIVED
	SUBJECT DOCUMENT FORWARDED TO:
	SUBJECT DOCUMENT RETURNED FOR
	SUBJECT DOCUMENT HAS BEEN REQUESTED, AND WILL BE FORWARDED WHEN RECEIVED
	COPY OF THIS CORRESPONDENCE WITH YOUR REPLY
	ENCLOSURE NOT RECEIVED
	ENCLOSURE FORWARDED AS REQUESTED
	ENCLOSURE RETURNED FOR CORRECTION AS INDICATED
	CORRECTED ENCLOSURE AS REQUESTED
	REMOVE FROM DISTRIBUTION LIST
	REDUCE DISTRIBUTION AMOUNT TO:

	CONTRACT ADMINISTRATION
	NAME & LOCATION OF SUPPLIER OF SUBJECT ITEMS
	SUBCONTRACT NO. OF SUBJECT ITEM
	APPROPRIATION SYMBOL, SUBHEAD, AND CHARGEABLE ACTIVITY
	SHIPPING AT GOVERNMENT EXPENSE ☐ YES ☐ NO
	A CERTIFICATE, VICE BILL OF LADING
	COPIES OF CHANGE ORDERS, AMENDMENT OR MODIFICATION
	CHANGE NOTICE TO SUPPLIER
	STATUS OF MATERIAL ON PURCHASE DOCUMENT

	PERSONNEL
	REPORTED TO THIS COMMAND:
	DETACHED FROM THIS COMMAND
	OTHER

REMARKS (*Continue on reverse*)

Enclosure (1) is another publication in the Navy Tactical Applications Guides (NTAG) series.

SIGNATURE & TITLE
R.P. HUFF, By direction

COPY TO:

CLASSIFICATION (*UNCLASSIFIED when detached from enclosures, unless otherwise indicated*)
UNCLASSIFIED

★ G.P.O.: 1982-587-016/5340

** MAY CONTAIN EXPORT CONTROL DATA **
ADAxxxxxx MICROFICHE ARE HOUSED IN THE GENERAL MICROFORMS AM

AN (1) AD-A160 761
FG (2) 040200
FG (2) 080300
CI (3) (U)
CA (5) BOHAN (WALTER A) CO PARK RIDGE IL
TI (6) Navy Tactical Applications Guide. Volume 5, Part 2. Indian Ocean (Arabian Sea/Bay of Bengal) Weather Analysis and Forecast Applications.
TC (8) (U)
DN (9) Technical rept.,
AU (10) Fett,R. W.
AU (10) Bohan,W. A.
AU (10) Englebretson,R. E.
RD (11) Feb 1985
PG (12) 235p
CT (15) N00228-84-C-3207
PJ (16) PE62759N
TN (17) WF59553
RN (18) NEPRF-TR-85-01
RC (20) Unclassified report
NO (21) See also Volume 5, Part 1, AD-A154 718.
DE (23) *WEATHER FORECASTING, *MARINE METEOROLOGY, * METEOROLOGICAL DATA, AIR WATER INTERACTIONS, ARABIAN SEA, PATTERNS, CASE STUDIES, FORECASTING, ARTIFICIAL SATELLITES, METEOROLOGICAL SATELLITES, MONSOONS, ENVIRONMENTS, BENGAL BAY, COASTAL REGIONS, INDIAN OCEAN, WEATHER
DC (24) (U)
ID (25) PE62759N, WU629
IC (26) (U)
AB (27) Case studies describing regional environmental analysis and forecast applications are based on satellite data and conventional meteorological observations for the Indian Ocean area are presented. Topics include Northeast Monsoon, Southwest Monsoon, coastal zone phenomena, and ocean-atmosphere interaction. The studies provide insights into identifiable patterns of weather development that occur frequently, so that once the basic pattern is recognized at an early stage this information can be used for improved weather analysis and forecasting. Originator-supplied keywords: Arabian Sea; Bay of Bengal; Meteorological satellite systems; Analysis and Forecast Applications; Indian Ocean; Northwest Monsoon; Southwest Monsoon; Coastal Zone Phenomena; Ocean-atmosphere interaction.
AC (28) (U)
DL (33) 01
SE (34) 5
CC (35) 059910

#

NAVY TACTICAL APPLICATIONS GUIDE

VOLUME 5
PART 2

INDIAN OCEAN
Arabian Sea/Bay of Bengal
WEATHER ANALYSIS AND FORECAST APPLICATIONS

METEOROLOGICAL
SATELLITE SYSTEMS

Prepared under the direction of
Robert W. Fett
Tactical Applications Department
Naval Environmental Prediction Research Facility

Scientific Coordinator
Walter A. Bohan
The Walter A. Bohan Company

1985

THE WALTER A. BOHAN COMPANY
2026 OAKTON STREET, PARK RIDGE, ILLINOIS 60068
APPLIED RESEARCH IN SATELLITE METEOROLOGY AND OCEANOGRAPHY

List of Contributors

Robert W. Fett, Head
Tactical Applications Department
Naval Environmental Prediction Research Facility
Monterey, California

Walter A. Bohan, Certified Consulting Meteorologist
The Walter A. Bohan Company
Park Ridge, Illinois

Ronald J. Englebretson, Research Scientist
Science Applications, Inc.
Monterey, California

Sherree L. Tipton, Meteorologist
The Walter A. Bohan Company
Park Ridge, Illinois

Foreword

Volume 5 of the Navy Tactical Applications Guide (NTAG) series is devoted to regional weather analysis and forecast applications in the northern Indian Ocean. Part 1 of Volume 5 is dedicated to operationally important weather phenomena affecting the region surrounding and including the Red Sea and Persian Gulf. Part 2 extends the area of interest to the Arabian Sea and Bay of Bengal. The case study technique of relating weather satellite imagery to concurrent conventional weather data and analyses from the surface to the upper troposphere, along with available numerical guidance products, is continued, focusing on the unique weather characteristics of the Indian Ocean region.

Whereas the topics of blocking and cyclogenesis were emphasized in previous volumes, it is the powerful monsoon influences of winter and summer that become the dominant interest in the Indian Ocean. Duststorm generation is a subject of major interest because of its effect on operations thoughout the northern portion of the Indian Ocean region. The ability to detect duststorms over land areas at the time of earliest inception in satellite data, and to forecast the areas most likely to be influenced by the dust, is given special attention.

The Indian Ocean volumes are intended as an evolving series which will be supplemented with additional material presently under development. The initial material is being distributed to the fleet to expedite access of completed work for operational use.

As with case studies developed for previous volumes, many of the principles derived for Indian Ocean weather analysis and forecasting are general in nature and equally applicable to similar weather events in other areas of the world.

It is anticipated that these guides will be useful supplements to other material available for the Indian Ocean region in their emphasis on new aspects of weather satellite interpretation for improved weather analysis and forecasts.

Kenneth L. Van Sickle

KENNETH L. VAN SICKLE
Captain, U.S. Navy
Commanding Officer, NEPRF

Acknowledgments

This volume could not have been published without the devoted effort of the NEPRF Meteorological Laboratory personnel who obtained required documentation, and who spent many hours on the computer terminal entering information for the analyses utilized in the studies. Directed by AGCM M. Shelton, the following personnel: AG1 E. Danielson, AG3 D. Haynes, AG3 B. Langan, and AG3 L. Livingston, did an outstanding job in supporting the work effort required for this volume.

PH2 M. Rutschky processed many of the original photos utilized. The correlative meteorological data were provided by the Fleet Numerical Oceanography Center, Monterey, CA, and the U.S. Naval Oceanographic Detachment, Asheville, N.C.

Additional satellite imagery was supplied by the National Environmental Satellite Data and Information Service (NESDIS) of the National Oceanic and Atmospheric Administration (NOAA). METEOSAT imagery was supplied by the European Space Agency.

The assistance of the staff of the Walter A. Bohan Company is again acknowledged; in particular, Lido A. Andreoni for design of the format of the publication and layout of the case studies. Gregory E. Terhune assisted in the preparation of case study graphics and preparation in the editing and formating of the text. The high quality of the reproduction of the satellite imagery used in the case studies and the excellent printing of the publication are due to the combined efforts of Peter M. Samorez and Michael E. Brock.

Upper-air streamline analyses from the T. N. Krishnamurti "Quick Look Summer Monex Atlas" have provided the type of detailed data needed for presenting some of the concepts discussed in this volume. A special acknowledgment is due to Dr. T. N. Krishnamurti and his staff at Florida State University for the excellent documentation provided by the Summer Monex Atlas.

Introduction

Seasonal Circulation Patterns of the Indian Ocean

The northern Indian Ocean is located within the world's most notorious monsoon regime. The term monsoon is a name for seasonal winds and is derived from the Arabic word *mausim*, meaning season. In general, the term describes a regime where there are highly persistent winds from nearly opposite directions in summer and winter and which are not the result of shifting migratory storm tracks. The basic cause of such a wind pattern is the differential heating and cooling of adjacent large land and sea areas. The land masses are warmer than the ocean areas in summer and cooler in winter, resulting in relatively lower pressure over the land in summer and higher in the winter. These pressure differences cause winds to blow primarily onshore (summer) and offshore (winter). The size, shape and orientation of the adjoining land/ocean areas play important roles in determining the specific monsoon characteristics of a given region.

The low-level circulation pattern for the Indian Ocean consists of southwest flow during the summer period and northeast flow during the winter period. When combined with the two intervening transitional periods it is convenient to use the mid-latitude convention of summer, autumn, winter, and spring season titles. It must by realized, however, that these terms applied to the tropics do not have the same connotations as when applied to the harsher extremes of mid latitudes. The approximate months of the four seasons are:

Autumn Transition—October through November
Winter Monsoon—December through March
Spring Transition—April through May
Summer Monsoon—June through September

Section 1

Arabian Sea/Bay of Bengal

Introduction

Case Studies

1B Autumn Transition

1C Winter

1D Spring Transition

1E Summer

Arabian Sea/Bay of Bengal Introduction

Arabian Sea/Bay of Bengal Autumn Transition

October–November

The autumn transition period precedes the northeast monsoon season. During that time, the northern near-equatorial trough (NET), which during the summer (southwest monsoon) is located over northern India, moves southward to near the Equator (1A-1a). The upper-level Tibetan anticyclone at the same time recedes southeastward to a position over Indo-China (1A-1b). This permits westerly flow and a branch of the polar jet stream to become active south of the Himalayas (near 25° N).

References

Findlater, J., 1971: Mean monthly airflow at low levels over the western Indian Ocean. *Geophys. Mem. London*, **16**, 53 pp.

Ramage, C. S., and C. R. V. Raman, 1972: Meteorological atlas of the international Indian Ocean expedition, Vol. 2: Upper air. National Science Foundation, Washington, D. C.

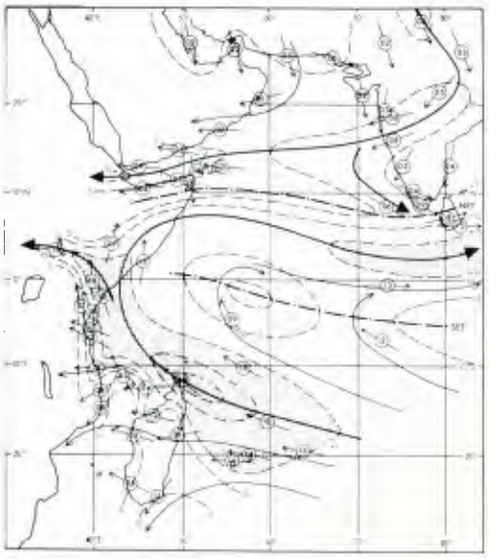

1A-1a. Monthly mean streamline analysis for October at the 3000 ft/1 km level (from Findlater, 1971).

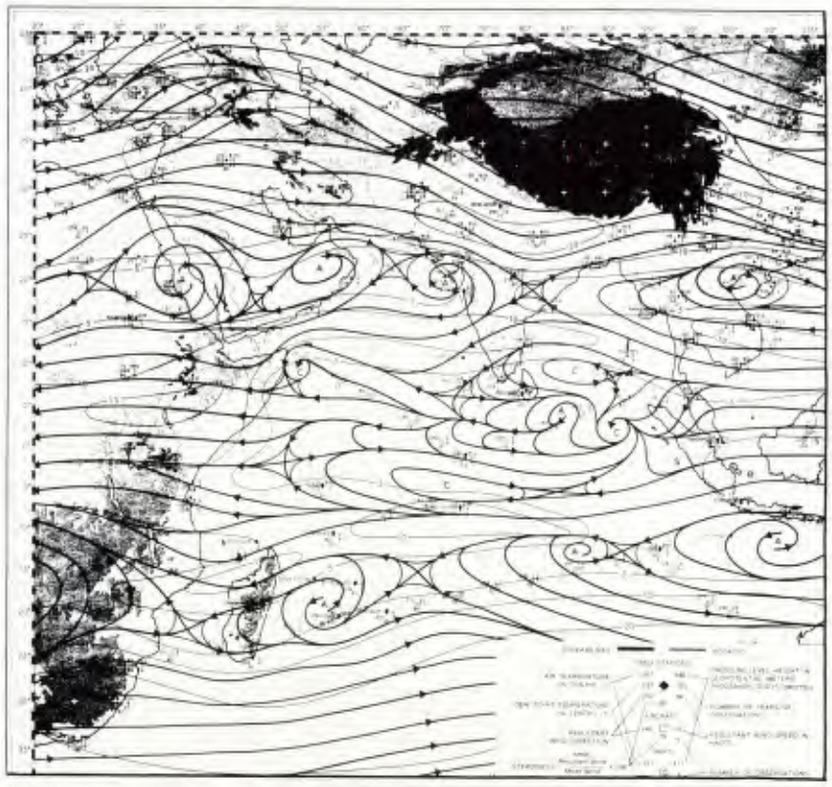

1A-1b. Monthly mean streamline analysis for October at the 500-mb level (from Ramage and Raman, 1972).

Arabian Sea/Bay of Bengal Northeast Monsoon

December–March

During the Northern Hemisphere winter, the low-level atmosphere over the land masses of Europe and Asia is much colder than that over the northern Indian Ocean. This results in the development of a strong high-pressure system (anticyclone) over land and a pressure gradient that creates northerly low-level flow into the subtropical regions. Over the northern Indian Ocean region, this low-level flow pattern is referred to as the northeast monsoon—the name reflects the prevailing low-level wind direction. Due to the east–west mountain ranges (Himalayas of Tibet, Taurus of Turkey, and Elburz of Iran), the cold surges from the Asiatic anticyclone are rather weak, as compared to surges over the South China Sea.

The undisturbed northeast monsoon weather is marked by a minimum of cloudiness and weak low-level winds. A branch of the polar jet stream is active south of the Himalayas. Because of the closer proximity to the east–west Himalayas, the northeast monsoon is typically weaker over the Bay of Bengal than over the Arabian Sea. This results in even fewer low-level clouds over the oceanic areas, and virtually no cyclonic disturbances or intrusions from mid latitudes.

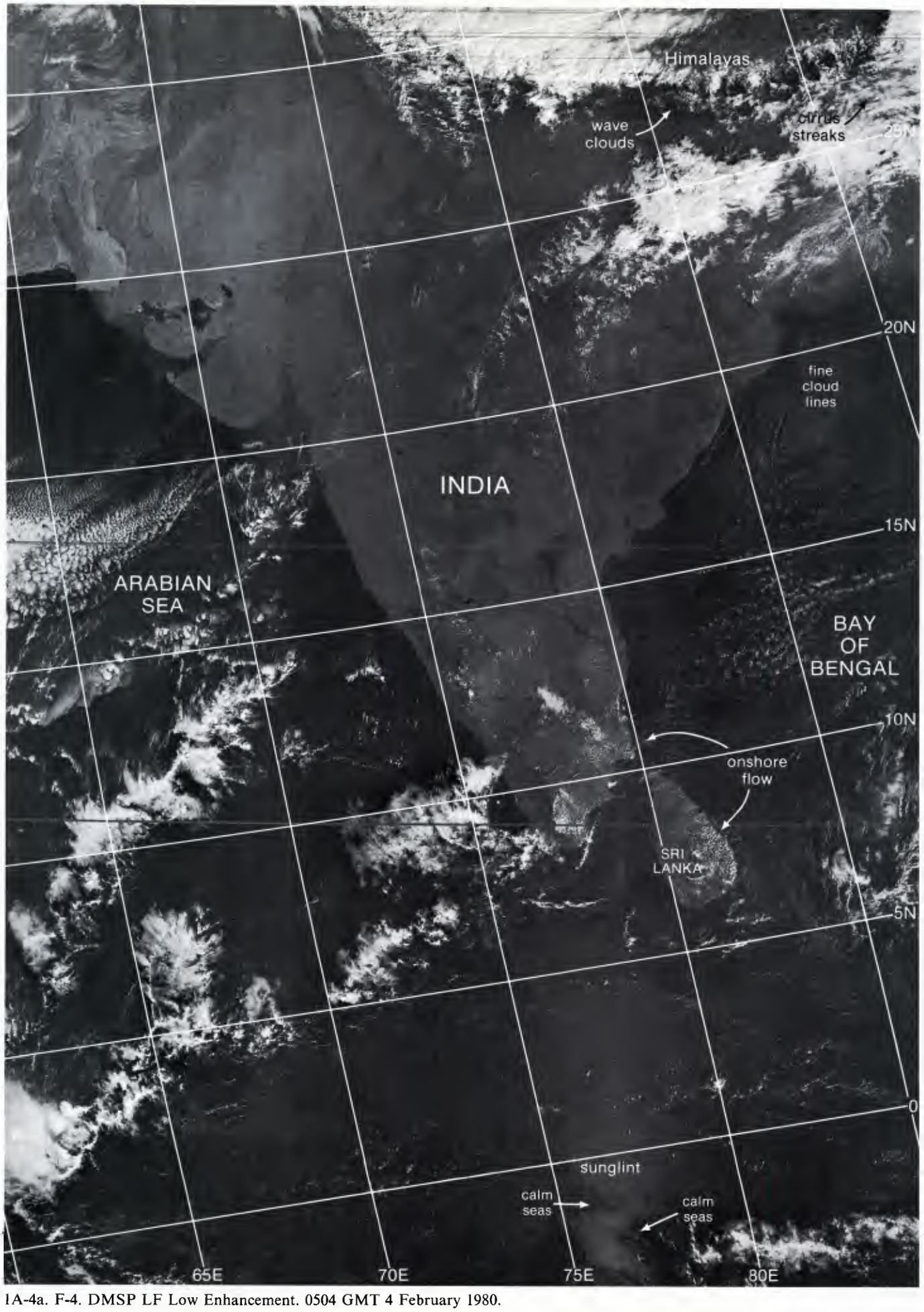

1A-4a. F-4. DMSP LF Low Enhancement. 0504 GMT 4 February 1980.

Northeast Monsoon
Prevailing Weather Patterns
Arabian Sea/Bay of Bengal

The Arabian Sea

The Arabian Sea is normally capped by an inversion during the northeast (winter) monsoon season. The depth of the planetary boundary layer and the height of the inversion increases from the northeastern to the southeastern portion of the Arabian Sea. Stratocumulus clouds form under the inversion and change from small to increasingly larger closed-cell cloud elements. For the southernmost extremity, cloud types change to cumuliform, reflecting the more unstable atmospheric conditions of the tropics and, specifically, the NET region.

The DMSP visible picture at 0504 GMT 4 February (1A-4a) shows the northeastern portion of the Arabian Sea, where a change in the size of cloud elements is particularly noticeable. Dark patches in the sunglint pattern south of India, near the bottom of the picture, indicate calm seas and the location of the near-equatorial trough axis. India is largely cloud free, which is typical of the winter season. The exceptions in this example are over the Himalayas, the northeast sector, and southern India. The cloud areas to the north occur under mid-latitude westerly flow; in this case a westerly disturbance is reflected by the clouds over northeast India and the Himalayas. Westerly flow is indicated by wave cloud patterns and cirrus streaks evident over the northern region. Weak northerly flow over the Bay of Bengal is implied by the fine cloud line pattern, while fair weather cumulus cloud lines observed over southeastern India and eastern Sri Lanka result from the onshore flow that is an extension of the general northeasterly monsoon through that region.

The surface streamline analysis at 0000 GMT 4 February (1A-5d) shows extremely light flow conditions, also suggested by the lack of pronounced cloud banding in the DMSP picture. The intensity and southerly penetration of the westerlies into India are clearly shown at 250 mb (1A-5a), 500 mb (1A-5b), and 700 mb (1A-5c). All three analyses indicate a trough **T1** approaching northwestern India. The cloudiness over the Himalayas is in the vorticity advection region in advance of this trough and in the left front quadrant of a jet streak at 250 mb. The extreme upper-level jet stream speeds, south of the Himalayas and extending over portions of the Arabian Sea and the Bay of Bengal, are characteristic of the northeast monsoon, and are of particular interest when contrasted to the light and variable wind conditions of the spring and fall transition periods, or to the southwest monsoon, when the upper-level jet comes from the opposite direction.

The Bay of Bengal

The DMSP visible picture at 0359 GMT 28 January (1A-6a) shows a full view of the Bay of Bengal. Sunglint is evident in this late morning (1000 LST) picture east of the center of the image, extending from the Southern Hemisphere northward past the tip of Sumatra and west of the Malay Peninsula. Interruption of the sunglint pattern in an east-northeast/west-southwest indentation, just north of the west tip of Sumatra, indicates a minimum wind speed region, likely associated with the NET. The NET would be expected to extend westward to the region south of the cloud band off the east coast of Sri Lanka (see Sec. 1C, Case 4). Anomalous gray shades off the east coast of India indicate poor visibilities due to fog and haze, becoming increasingly poorer near the coastline.

The surface analysis at 0000 GMT 28 January (not shown) shows no surface data over the Bay of Bengal, but numerous reports of fog and haze in the coastal regions surrounding the bay. High pressure is indicated over the center of the bay, with no indication of the NET. By 1200 GMT (1A-7d), however, a few reports provide evidence of a trough in the position suggested by the DMSP imagery. Note that the superimposed windflow field on the DMSP data (1A-6a, based on the calm effect in the lee of Great Nicobar Island; the offshore flow from Sri Lanka producing cloud lines southeast and southwest; and an analysis of the alignment of cloud streets in the region in conjunction with the ship reports) provides clear evidence that the NET does exist on this date. The NET is a persistent feature during the northeast monsoon and is frequently more active than in this example. The trough lies along the shipping route from southern India to the Strait of Malacca.

The penetration of the upper-level westerlies south of the Himalayas is clearly indicated by the wave cloud patterns north of the Bay of Bengal. The deep, broad belt of westerlies found south of the Himalayas during this season is shown at 250 mb (1A-7a), 500 mb (1A-7b), and 700 mb (1A-7c). The main core of the polar jet is depicted south of the Himalayas at 250 mb. This complete reversal from the southwest monsoon upper-level easterly flow cannot be over-emphasized to forecasters new to the area.

250 mb

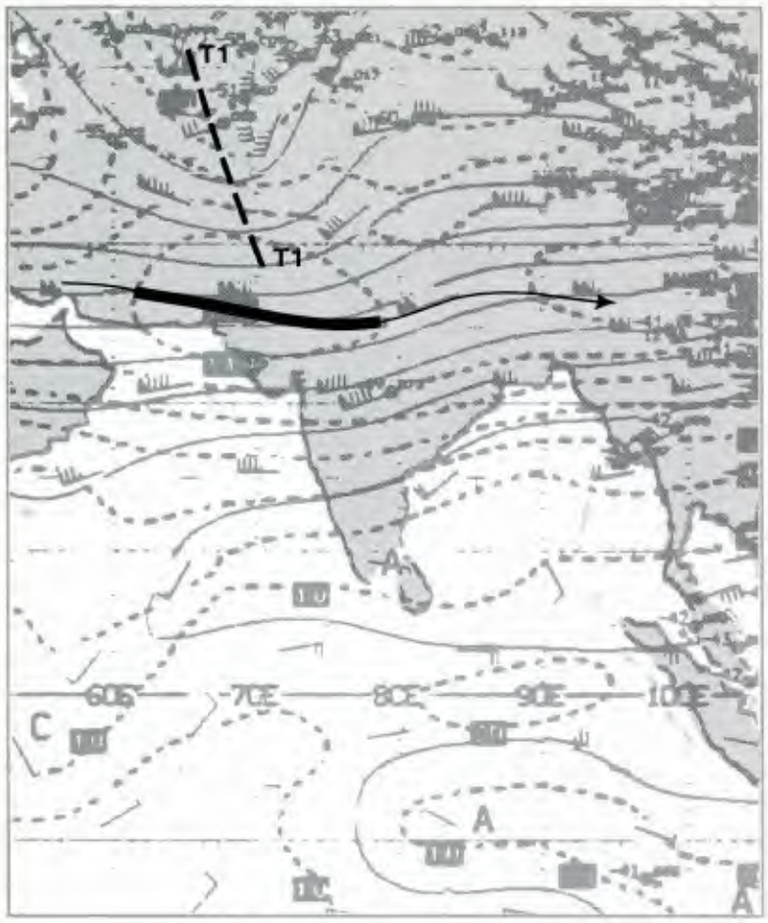

1A-5a. NMC Tropical 250-mb Streamline Analysis. 0000 GMT 4 February 1980.

500 mb

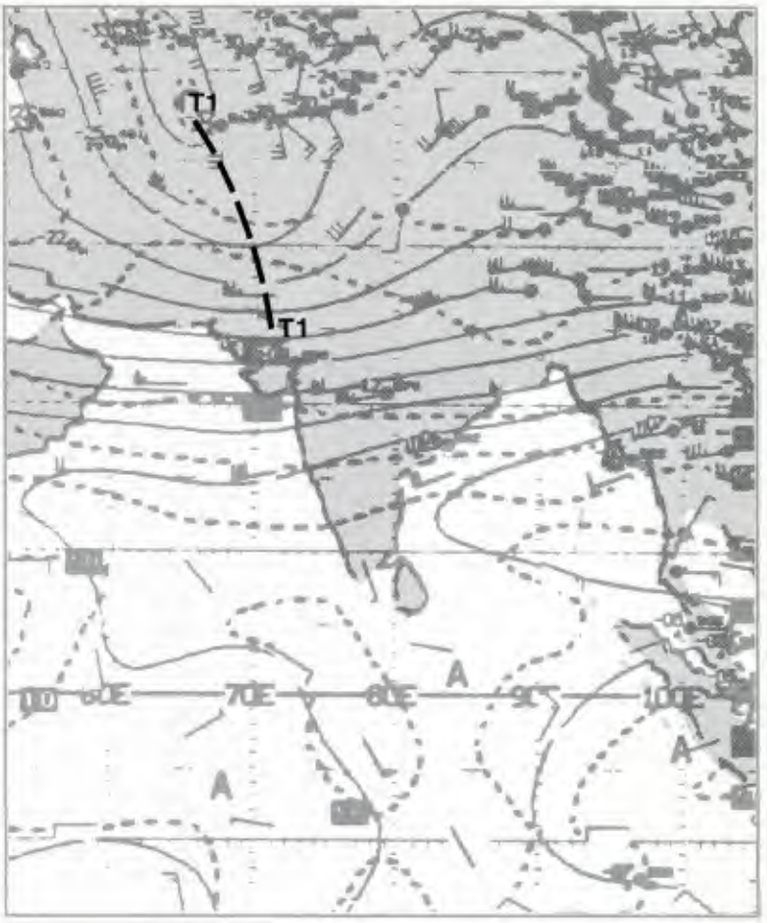

1A-5b. NMC Tropical 500-mb Streamline Analysis. 0000 GMT 4 February 1980.

700 mb

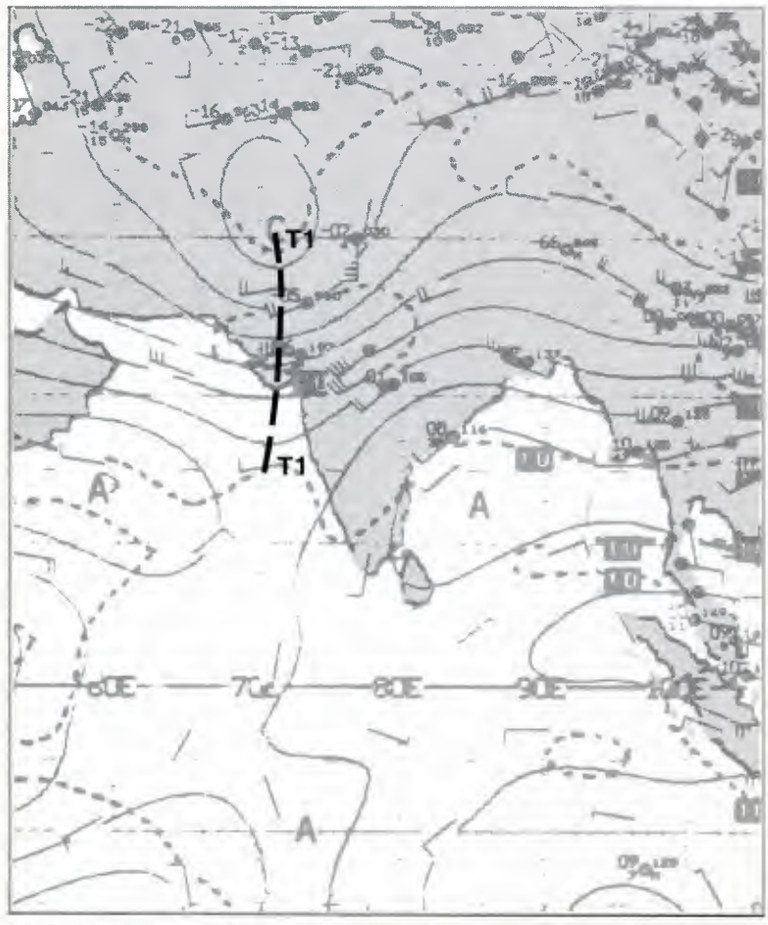

1A-5c. NMC Tropical 700-mb Streamline Analysis. 0000 GMT 4 February 1980.

surface

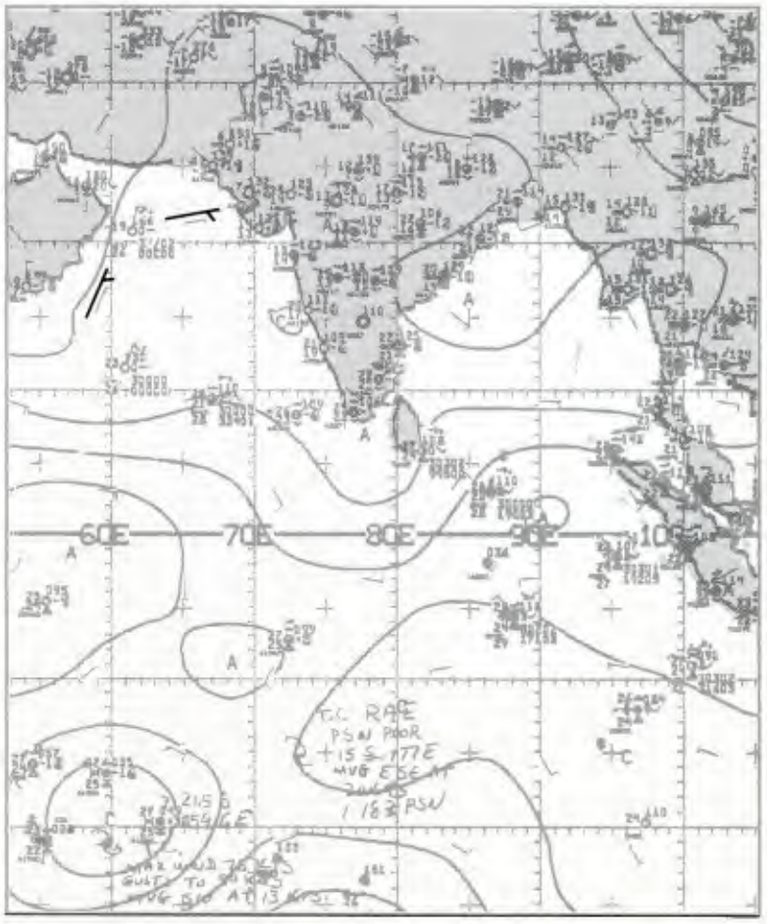

1A-5d. NMC Tropical Surface Streamline Analysis. 0000 GMT 4 February 1980.

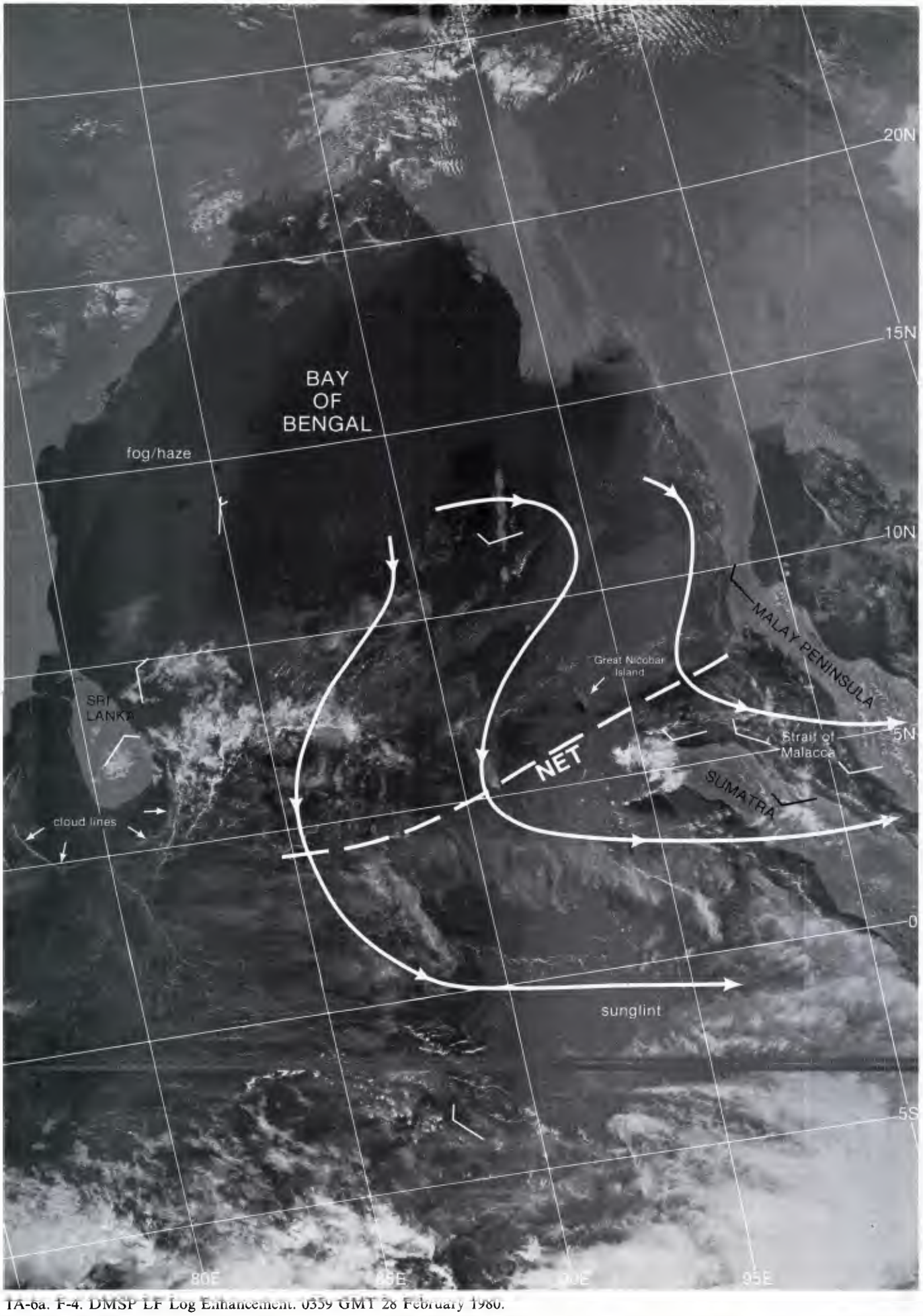

1A-6a. F-4. DMSP LF Log Enhancement. 0359 GMT 28 February 1980.

250 mb

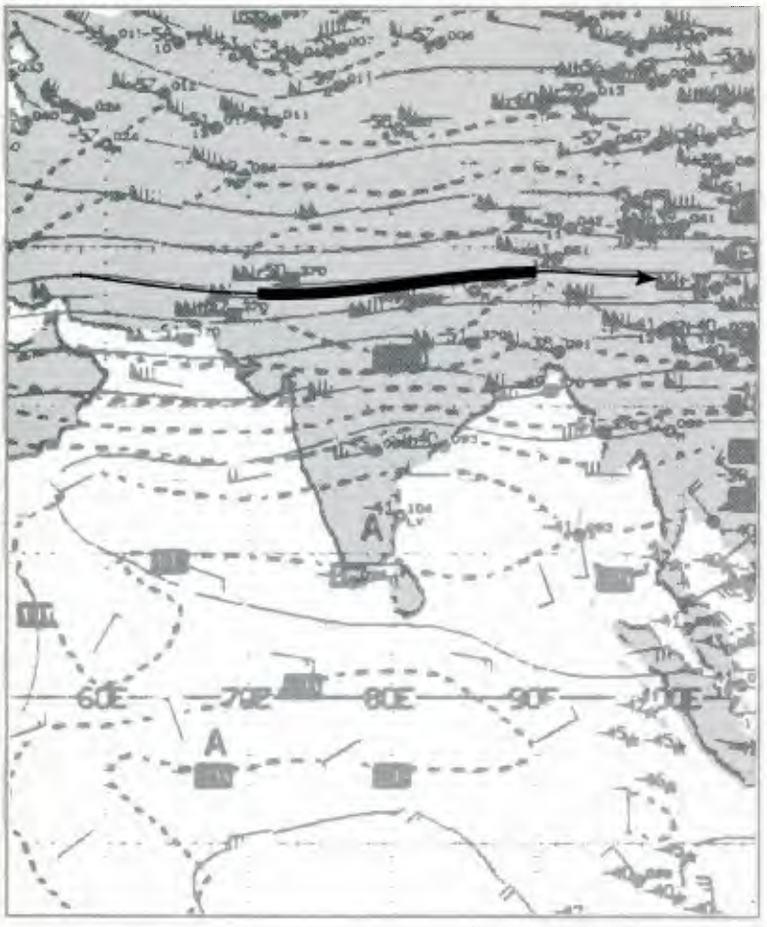

1A-7a. NMC Tropical 250-mb Streamline Analysis. 0000 GMT 28 January 1980.

500 mb

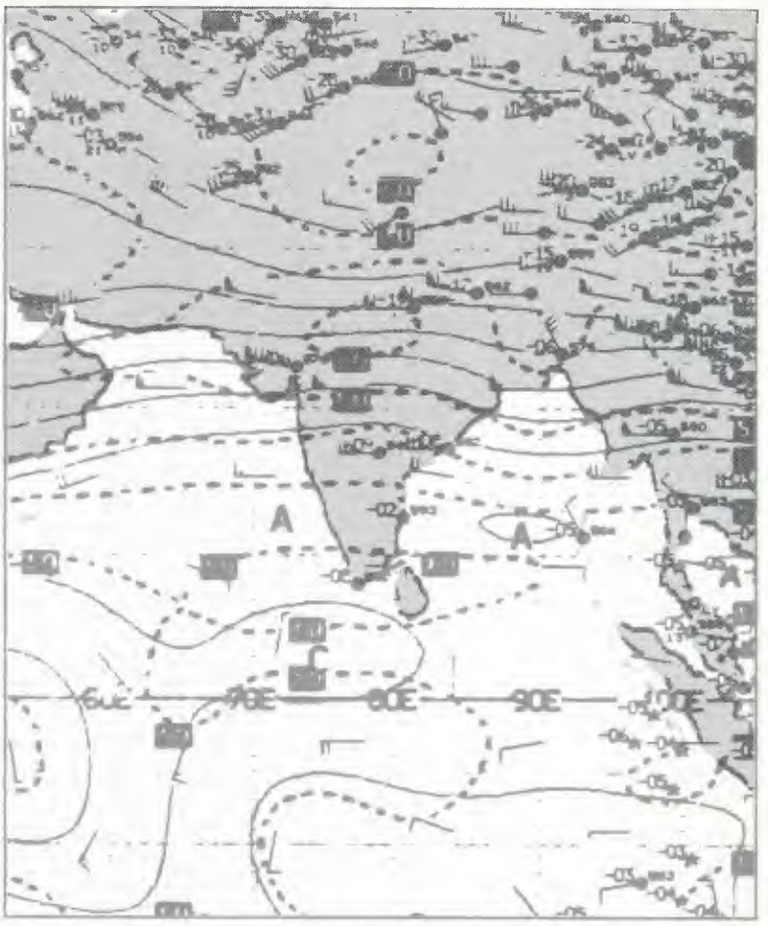

1A-7b. NMC Tropical 500-mb Streamline Analysis. 0000 GMT 28 January 1980.

700 mb

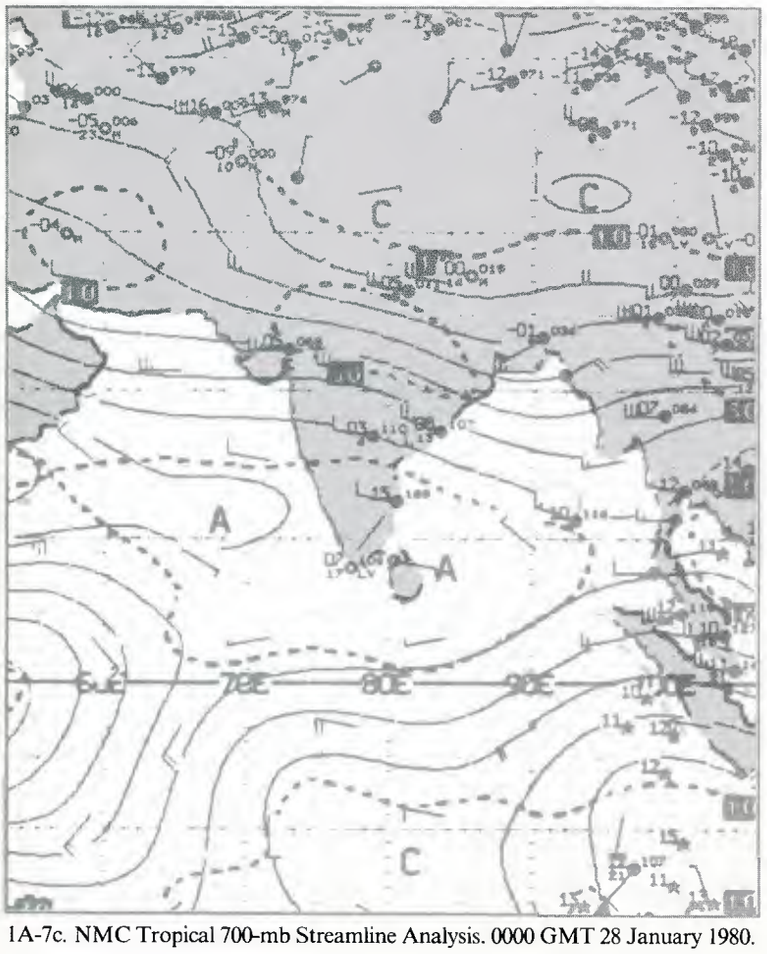

1A-7c. NMC Tropical 700-mb Streamline Analysis. 0000 GMT 28 January 1980.

surface

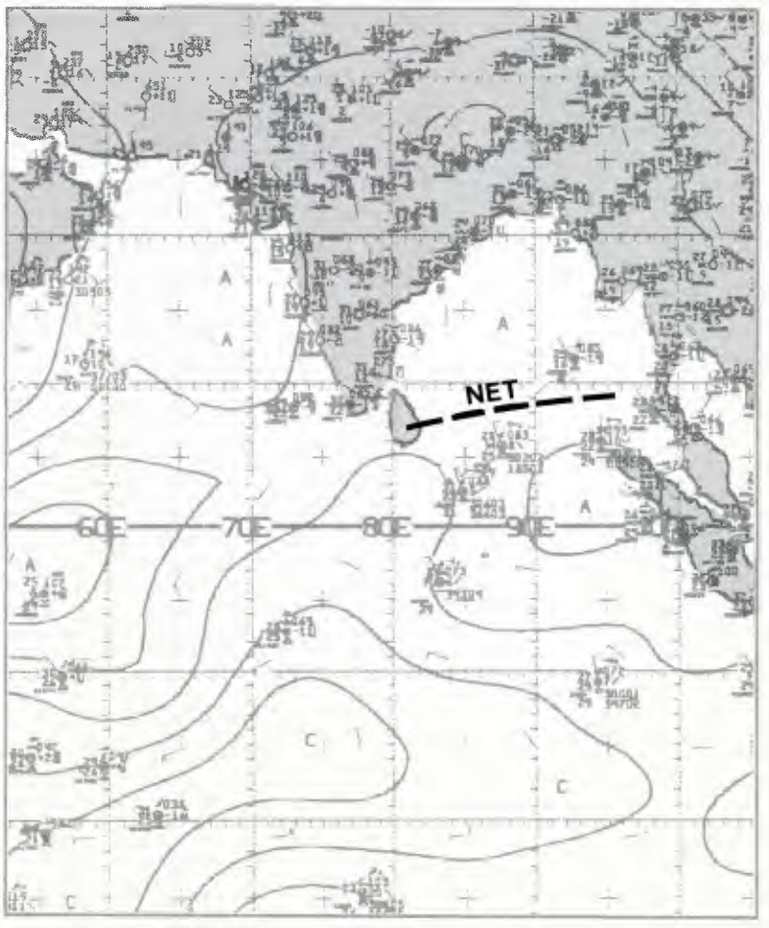

1A-7d. NMC Tropical Surface Streamline Analysis. 1200 GMT 28 January 1980.

Arabian Sea/Bay of Bengal Spring Transition—Early Phase

April–May

The spring transition from the northeast to the southwest monsoon over the northern Indian Ocean region is due to the increased heating of the land areas, which results in relatively lower pressure over land in comparison to that over the water. This constitutes a complete reversal from the winter northeast monsoon regime so that air that had been flowing offshore toward lower pressure now flows onshore toward lower pressure. A very shallow surface heat trough is formed over northern India which extends westward over Pakistan, Iran, Saudi Arabia, and across the Red Sea into Africa.

surface

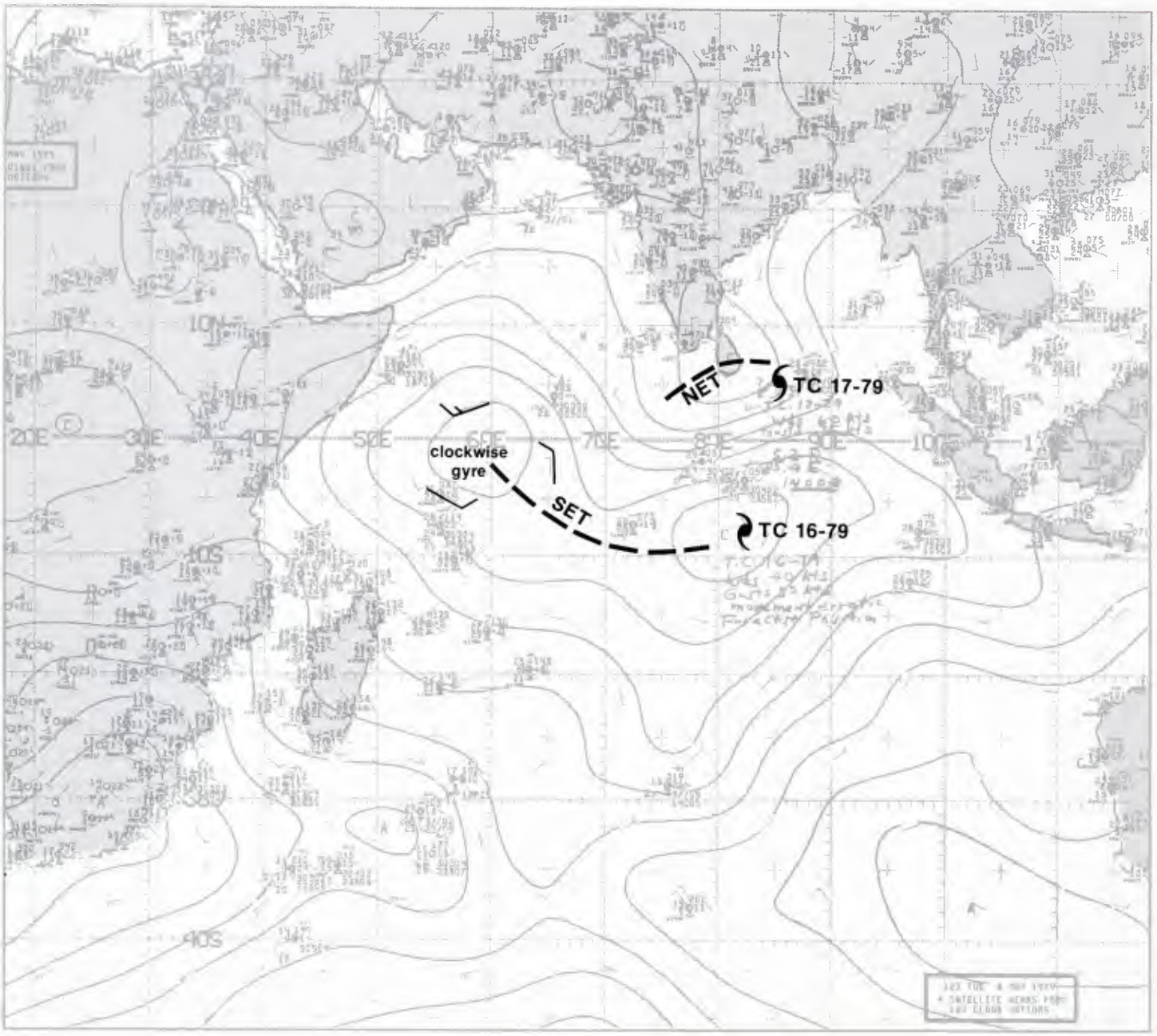

1A-10a. NMC Tropical Surface Streamline Analysis. 1200 GMT 8 May 1979.

Spring Transition—Early Phase
Prevailing Weather Patterns
Arabian Sea/Bay of Bengal
May 1979

8 May

The surface streamline analysis at 1200 GMT 8 May (1A-10a) shows the typical circulation features of the spring transition season. Cyclonic circulations are observed ringing the Arabian Sea region from southern India, Pakistan, Saudi Arabia, and across the Red Sea into the Sudan region of Africa. A clockwise gyre centered over the equator taps the southeasterly trades of the Southern Hemisphere. This creates a condition of cross-equatorial southerly flow near east Africa which, under the Coriolis influence, turns anticyclonically into the northern Arabian Sea.

The trough connecting the clockwise gyre with the Southern Hemisphere tropical cyclone (TC 16-79) is termed the southern near-equatorial trough (SET). Its counterpart, the NET is mainly evident in the region southeast of the southern tip of India, also extending to a tropical cyclone (TC 17-79).

Findlater (1971) shows the mean monthly positions and northward progression of these troughs for March, April, May, and June (1A-11a, 11b, 11c, and 11d). By June, the NET begins to merge with the thermal trough over land and becomes indistinguishable from this feature. The merged NET is commonly referred to as simply the "monsoon trough" throughout the southwest monsoon regime.

Major convection is commonly found on the north side of the SET while much of the NET or monsoon trough remains generally cloud free. The cloud-free condition is a result of the shallow nature of the trough which is normally capped by higher pressure aloft, commencing at the 850-mb level.

Cyclonic vortices of various intensities tend to develop within the NET and SET. This includes tropical cyclones which are notable features of the spring and autumn transition seasons, normally not in evidence during the height of the northeast or southwest monsoon periods. Couplets of such systems, one north and one south of the Equator (1A-10a), are a common occurrence. The surface analysis also shows the first tropical cyclone in the Bay of Bengal during the transition season. This cyclone produces the flow conditions that initiate the southwest monsoon over Indo-China. Onset of the southwest monsoon in this region, which occurred on 12 May, precedes that of the Indian subcontinent by more than 30 days.

The mean 850-mb (1A-12c) and 700-mb (1A-12b) streamline analyses, based on MONEX data for the 1–15 May 1979 transition period (Krishnamurti, 1979), depict a strong anticyclonic flow field extending over Saudi Arabia, with ridging into northern India. The analyses confirm the shallow nature of the surface heat low which occupies only the lowest kilometer of the atmosphere and does not extend upward even to the 850-mb level.

Cross-equatorial flow is observed to be minimal during this period, except at the 850-mb level off the east coast of Africa and in the Bay of Bengal where such flow is established following the passage of the tropical cyclone through the region.

The mean streamlines at 200 mb (1A-12a) show that the huge anticyclonic cell centered in the eastern Bay of Bengal, near Burma, completely dominates the flow at this level. The divergent northeasterly upper-level winds over Indo-China couple with lower-level southwesterly flow to provide an efficient outflow mechanism aloft, to promote heavy convection associated with the southwest monsoon over that region. These winds continue in a cross-equatorial direction and merge with the flow pattern of the Southern Hemisphere near-equatorial ridge.

A notable convergence asymptote is apparent over the northern Arabian Sea. This feature provides upper-level convergence over the lower-level divergent anticyclone in that area (1A-12a, 12b, and 12c). Zonal westerlies are observed in the region from 20° to 30° N. Short-wave disturbances penetrate at times into the southern portion of this belt, giving rise to severe weather and duststorms.

The DMSP visible picture at 0528 GMT 8 May, over the Bay of Bengal (1A-13a) shows that the tropical cyclone (TC 17-79) has a well-defined eye and central dense overcast, suggesting a fully-developed storm. Maximum winds of 60 kt are indicated on the surface analysis (1A-10a), approximately 7 hours after the time of the DMSP picture. The Southern Hemisphere vortex (TC 16-79) is also observed in the DMSP picture. This storm appears of much lesser intensity and is evaluated as having maximum sustained winds of 40 kt.

Note the general absence of cloudiness over India, with relatively weak onshore flow along the west coast depicted on the surface analysis (1A-10a). Such a condition, except for migratory mid-latitude disturbances which affect the northern region of India, is typical of the spring transition period to the southwest monsoon.

References

Findlater, J., 1971: Mean monthly airflow at low levels over the western Indian Ocean. *Geophys. Mem. London*, **16**, 53 pp.

Krishnamurti, T. N., P. Ardanuy, Y. Ramanathan, and R. Pasch, 1979: Quick look summer MONEX atlas. Part II: The onset phase. FSU Report No. 79-5, Florida State University, Tallahassee, FL, 205 pp.

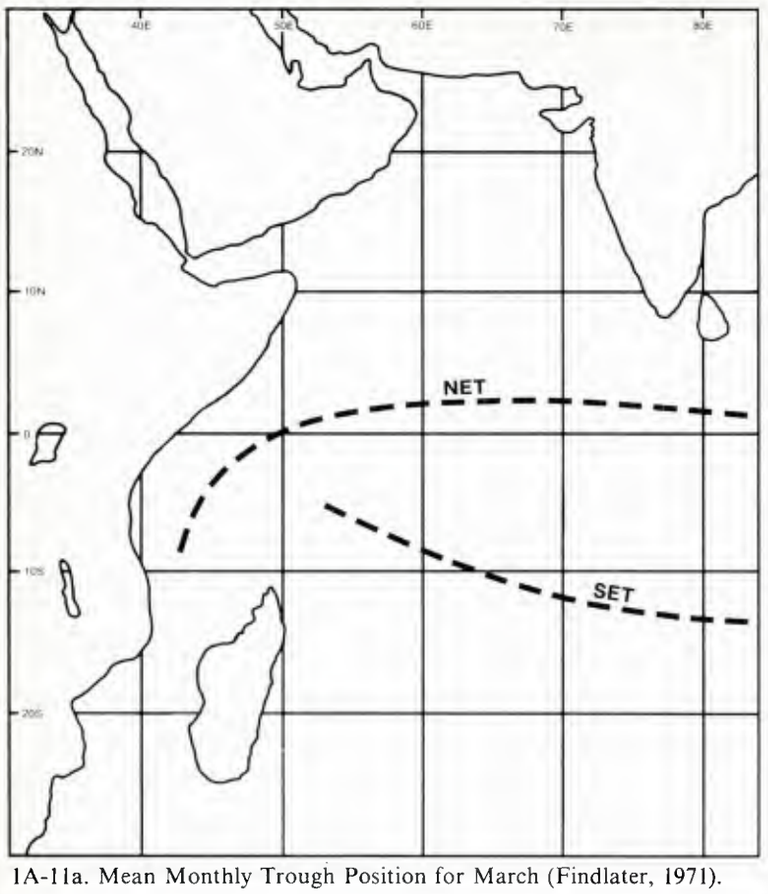

1A-11a. Mean Monthly Trough Position for March (Findlater, 1971).

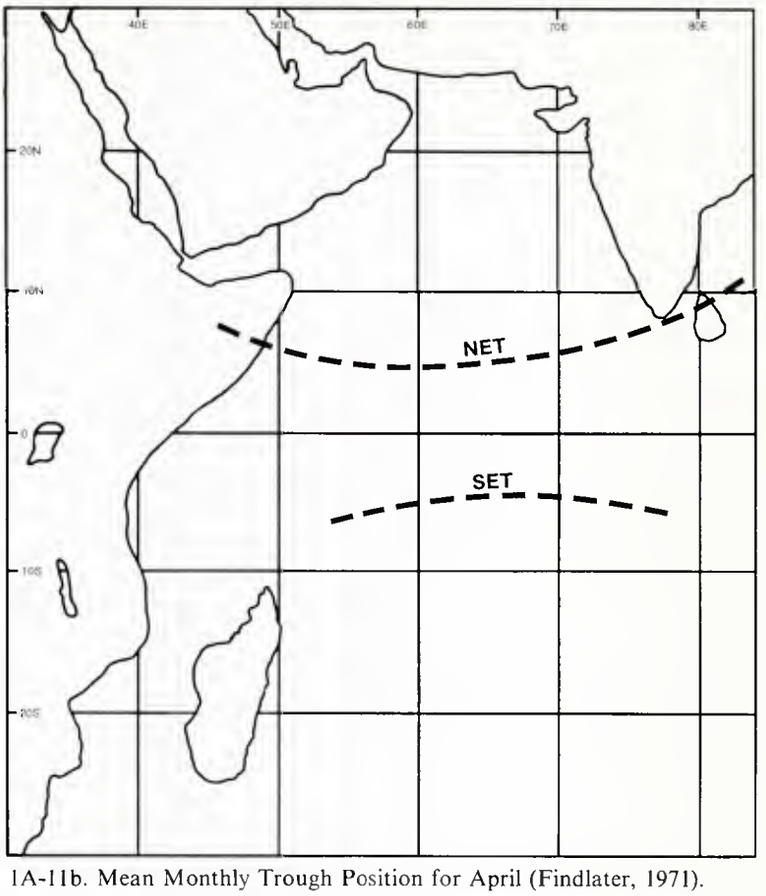

1A-11b. Mean Monthly Trough Position for April (Findlater, 1971).

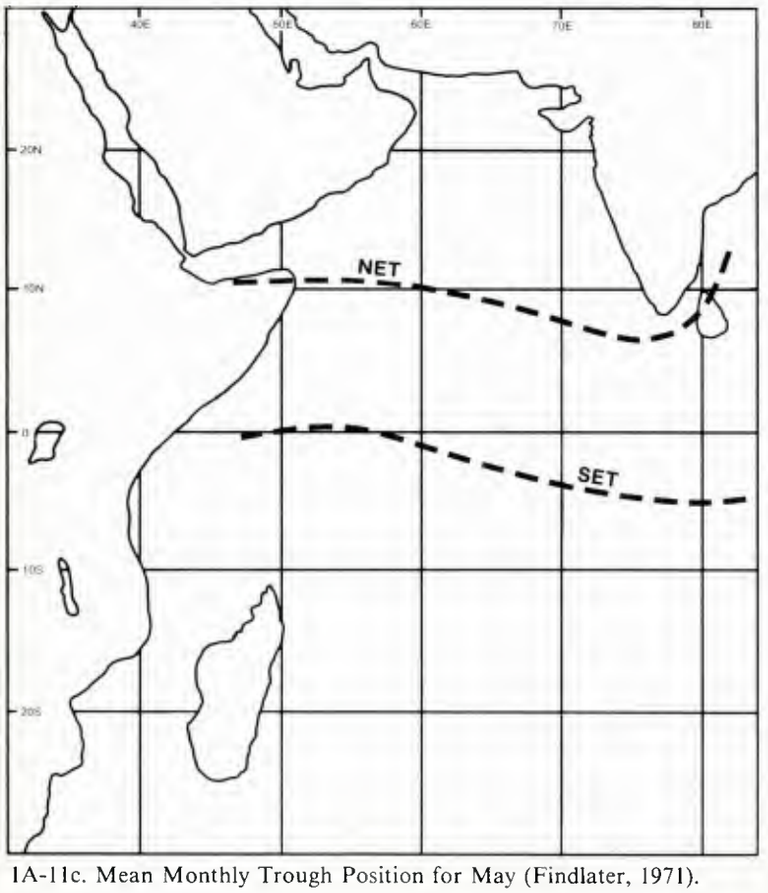

1A-11c. Mean Monthly Trough Position for May (Findlater, 1971).

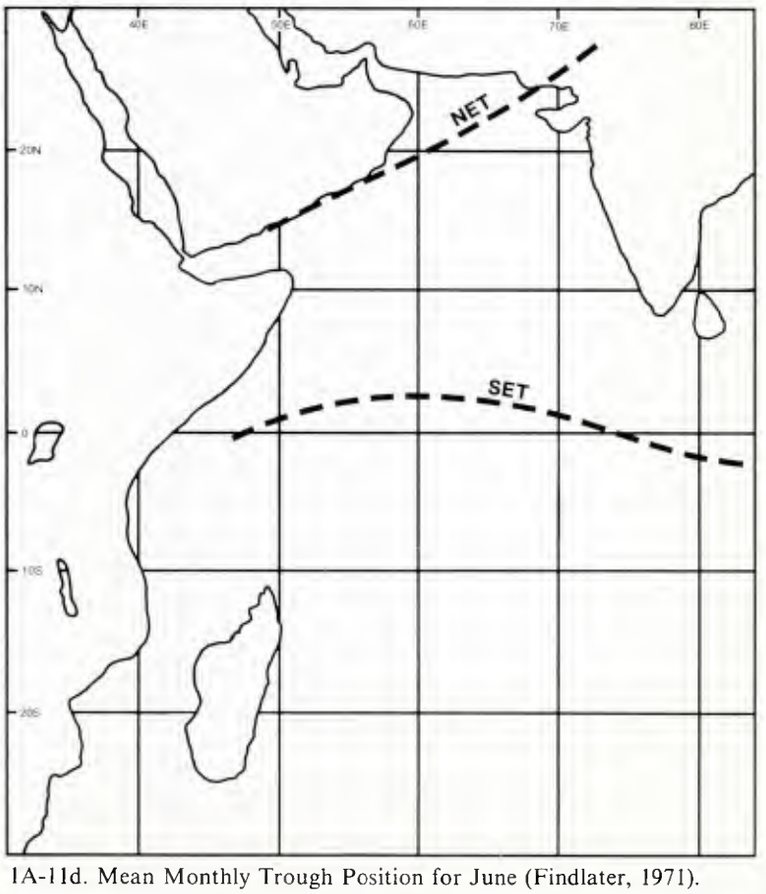

1A-11d. Mean Monthly Trough Position for June (Findlater, 1971).

200 mb

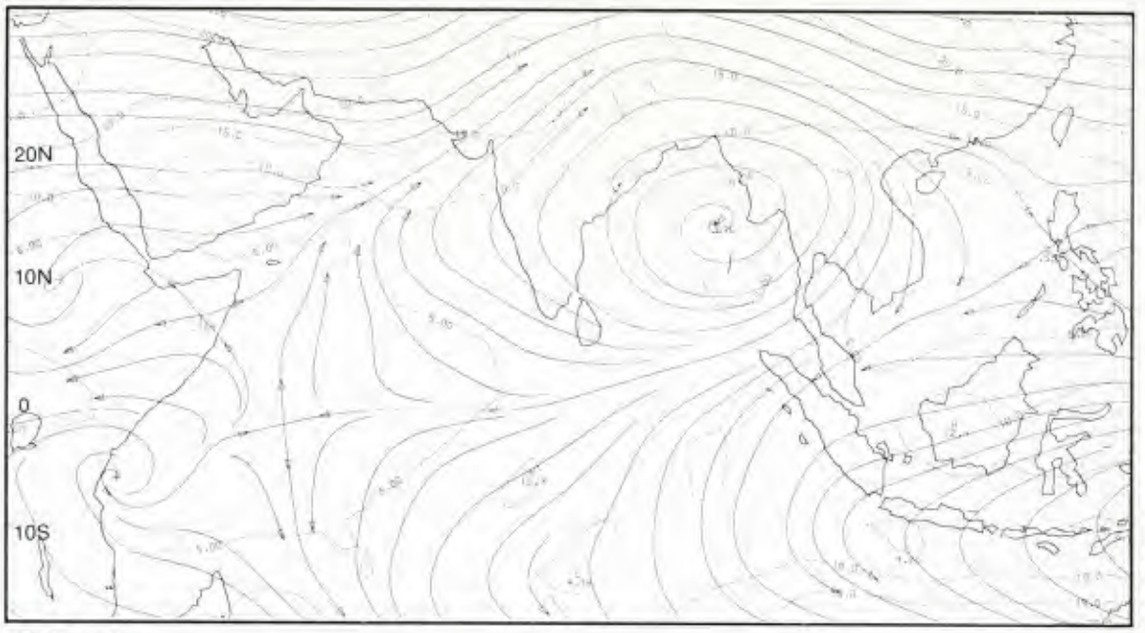

1A-12a. MONEX Mean 200-mb Analysis. 1–15 May 1979.

700 mb

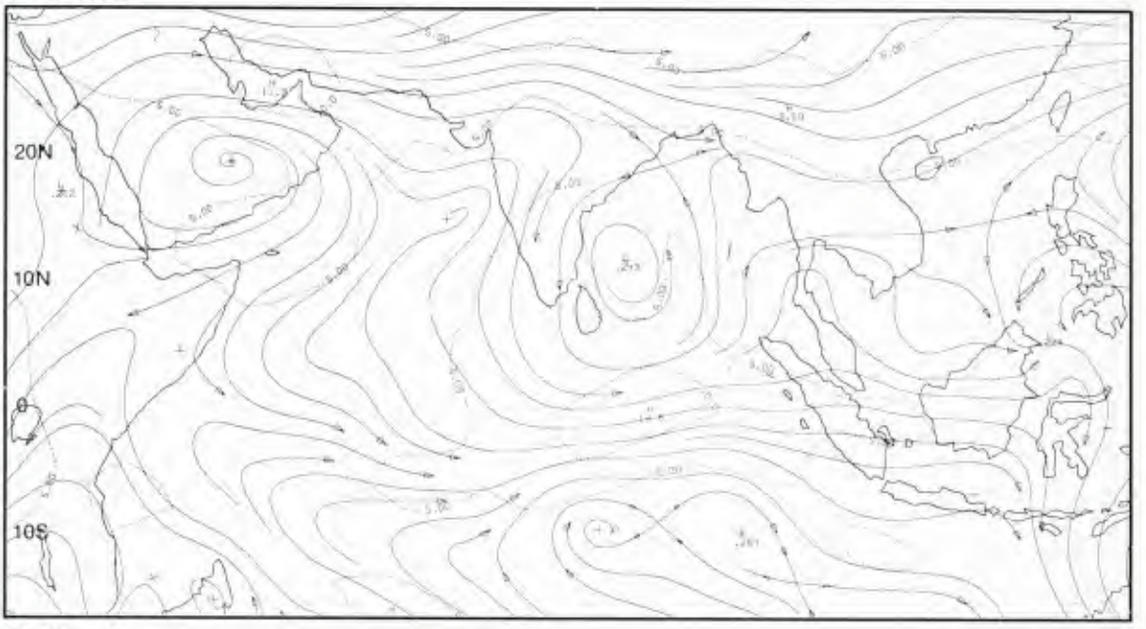

1A-12b. MONEX Mean 700-mb Analysis. 1–15 May 1979.

850 mb

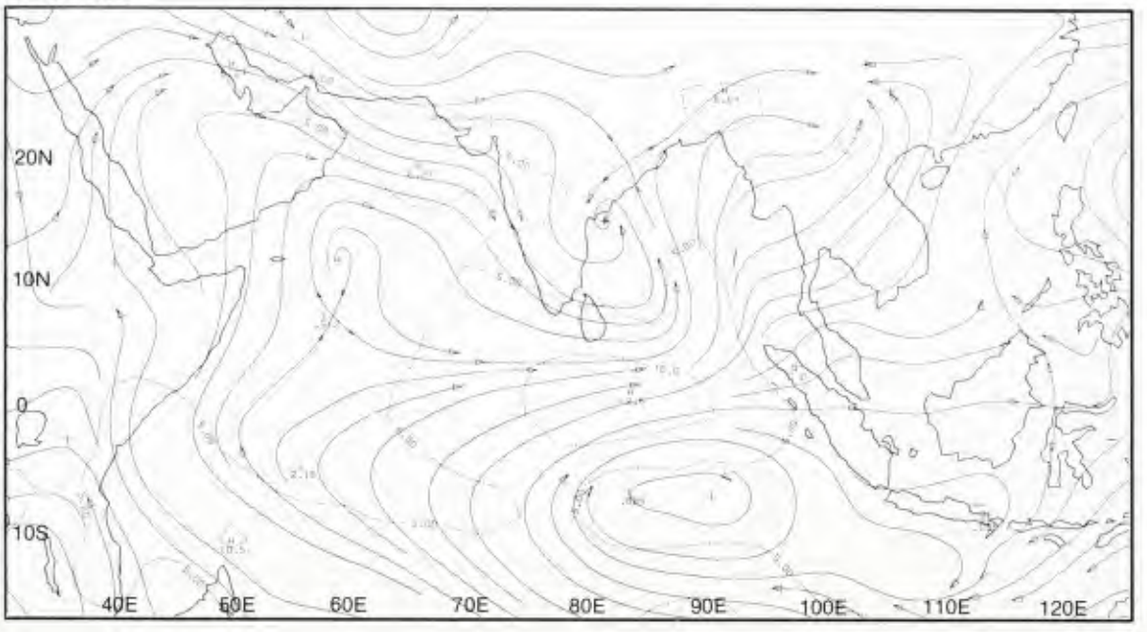

1A-12c. MONEX Mean 850-mb Analysis. 1–15 May 1979.

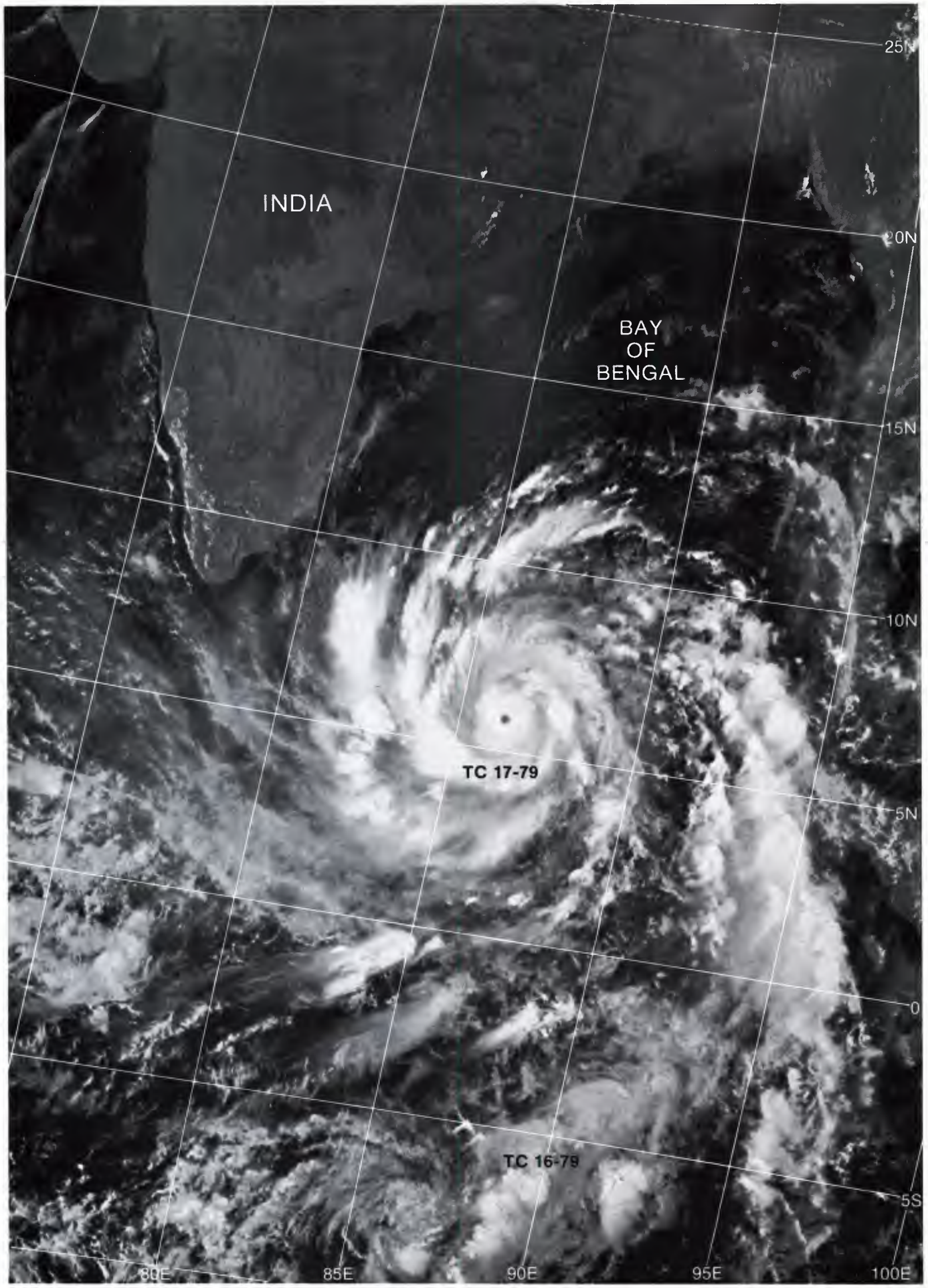

1A-13a. F-1. DMSP LS Low Enhancement. 0528 GMT 8 May 1979.

Arabian Sea/Bay of Bengal Spring Transition—Late Phase

May–June

During the late phase of the spring transition, southwest monsoon conditions become firmly established over Indo-China. However, the pattern over India remains less organized and is still subject to the effects of mid-latitude systems moving over the region.

Elsewhere, the low-level flow over the northern Indian Ocean begins to take on the pattern, but not the speed, of the southwest monsoon circulation. Two important ingredients of the active monsoon are lacking. First, there is inadequate well-established, cross-equatorial low-level flow. Such flow coming around the west side of the SET is required to provide the warm moist air that acts as a source of energy to encourage the large-scale cloud and precipitation pattern typical of the southwest monsoon regime. Second, strong upper-level easterly and northeasterly flow, required to couple with the lower-level southwesterlies and provide an efficient upper-level divergence mechanism to stimulate convection, has not yet developed.

250 mb

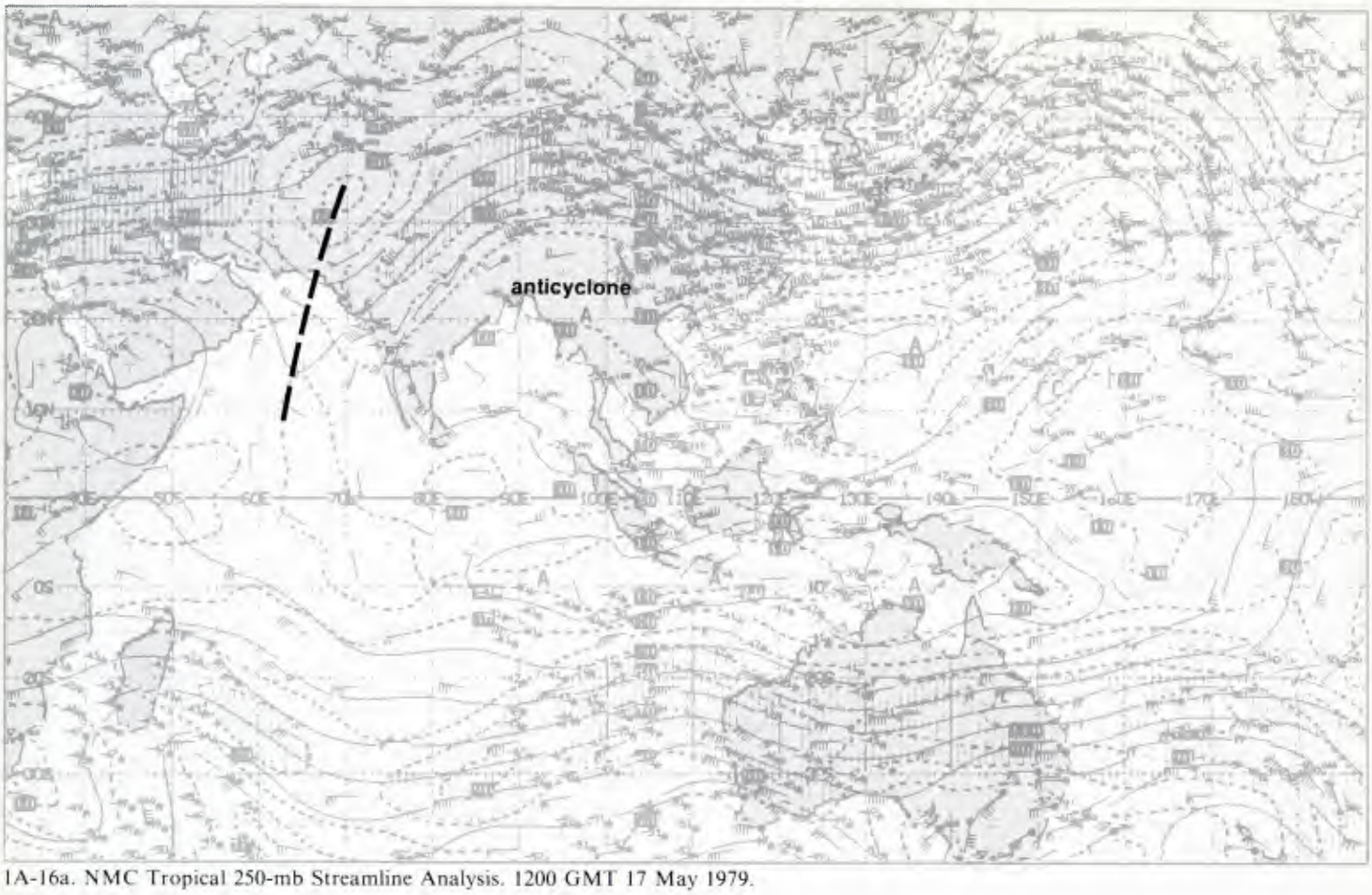

1A-16a. NMC Tropical 250-mb Streamline Analysis. 1200 GMT 17 May 1979.

500 mb

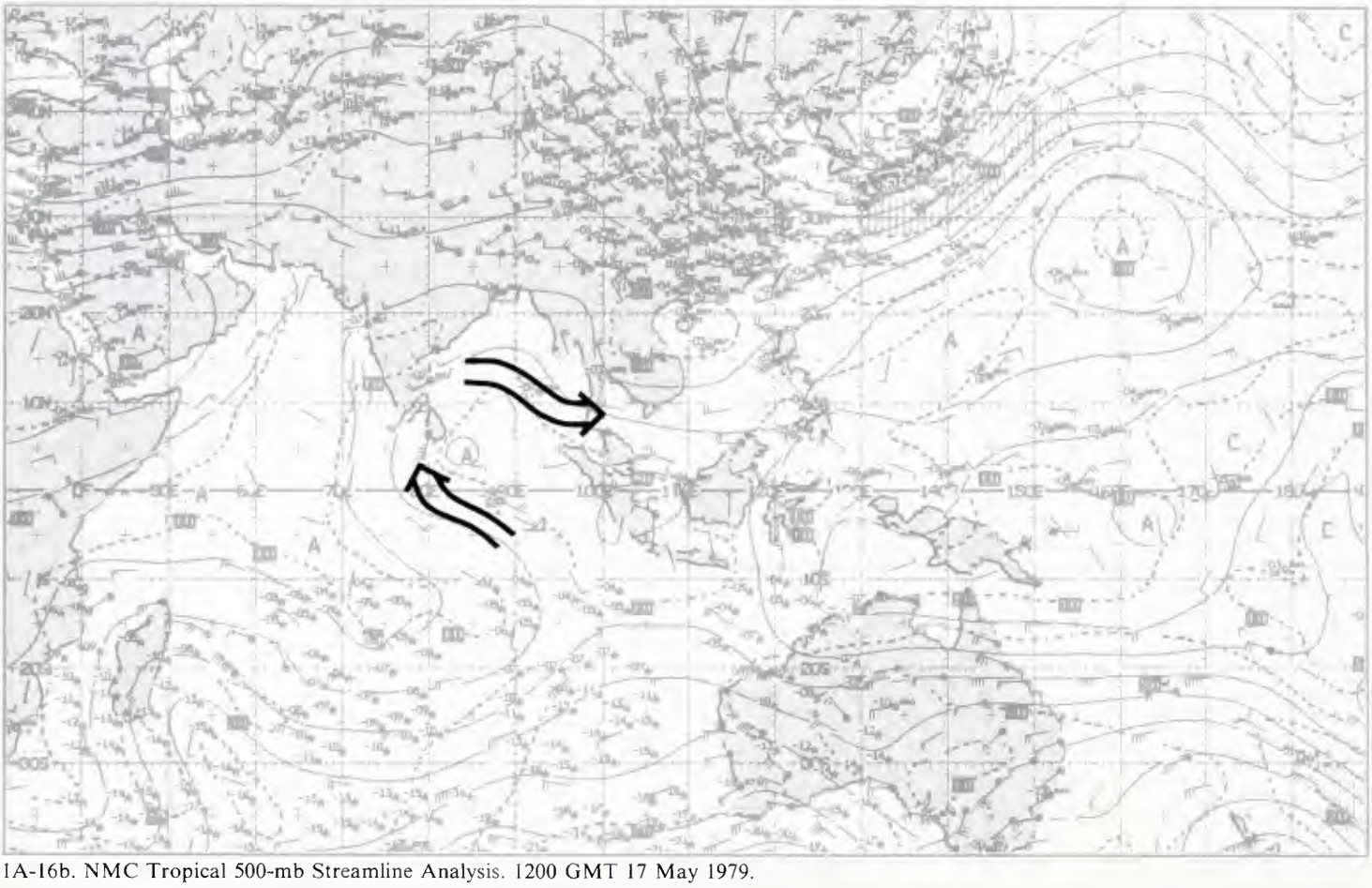

1A-16b. NMC Tropical 500-mb Streamline Analysis. 1200 GMT 17 May 1979.

Spring Transition—Late Phase
Prevailing Weather Patterns
Arabian Sea/Bay of Bengal
May/June 1979

17 May

The NMC surface streamline analysis at 1200 GMT (1A-17c) shows thunderstorms and shower activity over Indo-China, where the southwest monsoon is already established. However, India remains generally clear despite indications of a weak trough through the area. Cross-equatorial flow around the SET is quite light and does not cover a large area in its eastward extension. Easterly flow exists in the Gulf of Aden, implying southerly flow into the southern part of the Red Sea. This type of flow is characteristic of the northeast monsoon, and is a definite indicator that the southwest monsoon has not yet become established. Note that the cyclone over northern India is surrounded by fair weather conditions, typical of a thermal low.

The cyclone over southern India (1A-17c) is a deep system and is associated with a well-defined trough at 850 mb (1A-17b). Slight troughing is also observed in the region of the desert front over central Saudi Arabia. Note that a 20- to 25-kt wind maximum at 850 mb overlies the region of the established monsoon over Indo-China—the remainder of the northern Indian Ocean region shows winds of only 5–15 kt. These wind speeds will increase dramatically at the 850-mb level, and at lower levels, as the southwest monsoon becomes established over that area.

In the Southern Hemisphere, the low-level circulation over the central Indian Ocean is dominated by weak cyclonic flow centered near 5° S, 66° E on the surface analysis (1A-17c) and near 12° S, 66° E on the 850-mb analysis (1A-17b). This causes westerly flow in the region where southeasterly trades are typically found during the southwest monsoon regime. A migratory anticyclone is currently shown south of Madagascar (1A-17c). The flow about this system is causing southerly flow in the Mozambique Channel region. In general, the advection of mid-latitude air into the tropical region tends to delay or disrupt the southwest monsoon regime.

The upper-level tropospheric wind conditions as shown at 250 mb (1A-16a) reflect a more complex pattern than at 500 mb. The mid-tropospheric wind conditions, as shown at 500 mb (1A-16b) are light throughout the northern Indian Ocean. Cross-equatorial flow is limited to a small zone between 75° E and 90° E. This flow curves anticyclonically over the southern Bay of Bengal and feeds into the Indo-China region of convective activity. At 250 mb (1A-16a), the anticyclone over Indo-China has expanded in size and moved northwestward (compared to the conditions of the spring transition—early phase). This provides a larger region of upper-level divergence over the eastern Bay of Bengal and accounts for the enhanced convective activity apparent in that region.

The easterly flow on the equatorial side of the anticyclone extends to near 70° E. A trough in the westerlies located over the central Arabian Sea at 250 mb extends southward to near the Equator. The penetration of westerly disturbances to such low latitudes is an indicator that the southwest monsoon is not yet established over the region. During the developed southwest monsoon the upper-level cross-equatorial flow has a northerly component, the reverse of the low-level flow.

The GOES-Indian Ocean picture at 0930 GMT 17 May (1A-17a) reveals the intense convective activity associated with the southwest monsoon over Indo-China and with the cyclonic circulation at the south end of the trough over southern India. Higher reflectance from the waters surrounding Somalia is a sunglint effect, possibly modulated by sea state changes or dust in the atmosphere.

In the satellite picture, the clear zone off the east coast of India reflects the dry westerly offshore flow of continental air, shown particularly well on the 850-mb analysis (1A-17b). Conversely, the onshore component of flow from the high south of Madagascar has provided a moist source of air giving rise to widespread cloudiness and showers spreading inland in the coastal region from southern Africa to Somalia. Scattered to thin broken cloud conditions are seen over the remainder of the northern Indian Ocean.

9 June

The surface analysis at 1200 GMT (1A-19b) shows some distinctive changes near the end of the pre-monsoon period. The SET has intensified and appears better organized. Windflow around this feature has increased in speed, particularly noticeable off the coast of Somalia, where southwesterly flow of 15–25 kt is reported. Convective cloudiness in this region is also reported with intermittent heavy rain under obscured skies. Elsewhere over Saudi Arabia, Iran, Pakistan, and Afghanistan, generally clear sky conditions prevail. Fairly extensive cloudiness is reported over India with some shower activity. To the east, continued evidence of the southwest monsoon over Indo-China is shown by convective activity and showers in that region.

The 850-mb analysis (1A-19a), when compared to the 850-mb analysis for 17 May (1A-17a), enforces the low-level indication of a better organized southwest monsoon type flow pattern. The winds off Somalia have doubled in strength (isotachs are in m/sec) with 20-kt winds extending to near the central Arabian Sea. The pattern of cross-equatorial flow is now well organized, while it barely existed on the 17th. Troughing at the 850-mb level over India (1A-19a) appears to be the result of the penetration of a migratory mid-latitude trough into the region, and is responsible for enhanced cloudiness and convective activity over India, which cannot at this stage be attributed to a monsoonal influence. Modification of the thermal troughs over Pakistan and northern India by mid-latitude migratory systems is a characteristic feature of the pre-monsoon period.

9 June continued on page 1A-19

surface

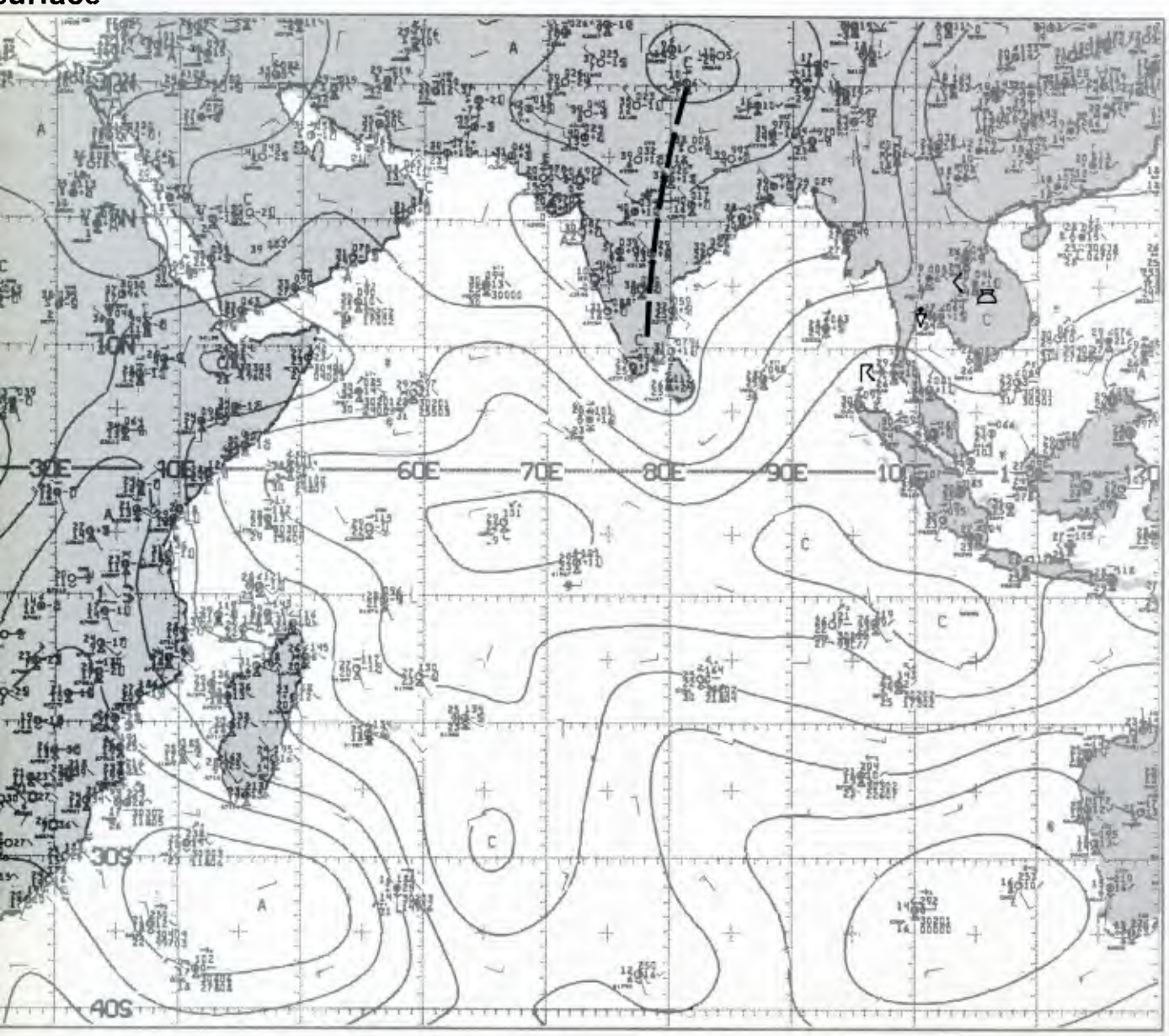

A-17c. NMC Tropical Surface Streamline Analysis. 1200 GMT 17 May 1979.

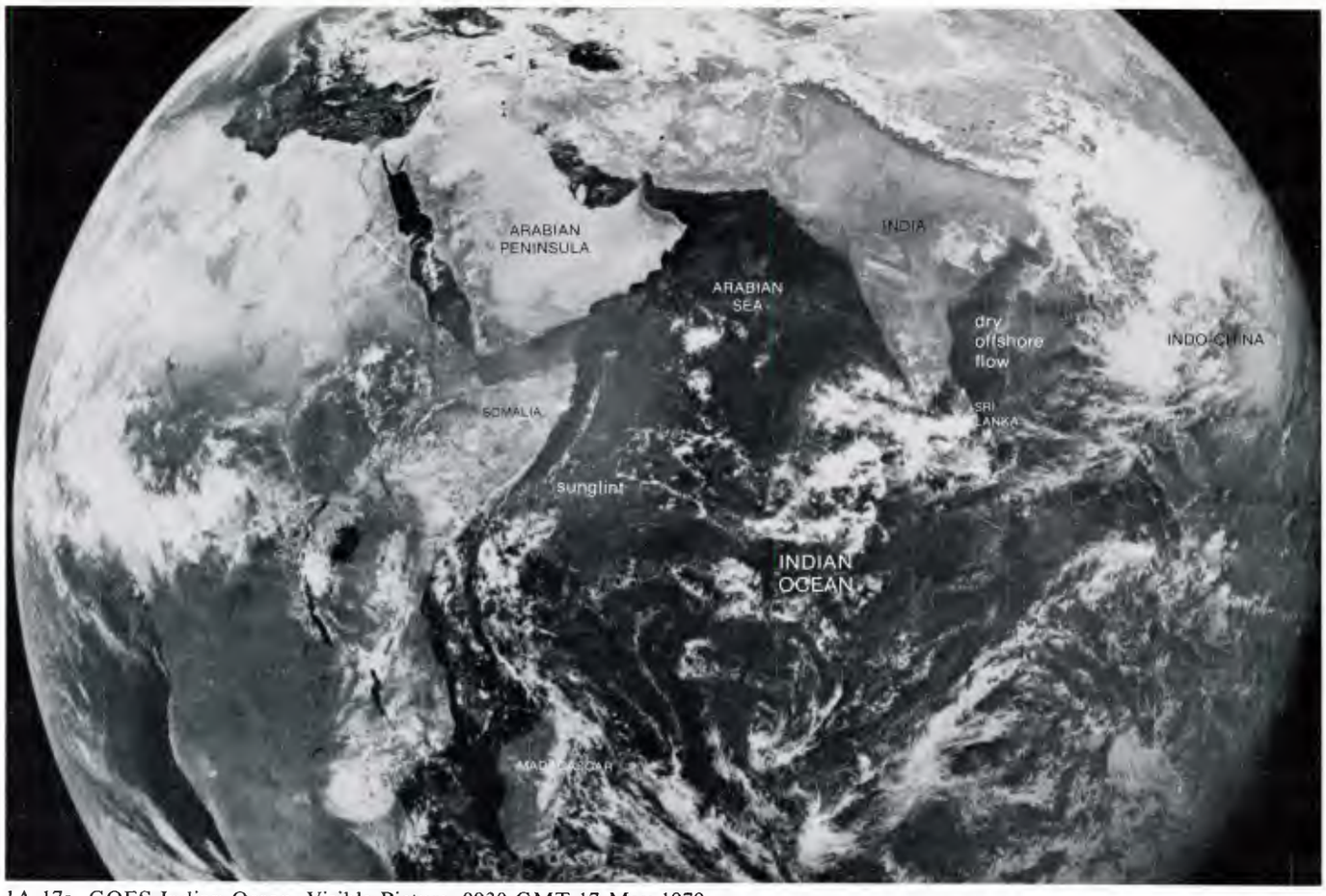

1A-17a. GOES-Indian Ocean. Visible Picture. 0930 GMT 17 May 1979.

850 mb

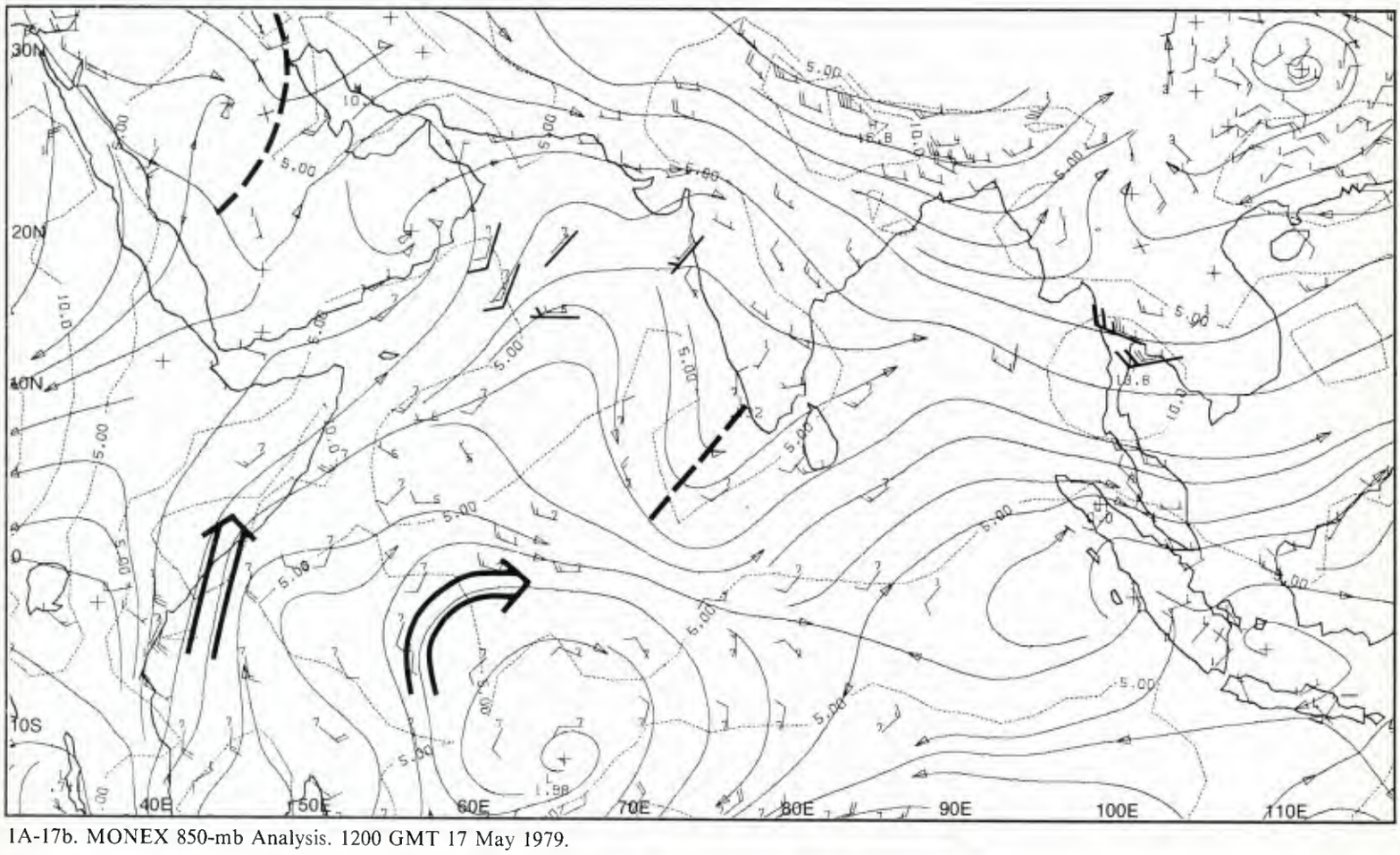

1A-17b. MONEX 850-mb Analysis. 1200 GMT 17 May 1979.

250 mb

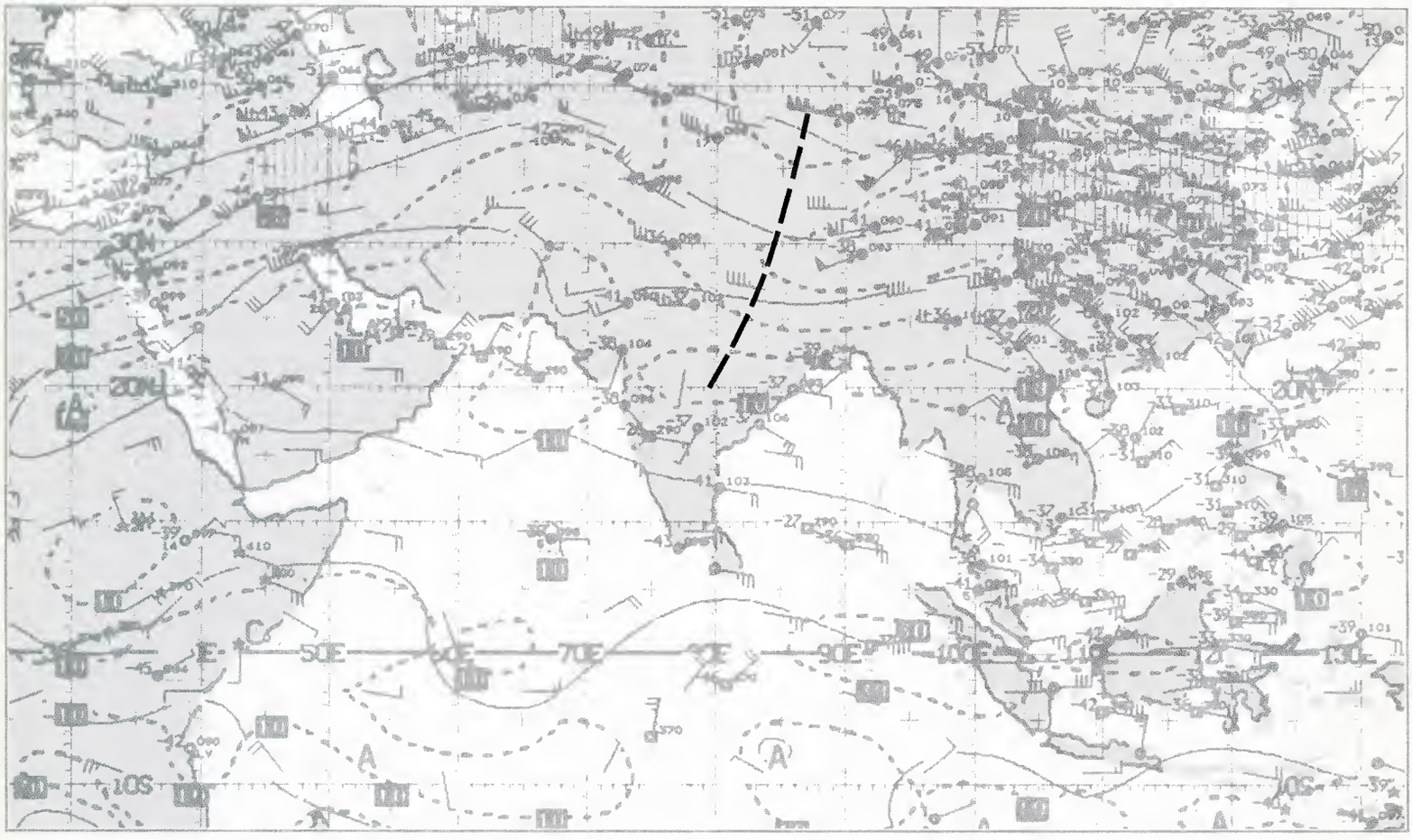

1A-18a. NMC Tropical 250-mb Streamline Analysis. 1200 GMT 9 June 1979.

500 mb

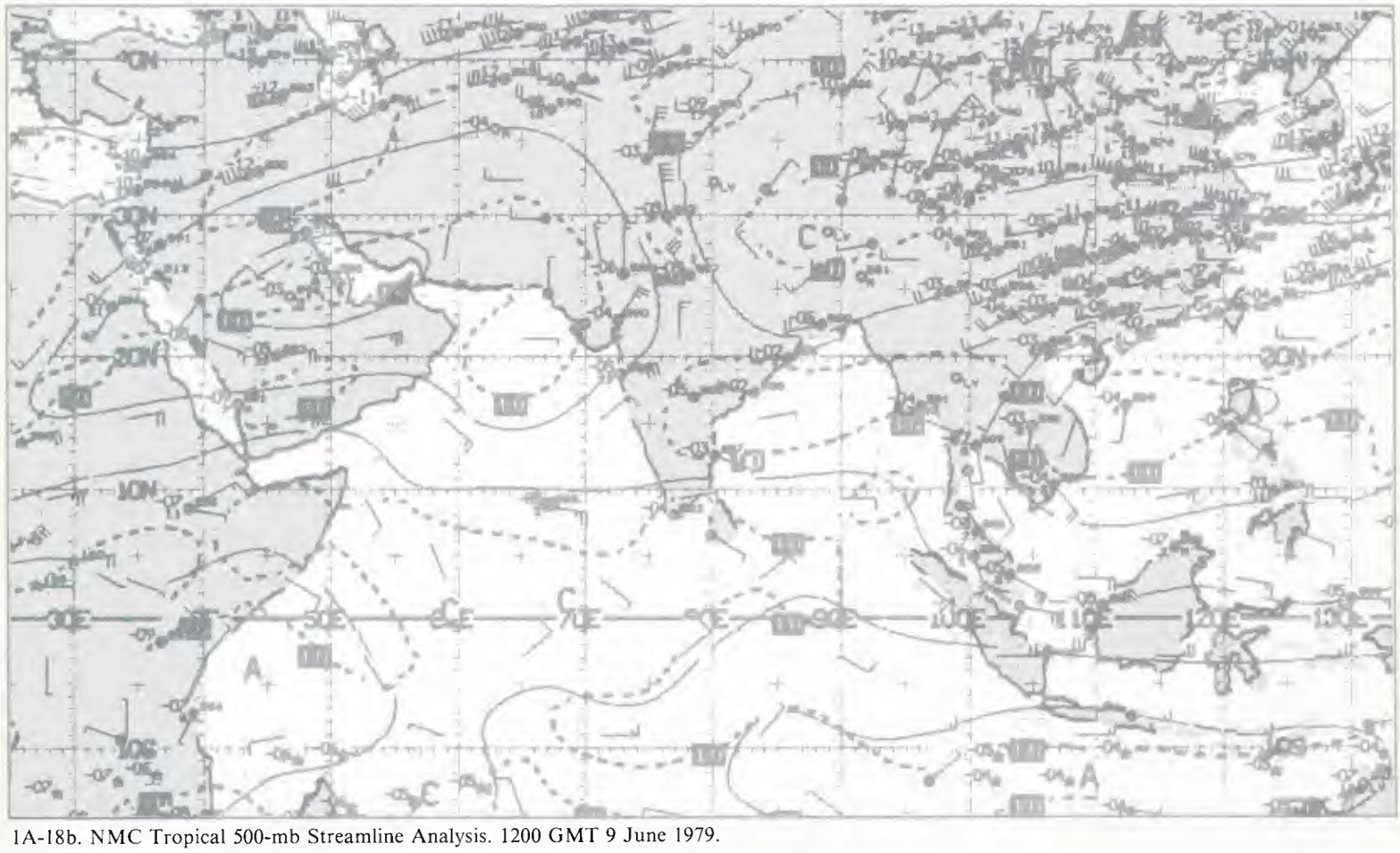

1A-18b. NMC Tropical 500-mb Streamline Analysis. 1200 GMT 9 June 1979.

The 250-mb (1A-18a) and 500-mb analyses (1A-18b) now show easterlies across the entire northern Indian Ocean except for a small region north of 20° N. Southeasterly flow is an essential ingredient of the southwest monsoon which was lacking in the early portion of the pre-monsoon period.

The GOES-Indian Ocean visible picture at 0500 GMT (1A-19c) reveals the intensified convection which develops north of the SET near the conclusion of the pre-monsoon period. The thunderstorm cell appearing as a circular mass off the coast of Somalia appears so frequently at that same location (the mouth of the Nogal River Valley) that we have named it the Nogal Valley thunderstorm (see Sec. 1D, Case 2).

A large thunderstorm cell is also apparent near Khartoum, Sudan. Such convective activity in this region often initiates intense down-draft produced duststorms which can advect across the Red Sea into Saudi Arabia (see NTAG Vol. 5, Part 1, Sec. 1E, Case 2).

9 June continued on page 1A-20

1A-19c. GOES-Indian Ocean. Enlarged View. Visible Picture. 0500 GMT 9 June 1979.

850 mb

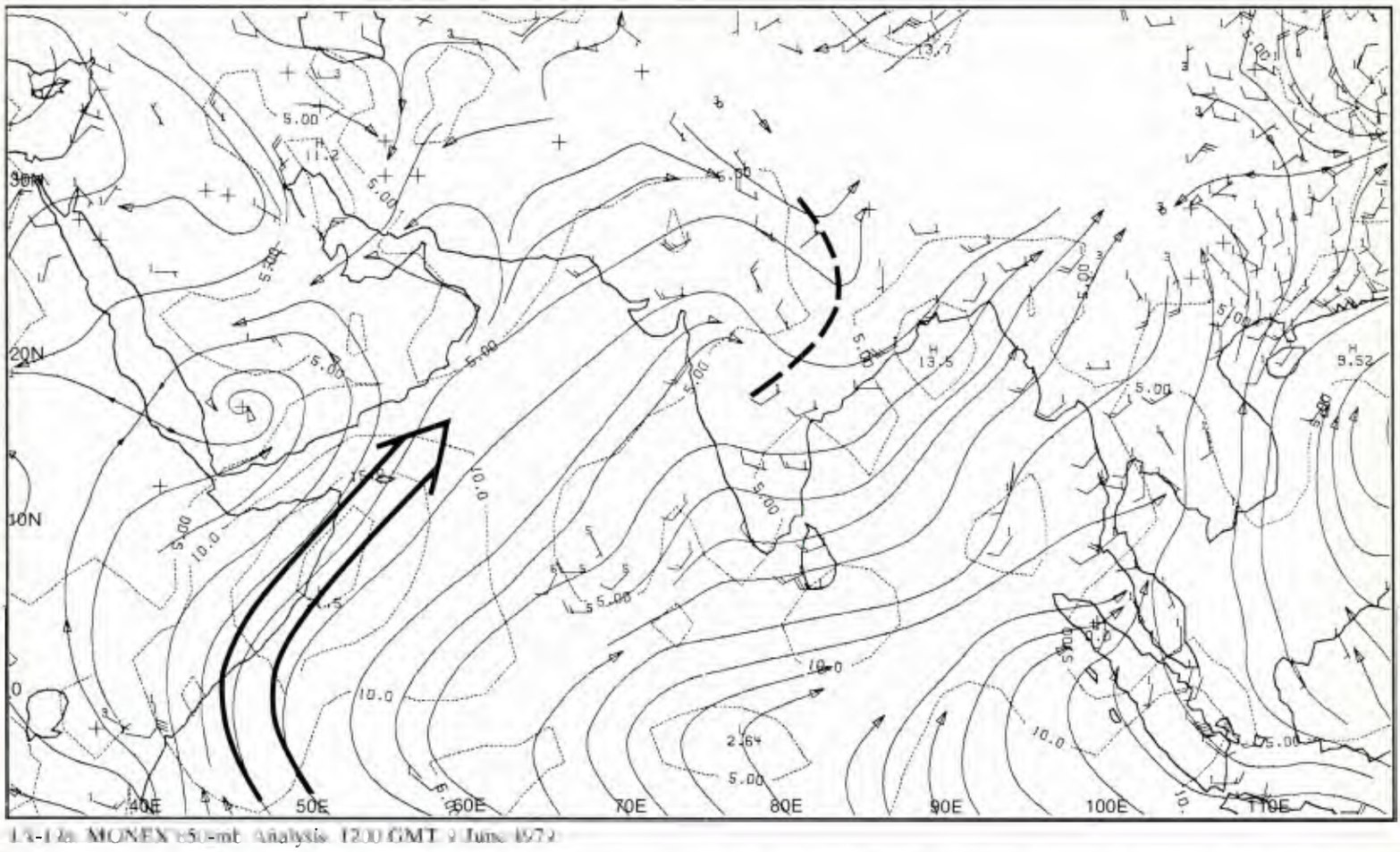

1A-18. MONEX 850-mb Analysis 1200 GMT 9 June 1979

surface

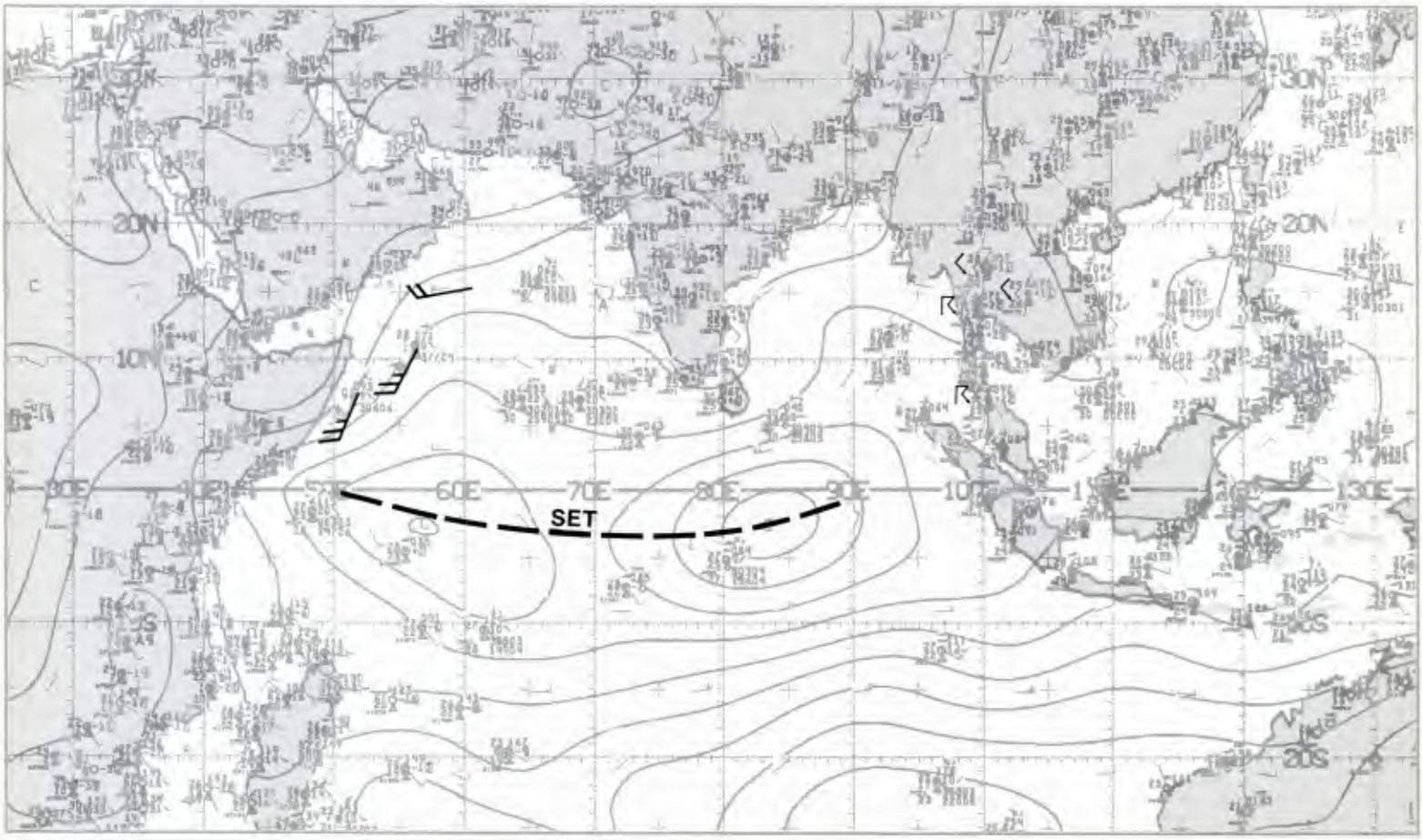

1A-19b. NMC Tropical Surface Streamline Analysis. 1200 GMT 9 June 1979.

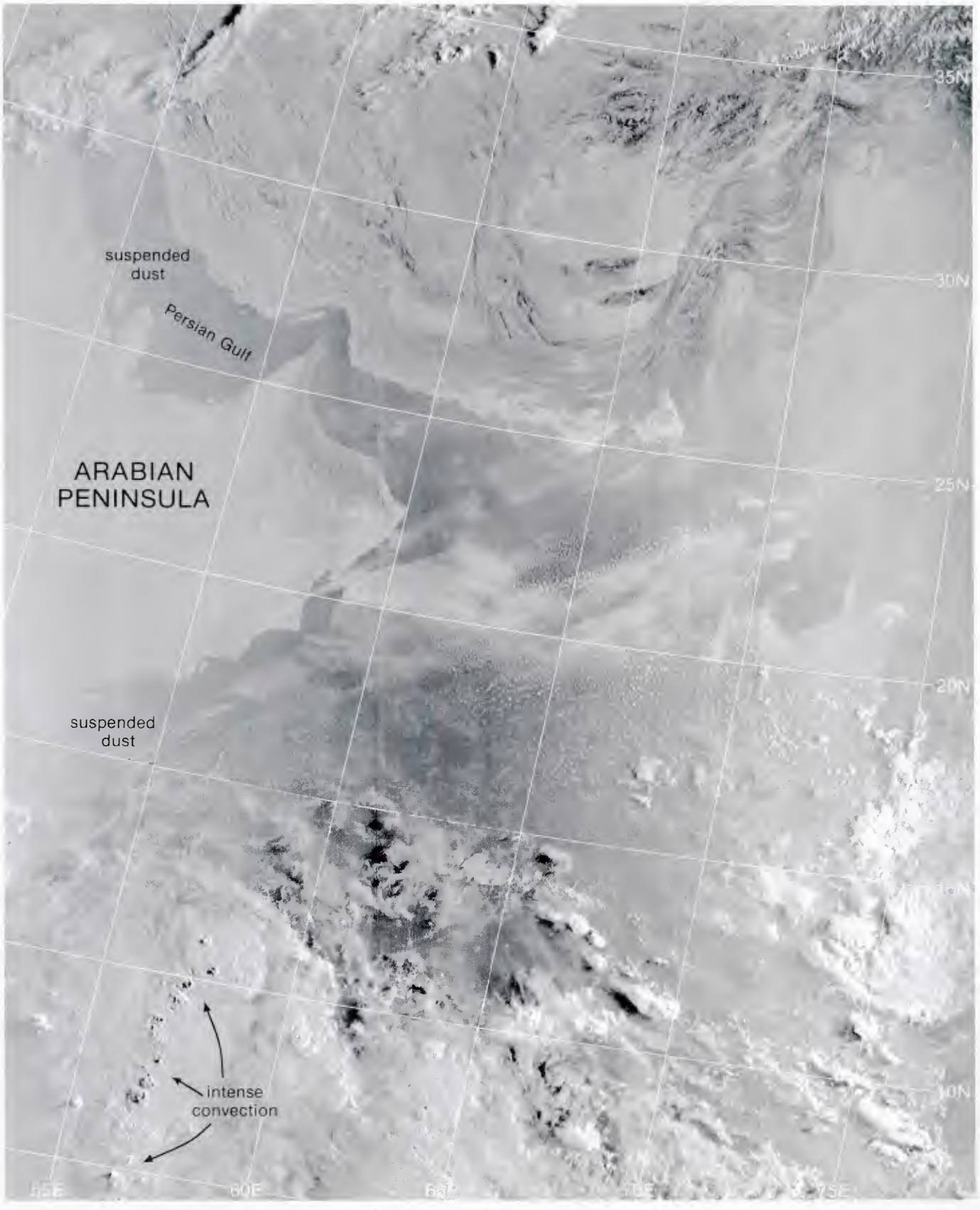

1A-20a. F-3. DMSP LF Low Enhancement. 0208 GMT 9 June 1979.

The DMSP visible picture at 0208 GMT (1A-20a) shows the intense nature of convection north of the SET and also the general degradation of contrast over non-cloudy areas caused by the large amount of suspended dust in the atmosphere resulting from winds associated with frontal penetration into the region. Only to the northeast over high Himalayan terrain, which projects above most of the dust, does increased clarity prevail.

Finally, the mean 850-mb, 700-mb and 200-mb MONEX analyses, for the period 16 to 31 May 1979, show the major changes in the upper-air circulation patterns. The 850-mb analysis (1A-21c) shows the change to more southwesterly flow over the western and northern Arabian Sea and on entry into northern India. Continued high pressure at this level prevails in the region of the thermal low over Arabia. Strong westerly flow is indicated crossing the Malay Peninsula into Indo-China.

At 700 mb (1A-21b) the southwesterly low-level flow over the northern Arabian Sea continues to be over-run by northeasterly winds from a dominant high pressure cell in southern Saudi Arabia. A high pressure cell is also located over central India, while westerly flow drops southward to reinforce the southwest monsoon over Indo-China.

The 200-mb analysis (1A-21a) continues to show two anticyclonic cells separated by a trough extending into the northern Arabian Sea. The confluence zone over the northern Arabian Sea also continues as a well-defined feature, while easterly flow is the dominant feature over the southern Bay of Bengal.

200 mb

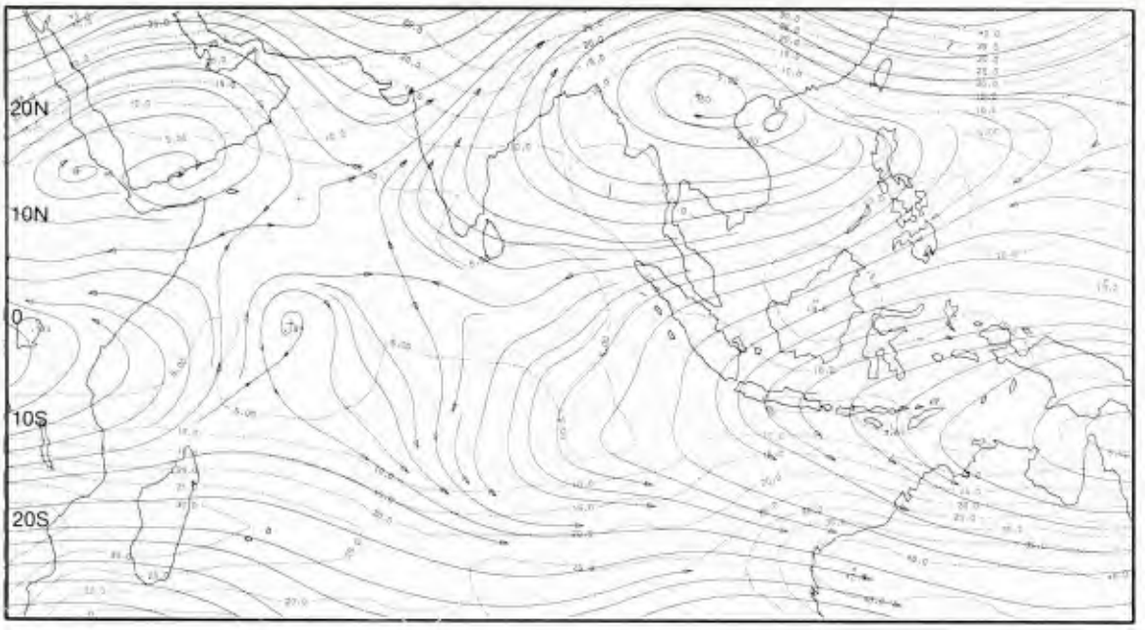

1A-21a. MONEX Mean 200-mb Analysis. 16–31 May 1979.

700 mb

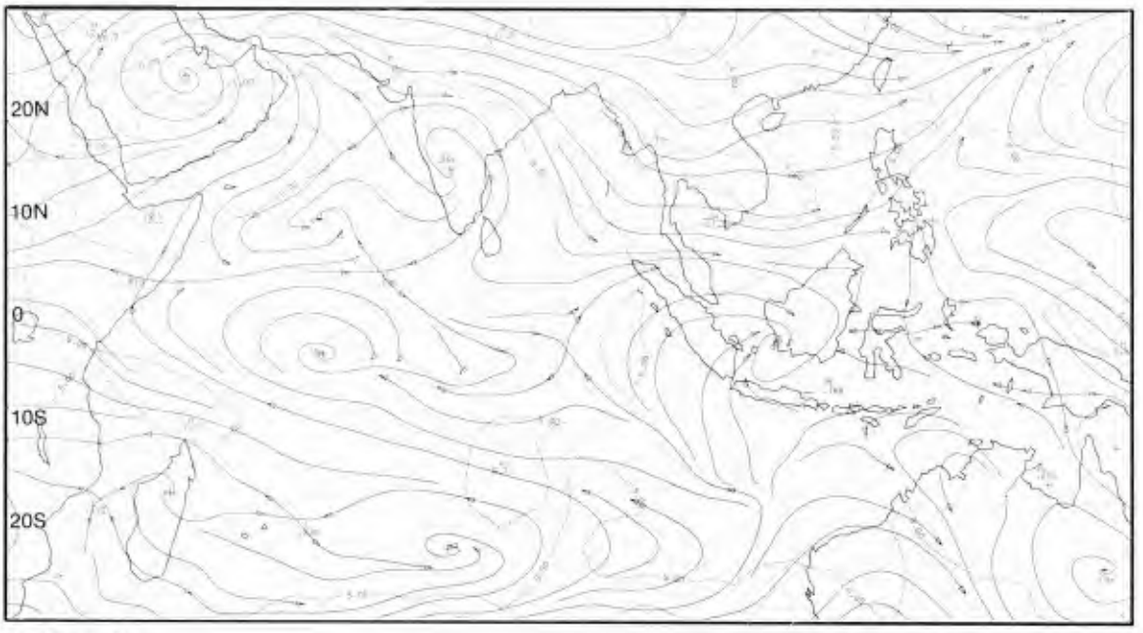

1A-21b. MONEX Mean 700-mb Analysis. 16–31 May 1979.

850 mb

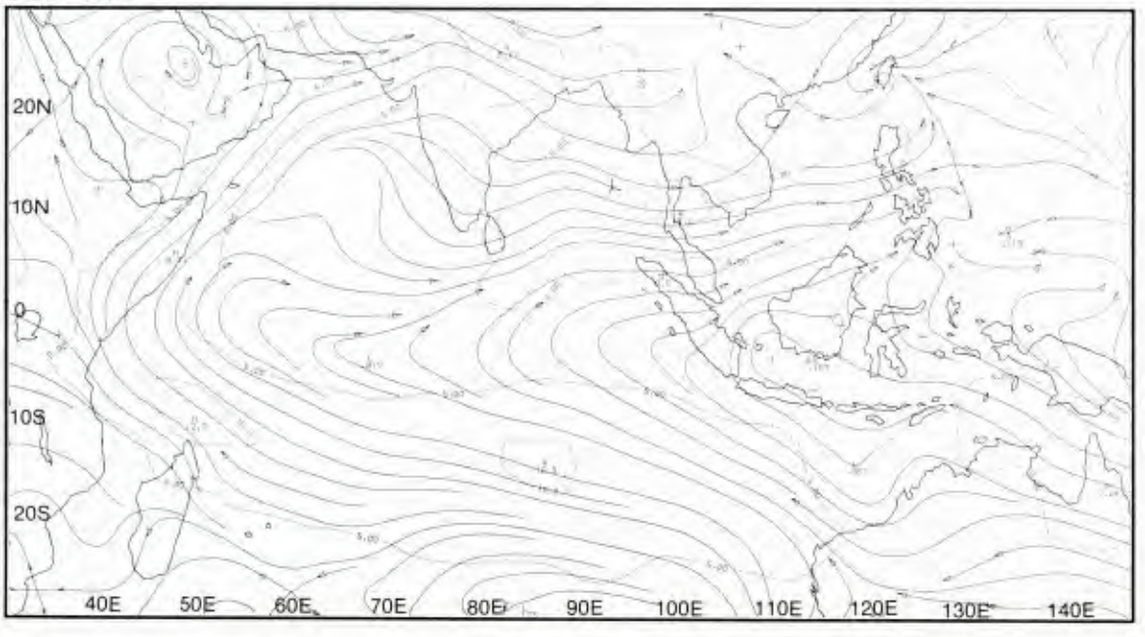

1A-21c. MONEX Mean 850-mb Analysis. 16–31 May 1979.

Arabian Sea/Bay of Bengal Spring Transition—Late Phase

May–June

The Burst of the Monsoon

The onset of the low-level southwest flow and the related monsoon cloudiness and rain over the Northern Hemisphere Indian Ocean region is known to occur abruptly, and is called the "burst of the monsoon". The general development of the southwest monsoon shows an increase in the Southern Hemisphere trade winds (intensification of the Mascarene high); followed in a couple of days by increased cross-equatorial flow (establishment of the low-level Somali jet); followed a few days later by increased westerly flow across the Arabian Sea (frequently leading to the development of an onset vortex off southwest India); and then abrupt increases in cloudiness and precipitation along the southwestern coast of India. Cadet (1979) shows the average onset dates of the rainy season as a function of location (1A-23a).

Reference

Cadet, D., 1979: Meteorology of the Indian summer monsoon. *Nature*, **279**, 761–767.

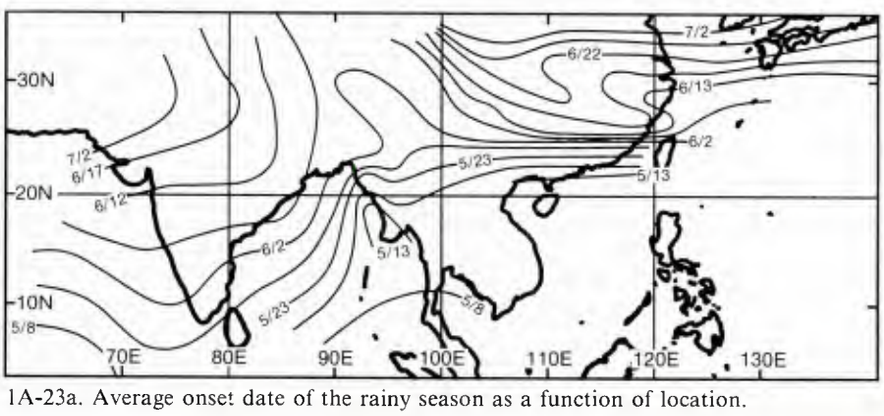

1A-23a. Average onset date of the rainy season as a function of location.

Spring Transition—Late Phase
Burst of the Monsoon
Arabian Sea
May 1978

10–16 May

The following examples of the low-level wind fields off eastern Africa depict the monsoon burst development in 1978 (Cadet, 1980). The 10 May wind field (1A-25a) shows the typical pre-monsoon conditions. The Southern Hemisphere trade winds enter east Africa and maintain their easterly component. Light westerly flow is seen off Somalia in the western Arabian Sea. Two days later, on 12 May (1A-25b), a marked change can be seen in the flow pattern. The cross-equatorial flow (Somali jet) is established. On 16 May (1A-25c) the Somali jet has intensified, southerly winds exist farther south along the African coast, and strong southwesterly winds are seen over the western Arabian Sea.

Reference

Cadet, D., and M. Desbois, 1980: The burst of the 1978 Indian summer monsoon as seen from METEOSAT. *Mon. Wea. Rev.*, **108**, 1697–1701.

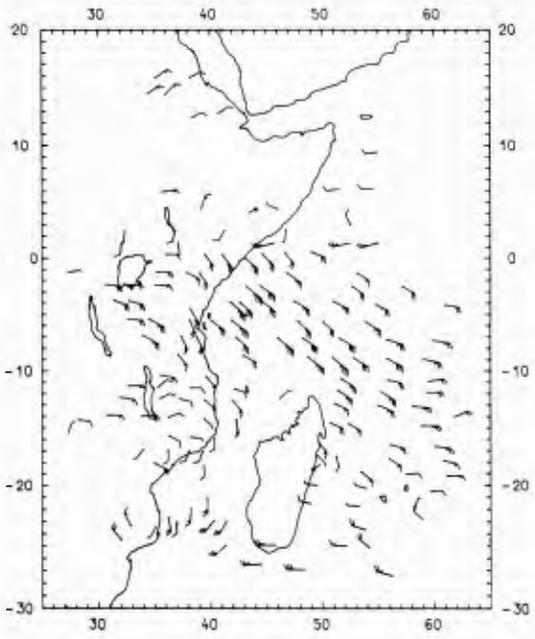

1A-25a. Low-level wind field. 10 May 1978 (Cadet and Desbois, 1980).

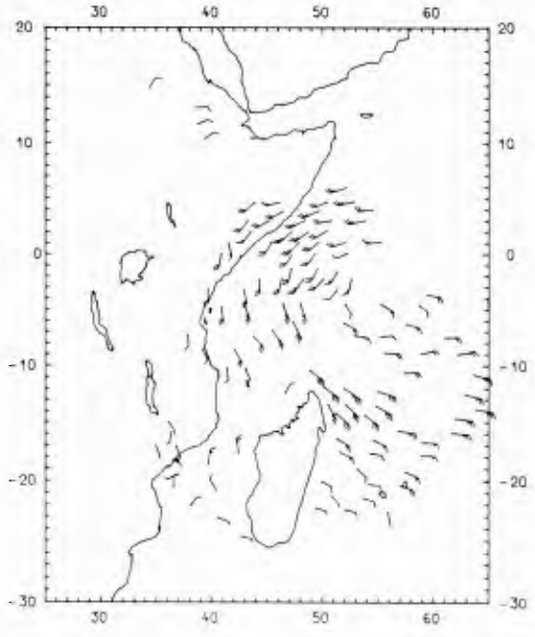

1A-25b. Low-level wind field. 12 May 1978 (Cadet and Desbois, 1980).

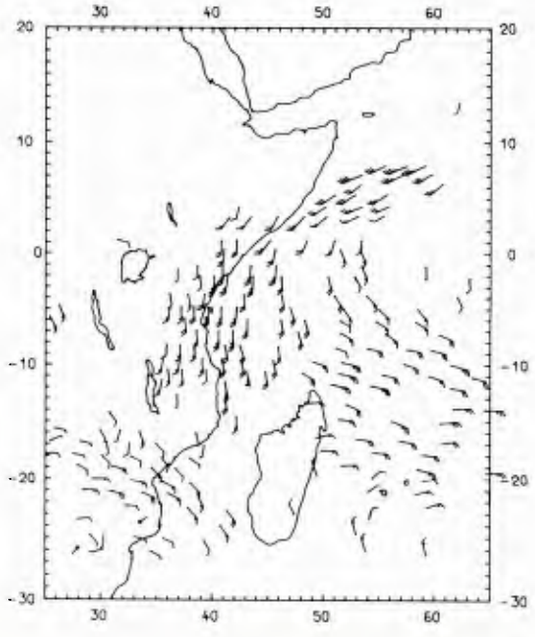

1A-25c. Low-level wind field. 16 May 1978 (Cadet and Desbois, 1980).

Arabian Sea/Bay of Bengal Spring Transition—Late Phase

May–June

Southwest Monsoon Onset Vortex

A vortex generated off the southwest coast of India has repeatedly been noted a few days prior to the commencement of the southwest monsoon over India. Because of its apparent role in the initiation of the southwest monsoon in that region, it has been termed the "onset vortex" (Krishnamurti, 1981). In a review of past years, clear evidence of such formations was apparent in 37 out of 68 cases. In cases where it was not noted, data deficiency may have posed a problem for proper analyses. The date of formation for those cases where the onset vortex was detected ranged from 14 May to 16 June. The vortex tends to move generally west-northwestward toward the Arabian coast.

Reference

Krishnamurti, T. N., 1981: On the onset vortex of the summer monsoon. *Mon. Wea. Rev.*, **109**, 344–363.

Spring Transition—Late Phase
Southwest Monsoon Onset Vortex
India
June 1979

11–14 June

Krishnamurti (1981) shows that the onset vortex is a deep three-dimensional phenomenon with a closed circulation extending from the surface up to 300 mb. In the 1979 development, prior evidence of the vortex was first noted at 300 mb on 11 June (not shown). No evidence of the vortex on this date appears at 200 mb or higher (1A-29a). The vortex subsequently formed at 700 mb (1A-29b) on 13 June, and at 850 mb (1A-29c) on 14 June, on the cyclonic shear side of the low-level jet along the low-level east–west asymptote of convergence that separates the dry air of the Arabian deserts from the moist cross-equatorial monsoon current. Note in the GOES-Indian Ocean picture on 14 June (1A-29d) that despite well-developed convection, the vortex center was not yet well defined. Krishnamurti concludes that the strong horizontal shear flow in the low levels provides energy for the maintenance of the vortex near the surface, and that the barotropic instability, resulting from the strong horizontal shear in the lower levels, may have been initiated (or triggered) by the gradual descent of the mid-tropospheric circulation.

Reference

Krishnamurti, T. N., 1981: On the onset vortex of the summer monsoon. *Mon. Wea. Rev.*, **109**, 344–363.

A-29d. GOES-Indian Ocean. Enlarged View. Visible Picture. 0400 GMT 14 June 1979.

200 mb

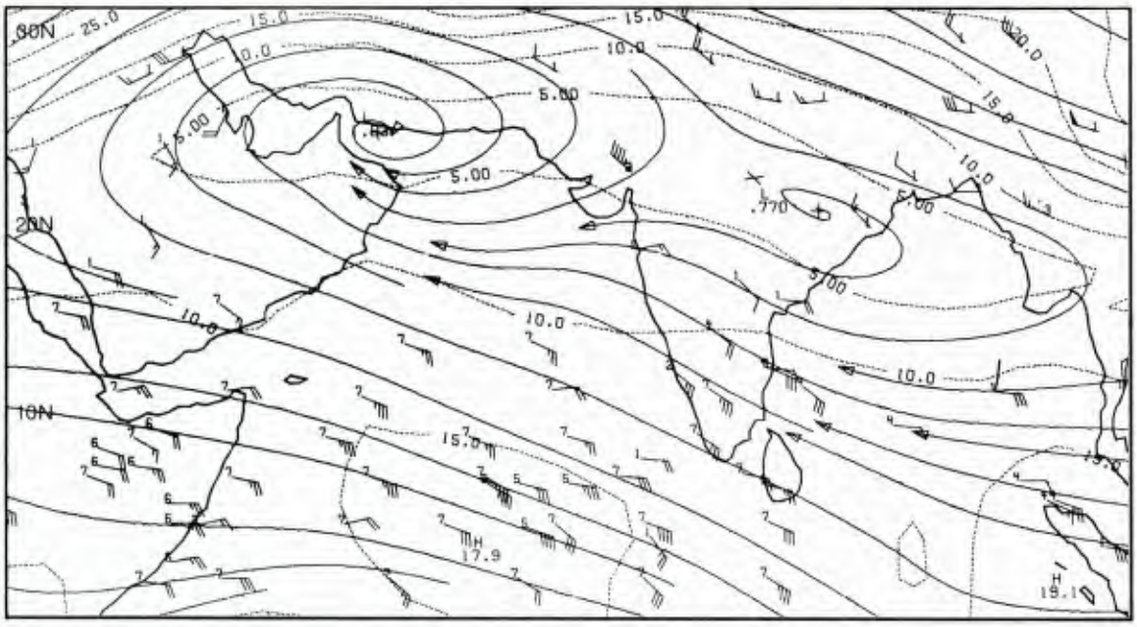

1A-29a. MONEX
200-mb Analysis.
1200 GMT
11 June 1979.

700 mb

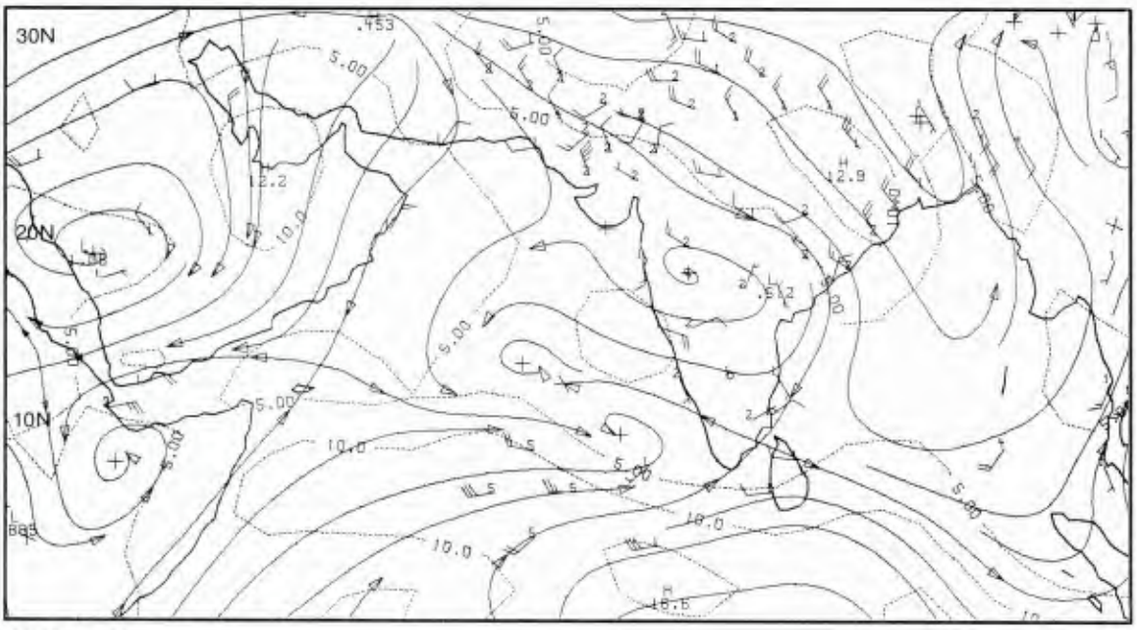

1A-29b. MONEX
700-mb Analysis.
1200 GMT
13 June 1979.

850 mb

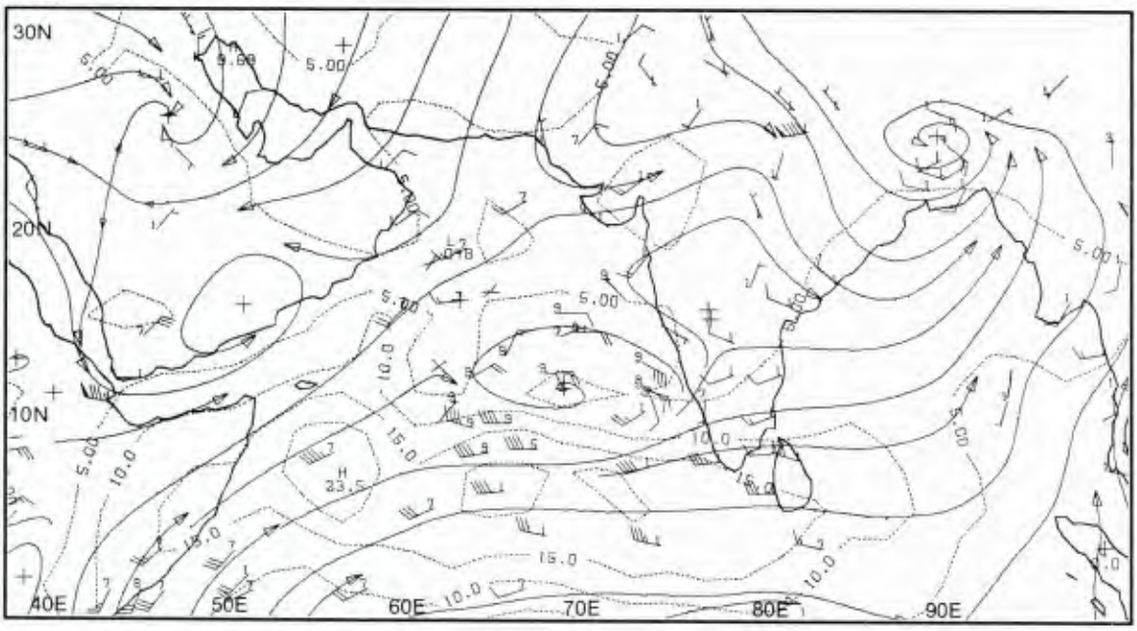

1A-29c. MONEX
850-mb Analysis.
1200 GMT
14 June 1979.

Arabian Sea/Bay of Bengal Southwest Monsoon

July–September

Characteristic Features

Krishnamurti and Bhalme (1976) define nine elements of the broad-scale southwest monsoon system (1A-31a). The elements are as follows:

1. **Monsoon trough**
2. **Mascarene high**
3. **Low-level jet**
4. **Tibetan high**
5. **Tropical easterly jet**
6. **Monsoon cloud cover**
7. **Monsoon rainfall**
8. **Dry static stability**
9. **Moist static stability**

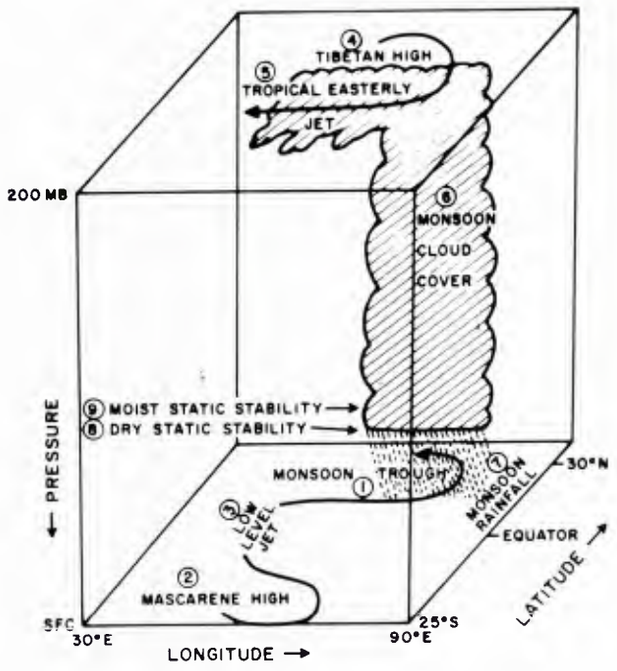

1A-31a. Schematic diagram of the nine elements of the monsoon system considered in this study (Krishnamurti and Bhalme, 1976).

Reference

Krishnamurti, T. N., and H. N. Bhalme, 1976: Oscillations of a monsoon system. Part I: Observational aspects. *J. Atmos. Sci.*, **33**, 1937–1954.

7. Monsoon Rainfall

Rainfall characteristics over the ocean cannot be directly addressed due to lack of data. A direct correlation to convective cloud activity is expected. Over India there are considerable variations in the monsoon rainfall from day-to-day and year-to-year. Those differences are illustrated (1A-33b) to show the contrasts in daily rainfall over central India (15° to 25° N, 75° to 85° E) during 1972 (a drought year) and 1973 (near normal rainfall year).

The nature of the commencement of the southwest monsoon is markedly different from the start of the northeast monsoon. While a gradual onset of light westerly flow takes place over the Arabian Sea and

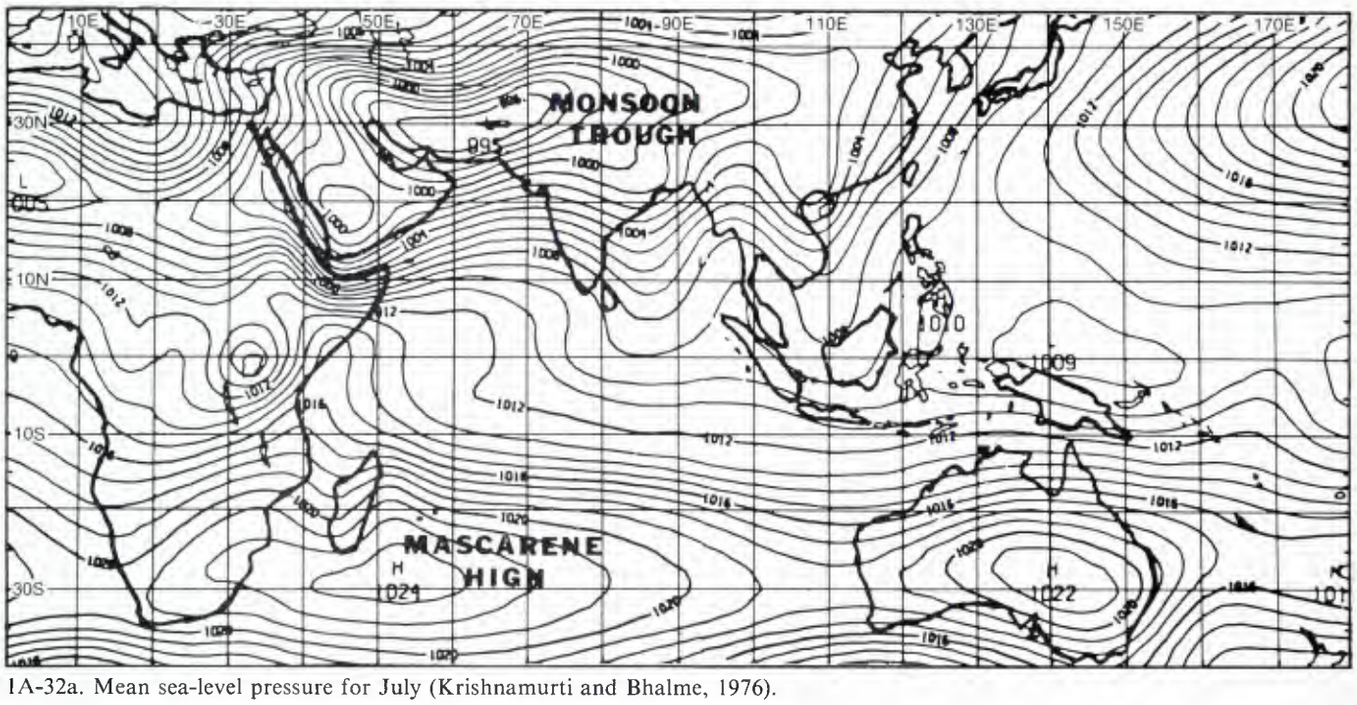

1A-32a. Mean sea-level pressure for July (Krishnamurti and Bhalme, 1976).

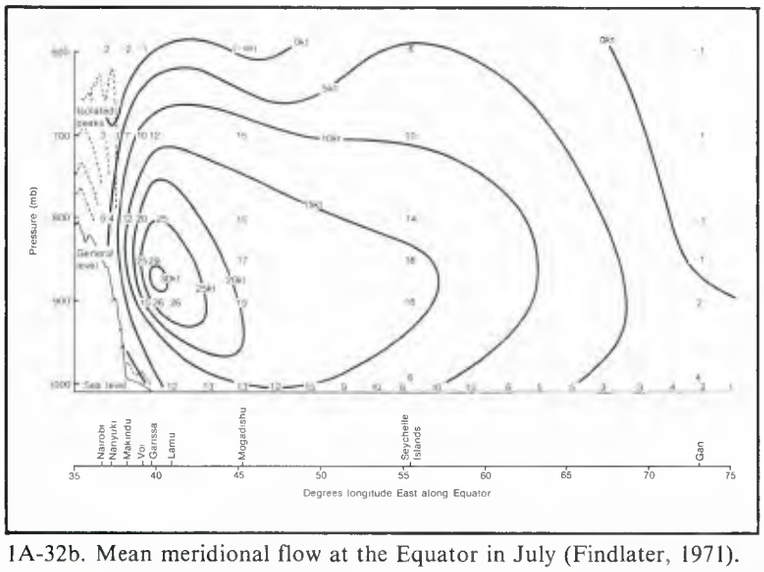

1A-32b. Mean meridional flow at the Equator in July (Findlater, 1971).

1A-32c. Month by month progress of the axis of the low-level cross-equatorial jet. Note the split in the axis of the jet in June and July. The east African mountains are also indicated in this diagram (Krishnamurti and Bhalme, 1976).

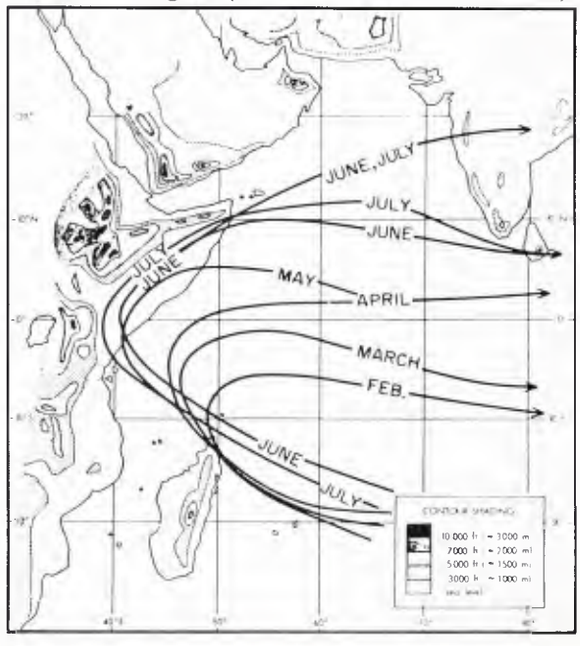

Characteristics of the Mature Phase

Seven of the nine elements listed by Krishnamurti and Bhalme (1976) are described to define the broad-scale features of the mature phase of the southwest monsoon.

1. Monsoon Trough

This low-pressure trough (1A-32a), located near 30° N, 65° E at sea level, is a part of the global thermal equatorial trough of the northern summer season. It is the axis of the area of low pressure caused by surface heating and includes the northern equatorial trough during the period of a well-established southwest monsoon.

2. Mascarene High

This is the Southern Hemisphere high pressure system (1A-32a) located near 30° S, 50° E. Its name comes from the Mascarene Islands east of Madagascar. The easterly flow on the equatorward side of this high feeds the cross-equatorial current of the southwest monsoon.

3. Low-Level Cross-Equatorial Jet

This is the low-level Somali jet first documented by Findlater (1971). Maximum winds occur near 5000 feet (1.5 km) and have been reported to speeds of 100 kt near Madagascar and off the Somalia coast. The mean structure of the Somali jet for July (1A-32b) and the month-by-month progress of its axis (1A-32c) show the evolution of this most important jet stream feature.

4. Tibetan High

A large anticyclone is best developed at 200 mb during the Northern Hemisphere summer months. It first forms in April just north of Borneo, is over southern Indo-China by May, over northern Burma in June and thereafter moves over the Tibetan highlands. It starts moving south-southeast in September, and is found over Malaysia in November; thereafter it loses its identity until the following April.

5. Tropical Easterly Jet

This upper-tropospheric feature is found near 150 mb and has winds of 80–100 kt, with the strongest winds being found just to the west of the southern tip of India over the Arabian Sea. It lies on the equatorward side of the Tibetan High. The jet forms in June and is present until September.

6. Southwest Monsoon Cloudiness

The onset of the southwest monsoon, frequently referred to as the burst of the monsoon, is marked by a progression of convective cloudiness from the western equatorial portion of the Indian Ocean northeastward toward southwestern India. This general cloudiness then progresses northward over the Arabian Sea and subcontinent of India. Under the fully developed southwest monsoon flow, the western Arabian Sea (west of about 60° E) is generally cloud free, while the eastern Arabian Sea exhibits general cloudy conditions. The cloud cells become larger and more vertically developed as the west coast of India is approached. Over India general cloudiness exists with enhanced activity over the mountainous areas. An analysis of satellite brightness (1A-33a) has been used to identify cloud cover conditions (Krishnamurti and Bhalme, 1976). In the illustration, the brightness conditions for a "break" monsoon day and an active monsoon day are depicted. High values indicate increased convective cloud conditions. The term "break" refers to an inactive spell in the monsoon rainfall over central India. In his text on Southwest Monsoons, Krishnamurti (1981) provides the following definition for this phenomenon: There are periods when the monsoon trough is located close to the foot of the Himalayas which leads to a striking decrease of rainfall over most of the country, but an increase along the Himalayas and the southern peninsula. Such a situation is referred to as the "Break in the Monsoon".

India subcontinent during the April through May transition period, the onset of increased southwesterly flow, cloudiness, and rainfall occurs so abruptly and spectacularly that it is known as the "burst of the monsoon". This "burst" phenomenon appears related to the establishment of cross-equatorial flow and intrusion of moist equatorial-maritime Southern Hemisphere air into the Northern Hemisphere monsoon circulation.

References

Findlater, J., 1971: Mean monthly airflow at low levels over the western Indian Ocean. *Geophys. Mem. London*, **16**, 53 pp.

Krishnamurti, T. N., and H. N. Bhalme, 1976: Oscillations of a monsoon system. Part I: Observational Aspects. *J. Atmos. Sci.*, **33**, 1937–1954.

Krishnamurti, T. N., 1981: On the onset vortex of the summer monsoon. *Mon. Wea. Rev.*, **109**, 344–363.

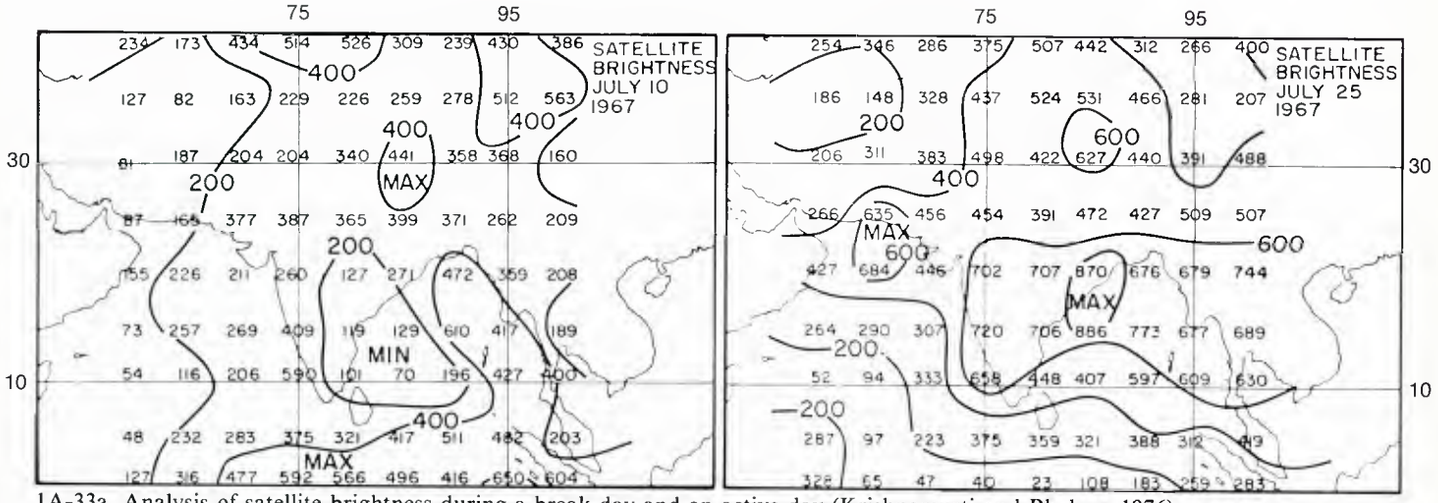

1A-33a. Analysis of satellite brightness during a break day and an active day (Krishnamurti and Bhalme, 1976).

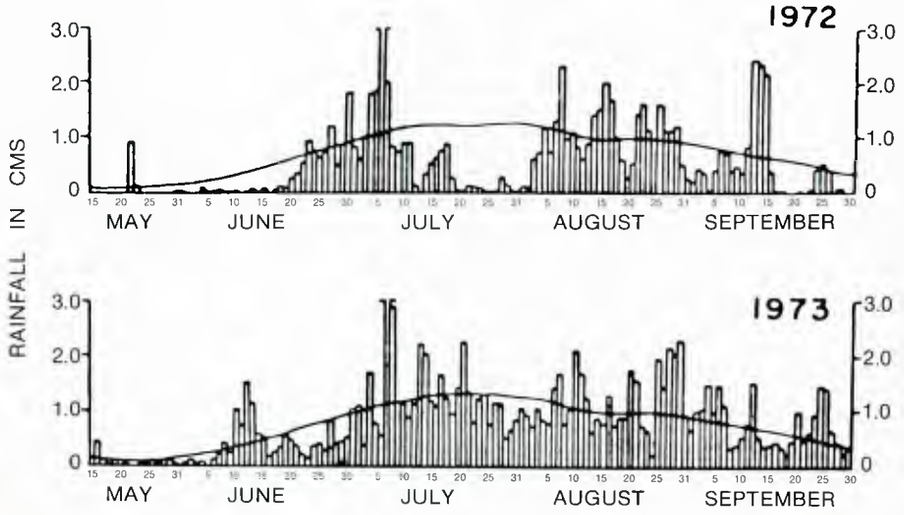

1A-33b. Daily rainfall over central India (75° to 85° E, 15° to 25° N) during a drought year (1972) and a near-normal rainfall year (1973). The envelope line is the daily long-term normal rainfall (Krishnamurti and Bhalme, 1976).

Arabian Sea/Bay of Bengal Southwest Monsoon

July–September

Breaks in the Southwest Monsoon

A break in the southwest monsoon is said to occur when rainfall amounts over central India diminish drastically from normal monsoon conditions. This brings summer drought conditions over the region.

The 1979 MONEX year was one of the 5 worst drought years (1877, 1899, 1918, 1972, and 1979) in the last 100 plus years in terms of severe and widespread drought over India. Recent drought years (1979, 1972, 1966, and 1965) were found to be associated with a mid-latitude circulation pattern of upper-tropospheric blocking ridges near 100° E over Asia (Raman, Rao, and Alvi, 1980). Under blocking ridge patterns the troughs in the westerlies are not progressive but rather exhibit locked positions east and west of the blocking ridge. With a blocking ridge near 100° E, a stationary trough pattern is found to the west of the ridge, near 80° E.

The upper-level trough brings cold air and reduced upper-level thicknesses over northwest India. It has been suggested by Verma (1980) that upper-level temperature and thickness anomalies of the spring transition period (April–May) persist during the subsequent monsoon months and that such anomalies may be useful in long-range prediction of the following monsoon season activity.

The following results summarize Verma's findings.

1. Warming/cooling of the upper troposphere over central and northern India, as observed during the pre-monsoon period, generally persists through the early monsoon months.
2. A warmer (cooler) upper troposphere over northern India during the pre-monsoon period is linked with above-normal (below-normal) rainfall activity during the ensuing summer monsoon season over India.

Blocking ridges tend to be of large latitudinal extent; Raman and Rao (1980) found those during the drought years to extend from 35° to 70° N. Under a large amplitude blocking ridge and stationary trough pattern, the equatorward portion of the trough is near the location typically occupied by the Tibetan anticyclone. This leads to the obvious breakdown or displacement of the Tibetan anticyclone and the associated weakening of the upper-level easterly jet and, in turn, the demise of the southwest monsoon regime.

An examination of rainfall records during an 80 year period (1888–1967) over India led Ramamurthy (1969) to conclude that:

1. The most frequent duration of breaks is 3 to 4 days.
2. The longest breaks last from 17 to 20 days.
3. The average duration of breaks is around 6 days.
4. Breaks are more common in August than in other months of the monsoon season.
5. Pressure rise of the order of 4 mb is noted during breaks over central India.
6. During 12 out of a total of 80 years there were no reported breaks in the monsoons.

From a synoptic perspective, the axis of the monsoon trough tends to move northward toward the mountains as the break begins. The rainfall belt around 20° N also moves northward to the foothills of the

Himalayas with the migration of the trough. This is associated with the northward propagation of a lower-tropospheric anticyclonic belt from the near-equatorial latitudes towards central India (Rao, 1976). During the breaks, two rainfall belts are usually observed. One of these is located near 25° N and the other is found near 7° N.

The reduced north–south pressure gradient over central India as a result of the above effects results in a northward shift and weakening of the subtropical easterly jet. It is also noted, in conjunction with the above effects, that the northern branch of the low-level jet over the Arabian Sea becomes dominant and wind velocities to the south become significantly decreased. This change in low-level windflow conditions reflects the northward shift of the upper-level divergence patterns and resultant convective activity spawned by the upper-level easterly jet.

Finally, Raman, Rao, and Alvi (1980) conclude that:

1. Free and unimpeded passage of westerly wave troughs across the longitudinal belt 90° E through 120° E (between 40° N and 50° N) is essential for the maintenance of good monsoon activity.
2. Movement of such troughs from the west across 120° E sets the stage for monsoon depression formation in the north Bay of Bengal.
3. Development of a blocking ridge between 90° E and 115° E leads to the anchoring of troughs to its west and inhibits the monsoon activity over central and northern India.
4. The persistence of this blocking ridge and the consequent stagnation of westerly troughs lead to monsoon droughts.

References

Ramamurthy, K., 1969: Some aspects of the break in the Indian summer monsoon during July and August. Forecasting Manual No. IV. India Meteorological Department, Poona, India, 57 pp.

Raman, C. R. V., and Y. P. Rao, 1980: Blocking highs over Asia and monsoon droughts over India. *Nature*, **289**, 271–273.

Raman, C. R. V., Y. P. Rao, and S. M. A. Alvi, 1980: The role of interaction with middle-latitude circulation in the behavior of the southwest monsoon of 1972 and 1979. *Curr. Sci.*, **49**, 112–129.

Rao, Y. P., 1976: Southwest monsoons. Meteorological Monograph No. 1. India Meteorological Department, New Delhi, India, 367 pp.

Verma, R. K., 1980: Importance of upper-tropospheric thermal anomalies for long-range forecasting of Indian summer monsoon activity. *Mon. Wea. Rev.*, **108**, 1072–1075.

Arabian Sea/Bay of Bengal
Sunglint Patterns
Winter, Spring, Summer

The Use of Sunglint Patterns in Determining the Surface Location of the Northern and Southern Near-Equatorial Troughs

Location of the Northern and Southern Near-Equatorial Troughs over the Indian Ocean

During winter, in the Northern Hemisphere, the NET is located on or slightly north of the Equator in the Indian Ocean region. The SET extends northwestward from Australia and then runs parallel to the Equator across the Indian Ocean at about 10° to 12° S (1A-39a), according to Atkinson and Sadler (1970).

As time progresses through the spring transition to the southwest monsoon, both the NET and SET move northward (1A-39b). Ultimately, the NET lies over northern India and is referred to as the monsoon trough, while the SET moves to a position near or slightly south of the Equator (1A-39c), where it is established as a dominant clockwise gyre.

Because of the sparcity of data over the Indian Ocean region, it is often difficult to locate the position of these features on any given day. However, high-quality satellite imagery provides many additional details that make it possible to locate them with a high degree of accuracy.

Low-level cloud streets appearing in satellite imagery normally align with the wind in tropical latitudes, although in some regions the normal mode is also observed. The tendency for tropical cloud lines to branch at their downwind end in a "Y-shaped" pattern is information that can sometimes be used to resolve the 180° ambiguity and determine the actual direction of flow. This method has not been previously described, but can be observed in some published examples (see NTAG Vol. 2, Sec. 1D, Case 1).

The near-equatorial trough axes are also minimum wind speed axes and, therefore, cause changes in sea surface roughness that influence sunglint patterns in satellite imagery in precisely the same manner as ridge line axes do in mid latitudes (see NTAG Vol. 1, Sec. 2A).

Knowledge of the location of the NET and SET trough axes is important from an operational point of view for many reasons. For aircraft carriers, these minimim wind speed regions are often avoided because of the expense in running launch and recovery operations under little or no wind conditions.

Movement of the trough axes also results in movement of associated convergence regions which can bring unexpected convective activity and/or change in wind direction that could affect planned operations. It is important to note, as suggested above, that the location of the near-equatorial convergence (NEC), a cloudy zone, and the NET and SET are not co-terminous, but typically separated by several degrees of latitude.

Reference

Atkinson, G. O., and J. C. Sadler, 1970: Tropical cloudiness and gradient-level wind charts over the tropics. AWS Technical Report 215, Vol. I (Text), and Vol. II (Charts).

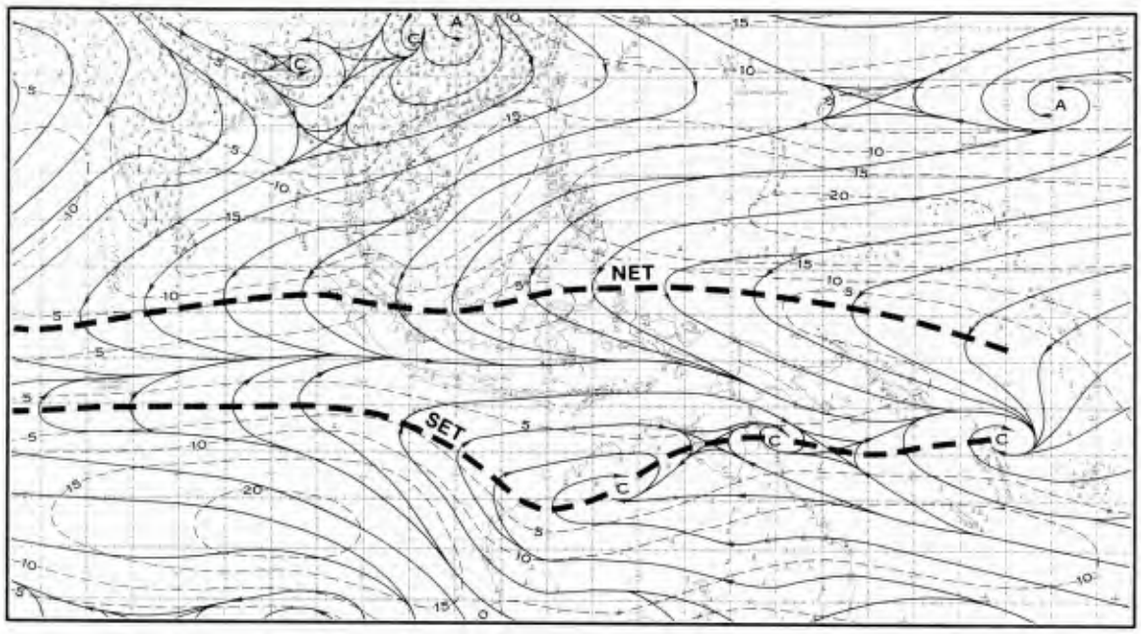

1A-39a. NET/SET Locations—January. (Note, dashed lines indicate gradient-level winds.)

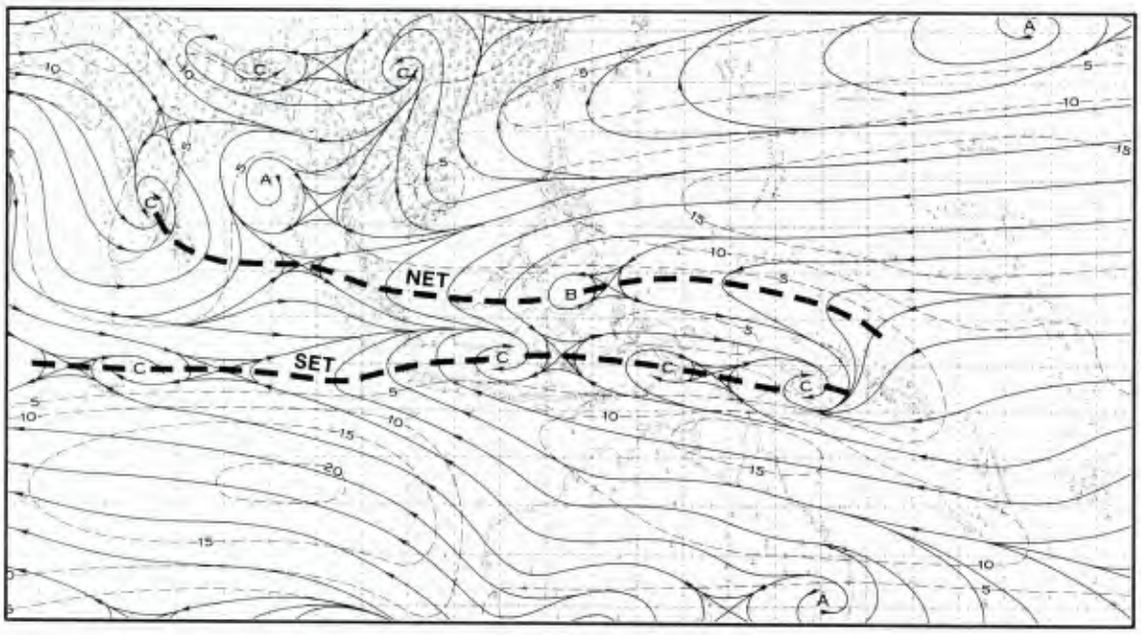

1A-39b. NET/SET Locations—April.

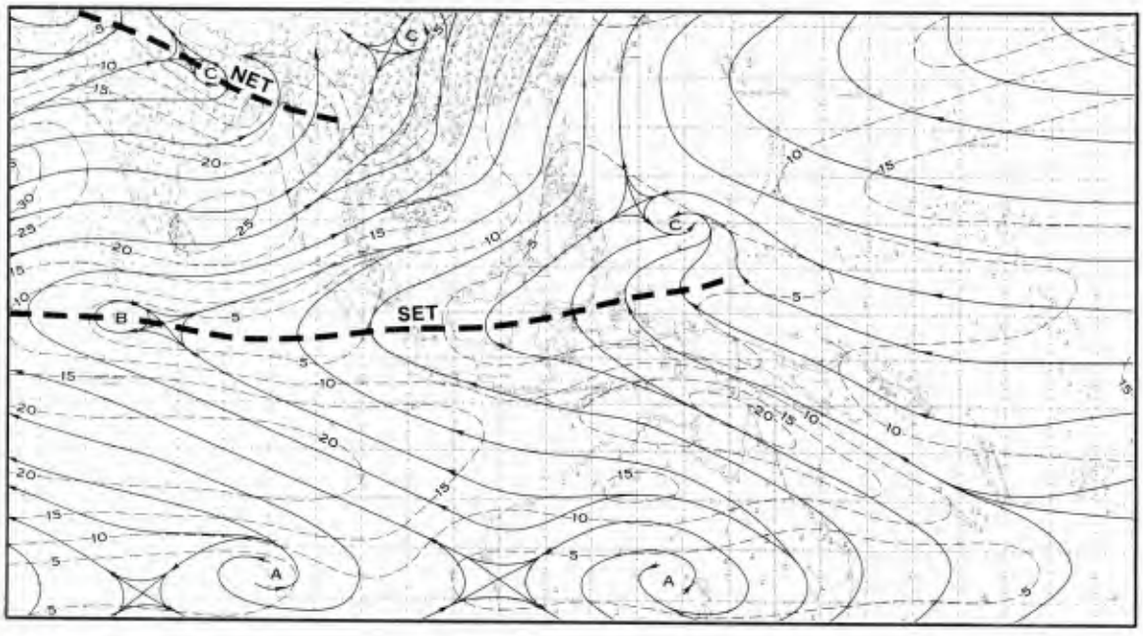

1A-39c. NET/SET Locations—July.

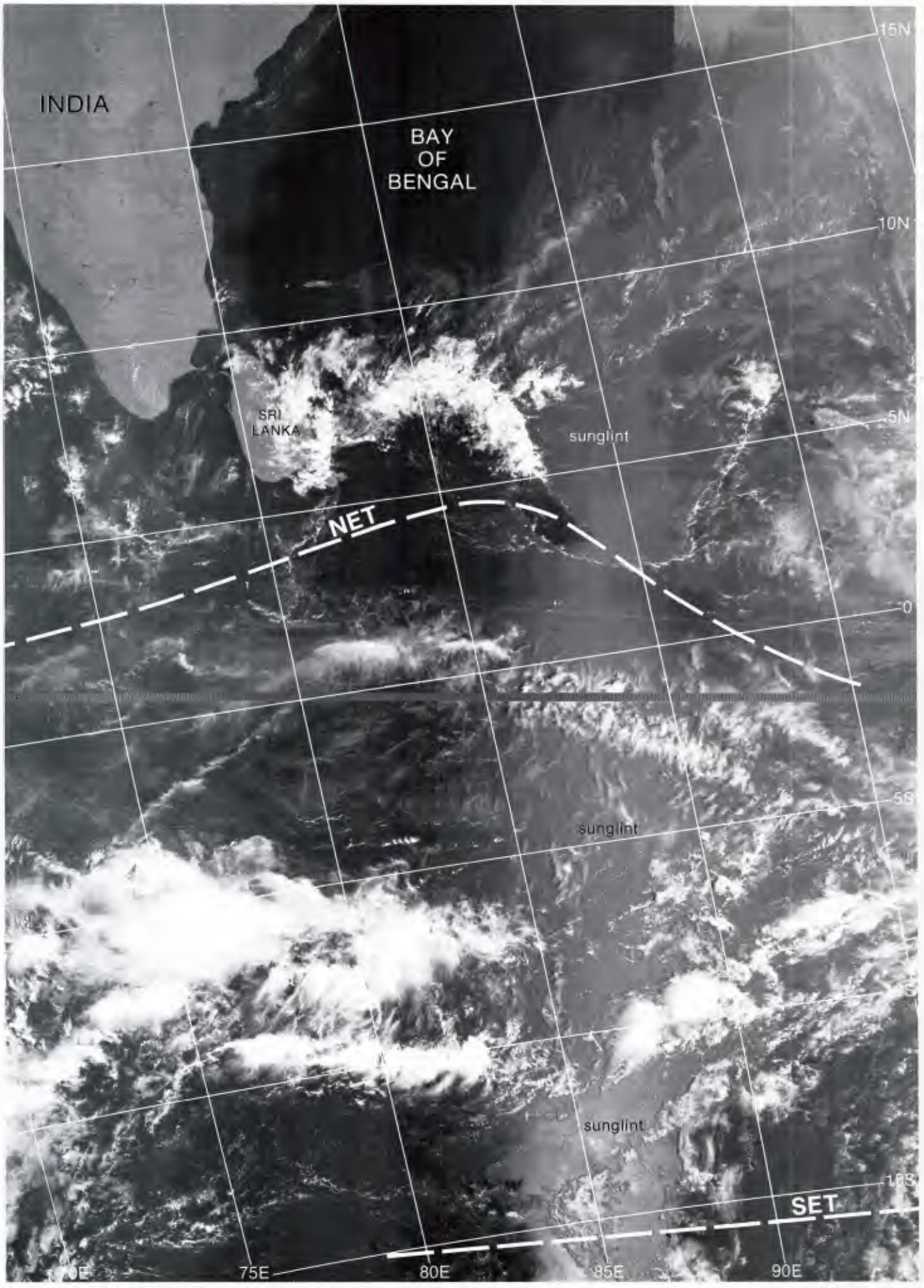

1A-40a. F-4. DMSP LF Log Enhancement. 0426 GMT 27 January 1980.

Bay of Bengal—Winter, 27 January 1980

During January, the northeast monsoon brings cool, dry winds over the Bay of Bengal which turn counterclockwise near the Equator around the NET (1A-39a). The SET is well to the south, near 10° to 15° S.

The DMSP visible picture at 0426 GMT (1A-40a) shows that cloudiness is minimal over the Bay of Bengal, except for the region extending eastward from Sri Lanka which shows heavy convection. Another convective cloud maximum is observed well to the south. The sunglint region extending through the right center of the picture provides immediate clues as to the location of the NET and SET. Dark indentations in the pattern south-southeast of Sri Lanka, and at the extreme southern end of the picture, suggest that these are the locations of the NET and SET, respectively, since the remainder of the sunglint pattern is rather uniform. To the north, northeasterlies would be expected, turning to northwesterlies in the area south of Sri Lanka (1A-39a). To the south, southeasterlies would be expected, turning to southwesterlies north of the sunglint indentation. The two flow patterns would be expected to merge along an asymptote of convergence very near the convective cloud clusters located in the southern portion of the picture.

Surface reports and a suggested streamline analysis superimposed on the DMSP picture (1A-41a) indicate that the flow pattern conforms closely to the mean January pattern (1A-39a). Note that in this example parallel-mode cloud lines (near 0° N, 74° E) and normal-mode cloud lines (near 5° S, 88° E) are both observed. Knowledge of the locations of the NET and SET and asymptotes of convergence, along with a few ship reports, helps resolve the basic flow pattern.

Bay of Bengal—Spring, 8 April 1978

By April, the NET has typically moved northward to a position between the southern portion of the Malay Peninsula and the southern tip of India (1A-39b). The northeasterly flow pattern over the Bay of Bengal changes rather drastically compared to the winter pattern, with a large anticyclone centered over the area bringing southeasterly flow along the eastern coastal area of India and westerly or northwesterly flow into Burma.

The DMSP visible picture at 0503 GMT (1A-42a) reveals scattered to broken cloudiness over the northern portion of the Bay of Bengal, with cloud alignment suggesting an anticyclonic center in the middle of the bay (delineated by the dark-toned gray shades).

Brilliant sunglint, with the typical dark regions in either side due west of the Malay Peninsula, identifies the NET axis. There is no clear evidence of an interruption in the sunglint pattern to the south. Flow toward Sumatra should therefore be from the west or southwest.

Based on these considerations, and using available surface reports, a streamline analysis is derived and superimposed on the DMSP picture (1A-43a). Special care has been taken to utilize cloud street alignment for direction of surface flow. This is extremely reliable in some areas, such as over Indo-China and around the periphery of the anticyclone, but less so in more confused regions, such as that due west of Sumatra. Nevertheless, a comparison of this analysis and the NMC surface streamline analysis for 0000 GMT (1A-43b), about four hours before the DMSP picture, leaves little doubt that a significant improvement in delineating the nature of the flow through this region has been achieved by using satellite imagery.

Arabian Sea—Summer, 3 June 1979

The summer period features the SET near or slightly south of the Equator (1A-39c). The NET (monsoon trough) lies over northern India. The DMSP visible picture at 0558 GMT (1A-44a) reveals a sunglint pattern off the southern tip of India which ends abruptly south of Sri Lanka. This sudden termination suggests calm seas normally co-located with the NET axis. The detection of sunglint termination was also observed in the GOES-Indian Ocean visible picture at 0400 GMT (1A-45a), approximately two hours prior to the time of the DMSP picture. Note that the sunglint termination occurs at exactly the same location.

Further to the north, in the Arabian Sea, the GOES-Indian Ocean visible picture at 0740 GMT (1A-45b) displays another dark-line feature traversing the Arabian Sea. This feature corresponds to the location of the ridge line of the pre-monsoon Arabian Sea anticyclone.

A streamline analysis of the surface reports and cloud motion winds superimposed on the DMSP picture (1A-46a) confirms the location of both features. The surface streamline analysis for 0600 GMT (1A-47a), closest to the time of the DMSP picture (1A-46a), verifies the general location of the NET and of the ridge line axis over the Arabian Sea.

The ridge line feature was also suggested in the DMSP picture on the previous day (1A-48a), by cloud street alignment, the barrier effect at Socotra, and the dark indentation into the sunglint pattern on the right side of the image in this early morning (0647 LST) pass. A streamline analysis superimposed on the DMSP picture (1A-49a) confirms the placement of the ridge line axis.

Note that the location of the NET and the ridge line axis over the Arabian Sea is much more precisely defined by the satellite imagery, using sunglint analysis, cloud street alignment, barrier effect indications, and available wind reports from ships and land stations, than by the conventional analysis alone.

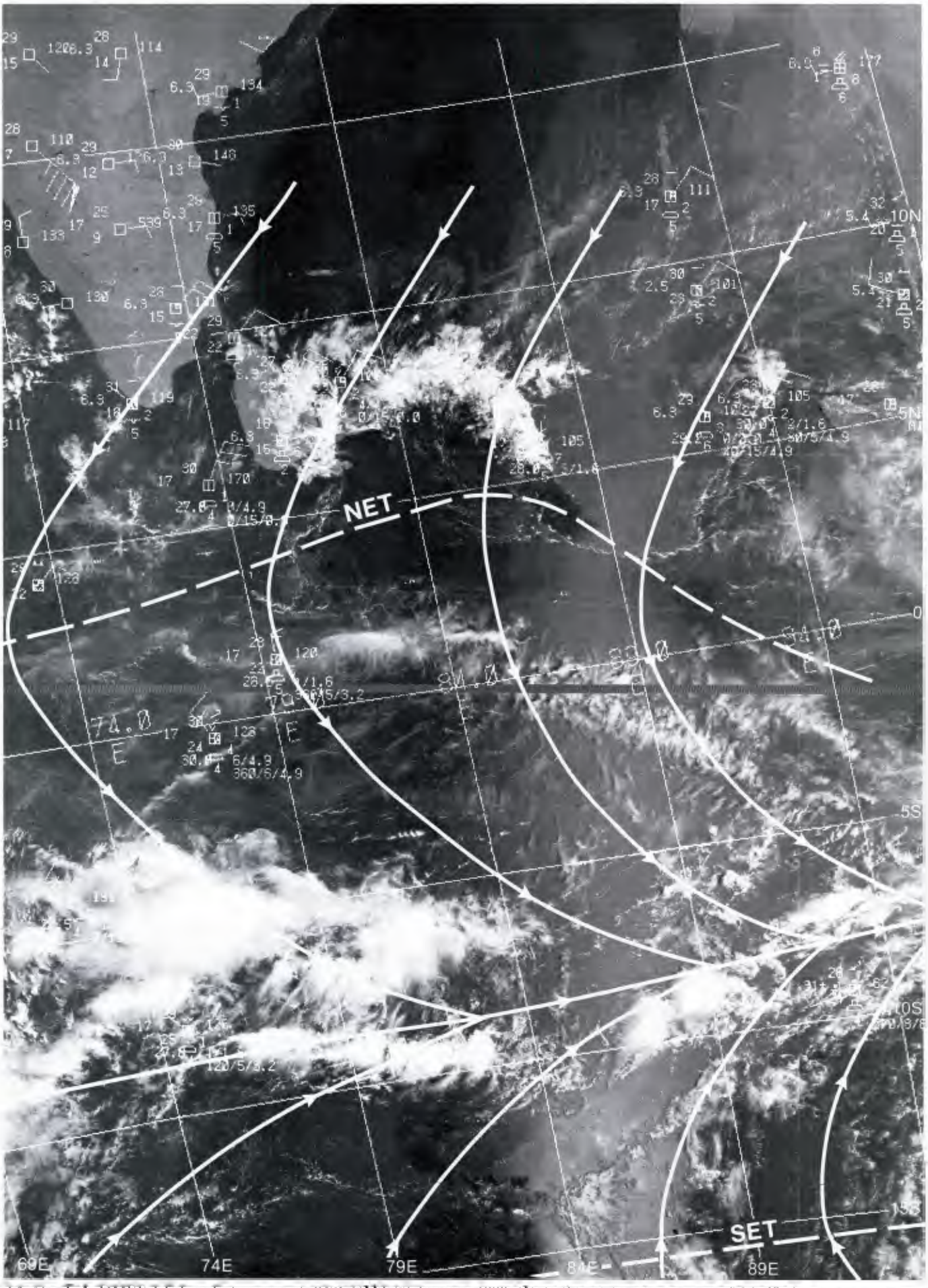

1A-41a. F-4. DMSP LF Log Enhancement. 0426 GMT 27 January 1980. (Note this picture is a repeat of 1A-40a.)
Surface Wind Reports and Streamline Analysis. 0600 GMT 27 January 1980.

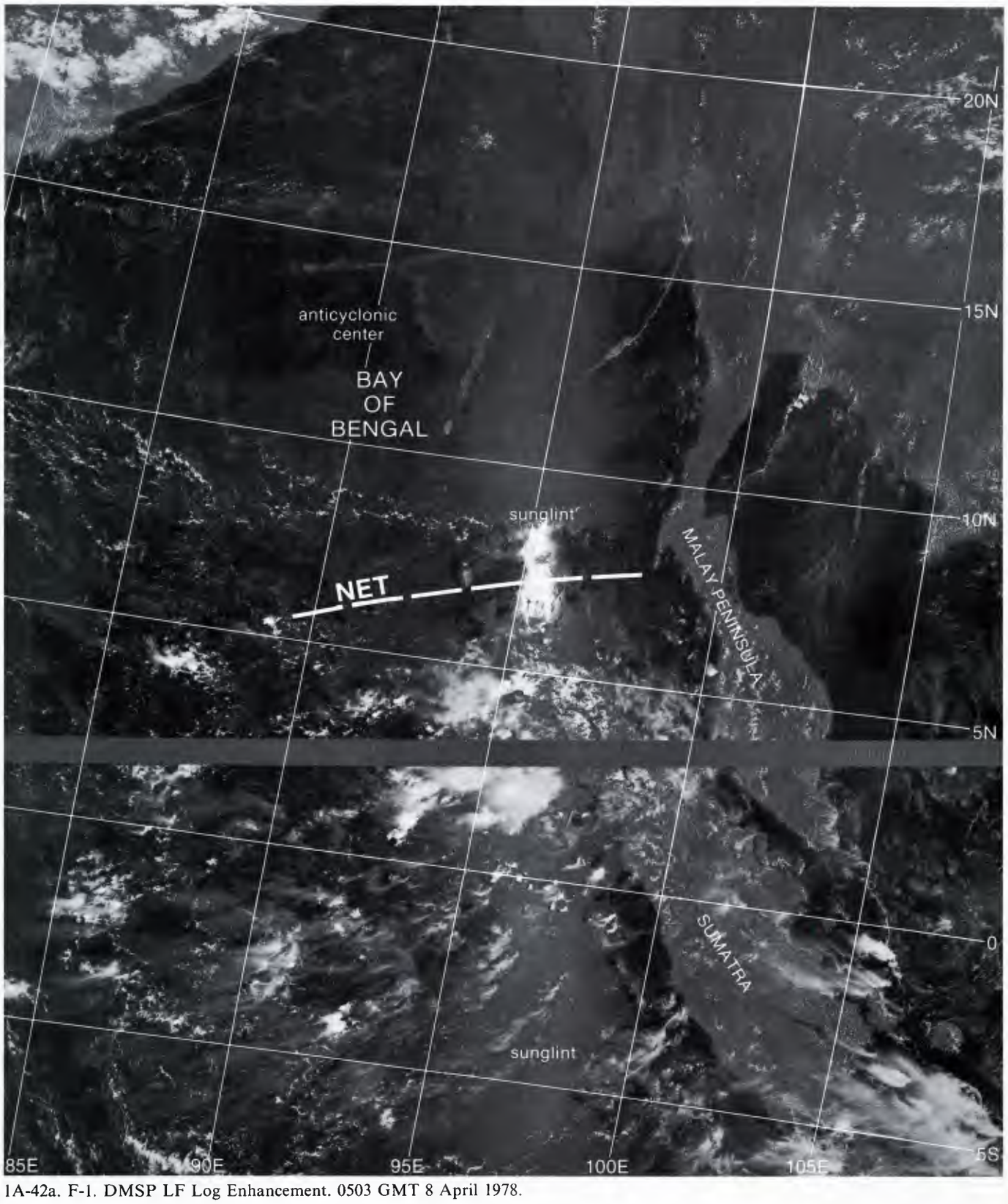

1A-42a. F-1. DMSP LF Log Enhancement. 0503 GMT 8 April 1978.

surface

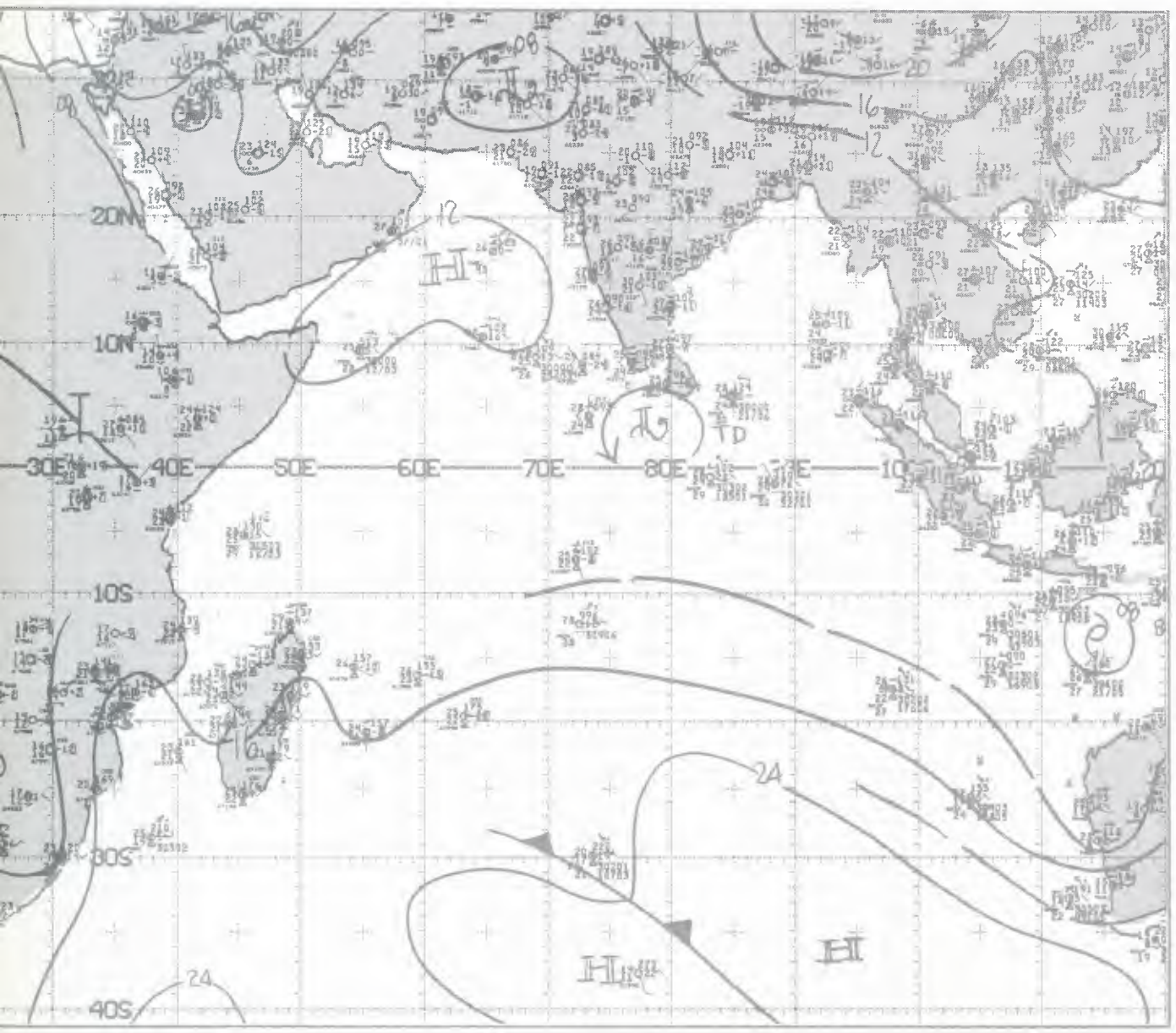

A-43b. NMC Tropical Surface Streamline Analysis. 0000 GMT 8 April 1978.

1A-43a. F-1. DMSP LF Log Enhancement. 0503 GMT 8 April 1978. (Note this picture is a repeat of 1A-42a.)
Surface Wind Reports and Streamline Analysis. 0600 GMT 8 April 1978.

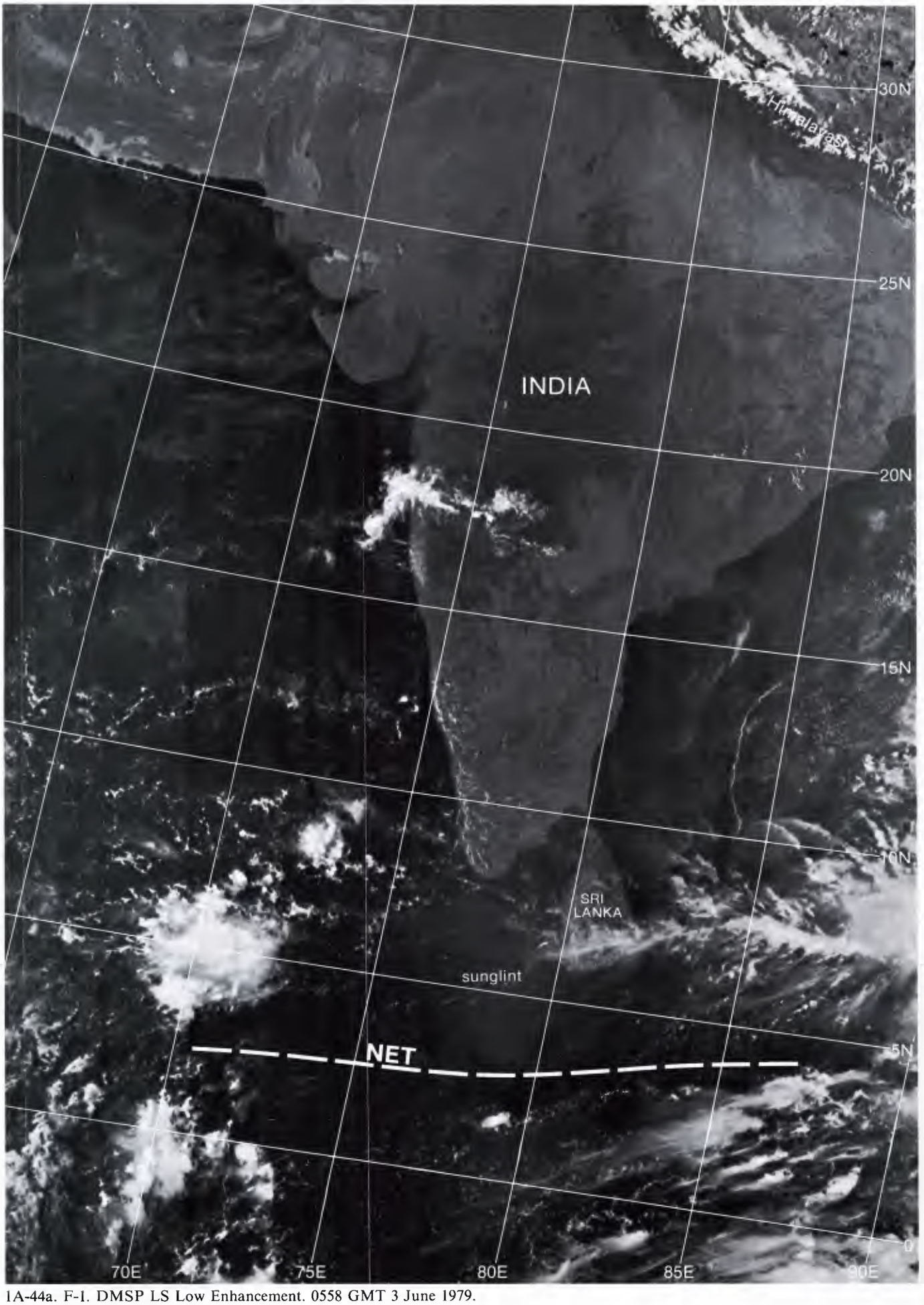

1A-44a. F-1. DMSP LS Low Enhancement. 0558 GMT 3 June 1979.

surface

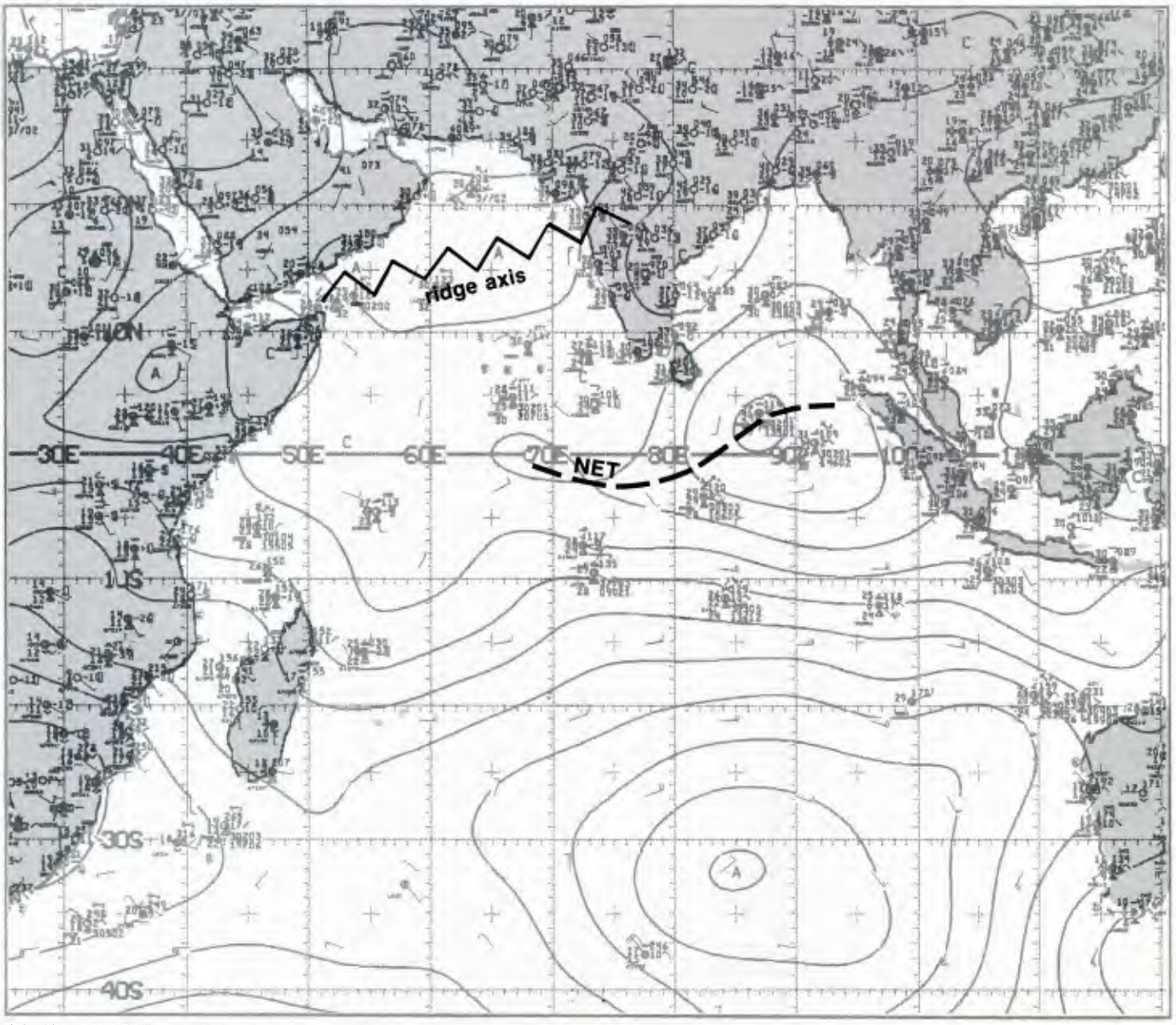

1A-47a. NMC Tropical Surface Streamline Analysis. 0600 GMT 3 June 1979.

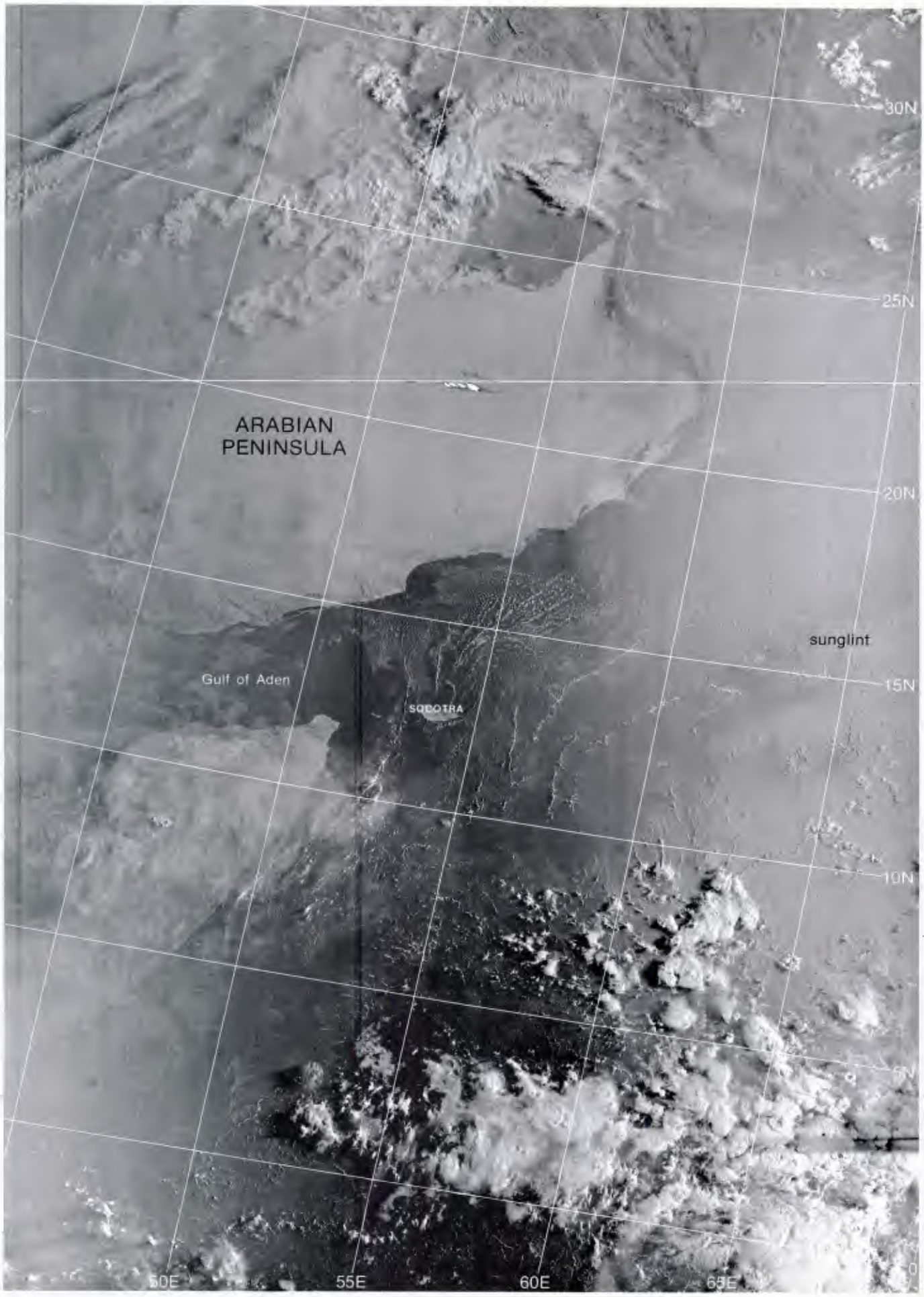

1A-48a. F-3. DMSP LF Normal Enhancement. 0247 GMT 2 June 1979.

1A-49a. U.S. DMSP LF Normal Enhancement. 0247 GMT 2 June 1979. (Note this picture is a repeat of 1A-48a.)
Surface Wind Reports and Streamline Analysis. 0600 GMT 2 June 1979.

Case 1 Arabian Sea/Bay of Bengal—Autumn Transition

Land Breeze Cloud Line Development

All around the world, wherever there is a distinct boundary between land and water, land and sea breezes develop. These circulations are strictly localized mesoscale phenomenon; however, they can be useful indicators of changes in the large-scale, low-level flow features, particularly over the Arabian Sea during the transition period between the southwest and northeast monsoons.

The southwest monsoon over the Arabian Sea brings steady, moderate force winds across India and into the Bay of Bengal. As a result, strong land breezes cannot develop along the west coast of India because they are overpowered by the onshore winds of the southwest monsoon. As the southwest monsoon subsides (autumn transition), land breezes develop along the west coast of India which are enhanced by cool air flowing down the slopes of the Western Ghats Mountains. As the land breeze moves offshore, it converges with the slow prevailing westerlies associated with the weakening southwest monsoon over the Arabian Sea. The convergence of the land breeze and the weak westerlies produces one of the most distinctive land breeze cloud lines observed anywhere in the world.

In contrast, as the northeast monsoon becomes established over the Arabian Sea, and the prevailing wind direction shifts to offshore from India across the Arabian Sea, any land breezes forming along the west coast of India are augmented by the offshore flow. Under these circumstances, the land breeze cloud line does not appear, due to the absence of the convergence zone which forms between the prevailing westerlies of the southwest monsoon and the easterlies of the land breeze. The presence or absence of the land breeze cloud line along the west coast of India in satellite imagery, therefore, can be a useful indicator of seasonal differences in the flow pattern (southwest or northeast monsoon) over the Arabian Sea and India.

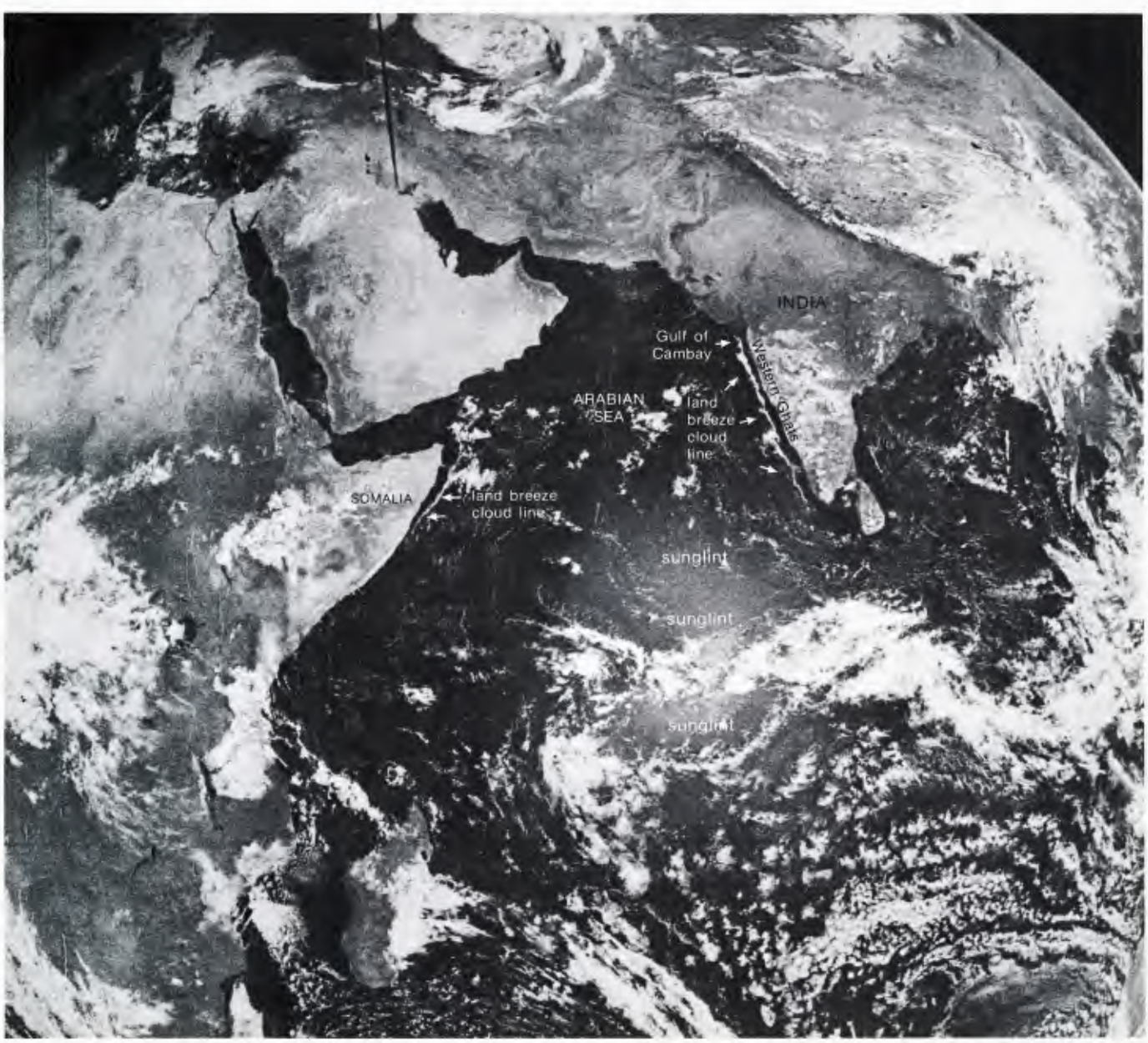

1B-2a. GOES-Indian Ocean. Enlarged View. Visible Picture. 0630 GMT 8 October 1979.

Land Breeze Cloud Lines
West Coast of India/Somalia Coast
October 1979/December 1978

8 October 1979

The GOES-Indian Ocean visible picture at 0630 GMT (1B-2a) shows a land breeze cloud line extending along the west coast of India from the Gulf of Cambay, in the north, to the southern tip of India. It is to be noted that the northern extent of the cloud line coincides roughly with the northern limit of the Western Ghats coastal mountain range. Cool air coming down the along-shore coastal mountain slopes during the nighttime hours enhances the strength of the land breeze sufficiently to produce the offshore convergence zone (light, prevailing northwesterlies over the open seas converging with the enhanced land breeze) needed to form the land breeze cloud line observed on the satellite picture. This indicates that the presence of coastal mountain ranges are an important factor (source of downslope winds) in enhancing the strength of land breezes.

In the satellite picture, another land breeze cloud line is observed off the northern tip of Somalia. The Somalia coast also has higher terrain just inland from the coastline. For reference purposes, the satellite picture time is 1230 LST over India and 0930 LST over Somalia. During the morning hours, as the land breeze diminishes and the sea breeze develops, the land breeze cloud line advances toward the coast. Occasionally, the land breeze cloud line crosses the coastline and moves inland as a miniature cold front with shower activity.

The NMC surface streamline analysis for 0600 GMT (1B-3a) displays anticyclonic flow over the northern Arabian Sea—nearly parallel to the Somalia coast, but with a pronounced onshore component along the west coast of India. Winds over India are light and variable, which is favorable for land breeze development during the nighttime hours.

9 October 1979

On the following day, the GOES-Indian Ocean visible picture at 0800 GMT (1B-4a) shows a land breeze cloud line (with increased convective activity) along the west coast of India. The Somalia land breeze cloud line is also present. This indicates that the basic low-level flow pattern over the Arabian Sea (weak southwest monsoon) has not changed. The dark patch appearing on the north side of the sunglint pattern in the central Arabian Sea suggests the presence of a southwest to northeast oriented ridge line **R1**. The surface analysis for 0600 GMT (1B-5a) shows a ridge line **R1** (as interpreted in the satellite picture), and the general anticyclonic flow pattern over the northern Arabian Sea giving rise to the land breeze cloud lines off Somalia and India.

6 December 1978

About one year earlier, but later in the year (December vs. October), the GOES-Indian Ocean visible picture at 0730 GMT (1B-6a) shows no evidence of a land breeze cloud line along the west coast of India or the northern tip of Somalia. This implies a different synoptic-scale flow pattern over the Arabian Sea/Indian Continent. Note that the western coastal region of India is cloud free, whereas the eastern coastal region is cloud covered. This cloudiness pattern *in toto* implies the onset of the northeast monsoon. Note also that the sunglint area has shifted from the central Arabian Sea to a location considerably to the south, in comparison to the October satellite pictures, reflecting the change to the cooler season of the year over the region.

The surface analysis for 0600 GMT (1B-7a) confirms the presence of a moderate northeasterly or easterly flow pattern characteristic of an established northeast monsoon regime over the Arabian Sea and the adjacent Indian Continent.

Important Conclusions

1. The land breeze cloud line is observed primarily offshore of coastal mountain ranges when the prevailing flow is onshore, or has a converging component with the land breeze.

2. The presence or absence of the land breeze cloud line, as it appears in satellite imagery over the Indian Ocean, is useful for identifying seasonal differences in the synoptic circulation pattern (southwest monsoon vs. northeast monsoon) over the Arabian Sea/Indian Continent region.

surface

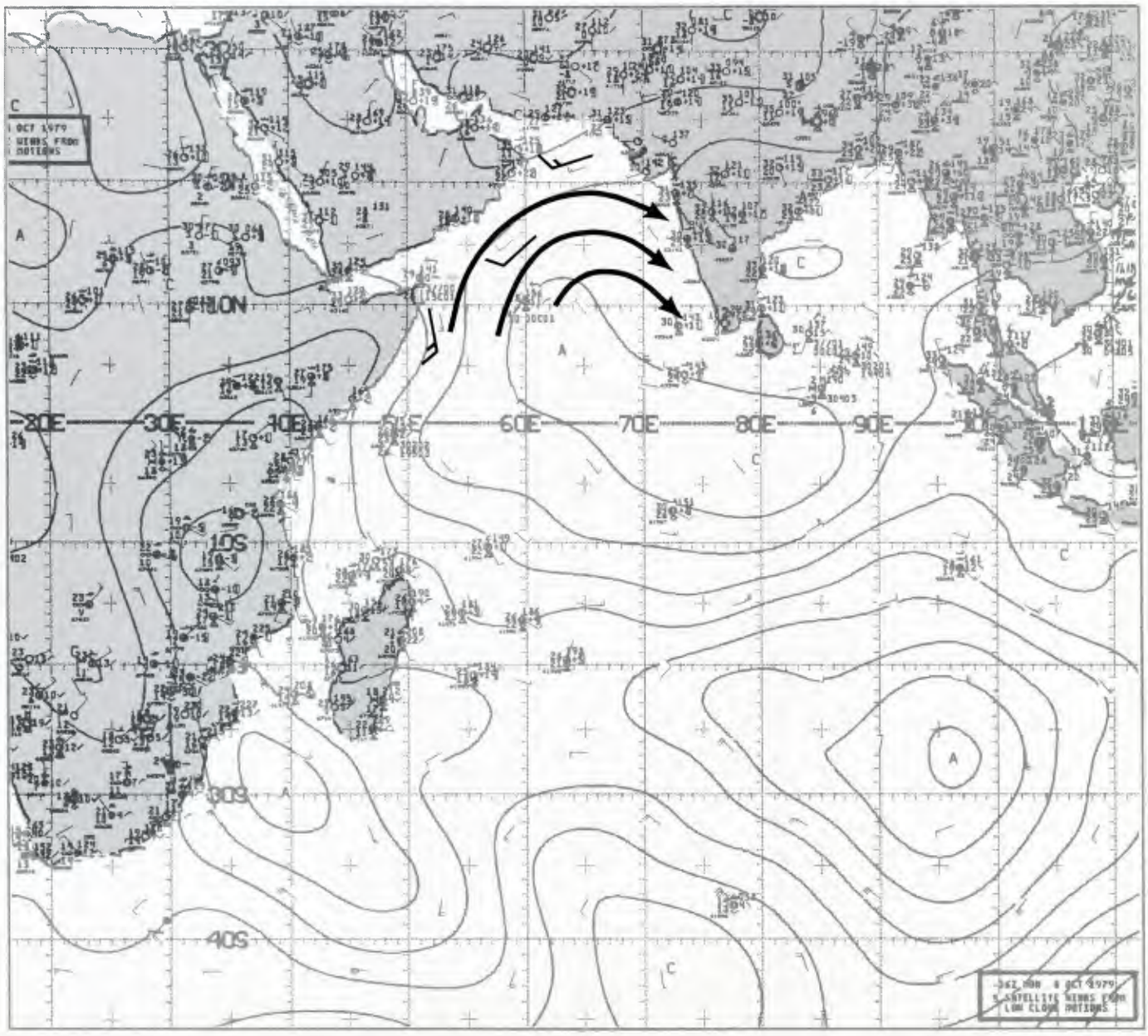

1B-3a. NMC Tropical Surface Streamline Analysis. 0600 GMT 8 October 1979.

1B-4a. GOES-Indian Ocean. Enlarged View. Visible Picture. 0800 GMT 9 October 1979.

surface

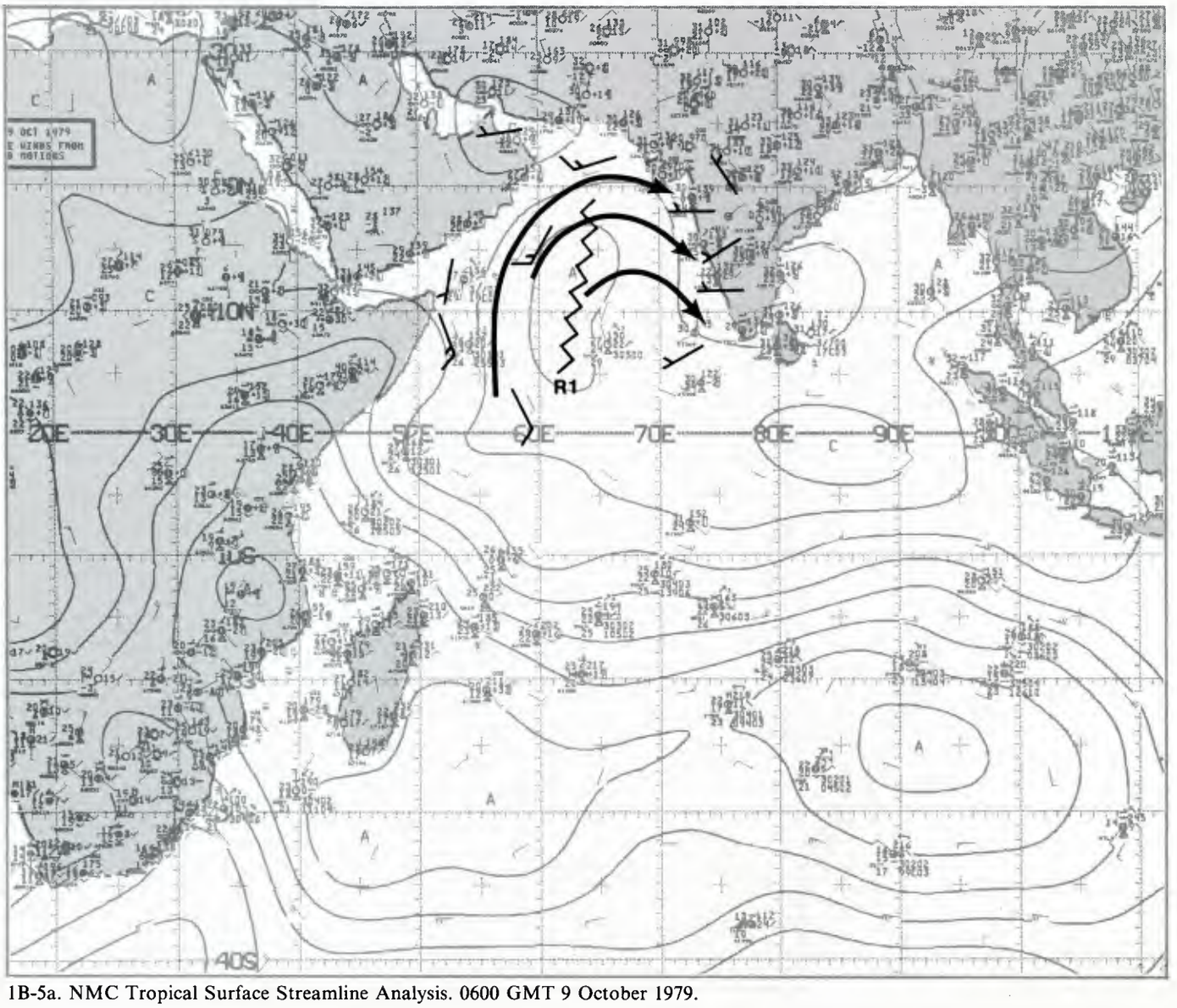

1B-5a. NMC Tropical Surface Streamline Analysis. 0600 GMT 9 October 1979.

1B-6a. GOES-Indian Ocean. Enlarged View. Visible Picture. 0730 GMT 6 December 1978.

surface

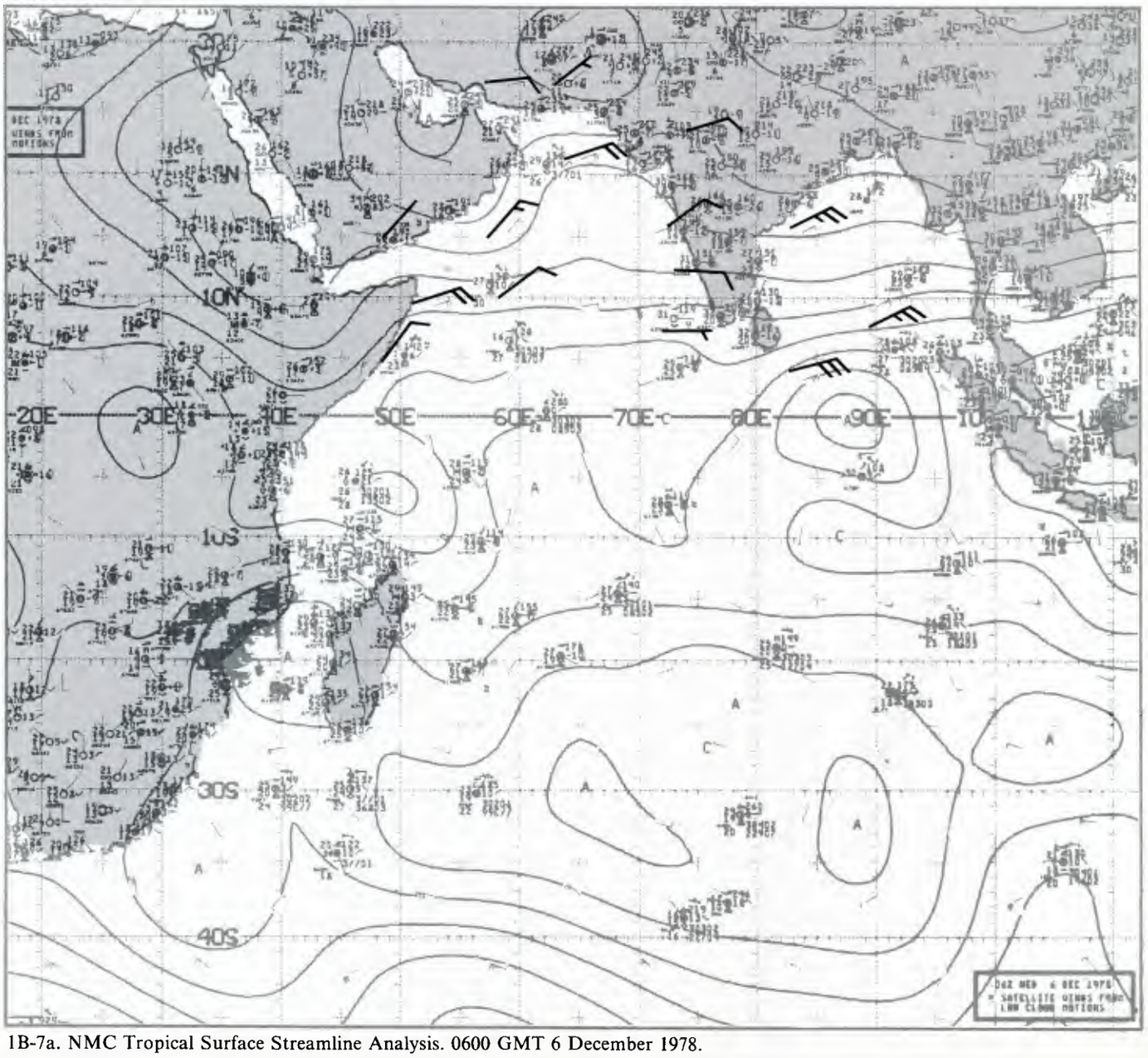

1B-7a. NMC Tropical Surface Streamline Analysis. 0600 GMT 6 December 1978.

Case 2 Arabian Sea/Bay of Bengal—Autumn Transition

Tropical Cyclones in the Arabian Sea

Tropical cyclone development in the Arabian Sea is a dominant feature of the spring and fall transition periods. Formation occurs within the near-equatorial trough as it advances northward in the spring and retreats southward in the fall toward its position near the Equator.

In order for conditions to be favorable for storm development, sea surface temperatures must be at least 26° C (78.8° F); vertical shear from lower levels to about the 200-mb level should be small; and a favorable upper-level divergence pattern should exist or be initiated during the storm's formative stage. Lack of such conditions will either prevent storm formation or cause an initial storm development to weaken so that tropical cyclone intensity (winds greater than 64 kt) will not be achieved.

250 mb

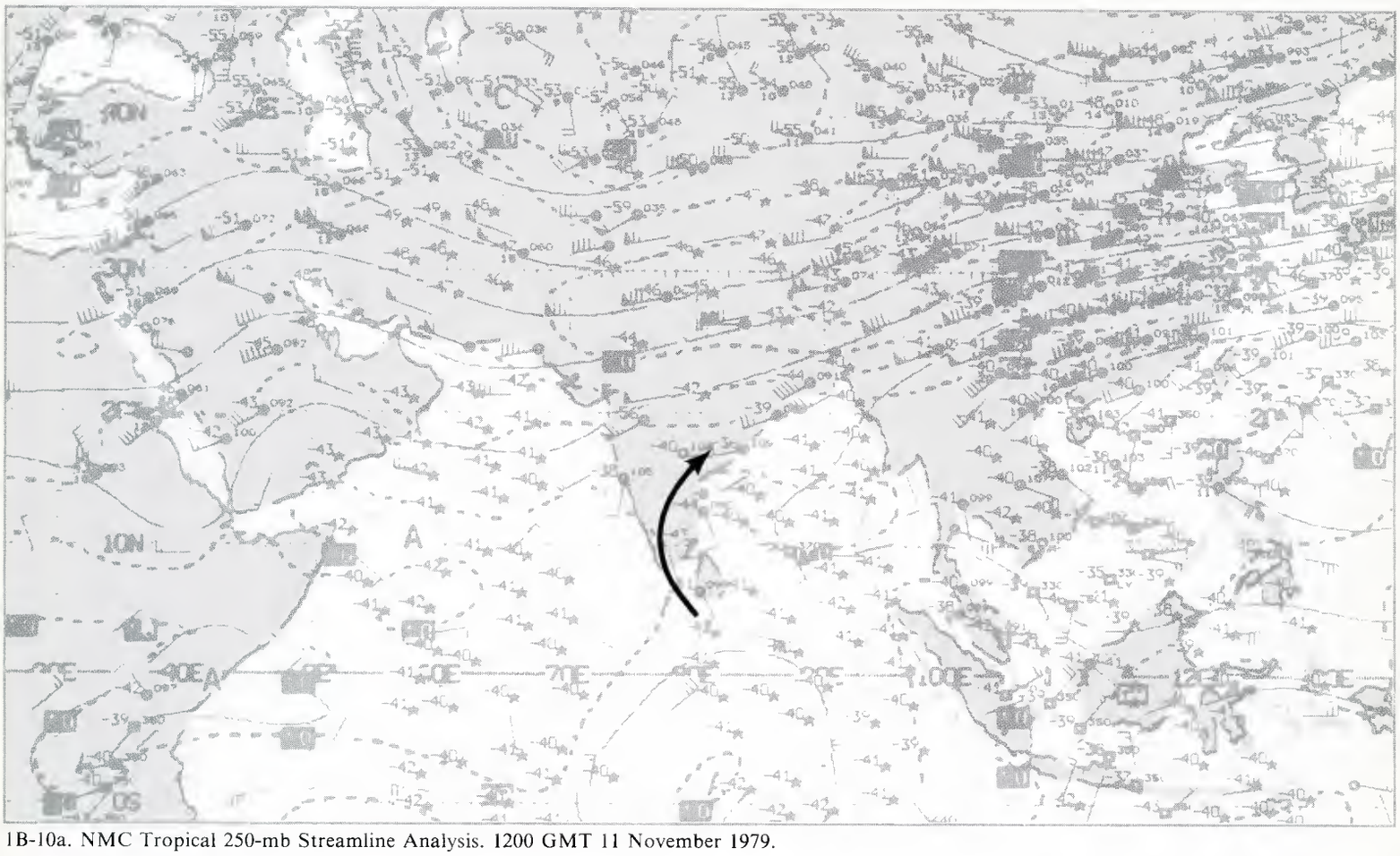

1B-10a. NMC Tropical 250-mb Streamline Analysis. 1200 GMT 11 November 1979.

700 mb

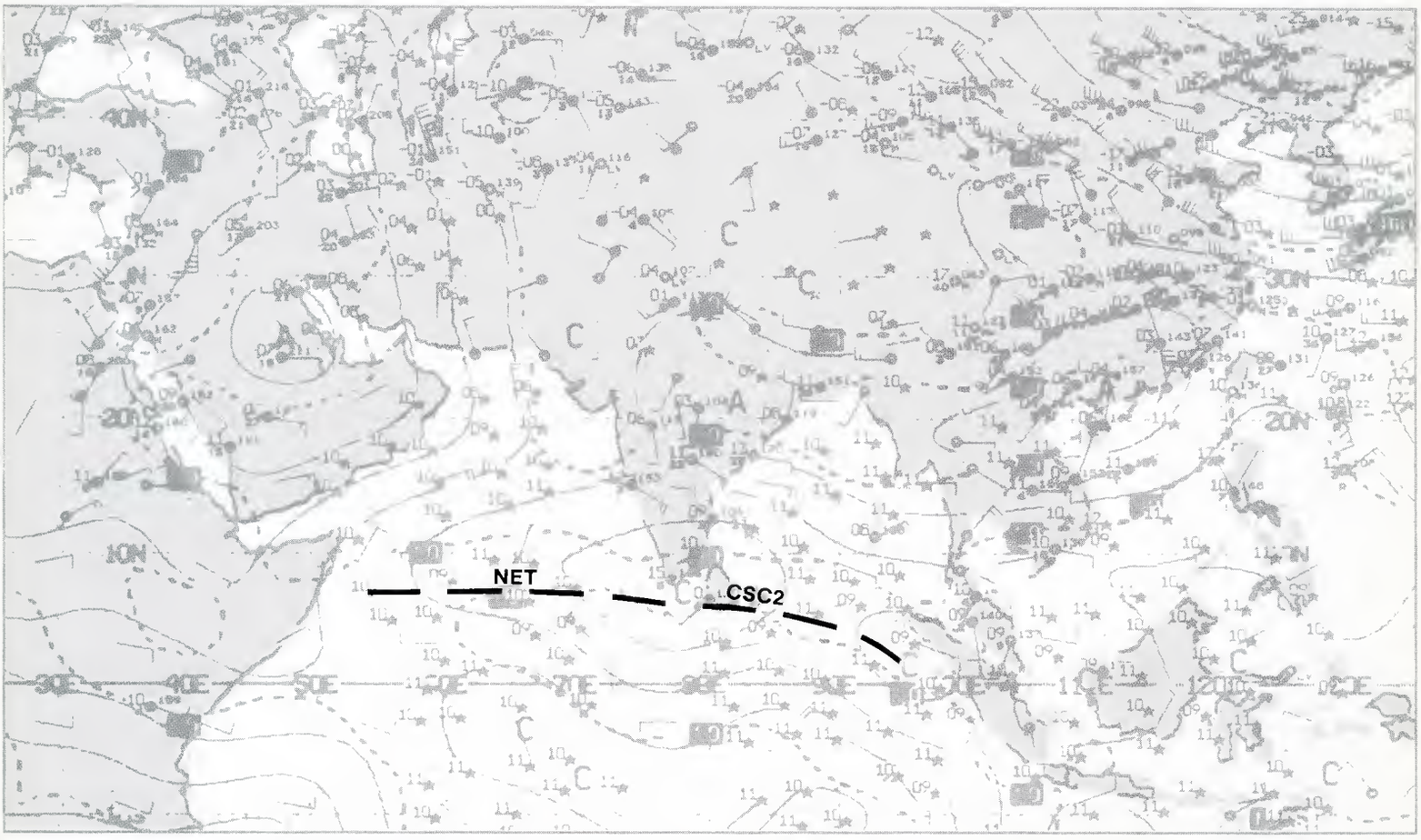

1B-10b. NMC Tropical 700-mb Streamline Analysis. 1200 GMT 11 November 1979.

11 November

The NMC surface streamline analysis for 0600 GMT (1B-11b) shows that the near-equatorial trough (NET) is located across the southern tip of India and angles sharply southward on either side toward the Equator. The GOES-Indian Ocean visible picture at 0730 GMT (1B-11a) displays convergence zone (CZ) cloudiness centered largely south of the NET surface position in a region of westerly winds. It is therefore on the north side of the CZ that cyclonic vortices would be expected to develop and, in fact, a cyclonic streamline center **CSC1** is analyzed north of the CZ just to the west of the southern tip of India on the surface chart. This cyclonic circulation, however, is not reflected in the NET cloudiness on the satellite picture.

An examination of the 700-mb streamline analysis for 1200 GMT (1B-10b) shows the NET near the southern tip of India—roughly in the same location as at the surface. At this level, a cyclonic streamline center **CSC2** is located over the southern tip of India. Since there is a difference of six hours between the surface analysis (1B-11b) and the 700-mb analysis, the identification and tracking of cyclonic centers in the NET is difficult. The task is made somewhat easier when satellite imagery is available because clouds tend to become organized in a cyclonic pattern in areas of concentrated cyclonic rotation. This is not the case on this day. At 250 mb (1B-10a), the streamline analysis shows weak anticyclonic flow over the lower-level, near-equatorial trough and zonal westerlies with embedded troughs to the north.

12 November

The surface analysis (1B-13b) again reveals the NET in roughly the same location. Wind reports suggest a cyclonic center **CSC3** just west of the southern tip of India. Drizzle and rain showers in that region attest to the unsettled conditions over the area. The satellite picture (1B-13a) now also reveals banding effects suggesting the possibility of a weak closed circulation, with a center southwest of the southern tip of India. The cloud pattern has intensified in appearance and now suggests two separate clusters of convective activity—one to the south of India and the other over the Bay of Bengal.

Wisps of cirrus turning anticyclonically north of the convection region suggest the presence of an upper-level anticyclone. This condition is favorable for continued development and intensification of any low-level cyclonic vortex by providing an upper-level divergence outflow mechanism.

The 700-mb analysis (1B-12b) continues to reveal the position of the NET quite well and shows two separate embedded vortices, one west of the southern tip of India **CSC3**, and the other just north of the Equator over the Bay of Bengal **CSC4**, well to the south of the satellite-observed cloud mass in that region. At 250 mb (1B-12a), a large anticyclonic cell is seen to overlie both disturbed regions. Speed divergence on the west side of the cell favors intensification of the vortex in the Arabian Sea.

13 November

The cyclonic vortex **CSC3** in the Arabian Sea dominates the flow pattern over the entire region, as shown on the surface analysis (1B-15b). A pronounced north-northeast to south-southwest oriented trough line **T1** extends into northern India from the vortex center. Wind speeds, however, appear rather light, although no reports are available near the cyclonic center. A GOES-Indian Ocean visible picture is not available for this date; however, the corresponding infrared picture (1B-15a) shows an impressive cold cloud mass with cirrus radiating out from the edge of the system, providing evidence of continued anticyclonic outflow aloft.

The 700-mb analysis (1B-14b) reveals a large vortex **CSC3** over the Arabian Sea, with a trough line extending east-southeast to a low centered near the Malay Peninsula. At 250 mb (1B-14a), anticyclonically-turning flow, with continued speed divergence, is seen to overlie the lower-level vortex region.

14 November

The vortex **CSC3** in the Arabian Sea appears well defined on the surface analysis (1B-17b). Winds of 20 to 25 kt encircle the vortex out to a large radius. A trough line **T1** continues to extend northeastward from the vortex into northern India. The satellite picture (1B-17a) reveals a curved cloud band in the shape of an inverted V or U pattern. A center of circulation is not apparent in the cloud banding, but would lie in the western portion of the cloud mass, judging from the surface analysis.

The vortex **CSC3** is also shown on the 700-mb analysis (1B-16b), with a center near the surface position. Strong 30-kt southerly winds associated with the vortex circulation are apparent along the west coast of India. At 250 mb (1B-16a), anticyclonic flow continues to override the lower-level vortex. However, the trough **T2** located over Saudi Arabia is advancing eastward and could bring strong southwesterly flow over the developing vortex. If this occurs, strong vertical wind shear would arrest the storm's development or cause dissipation.

1B-11a. GOES-Indian Ocean. Enlarged View. Visible Picture. 0730 GMT 11 November 1979.

surface

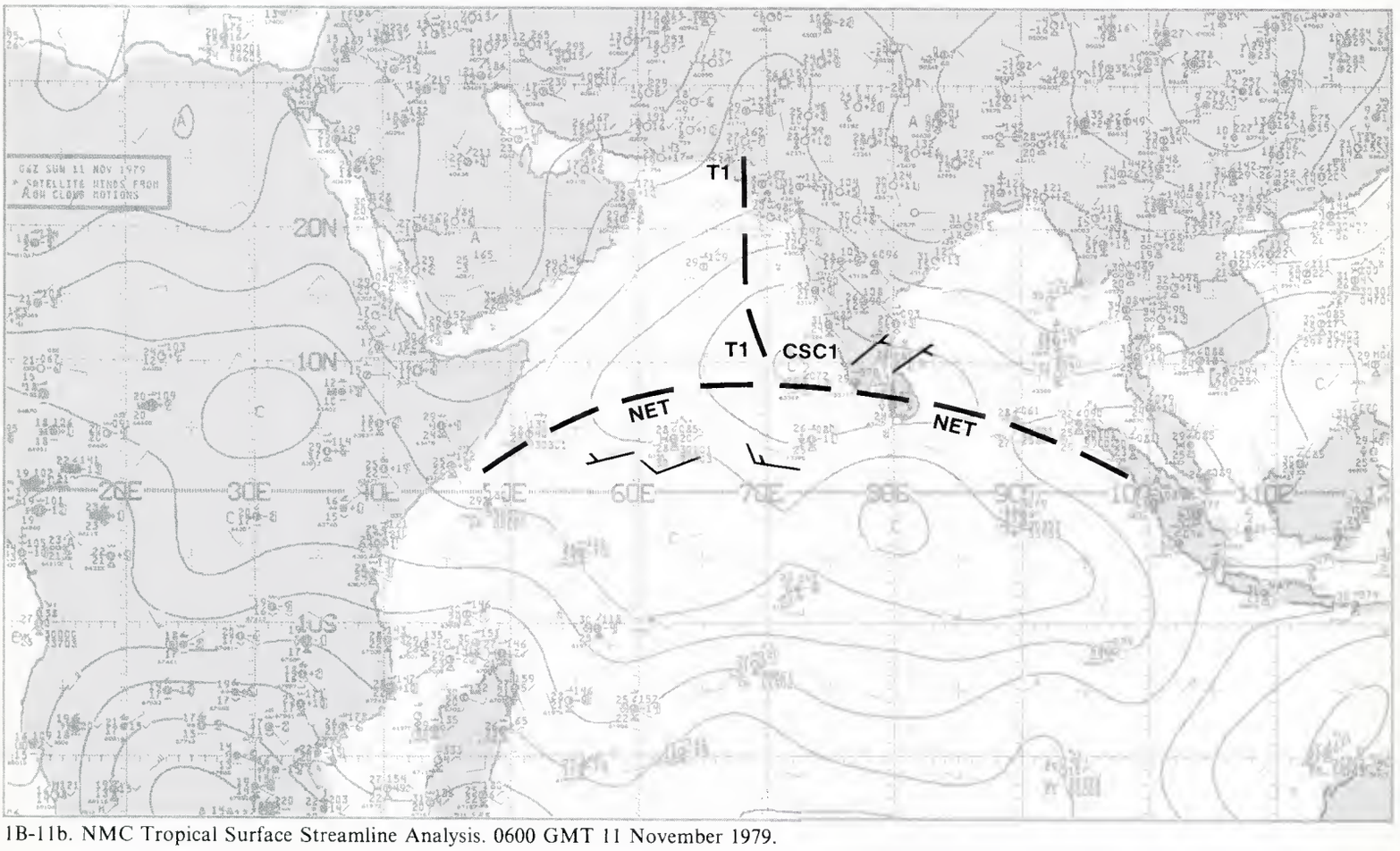

1B-11b. NMC Tropical Surface Streamline Analysis. 0600 GMT 11 November 1979.

250 mb

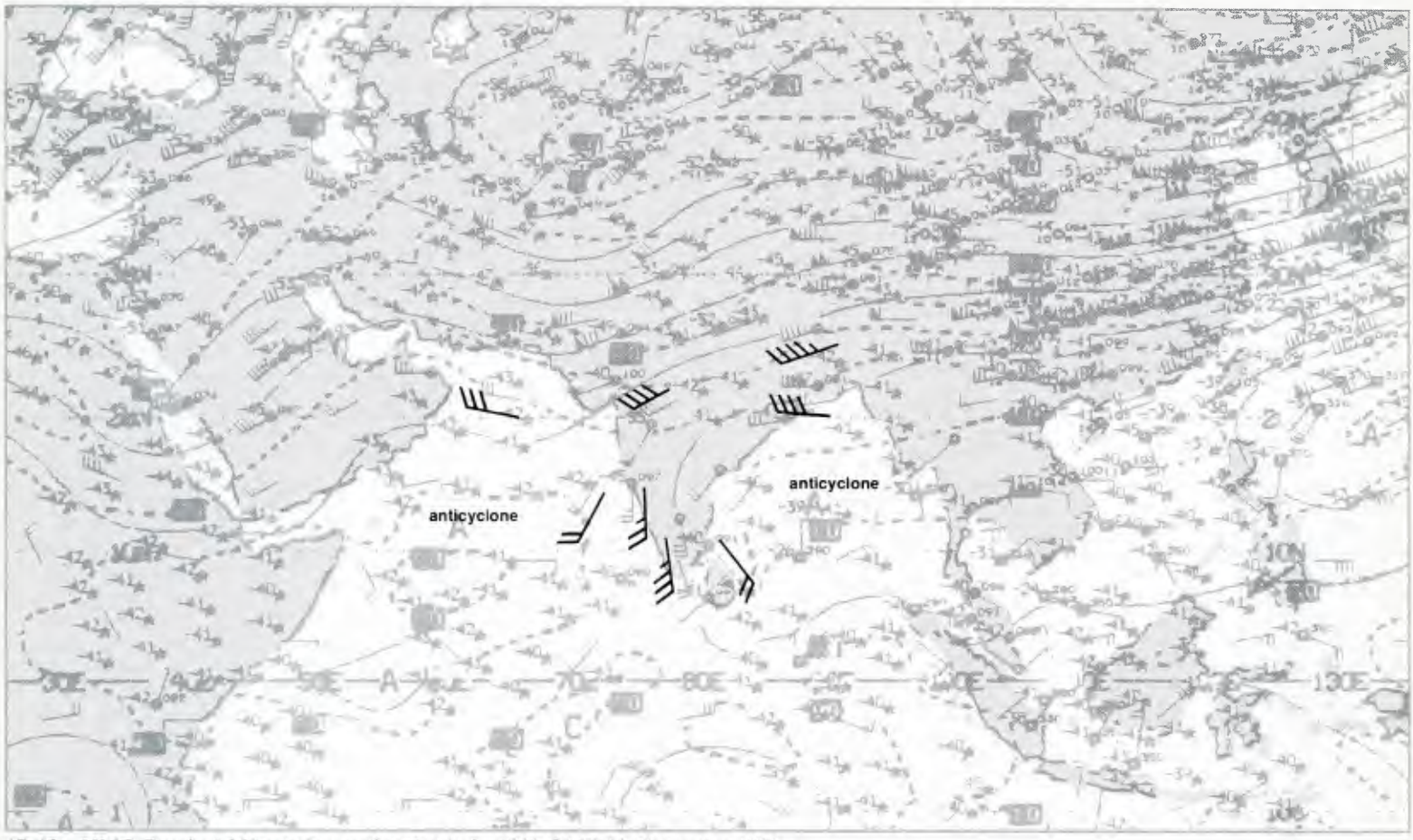

1B-12a. NMC Tropical 250-mb Streamline Analysis. 1200 GMT 12 November 1979.

700 mb

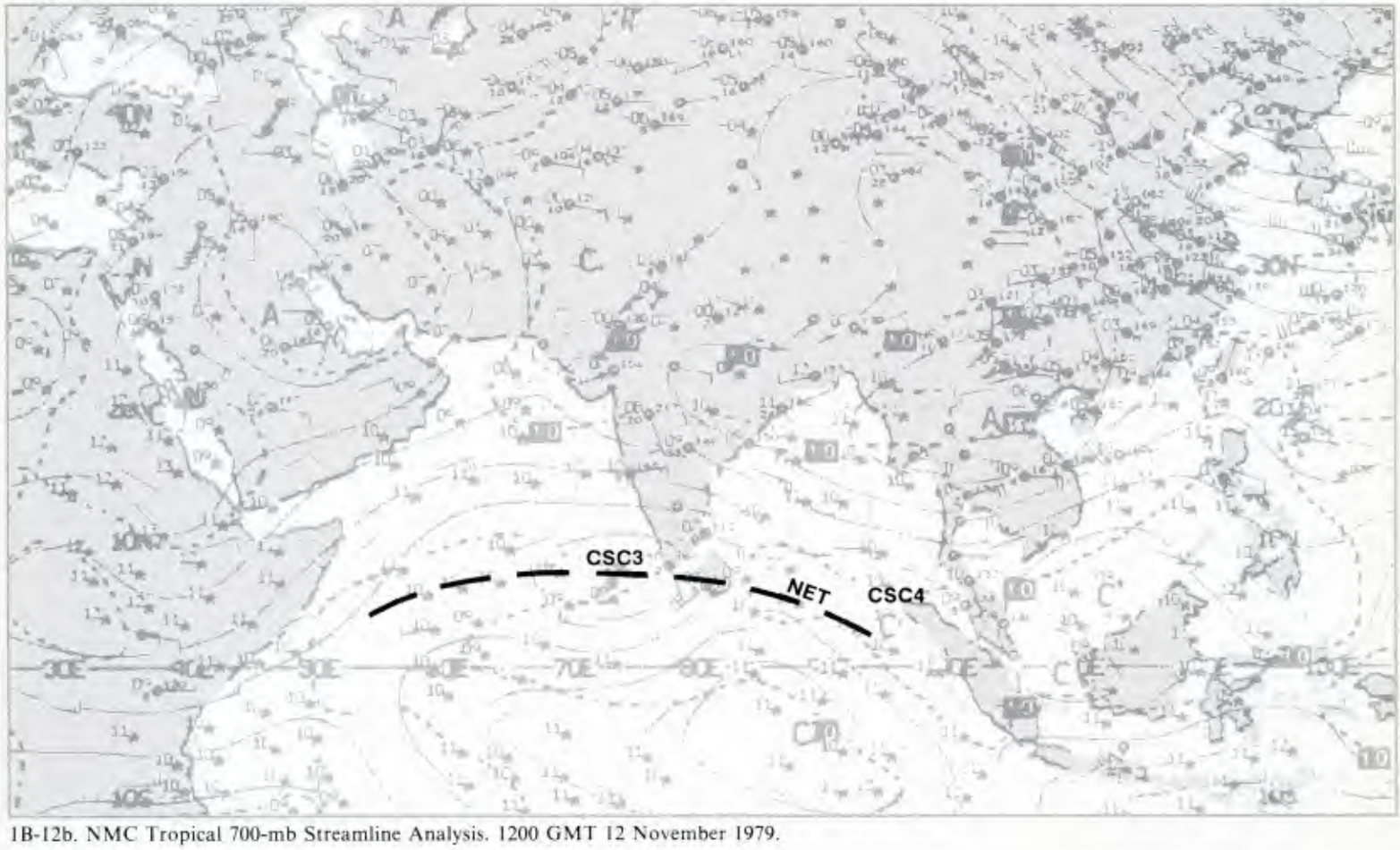

1B-12b. NMC Tropical 700-mb Streamline Analysis. 1200 GMT 12 November 1979.

1B-13a. GOES-Indian Ocean. Enlarged View. Visible Picture. 0730 GMT 12 November 1979.

surface

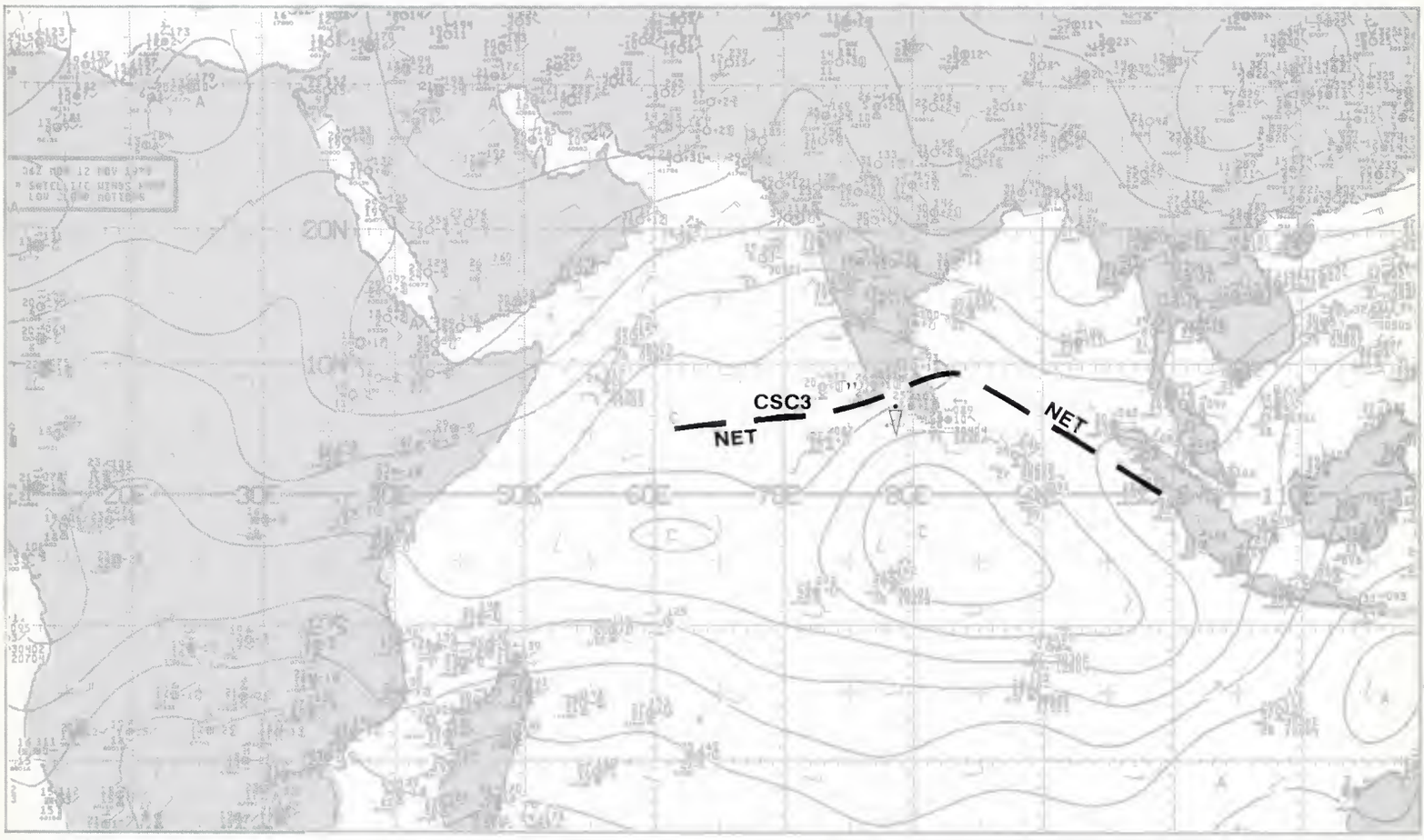

1B-13b. NMC Tropical Surface Streamline Analysis. 0600 GMT 12 November 1979.

250 mb

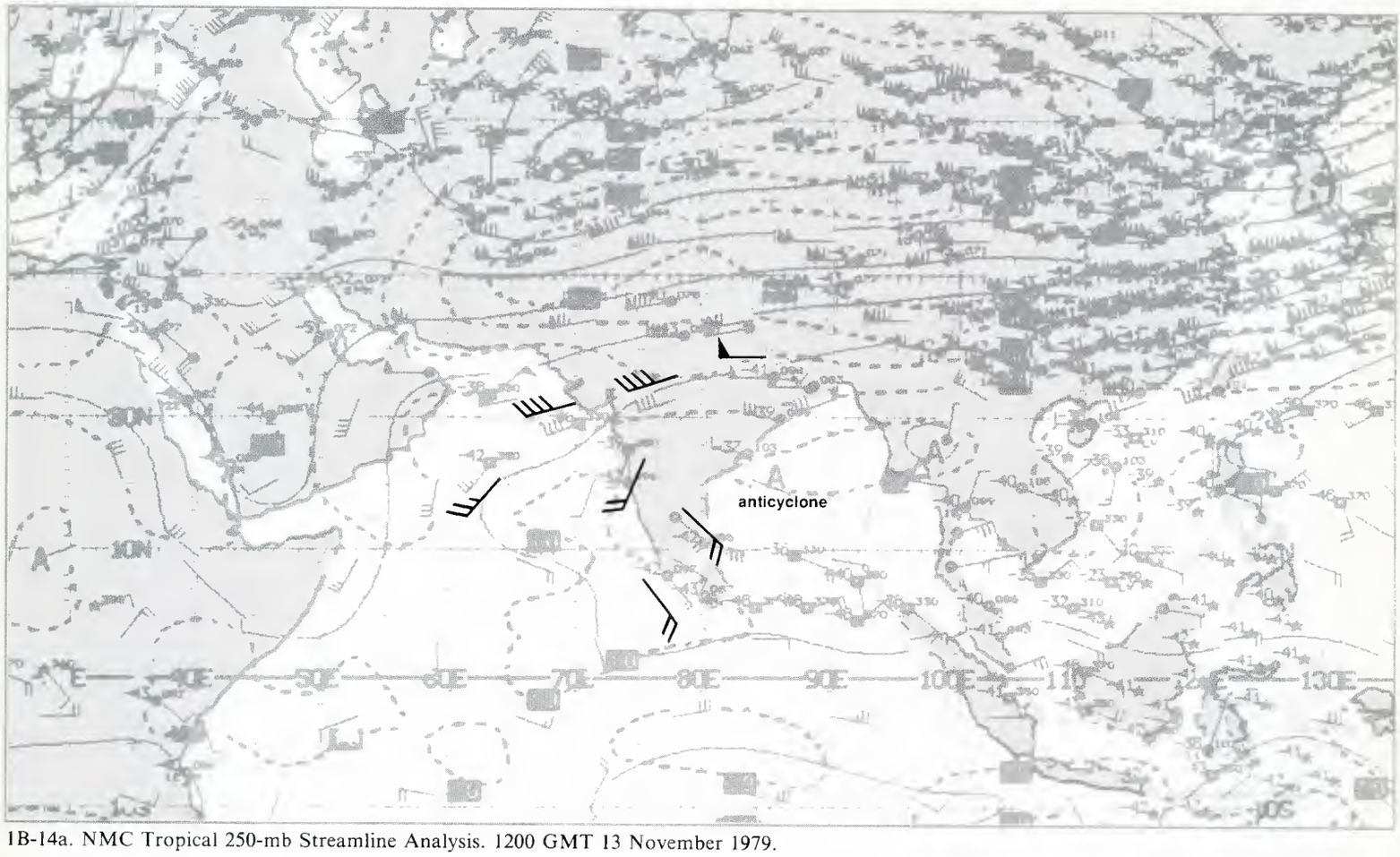

1B-14a. NMC Tropical 250-mb Streamline Analysis. 1200 GMT 13 November 1979.

700 mb

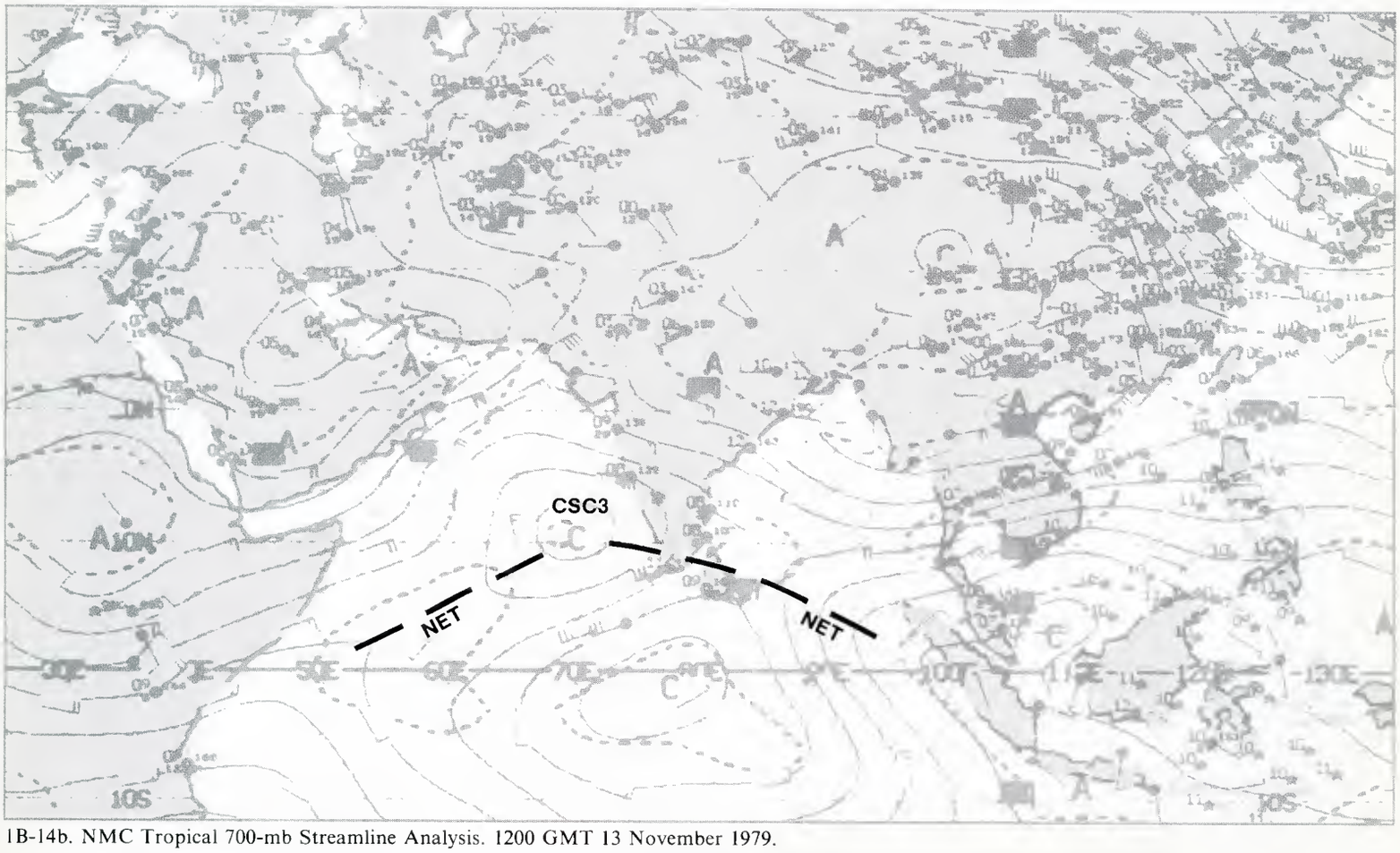

1B-14b. NMC Tropical 700-mb Streamline Analysis. 1200 GMT 13 November 1979.

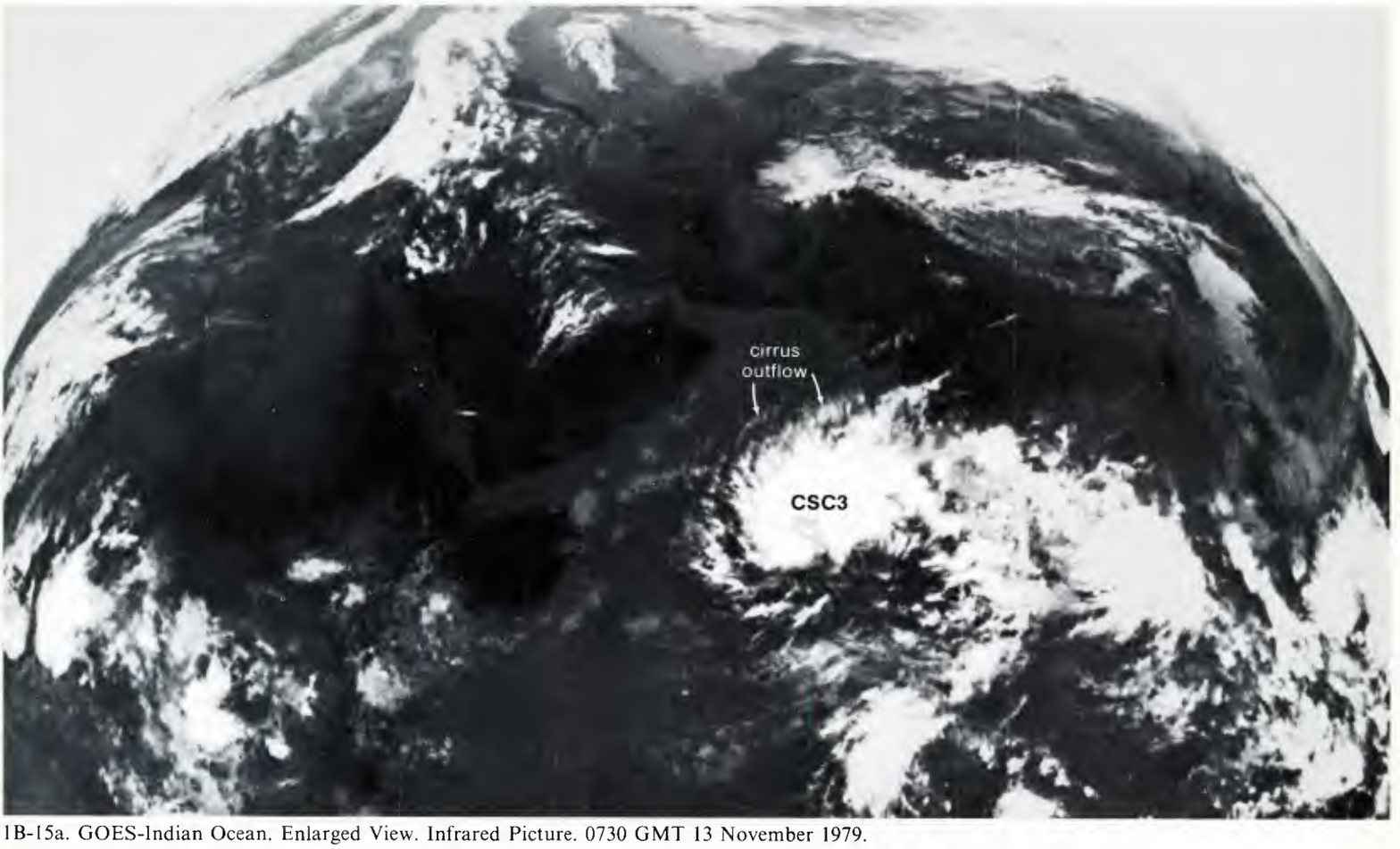

1B-15a. GOES-Indian Ocean. Enlarged View. Infrared Picture. 0730 GMT 13 November 1979.

surface

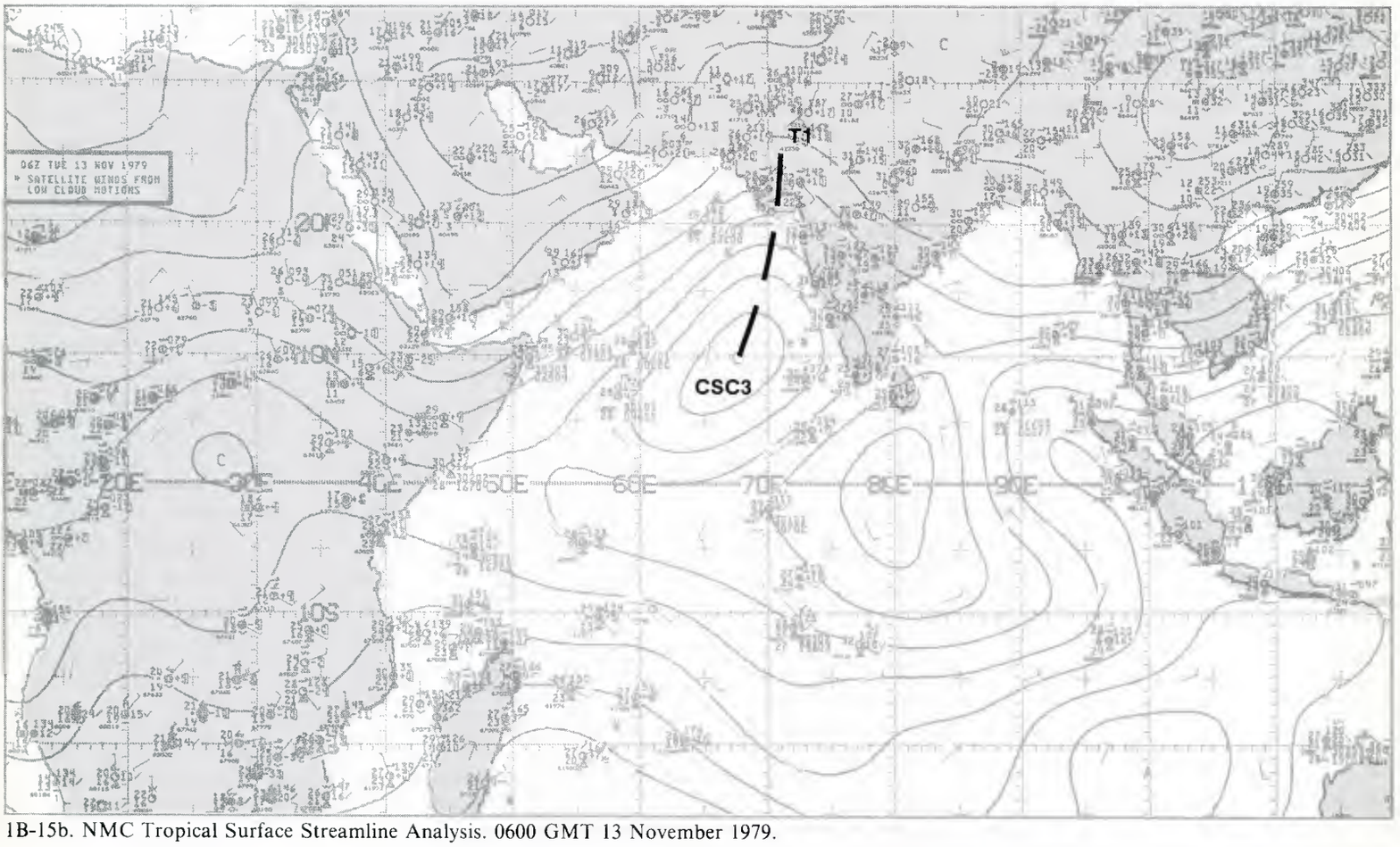

1B-15b. NMC Tropical Surface Streamline Analysis. 0600 GMT 13 November 1979.

250 mb

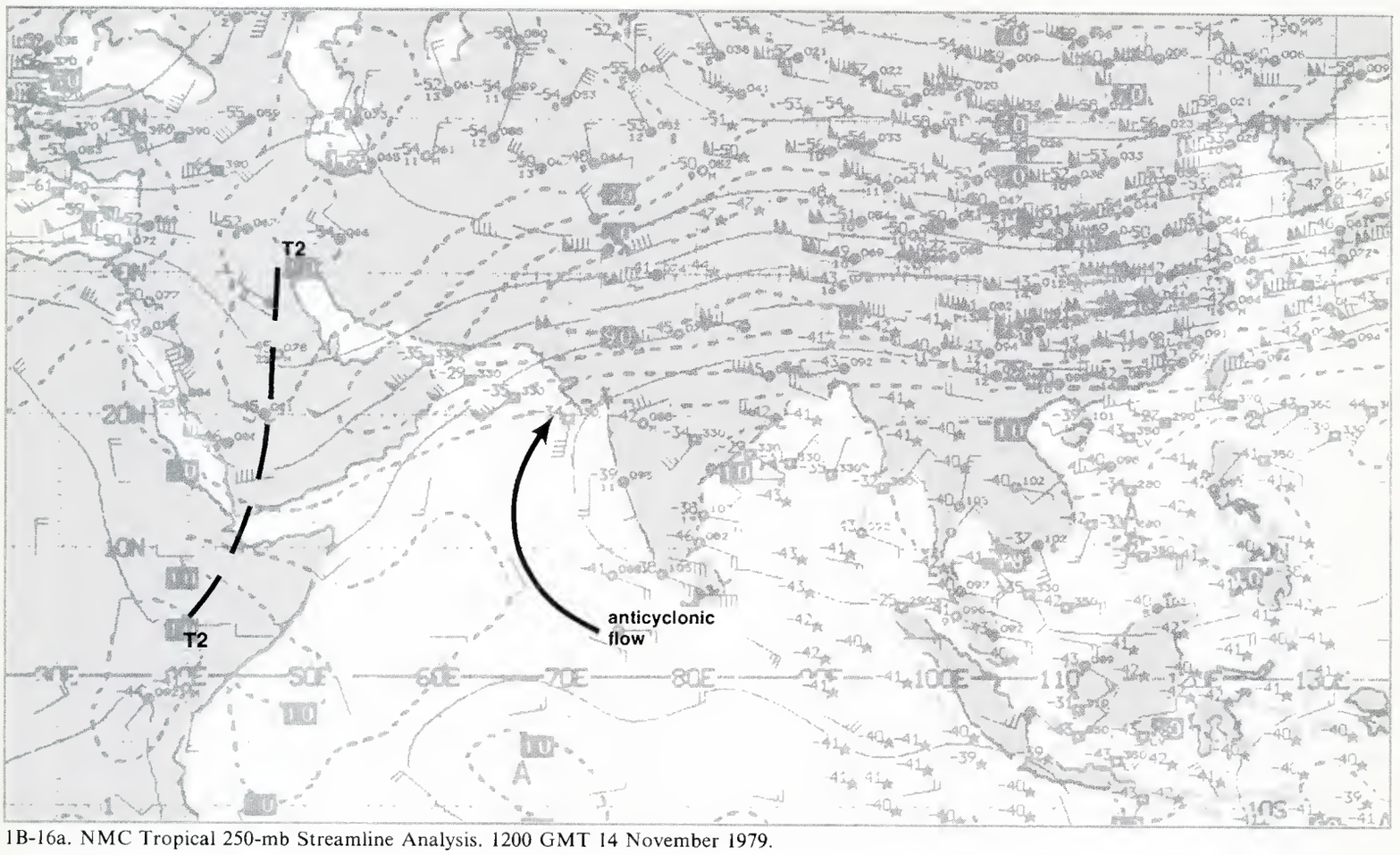

1B-16a. NMC Tropical 250-mb Streamline Analysis. 1200 GMT 14 November 1979.

700 mb

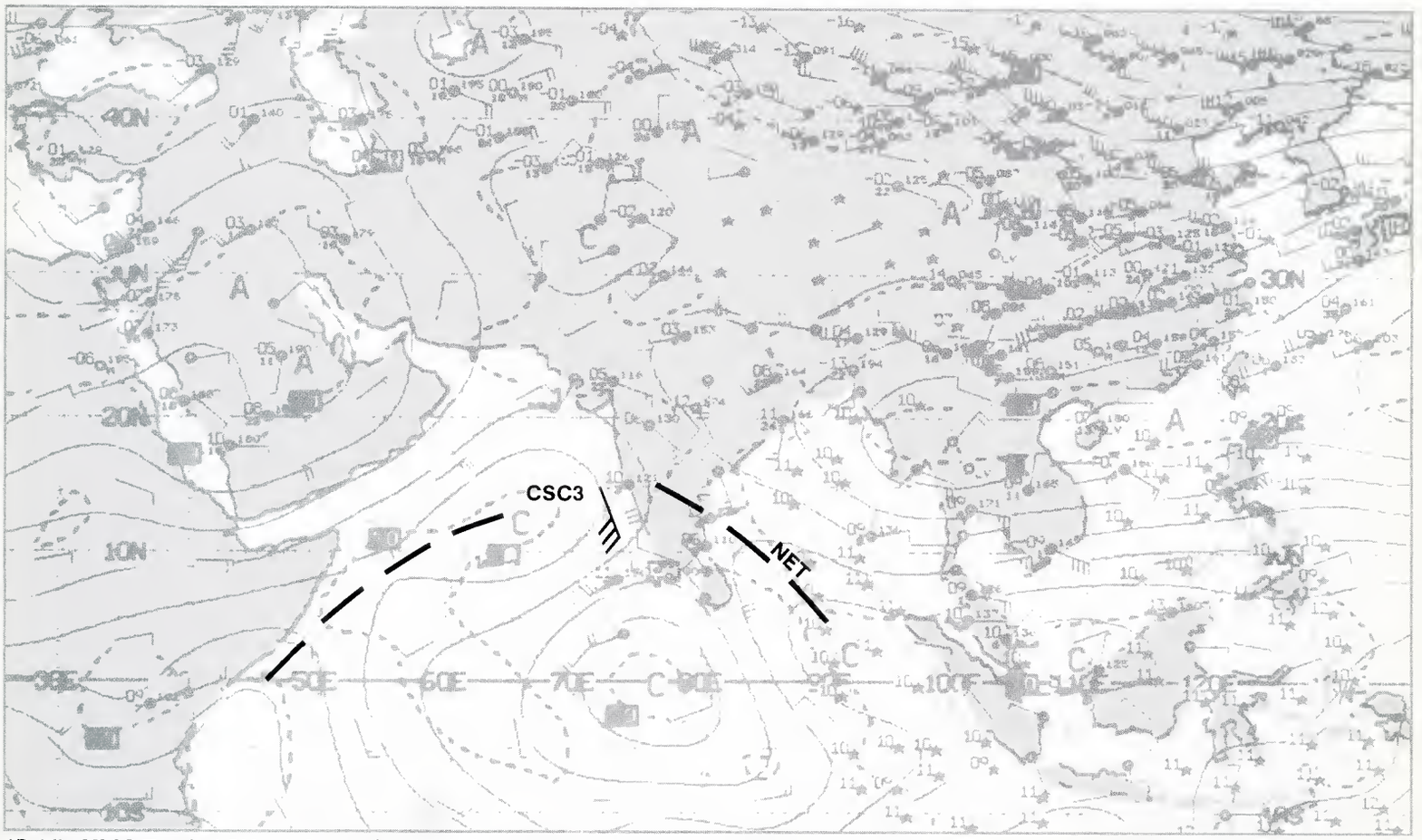

1B-16b. NMC Tropical 700-mb Streamline Analysis. 1200 GMT 14 November 1979.

1B-17a. GOES-Indian Ocean. Enlarged View. Visible Picture. 0700 GMT 14 November 1979.

surface

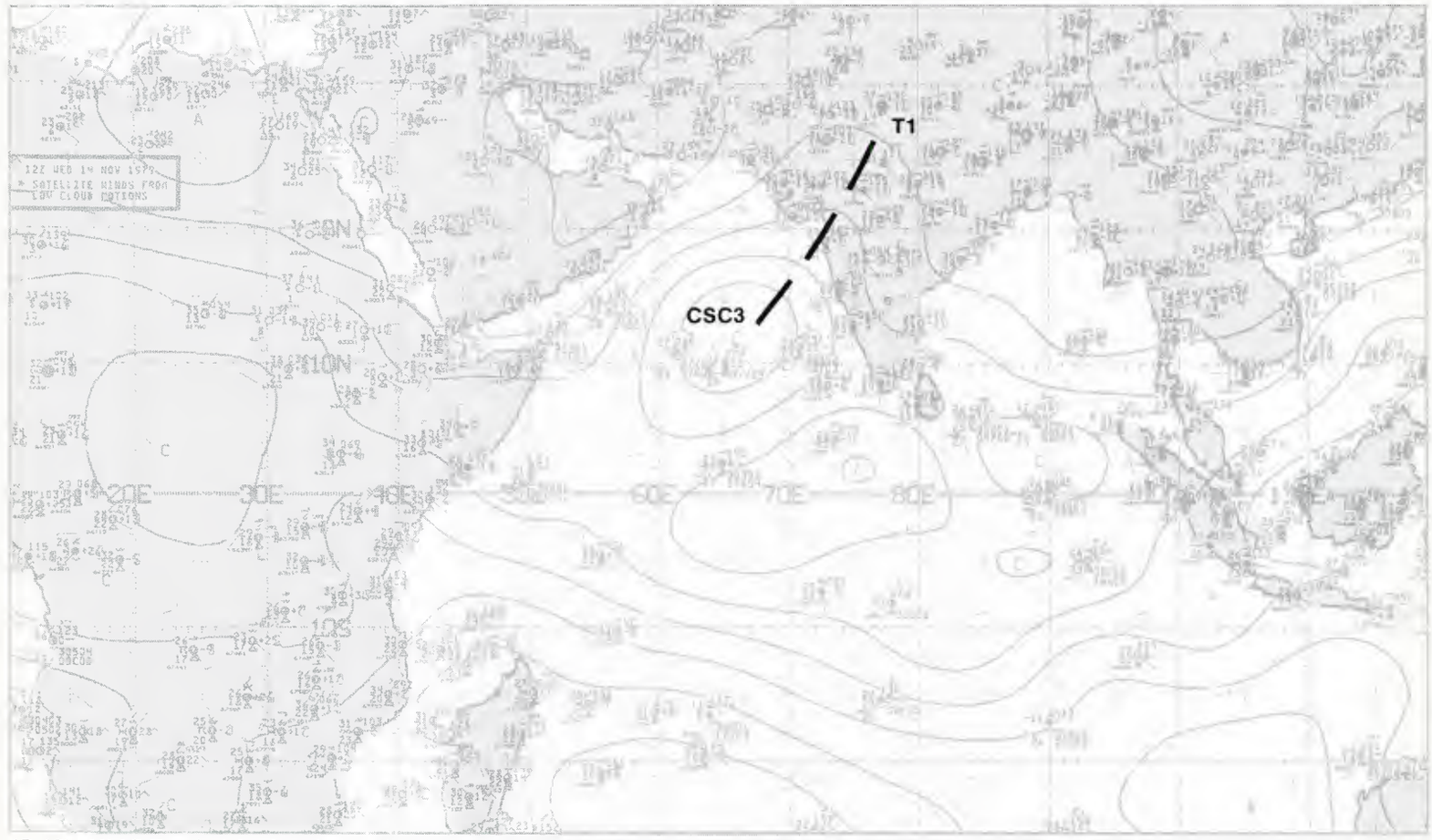

1B-17b. NMC Tropical Surface Streamline Analysis. 1200 GMT 14 November 1979.

250 mb

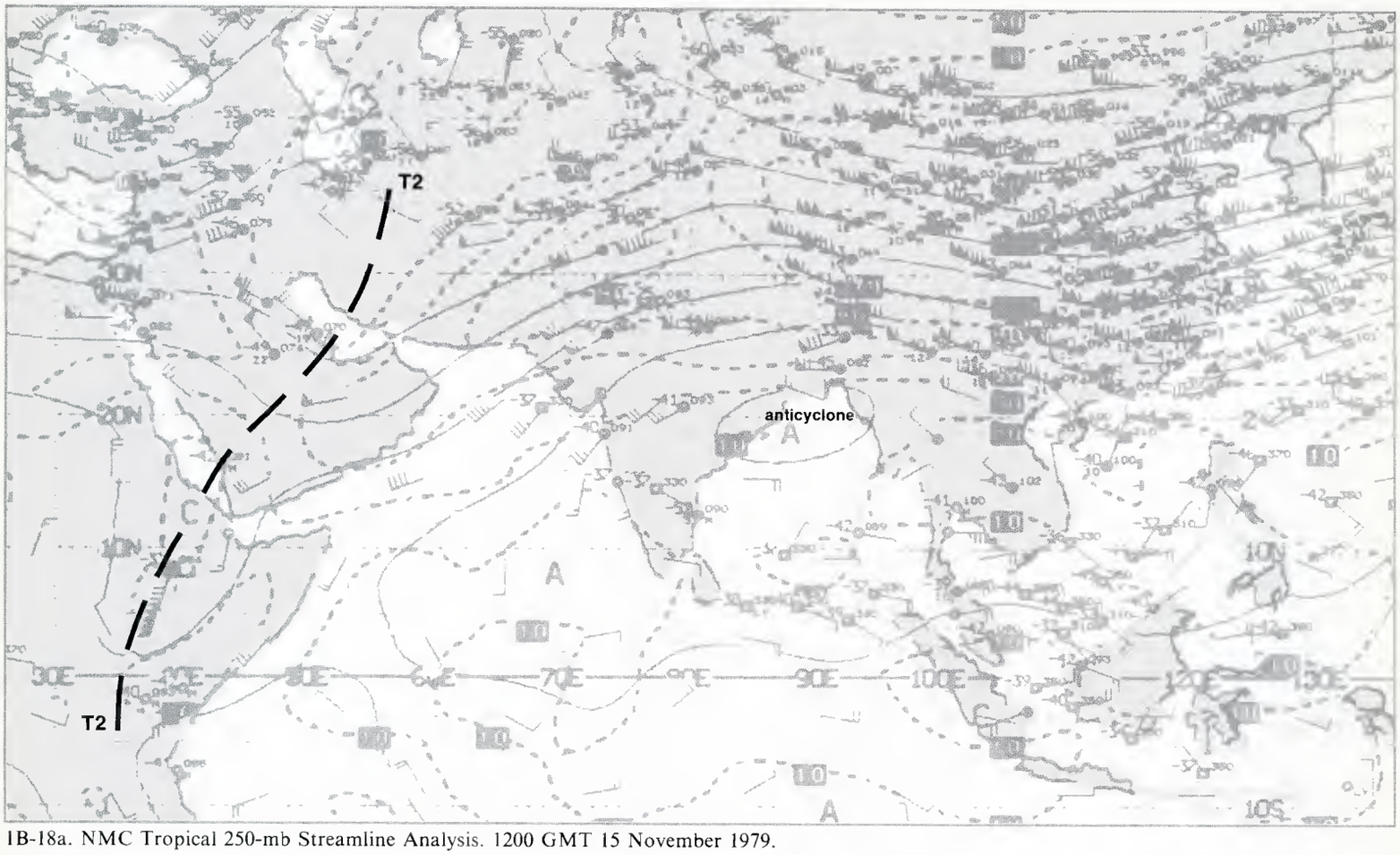

1B-18a. NMC Tropical 250-mb Streamline Analysis. 1200 GMT 15 November 1979.

700 mb

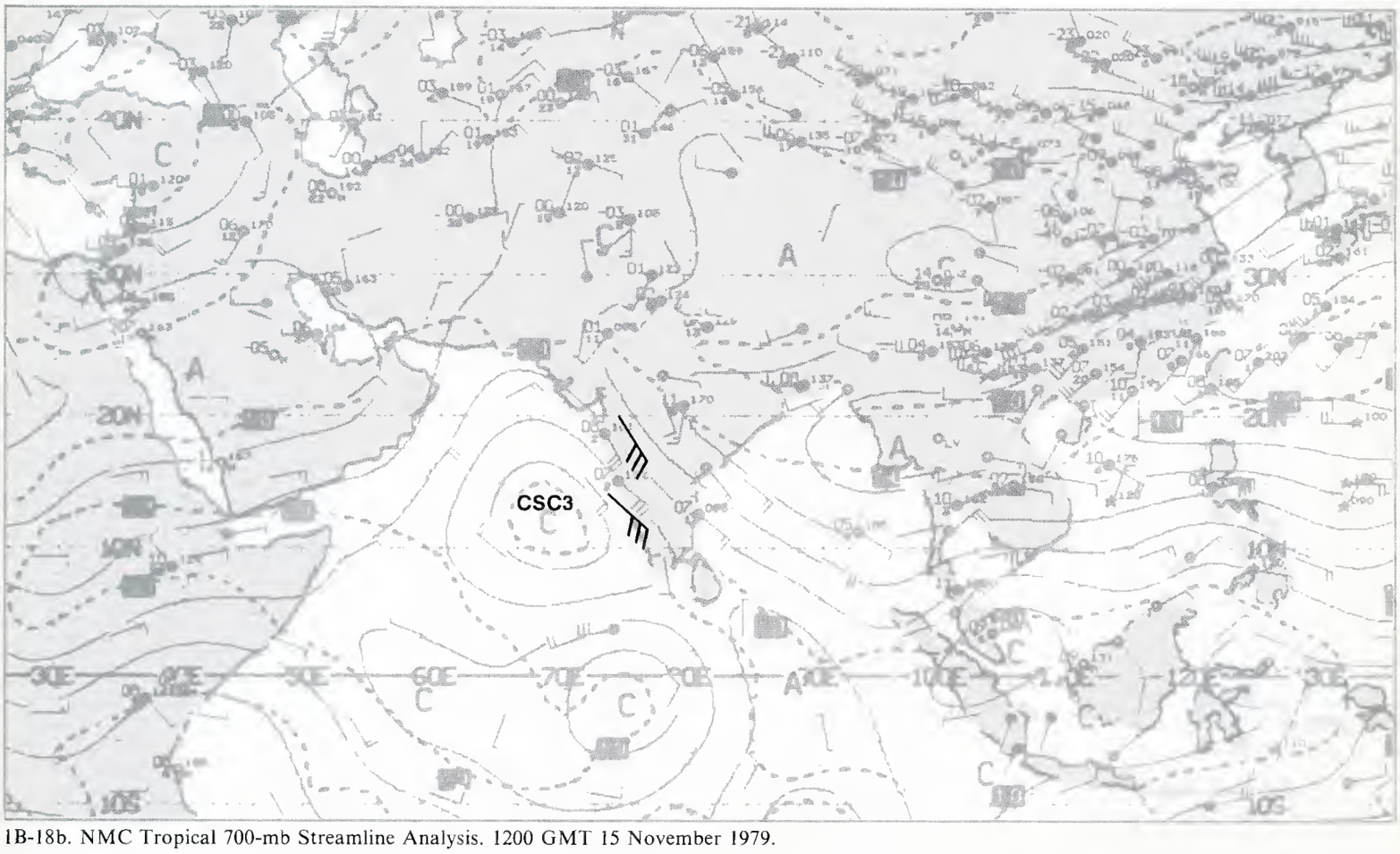

1B-18b. NMC Tropical 700-mb Streamline Analysis. 1200 GMT 15 November 1979.

15 November

The vortex **CSC3** shows some northward movement and intensification on this date, based on the surface analysis (1B-19b). A 35-kt wind report is shown north of the storm center, while a trough line **T1** continues to extend north-northeastward into northern India from the vortex.

The satellite picture (1B-19a), for the first time, shows banding features typical of early tropical storm development, with a suggested center of circulation. The northern edge of the cloudiness, however, is being sheared toward the northeast by strong upper-level flow, apparently under the influence of the upper-level trough **T2** at 250 mb (1B-18a), approaching from the west (1B-16a). Strong upper-level flow so near the storm center in an early formative stage produces a vertical shear not conducive to further intensification.

The storm is well defined by reports at the 700-mb level (1B-18b), with 30-kt southeasterly winds apparent along the west coast of India. In the satellite picture (1B-19a), the movement of cirrus to the northeast from the storm area is due to the strong winds at 250 mb (1B-18a). Note also that the surface storm center is located well to the west of the 250-mb anticyclonic center, which is now located over the northern Bay of Bengal.

16 November

The first warning of the development of a tropical depression (TC 25-79) was issued by the Joint Typhoon Warning Center (JTWC) at 0200 GMT (1B-21c). This chart also shows the "Best Track", wind information, and storm evolution. The surface analysis (1B-21b) shows the position of the depression, with a wind warning indicating maximum winds of 40 kt and gusts to 50 kt.

The satellite picture (1B-21a) reveals the storm with an apparent center of circulation still outside of the major overcast region, implying a tropical depression condition and little change in intensity from the preceding day. Cirrus clouds continue to be advected east-northeastward by apparently strong upper-level winds.

The 700-mb analysis (1B-20b) indicates that the vortex circulation **CSC3** dominates the entire Arabian Sea region, although wind speeds are not especially strong. The 250-mb analysis (1B-20a) shows that strong southwesterly winds are beginning to advance over the vortex center. This condition is not favorable for development, and a decrease in storm intensity might be anticipated for the following day.

17 November

The surface analysis (1B-23b) shows the storm TC 25-79 located near the southern tip of India; however, the storm is much further north, as indicated by the satellite picture (1B-23a). The storm is very weak—at the surface very light winds are reported to the east of the storm along the coast. The satellite picture also suggests a weak storm system, diminished in intensity from the preceding day (1B-21a). In particular, cloud banding in the area defining the center to the south of the major overcast region appears weak and lacking strong symmetry or spiral characteristics that would imply a greater intensity. One small spiral cloud complex is apparent, however, that seems to define the exact center. The overcast cloud area also is not as intense as earlier—some breaks appear and there is a lack of cirrus outflow that would be characteristic of strong convection.

At 700 mb (1B-22b), the circulation appears less dominant over the Arabian Sea and is suggesting a dissipative tendency. The 250-mb analysis (1B-22a) reveals even stronger southwesterly windflow over the vortex center than on the preceding day. The indication is that winds of 50 kt, or greater, are blowing directly over the storm center. The prognosis for dissipation on the following day is excellent. At 2000 GMT, the JTWC issued its last warning on this storm (1B-21a).

18 November

The surface analysis (1B-25b) fails to indicate even a vortex remnant of TC 25-79, although a long trough axis is shown extending northward from a new cyclonic streamline center **CSC4**. The satellite picture (1B-25a), however, does reveal the dissipating cloud vortex TC 25-79. Banding and cloudiness does not extend more than a degree or so from this center, and its potential for further development at this stage is negligible.

The 700-mb analysis (1B-24b) shows only a weak trough **T3** in the region of the dissipating storm. In addition, the 250-mb analysis (1B-24a) continues to show anticyclonically turning flow over the storm remnants; however, loss of circulation at low levels and its proximity to land, where it is being steered, precludes further development.

Important Conclusions

1. Tropical cyclones in the Arabian Sea are especially favored during the spring and fall transition seasons to the southwest and northeast monsoons.

2. The storms develop in the near-equatorial trough (NET) as it moves to its position over northern India in the spring, and retreats to its position near the Equator in the fall.

3. Strong upper-level winds moving near or over the vortex center create pronounced vertical shear not conducive to further development.

4. The surface and 700-mb analyses are reasonably accurate in portraying the position of the near-equatorial trough, and in the development of disturbances and tropical depressions within that region.

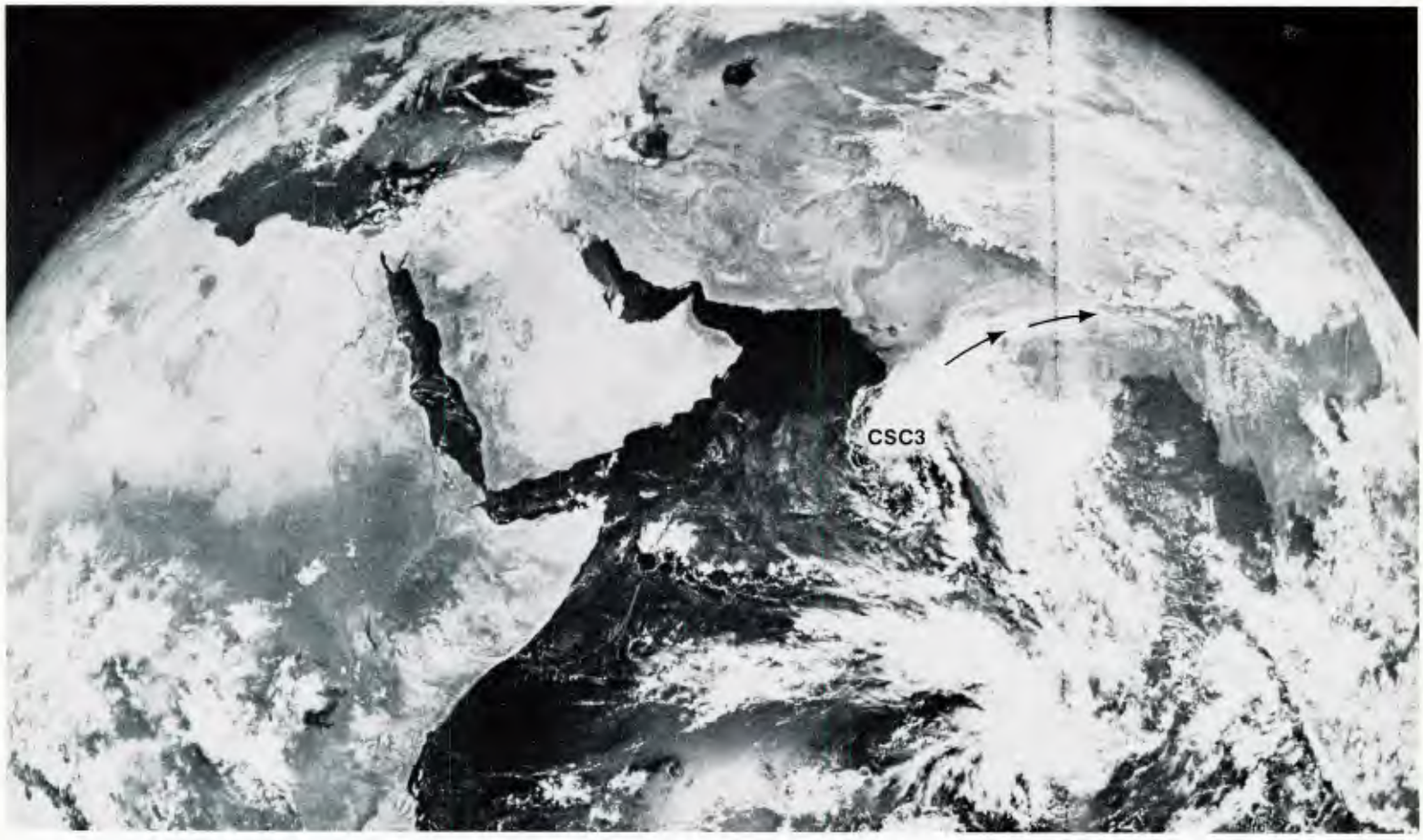

1B-19a. GOES-Indian Ocean. Enlarged View. Visible Picture. 0730 GMT 15 November 1979.

surface

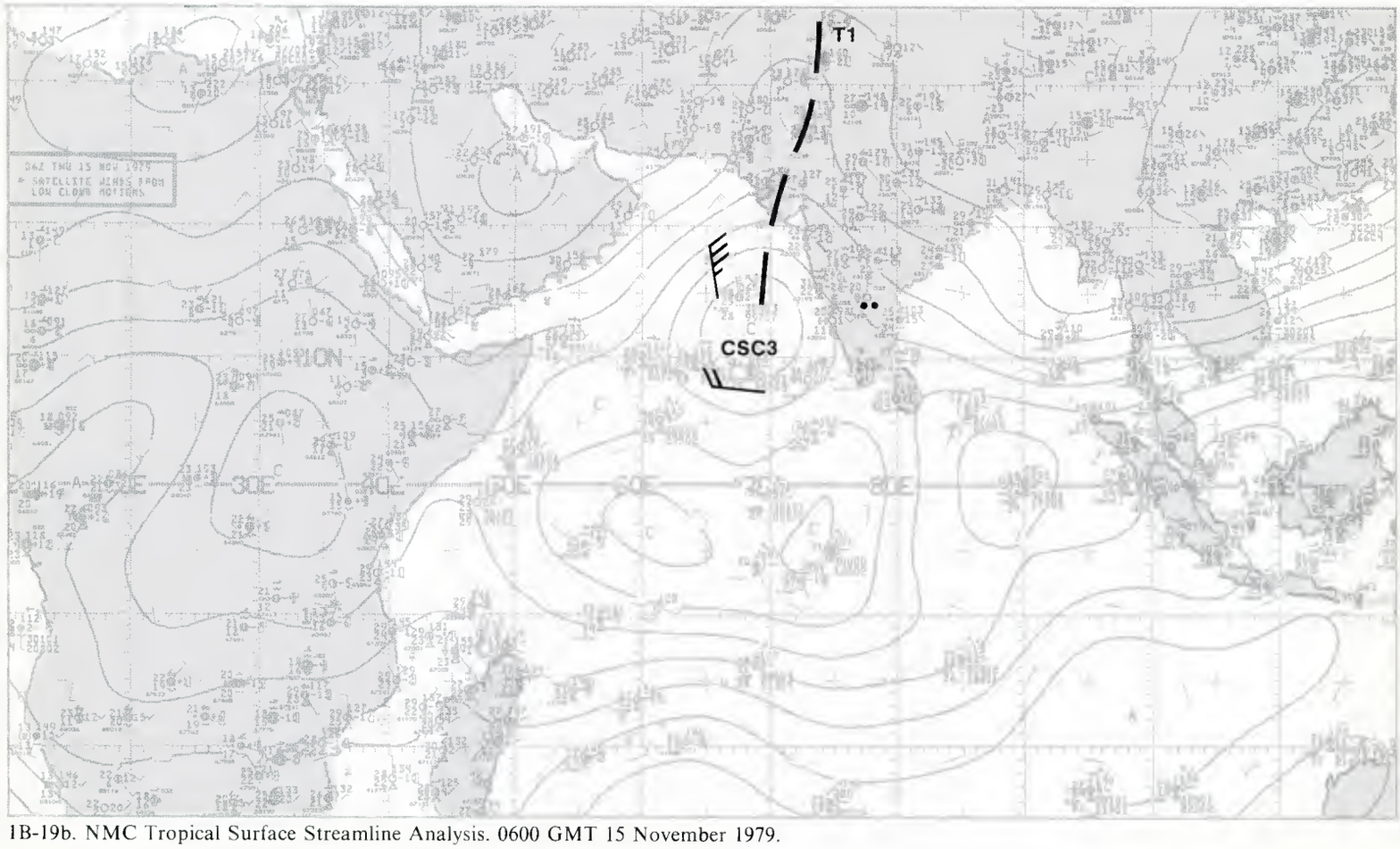

1B-19b. NMC Tropical Surface Streamline Analysis. 0600 GMT 15 November 1979.

250 mb

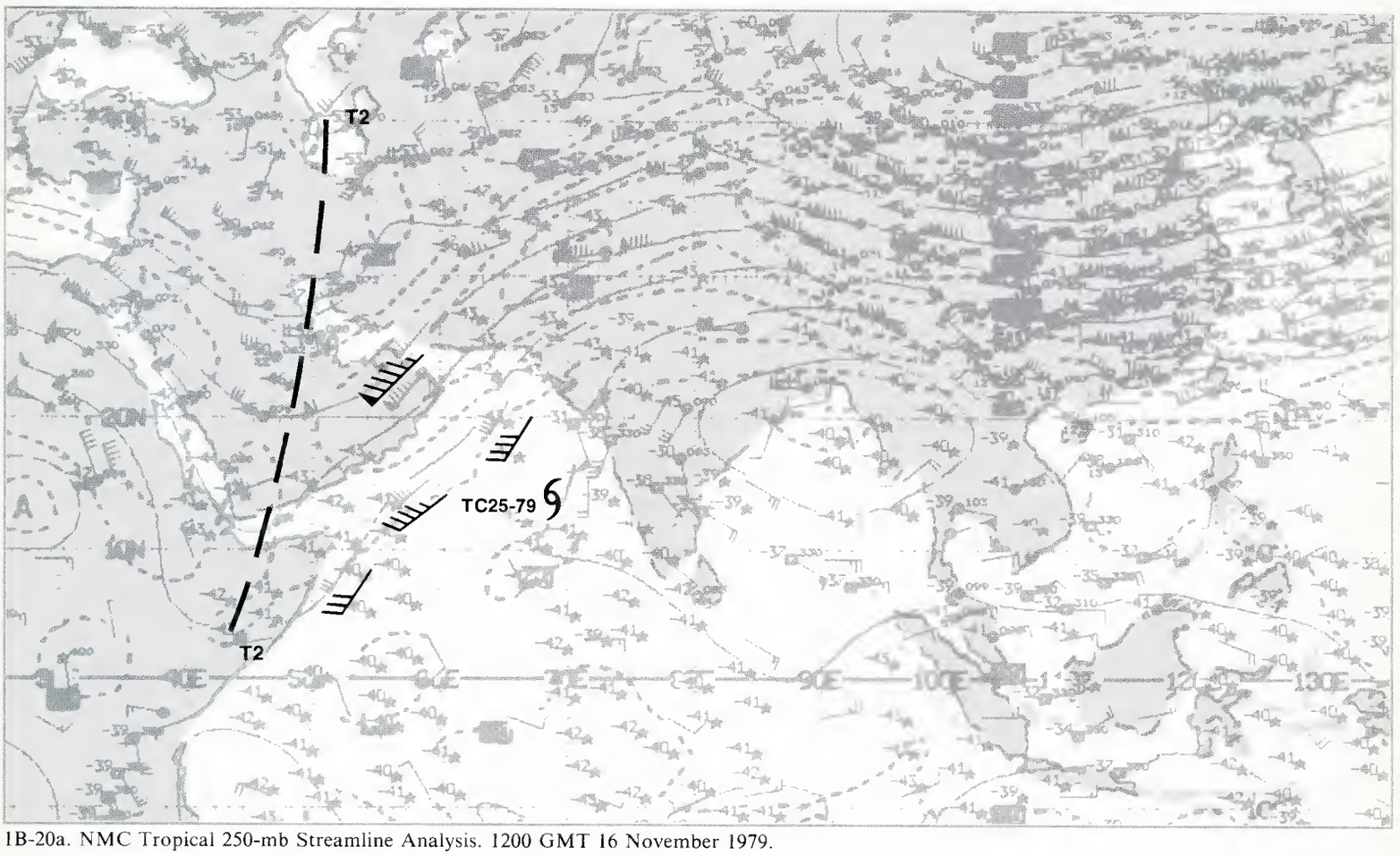

1B-20a. NMC Tropical 250-mb Streamline Analysis. 1200 GMT 16 November 1979.

700 mb

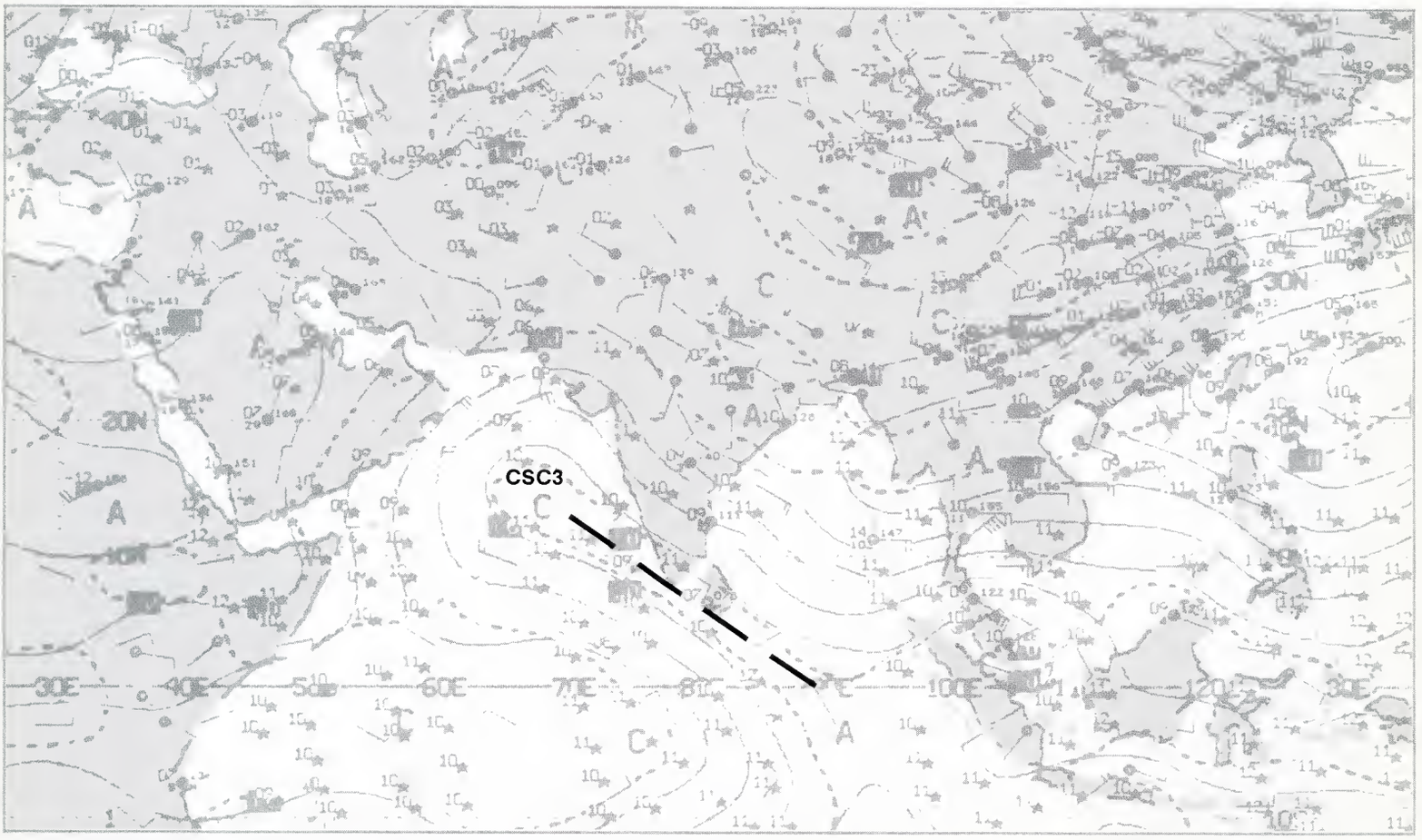

1B-20b. NMC Tropical 700-mb Streamline Analysis. 1200 GMT 16 November 1979.

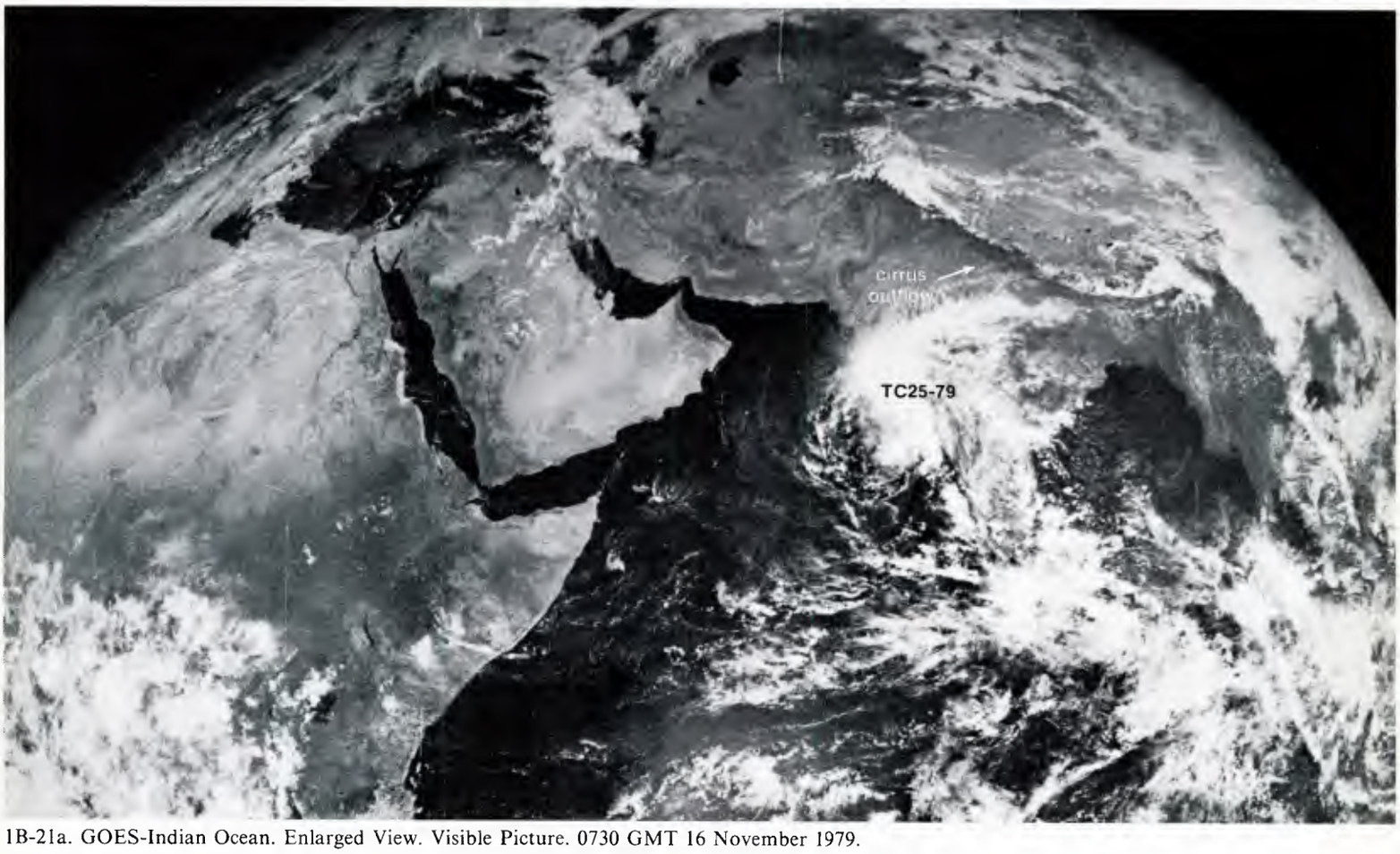

1B-21a. GOES-Indian Ocean. Enlarged View. Visible Picture. 0730 GMT 16 November 1979.

surface

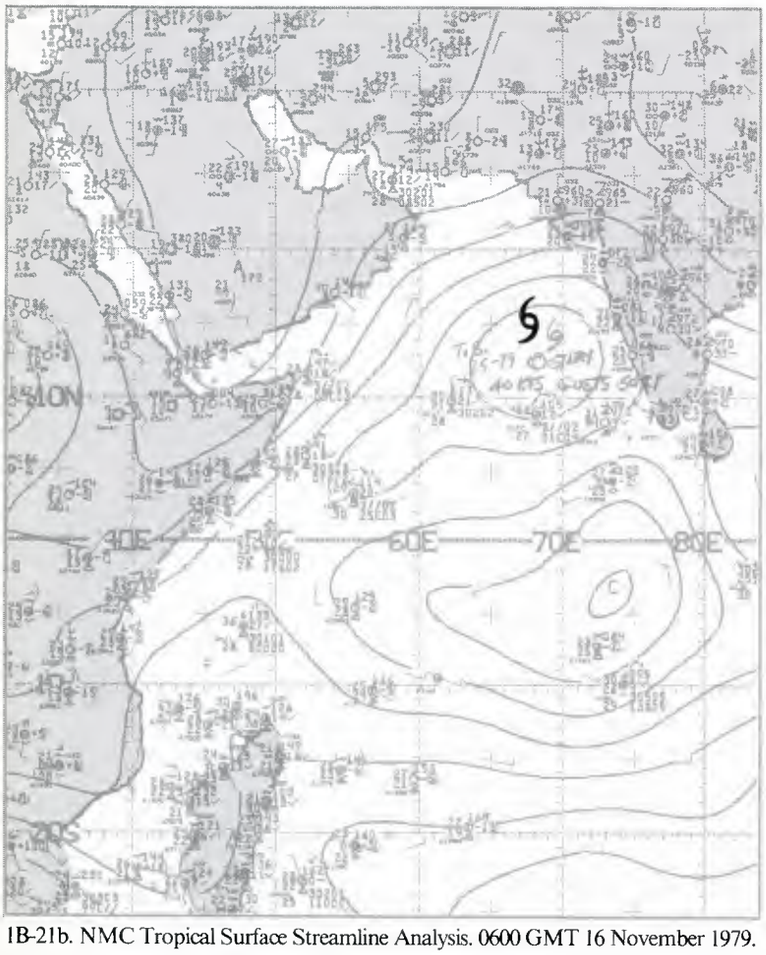

1B-21b. NMC Tropical Surface Streamline Analysis. 0600 GMT 16 November 1979.

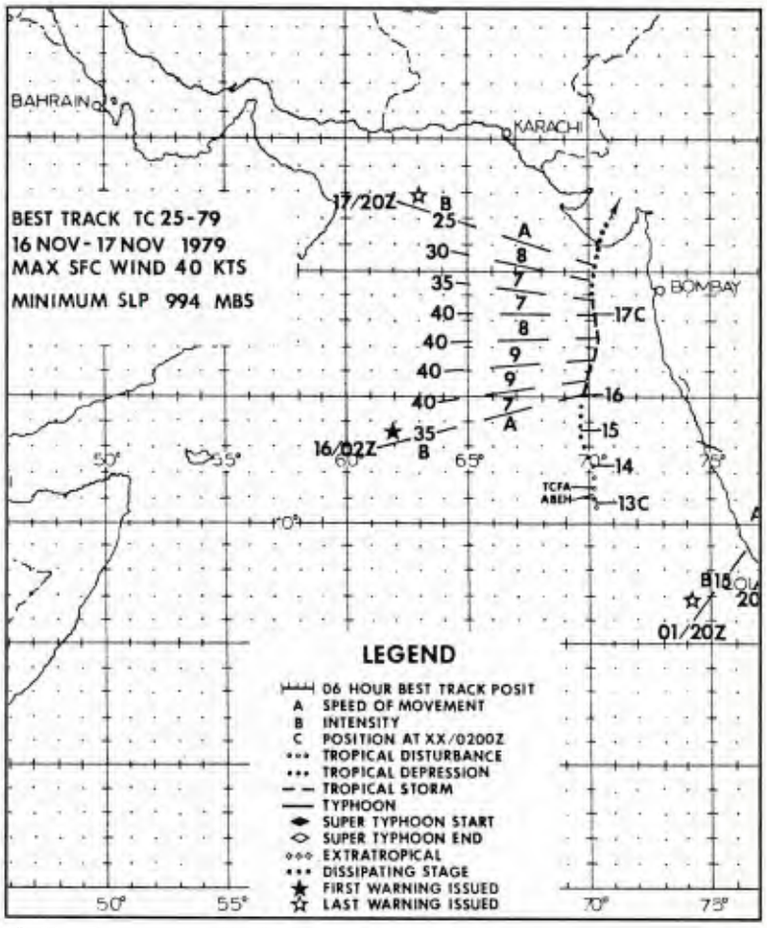

1B-21c. Best Track—TC 25-79. 16–17 November 1979.

250 mb

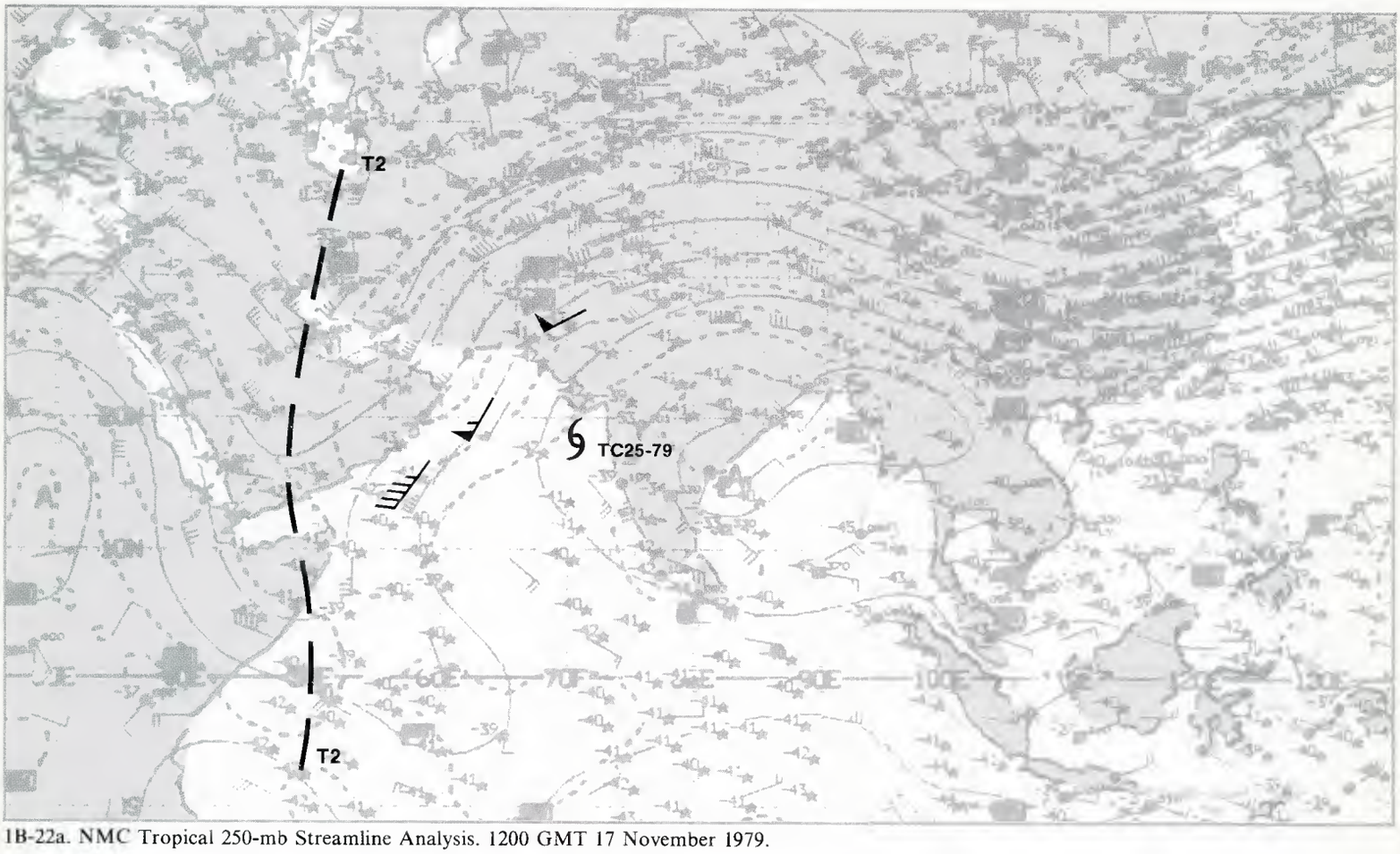

1B-22a. NMC Tropical 250-mb Streamline Analysis. 1200 GMT 17 November 1979.

700 mb

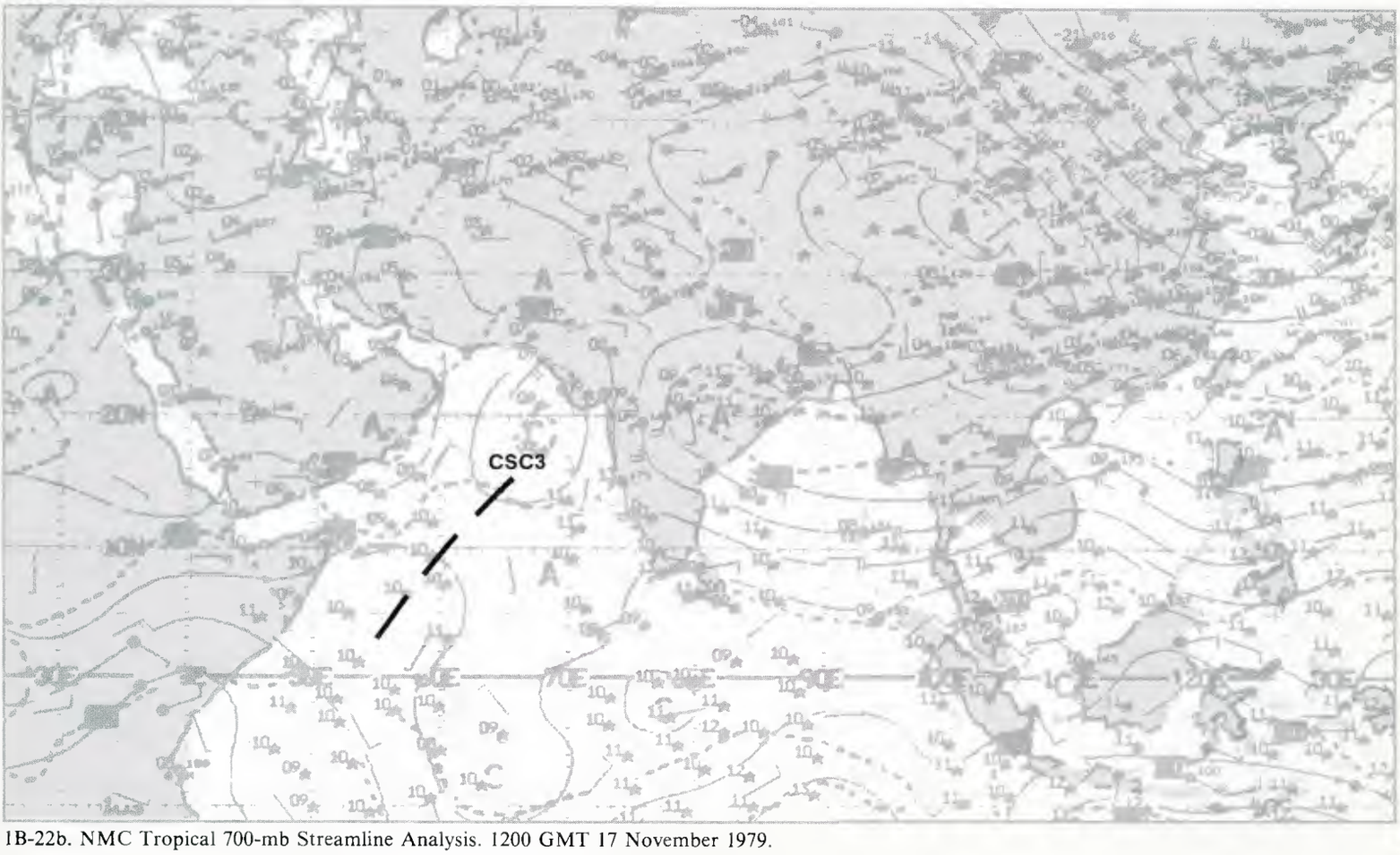

1B-22b. NMC Tropical 700-mb Streamline Analysis. 1200 GMT 17 November 1979.

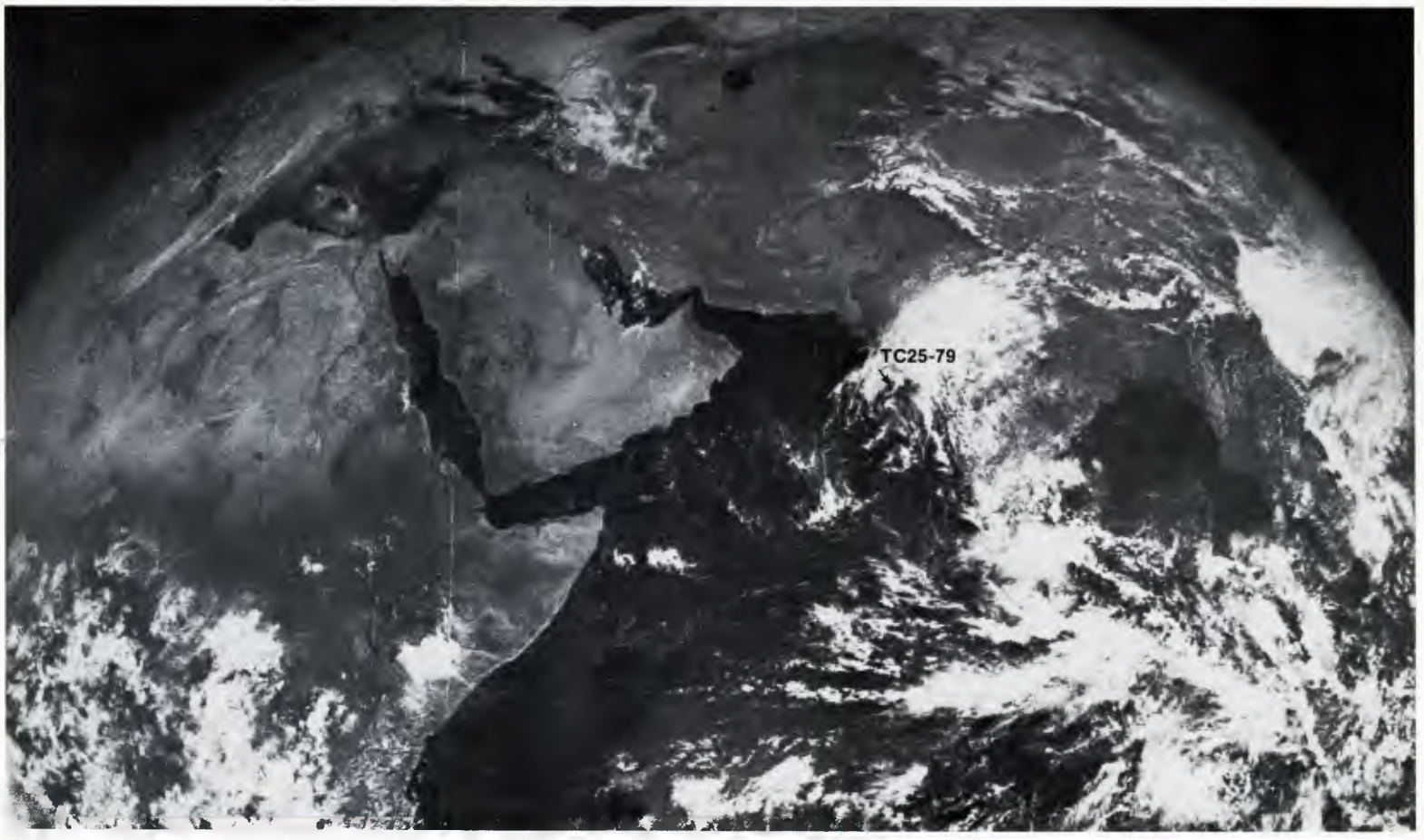

1B-23a. GOES-Indian Ocean. Enlarged View. Visible Picture. 0730 GMT 17 November 1979.

surface

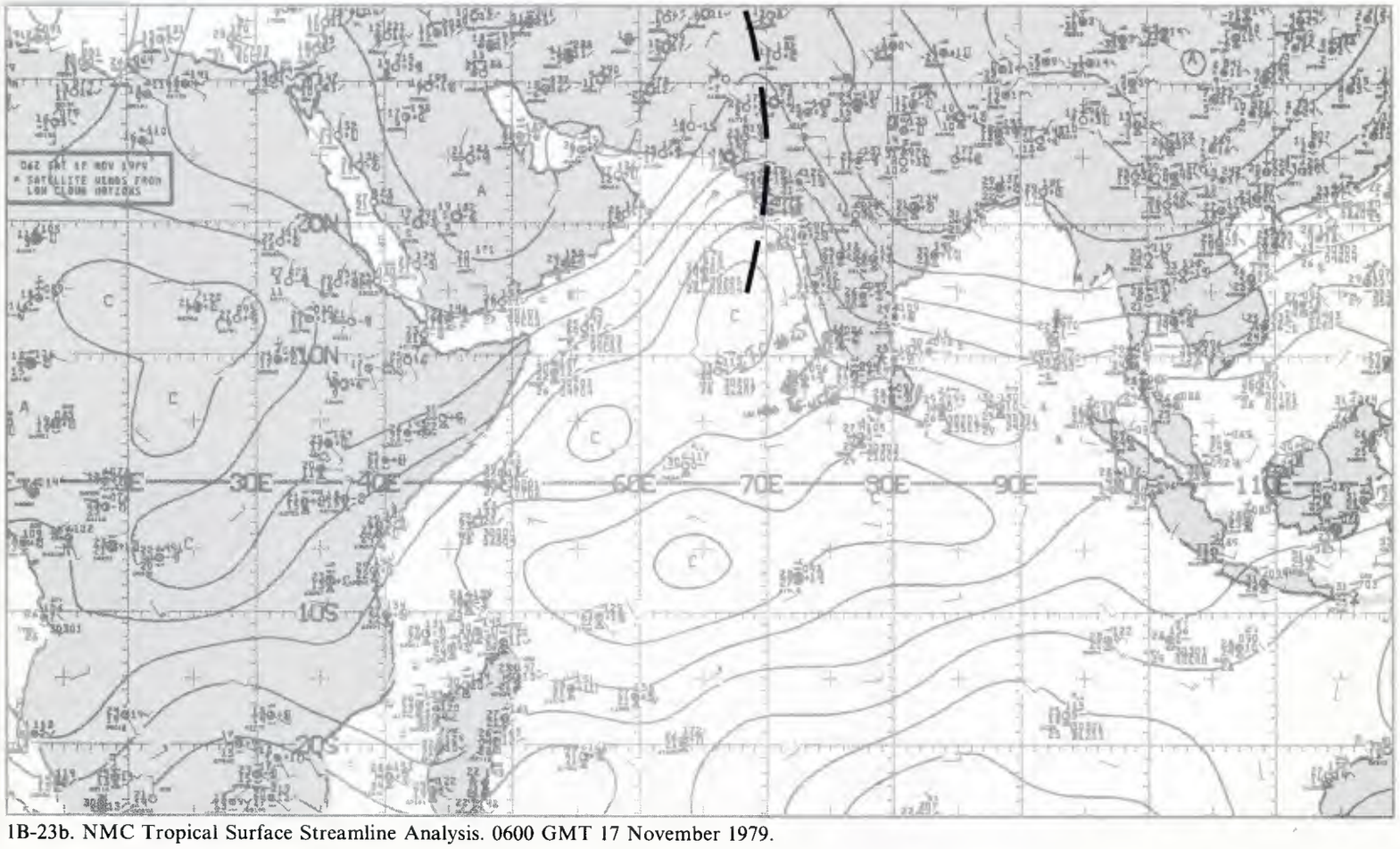

1B-23b. NMC Tropical Surface Streamline Analysis. 0600 GMT 17 November 1979.

250 mb

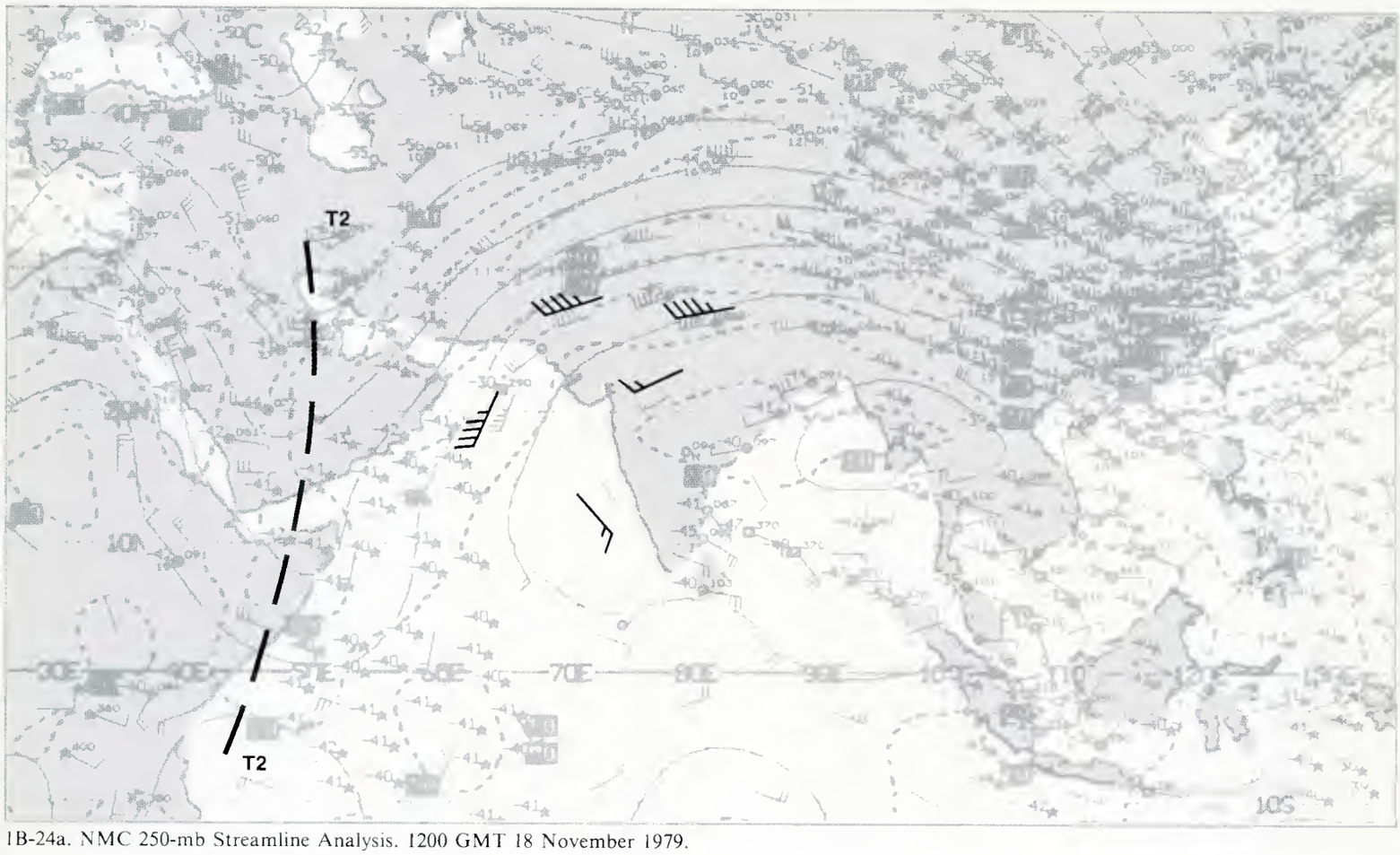

1B-24a. NMC 250-mb Streamline Analysis. 1200 GMT 18 November 1979.

700 mb

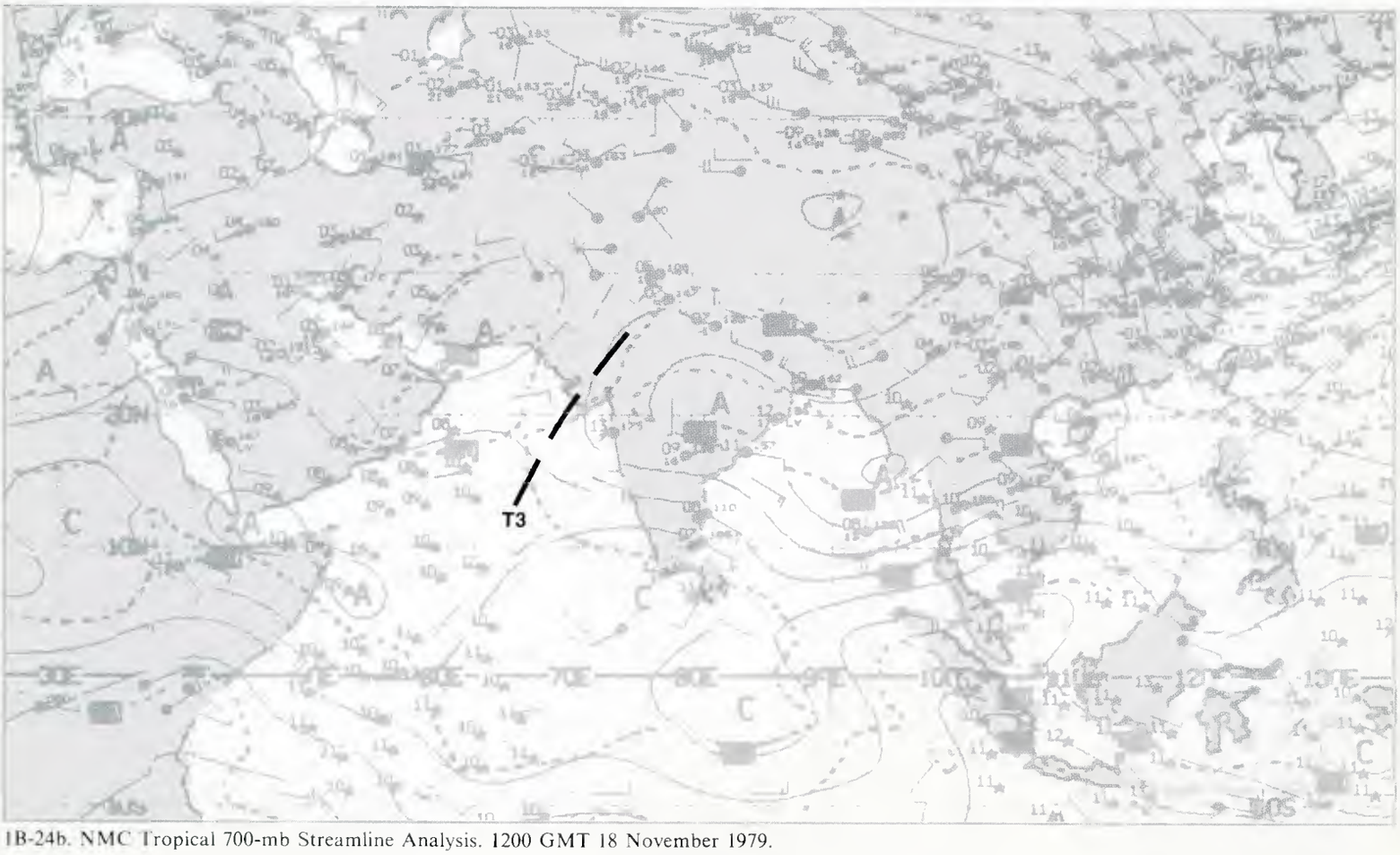

1B-24b. NMC Tropical 700-mb Streamline Analysis. 1200 GMT 18 November 1979.

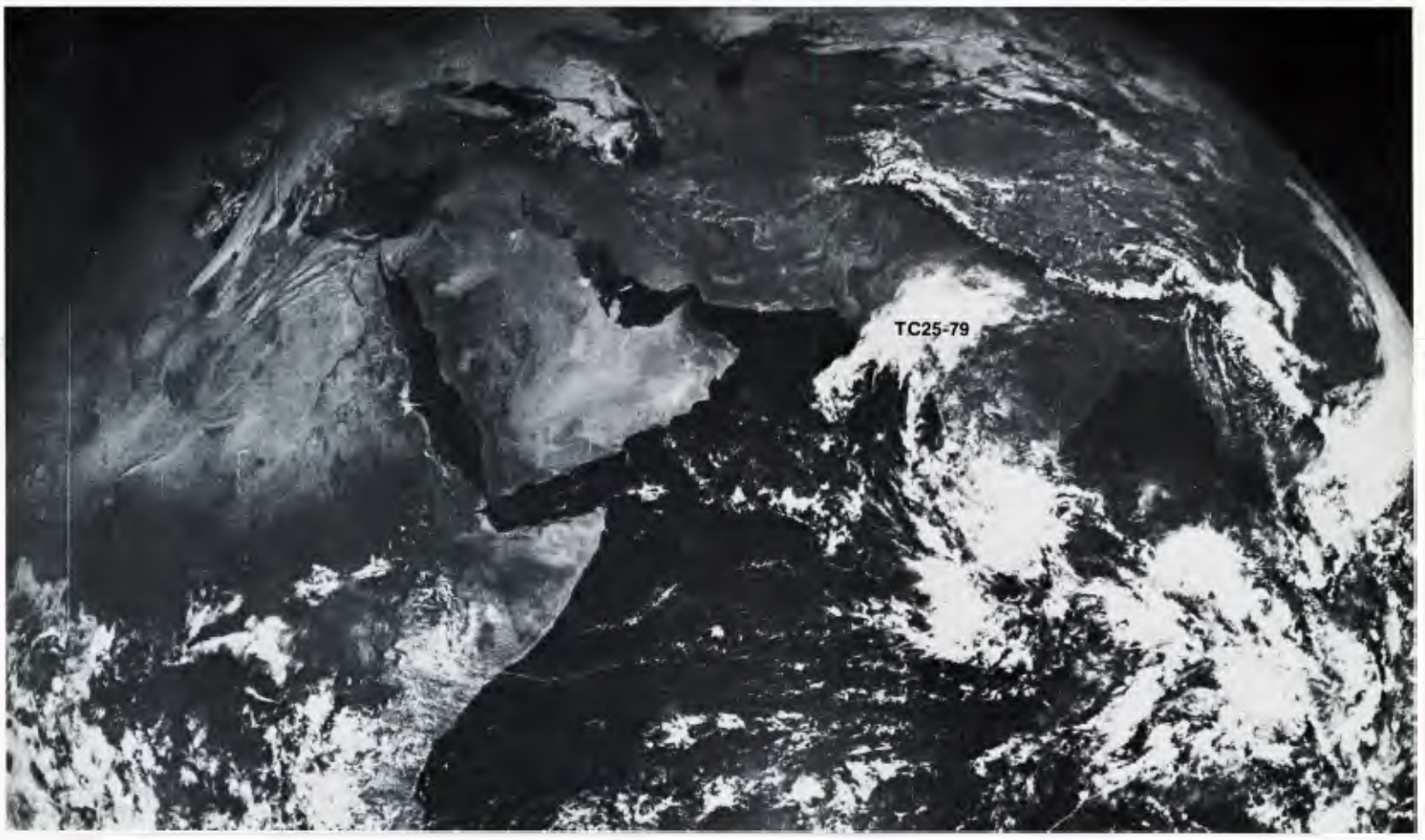

1B-25a. GOES-Indian Ocean. Enlarged View. Visible Picture. 0700 GMT 18 November 1979.

surface

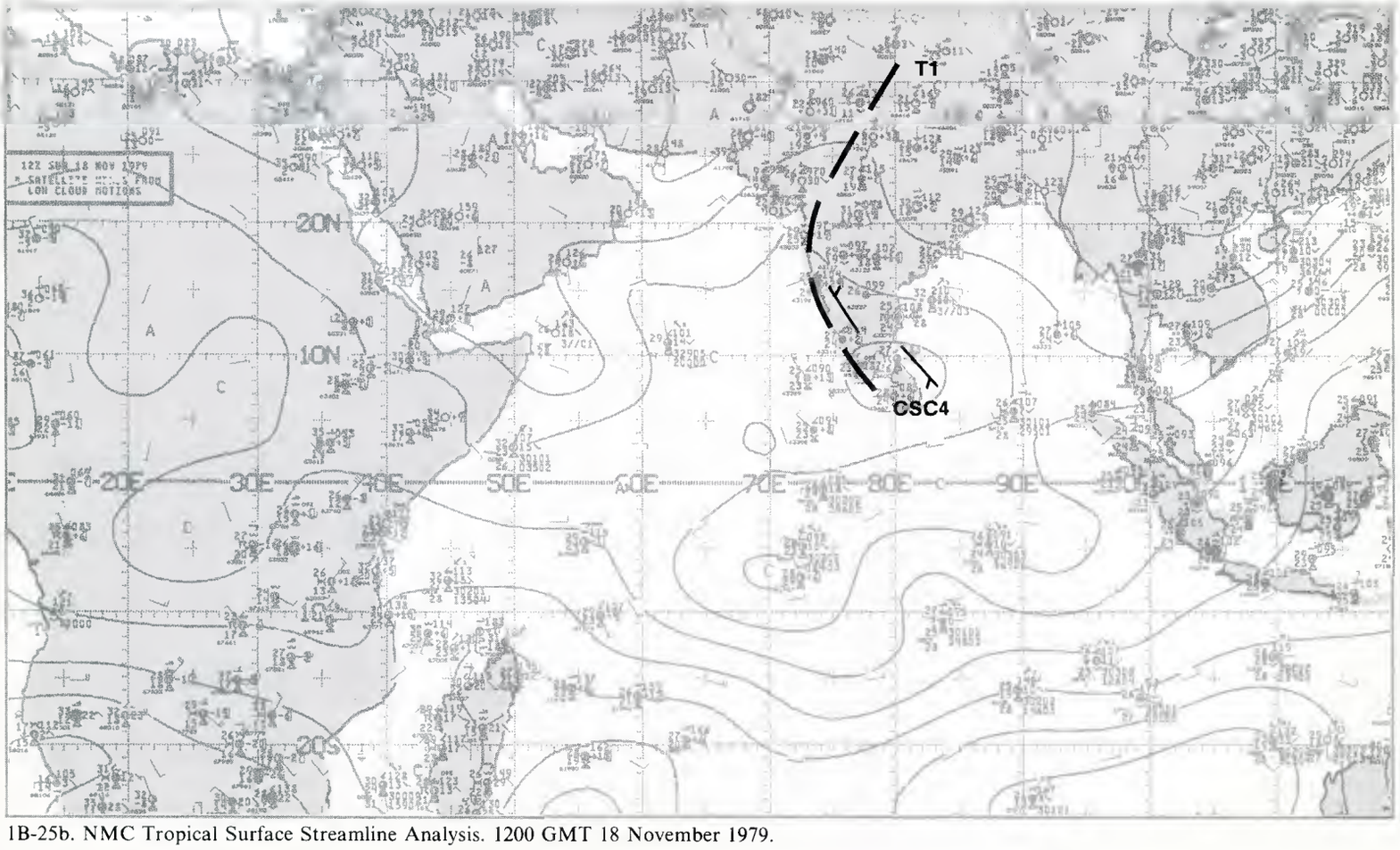

1B-25b. NMC Tropical Surface Streamline Analysis. 1200 GMT 18 November 1979.

Case 1 Arabian Sea/Bay of Bengal—Winter

Cold Air Outbreaks over the Northern Arabian Sea During the Winter Monsoon

The criteria for a region to be considered monsoonal is highly persistent winds from different directions in summer and winter (Ramage, 1971); however, it specifically excludes areas in which the seasonal wind shift only reflects the movement in the mean tracks of weather systems (cyclone–anticyclone alternations). This is not to say that fronts do not affect a monsoon region—cold fronts push into the northern Arabian Sea several times each winter (Brody, 1977).

There are two potential sources for cold air surges into the northern Arabian Sea—the Siberian polar anticyclone and polar air to the rear of disturbances moving from the Mediterranean. The cold air from the Siberian polar anticyclone is effectively cut off from the Arabian Sea by the Himalayas and the Zagros mountain ranges of Afghanistan and Iran. Polar troughs in the westerlies are forced to low latitudes when a block develops over northern Europe, and there is a split in the westerlies upstream of the block. Polar troughs in the southern branch of the split in the westerlies cross the Mediterranean into eastern Asia (Iran and Afghanistan). As the disturbances pass to the north of the Persian Gulf, cold air surges to the rear of the disturbances, penetrating southward over the Arabian Peninsula and the Persian Gulf into the northern Arabian Sea. The strongest and most persistent cold air surges occur from mid-December to early March.

References

Brody, L. R., 1977: Meteorological phenomena of the Arabian Sea. NAVENVPRED-RSCHFAC Applications Report 77-01. Monterey, CA.

Perrone, T. J., 1979: Winter shamal in the Perisan Gulf. NAVENVPREDRSCHFAC Technical Report TR 79-06. Naval Environmental Prediction Research Facility, Monterey, CA, 180 pp.

Ramage, C. S., 1971: Monsoon Meteorology. Academic Press, New York, 296 pp.

200 mb

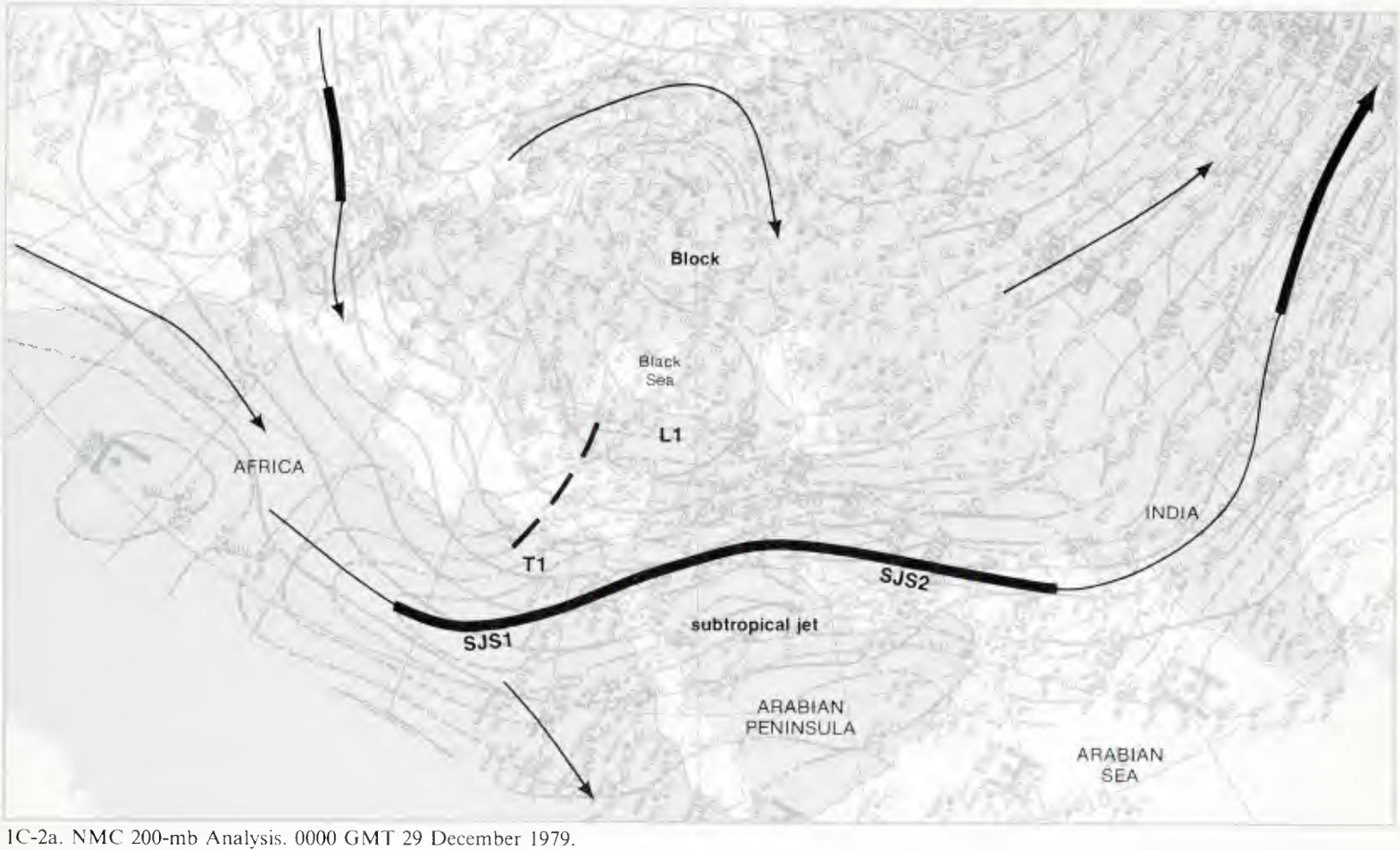

1C-2a. NMC 200-mb Analysis. 0000 GMT 29 December 1979.

500 mb

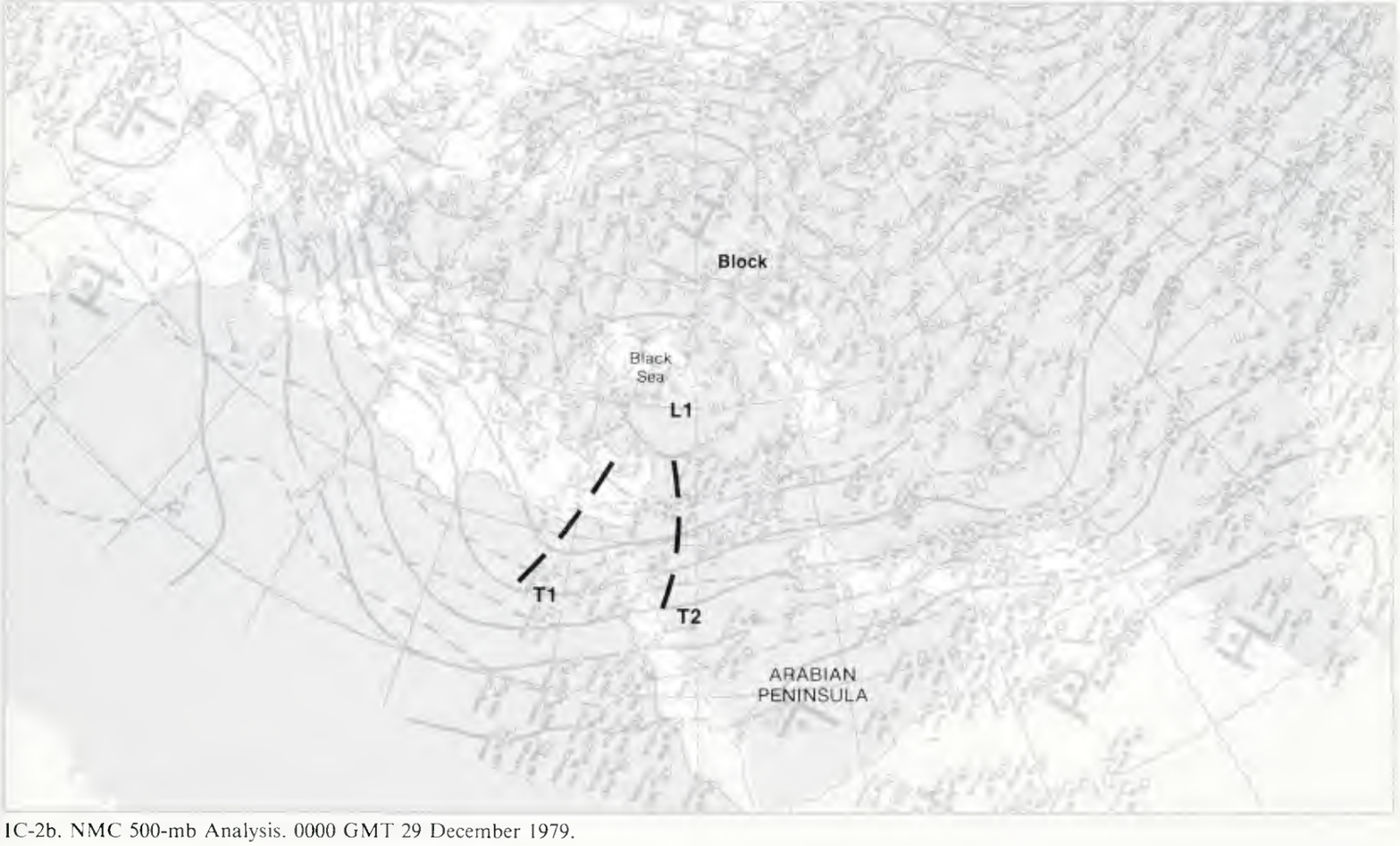

1C-2b. NMC 500-mb Analysis. 0000 GMT 29 December 1979.

Cold Air Outbreak Following the Passage of a Polar Trough
Gulf of Oman/Northern Arabian Sea
December 1979

29 December

The NMC 200-mb analysis (1C-2a), at 0000 GMT, shows a very strong, zonal, subtropical jet stream extending from north-central Africa, across the Arabian Peninsula and India, to China. Note the broad, anticyclonic turning (ridging) of the subtropical jet from Africa to the northern Arabian Sea—this is typical of the subtropical jet in this region when a deep polar trough upstream, such as the trough **T1**, has advanced to low latitudes. A characteristic feature of this subtropical jet is that the highest wind speeds, or jet streaks, **SJS1** (150 kt) and **SJS2** (150 kt) are located along the crest of the anticyclonic pattern. The 200-mb analysis also shows a blocking anticyclone over northern Europe, with a trapped low **L1** to the south over the Black Sea. To the west of the block, the westerlies split into two branches: a northern branch moving over the block and a southern branch merging with the subtropical jet flow in the vicinity of the deep polar trough **T1**.

A comparison of the location and circulation features of the block over northern Europe and the trapped low **L1** over the Black Sea on the 500-mb analysis (1C-2b) with their counterparts at 200 mb (1C-2a), reveals the nearly vertical structure of these systems. This indicates that they are persistent, slowly moving synoptic features. It is also important to note that the southern branch of the polar westerlies is a nearly continuous, high-speed band (closely-spaced height contour lines) extending from the eastern Atlantic southward around the base of the low **L1** and across the Arabian Peninsula. The deep polar trough **T1** and the minor trough **T2** are migratory disturbances embedded in this high-speed westerly current.

On the early morning DMSP visible picture (1C-3a), the appearance of numerous convective cloud lines over the northern Arabian Sea is typical of weak, undisturbed winter monsoon flow. These cloud lines have formed in the northeasterly flow around the eastern periphery of the winter surface anticyclone over the southern Arabian Peninsula and Iran/Pakistan (1C-3e). The lack of north/south oriented low-level cumulus cloud lines in the Persian Gulf similarly implies undisturbed conditions with no evidence of a shamal in progress. Over the northern Arabian Peninsula there is a cirrus shield that shows the distinct poleward edge characteristic of polar jet stream or merged polar/subtropical jet stream-associated cirrus.

An examination of the NMC 700-mb (1C-3c) and 500-mb (1C-2b) analyses shows that the cirrus is located in the southwesterly flow ahead of the troughs **T1** and **T2**. The density, smoothness, striations, and distinct poleward edge of the cirrus shield in the satellite picture (1C-3a) suggest that a disturbance to the west is generating the cirrus. On the 200-mb analysis (1C-2a) note that there is a subtropical jet streak **SJS1**, and at 300 mb (1C-3b) a merged subtropical/polar jet streak **SJS/PJS1** (140 kt) located in the southwesterly flow ahead of the deep polar trough **T1**. The disturbed area generating the cirrus observed on the satellite picture is located in the left front quadrant of the merged jet streaks **SJS/PJS1**—an area favorable for cyclogenesis. The surface analyses (1C-3d and 3e) show a weak low pressure area over the northern Arabian Peninsula, but no surface disturbance at this time. The disturbance suggested by the satellite picture, therefore, appears to be an upper-level development.

The late afternoon DMSP infrared picture (1C-5a) shows that the cloudiness (see 1C-3a) over the northern Arabian Peninsula has evolved into a well-defined, comma cloud pattern characteristic of a short-wave development. The comma head shows a solid overcast of middle and high clouds and a distinct western edge. The eastern edge is irregular and is feathered with plumes of convective debris. The comma tail does not show the typical solid cloud band defining a surface frontal zone trailing to the southwest; however, lines of globular cloudiness indicate convective activity is occurring along the comma tail. The axis of the merged subtropical/polar jet **SJS/PJS1** is located just poleward of the northern edge of the transverse band of cirrus extending across the central Arabian Peninsula.

The enhanced convective activity observed on the satellite picture is confirmed by surface reports. On the 1200 GMT surface analysis (1C-5d), a few hours prior to the satellite picture time, Basra, Iraq **O1** reports cumulonimbus and a thunderstorm in progress. There are other reports of convective activity and precipitation northwest of Basra. Although there is no surface disturbance indicated, winds show a definite tendency to turn cyclonically to the northwest of Basra. Note that the surface streamline analysis (1C-5e), close to the picture time, shows a cyclonic circulation **C1** to the west of Basra **O1**, with reports of precipitation in the area. The low-level cyclonic circulation is bringing warm, moist air northward (note 100% relative humidity at Basra and high humidities at stations to the south) so that continued convective activity can be expected.

An examination of the flow pattern over the northern Arabian Peninsula on the 700-mb (1C-5c), 500-mb (1C-4b), and 300-mb (1C-5b) analyses indicates that the comma cloud has developed in the southwesterly flow ahead of the deep polar trough **T1** and in the left front quadrant of the merged subtropical/polar jet streaks **SJS/PJS1**. This trough has moved rapidly eastward in the southern branch of the westerlies associated with the block over northern Europe and the trapped low **L1** to the south of the block. A new polar trough **T3** is also observed in the westerlies over central Africa (1C-4b). The merged **SJS/PJS1** at 300 mb has advanced eastward and maintained its intensity, where the subtropical jet streak **SJS1** has weakened from 150 kt (1C-2a) to 130 kt (1C-4a) and retrograded westward. This confirms that the comma cloud development is associated with the merged subtropical/polar jet streaks **SJS/PJS1** at 300 mb. The appearance of the polar jet streak **PJS3** to

29 December continued on page 1C-5

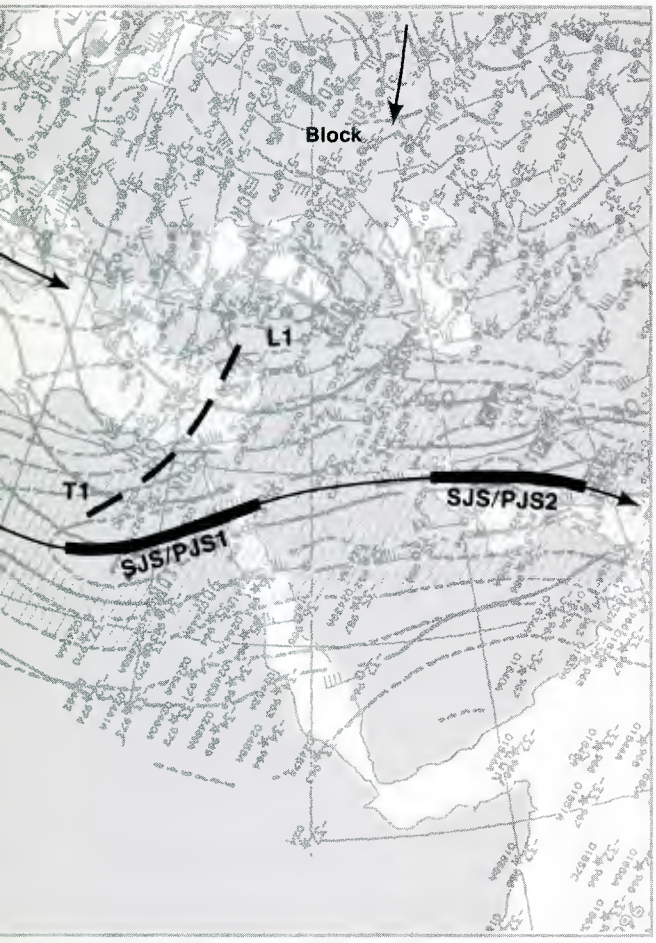

NMC 300-mb Analysis. 0000 GMT 29 December 1979.

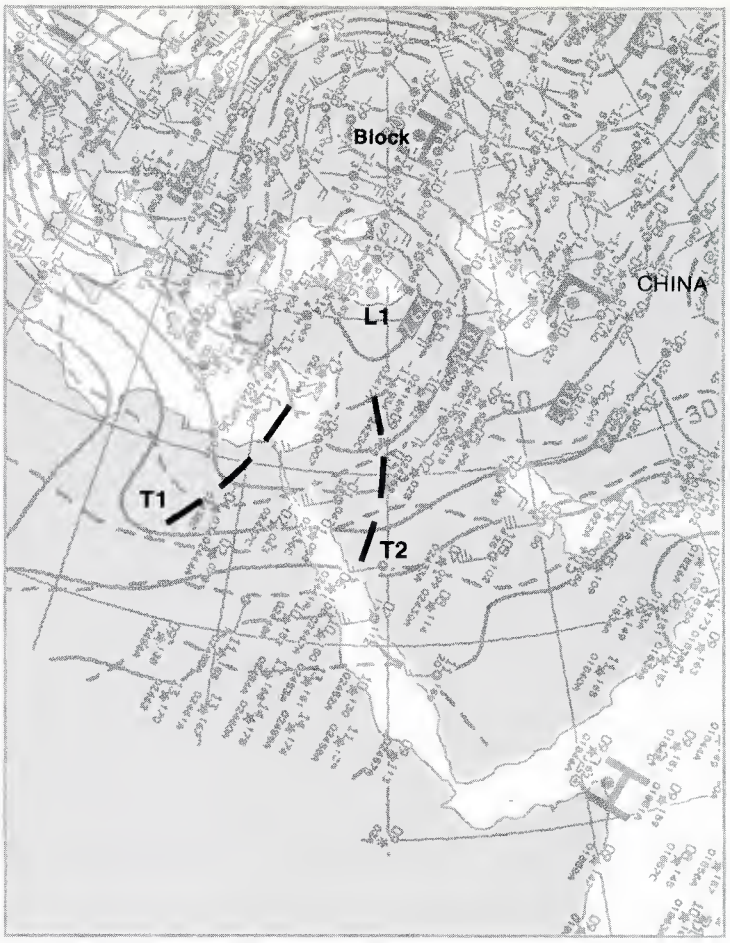

1C-3c. NMC 700-mb Analysis. 0000 GMT 29 December 1979.

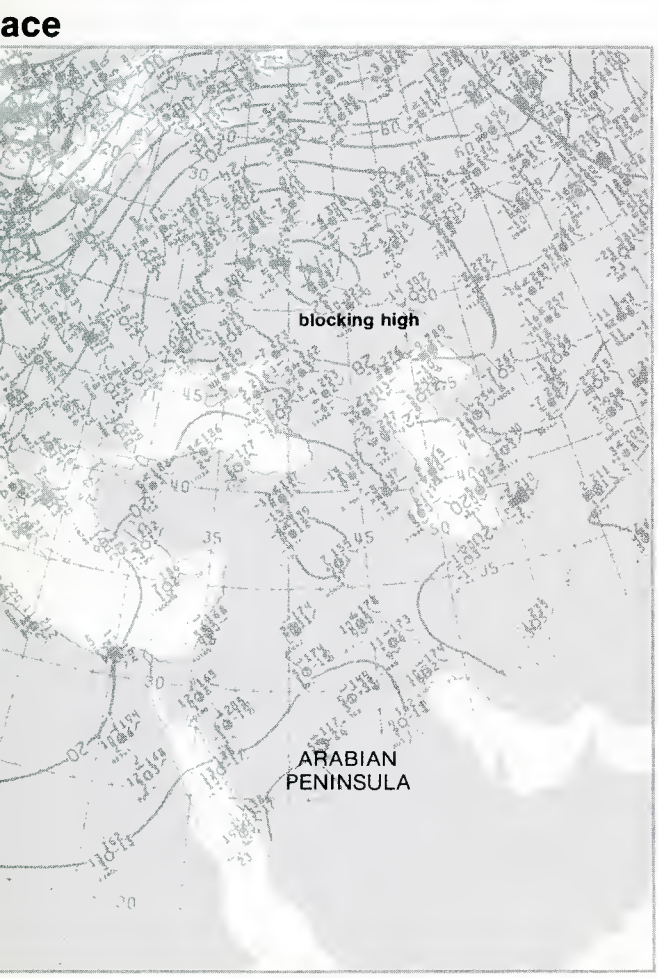

NMC Surface Analysis. 0000 GMT 29 December 1979.

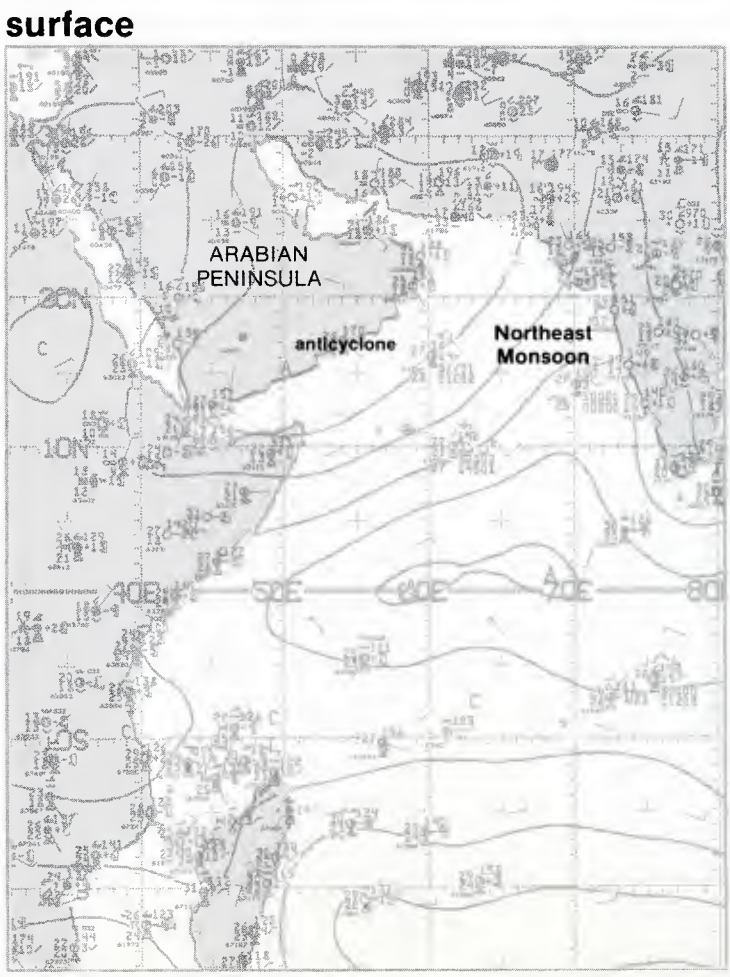

1C-3e. NMC Tropical Surface Streamline Analysis. 0600 GMT 29 Dec 1979.

1C-3a. F-2. DMSP LF Normal Enhancement. 0527 GMT 29 December 1979.

200 mb

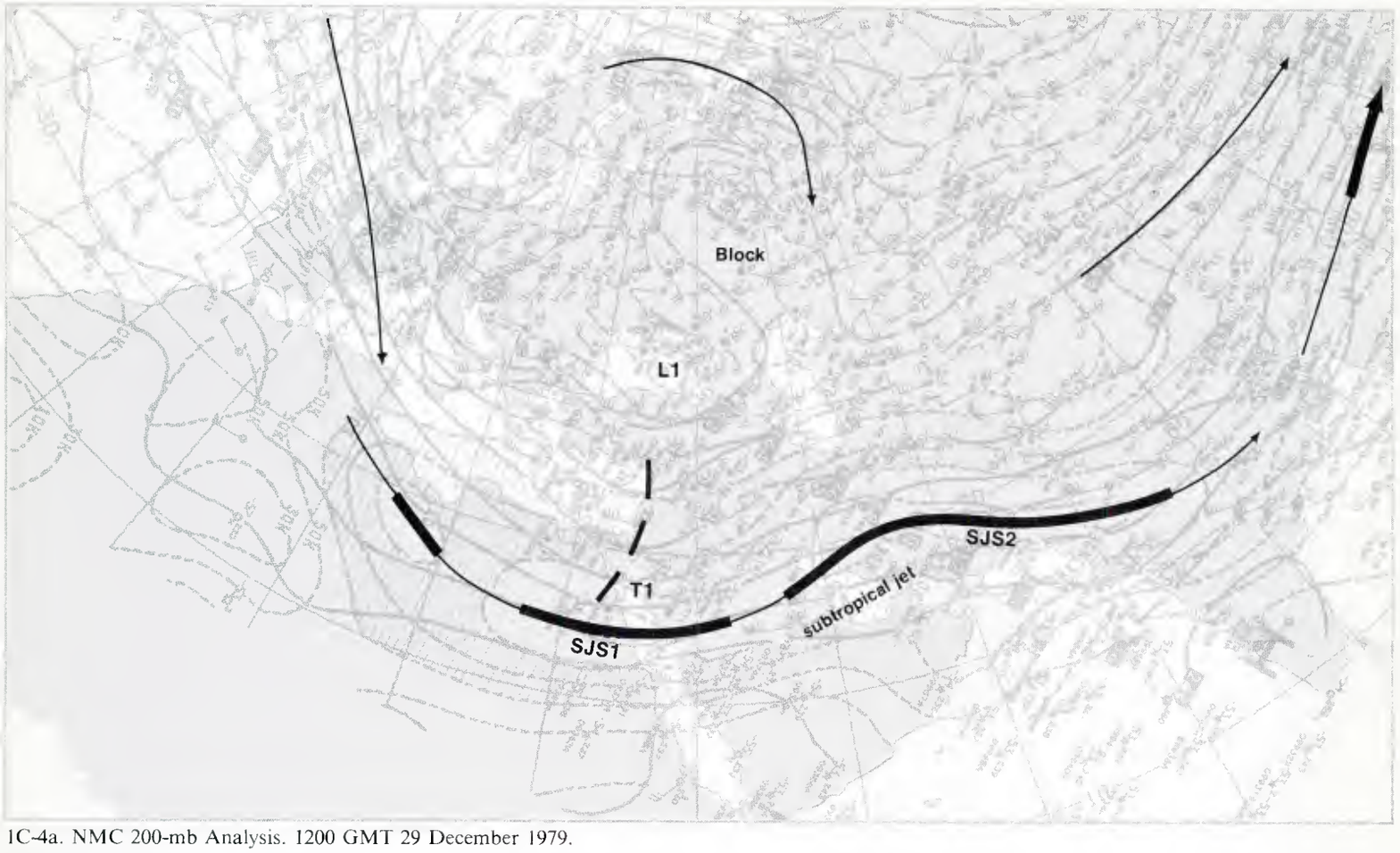

1C-4a. NMC 200-mb Analysis. 1200 GMT 29 December 1979.

500 mb

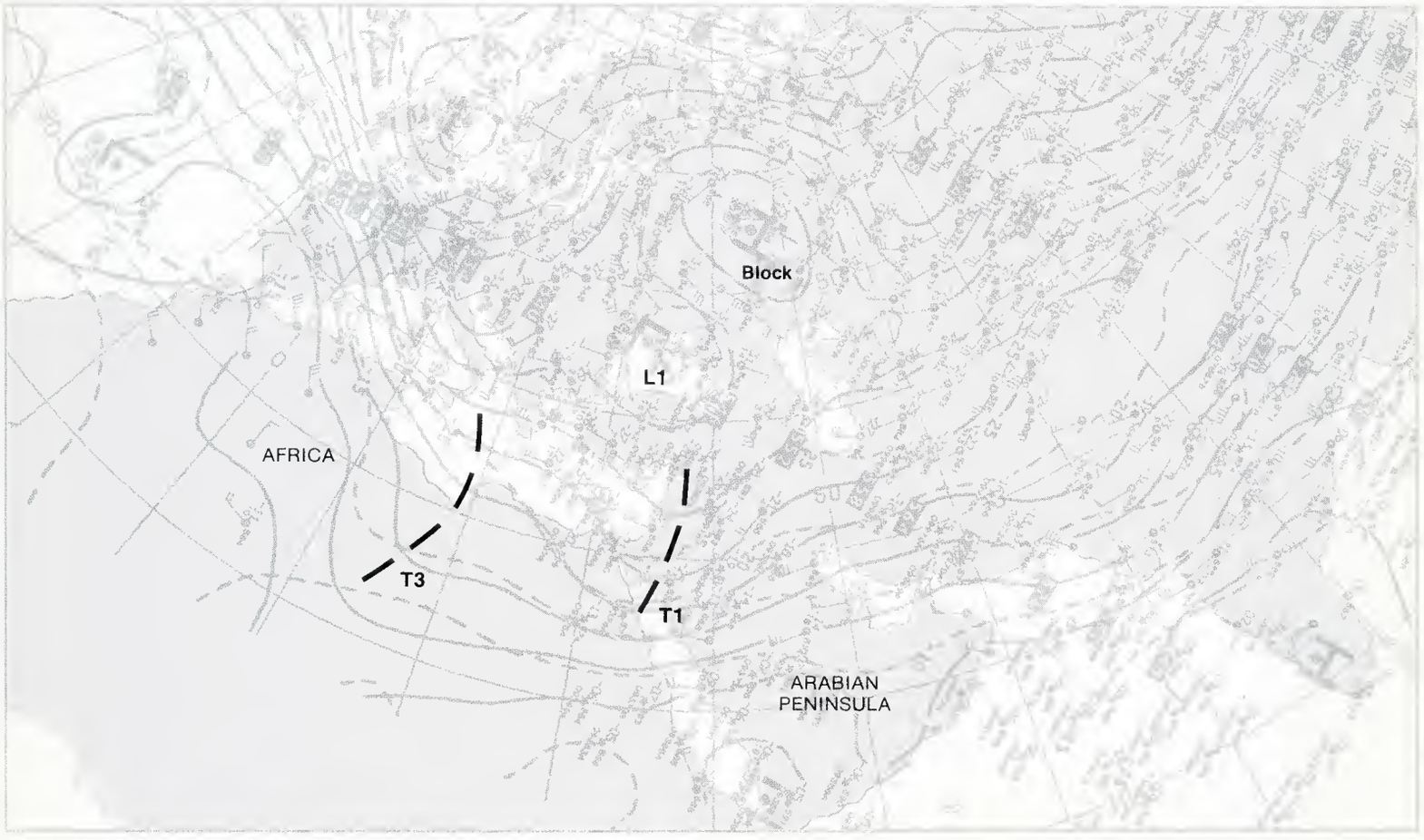

1C-4b. NMC 500-mb Analysis. 1200 GMT 29 December 1979.

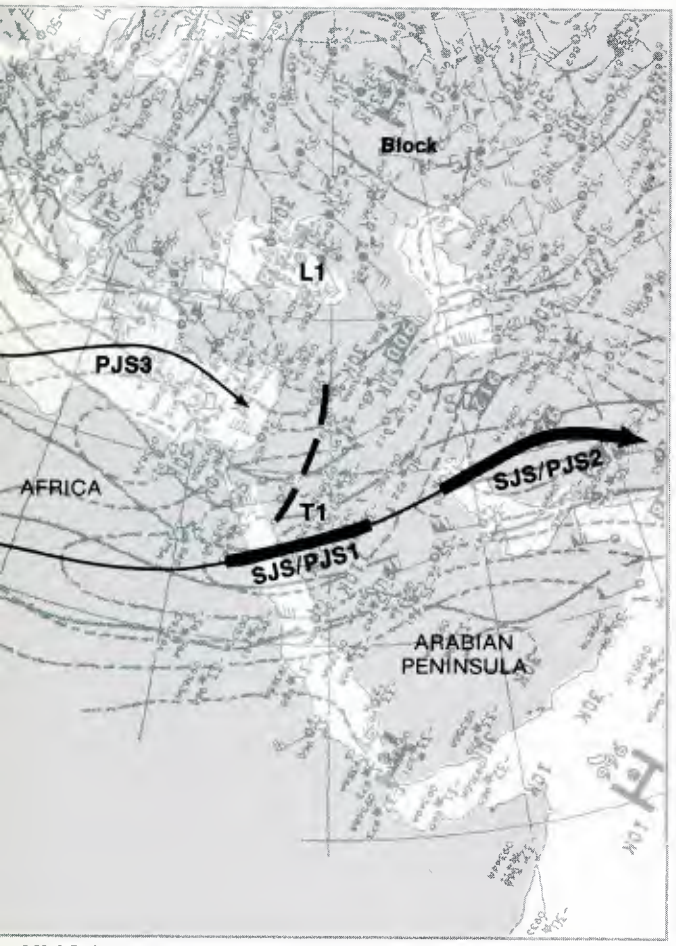

b. NMC 300-mb Analysis. 1200 GMT 29 December 1979.

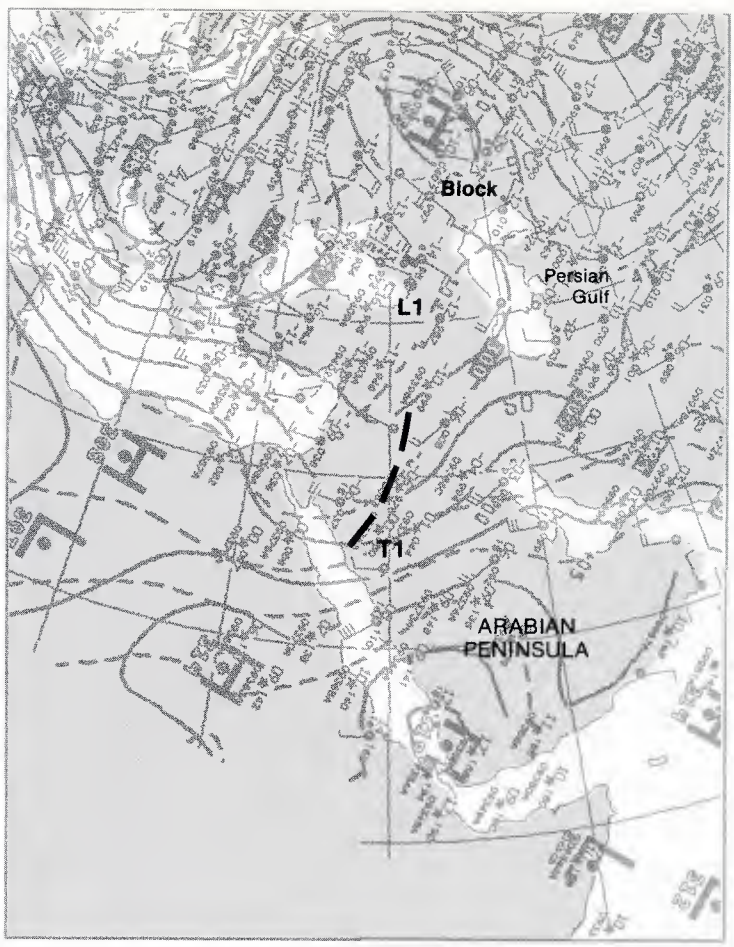

1C-5c. NMC 700-mb Analysis. 1200 GMT 29 December 1979.

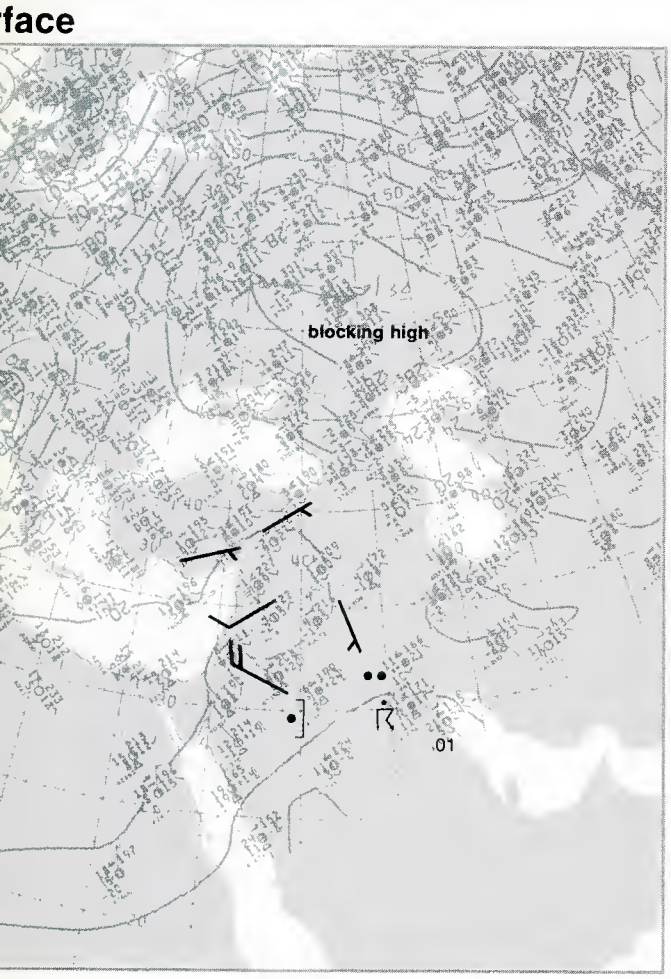

l. NMC Surface Analysis. 1200 GMT 29 December 1979.

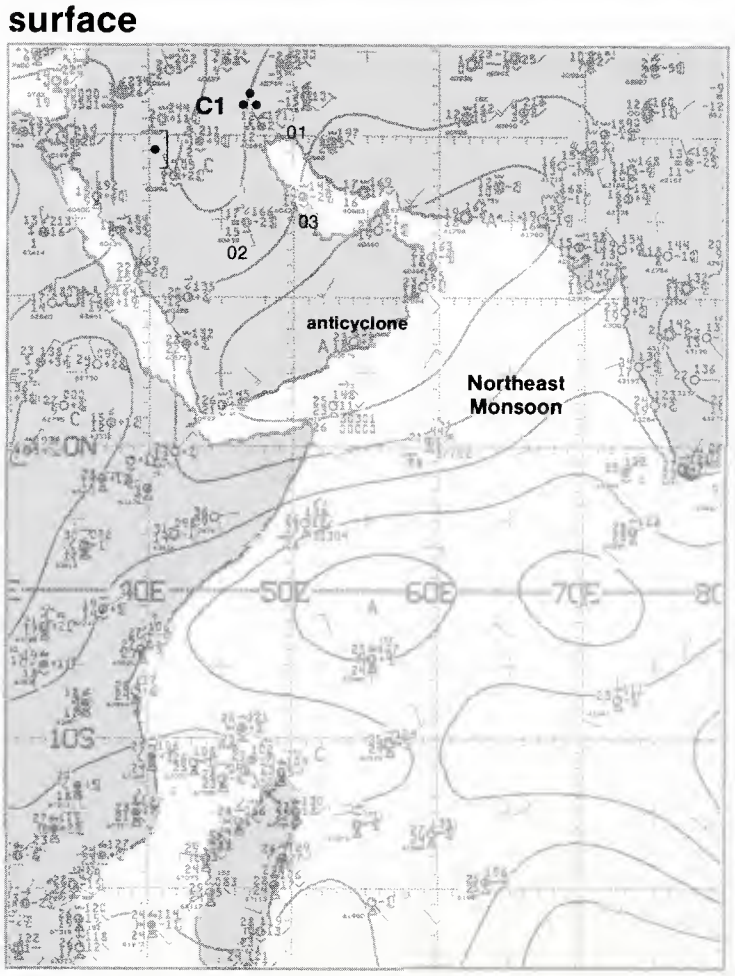

1C-5e. NMC Tropical Surface Streamline Analysis. 1800 GMT 29 Dec 1979.

the northwest of the comma cloud, however, is not favorable for further storm intensification. The cold air surge advected into the southwest quadrant of the comma cloud by **SJS/PJS1**, which is necessary for the continued development of the comma cloud, will be disrupted by the cold air surge associated with **PJS3** coming into the comma head from the northwest.

29 December continued on page 1C-6

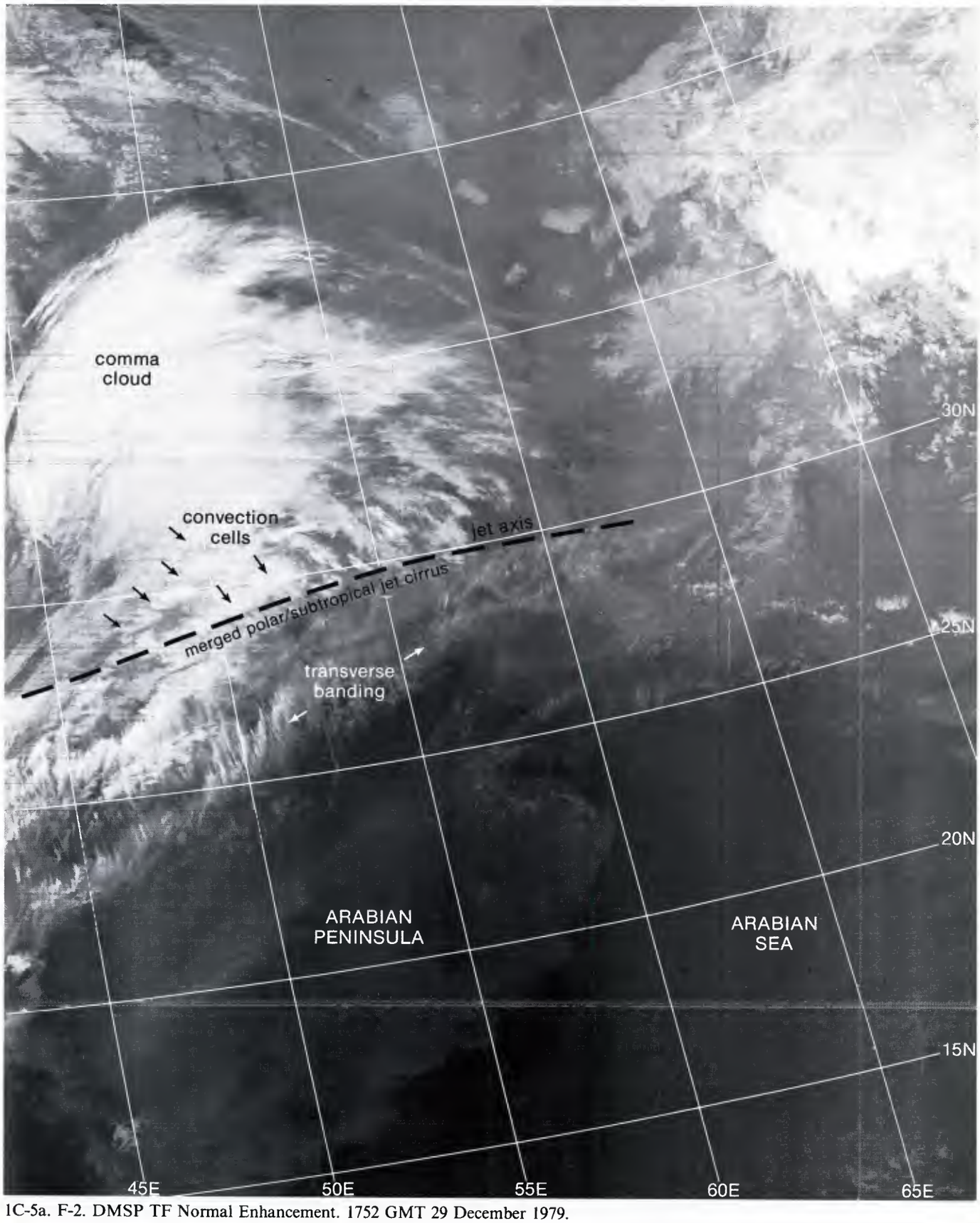

1C-5a. F-2. DMSP TF Normal Enhancement. 1752 GMT 29 December 1979.

The FNOC PE initial 500-mb analysis for 1200 GMT (1C-6a), provides a clear depiction of the large-scale circulation features observed on the corresponding NMC 500-mb analysis (1C-4b): the block over northern Europe, the split in the westerlies upstream with the southern branch passing to the south of the trapped low **L1**, and the deep polar trough **T1** moving eastward in the southern branch of the westerlies. The comma cloud pattern (1C-5a) has developed in the southwesterly flow ahead of the trough **T1**. The southwesterly flow is also responsible, in part, for the buildup of the ridge to the east over Iran (compare with 1C-2b).

The FNOC PE 36-hr 500-mb prognosis (1C-7a), based on the initial 500-mb analysis (1C-6a) shows that the block over northern Europe will move slowly eastward, with the trapped low **L1** to the south persisting and moving from the Black Sea to the vicinity of the Caspian Sea. Although strong westerlies (closely-spaced height contour lines) are forecast over western Europe, both northern and southern branches of the split flow in the westerlies upstream of the block will weaken considerably (more widely-spaced height contour lines). Note that the polar trough **T1** is forecast to advance rapidly eastward and weaken considerably.

continued on page 1C-8

500 mb

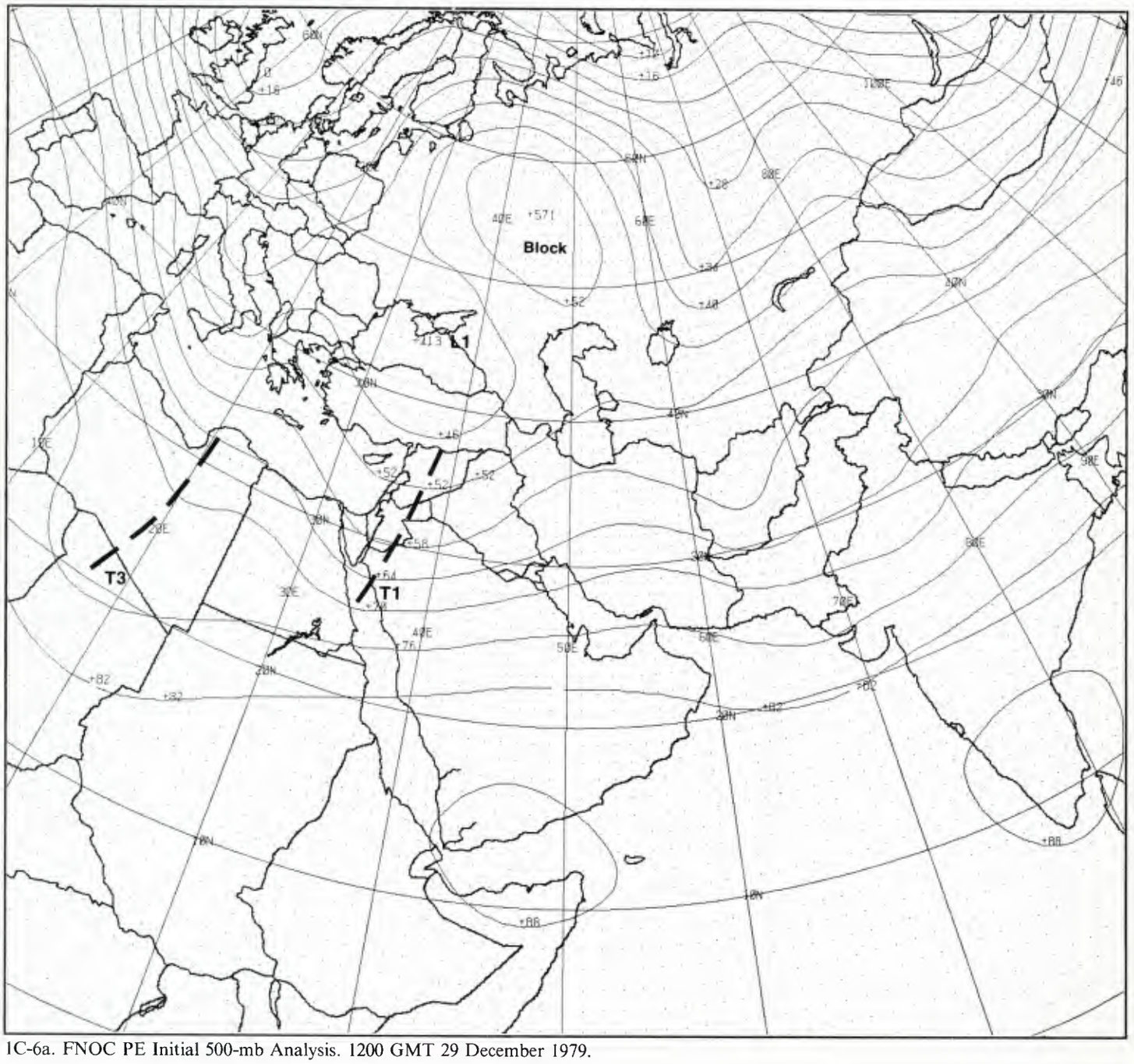

1C-6a. FNOC PE Initial 500-mb Analysis. 1200 GMT 29 December 1979.

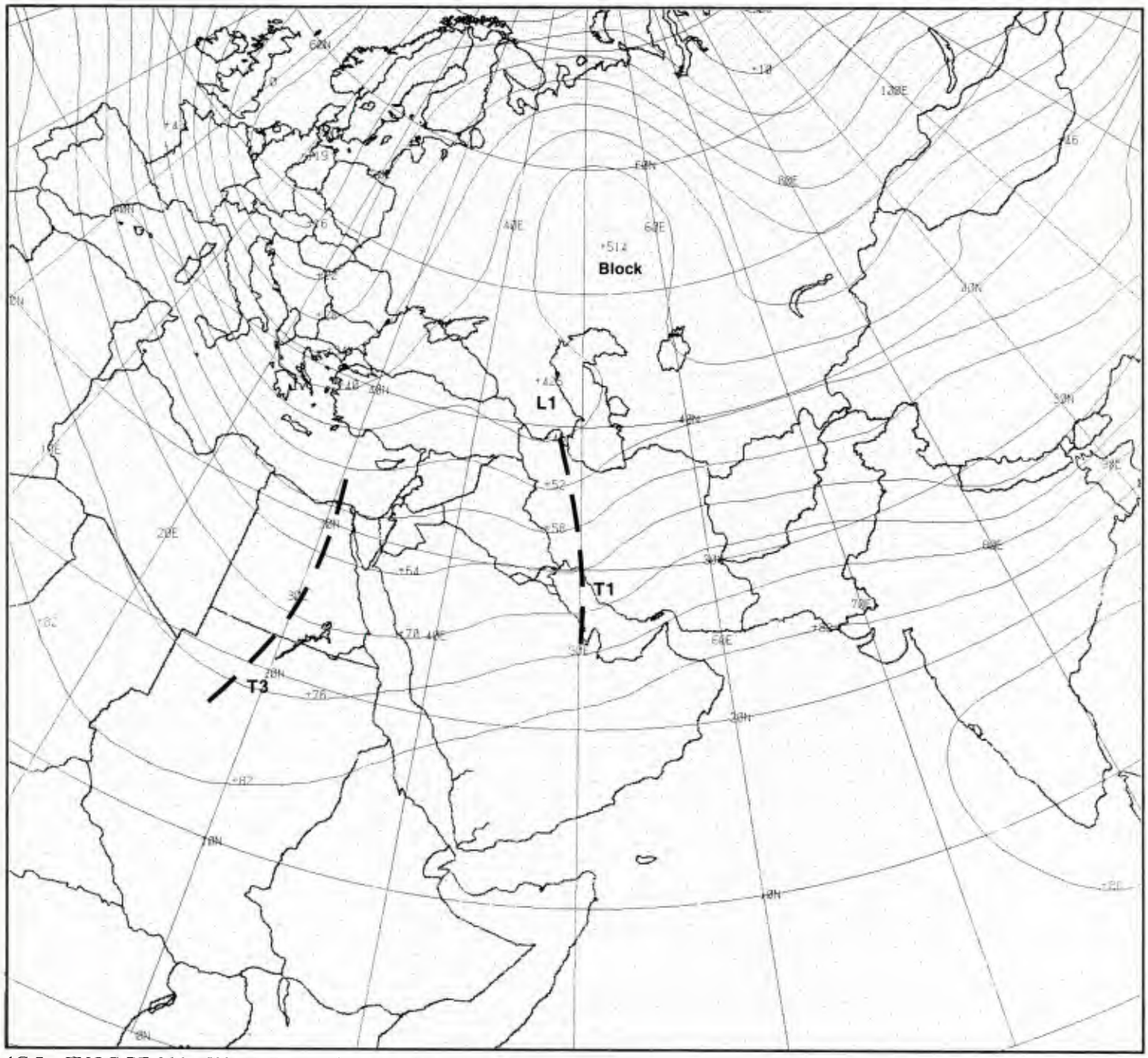

1C-7a. FNOC PE 36-hr 500-mb Prognosis. Valid 0000 GMT 31 December 1979.

200 mb

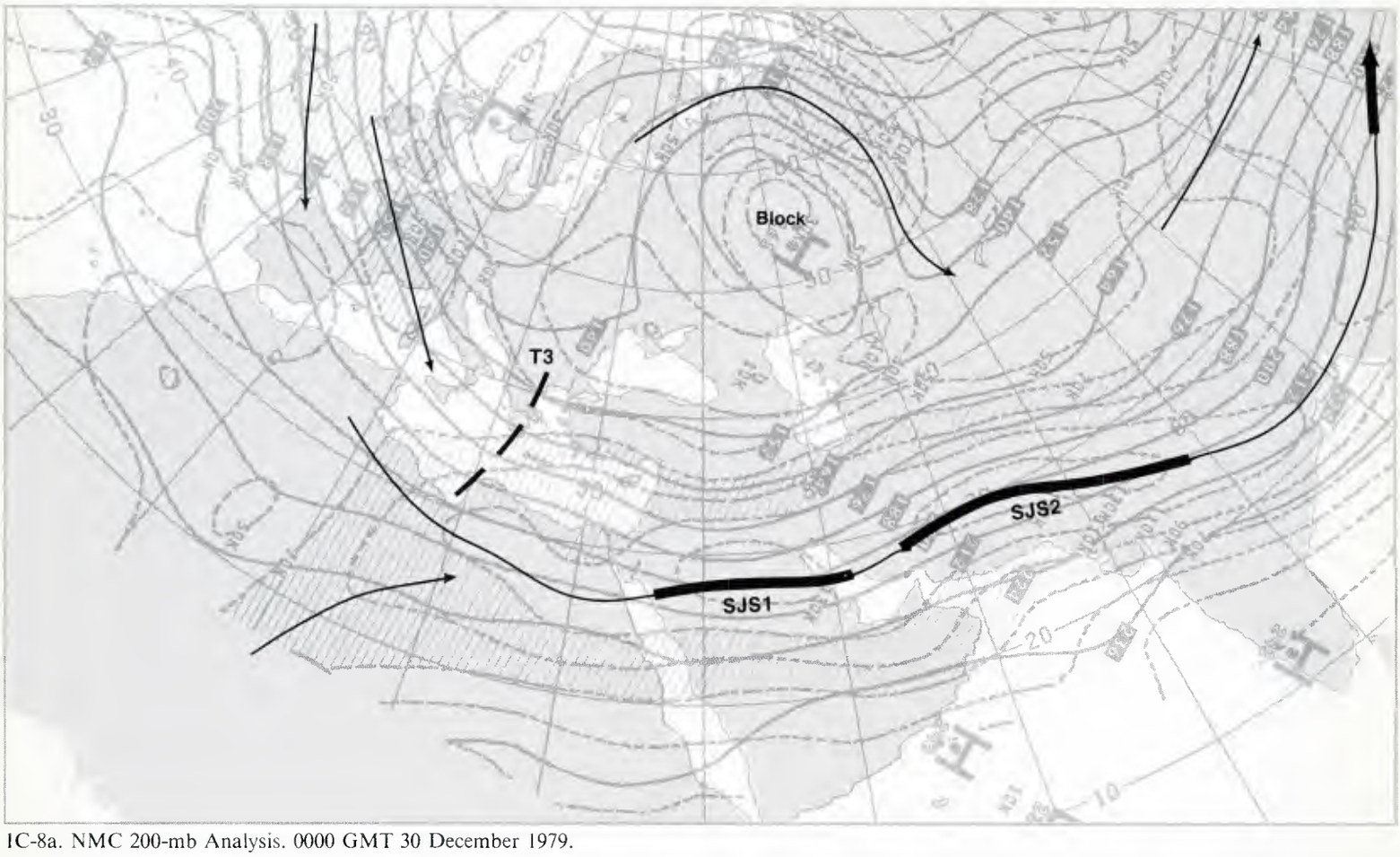

1C-8a. NMC 200-mb Analysis. 0000 GMT 30 December 1979.

500 mb

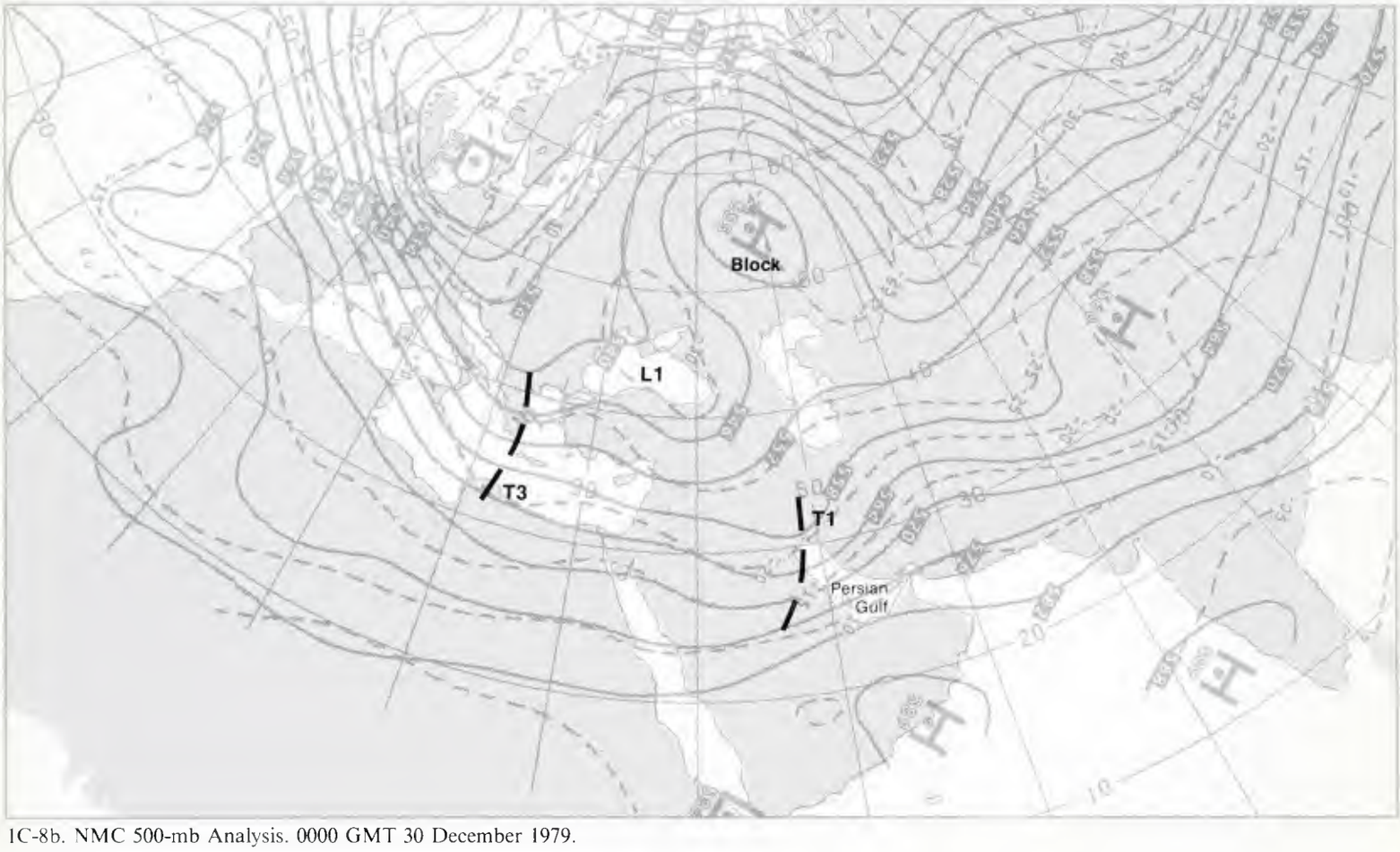

1C-8b. NMC 500-mb Analysis. 0000 GMT 30 December 1979.

30 December

The early morning DMSP visible picture (1C-9a) reveals that the comma cloud (1C-5a) did not continue to intensify—only a large cirrus arch cloud pattern over eastern Iran identifies the remains of the comma cloud pattern. The lack of further development is due to the disruption of the low-level circulation by the mountainous terrain (Zagros Mountains) of central Iran. Considerable moisture is present, however, since convective clouds are observed along the southern border of the cirrus arch cloud.

More important to the lack of intensification of the comma cloud is the appearance of the cirrus band over the southern Caspian Sea (note the pronounced shadow line along the poleward boundary of the cirrus band). This cirrus band indicates the location of the remnants of the polar jet streak **PJS3** (1C-5b) which advanced across the head of the comma cloud, causing it to shear out. The 300-mb analysis (1C-9b) does not show **PJS3**; however, note that the westerlies across the northern Persian Gulf connect with the westerlies over western Europe. On the previous 300-mb analysis (1C-5b), the westerlies approached the northern Persian Gulf from the southwest over Africa.

The persistence of the strong block at mid to upper levels over northern Europe (700 mb, 1C-9c; 500 mb, 1C-8b; and 300 mb, 1C-9b) continues to produce the split in the polar westerlies upstream, which maintains the southern branch of the westerlies from the eastern Atlantic to the Persian Gulf. The trough **T1** is moving rapidly eastward in this southern branch and, at 500 mb (1C-8b), the trough **T1** is located over the northern Persian Gulf. On the satellite picture (1C-9a), the approximate position of the trough **T1** is shown where it crosses the comma tail. At 200 mb (1C-8a), the subtropical jet streaks **SJS1** and **SJS2** have advanced eastward, and a new polar surge is moving toward the subtropical jet flow behind the polar trough **T3**.

The surface analysis (1C-9d) shows a closed isobar circulation center **C2**; however, an examination of the satellite picture (1C-9a) places the surface low at the more likely position—near the inflection point along the northern boundary of the cirrus arch over Iran. This position is marked as **C1** on the surface analysis, an area showing no surface reports for confirmation.

On the satellite picture (1C-9a), the cloud band extending across the central Persian Gulf identifies the comma tail associated with the cirrus arch over Iran. When the location of the comma tail is superimposed on the surface streamline analysis (1C-9e), it separates a region (reports **O1**, **O2**, and **O3**) of lower surface temperatures and strong northwesterly winds to the north from tropical air and southerly winds **O4** to the south, indicating cold frontogenesis in the region. Precipitation is occurring at **O4**, below the convective clouds indicated on the satellite picture just to the east of the central Persian Gulf. On the satellite picture, convective cloud lines over the northern Persian Gulf, which are typical of cold air outflow over a warmer sea surface, confirm the northerly flow and a cold air outbreak associated with shamal conditions extending down the central Persian Gulf. Although a cold front is not depicted on the surface analysis, it is not uncommon to observe the characteristic cold frontal effects (wind shift, precipitation, and temperature drop) during the passage of a comma tail associated with a comma cloud system (sheared-out comma cloud in this example).

31 December

The 500-mb analysis (1C-10b) shows the block over the eastern U.S.S.R., as forecast (1C-7a), with the open trough-trapped low **L1** near the Caspian Sea. The southern branch of the westerlies to the south of the block appears to be intact, and the polar trough **T1** has weakened and moved over Afghanistan. The polar trough **T1** cannot be detected at 300 mb (1C-11b) and is only weakly indicated on the 700-mb (1C-11c) analysis. At 200 mb (1C-10a), the deep polar low **L2** over northern Europe shows a strong polar jet, which has replaced the western portion of the southern branch of the westerlies associated with the block over eastern Russia. A strong subtropical jet has also formed over the northern Arabian Peninsula, and the polar jet over northern Europe appears on a track parallel to the subtropical jet instead of on a merging course, as noted on 29 December (1C-2a and 4a).

On the early morning DMSP visible picture (1C-11a), the solid overcast over northern Afghanistan and Pakistan is the location of the comma cloud system which had developed over the northern Arabian Peninsula about 34 hours earlier (1C-5a). The upper-level trough **T1** in which the disturbance formed has weakened considerably; however, the surface streamline analysis (1C-11e) shows a closed circulation center **C1**. Unfortunately, the NMC surface analysis (1C-11d) does not extend far enough to the south to confirm a surface low. There are no showers reported in the vicinity of the low center **C1** on the surface streamline analysis (1C-11e), but some buildups in the overcast on the satellite picture suggest precipitation in the area, although fog and low stratus predominate in this early morning pass.

Of particular significance on the satellite picture (1C-11a) is the evidence that the comma tail has moved from the central Persian Gulf (1C-9a), past the Gulf of Oman, into the northern Arabian Sea. Cold air advection cloud lines now extend into the southern Persian Gulf, indicative of a shamal in progress. This cold air outbreak followed the movement of the upper-level trough **T1** across the northern Persian Gulf. This southward advance is confirmed on the surface streamline analysis (1C-11e). Surface reports show strong northwesterly winds along the length of the Persian Gulf. Lower surface temperatures are reported along the coastal stations and over the central Arabian Peninsula (compare with 1C-9e). The typical winter surface anticyclone has also been reestablished over the central Arabian Peninsula (1C-11e), with its characteristic strong northeast winds **O5** over the southern Arabian Peninsula generating raised dust at **O6**. The cold air outbreak is short-lived, however, since the upper-level polar trough **T1** weakened as it moved across the northern Persian Gulf, minimizing the effect of the cold air advection following the trough. The coming end of this shamal event is signalled in the satellite data (1C-11a) by the formation of a convergence cloud line in the Gulf of Oman. Perrone (1979) first documented the formation of this cloud line as being a reliable indicator of the ending of shamal conditions in the Persian Gulf.

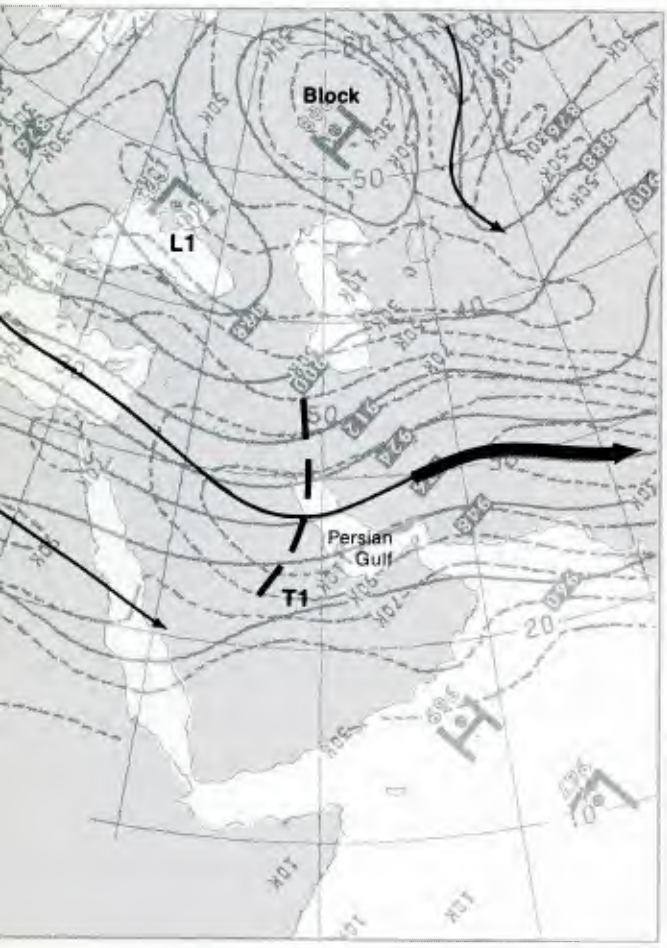

. NMC 300-mb Analysis. 0000 GMT 30 December 1979.

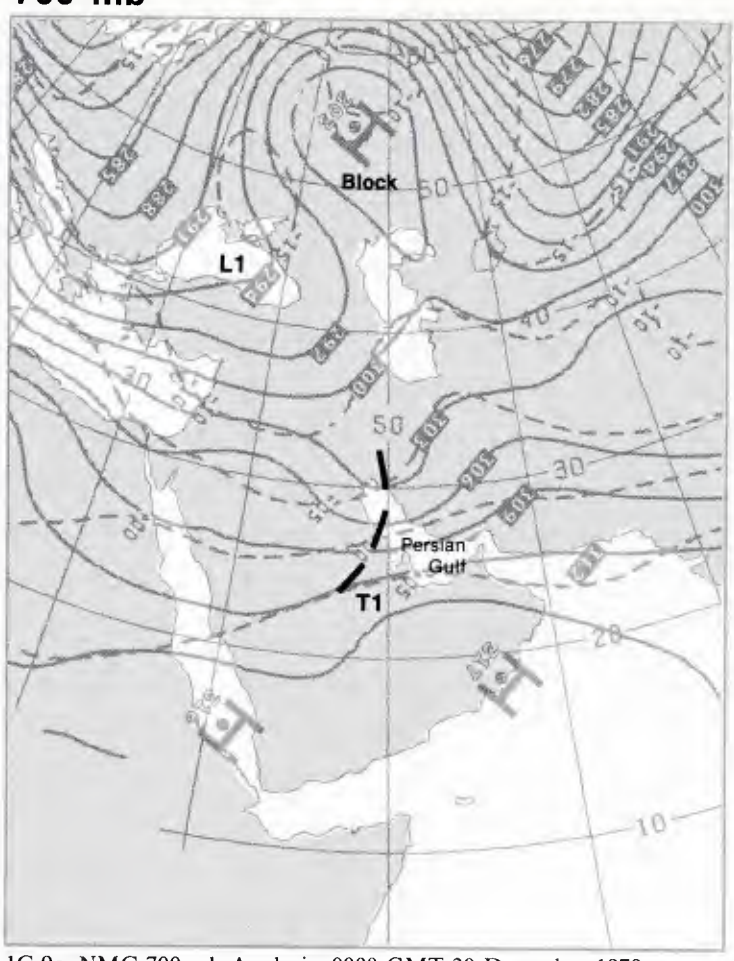

1C-9c. NMC 700-mb Analysis. 0000 GMT 30 December 1979.

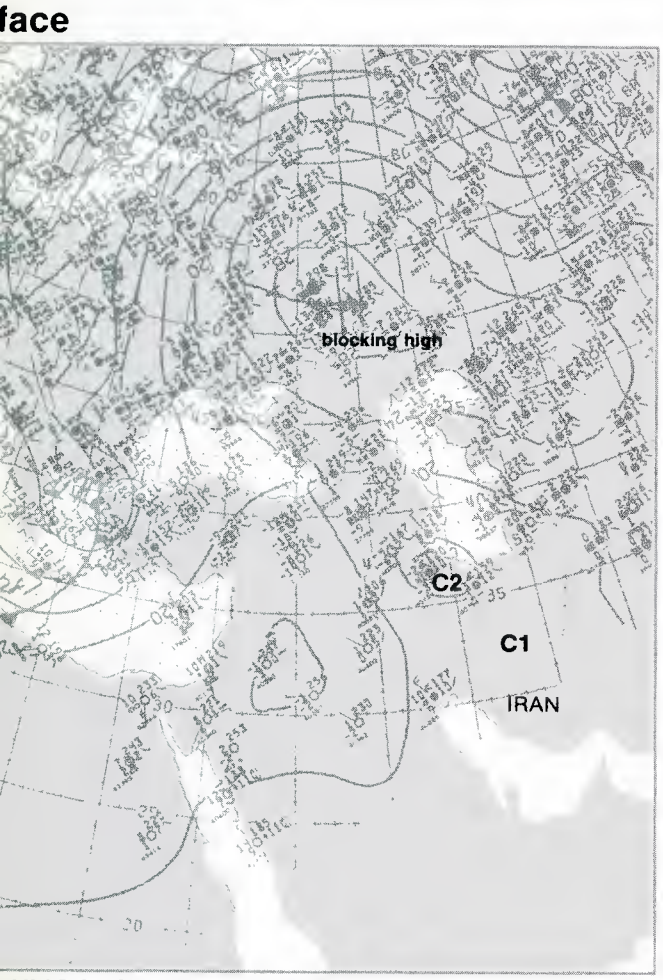

NMC Surface Analysis. 0000 GMT 30 December 1979.

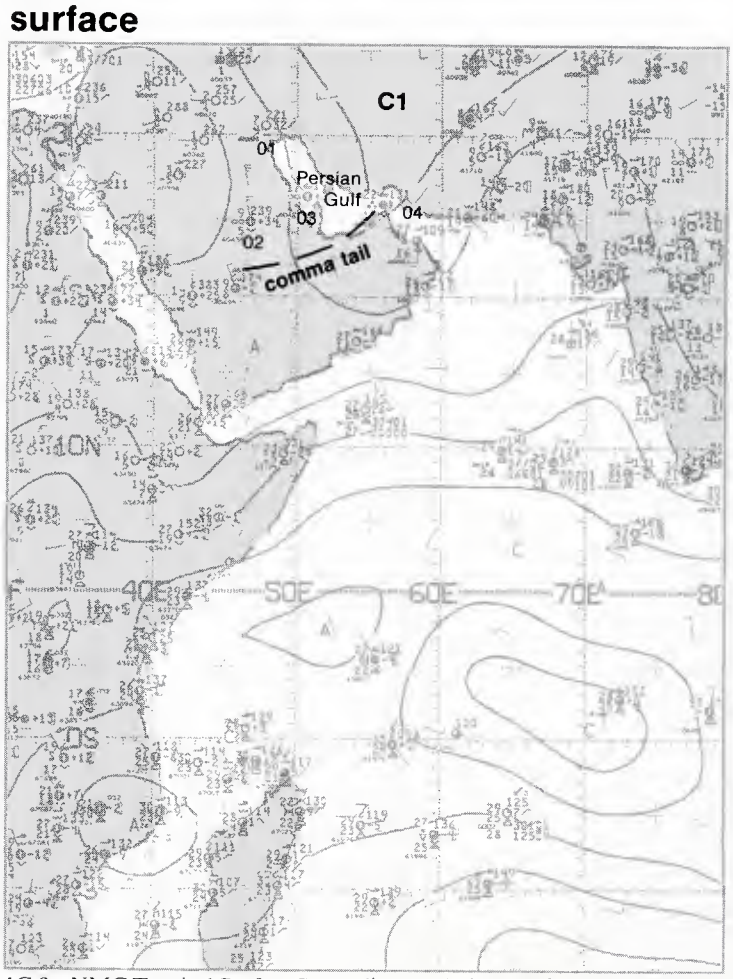

1C-9e. NMC Tropical Surface Streamline Analysis. 0600 GMT 30 Dec 1979.

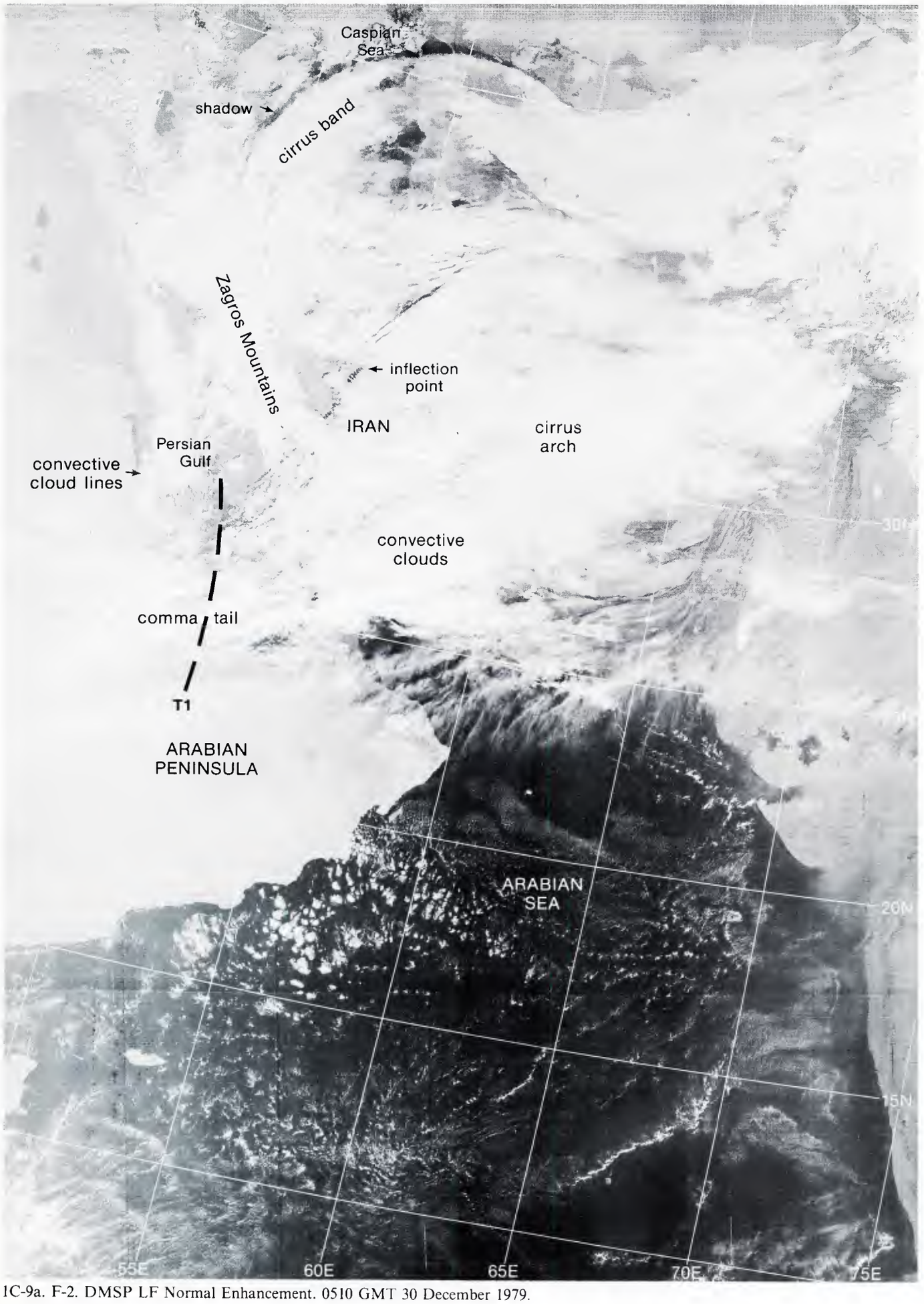

1C-9a. F-2. DMSP LF Normal Enhancement. 0510 GMT 30 December 1979.

200 mb

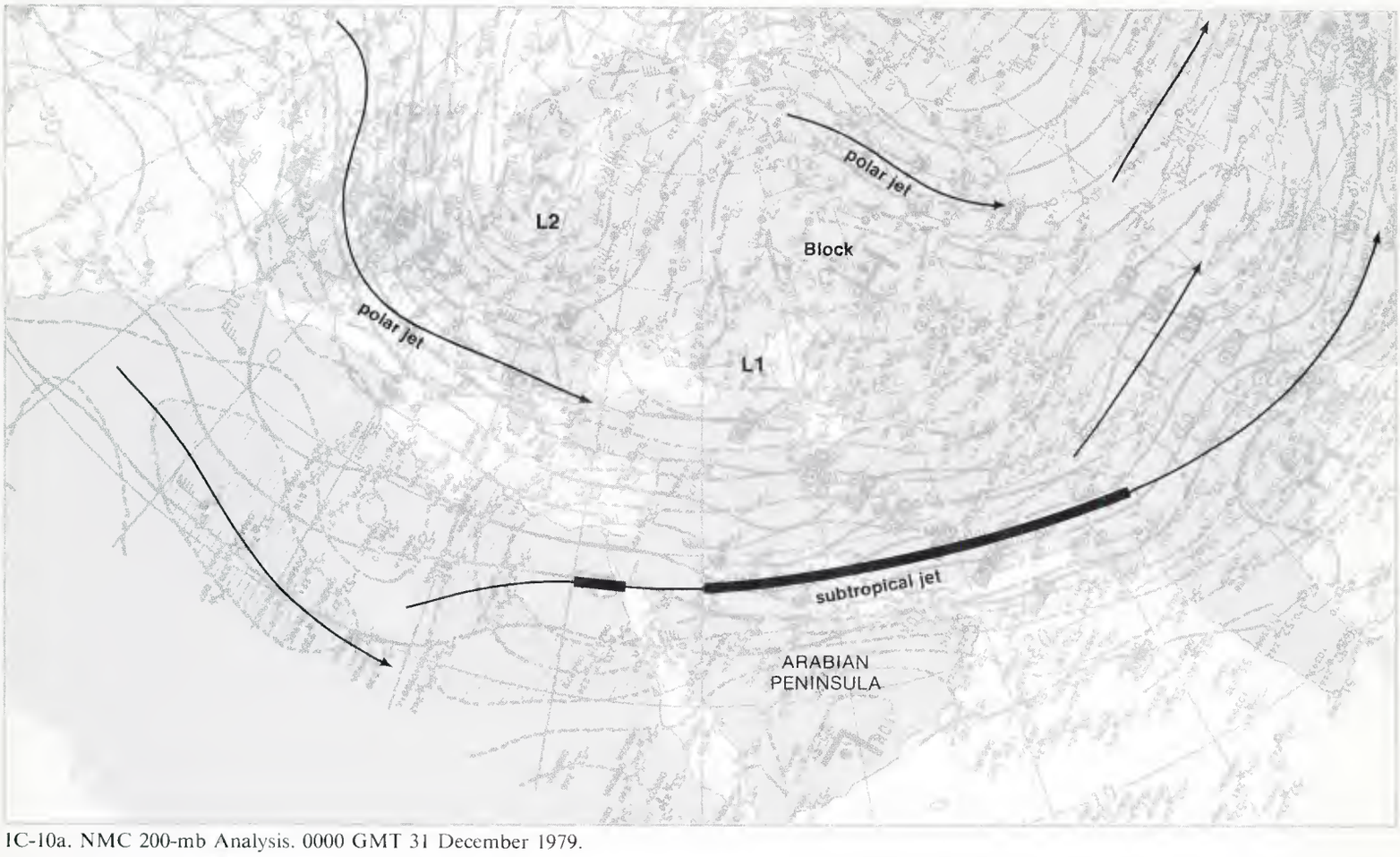

1C-10a. NMC 200-mb Analysis. 0000 GMT 31 December 1979.

500 mb

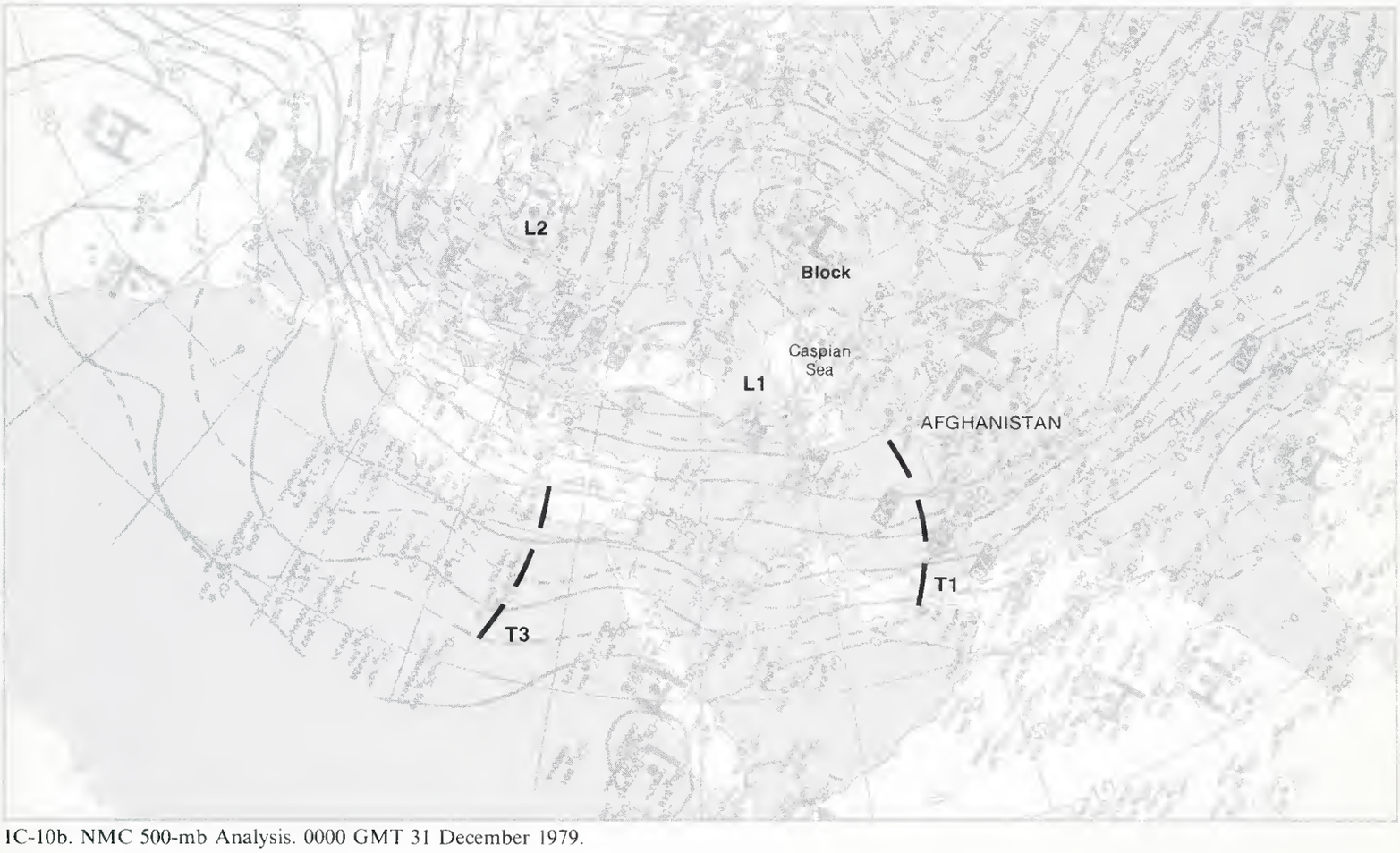

1C-10b. NMC 500-mb Analysis. 0000 GMT 31 December 1979.

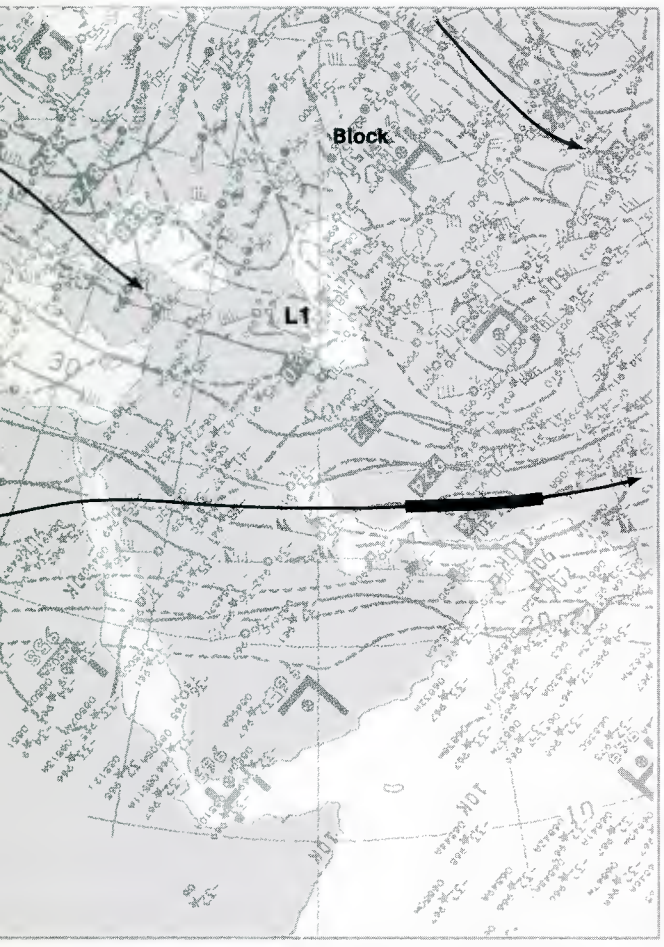

b. NMC 300-mb Analysis. 0000 GMT 31 December 1979.

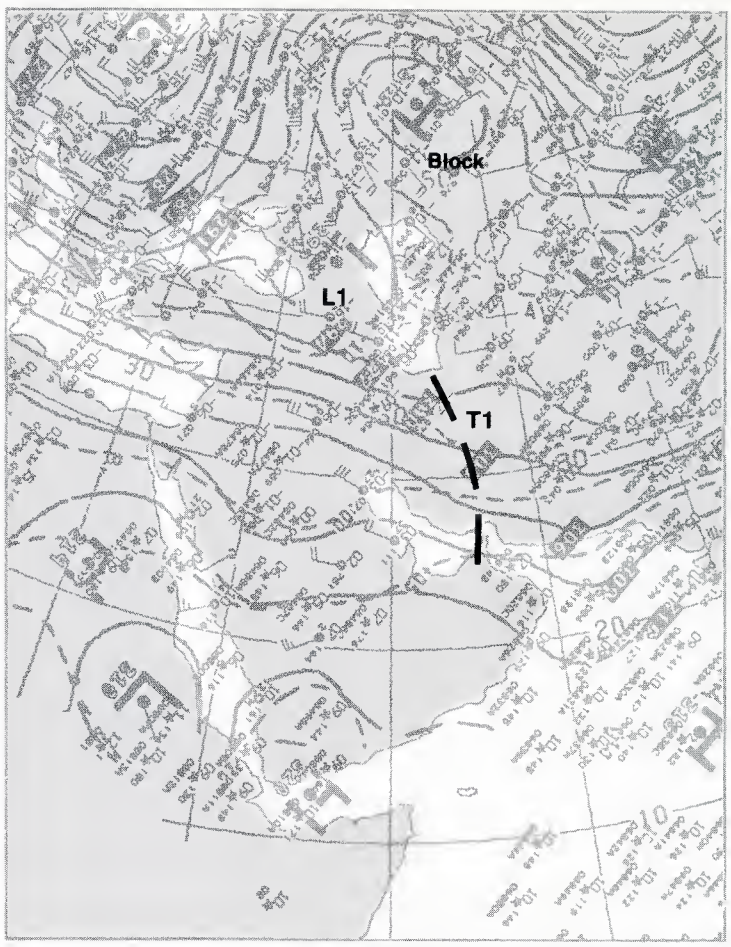

1C-11c. NMC 700-mb Analysis. 0000 GMT 31 December 1979.

d. NMC Surface Analysis. 0000 GMT 31 December 1979.

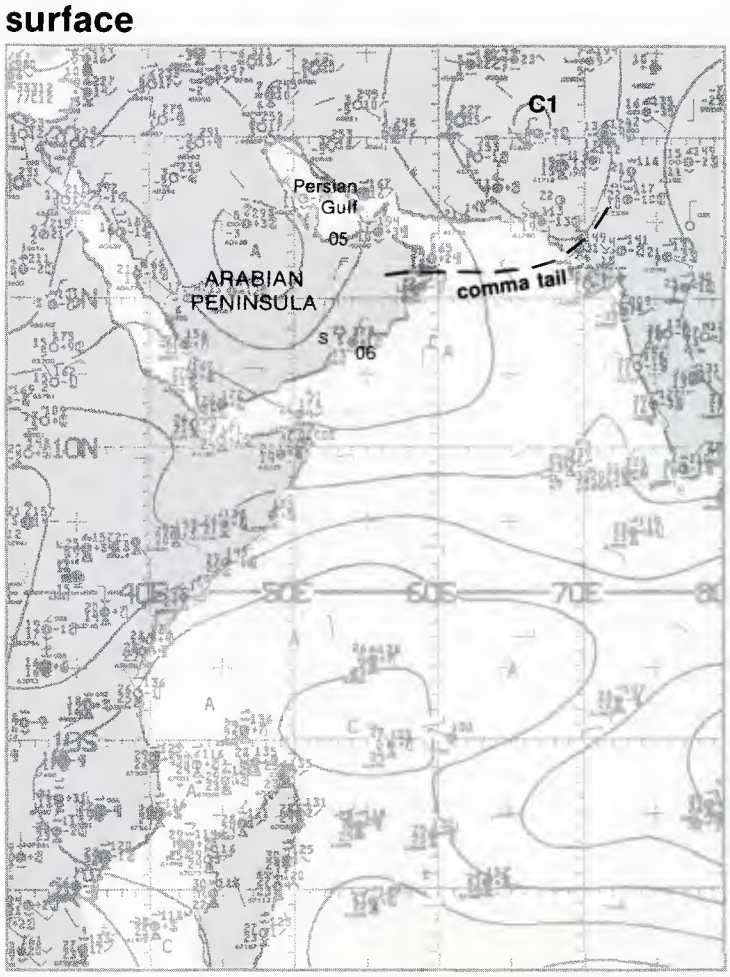

1C-11e. NMC Tropical Surface Streamline Analysis. 0600 GMT 31 Dec 1979.

Important Conclusions

1. It is possible using satellite data and conventional observations to track the passage of weak cold fronts through the Persian Gulf region.

2. Blocking situations over northern Europe establish the split-flow precursor condition of cold frontal penetration into the Persian Gulf region.

3. The left-front quadrant of jet streaks in advance of polar troughs is a favored location for storm intensification.

Reference

Perrone, T. J., 1979: Winter shamal in the Persian Gulf. NAVENVPREDRSCHFAC Technical Report TR 79-06. Naval Environmental Prediction Research Facility, Monterey, CA, 180 pp.

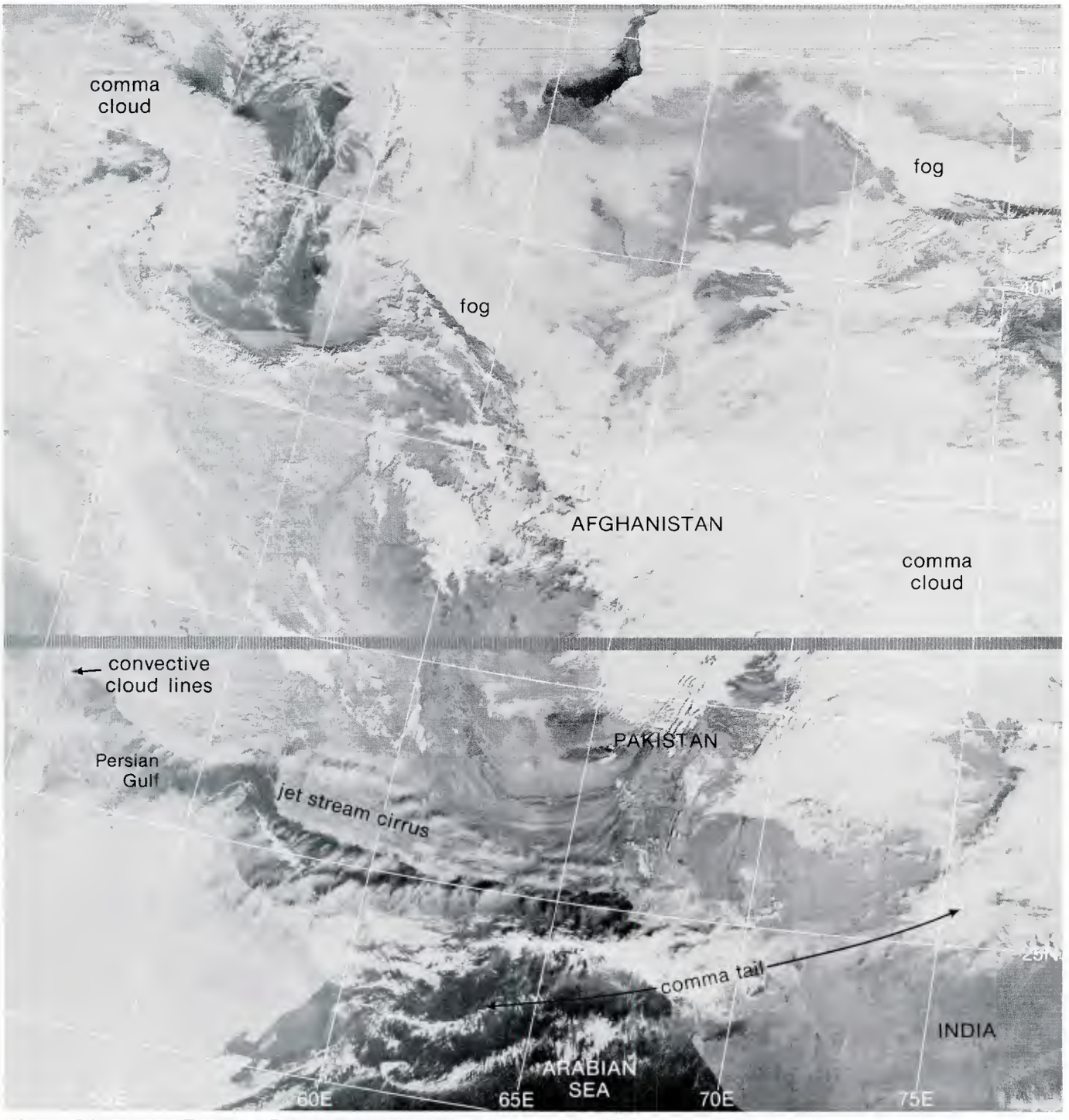

1C-11a. F-2. DMSP LF Normal Enhancement. 0350 GMT 31 December 1979.

Case 2 Arabian Sea/Bay of Bengal—Winter

Subtropical Jet Trough Development at Upper Levels

The baroclinic zone associated with the subtropical jet is found only in the upper troposphere, generally above 500 mb (Reiter, 1977). In order for strong low-level cyclogenesis/frontogenesis to occur in the area of the subtropical jet, interaction with the polar jet, which is characterized by strong baroclinicity in the lower and middle troposphere, is necessary. When these two jet streams interact, generally in the area of a long-wave trough, deep intense weather disturbances extending throughout the entire depth of the troposphere occur.

Upper-level troughs can develop independently of low level support and may produce potent-looking cloud signatures. These upper-level disturbances are related to the positive vorticity advection patterns of the subtropical jet streaks. The cloud signatures, as viewed in satellite imagery, can be misleading in that the existence of a low-level frontal zone cannot be assumed because the disturbed region is actually limited to the upper troposphere.

Reference

Reiter, E. R., 1977: Jet Stream Meteorology. The University of Chicago Press, Chicago and London, 515 pp.

200 mb

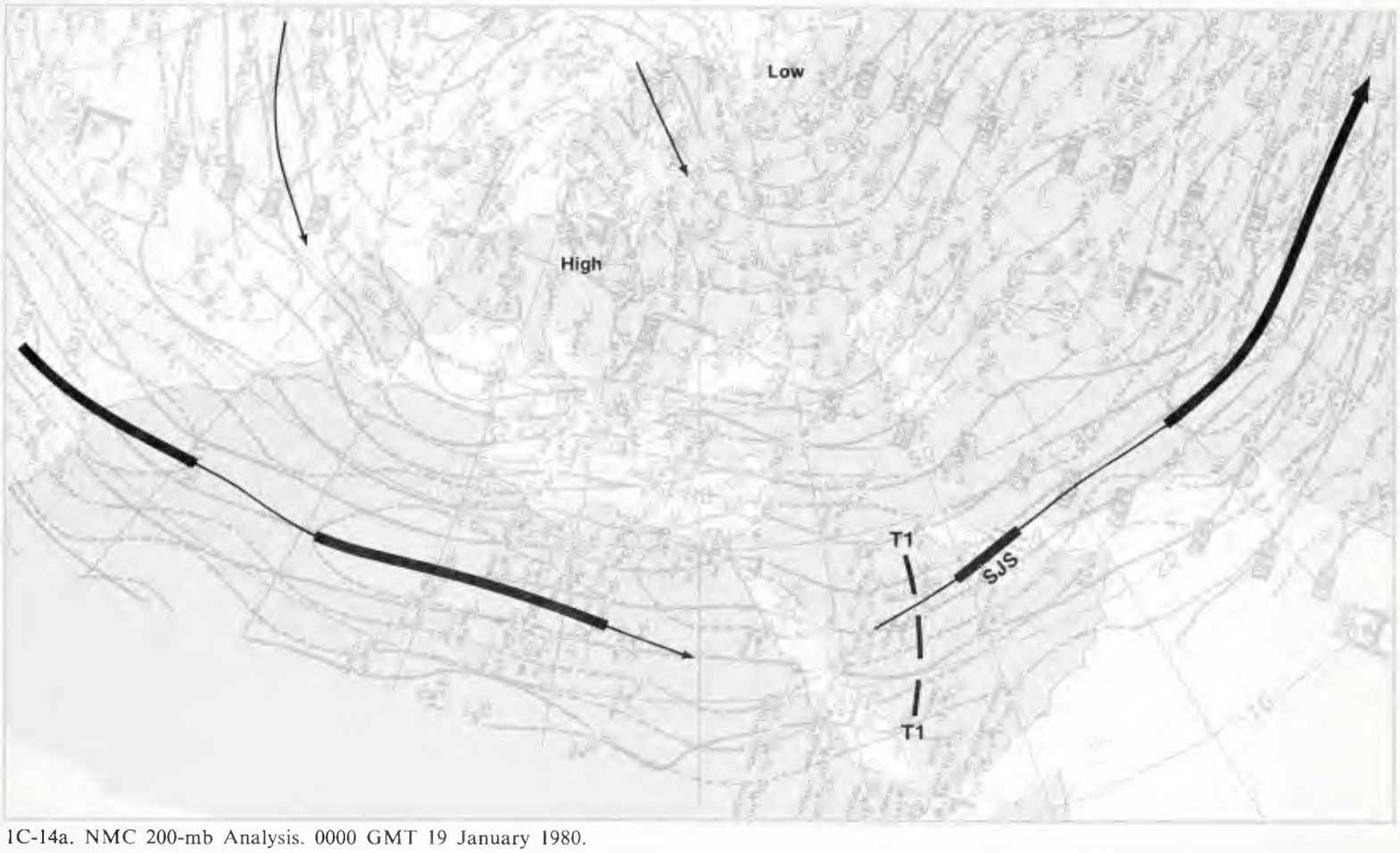

1C-14a. NMC 200-mb Analysis. 0000 GMT 19 January 1980.

500 mb

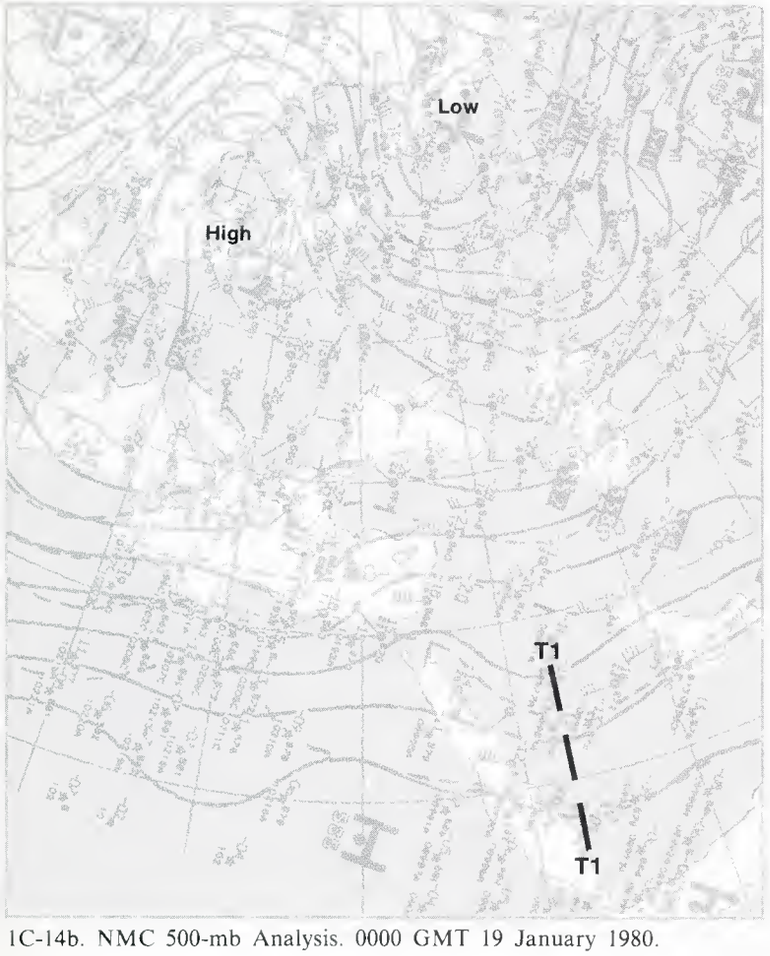

1C-14b. NMC 500-mb Analysis. 0000 GMT 19 January 1980.

surface

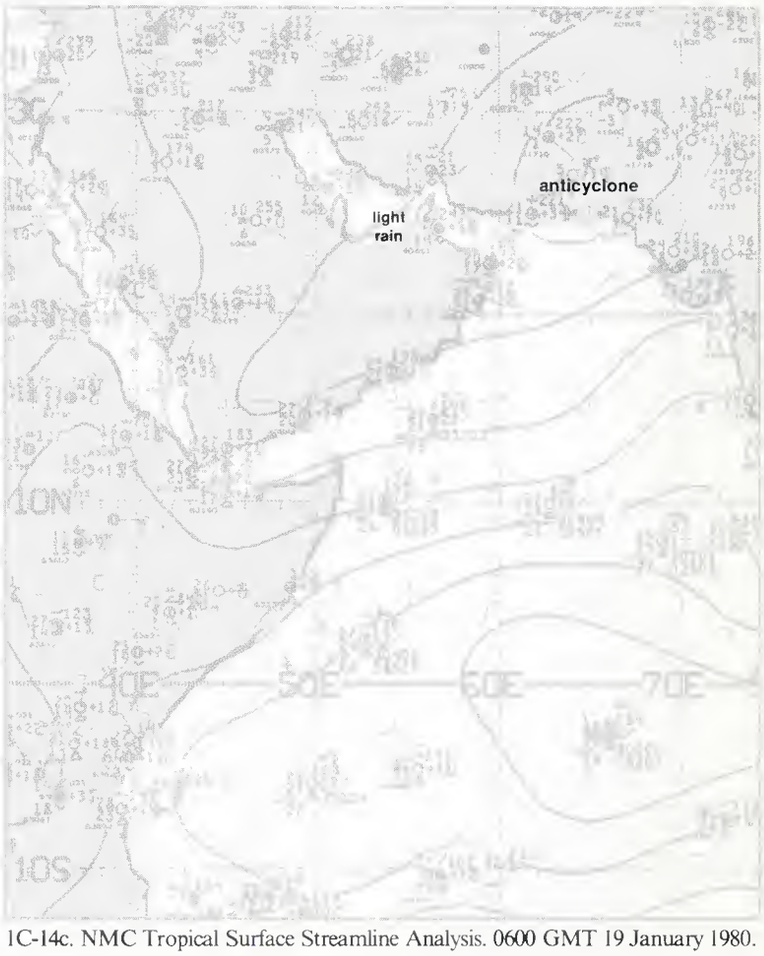

1C-14c. NMC Tropical Surface Streamline Analysis. 0600 GMT 19 January 1980.

Subtropical Jet Trough
Northern Arabian Sea
January 1980

19 January

On this date in January, the surface weather pattern of the northern Arabian Sea and bordering areas is dominated by anticyclonic circulation. The NMC surface streamline analysis for 0600 GMT (1C-14c) has an anticyclone centered over southern Pakistan. Station weather reports over southern Pakistan indicate generally clear skies, light winds, and some visibility restrictions due to haze and light fog.

A weak short-wave trough **T1** is noted at 500 mb (1C-14b) over the western Arabian Peninsula. At 200 mb (1C-14a), a weak, shallow-amplitude, short-wave trough **T1** is located slightly east of the 500-mb position. The subtropical jet core is located over central Saudi Arabia, flowing through the center of the short-wave trough. A 110-kt jet streak **SJS** is indicated east of the trough over the southern Persian Gulf.

The DMSP visible picture at 0545 GMT (1C-15a) shows a potent-looking cloud mass over the Gulf of Oman region. This system contains both cirrus and lower-level clouds and could be interpreted as a developing frontal wave. The surface analysis (1C-14c), however, did not provide any indication of disturbed weather, and in the picture there are no cloud lines to be seen over the Persian Gulf that would indicate cold northwesterly flow. Therefore, the cloud system is considered an upper-level feature associated with the subtropical jet streak **SJS** noted at 200 mb.

The FNOC surface analysis (1C-16b) shows that weak high-pressure systems dominate the pressure pattern at the surface over the Arabian Sea and the surrounding area. A blocking pattern centered over northwestern Europe with a broad band of westerlies flowing under the block over the Mediterranean and the area north of the Arabian Sea is shown at 500 mb (1C-16a). The FNOC 36-hour surface (1C-17b) and 500-mb (1C-17a) prognoses indicate no significant change. There is no cyclogenesis forecast for the Arabian Sea area and the block is forecast to be maintained.

Throughout the 19th of January the cloud pattern is maintained but nothing in the way of significant weather occurs at the surface. Light rain was reported by stations 40445 (24.4° N, 54.5° E) at 0000 and 0600 GMT and 40462 (23.6° N, 58.3° E) at 0900 and 1200 GMT (not shown), during the passage of the cloud system. These stations are located in the southern Persian Gulf and the Gulf of Oman. A wind shift from 290° to 330° occurred at station 40445 between 0900 and 1100 GMT, with winds at 9 kt. No other significant wind changes were noted in available surface reports. Sky conditions were reported as scattered stratocumulus and multi-layered broken altocumulus and cirrus.

20 January

Anticyclonic circulation continues at the surface over the northern Arabian Sea and surrounding area (1C-18c). A report of light rain is noted on the surface analysis near 30° N, 67° E, which is a mountainous region of extreme northwestern India. The short-wave trough **T1** at 500 mb (1C-18b) is located over southern Pakistan. A 110-kt subtropical jet streak **SJS** intersects this trough at the 200-mb level (1C-18a). The polar jet core **PJS** is located well to the north (near 40° N, 60° E), and there is no interaction between the subtropical jet and the polar jet in the Arabian Sea area. The cloud pattern over northern Pakistan remains potent looking in the DMSP infrared picture at 1810 GMT on 19 January (1C-19a), with well-organized cirrus and middle-level clouds.

The surface conditions remain undisturbed, under general anticyclonic circulation at 1200 GMT (1C-20c). The short-wave trough **T1** at 500 mb (1C-20b) has moved eastward to near 72° E. A 110-kt subtropical jet streak **SJS** and trough **T1** at 200 mb (1C-20a) continue to overlie the 500-mb trough. The DMSP visible picture at 0527 GMT (1C-21a) shows that the cloud system has moved eastward, out of the area of view, beyond 70° E, or has dissipated. The FNOC surface analysis (1C-21c) and 500-mb analysis (1C-21b), which are the verifying charts for the 36-hour prognoses (1C-17b and 17a), indicate no significant low-level development has occurred and the blocking pattern has been maintained, as forecast.

The cloud pattern first observed in the DMSP visible picture at 0545 GMT on 19 January (1C-15a), did not at that time or at any subsequent time during its passage through the Arabian Sea region produce any significant surface weather. The disturbed conditions were limited to the middle and upper portions of the troposphere, while surface conditions remained dominated by an anticyclonic circulation.

Both the conventional observations and satellite imagery provided evidence of the nature of this system. The observations supported the anticyclonic circulation and fair weather. The lack of cloud lines over the Persian Gulf, as seen in the imagery, indicated there was no cold air outbreak behind the cloud pattern.

Important Conclusions

1. Upper-level short-wave troughs which form as a result of subtropical jet stream activity can produce potent-looking cloud patterns.

2. The formation of these troughs is related to jet streaks embedded in the subtropical jet.

3. Extensive upper- and middle-level clouds are formed but no significant surface weather results.

4. Both conventional observations and satellite imagery provide useful information in determining the levels at which disturbed conditions exist.

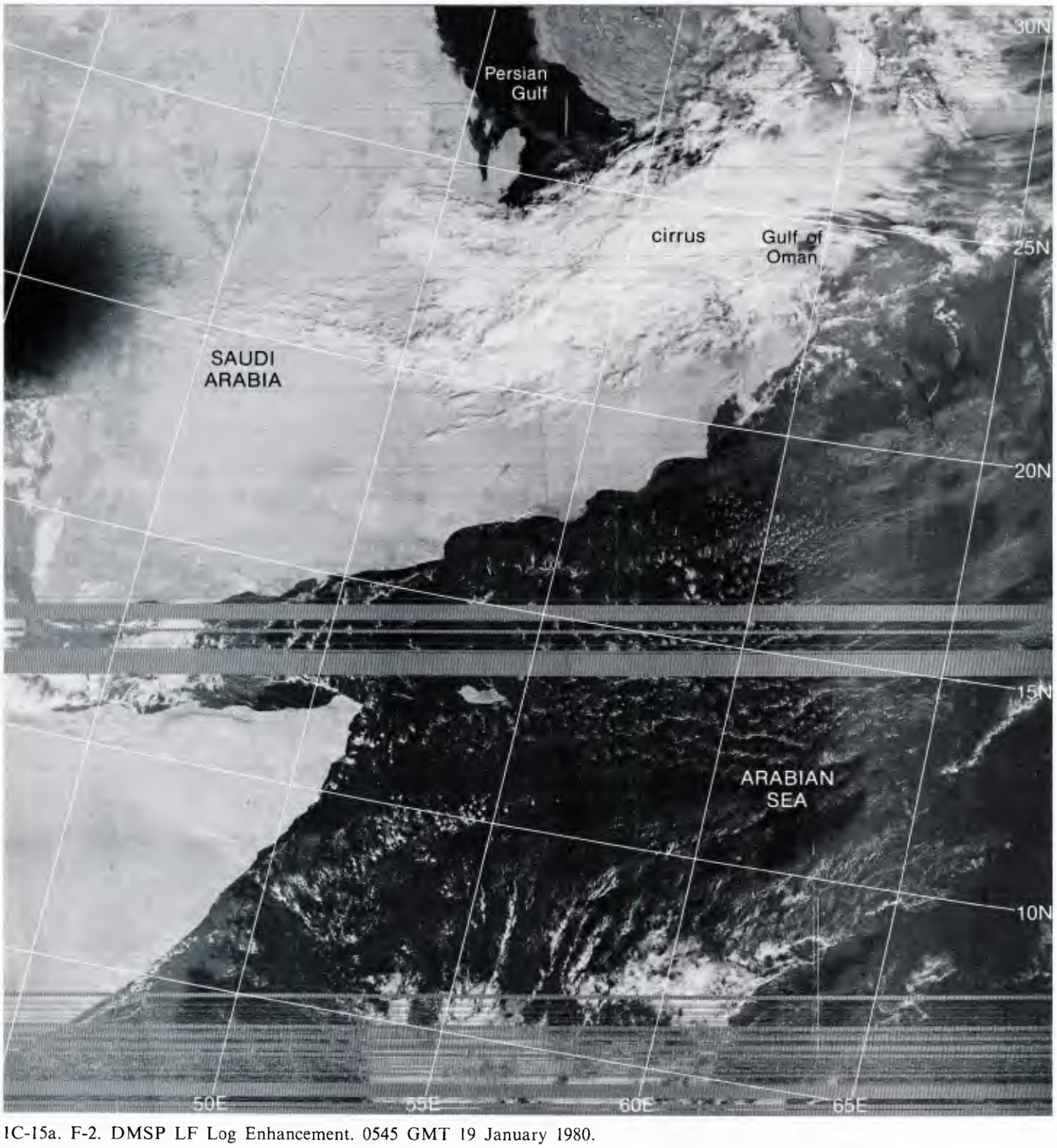

1C-15a. F-2. DMSP LF Log Enhancement. 0545 GMT 19 January 1980.

500 mb

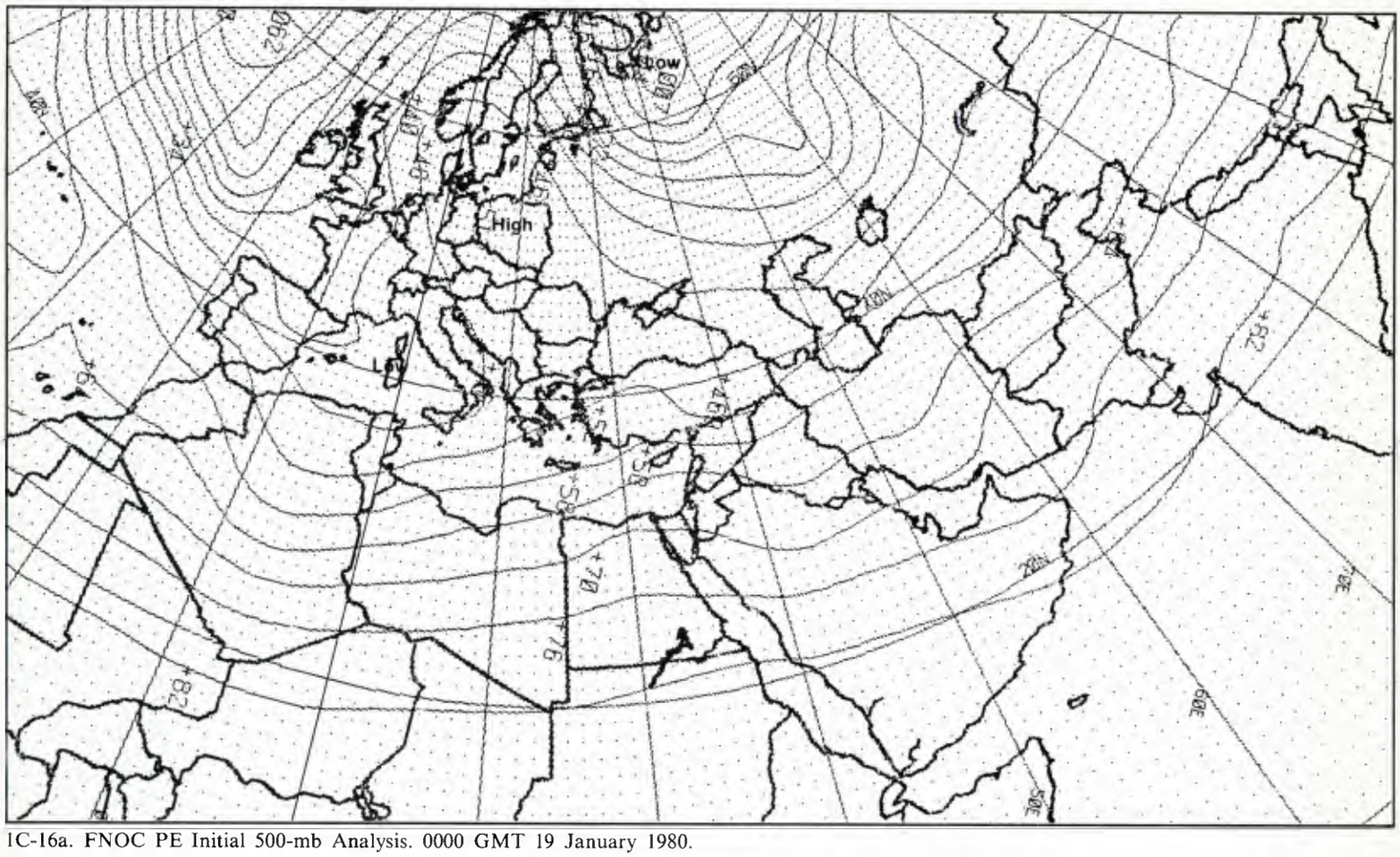

1C-16a. FNOC PE Initial 500-mb Analysis. 0000 GMT 19 January 1980.

surface

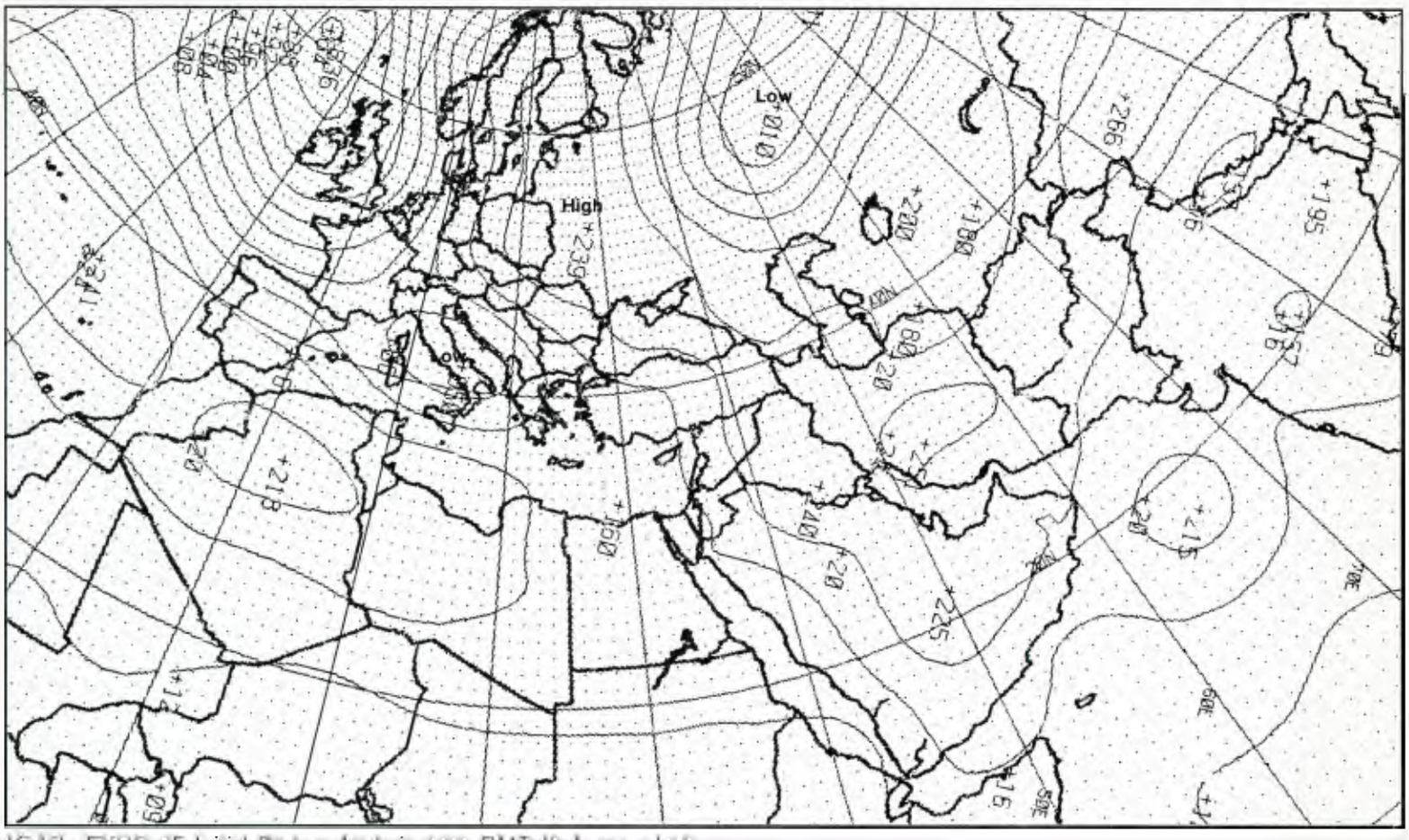

1C-16b. FNOC PE Initial Surface Analysis. 0000 GMT 19 January 1980.

500 mb

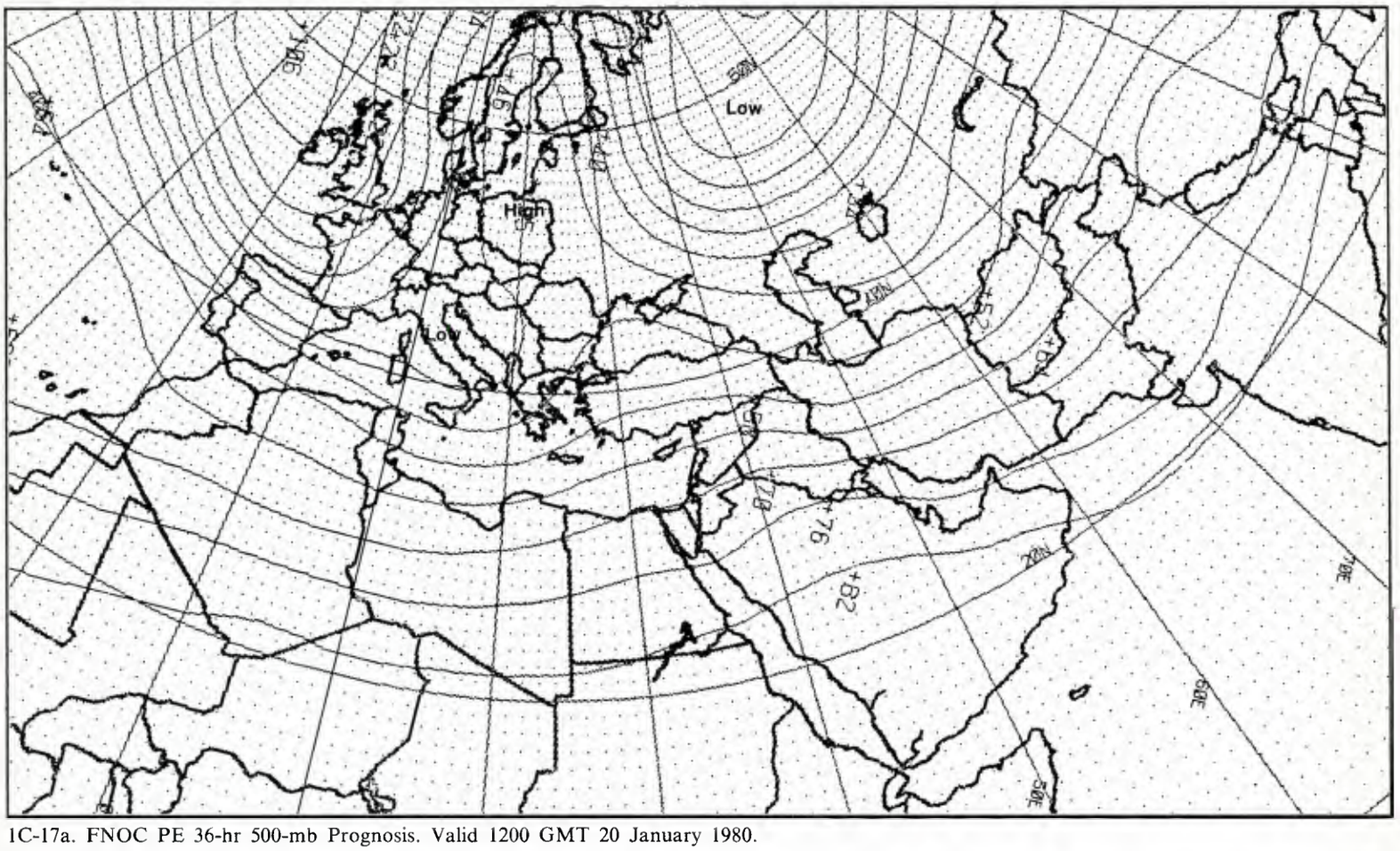

1C-17a. FNOC PE 36-hr 500-mb Prognosis. Valid 1200 GMT 20 January 1980.

surface

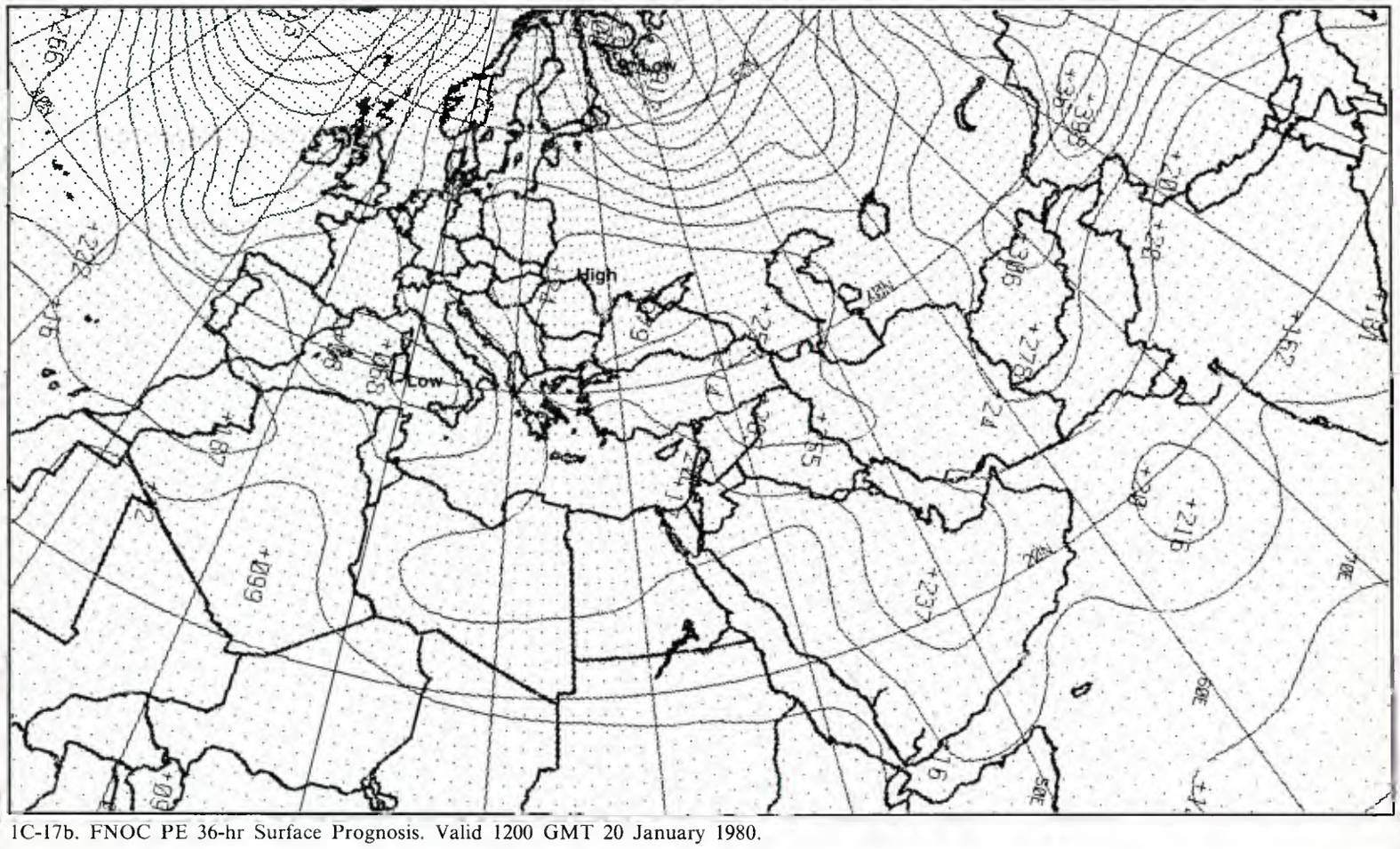

1C-17b. FNOC PE 36-hr Surface Prognosis. Valid 1200 GMT 20 January 1980.

200 mb

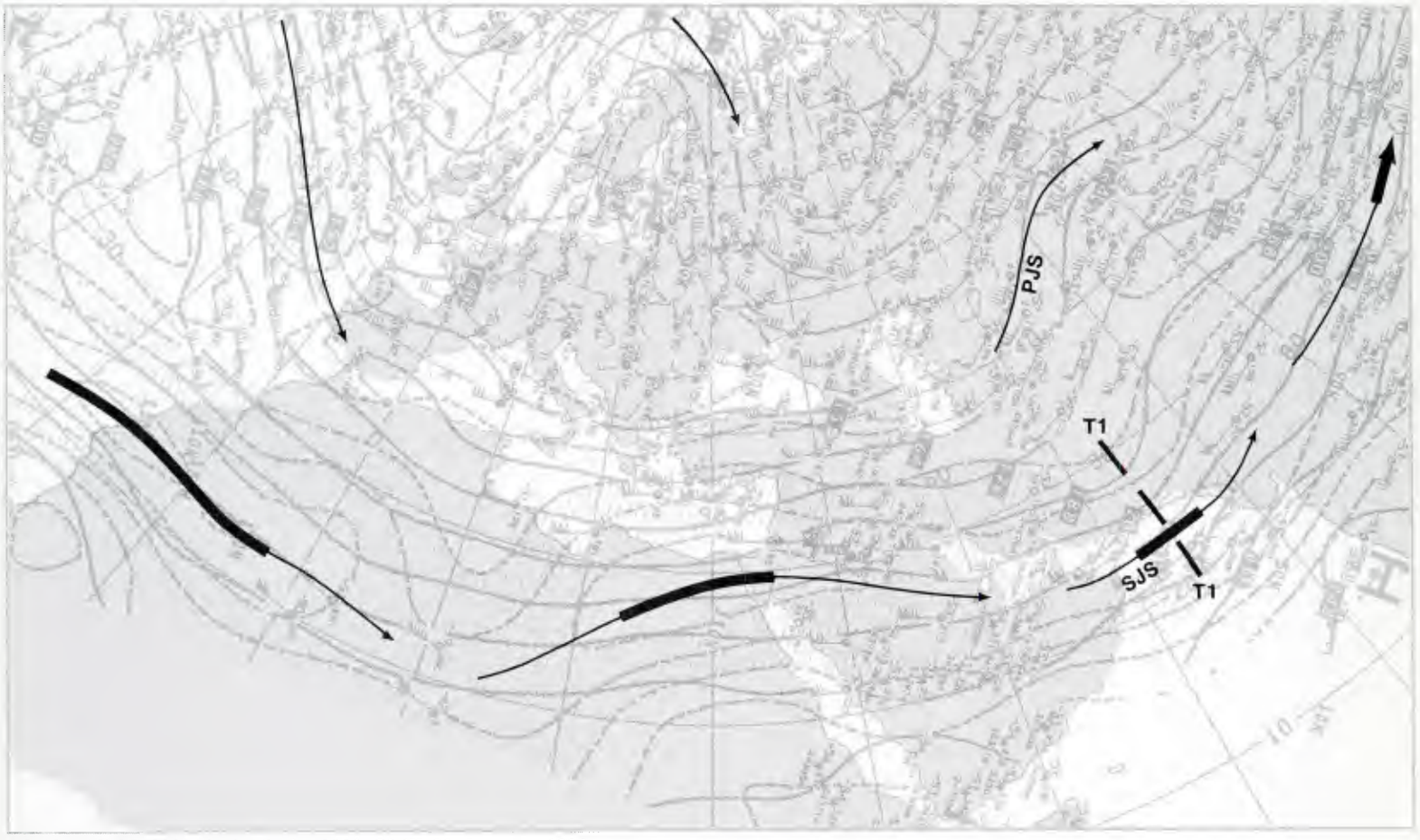

1C-18a. NMC 200-mb Analysis. 0000 GMT 20 January 1980.

500 mb

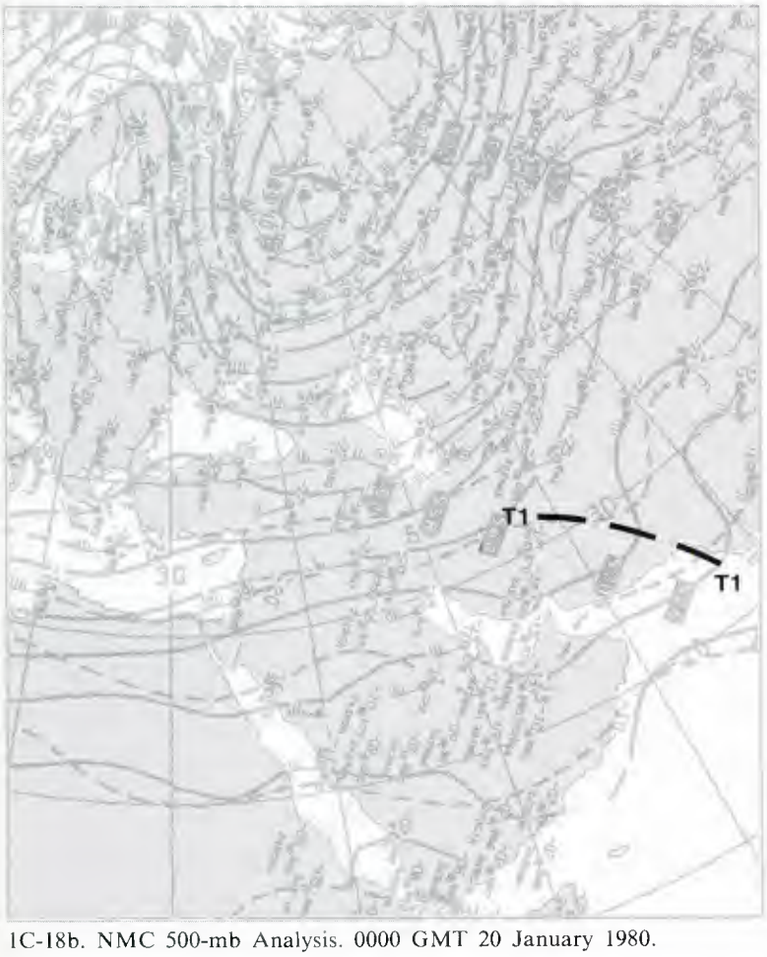

1C-18b. NMC 500-mb Analysis. 0000 GMT 20 January 1980.

surface

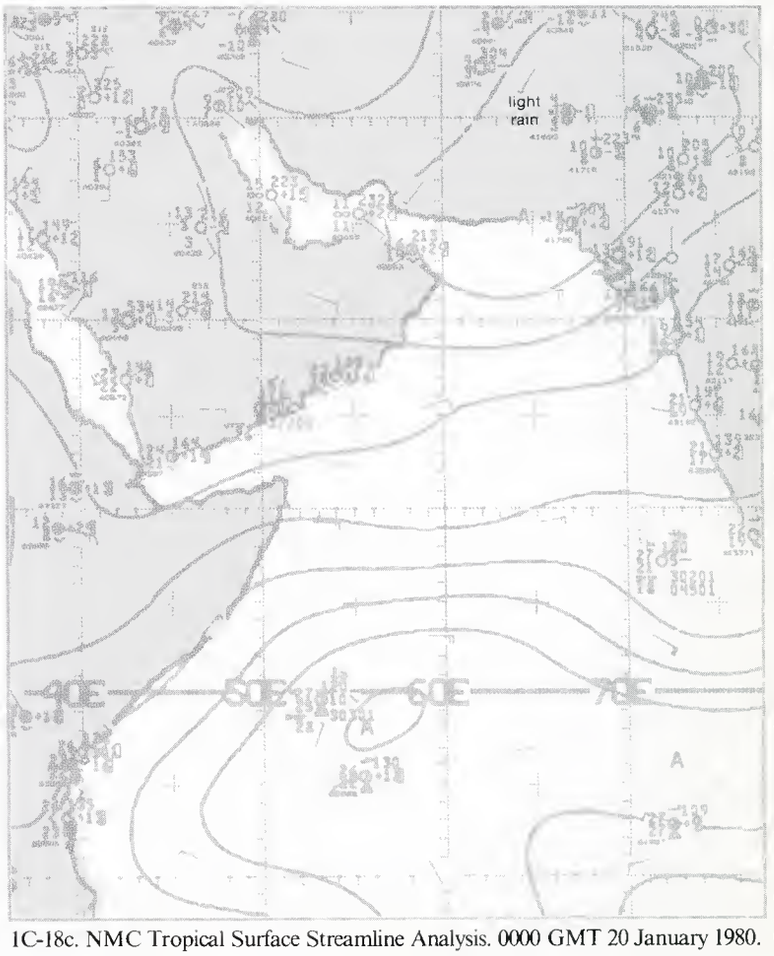

1C-18c. NMC Tropical Surface Streamline Analysis. 0000 GMT 20 January 1980.

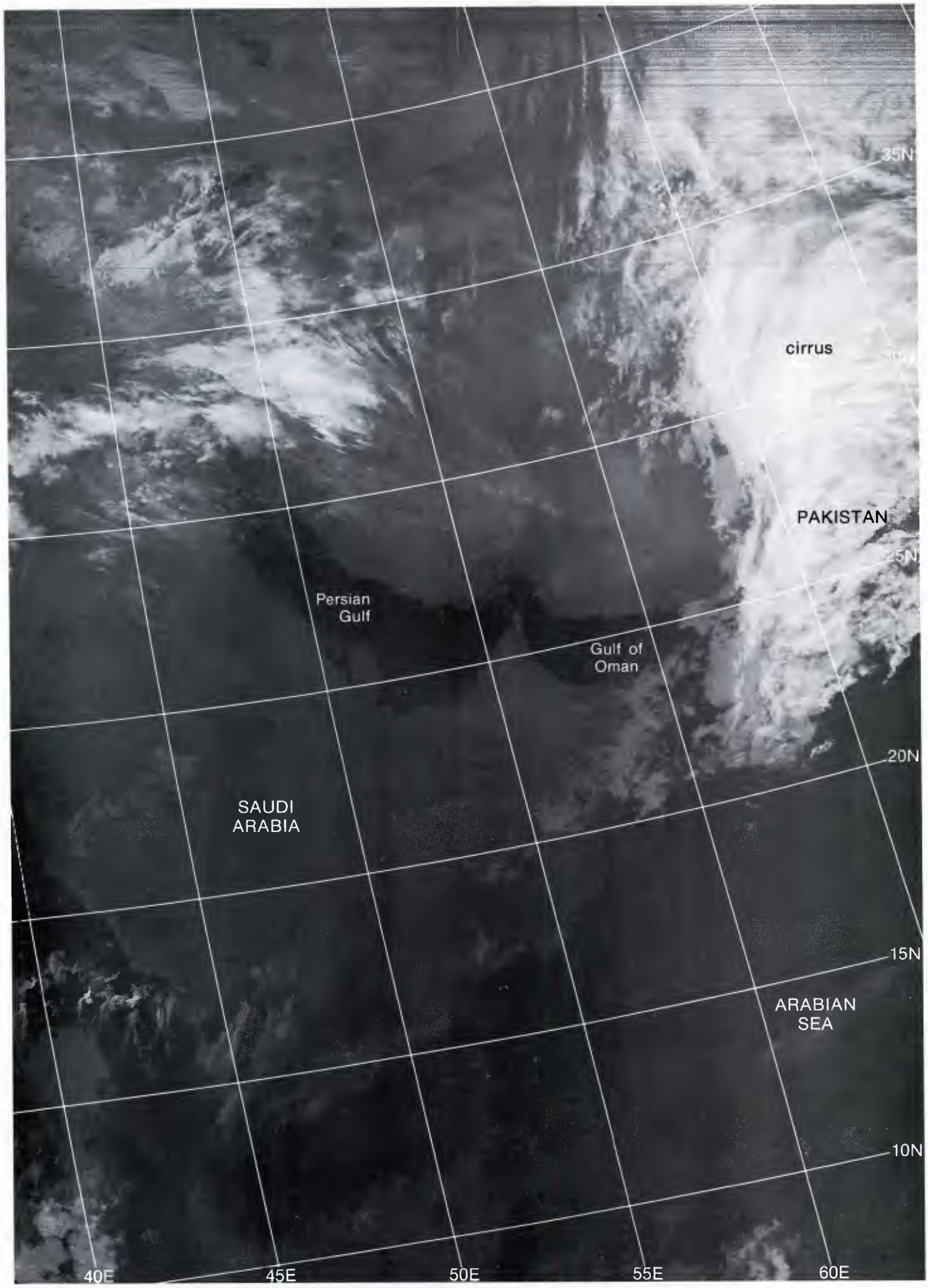

1C-19a. F-2. DMSP TF Normal Enhancement. 1810 GMT 19 January 1980.

200 mb

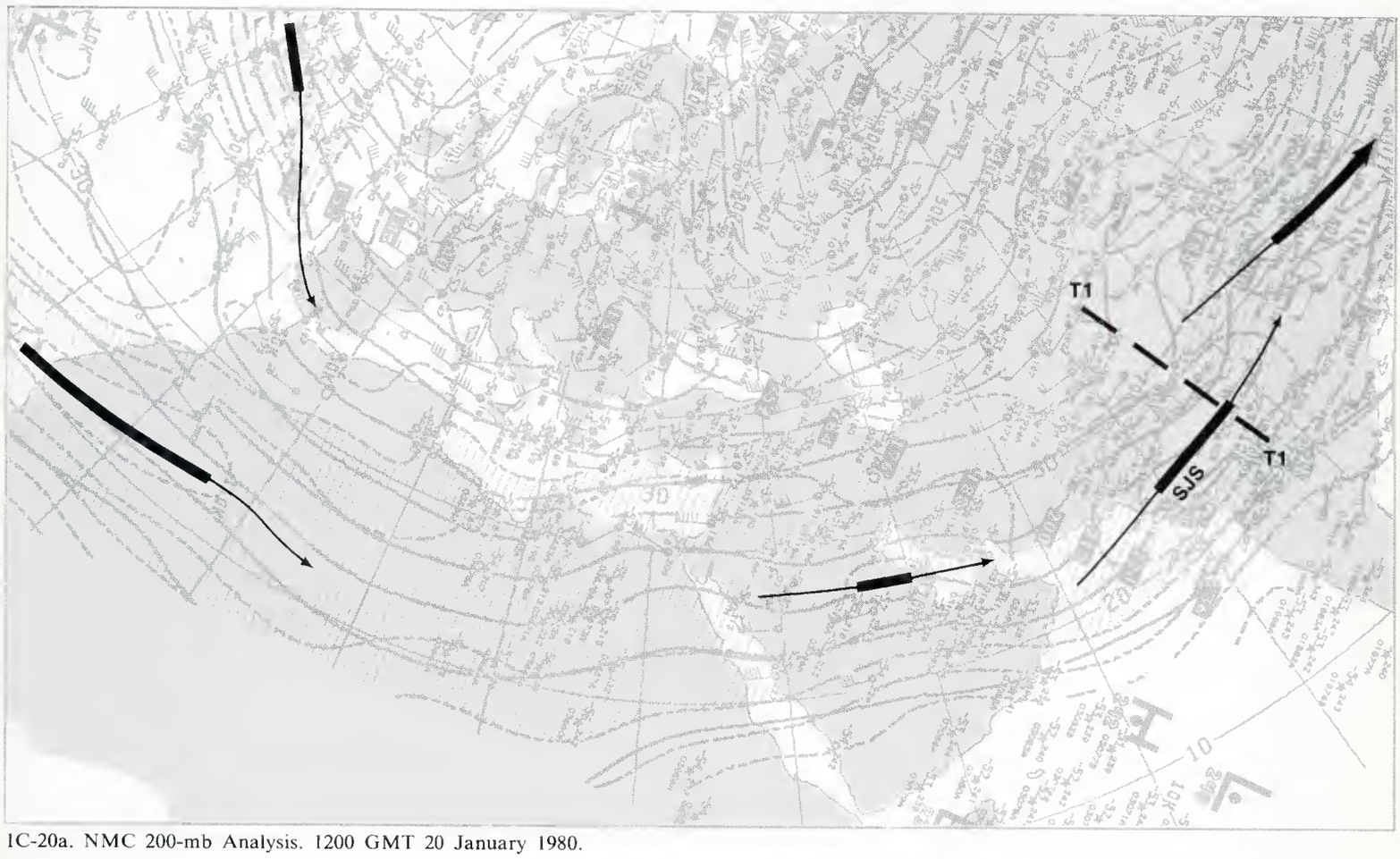

1C-20a. NMC 200-mb Analysis. 1200 GMT 20 January 1980.

500 mb

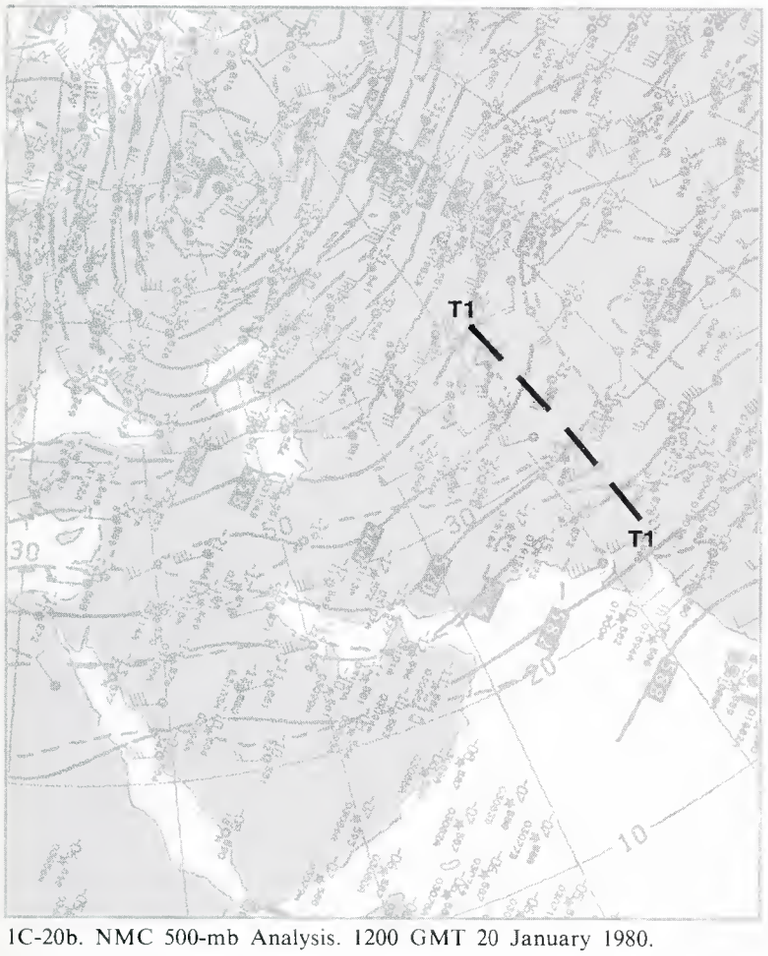

1C-20b. NMC 500-mb Analysis. 1200 GMT 20 January 1980.

surface

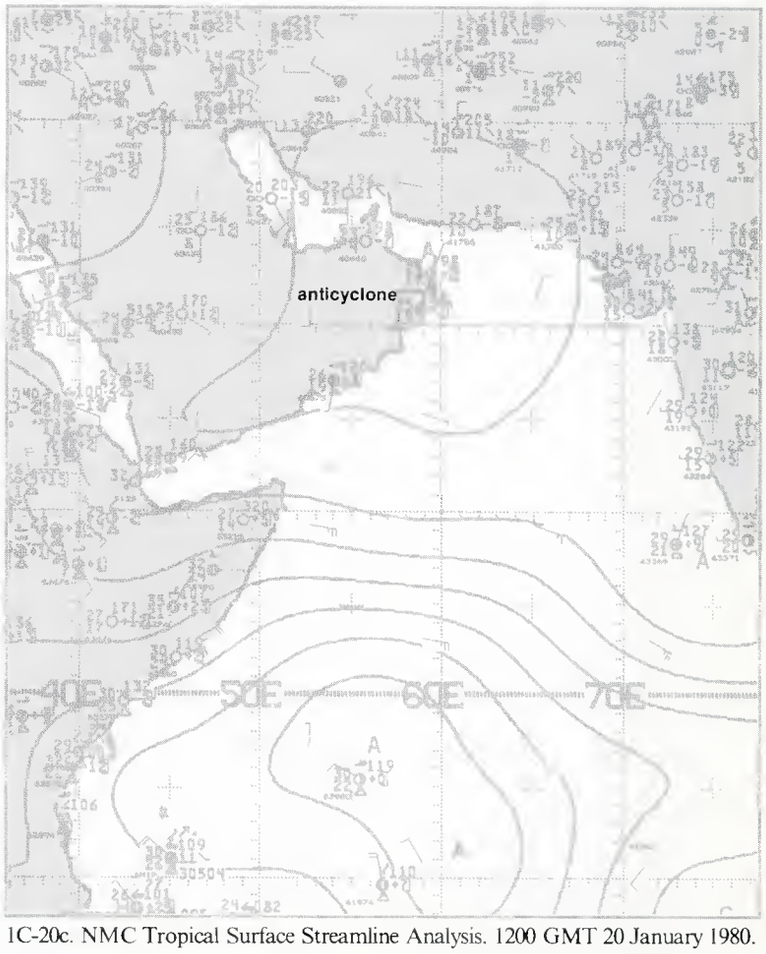

1C-20c. NMC Tropical Surface Streamline Analysis. 1200 GMT 20 January 1980.

mb

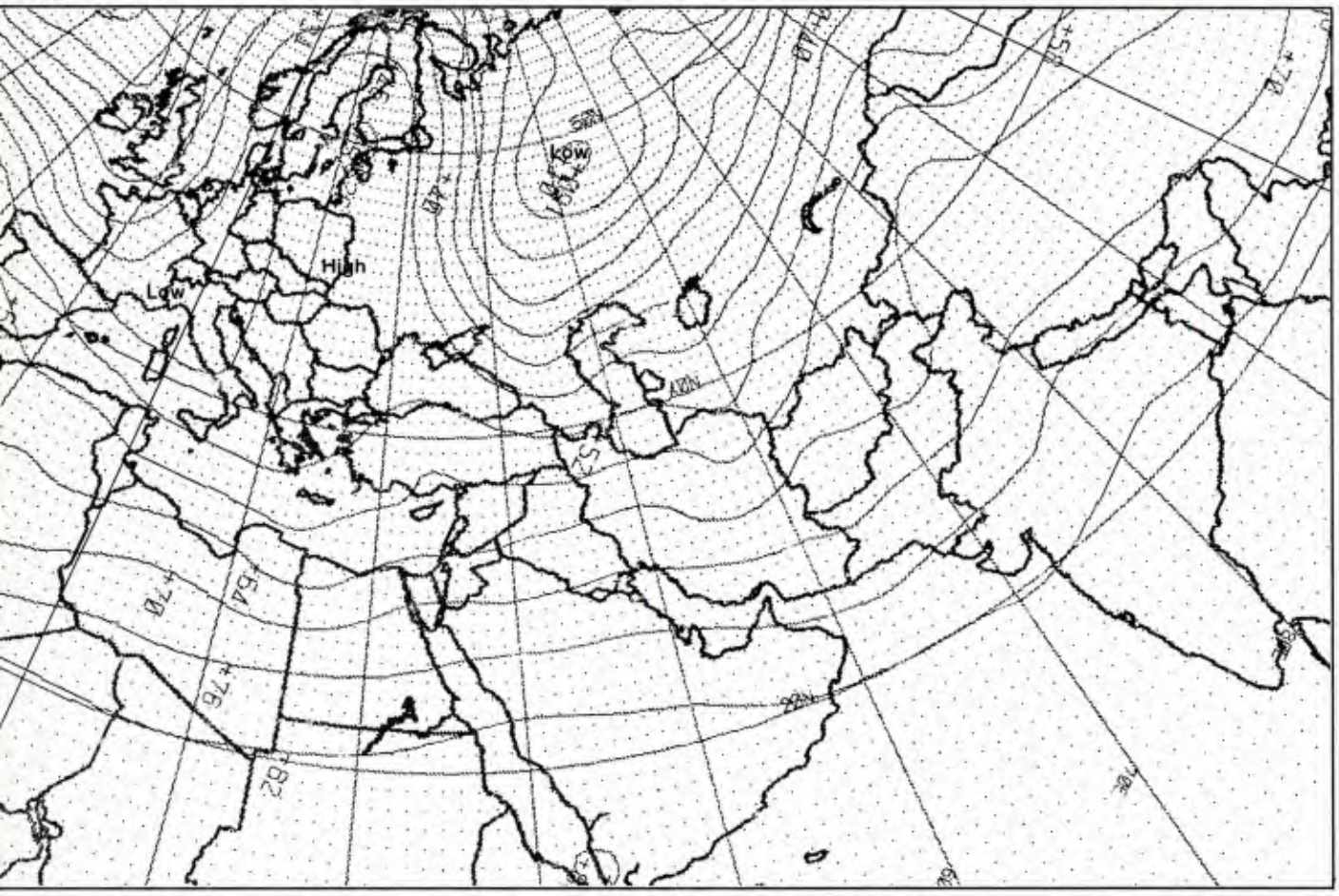

b. FNOC PE Initial 500-mb Analysis. 1200 GMT 20 January 1980.

face

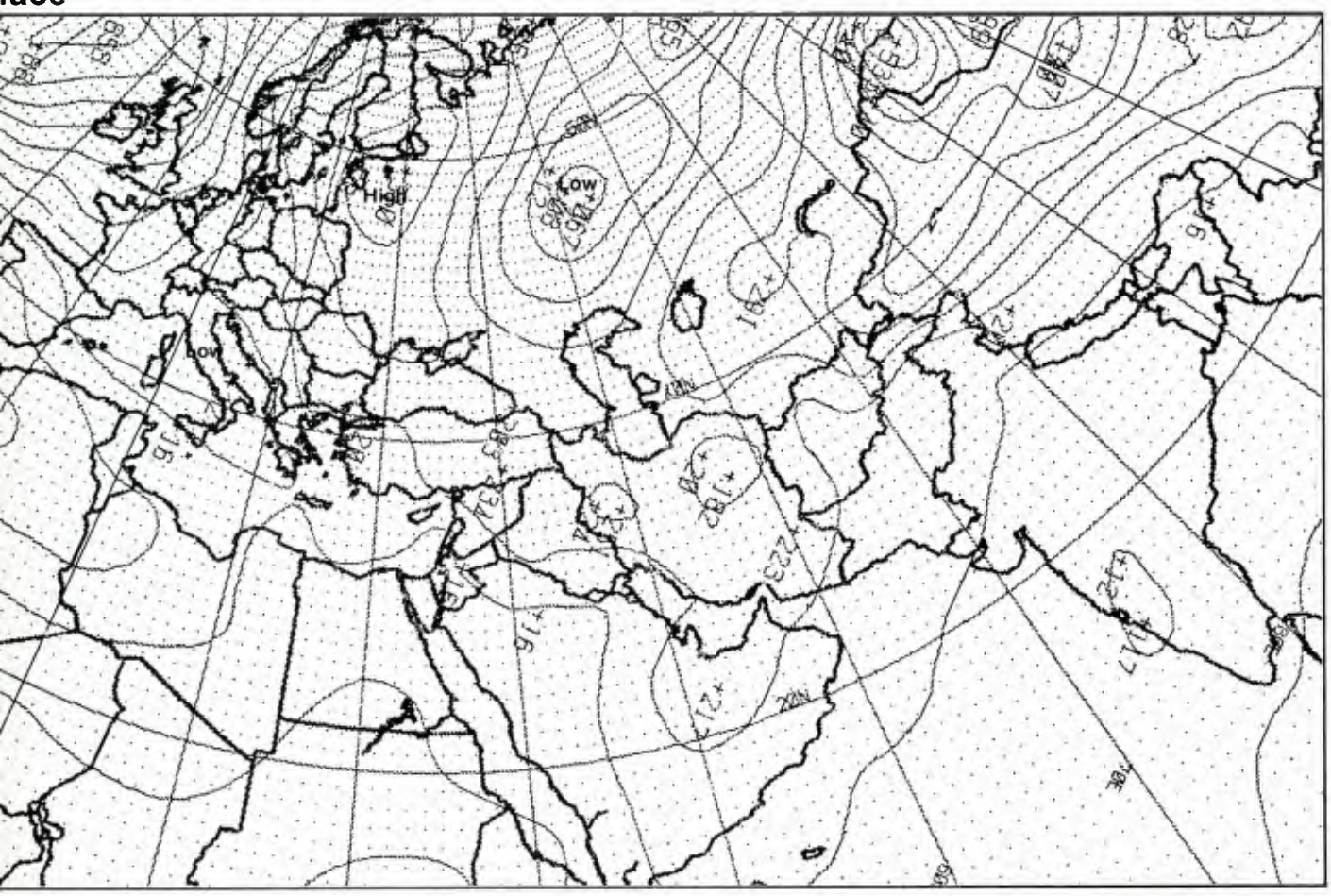

c. FNOC PE Initial Surface Analysis. 1200 GMT 20 January 1980.

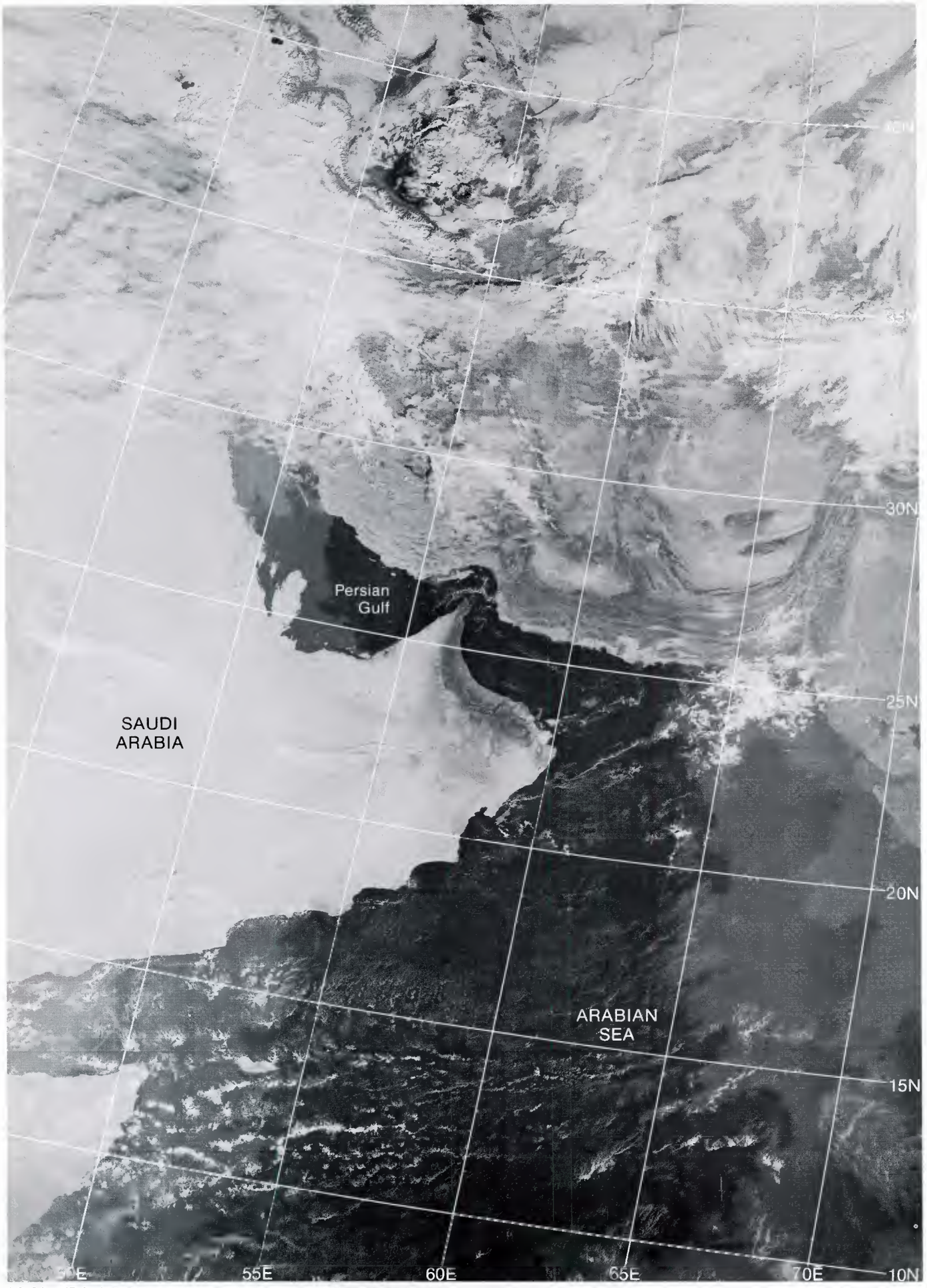

1C-21a. F-2. DMSP LF Log Enhancement. 0527 GMT 20 January 1980.

Case 3 Arabian Sea/Bay of Bengal—Winter

The Winter Shamal

The term "shamal" is an Arabic word meaning north and, in meteorology, refers to the seasonal north or northwesterly winds that occur over the Persian Gulf region during the summer and winter months (Perrone, 1979). The winter shamal is stronger than the summer shamal and normally has greater potential to create adverse weather conditions that would affect naval operations.

Perrone provides a detailed discussion of the characteristic features of the winter shamal and should be referred to for an in-depth discussion. The key elements are as follows: (1) A protrusion of high pressure over the Arabian Peninsula following a cold frontal penetration into the Arabian Sea; (2) An inverted trough east of the Persian Gulf; and (3) High pressure penetrating southward into Iran and western Pakistan. Strong shamal winds in the Persian Gulf are initiated as a long-wave upper-level trough moves southeastward over the Arabian Peninsula. The shamal can last as long as 3–5 days; however, more frequently it lasts from 24 to 36 hours, as the associated upper-level trough moves rapidly through the region rather than stalling in a position to cause the extended duration episodes. In both instances, continued shamal effects occur further east, off the coast of Iran and western Pakistan, as the surface low east of the Persian Gulf and the upper-level trough move eastward across those areas.

Under these conditions, the pressure gradient in the Persian Gulf lessens and strong upper-level northerly winds become superimposed over northerly surface flow in the Iran/Pakistan region. A strong offshore flow condition results which often raises sand and dust that can be advected long distances over the northern Arabian Sea. It was under such a circumstance that the aircraft carrier USS *Midway* (CV-41) encountered a severe sandstorm while operating near the Gulf of Oman, over 100 miles at sea (NEPRF, 1980).

To predict the shamal over the Persian Gulf, and later effects over the northern Arabian Sea, it is necessary to analyze maps over eastern Europe for cold frontal movement and cold air advection at low levels behind the front, having the potential to surge southward across the Arabian Peninsula. Satellite imagery is important and useful in judging frontal position and intensity. However, the tendency for cloudiness to dissipate as the front moves across the Arabian Peninsula makes the application of conventional satellite imagery (visible and infrared) less useful than normal, and a continuous monitoring of surface reports becomes essential to judge frontal location.

References

NEPRF, 1980: Sandstorm in the Arabian Sea. NAVENVPREDRSCHFAC Technical Bulletin 80-07. Naval Environmental Prediction Research Facility, Monterey, CA, 11 pp.

Perrone, T. J., 1979: Winter shamal in the Persian Gulf. NAVENVPREDRSCHFAC Technical Report TR 79-06. Naval Environmental Prediction Research Facility, Monterey, CA, 180 pp.

850 mb

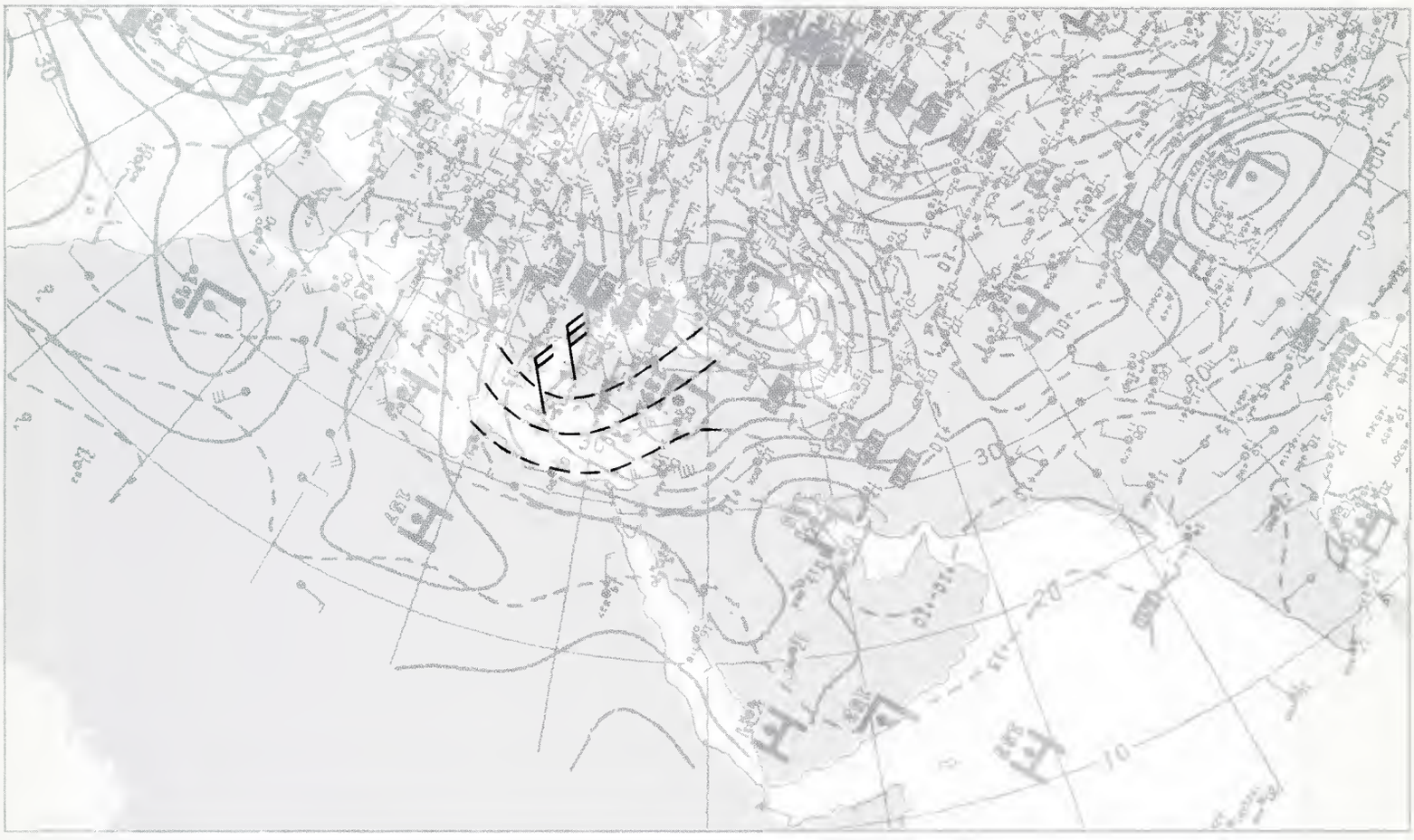

1C-24a. NMC 850-mb Analysis. 1200 GMT 28 January 1980.

surface

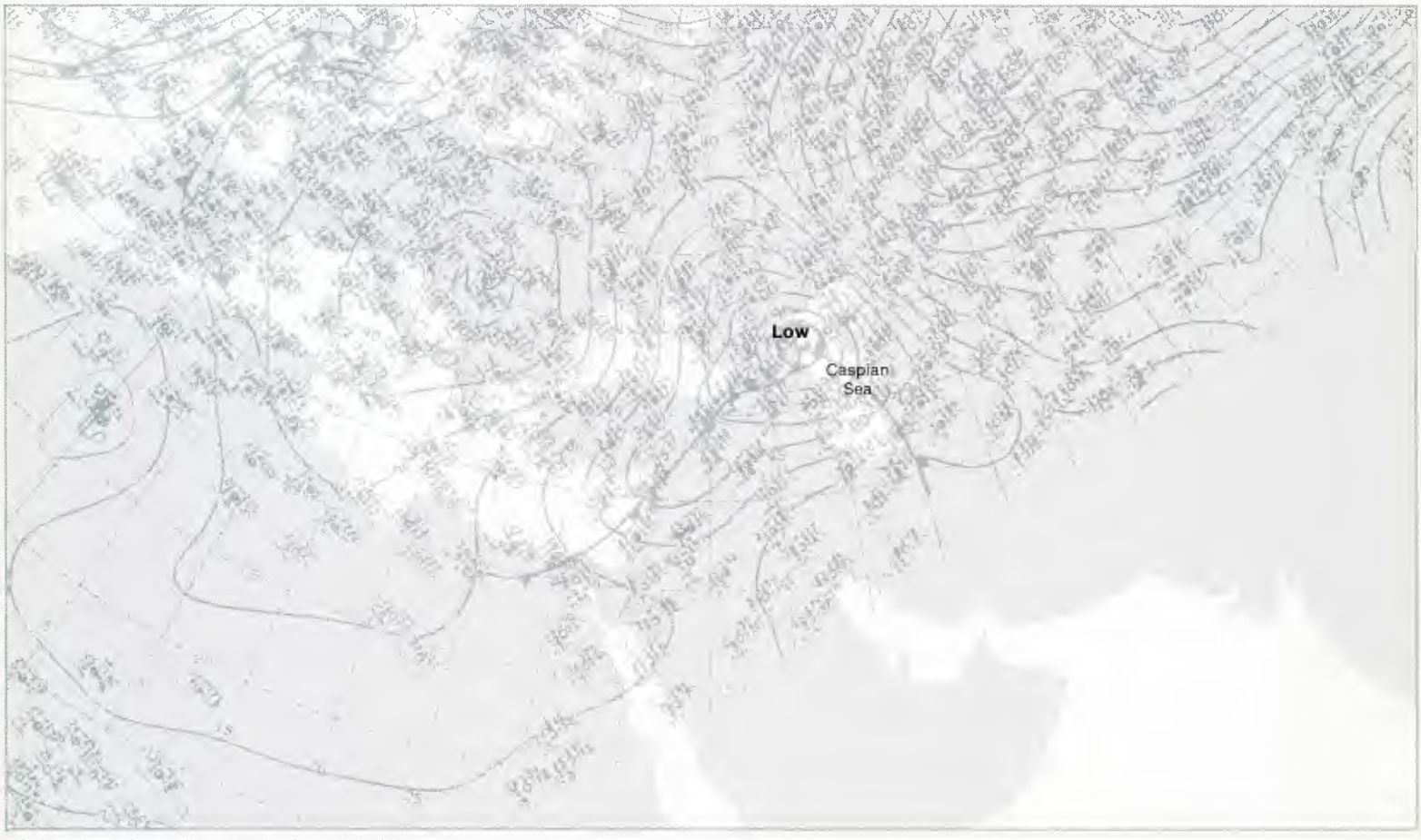

1C-24b. NMC Surface Analysis. 1200 GMT 28 January 1980.

28 January

The NMC surface analysis for 1200 GMT (1C-24b) reveals a cold front crossing the eastern Mediterranean, extending to a low centered near the Caspian Sea. Strong winds and very cold temperatures are evident behind the front.

The NMC 850-mb analysis (1C-24a) shows a packing of isotherms near the frontal position and strong northwesterly (20–30 kt) winds blowing perpendicular to the isotherms, indicating pronounced cold air advection toward the Arabian Peninsula. This provides over 48 hours advance warning of a potential for shamal winds in the Persian Gulf, assuming the front moves at a speed of 20–30 kt.

The DMSP infrared picture at 0723 GMT (1C-25a) reveals frontal cloudiness over the northern Arabian Peninsula. The front appears rather weak and it is in a dissipative state, based on the DMSP picture.

29 January

The 1200 GMT surface analysis (1C-26b) shows a small cold frontal section extending from the low just east of the Caspian Sea. High pressure is now seen moving into the northern Red Sea region, whereas 24 hours earlier (1C-24b) a trough was approaching. On the surface streamline analysis (1C-26c), northerly flow can be seen extending into the northern Arabian Peninsula while weak southerly flow is evident further south. A streamline trough separates the two flows and identifies the likely position of the cold frontal extension into this region. Note the weak southwesterly flow and falling pressure tendency at Riyadh in advance of the probable frontal position.

The 850-mb analysis for 1200 GMT (1C-26a) shows the continued strong cold air advection. The 0° C isotherm now extends to the Sinai Peninsula and into northern Iraq.

The DMSP infrared picture at 1830 GMT (1C-27a) shows the southward protrusion of dissipating cloudiness associated with the cold frontal system.

30 January

The surface analysis for 1200 GMT (1C-28b) shows the apparent southward progression of the low that had been near the Caspian Sea, and that now lies slightly to the northeast of the Persian Gulf. A new cold frontal development is analyzed extending to the west-northwest from this feature.

On the surface streamline analysis (1C-28c), reports show rising pressures over northern Saudi Arabia and falling pressures over the southern region. Winds at Riyadh, which had been continuously southerly for the past two days, have switched to northerly as have the winds over the northern Persian Gulf. The pressure tendency at Riyadh, which had been falling, now shows a strong rising tendency suggesting cold frontal passage.

The surface streamline analysis confirms this probability in revealing the southward progression of a trough past Riyadh and the likely position of the leading edge of the cold front at this time.

At 850 mb (1C-28a), the continued advection of cold air toward the Persian Gulf region is evident. The 0° C isotherm, which had been located 5° north of the Persian Gulf on 29 January, has now moved to only about 2.5° north of the gulf.

The DMSP infrared picture (1C-29a), about five hours prior to the analyses, shows a weak band of wispy cloudiness associated with the leading edge of the front.

continued on page 1C-30

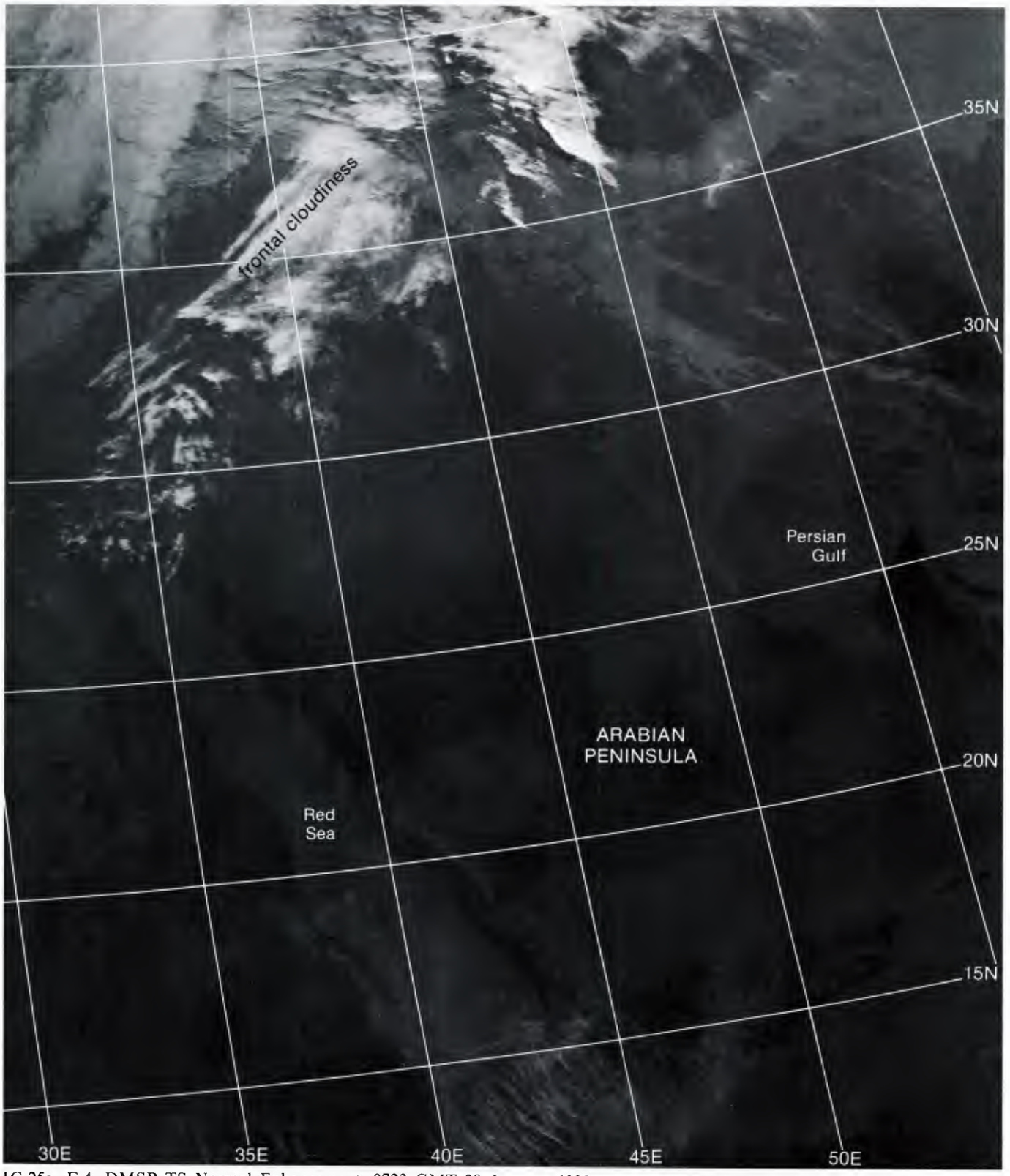

1C-25a. F-4. DMSP TS Normal Enhancement. 0723 GMT 28 January 1980.

850 mb

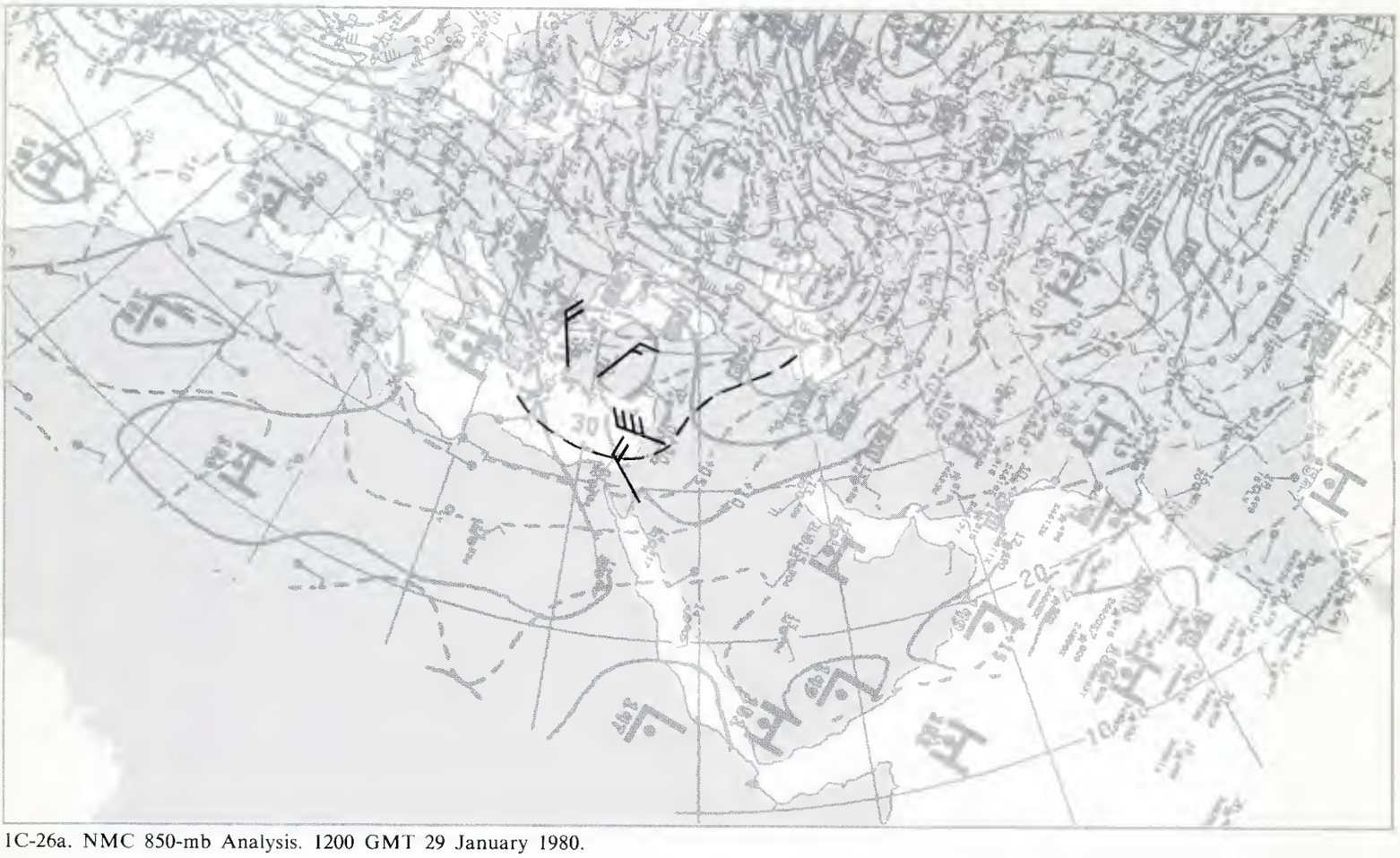

1C-26a. NMC 850-mb Analysis. 1200 GMT 29 January 1980.

surface

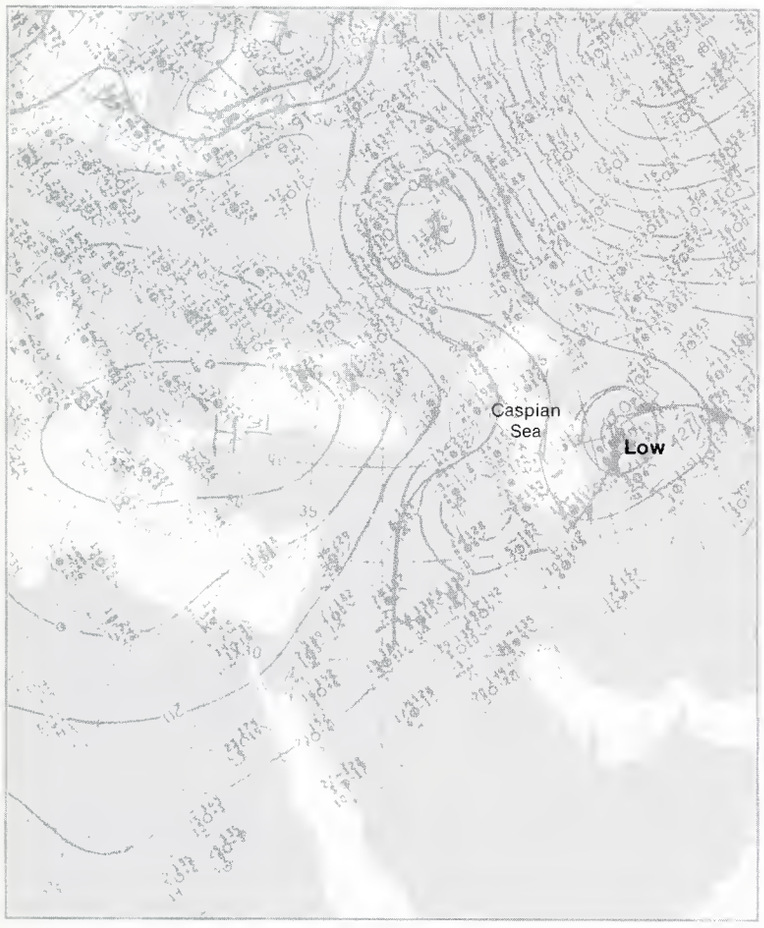

1C-26b. NMC Surface Analysis. 1200 GMT 29 January 1980.

surface

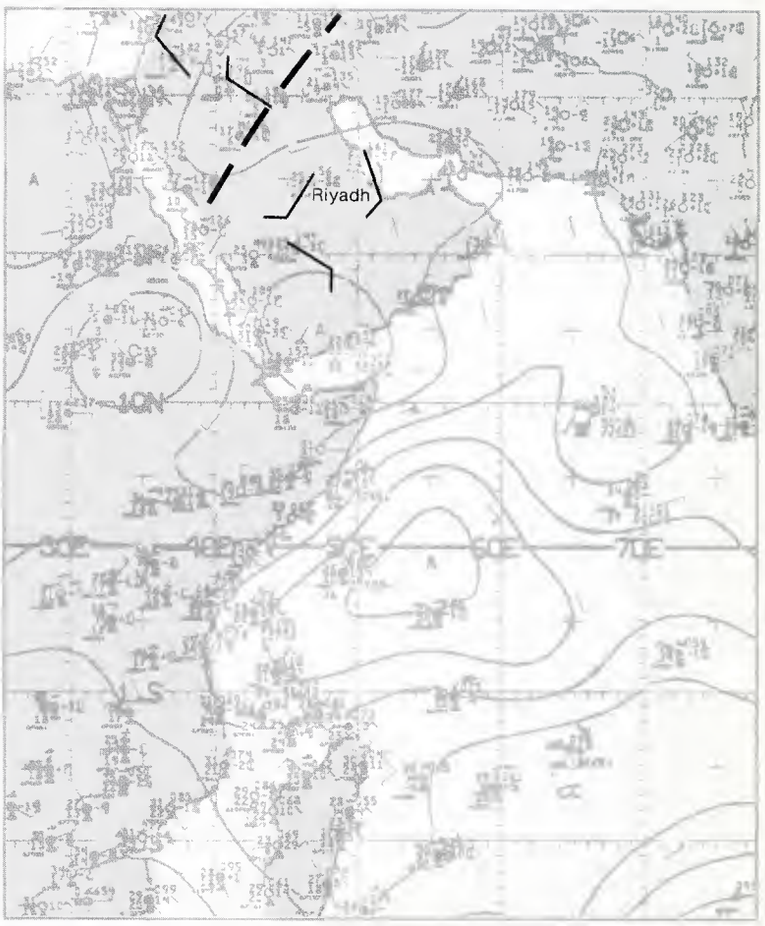

1C-26c. NMC Tropical Surface Streamline Analysis. 1200 GMT 29 January 1980.

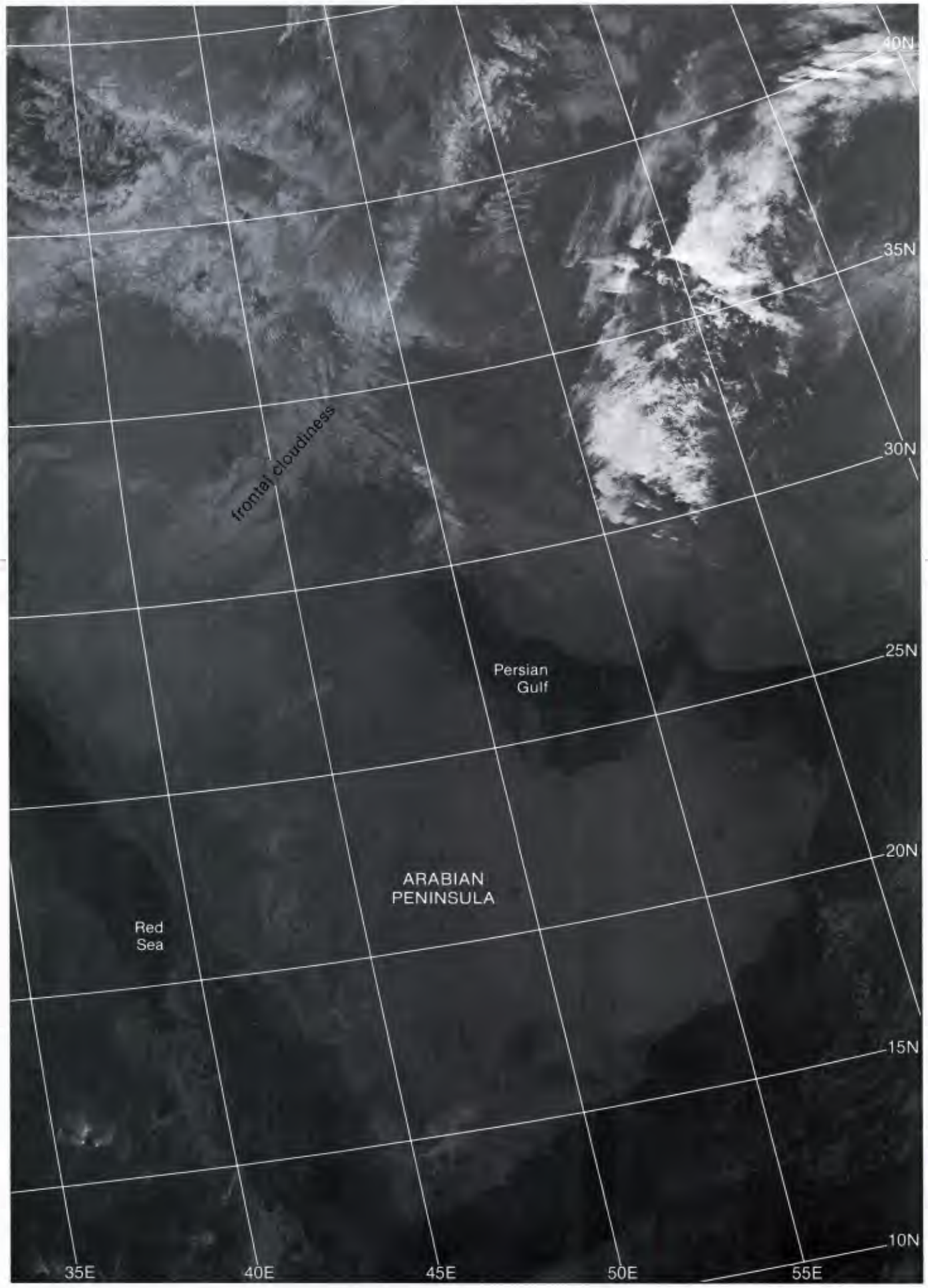

1C-27a. F-2. DMSP TF Normal Enhancement. 1830 GMT 29 January 1980.

850 mb

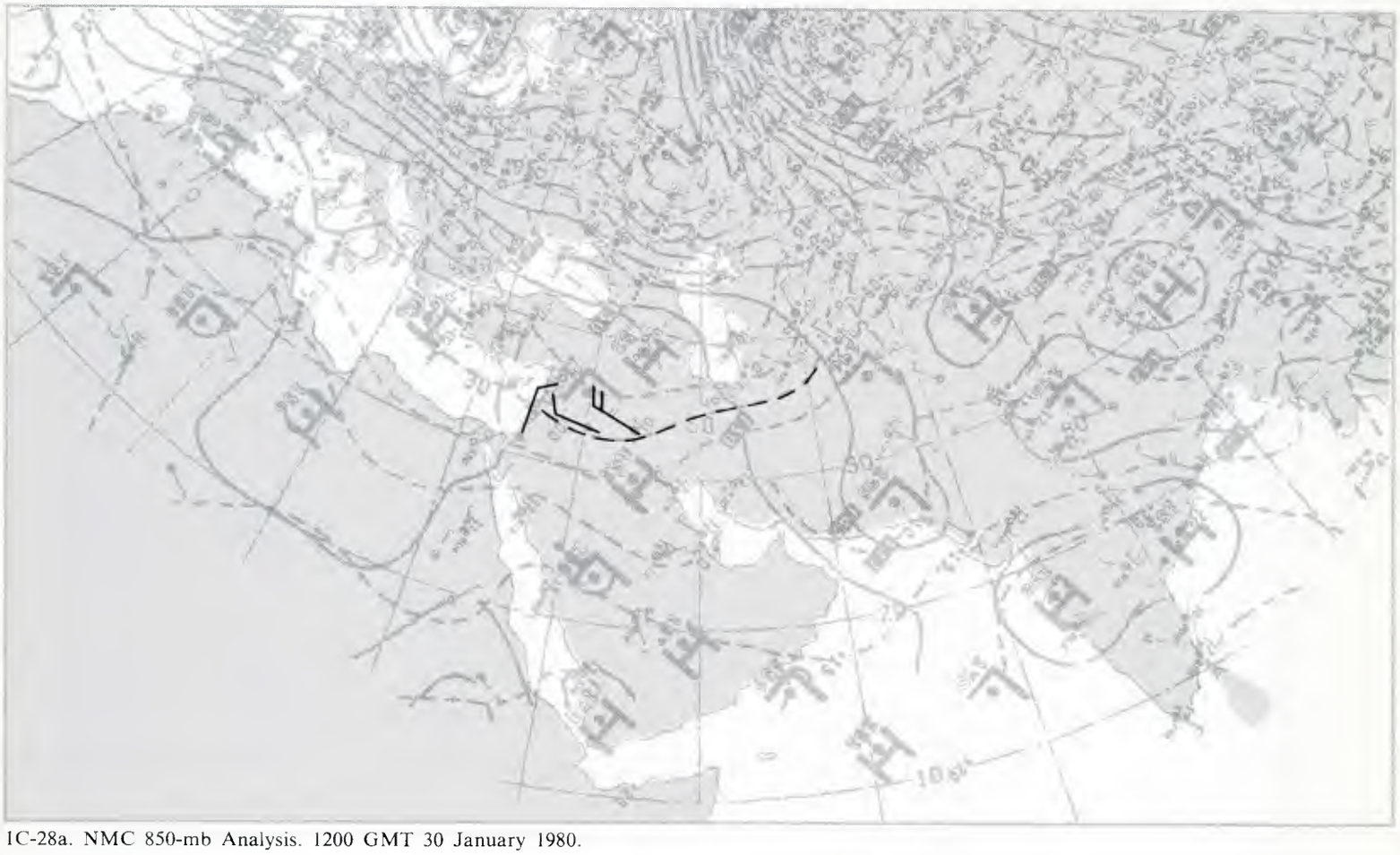

1C-28a. NMC 850-mb Analysis. 1200 GMT 30 January 1980.

surface

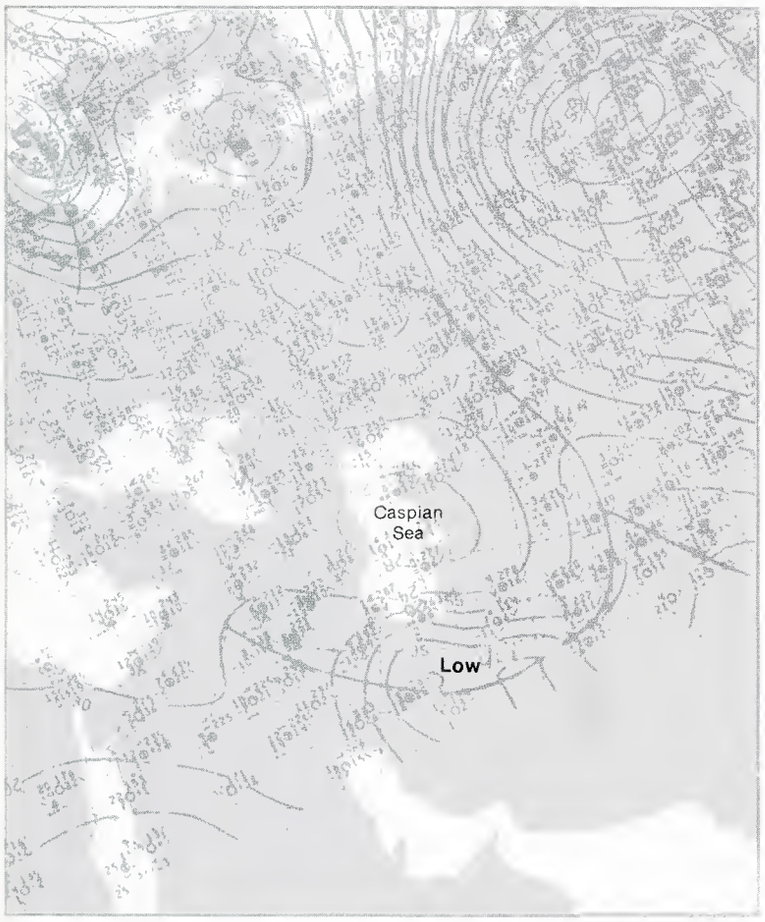

1C-28b. NMC Surface Analysis. 1200 GMT 30 January 1980.

surface

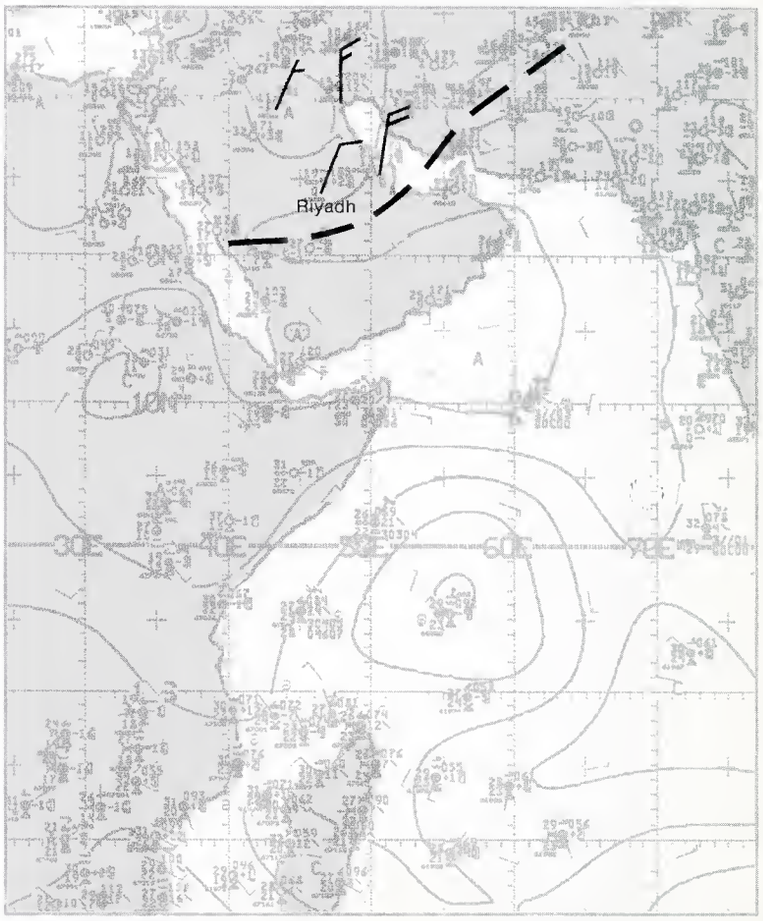

1C-28c. NMC Tropical Surface Streamline Analysis. 1200 GMT 30 January 1980.

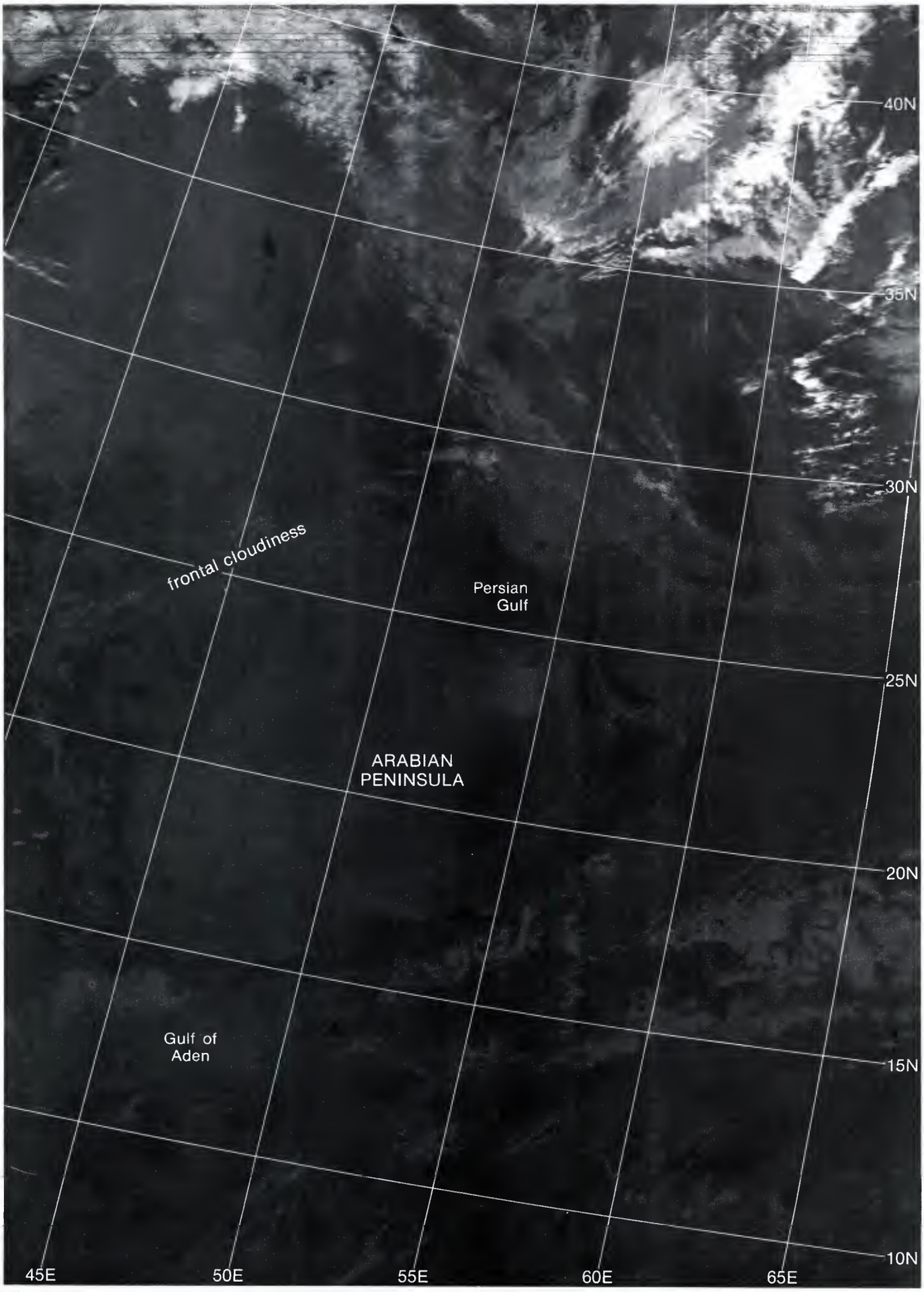

1C-29a. F-2. DMSP TS Normal Enhancement. 0545 GMT 30 January 1980.

850 mb

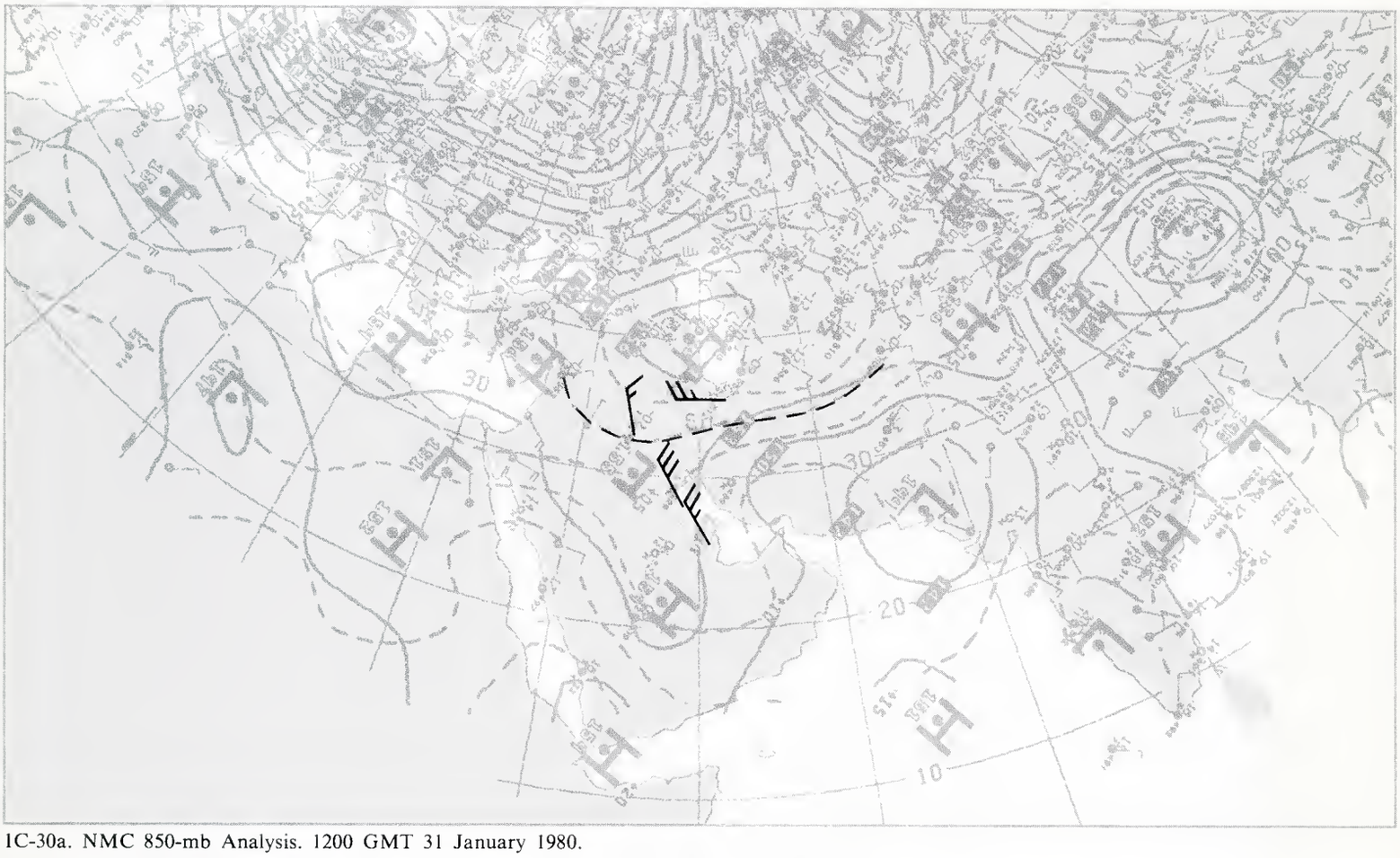

1C-30a. NMC 850-mb Analysis. 1200 GMT 31 January 1980.

surface

1C-30b. NMC Surface Analysis. 1200 GMT 31 January 1980.

surface

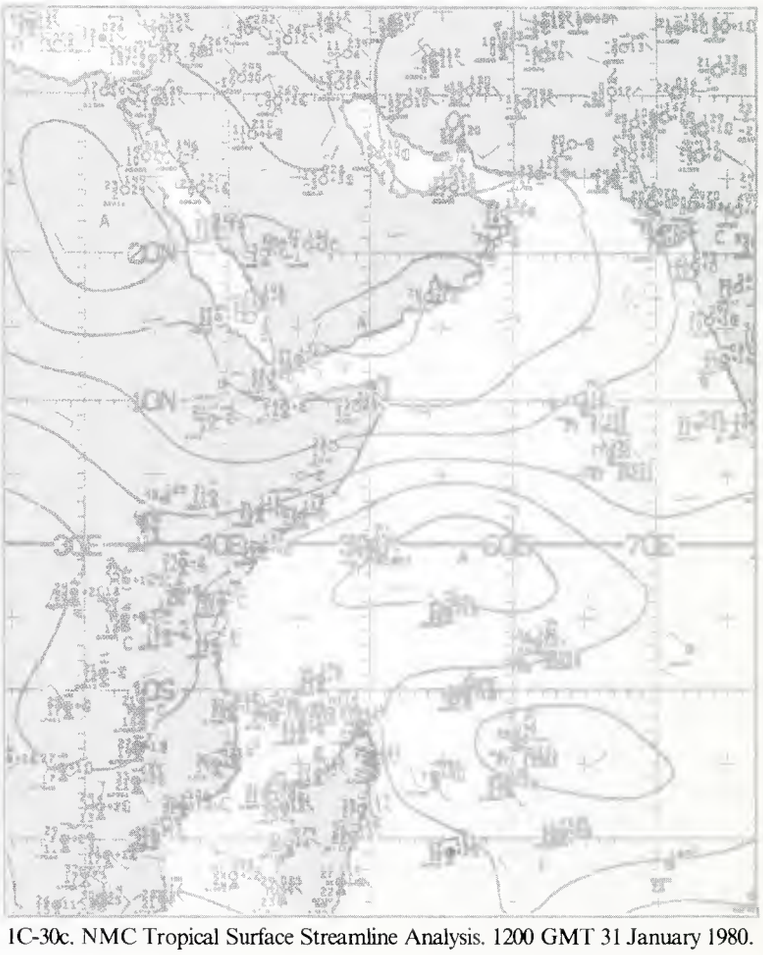

1C-30c. NMC Tropical Surface Streamline Analysis. 1200 GMT 31 January 1980.

31 January

The surface analysis for 1200 GMT (1C-30b) shows a bulge of high pressure extending southward into the Arabian Peninsula. Low pressure previously shown east of the Persian Gulf now appears well to the east as an inverted trough.

The surface streamline analysis (1C-30c) shows continuation of northerly flow and a rising pressure tendency at Riyadh. The pressure at this location, which was 1020.4 mb on 28 January at 1200 GMT, fell 10 mb to a low of 1010.7 mb on 29 January at 0000 GMT, then rose to the value of 1022.8 mb on 31 January at 1200 GMT, as high pressure moved in behind the front. High pressure over central Saudi Arabia (near 1023 mb) now contrasts with low pressure (near 1013 mb) just to the east of the Persian Gulf, where a low pressure center is analyzed. This pressure gradient has induced the beginning of the shamal in the northern Persian Gulf, where northerly winds in excess of 20 kt are reported.

At 850 mb (1C-30a), strong northwesterly flow over the northern Persian Gulf is also evident. It is the superposition of strong upper-level flow over low-level flow from the same direction that reinforces the strength of the shamal. Further progression of the cooling at this level, however, does not appear to have advanced very far in comparison with the previous 24-hour location (1C-28a).

The DMSP visible picture at 0623 GMT (1C-31a) shows the apparently benign conditions and few clouds associated with this event. The front has not moved offshore since local coastal effects in the Gulf of Aden produce cloud-free coastal corridors (land breeze effect) on both sides of the gulf.

By superimposing surface reports and a streamline analysis on the DMSP picture (1C-31b), a clear view of the weather and flow pattern can be seen. Solid contours without arrows are 500-mb contours. It is obvious that an upper trough extends over the Persian Gulf region, superimposing upper-level northerly winds on northerly surface flow. A wisp of dust off the central Persian Gulf coast of Iran attests to the beginning of a shamal event. Anticyclonically-turning flow over southern Saudi Arabia likely accounts for some of the tendency for frontal cloudiness to dissipate in this region.

1 February

The surface analysis for 1200 GMT (1C-32b) reveals that pressures, which had been rising over northern Saudi Arabia, are now beginning to fall as the ridge line **R1** moves eastward and brings higher pressures to Iran on the east side of the gulf.

The surface streamline analysis (1C-32c) shows that the surface low, previously due east of the central Persian Gulf has now moved east-southeastward to a position over western Pakistan. The pressure gradient over the central Persian Gulf has slackened as a result, and weaker wind speeds seem to signify the abatement of the shamal in that region. The 850-mb analysis (1C-32a) also shows high pressure and cold air advection extending into Iran. The 0° C isotherm has penetrated southward almost to 30° N in that region.

The DMSP visible picture at 0605 GMT (1C-33a) shows northwesterly flow effects in the southern portion of the Persian Gulf. Subtle gray shades protruding southward from the southern coast of Saudi Arabia and a clearing of cloudiness previously located in that region provide evidence that the cold front (with air temperature considerably modified by passage over the hot desert terrain) has passed out to sea. The gray shades likely are dust effects driven out to sea by northerly winds.

The convergence cloud line in the Gulf of Oman, noted by Perrone, is an indicator of the ending or last stage of the shamal over the Persian Gulf. According to Perrone, it indicates that "the shamal has ceased on the eastern side of the gulf, has diminished to the 15–20 kt range on the western side of the gulf, and will probably dissipate by evening".

Superimposing surface reports, streamlines, and 500-mb contours on the DMSP picture (1C-33b) reveals that Perrone's observations were probably correct. Winds of 10–20 kt exist in the southern Persian Gulf, but the upper-level trough has moved out over Iran and Pakistan. This foretells the ending of the shamal in the Persian Gulf. However, strong northerly flow now may be forecast offshore of Iran and Pakistan, as the trough progresses eastward.

2 February

The surface analysis for 1200 GMT (1C-34b) shows that there is even higher pressure extending into Iran, while flow entering the northern Persian Gulf appears quite weak.

The surface streamline analysis for 0000 GMT (1C-34c) shows that low pressure now has moved into northwest India, while high pressure dominates the Arabian Peninsula. The shamal over the Persian Gulf has ceased completely. However, note that strong (30 kt) offshore flow, with dust in suspension, is indicated at Jiwani, Pakistan (25.1° N, 61.8° E).

By 1200 GMT the surface streamline analysis (1C-34d) shows a lessening of northerly wind speeds, although suspended dust is still reported at Jiwani.

The 850-mb analysis for 1200 GMT (1C-34a) reveals the intense cooling that took place over Iran, with the 0° C isotherm reaching almost to the southern coast. Temperatures in this region, at 850 mb, dropped almost 10° C (18° F) in comparison to the conditions at 1200 GMT on 28 January (1C-24a).

The DMSP visible picture at 0450 GMT (1C-35a) reveals the position of the leading edge of the cold front most clearly at this time as a "rope-like" cloud structure crossing the northern Arabian Sea. A sand/duststorm of epic proportions can be seen behind the front extending southward from the coastline of Iran and Pakistan. This storm is shown more clearly in an enlargement (1C-36a) on which is superimposed the position of the aircraft carrier USS *Midway* (CV-41).

2 February continued on page 1C-36

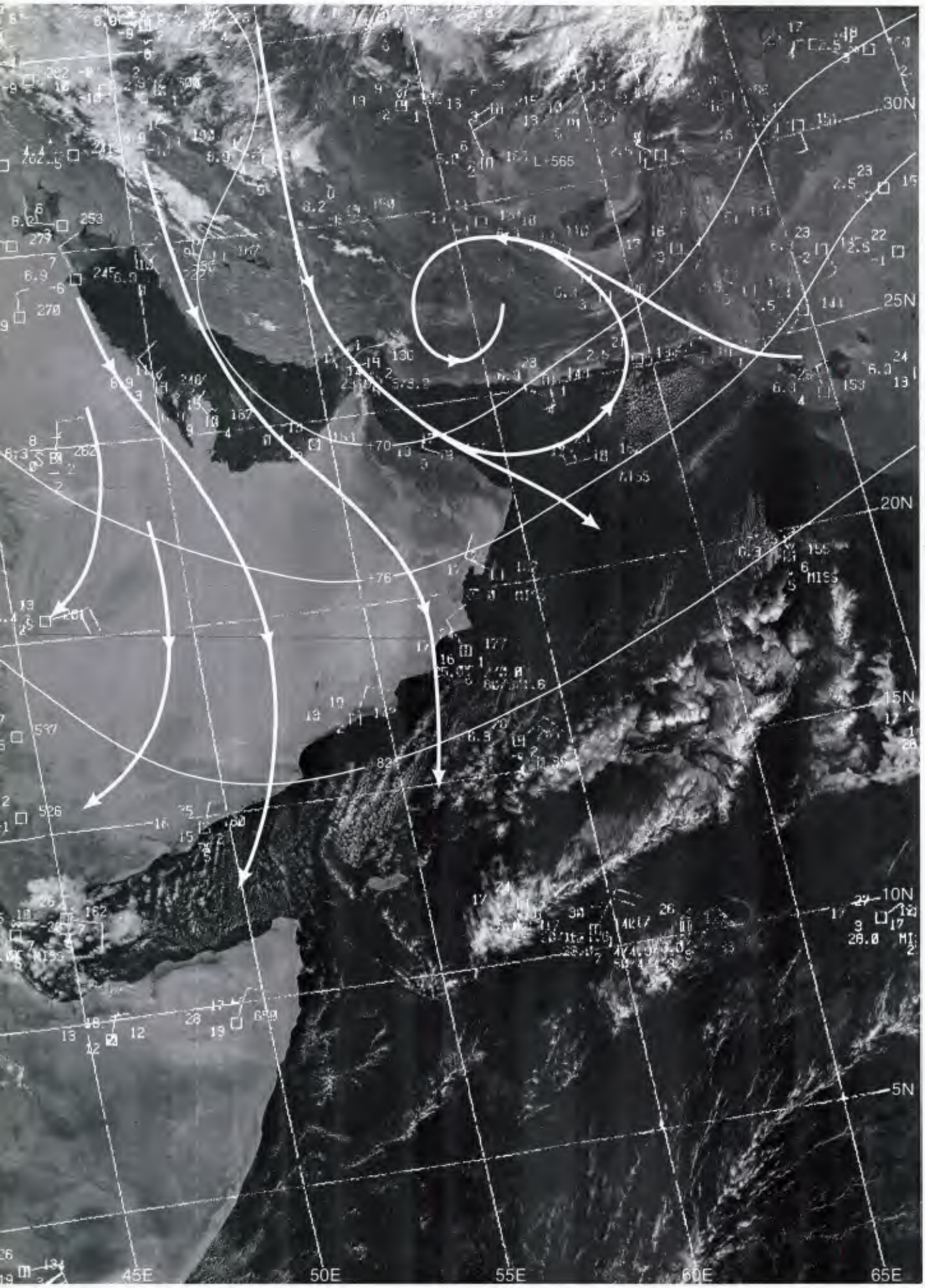

1C-31b. F-4. DMSP LF Low Enhancement. 0623 GMT 31 January 1980. (Note this picture is a repeat of 1C-31a.) Surface Wind Reports and Streamline Analysis. 0000 GMT 31 January 1980.

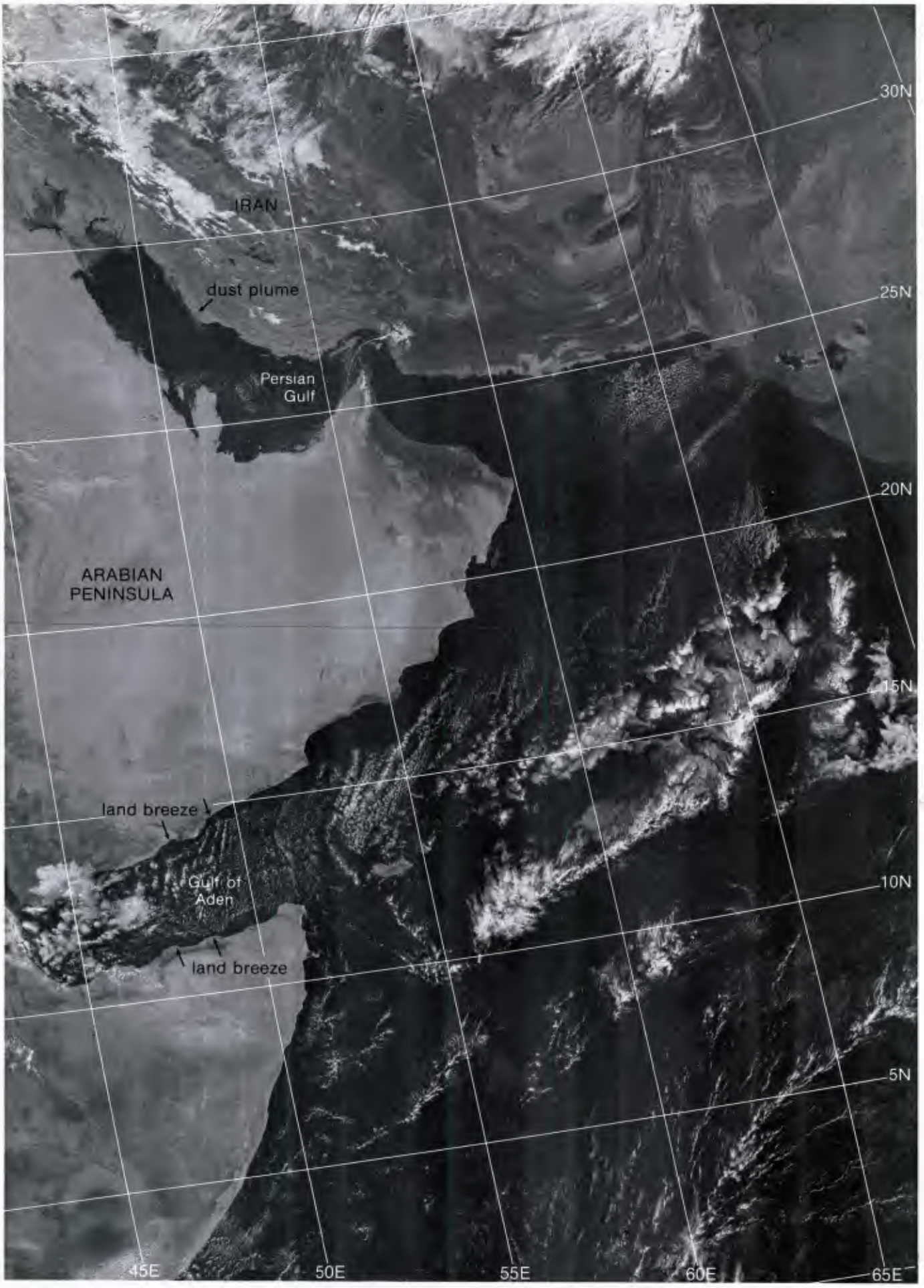

1C-31a. F-4. DMSP LF Low Enhancement. 0623 GMT 31 January 1980.

850 mb

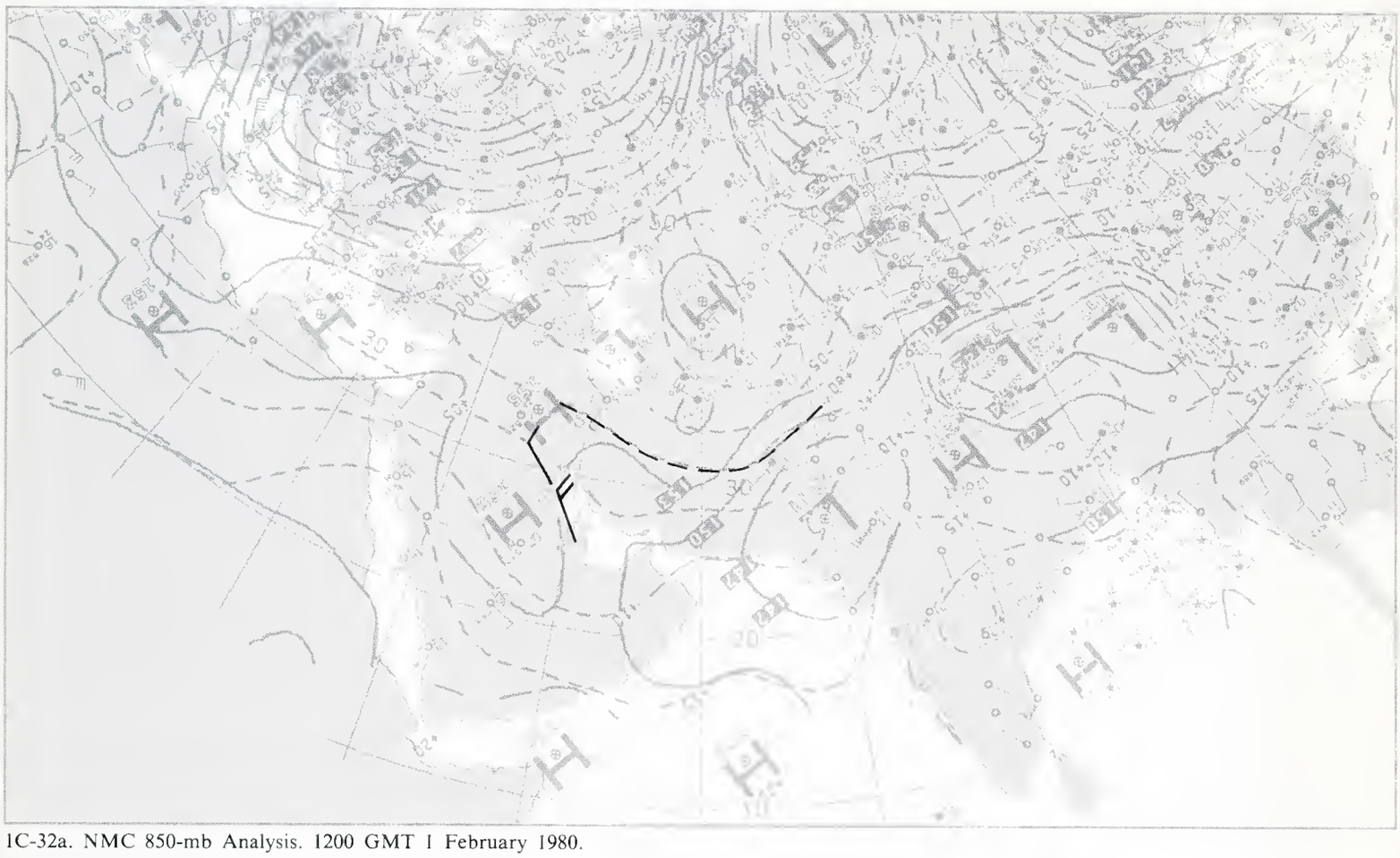

1C-32a. NMC 850-mb Analysis. 1200 GMT 1 February 1980.

surface

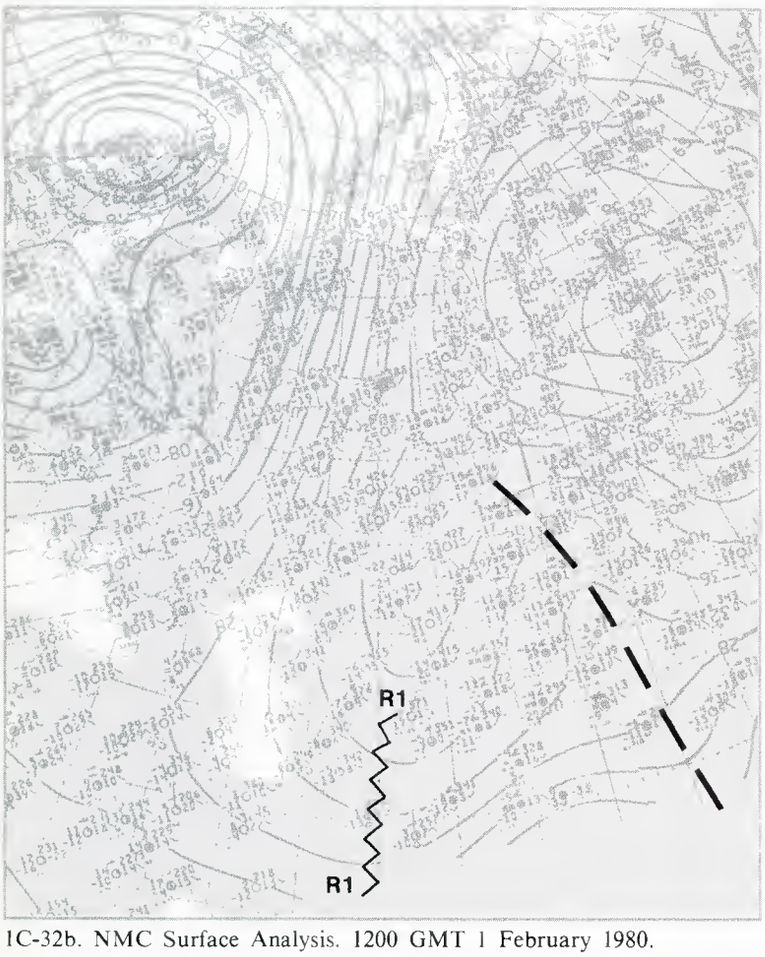

1C-32b. NMC Surface Analysis. 1200 GMT 1 February 1980.

surface

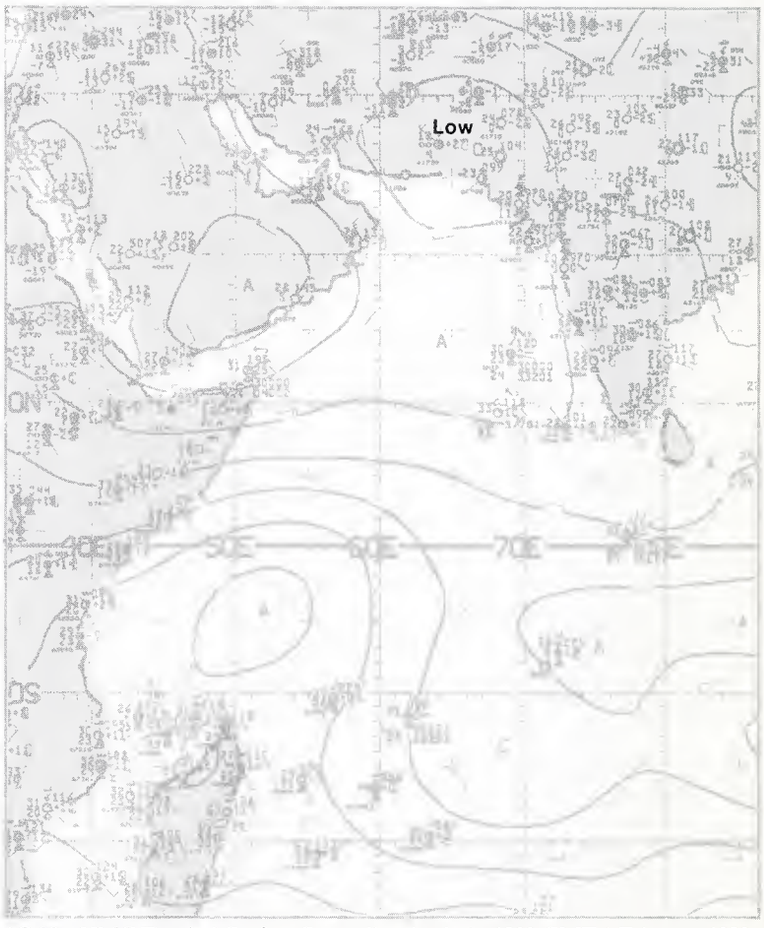

1C-32c. NMC Tropical Surface Streamline Analysis. 1200 GMT 1 February 1980.

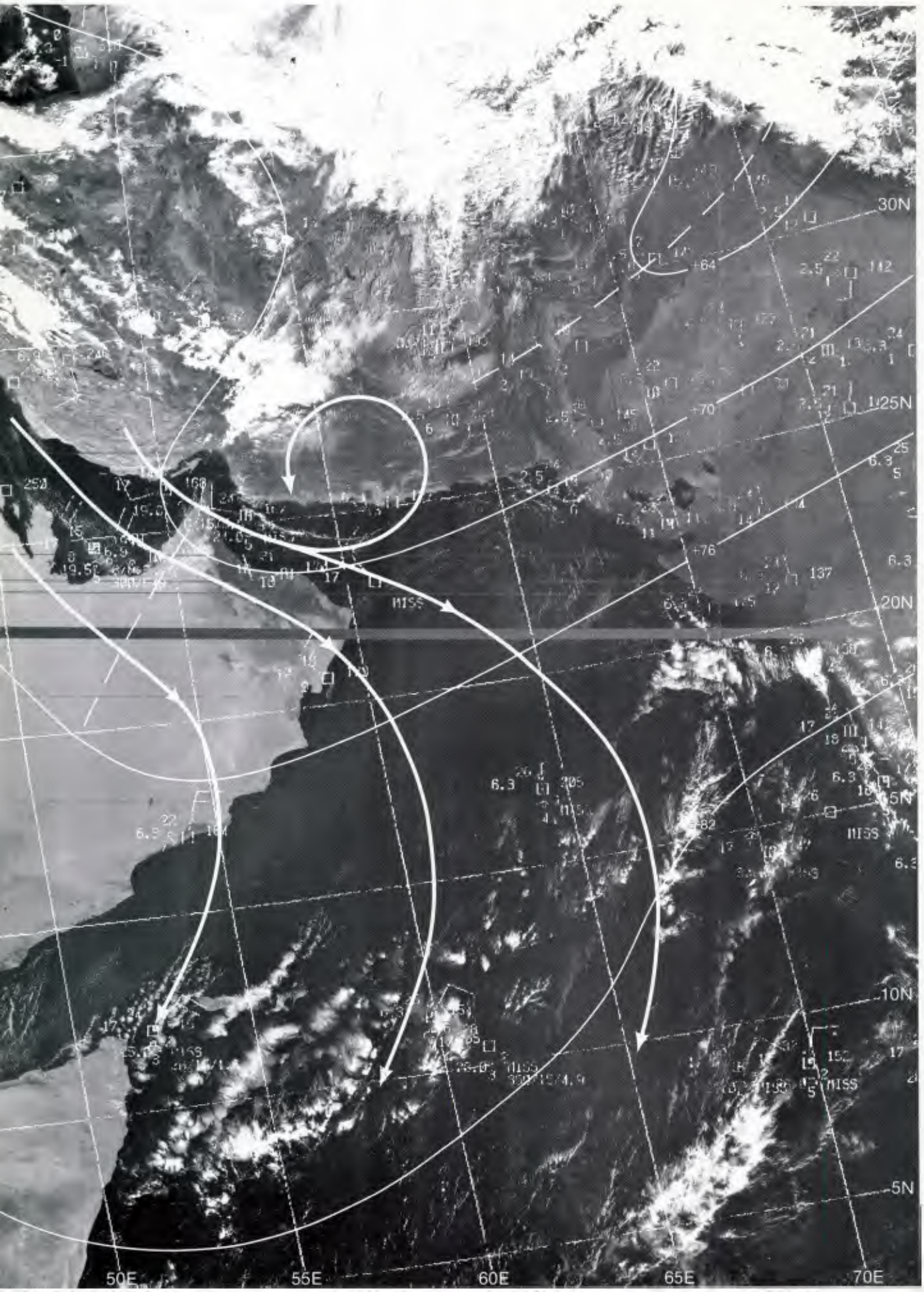

C-33b. F-4. DMSP LF Low Enhancement. 0005 GMT 1 February 1980. (Note this picture is a repeat of 1C-33a.)
Surface Wind Reports, Streamline Analysis, and 500-mb Contours. 0600 GMT 1 February 1980.

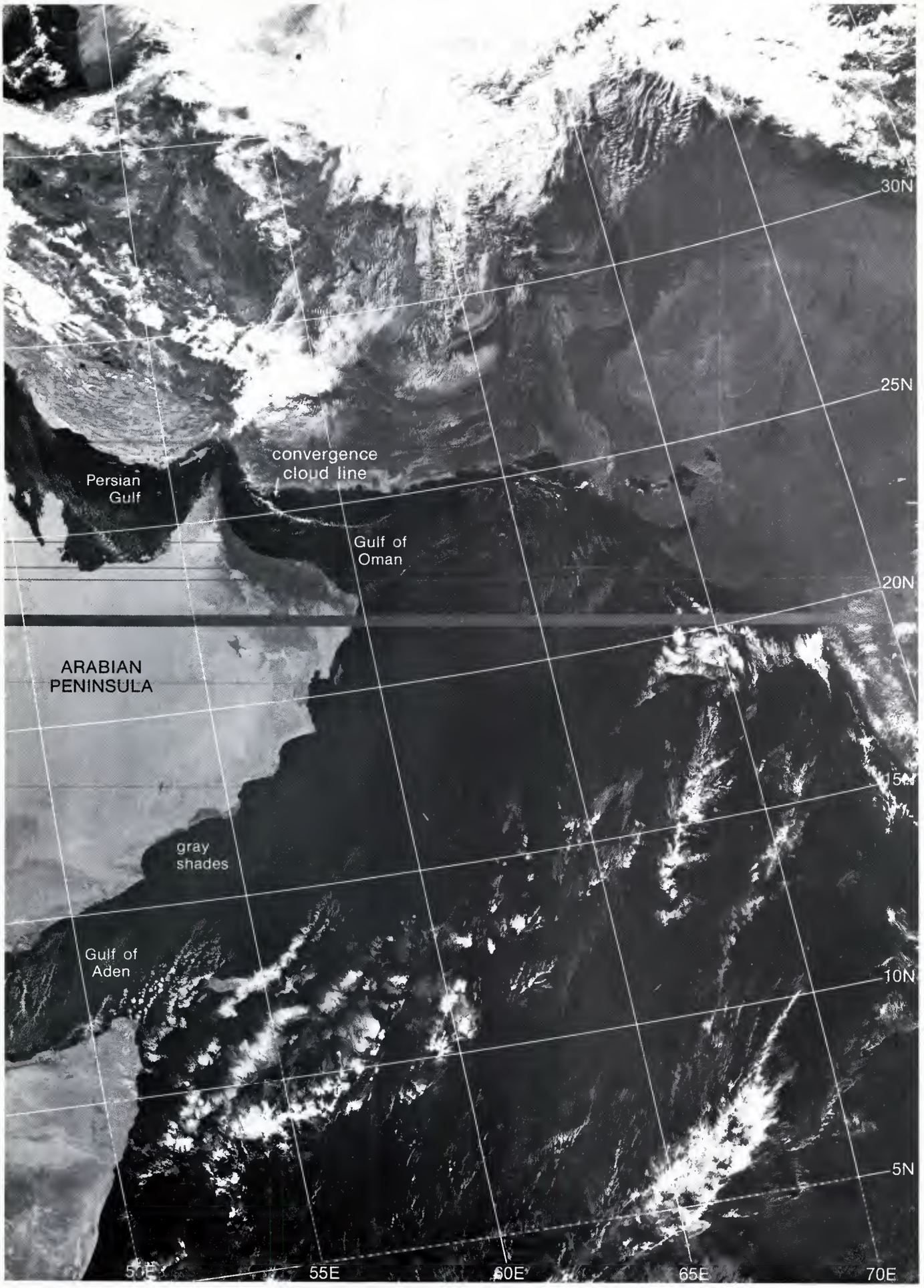

1C-33a. F-4. DMSP LF Low Enhancement. 0605 GMT 1 February 1980.

850 mb

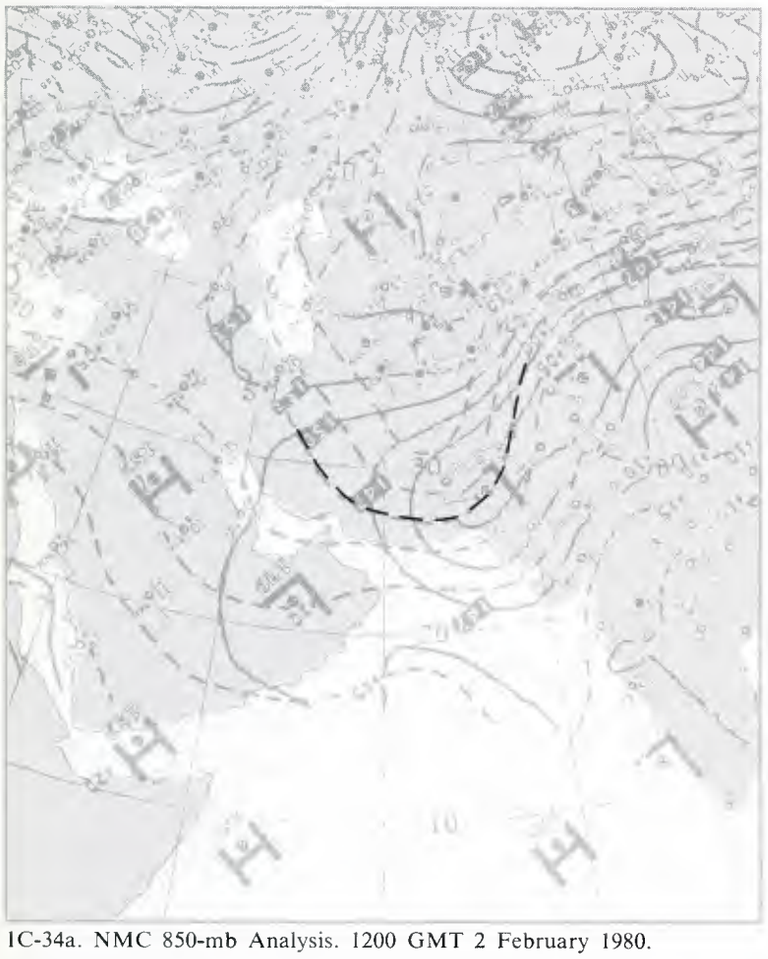

1C-34a. NMC 850-mb Analysis. 1200 GMT 2 February 1980.

surface

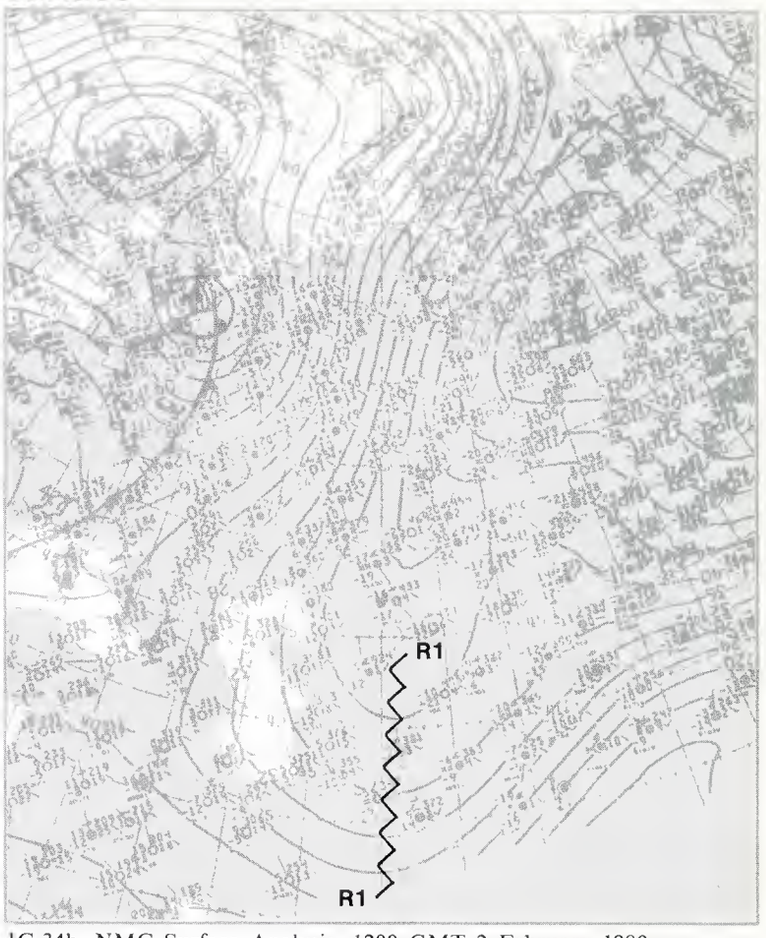

1C-34b. NMC Surface Analysis. 1200 GMT 2 February 1980.

surface

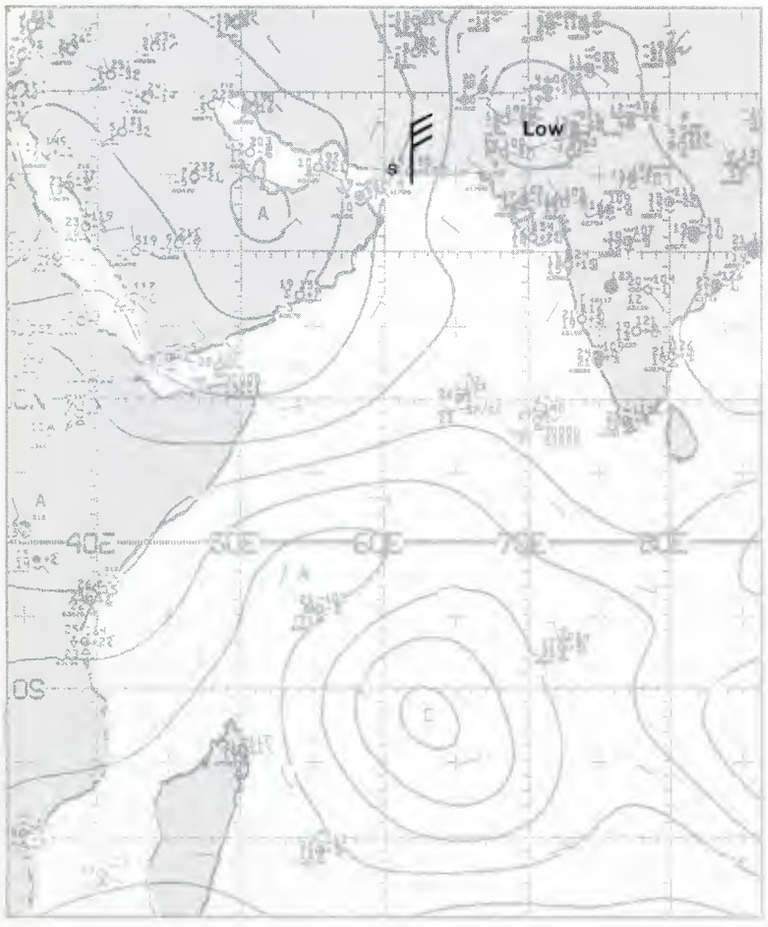

1C-34c. NMC Tropical Surface Streamline Analysis. 0000 GMT 2 February 1980.

surface

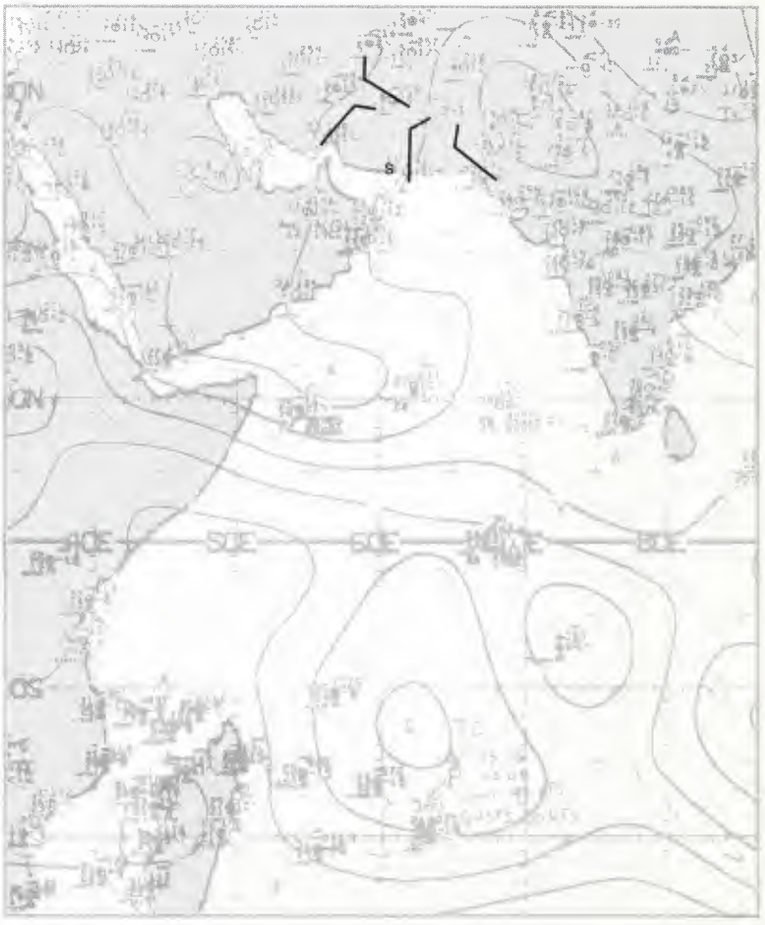

1C-34d. NMC Tropical Surface Streamline Analysis. 1200 GMT 2 February 1980.

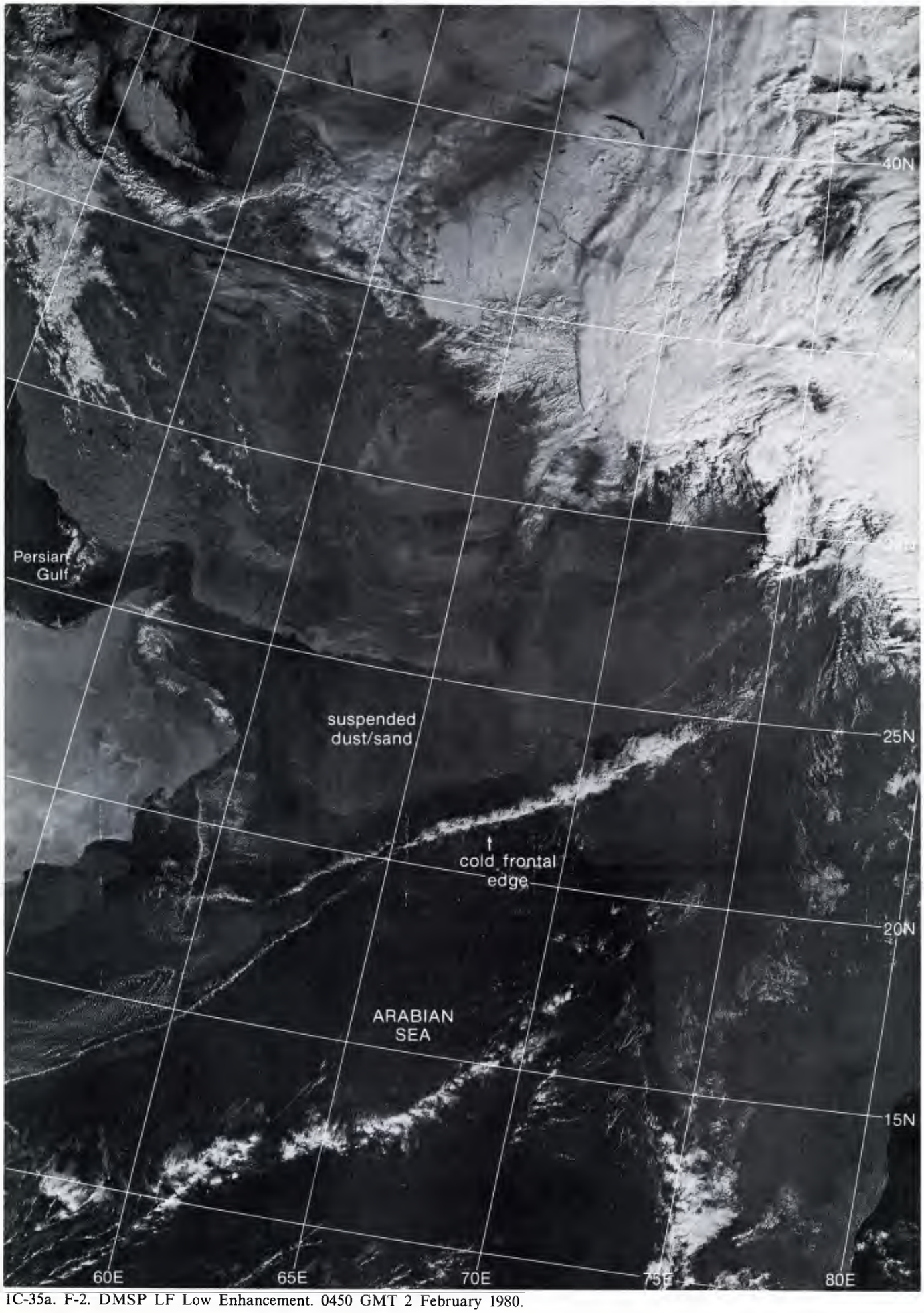

1C-35a. F-2. DMSP LF Low Enhancement. 0450 GMT 2 February 1980.

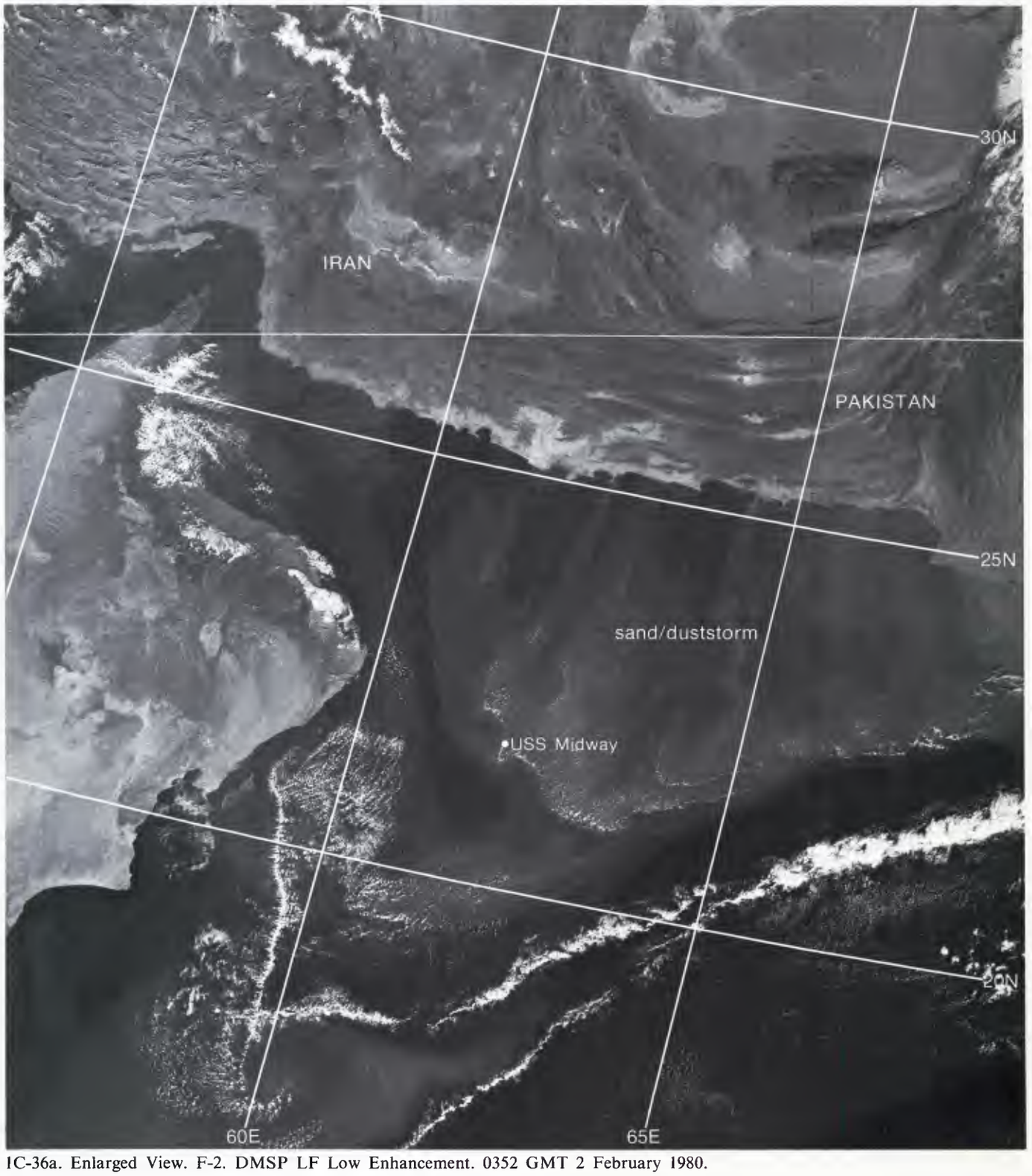

1C-36a. Enlarged View. F-2. DMSP LF Low Enhancement. 0352 GMT 2 February 1980.

It is notable that this sandstorm does not seem to obscure terrain features over Iran or Pakistan. This implies that the strong winds are picking up sand/dust at the coastline rather than in interior locations. Sand dune formations are located along the southern coast of Iran and West Pakistan. The dunes act as point sources for sand which is advected far out to sea by the strong winds. Moisture on the sand, which act as condensation nuclei, causes particle sizes to grow as the sand moves over the sea. Increased atmospheric reflection and scattering results, causing lighter gray shades to occur. Such areas are associated with poor visibility.

AG1 Michael E. Whitehead, aboard USS *Midway*, reported sand on the flight deck and aircraft, even though the ship was 100 miles from the coast. Visibilities fluctuated as the sand swept over the ship, with reduction of horizontal visibility to less than 3 miles and slant range visibility to less than 1 mile. Dust continued settling on the ship for over 24 hours.

Surface reports, streamlines, and 500-mb contours superimposed over the DMSP data (1C-37a) reveal the upper-level trough position and the flow characteristics producing this remarkable weather event.

Important Conclusions

1. To predict the shamal over the Persian Gulf over 48 hours in advance requires an analysis of surface and upper-level charts over eastern Europe.

2. The 850-mb level is an important level to analyze for effects of cold air advection associated with cold frontal movement over the Arabian Peninsula.

3. A convergence cloud line appearing in satellite data in the Gulf of Oman is a useful and reliable predictor of the ending of a shamal event.

4. Nearly cloud-free cold frontal zones can pass over Saudi Arabia. It is essential, therefore, to monitor surface reports for wind shifts and pressure tendency changes to detect frontal approach and passage.

5. After a shamal ends in the Persian Gulf, sand/duststorms may be produced in the Gulf of Oman and offshore of Iran and Pakistan.

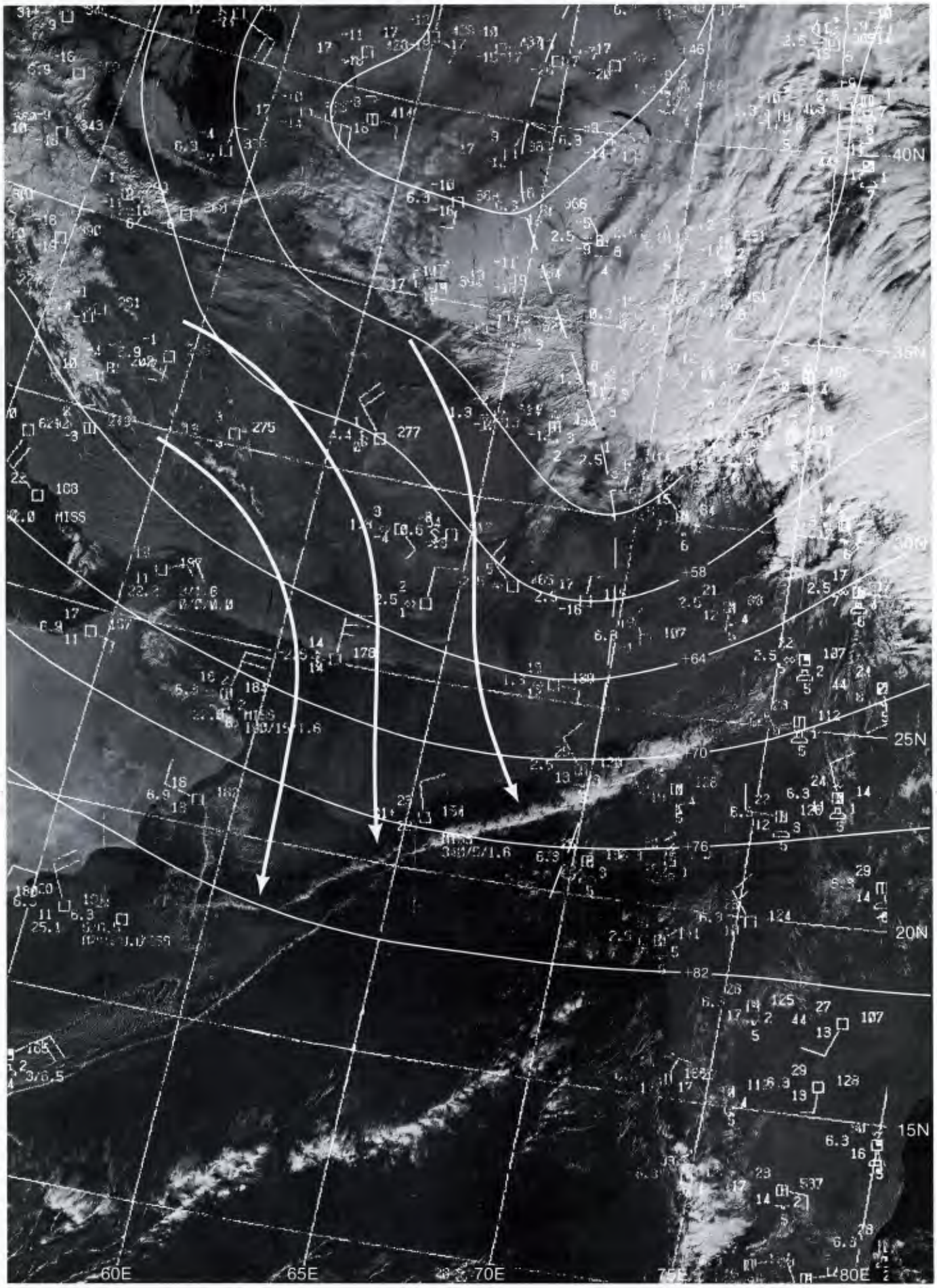

1C-37a. F-2. DMSP LF Low Enhancement. 0450 GMT 2 February 1980. (Note this picture is a repeat of 1C-35a.) Surface Wind Reports, Streamline Analysis, and 500-mb Contours. 0600 GMT 2 February 1980.

Case 1 Arabian Sea/Bay of Bengal—Spring Transition

The Arabian Sea Anticyclone
Spring Transition Circulation Features

The Monsoon Experiment (MONEX) over the Arabian Sea during April and May 1979 resulted in the gathering of a more extensive wind data set than had ever before been obtained over that area. A major input was satellite-derived winds which defined the flow at approximately the 850- and 200-mb levels for the spring transition period.

The mean 850-mb wind flow pattern for the period 1–15 May 1979 (1D-2a) and the corresponding mean flow at 200 mb (1D-3a) show the flow patterns that define the typical circulations at these levels during the spring transition to the southwest monsoon.

850 mb

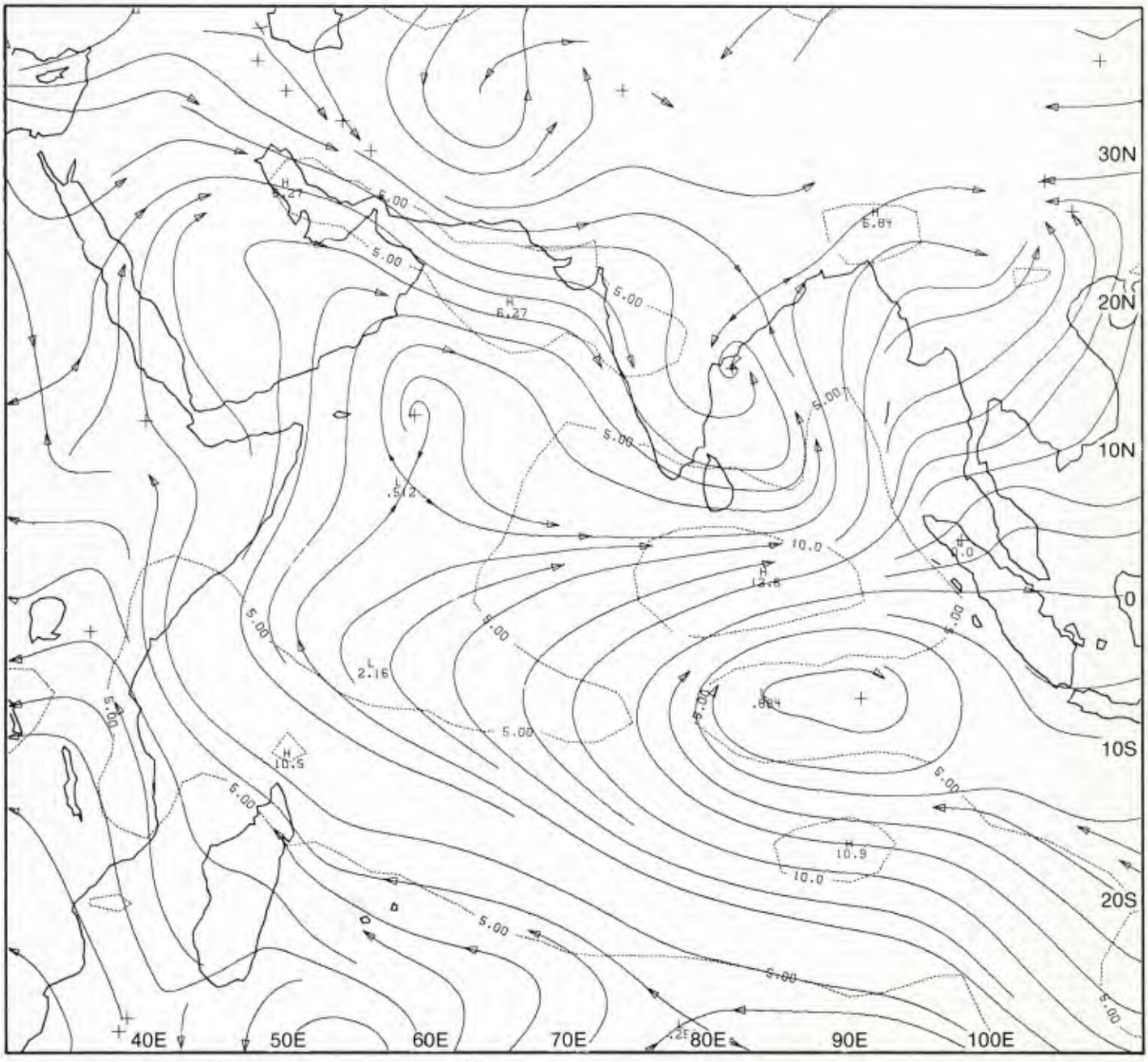

1D-2a. MONEX Mean 850-mb Analysis. 1–15 May 1979.

A dominant feature over the Arabian Sea at the 850-mb level (1D-2a) is an anticyclone which brings southerly flow past Somalia to Saudi Arabia, and northwesterly flow over the northern Arabian Sea into India.

An asymptote of convergence at the 200-mb level (1D-3a) overlies the low-level anticyclone. The suggestion of upper-level convergence and lower-level divergence, with pronounced subsidence from aloft, also implies that such an area should be quite cloud free, particularly along the ridge line extending from the anticyclone center where subsidence is always most pronounced. Thus, satellite evidence should be very helpful in locating such a feature and in determining the alignment of the ridge axis.

200 mb

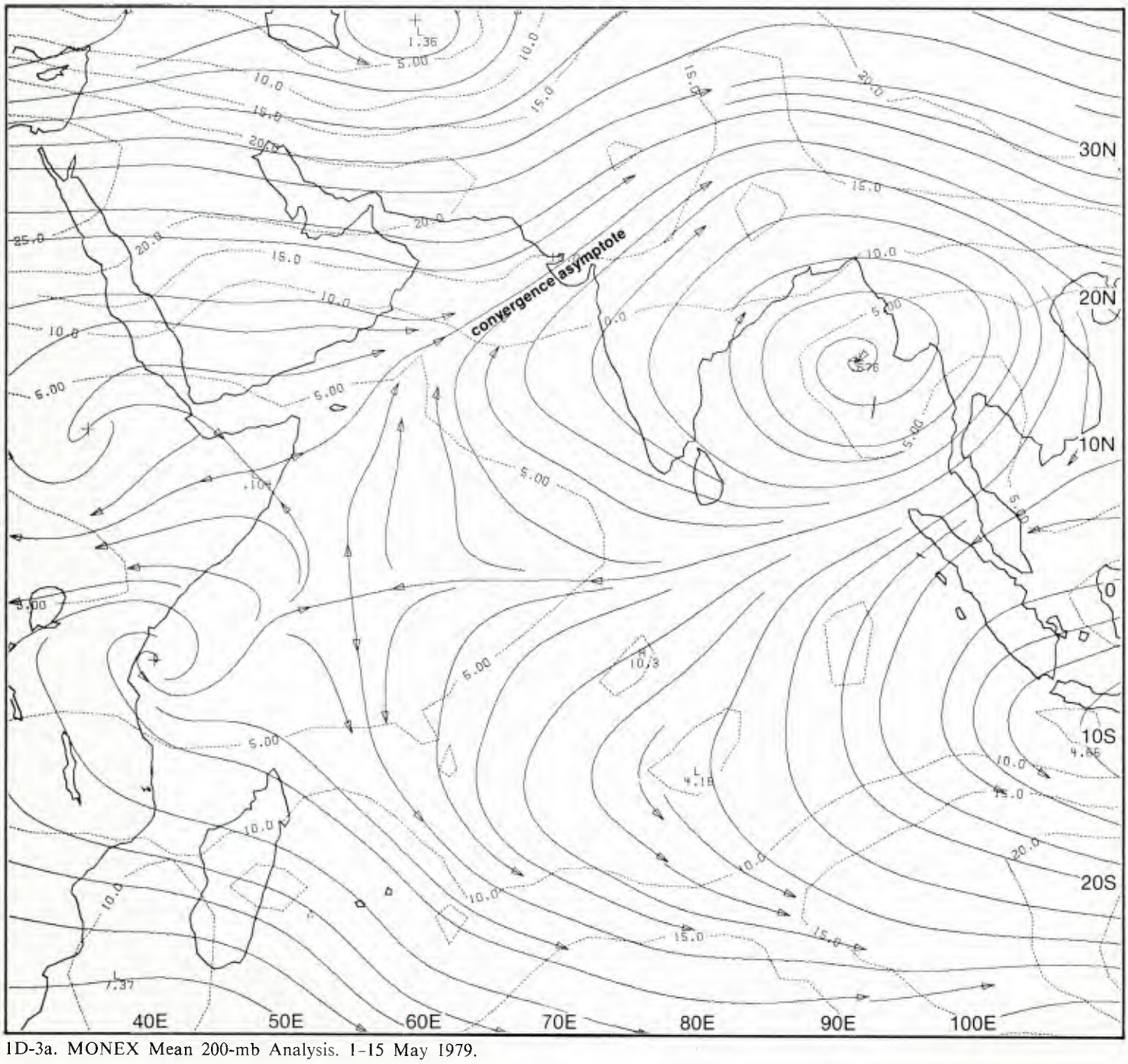

1D-3a. MONEX Mean 200-mb Analysis. 1-15 May 1979.

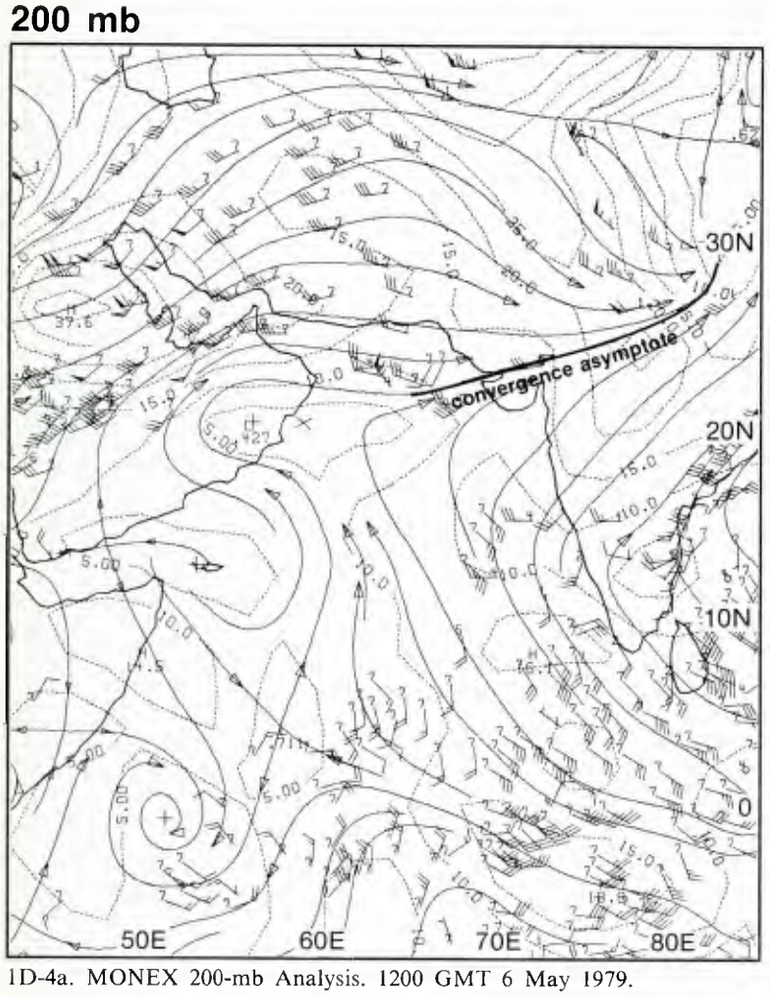

1D-4a. MONEX 200-mb Analysis. 1200 GMT 6 May 1979.

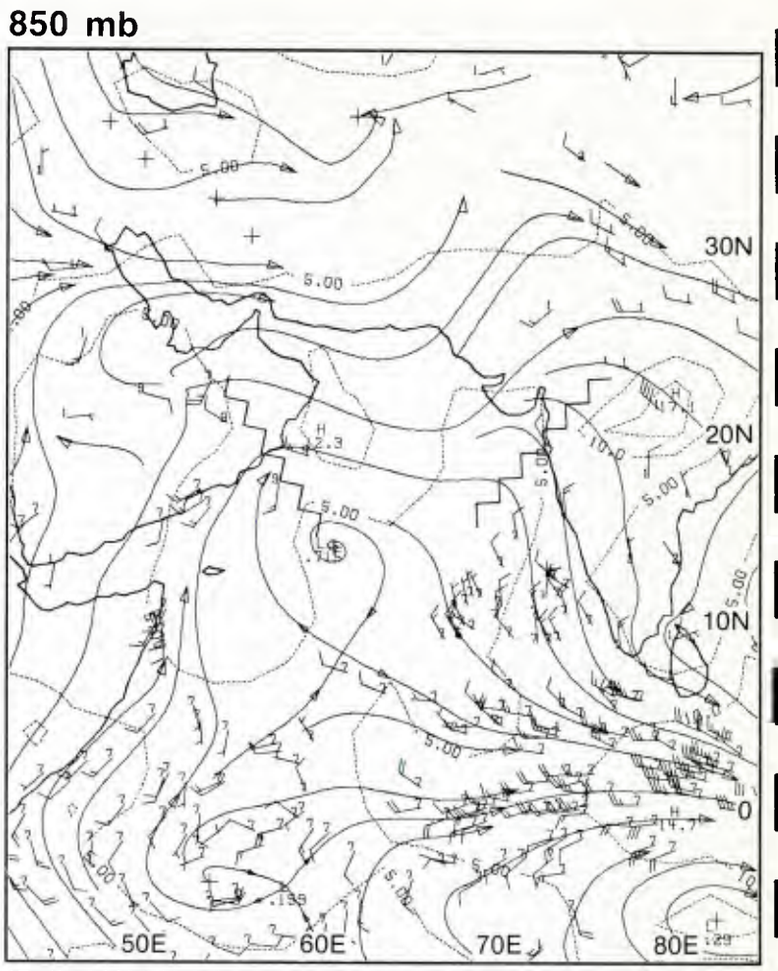

1D-4b. MONEX 850-mb Analysis. 1200 GMT 6 May 1979.

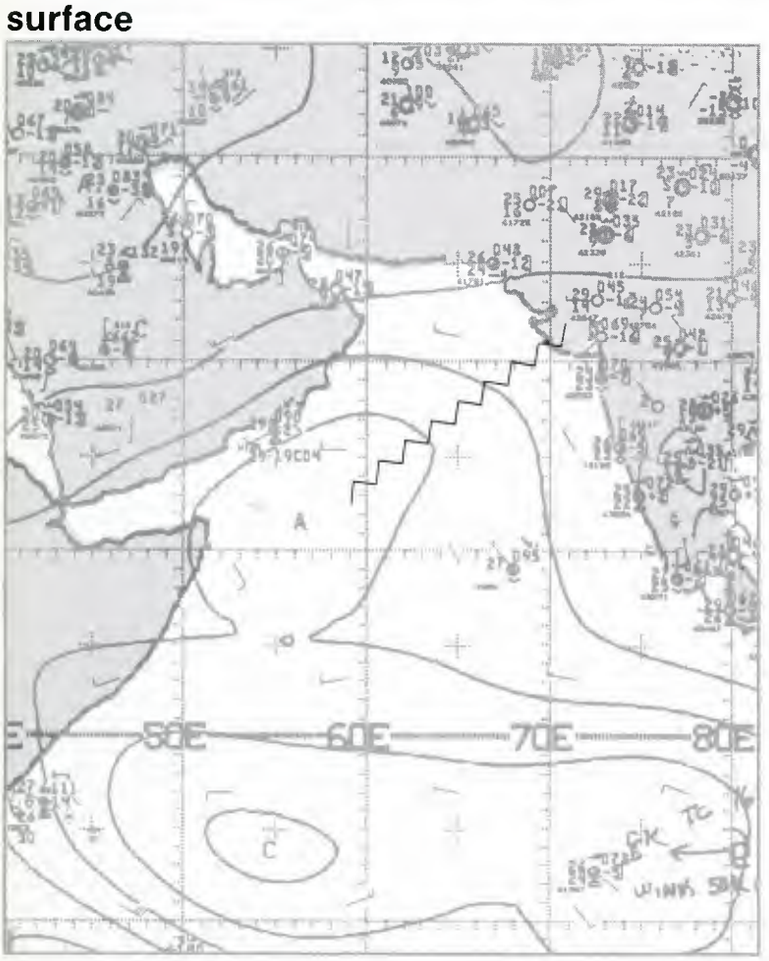

1D-4c. NMC Tropical Surface Streamline Analysis. 0000 GMT 6 May 1979.

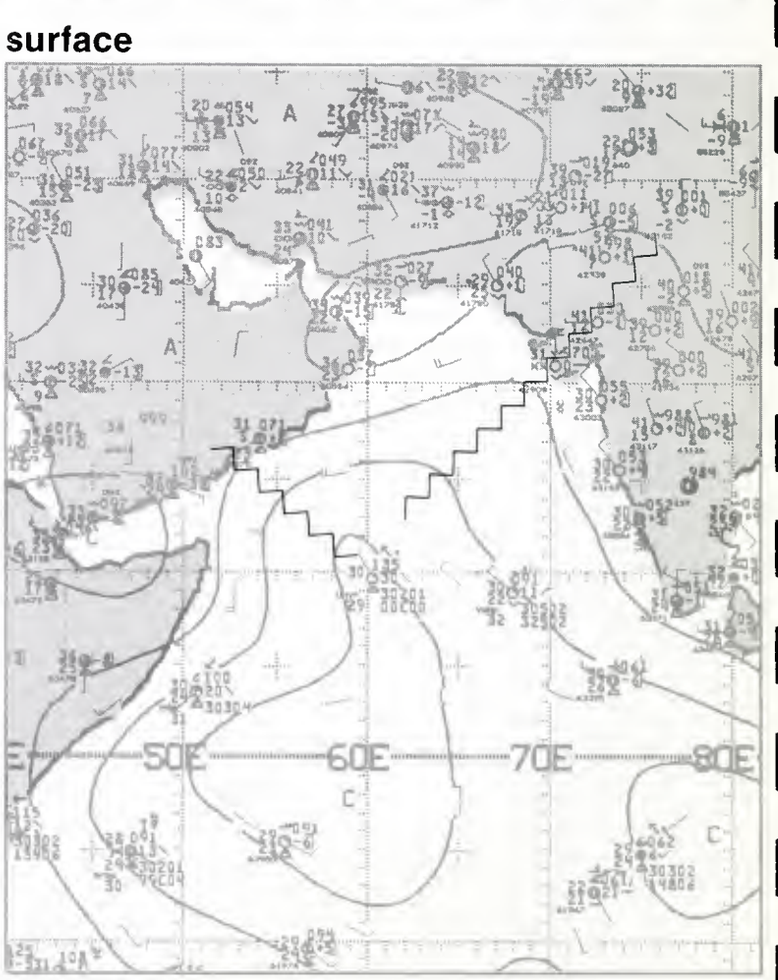

1D-4d. NMC Tropical Surface Streamline Analysis. 1200 GMT 6 May 1979.

6 May

The 0000 GMT (1D-4c) and 1200 GMT (1D-4d) NMC surface streamline analyses show an anticyclonic turning of the winds over the northern Arabian Sea with a ridge line oriented southwest to northeast, from the central Arabian Sea into the northwest portion of India. On the 1200 GMT analysis a second ridge line extends northwestward to the coast of the Arabian Peninsula.

This flow pattern and ridge line alignment is additionally verified by the MONEX 850-mb analysis (1D-4b), which includes many satellite cloud motion vectors. The MONEX 200-mb analysis (1D-4a) shows an asymptote of convergence which nearly overlies the position of the lower-level ridge line in the northern Arabian Sea.

The DMSP visible picture (1D-5a), with superimposed surface winds, reveals an especially clear area in the ridge line region. The absence of cloudiness in this region suggests pronounced subsidence. Heightened reflectivity along the coastline of India is caused by sunglint off calmer waters in the region of sea breeze subsidence.

The corresponding DMSP infrared picture (1D-5b) shows warmest temperatures (medium gray shades) coincident with the clear slot and along the coastline of the west coast of India, where sea breeze subsidence could be anticipated in this near-noon (LST) picture.

It is apparent that a meteorologist familiar with the climatology of the Arabian Sea during the spring transition season could use the satellite evidence to accurately locate the ridge line position and deduce direction and relative intensity of wind flow about the ridge line based purely on the satellite pictures, if deprived of other observations.

7 May

The surface streamline analyses for 0600 GMT (1D-6c) and 1200 GMT (1D-6d) reveal the continuation of the anticyclone over the Arabian Sea. The 850-mb analysis (1D-6b) shows ridging in alignment with the surface anticyclone, while at 200 mb (1D-6a), confluent flow from the surface anticyclone position into the west coast of northern India is apparent.

The DMSP visible picture, with superimposed surface winds (1D-7a), reveals a clear slot in the ridge line **R1** region. These data suggest that the ridge terminates, in its southward extremity, at about 5° N, 57° E. Data in the surface analyses are not sufficient to verify this condition, but can accomodate such a possibility. As on the previous date, the corresponding infrared picture (1D-7b) shows warmest temperatures (medium gray shades) over the clear region. Gradual cooling (light gray shades) of the infrared response to the northeast, even over an apparently clear area, indicates water vapor contamination and/or the presence of cloud particles too small to be resolved by the DMSP 2 n mi resolution LS sensor. The contours of temperature in the infrared data over that area correspond to gray shade contours in the DMSP visible data, lending support to the above argument. Note that the island of Socotra has produced a lee calming effect. The bright return north-northeast of the island is sunglint from calm seas and not a cloud, as can be verified by the infrared imagery which reveals very warm temperatures in that region.

8 May

Surface streamline analyses at 0000 GMT (1D-8c) and 1200 GMT (1D-8d) continue to show anticyclonic turning of the winds over the northern Arabian Sea with an anticyclonic center indicated at approximately 15° N, 60° E at 0000 GMT.

The 850-mb analysis (1D-8b) shows a north–south oriented ridge extending into the northern Arabian Sea near longitude 60° E, with a secondary ridge into northwest India. An anticyclonic couplet is apparent at the 200-mb level (1D-8a) over the northern Arabian Sea. Upper confluent flow is shown coming in from the southeast, over the low-level anticyclone (1D-8c and 8d).

The DMSP visible picture (1D-9a) shows a sunglint pattern through the Arabian Sea indicating a high center or ridge line extending from southwest to northeast through the area near 12° N, 60° E, just south of the anticyclonic center position indicated on the 0000 GMT surface analysis.

Superimposed surface winds and streamline analysis (1D-9a) show the dominance of the Arabian Sea anticyclone over the area at this time. Cloud lines are reliable indicators of the direction of low-level flow in the tropics and these have been used to verify: (a) The existence of the southeast trades to the southwest of the high; (b) Southwest flow past Somalia around the east portion of the high; and, (c) Northwest flow to the northeast of the high into India. These are characteristic features of the Arabian Sea area during the spring transition season.

The use of the sunglint pattern enables the meteorologist to determine a very close approximation of the location of the ridge line and is indicative of where sea state should be very close to calm, the calmest of the entire region.

The simultaneous DMSP infrared picture (1D-9b) reveals the warm temperatures (medium gray shades) outlining the clearest region associated with the surface anticyclone.

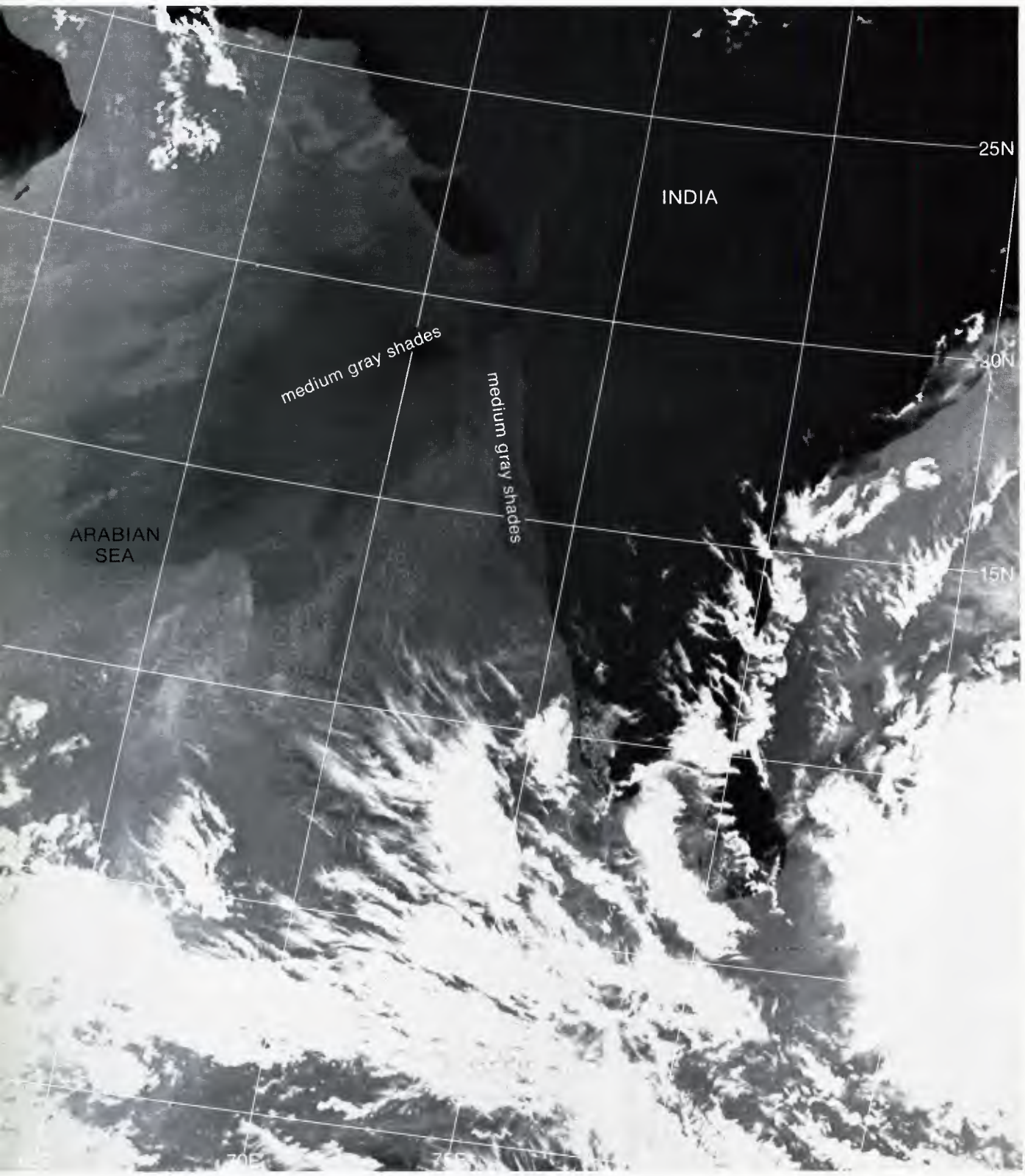

1D-5b. F-1. DMSP TS Low Enhancement. 0605 GMT 6 May 1979.

Important Conclusions

1. During the spring transition season to the summer southwest monsoon expect:
   a. Southeast trade wind flow around the southern portion of the Arabian Sea high in the region south of the Equator.
   b. Southwest flow around the west side of the high past Somalia.
   c. Northwest flow around the northeast portion of the high from near the Gulf of Oman into India.
2. DMSP visible and infrared imagery are useful in determining the ridge line axis associated with the high over the Arabian Sea.
3. Low-level cloud lines apparent in DMSP visible imagery are useful indicators of the direction of low-level flow and aid in determining the best possible streamline analysis for the region.

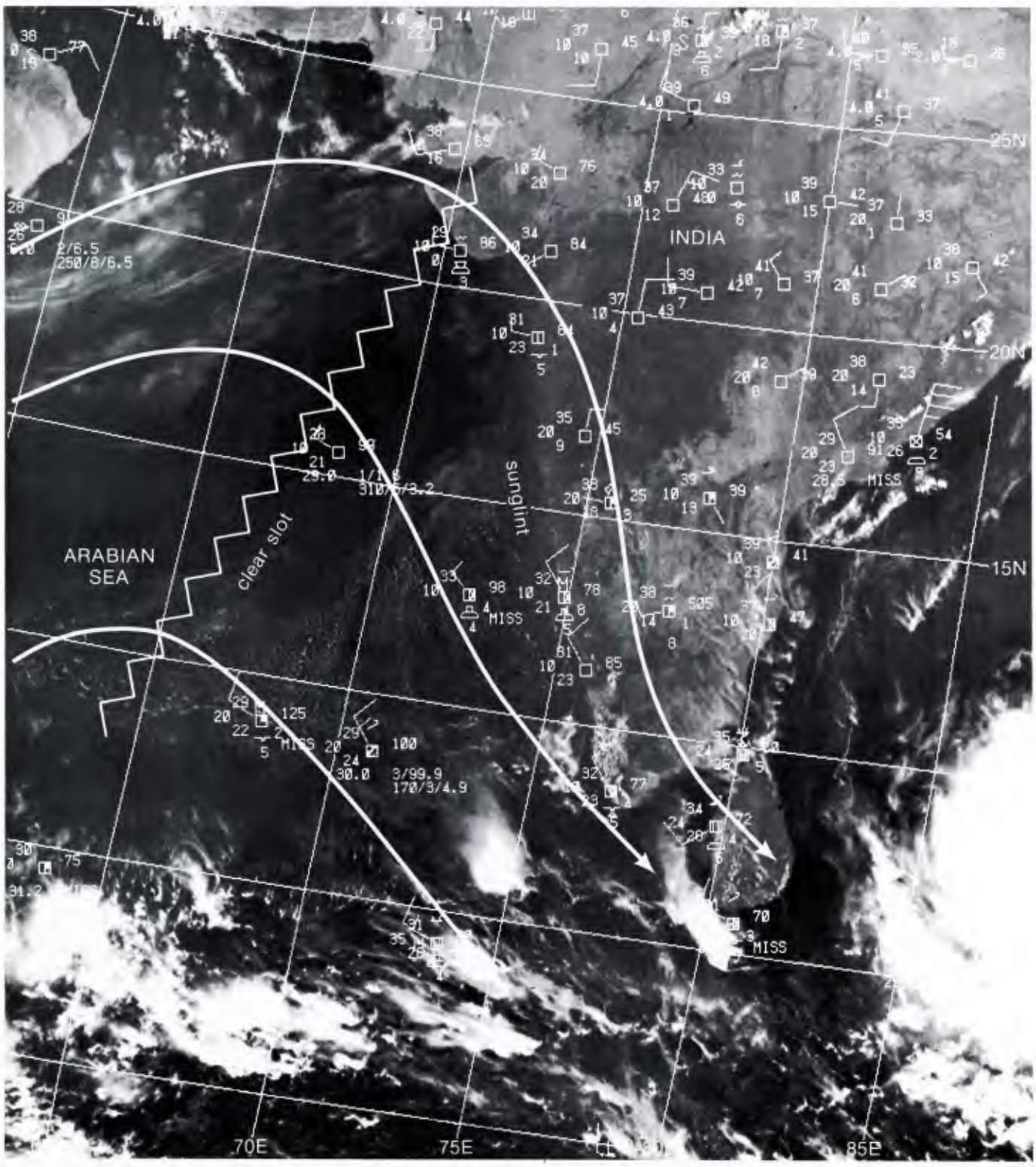

1D-5a. F-1. DMSP LS Low Enhancement. 0605 GMT 6 May 1979.
Surface Wind Reports and Streamline Analysis. 0600 GMT 6 May 1979.

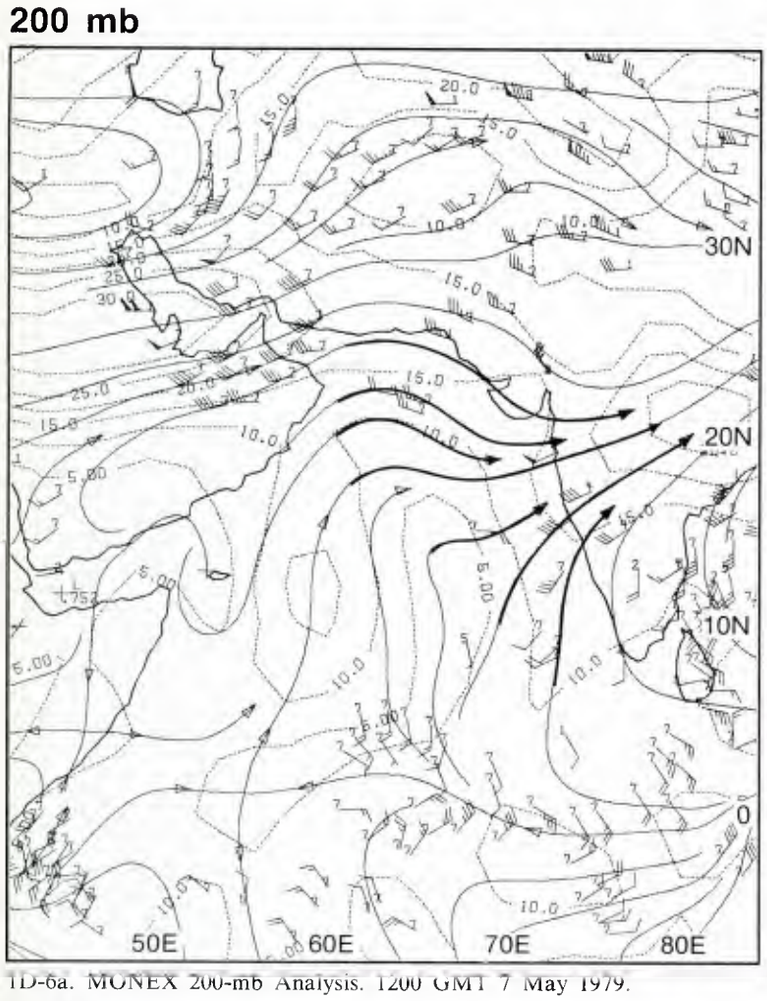

1D-6a. MONEX 200-mb Analysis. 1200 GMT 7 May 1979.

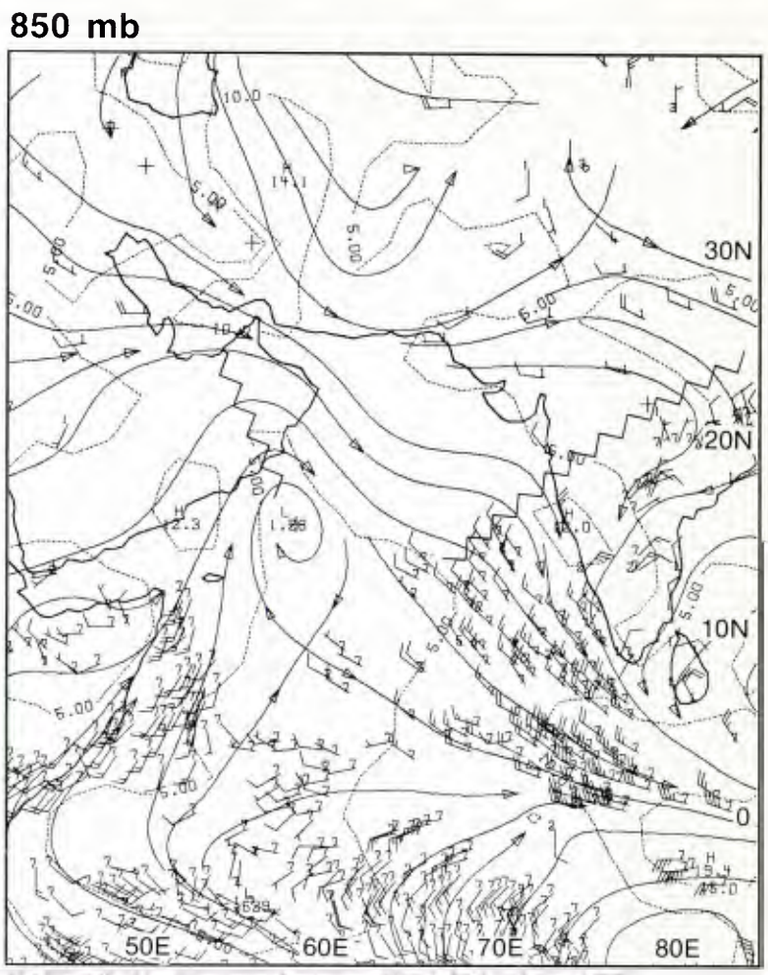

1D-6b. MONEX 850-mb Analysis. 1200 GMT 7 May 1979.

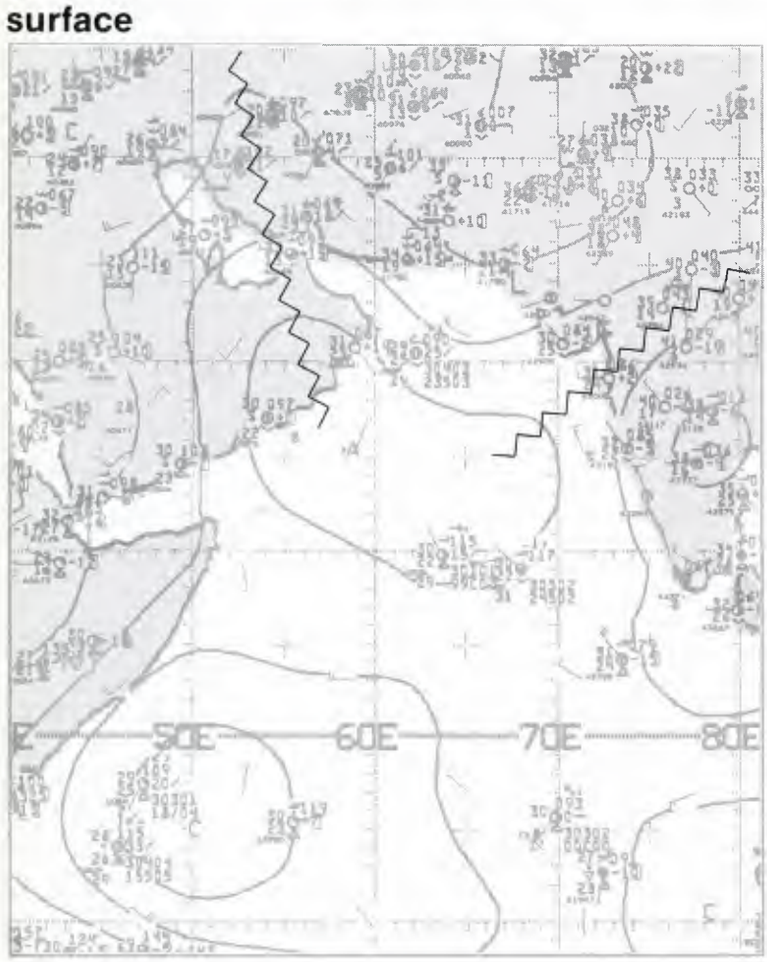

1D-6c. NMC Tropical Surface Streamline Analysis. 0600 GMT 7 May 1979.

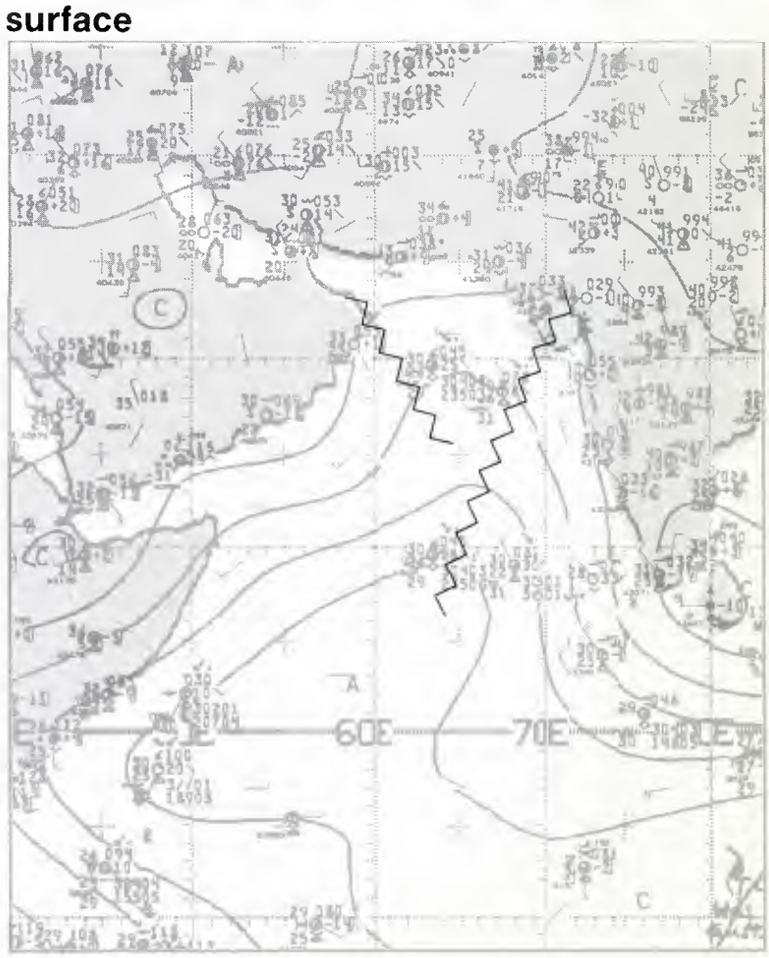

1D-6d. NMC Tropical Surface Streamline Analysis. 1200 GMT 7 May 1979.

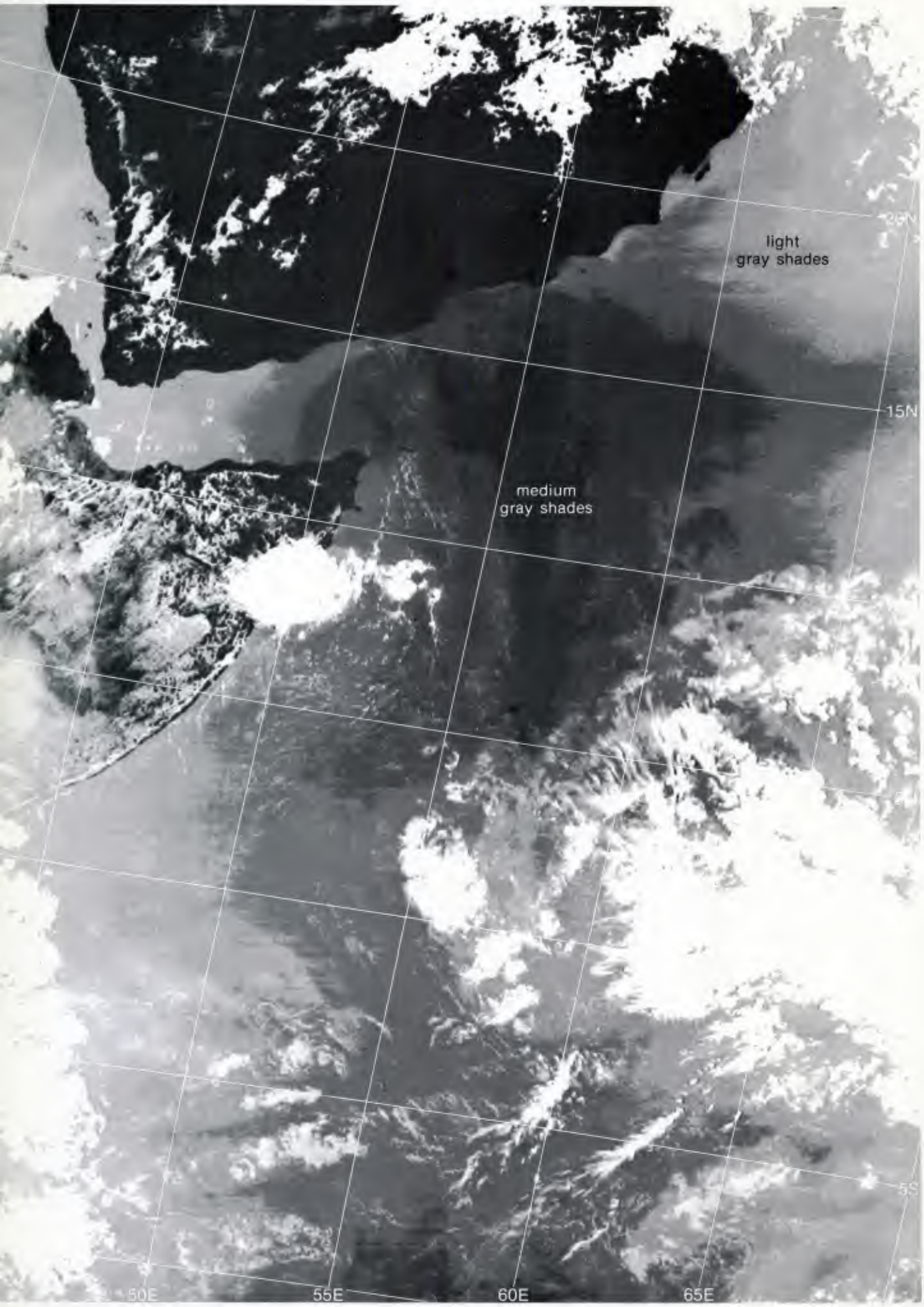

1D-7b. F-1. DMSP TS Low Enhancement. 0728 GMT 7 May 1979.

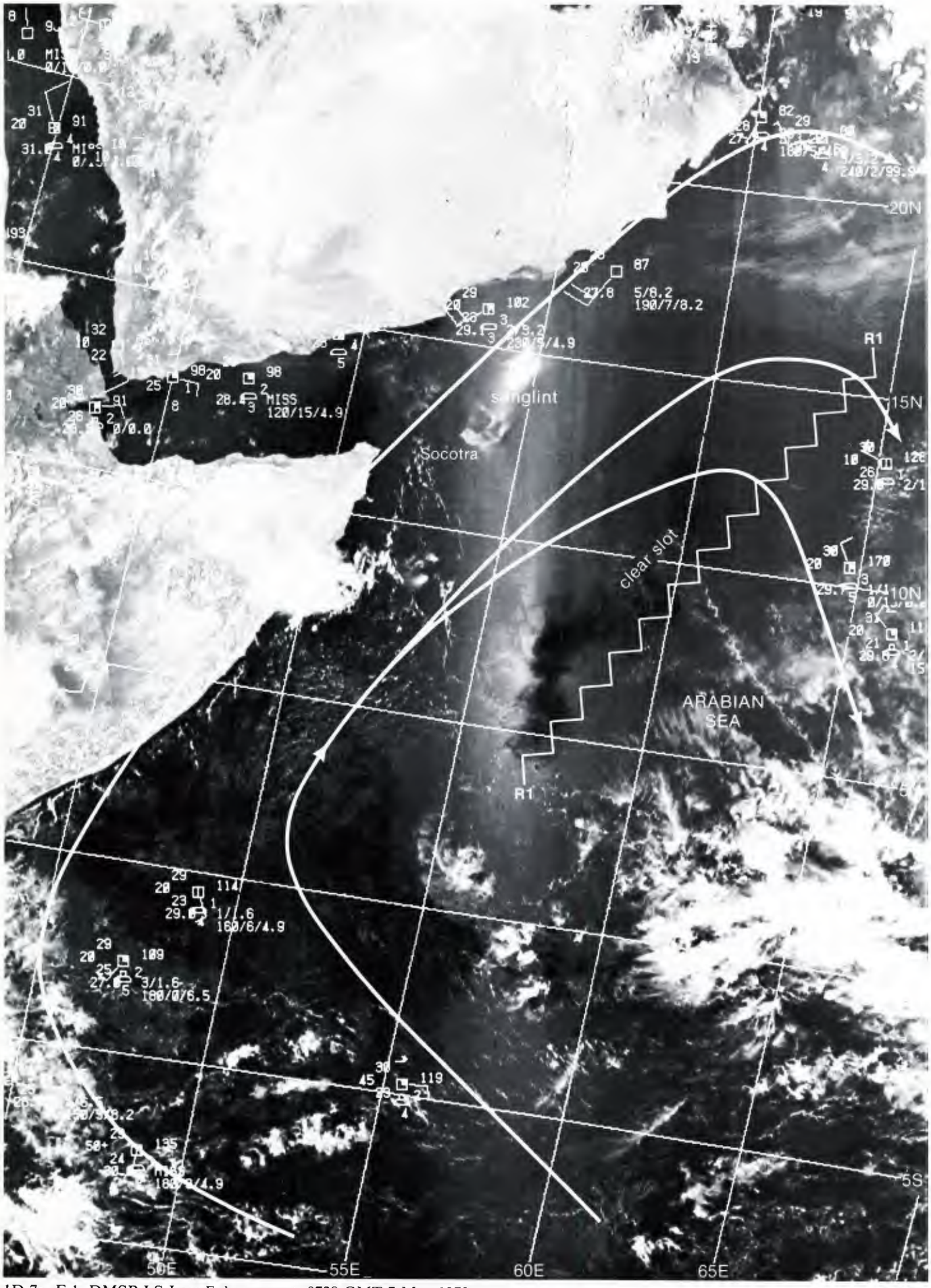

1D-7a. F-1. DMSP LS Low Enhancement. 0728 GMT 7 May 1979.
Surface Wind Reports and Streamline Analysis. 0600 GMT 7 May 1979.

200 mb

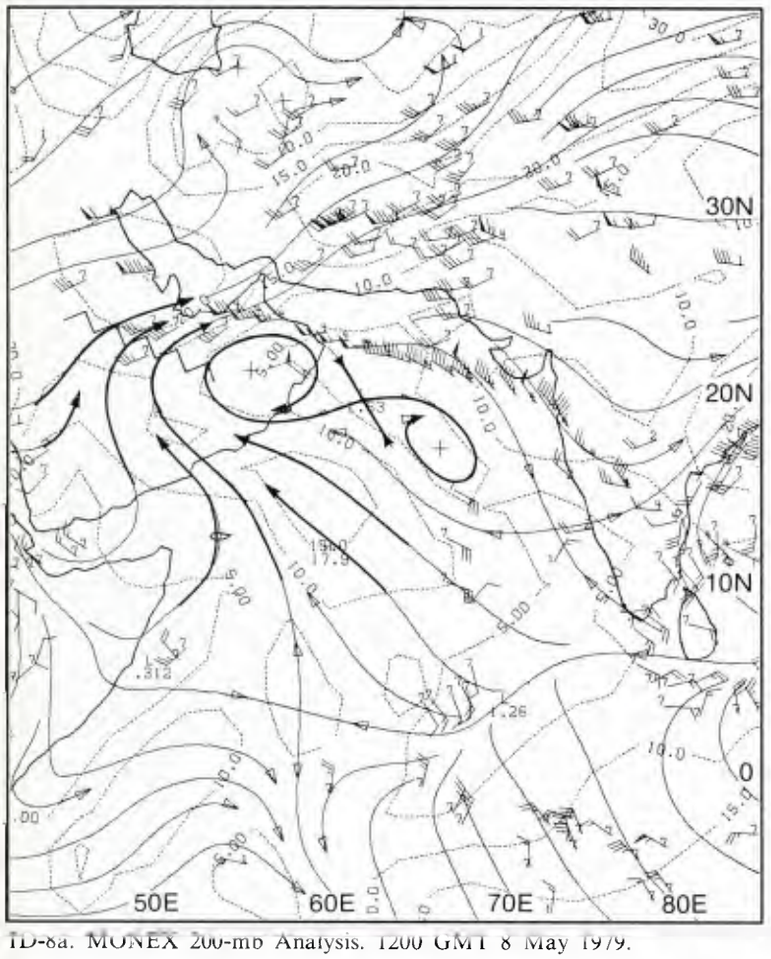

1D-8a. MONEX 200-mb Analysis. 1200 GMT 8 May 1979.

850 mb

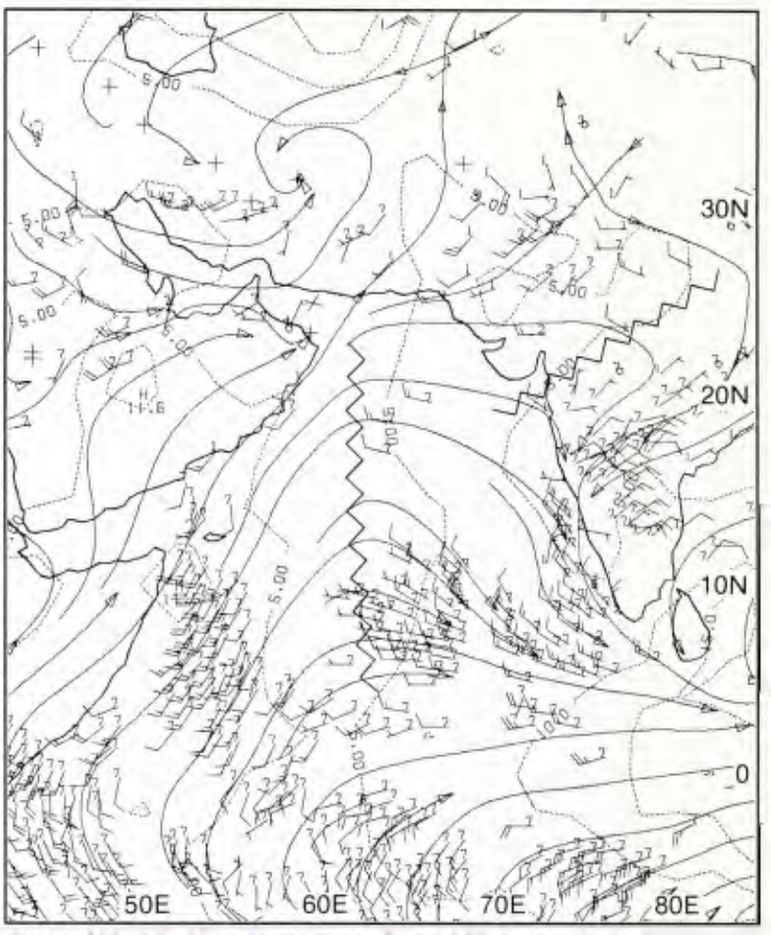

1D-8b. MONEX 850-mb Analysis. 1200 GMT 8 May 1979.

surface

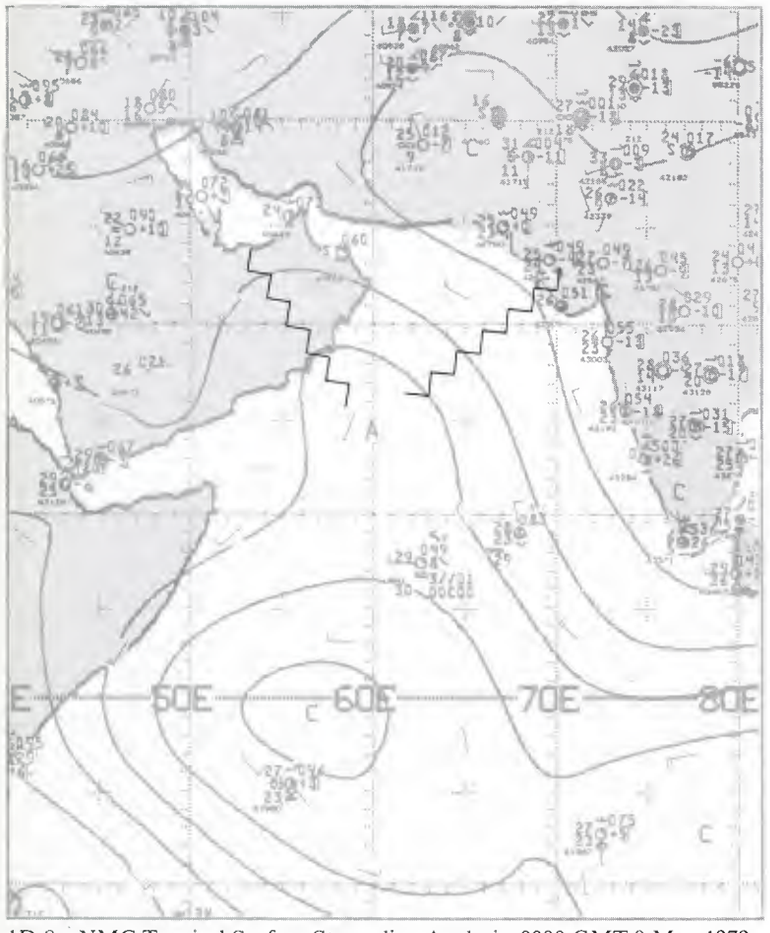

1D-8c. NMC Tropical Surface Streamline Analysis. 0000 GMT 8 May 1979.

surface

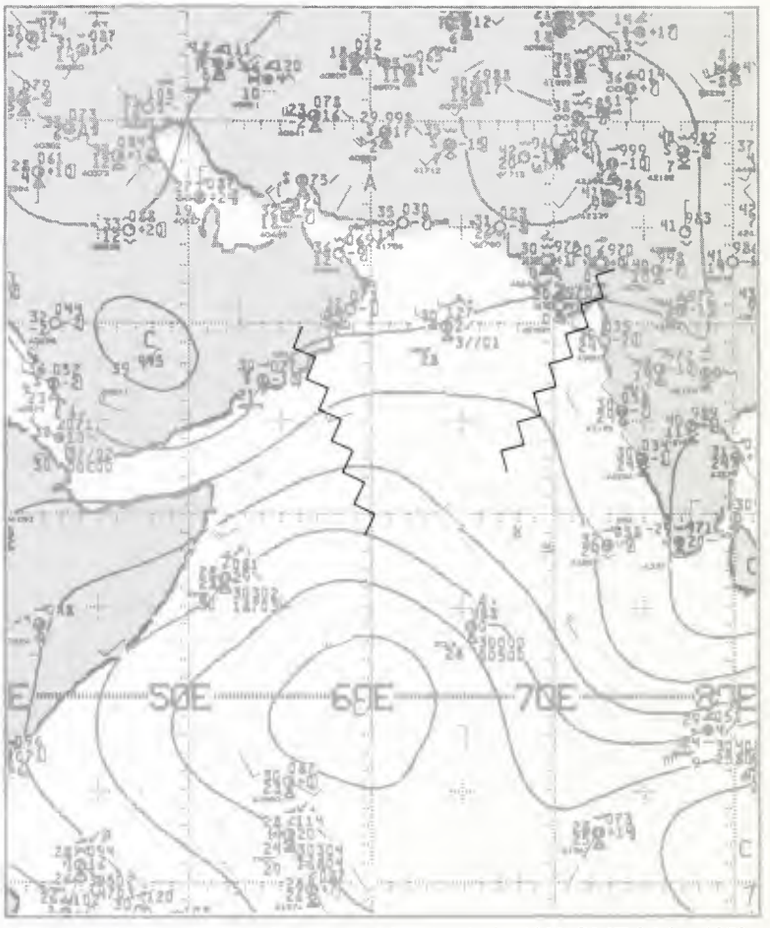

1D-8d. NMC Tropical Surface Streamline Analysis. 1200 GMT 8 May 1979.

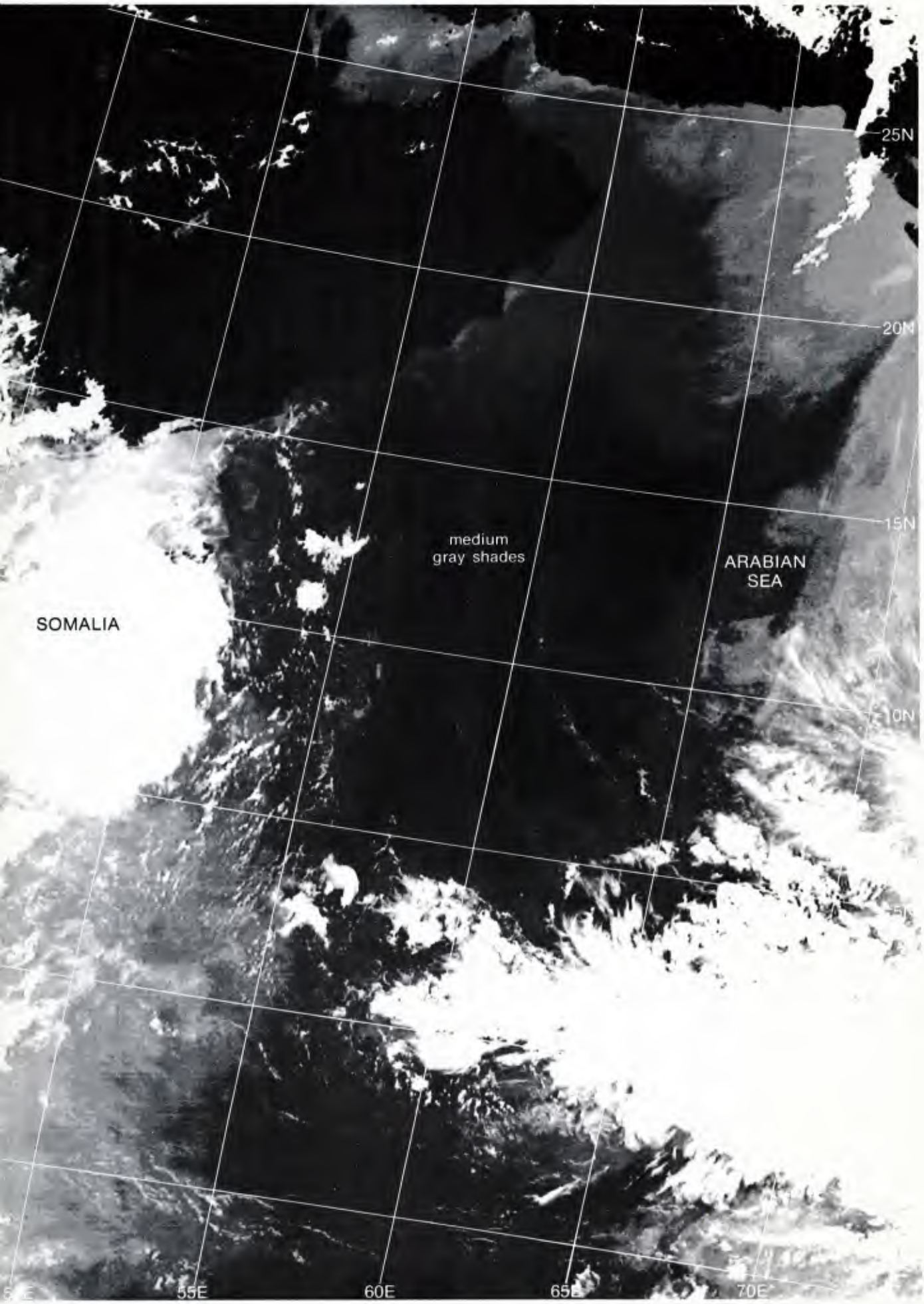

1D-9b. F-1. DMSP TS Low Enhancement. 0710 GMT 8 May 1979.

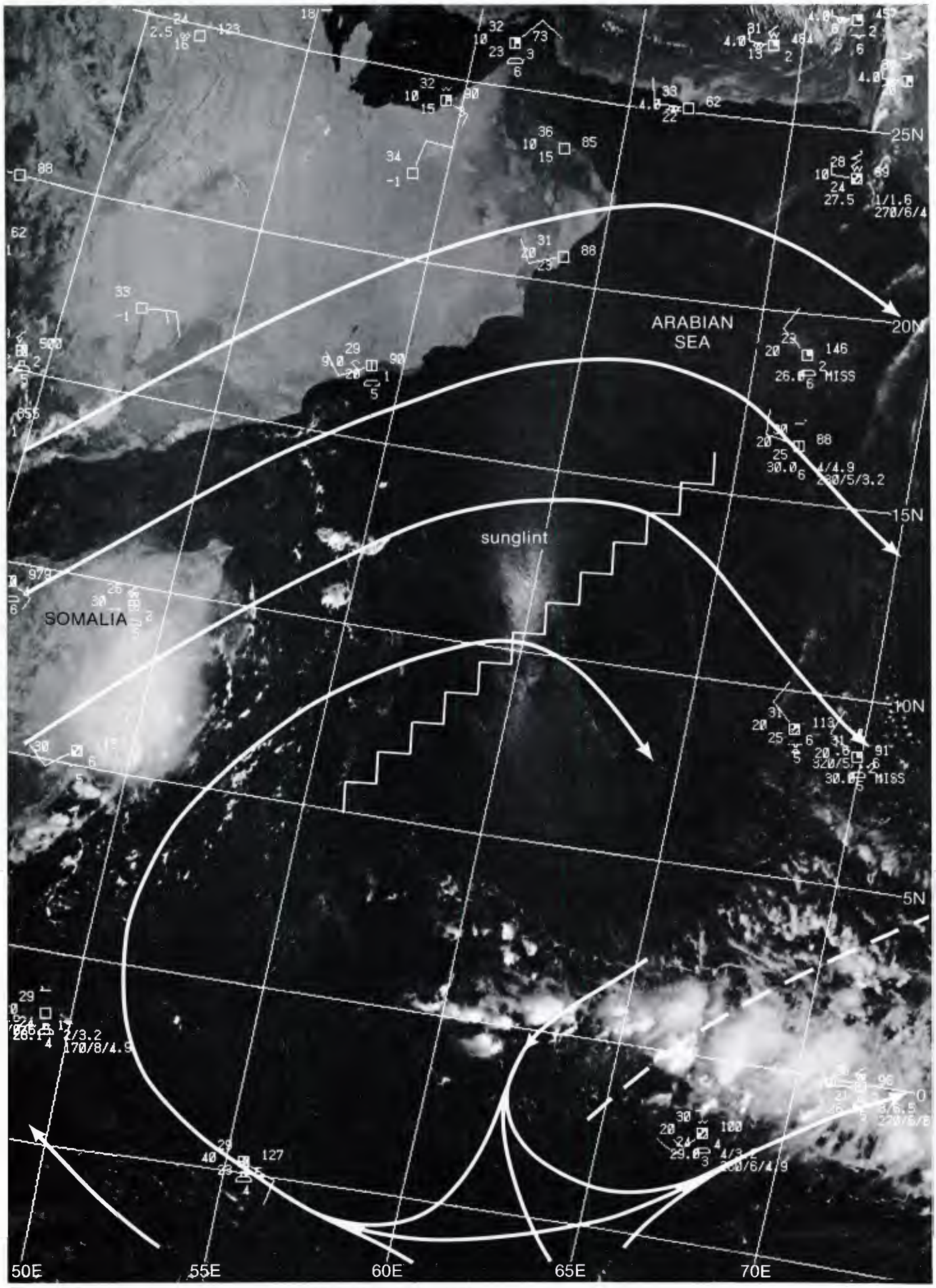

1D-9a. F-1. DMSP LS Low Enhancement. 0710 GMT 8 May 1979.
Surface Wind Reports and Streamline Analysis. 0600 GMT 8 May 1979.

Case 2 Arabian Sea/Bay of Bengal—Spring Transition

Somalia Coastal Thunderstorm

During the month of May, southerly or southwesterly flow of generally less than 15 kt commonly occurs at low levels off the coastline of Somalia. The stronger winds of the Somali jet have not yet arrived. A series of valleys lead down to the coastline of Somalia from high elevations (exceeding 7,000 ft) in the region to the northwest in what was formerly British Somaliland (1D-11a). During nighttime hours, as the earth cools due to radiation effects, a land breeze develops and is accentuated by the downward fall velocity of cold air from the high coastal elevations. An offshore cloud line often delineates the limit of the land breeze circulation, where the offshore flow converges with the prevailing synoptic-scale flow.

The Nogal Valley intersects the Somalia coastline at about 7.5° N (1D-11a). When the nighttime air flow down the Nogal Valley is pronounced, the cool air rushes over the coastal waters like a miniature cold front inducing intense convection, day after day, at nearly the same point on the land breeze cloud line. Convection is intensified since the temperature of the early morning air is much colder than that of the offshore water at this time of year (May), when coastal upwelling is at a minimum. The size of the thunderstorm cell or cells which this convergence gives rise to is very large, with the cirrus outflow from the convective top sometimes filling a 5 degree or more latitude/longitude square.

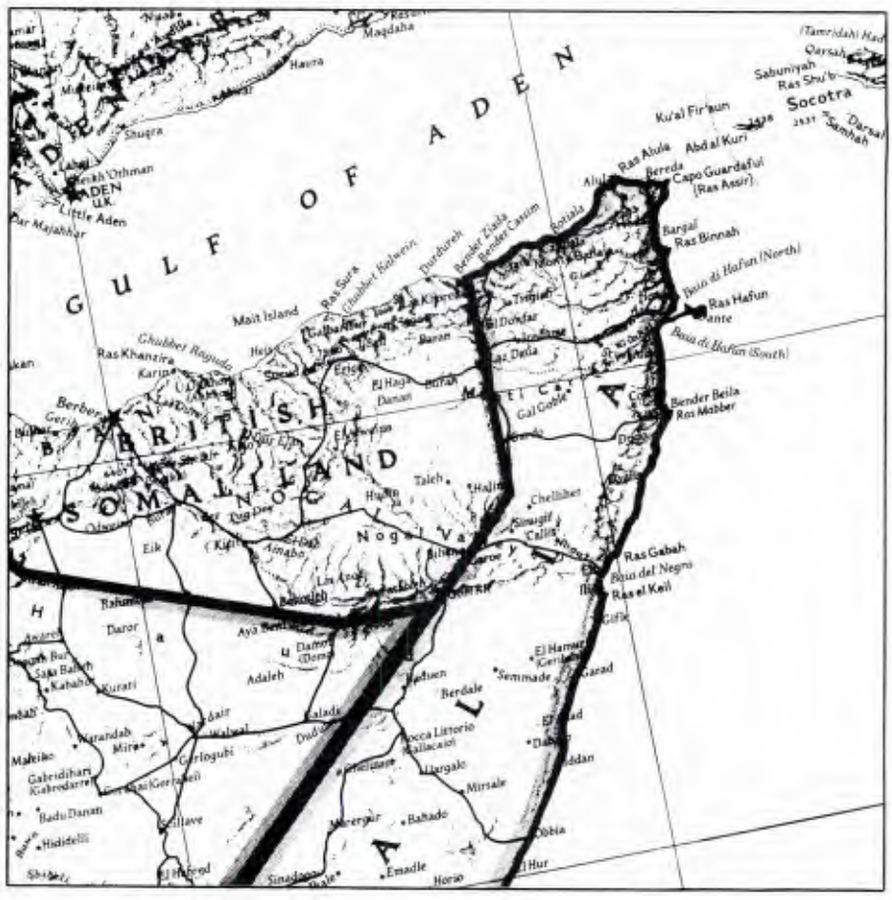

1D-11a. Map of Somalia.

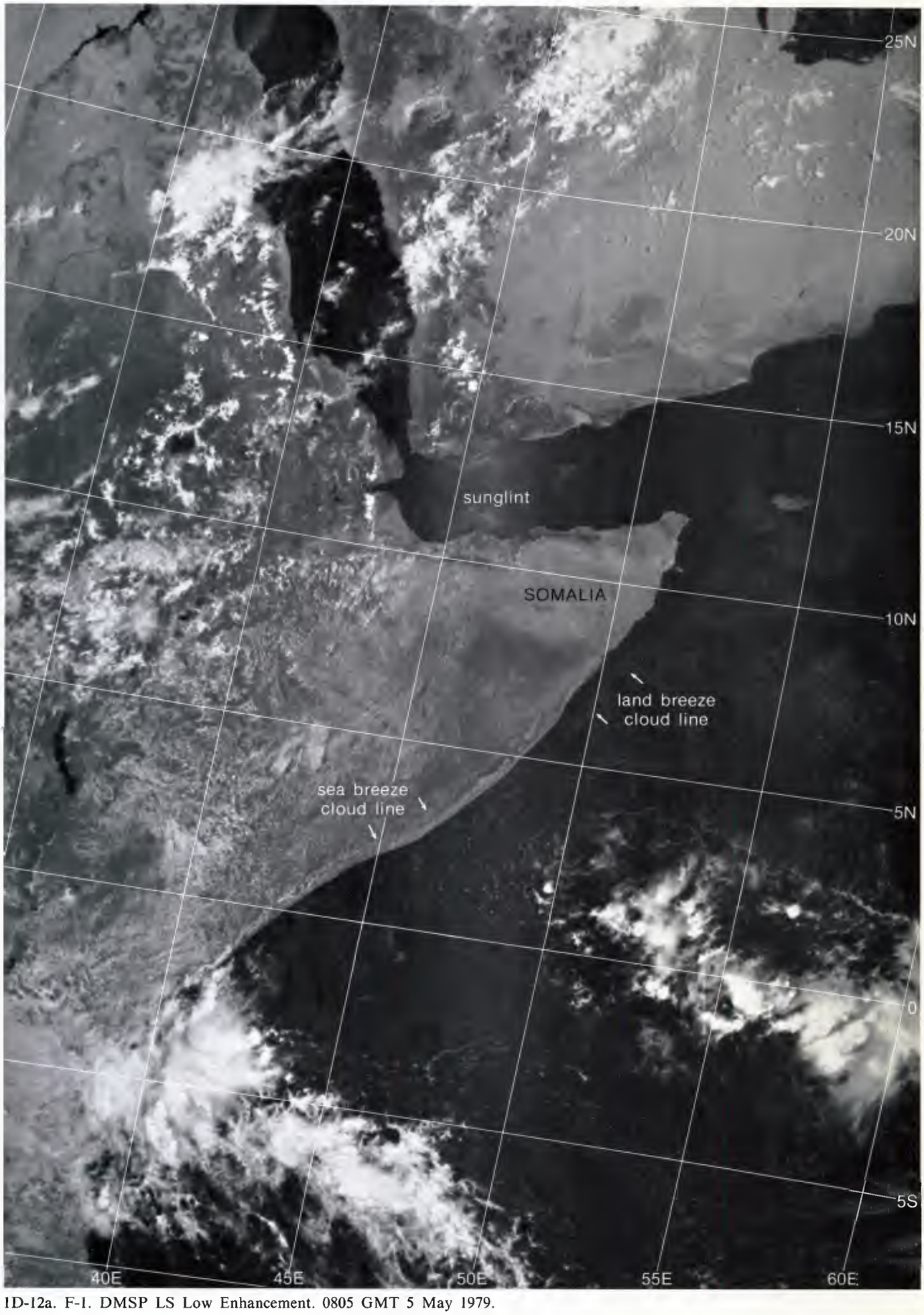

1D-12a. F-1. DMSP LS Low Enhancement. 0805 GMT 5 May 1979.

Nogal Valley Thunderstorm
Somalia
May 1979

5 May

The DMSP visible picture at 0805 GMT (1D-12a) shows the offshore land breeze cloud line, which delineates the limit of the land breeze circulation, in a very undeveloped form. Since this picture was acquired at 1105 LST, the land breeze has ceased to exist and a sea breeze effect in the form of an enhanced cloud line is beginning to appear in the coastal inland area south of Somalia. The land breeze cloud line remnant, offshore, often persists as in this example, even as the sea breeze circulation becomes established.

The DMSP infrared picture (1D-13a), concurrent with the visible picture, reveals warm temperatures (medium gray shades) from the Somalia coastline to the land breeze cloud line, with much cooler conditions further offshore. Although strong southwesterly flow, associated with the low-level Somali jet, has not yet occurred in the Somalia region to induce upwelling along the coast, sea surface temperatures are not warmer in the coastal region, as the DMSP picture might suggest. The effect is believed to be atmospheric, with the air between the offshore cloud line and the coast being drier than the air further out to sea. Hence, atmospheric water vapor absorption is reduced and a warmer temperature is observed in the imagery.

The coastal air is drier because of the land breeze which permits cool, dry, continental air to flow seaward to the cloud line limit of the land breeze circulation. The air remains drier as the sea breeze becomes established, and air subsides in the region between the offshore cloud line and the coast.

7 May

The thunderstorm observed in the DMSP picture just off the Somalia coastline (1D-15a) has apparently developed on the faint offshore land breeze cloud line which extends to the north and south along the coast. Simultaneous DMSP infrared imagery (1D-15b) reveals the rather large size of the cirrus top of the cumulonimbus. Note the short, clear warm slot (dark gray shade) extending west-northwest from the thunderstorm cluster. This is the Nogal Valley, believed responsible for the nighttime valley wind which caused the offshore convergence producing the thunderstorm.

The NMC surface streamline analysis (1D-14c) near the time of the satellite picture implies rather light, diffluent southerly flow past the offshore area of eastern Somalia. A similar low-level flow pattern is observed at 1200 GMT (1D-14d). However, the MONEX 850-mb analysis at 1200 GMT (1D-14b) shows light northwesterly winds from the Nogal Valley region converging with the along shore winds, which is favorable for development of the Nogal Valley thunderstorm. At 200 mb (1D-14a), winds over the area are very light and variable. The presence of very short cirrus streamers along the northwest quadrant of the thunderstorm (1D-15a) also indicates the absence of strong winds aloft.

8 May

On this day, the DMSP visible picture (1D-17a) shows a gigantic thunderstorm on the Somalia coast. The simultaneous DMSP infrared picture (1D-17b) shows an anvil top of about 8 degrees (500 n mi) in diameter!

The surface streamline analyses for 0000 GMT (1D-16c) and 1200 GMT (1D-16d) show moderate southwesterly flow over the Somalia coast, as on the previous day (1D-14c and 14d). The moderate southwesterly flow is also observed at 850 mb (1D-16b) with light, variable winds at 200 mb (1D-16a). Although wind observations are not available over the northern tip of Somalia, the localized nature of the thunderstorm indicates that it has developed as a result of the convergence of the Nogal Valley winds and the offshore flow.

10 May

The DMSP visible picture on this day (1D-19a) shows a clear view of the Somalia Peninsula, with a Nogal Valley thunderstorm in progress. Offshore cloud lines on the satellite picture indicate convergent flow associated with the thunderstorm, which is easily the most dominant convective effect in the entire picture.

The surface streamline analyses for 0600 GMT (1D-18c) and 1200 GMT (1D-18d) show a more coastally directed surface flow. By chance a ship was passing near the thunderstorm area (1D-18c) and reported a heavy thunderstorm with rain in progress. Note that a sea surface temperature of 30° C is reported, which is much warmer than the 25° C air temperature. This sea surface temperature reading is consistent with shipboard temperatures reported in the area by Brown (1980).

The simultaneous DMSP infrared picture (1D-19b) reveals the almost circular shape of the cirrus top of the thunderstorm. Such a circular shape implies very light winds at upper levels. This is verified at 200 mb (1D-18a) which reveals light winds in the region of the thunderstorm.

Important Conclusions

1. Drainage of cold air from mountain valleys to coastal areas can produce intense convection on offshore land breeze cloud lines.

2. Offshore areas between the land and the land breeze cloud line should be areas of drier low-level air having increased visibility in comparison to those regions further out to sea.

Reference

Brown, O. B., J. G. Bruce, and R. H. Evans, 1980: Evolution of sea surface temperature in the Somalia basin during the southwest monsoon of 1979. *Science*, **209**, 595–597.

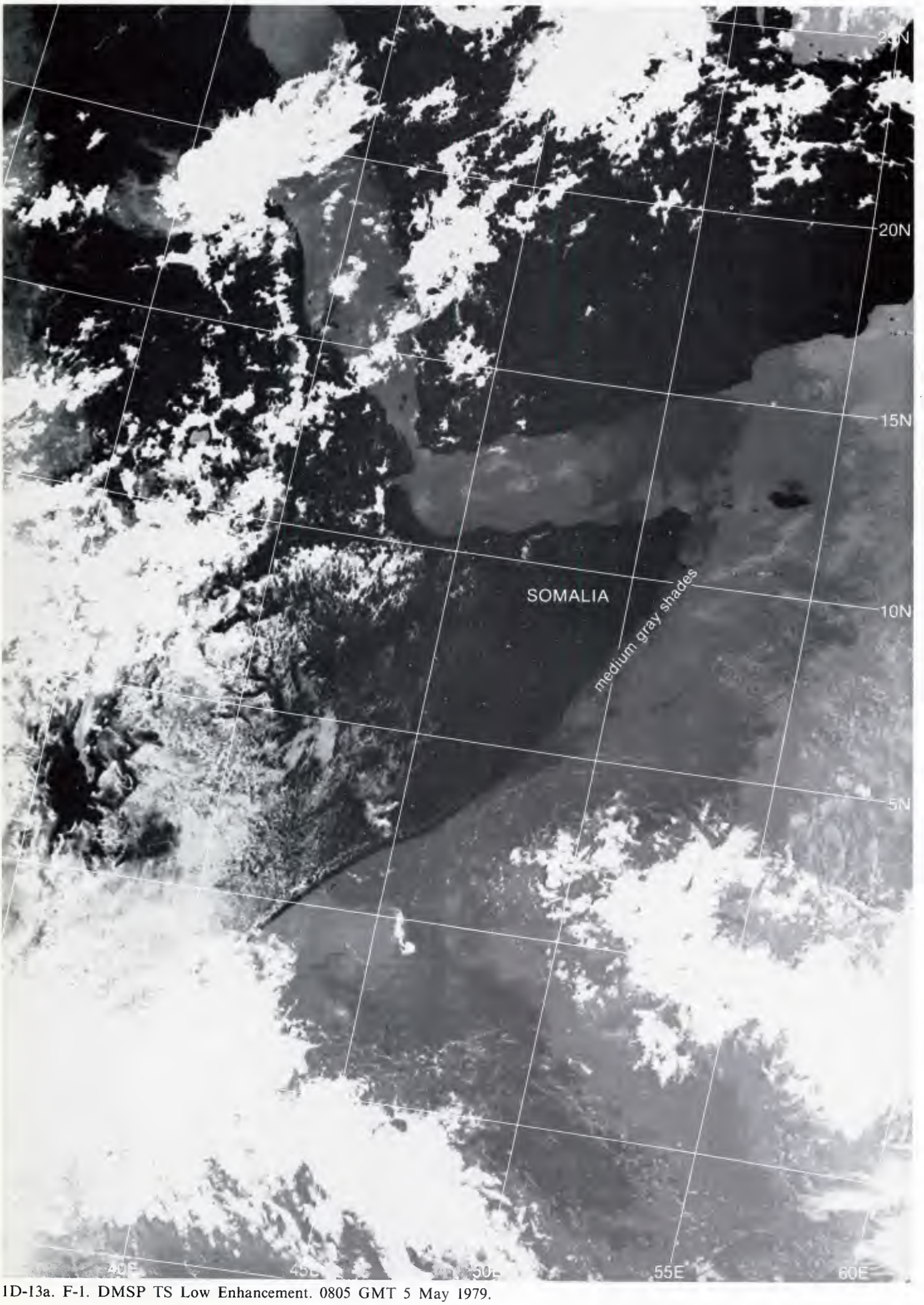

1D-13a. F-1. DMSP TS Low Enhancement. 0805 GMT 5 May 1979.

200 mb

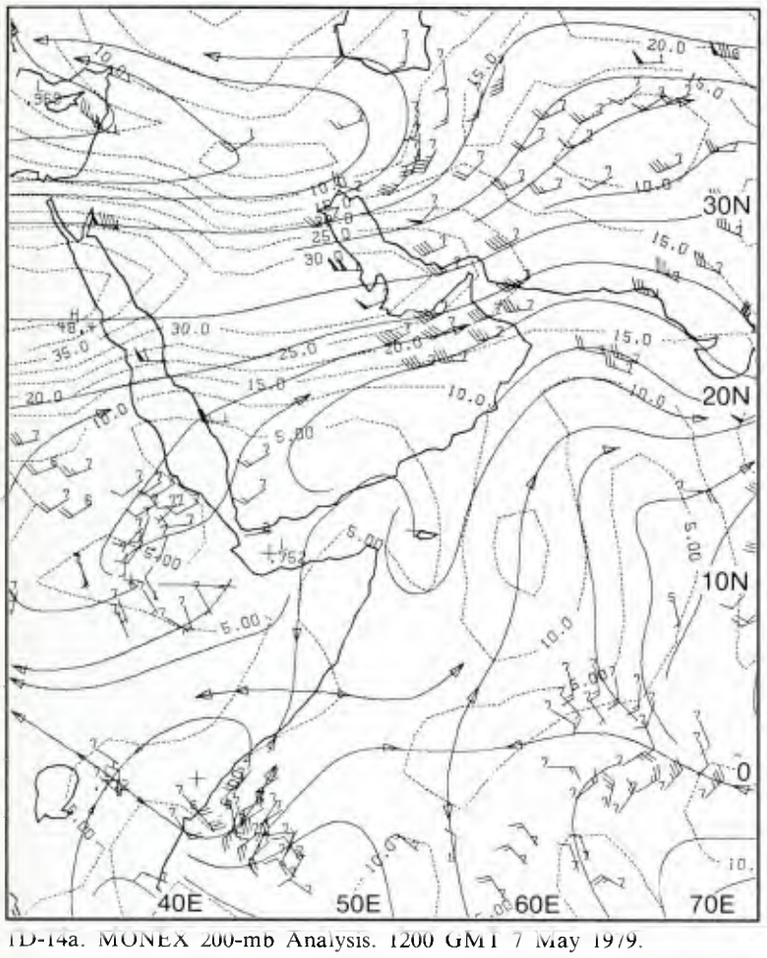

1D-14a. MONEX 200-mb Analysis. 1200 GMT 7 May 1979.

850 mb

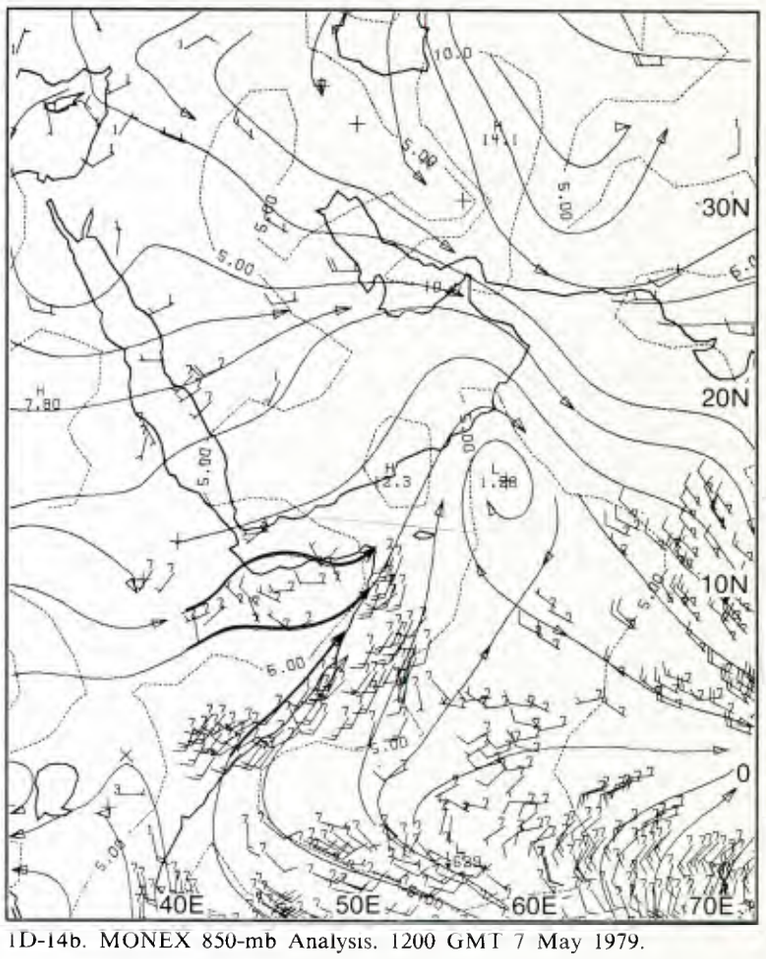

1D-14b. MONEX 850-mb Analysis. 1200 GMT 7 May 1979.

surface

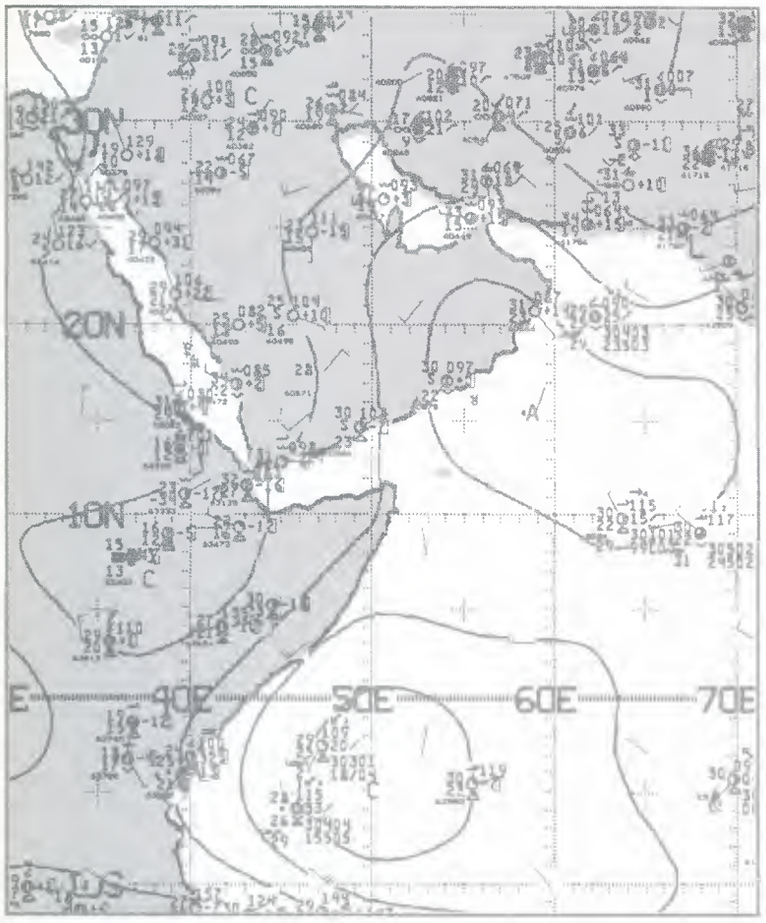

1D-14c. NMC Tropical Surface Streamline Analysis. 0600 GMT 7 May 1979.

surface

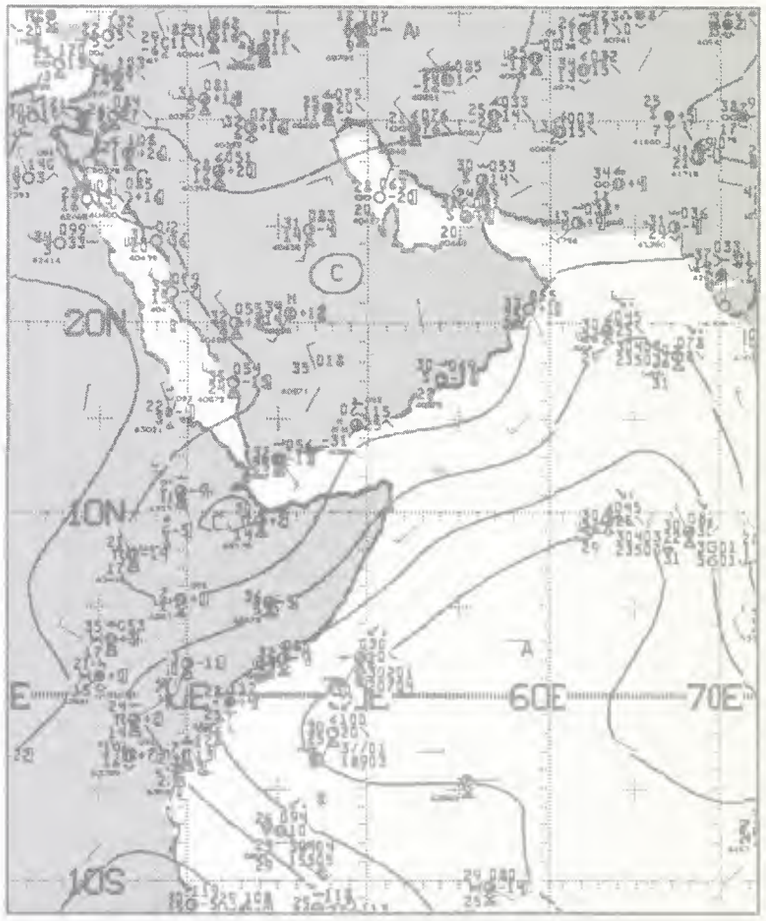

1D-14d. NMC Tropical Surface Streamline Analysis. 1200 GMT 7 May 1979.

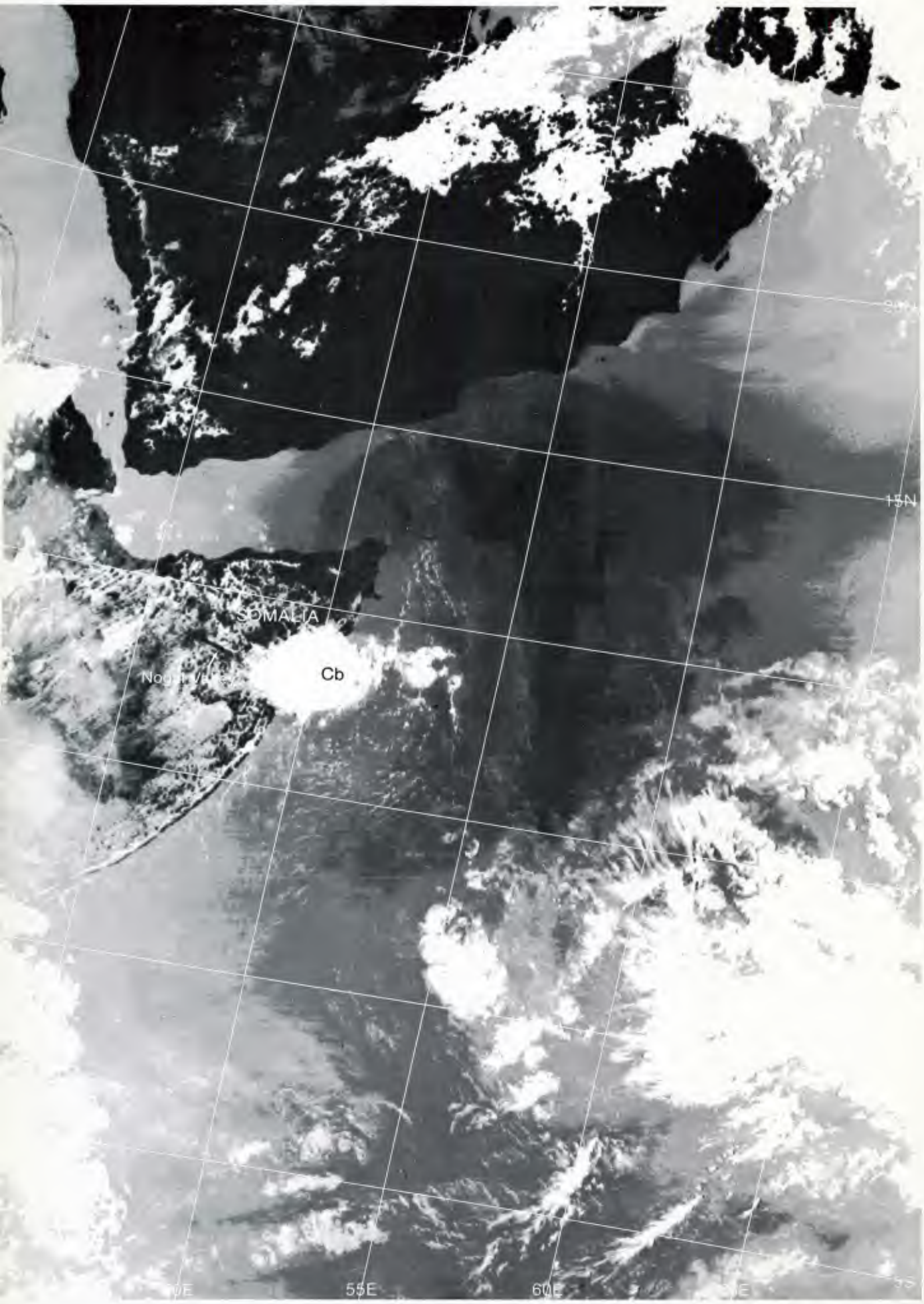

1D-15b. F-1. DMSP TS Low Enhancement. 0728 GMT 7 May 1979.

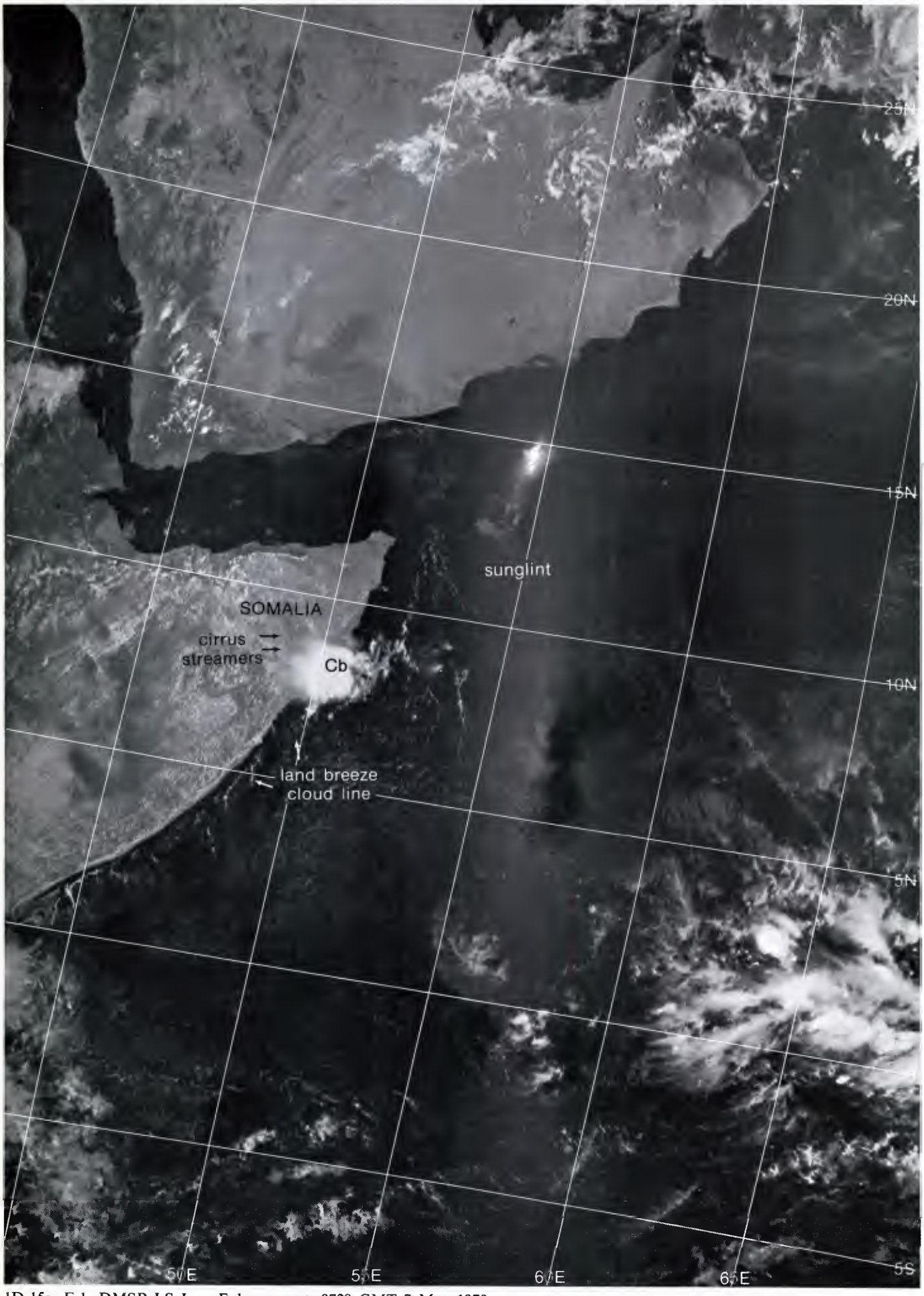

1D-15a. F-1. DMSP LS Low Enhancement. 0728 GMT 7 May 1979.

200 mb

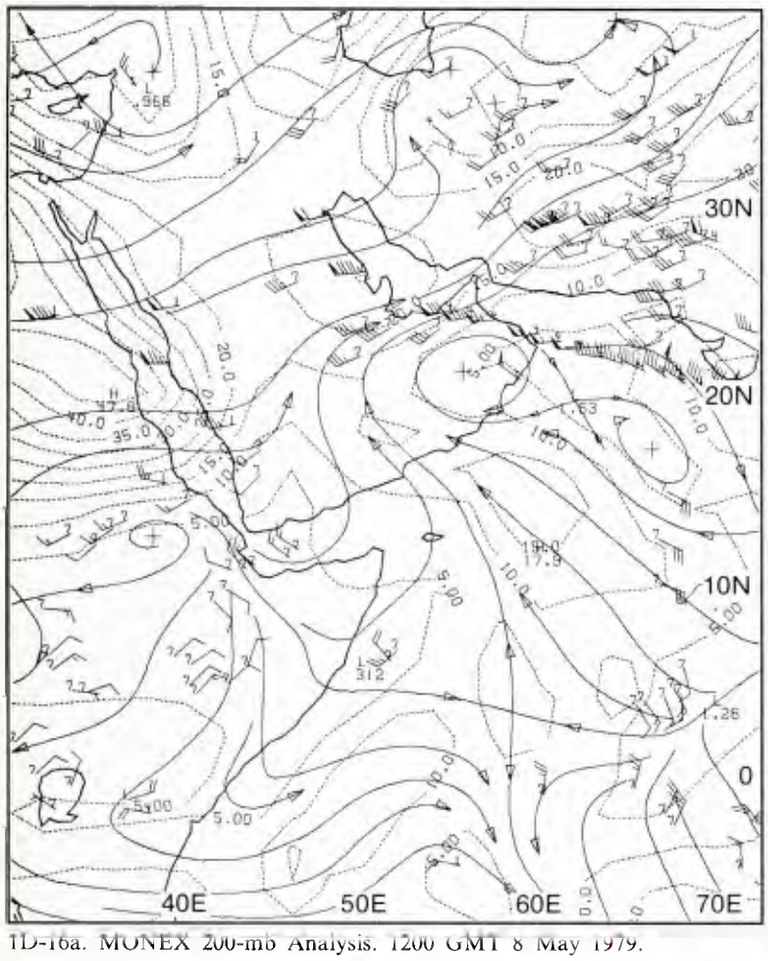

1D-16a. MONEX 200-mb Analysis. 1200 GMT 8 May 1979.

850 mb

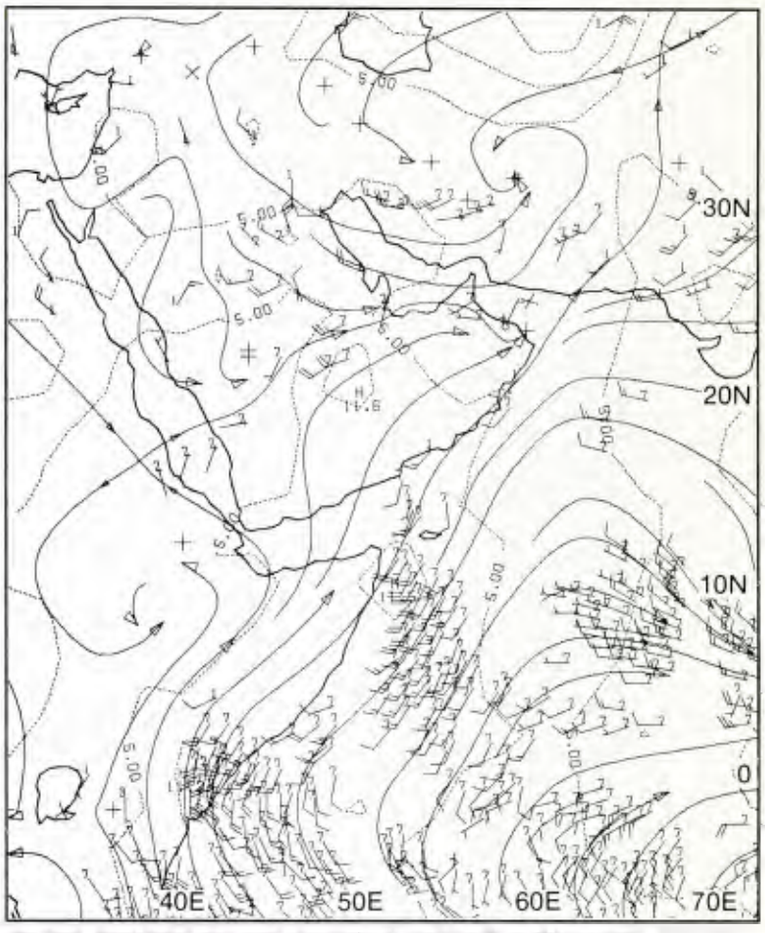

1D-16b. MONEX 850-mb Analysis. 1200 GMT 8 May 1979.

surface

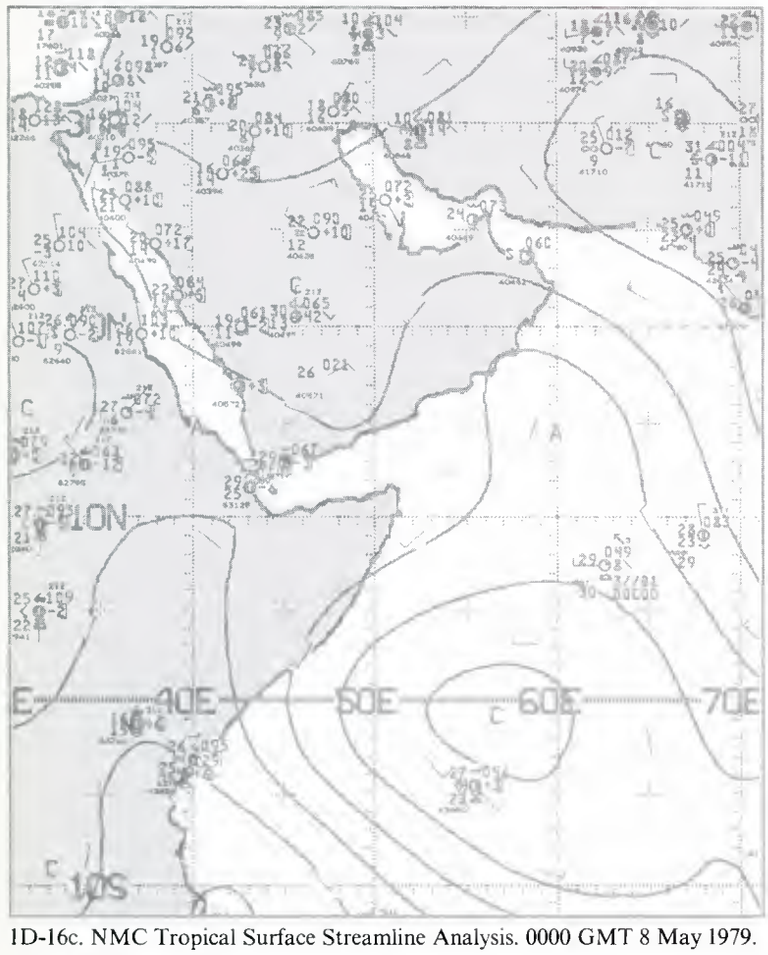

1D-16c. NMC Tropical Surface Streamline Analysis. 0000 GMT 8 May 1979.

surface

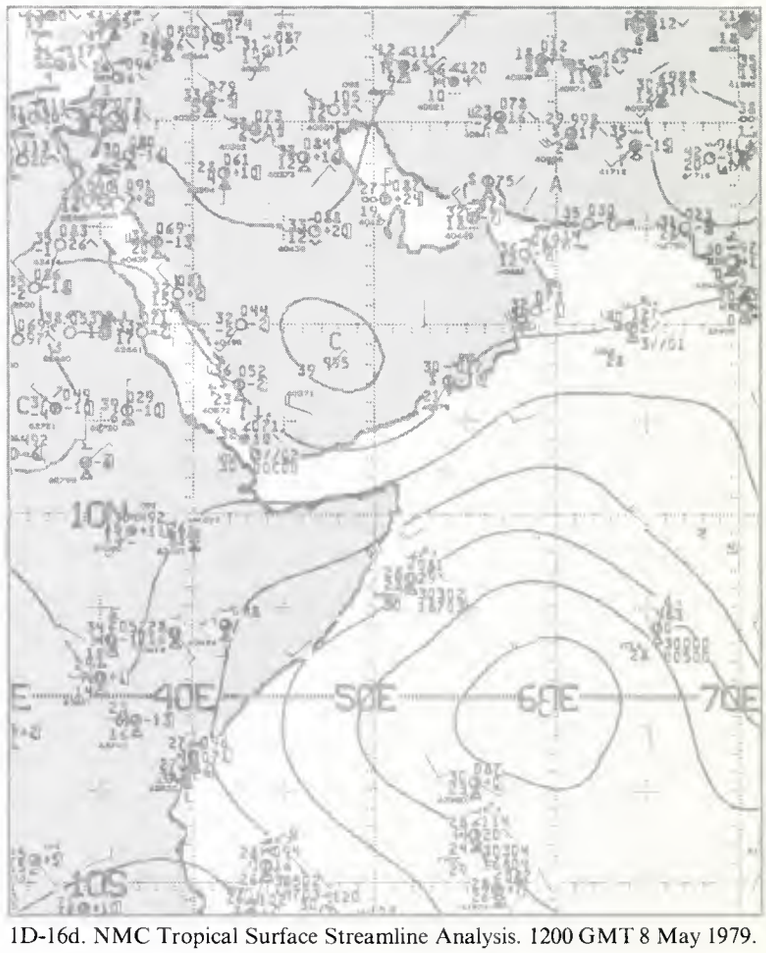

1D-16d. NMC Tropical Surface Streamline Analysis. 1200 GMT 8 May 1979.

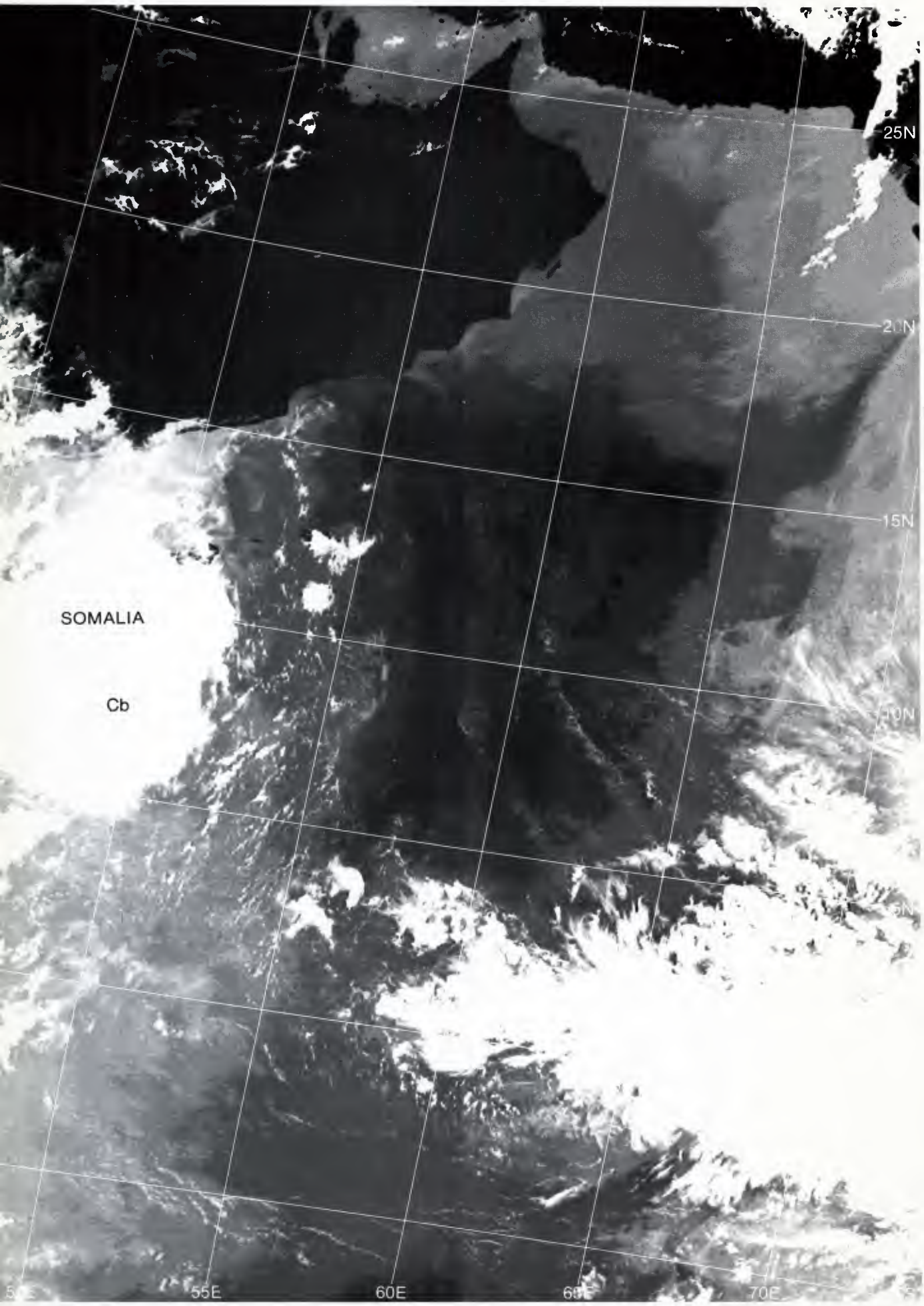

1D-17b. F-1. DMSP TS Low Enhancement. 0710 GMT 8 May 1979.

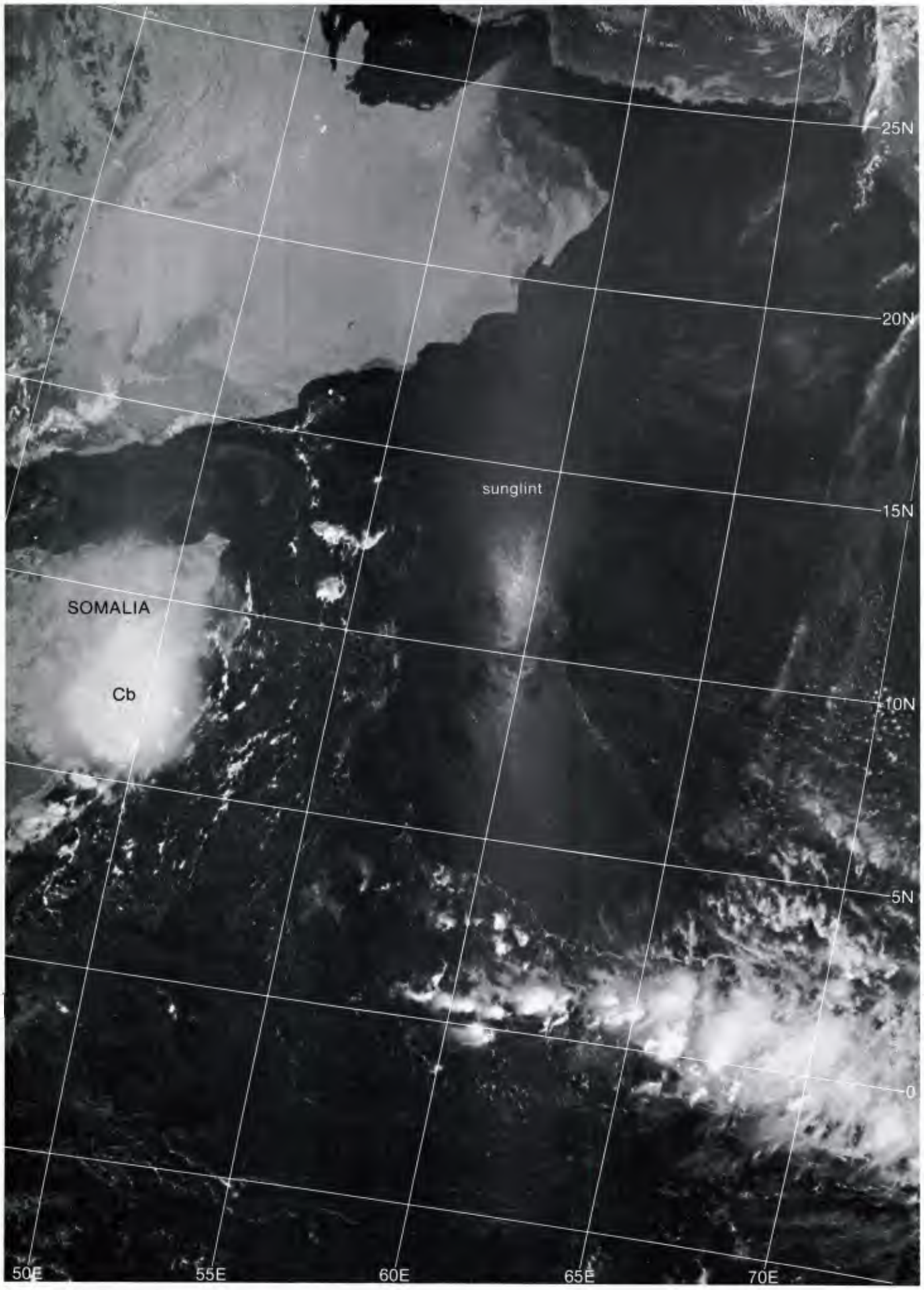

1D-17a. F-1. DMSP LS Low Enhancement. 0710 GMT 8 May 1979.

200 mb

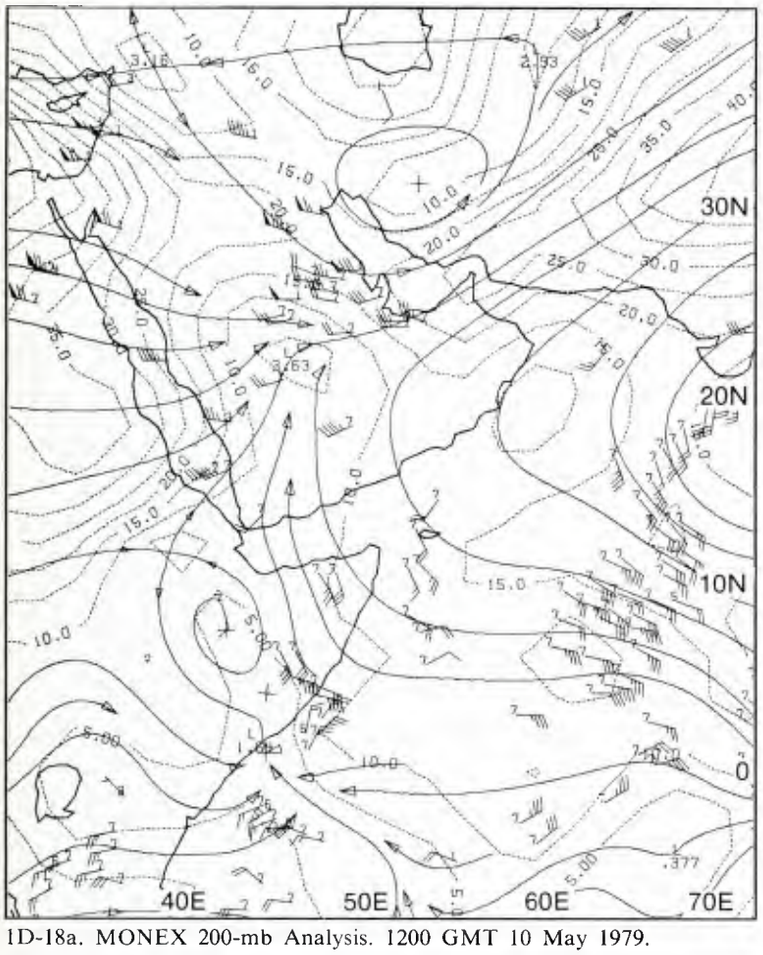

1D-18a. MONEX 200-mb Analysis. 1200 GMT 10 May 1979.

850 mb

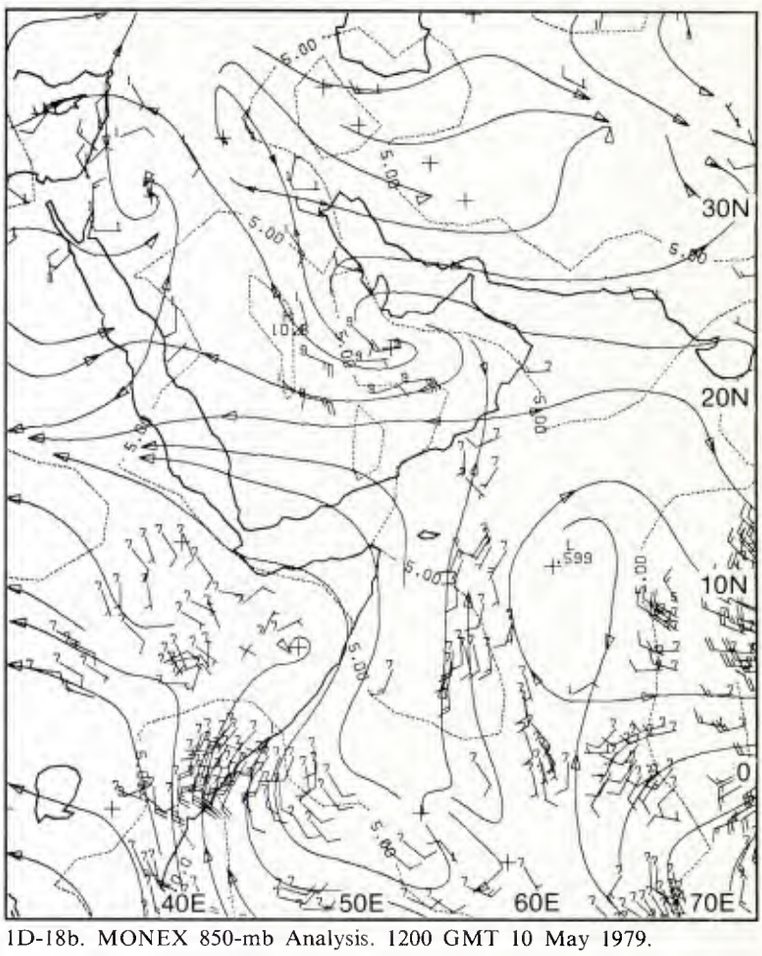

1D-18b. MONEX 850-mb Analysis. 1200 GMT 10 May 1979.

surface

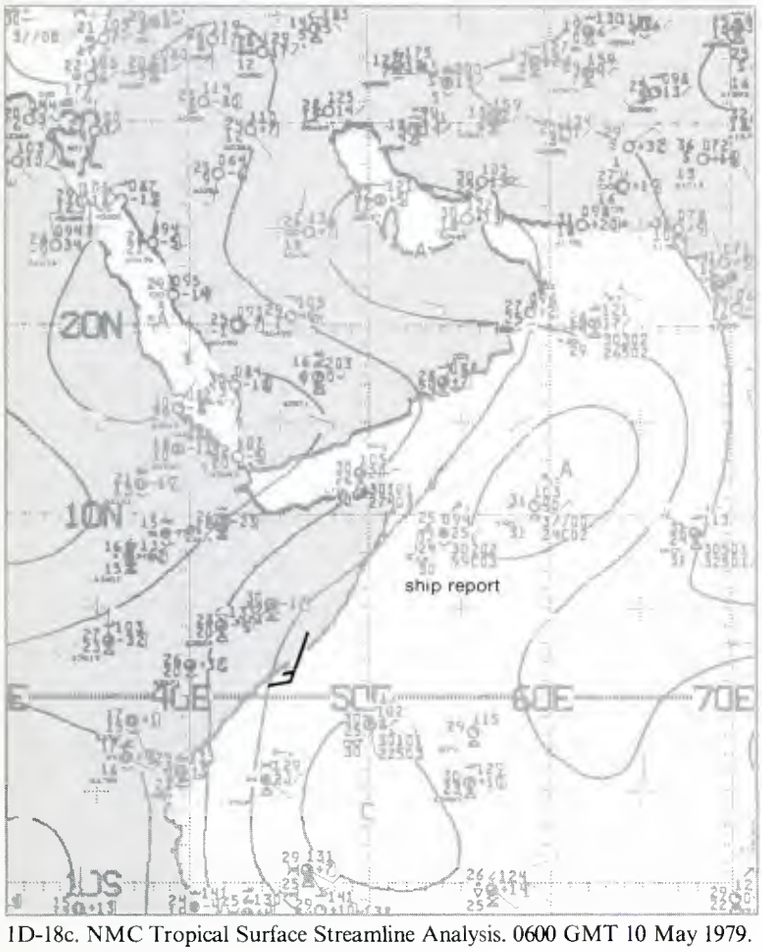

1D-18c. NMC Tropical Surface Streamline Analysis. 0600 GMT 10 May 1979.

surface

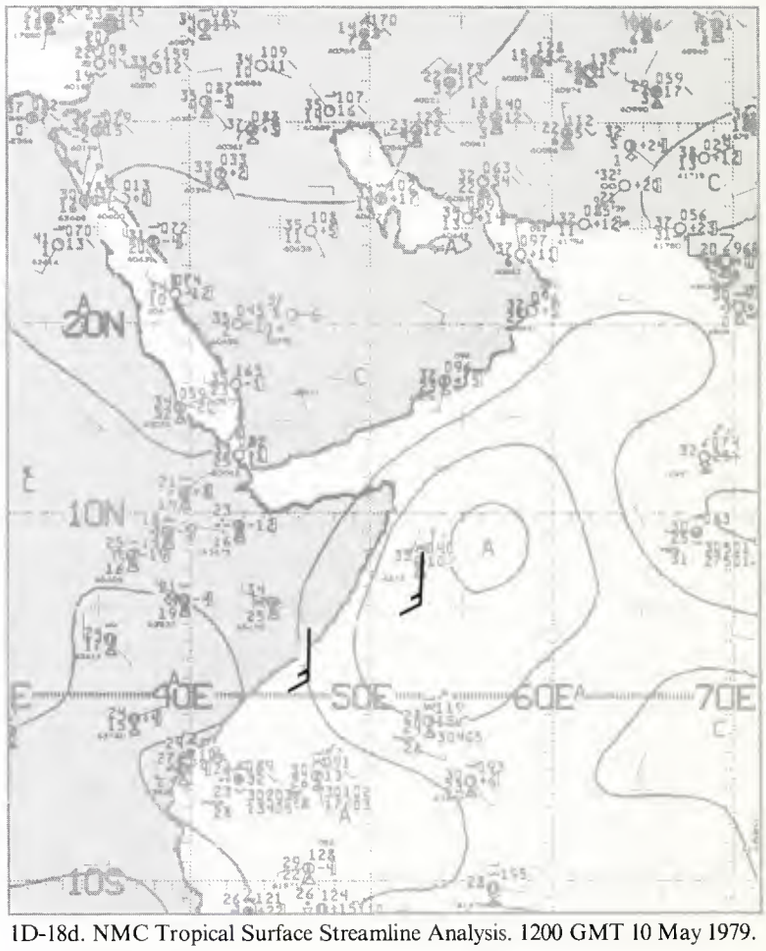

1D-18d. NMC Tropical Surface Streamline Analysis. 1200 GMT 10 May 1979.

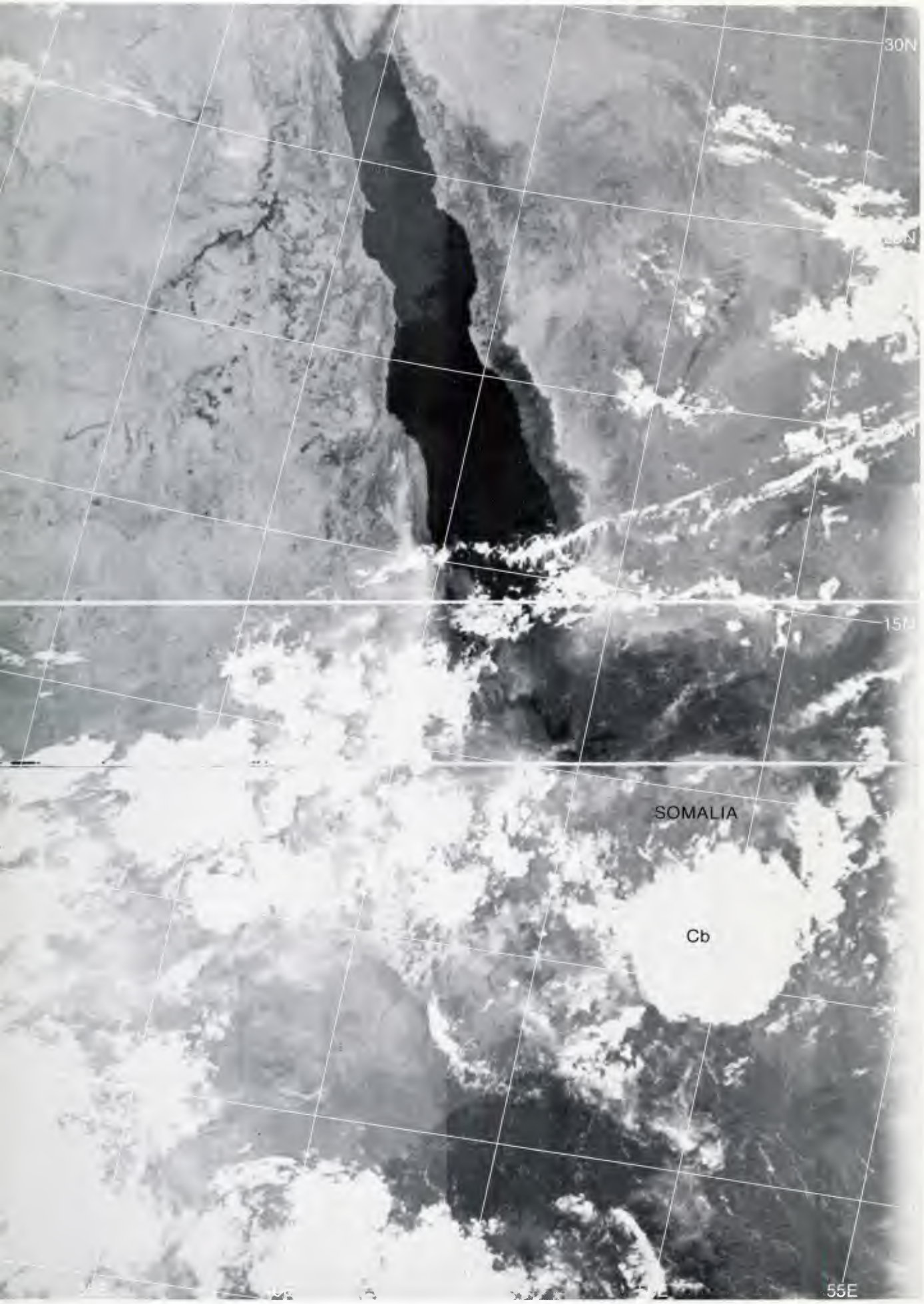

1D-19b. F-3. DMSP TS Low Enhancement. 0343 GMT 10 May 1979.

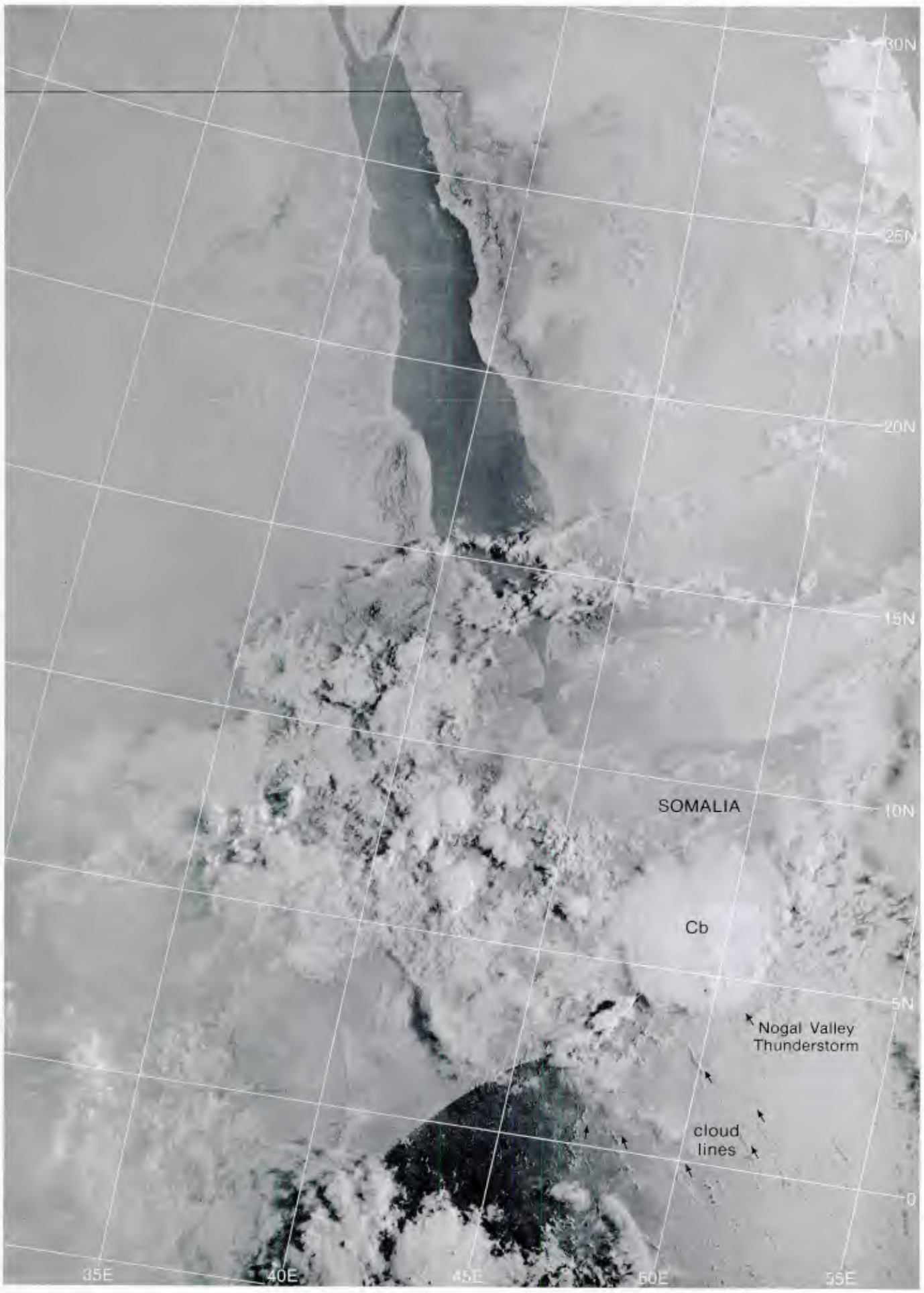

1D-19a. F-3. DMSP LF Low Enhancement. 0343 GMT 10 May 1979.

Case 1 Arabian Sea/Bay of Bengal—Summer

Burst of the Southwest Monsoon

The initial indication of the monsoon burst in the Northern Hemisphere is a marked increase in the southerly flow along the east African coast that accompanies the formation of the low-level Somali jet. This increased low-level flow then turns eastward, crossing the southern Arabian Sea in 3 to 4 days, bringing increased westerly flow and precipitation to southwestern India. The 3 to 4 day crossing period is based on the crossing times of constant-level balloons during the 1979 MONEX study. Following the onset of monsoon rain in southwestern India, the rainfall front propagates northward and after about one month all the Indian subcontinent is affected by the monsoon rains.

surface

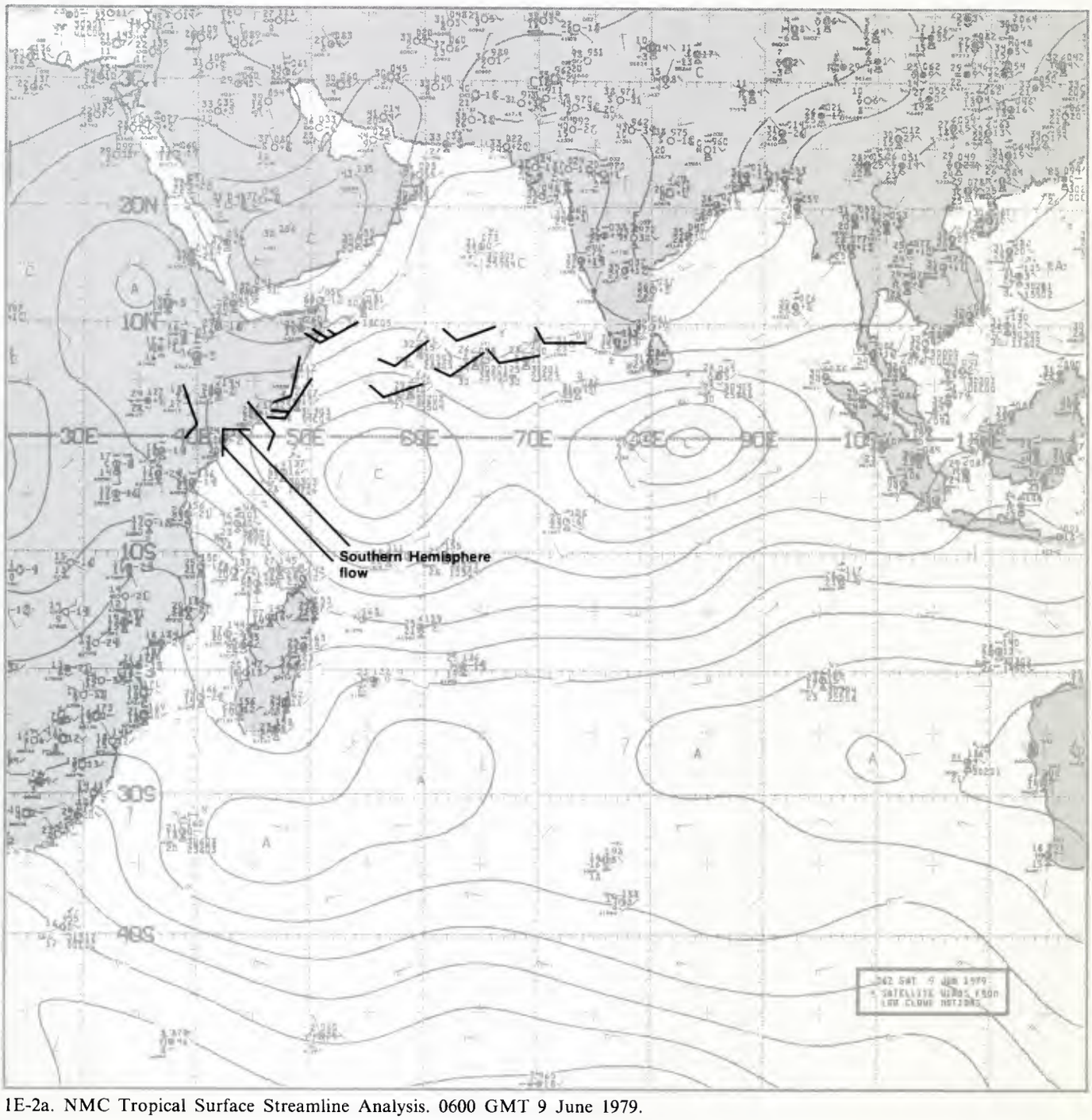

1E-2a. NMC Tropical Surface Streamline Analysis. 0600 GMT 9 June 1979.

Burst of the 1979 Southwest Monsoon
Arabian Sea
June 1979

The burst of the 1979 southwest monsoon occurred over the western and southern Arabian Sea on 10–12 June, followed by the onset vortex development during 13–16 June (see Sec. 1E, Case 2). The earliest southwest monsoon cloudiness occurred over the extreme southwestern part of India on the 12th, but cloudiness and rainfall did not become well established until after the onset vortex formation.

9 June

The NMC surface streamline analysis for 0600 GMT (1E-2a) depicts the pre-burst conditions. The Southern Hemisphere flow approaching the equatorial coast of east Africa does not turn northward to support the Somali jet, but rather retains an easterly component. The surface wind reports north of the Equator are generally light (10 kt), with the exception being two reports of 20 kt just off the Somalia coast. The 25-kt plotted wind near 9° N, 53° E is a gradient wind based on the analysis and not an actual report. The DMSP visible picture at 0731 GMT (1E-3a) is of the western Indian Ocean region. The easterly component of the Southern Hemisphere flow is advecting clouds onshore in the vicinity of the Equator. Scattered convective activity is occurring from near the Equator to 12° N. Weakly defined low-level cloud lines can be seen off the Somalia coast.

10 June

The 0600 GMT surface streamline analysis (1E-4a) indicates that the cross-equatorial low-level flow has become more southerly, and the easterly component of the Southern Hemisphere trade winds has been lost. The streamlines indicate a more organized westerly flow over the southern Arabian Sea. The beginning of an organized cloud line appears from the Somalia coast, and extends to the southeast, as seen in the 0712 GMT DMSP picture (1E-5a). The winds and low-level cloud lines off the east coast of Somalia still indicate relatively light southwesterly flow.

11 June

Surface wind reports of 10 to 20 kt are indicated in the region of the low-level Somali jet on the 0600 GMT surface streamline analysis (1E-6b). While not clearly indicated in this analysis, it was on this date that Krishnamurti (1981) found a dramatic increase in westerly kinetic energy over the Arabian Sea during the 1979 monsoon burst (1E-6a). The intensification of the westerly flow is clearly delineated starting on the 11th.

Low-level cloudiness can be seen off the Somalia coast in the DMSP picture at 0309 GMT (1E-7a). Closely-spaced cloud lines suggest stronger wind speeds. Upwelling is undoubtedly occurring, increasing the land/sea temperature contrast and horizontal pressure gradient, thereby strengthening the southwest monsoon flow. The amount of convective cloud cover in the southwestern Arabian Sea is increasing with a large overcast area shown near the Equator. Increased cloud amounts would be expected as a result of the increasing cross-equatorial flow advecting more moist low-latitude air poleward so that latitudinal convergence increases. In an enlargement of the satellite picture (1E-7b) of the Socotra Island area, note the leeward island barrier effects north of the island which indicate strong southerly flow in that area. This island (1E-7c) has elevated terrain features which produce the barrier effect. Note that strong winds (lighter sea surface) are shown in the bay area of the leeside and weak winds (darker sea surface) are shown in the lee of the mountains.

12 June

The 0600 GMT surface streamline analysis (1E-8a) gives a much better indication of the increased southwesterly and westerly flow over the southern Arabian Sea than the analysis twenty-four hours earlier. The increased cross-equatorial flow and the extent of cloudy conditions from Africa to India, near 10° N, is shown. Low-level cloud lines can be seen extending well off the east coast of Somalia in the DMSP picture at 0249 GMT (1E-9a). The overplotted surface observations indicate widespread enhanced convective activity extending across the southern Arabian Sea from about 3° to 13° N. A DMSP picture at 0636 GMT (1E-9b) indicates the convective activity is just approaching the extreme southwestern coast of India. The overplotted surface winds show the established westerly flow across the Arabian Sea.

At this time the burst of the monsoon has occurred from the east African equatorial region, across the southern Arabian Sea to southwestern India. During the immediate following period, 13 to 16 June, the onset vortex forms (see Sec. 1E, Case 2) and the march of the southwest monsoon eastward and northward over the subcontinent of India follows.

Reference

Krishnamurti, T. N., 1981: The 10- and 20-day westward propagating mode and "breaks in the monsoons". *Tellus*, **32**, 15–26.

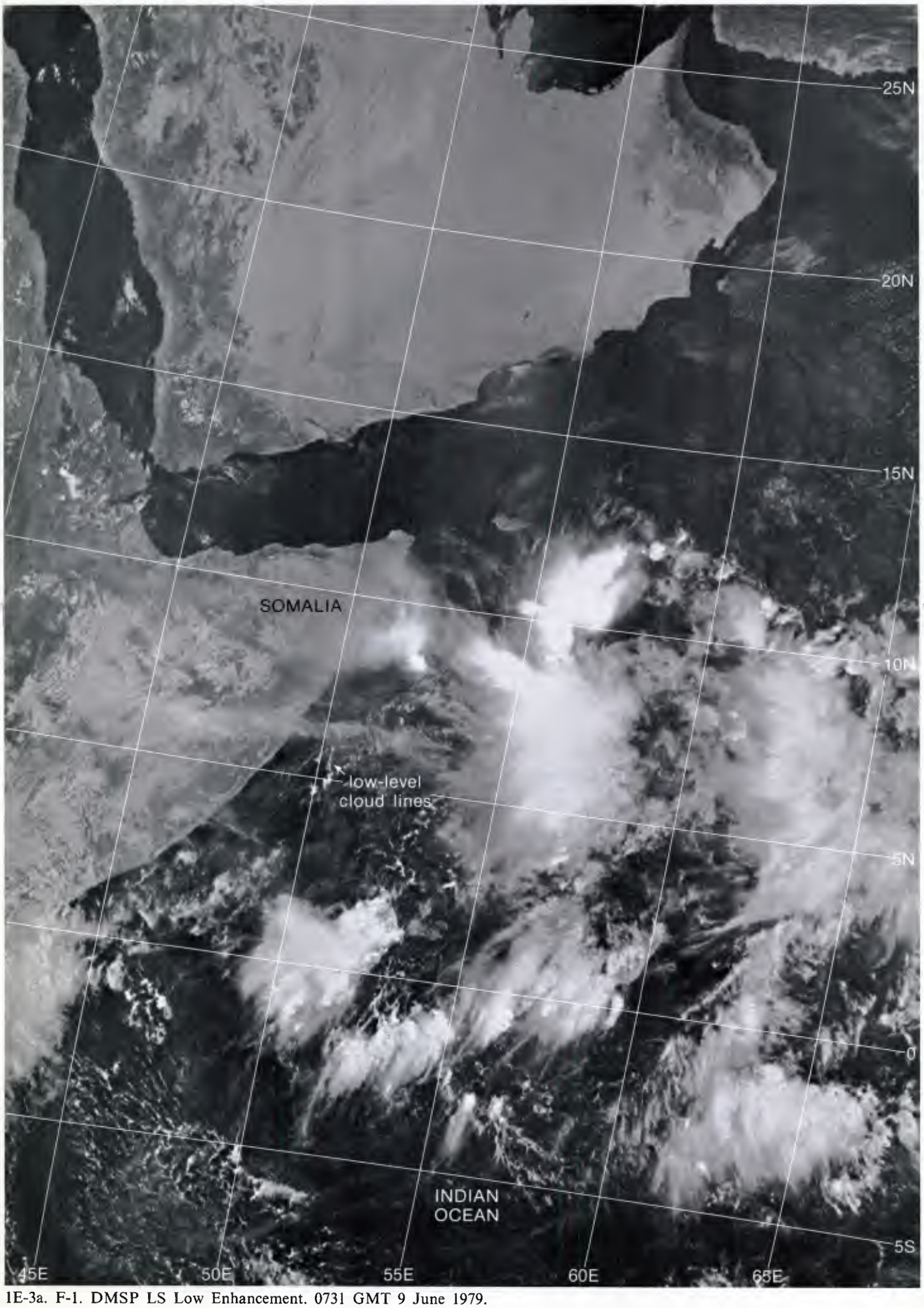

1E-3a. F-1. DMSP LS Low Enhancement. 0731 GMT 9 June 1979.

surface

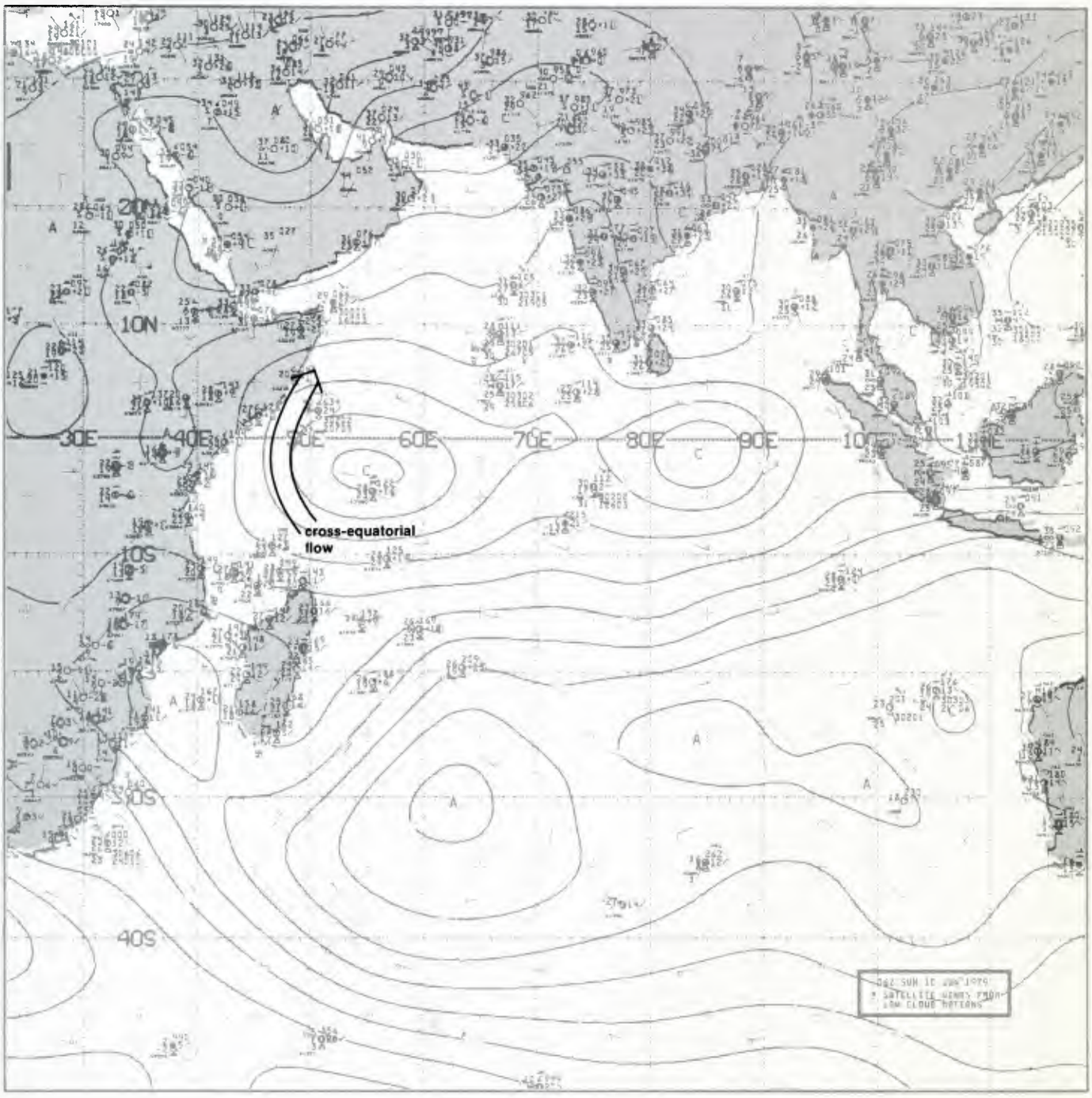

1E-4a. NMC Tropical Surface Streamline Analysis. 0600 GMT 10 June 1979.

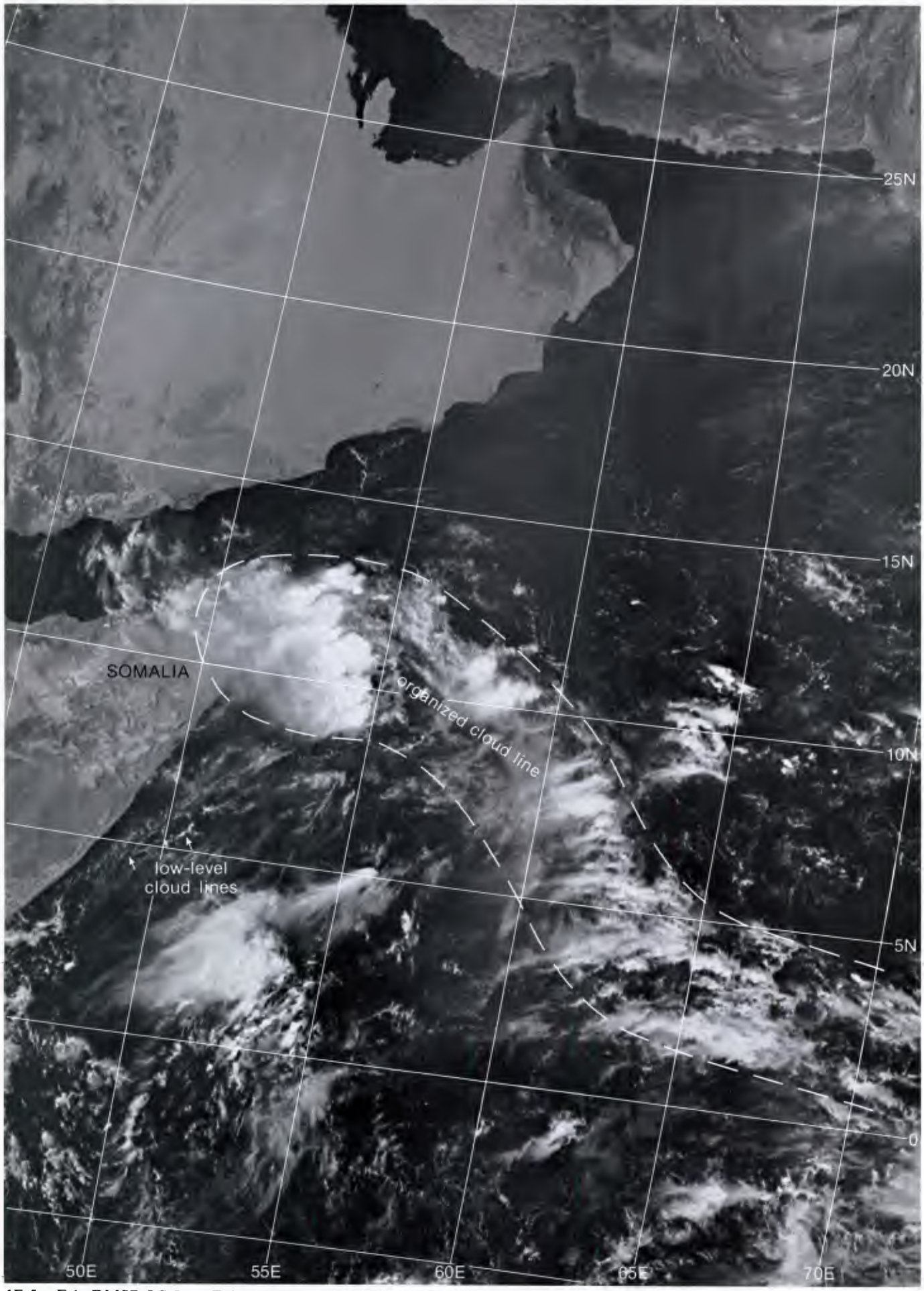

1E-5a. F-1. DMSP LS Low Enhancement. 0712 GMT 10 June 1979.

1E-6a. A plot of an area averaged value of a zonal kinetic energy as a function of time. The area encloses a large domain of the Arabian Sea north of 4° S at 850 mb.

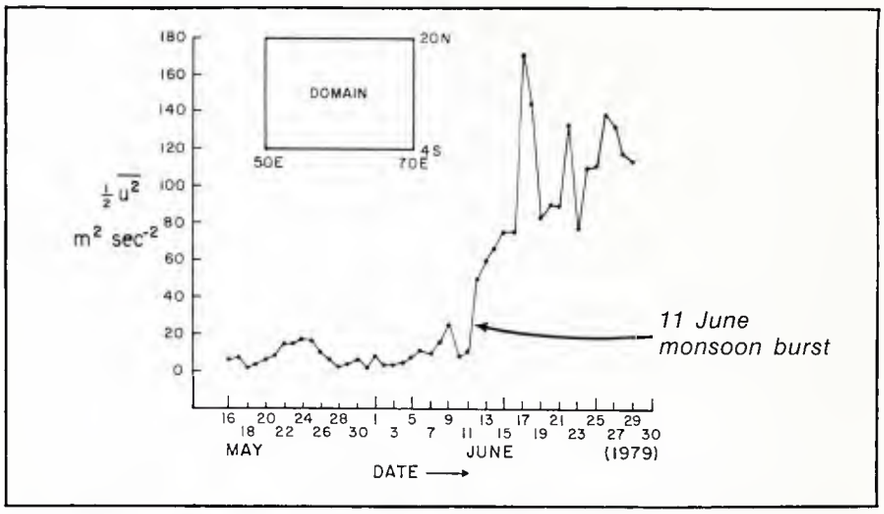

surface

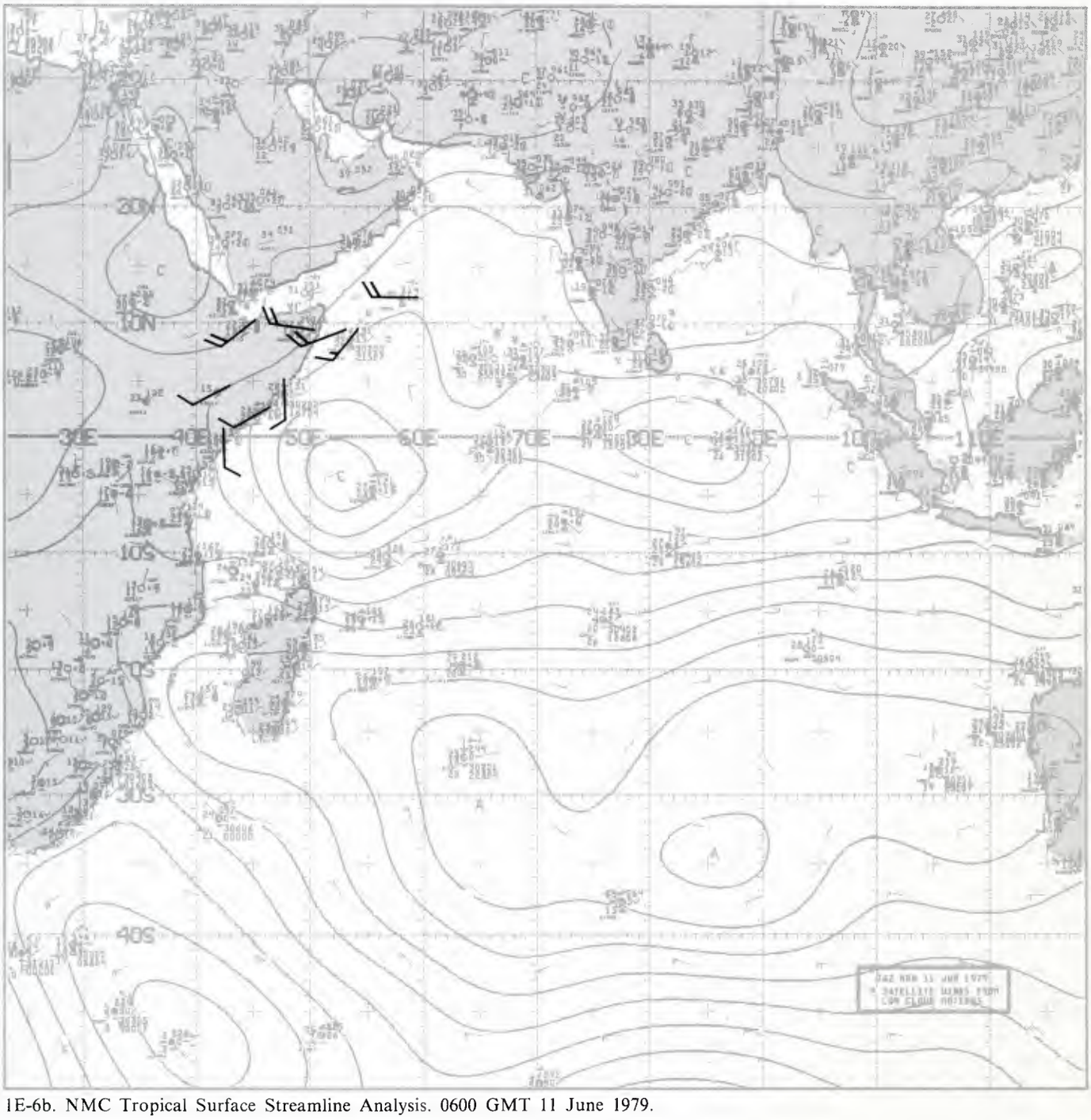

1E-6b. NMC Tropical Surface Streamline Analysis. 0600 GMT 11 June 1979.

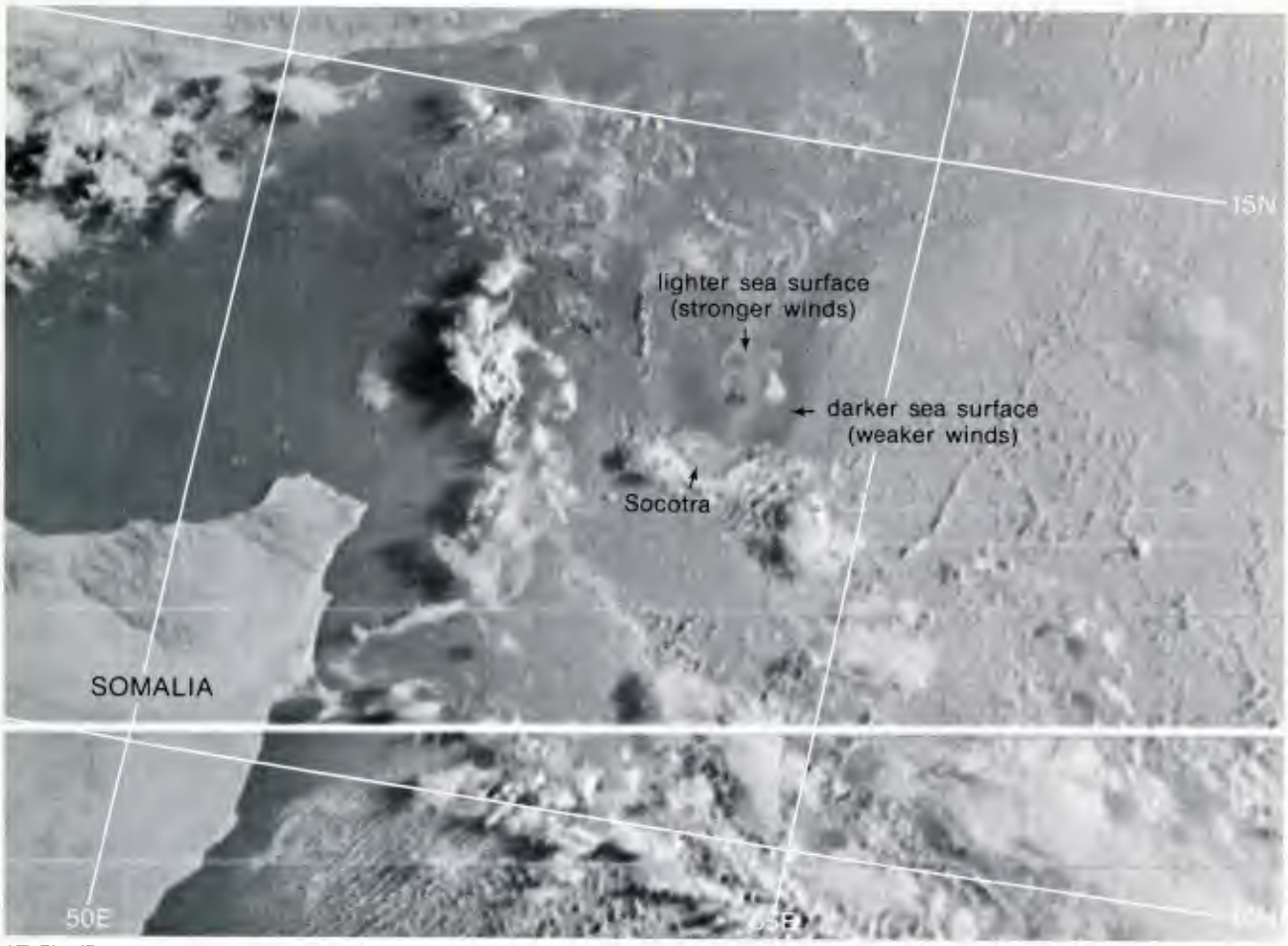

1E-7b. Enlarged View. F-1. DMSP LF Low Enhancement. 0309 GMT 11 June 1979.

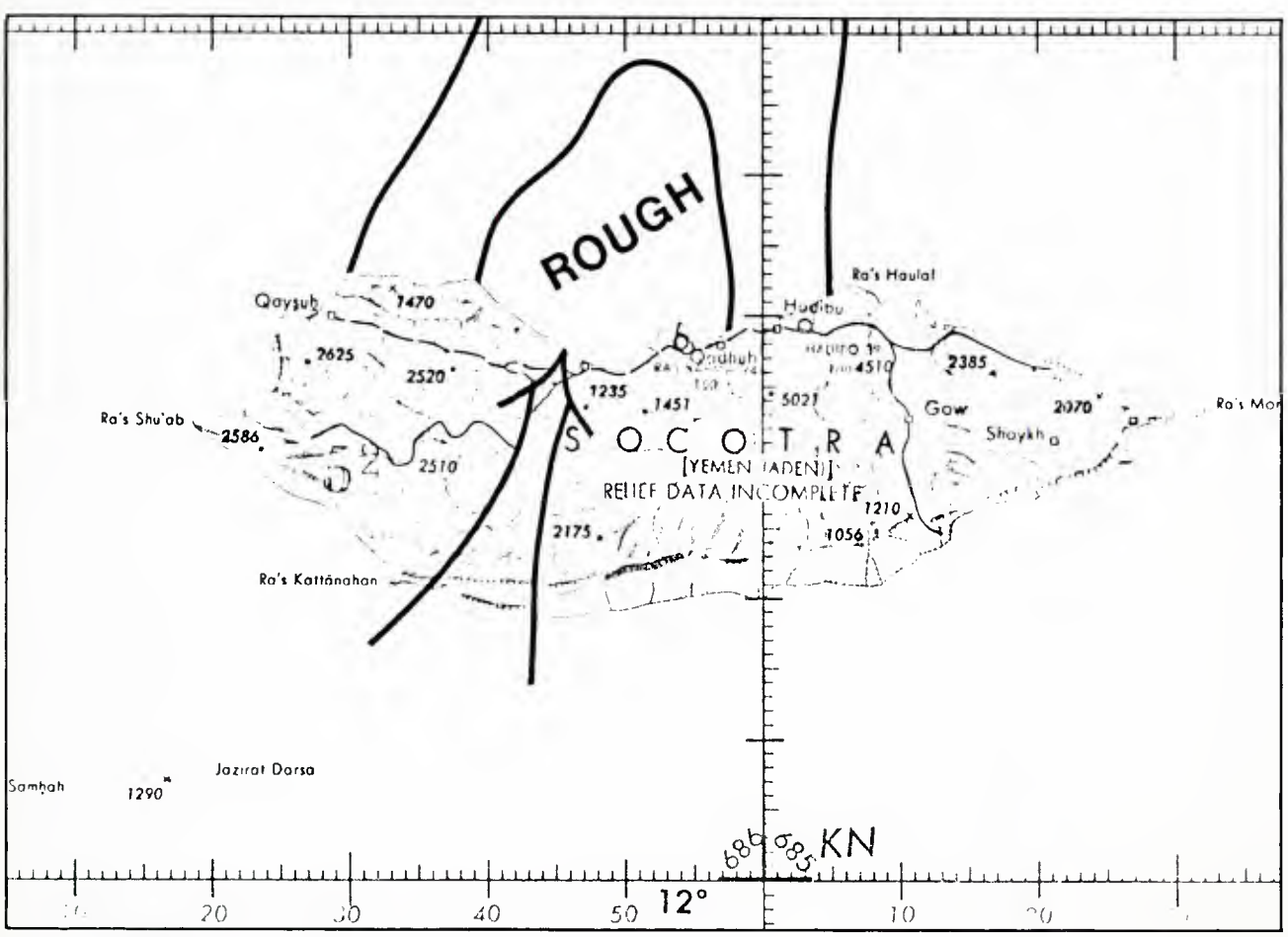

1E-7c. Relief Map of Socotra Island.

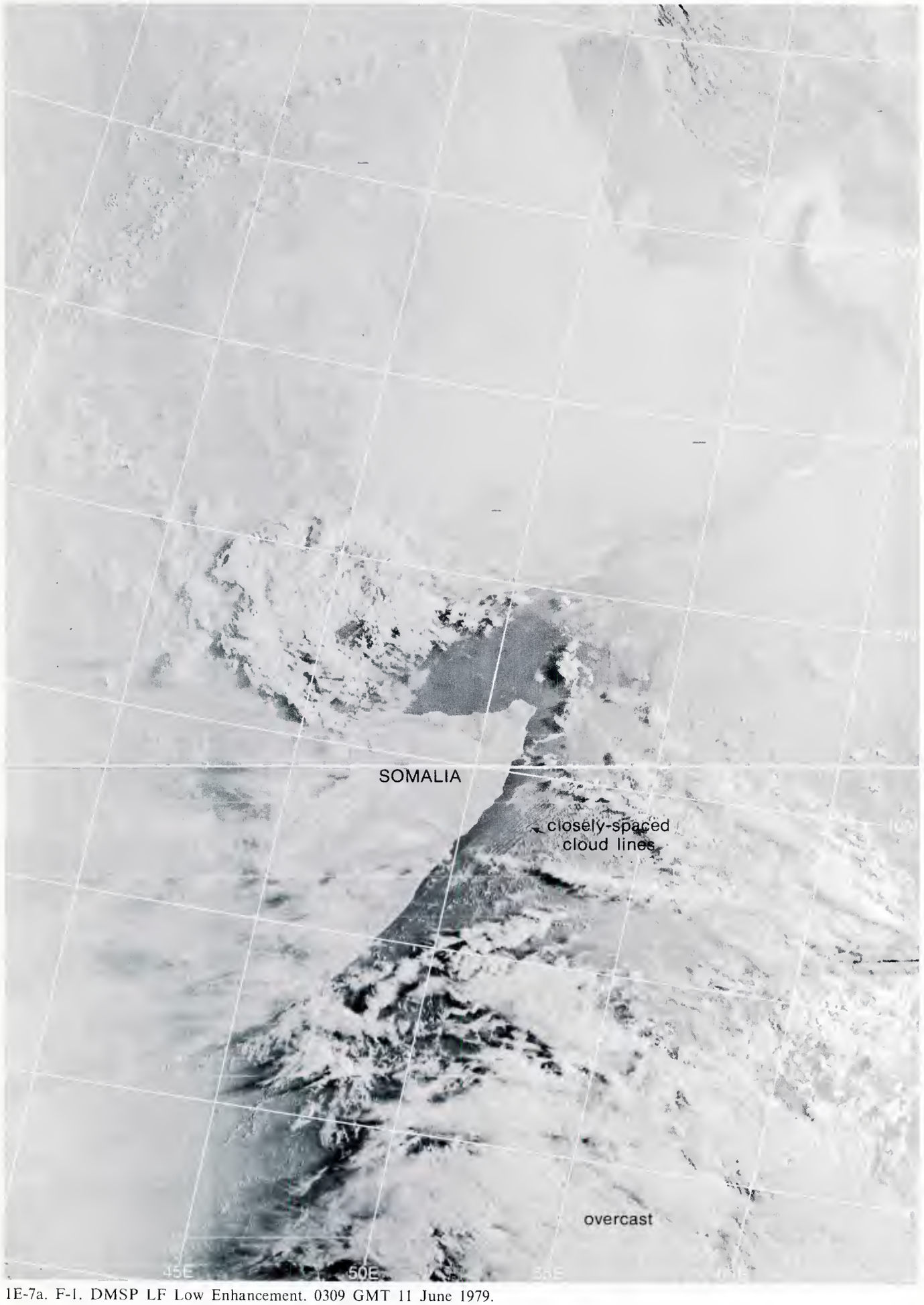

1E-7a. F-1. DMSP LF Low Enhancement. 0309 GMT 11 June 1979.

Important Conclusions

1. The onset or burst of the southwest monsoon occurs throughout the northern Indian Ocean in a rapid but organized manner.

2. The general development trend is for increased cross-equatorial flow, followed by increased westerly flow across the Arabian Sea, frequent development of an onset vortex, and then a steady northward and eastward progress of the southwest monsoon clouds and precipitation over India.

3. Several of the stages of the burst can be identified by cloud patterns in satellite imagery.
   (a) Cross-equatorial flow (Somali low-level jet) identified by low-level cloudiness parallel to the Somalia coast.
   (b) The area of increased westerly flow shown by a line or leading edge of convective activity.
   (c) The onset vortex which forms on the cyclonic shear side of the increased westerly flow (see Sec. 1E, Case 2).
   (d) The northward and eastward march of the southwest monsoon over India identified by the development of convective clouds.

4. The time of the onset of increased cross-equatorial flow until the increased westerly flow reaches extreme southwest India is on the order of 3 to 4 days.

5. Significant changes in environmental conditions will occur as the burst crosses the Arabian Sea, giving rise to vastly increased sea state conditions, increased occurrence and intensity of rain showers, and reduced visibility.

surface

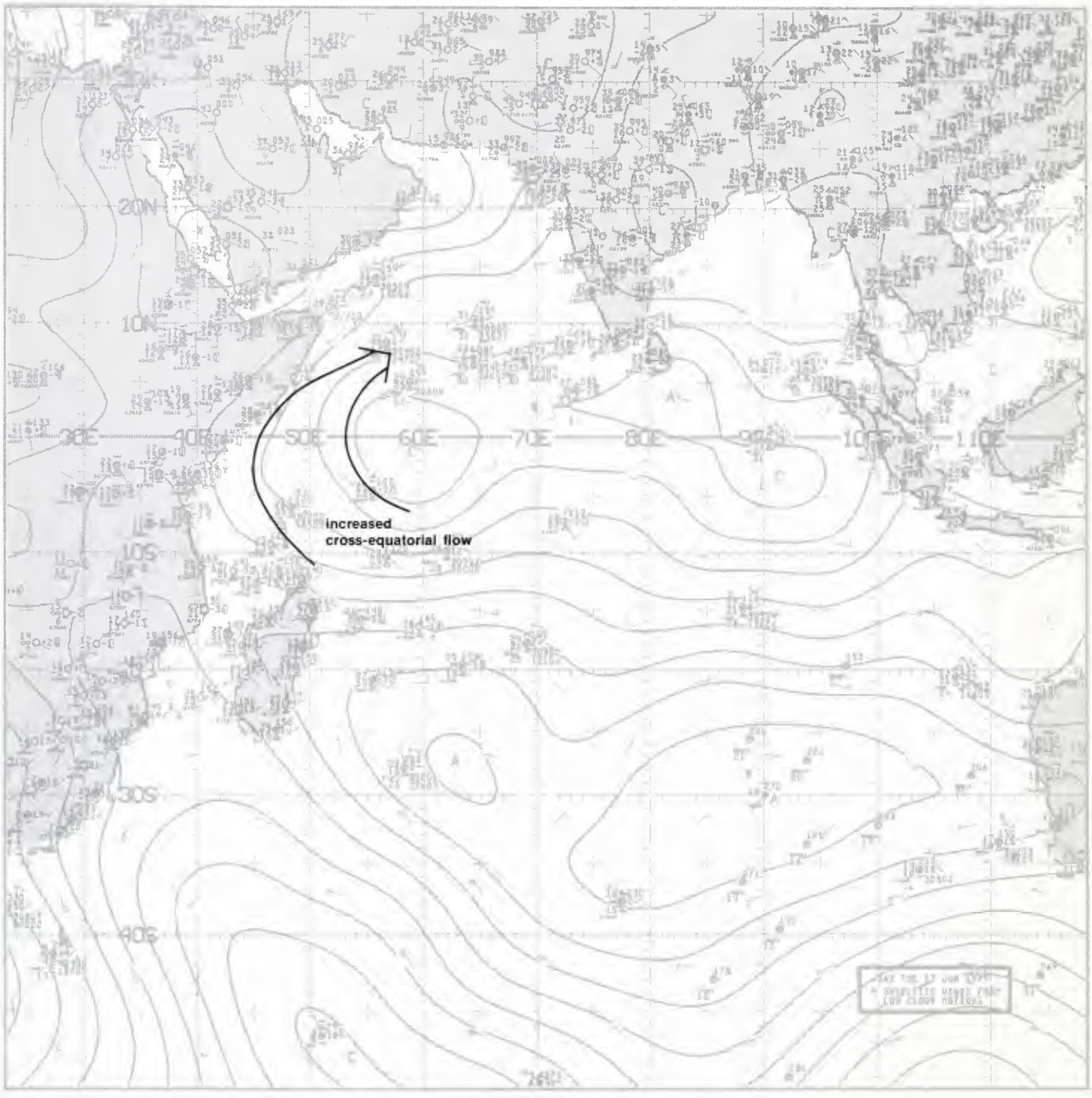

1E-8a. NMC Tropical Surface Streamline Analysis. 0600 GMT 12 June 1979.

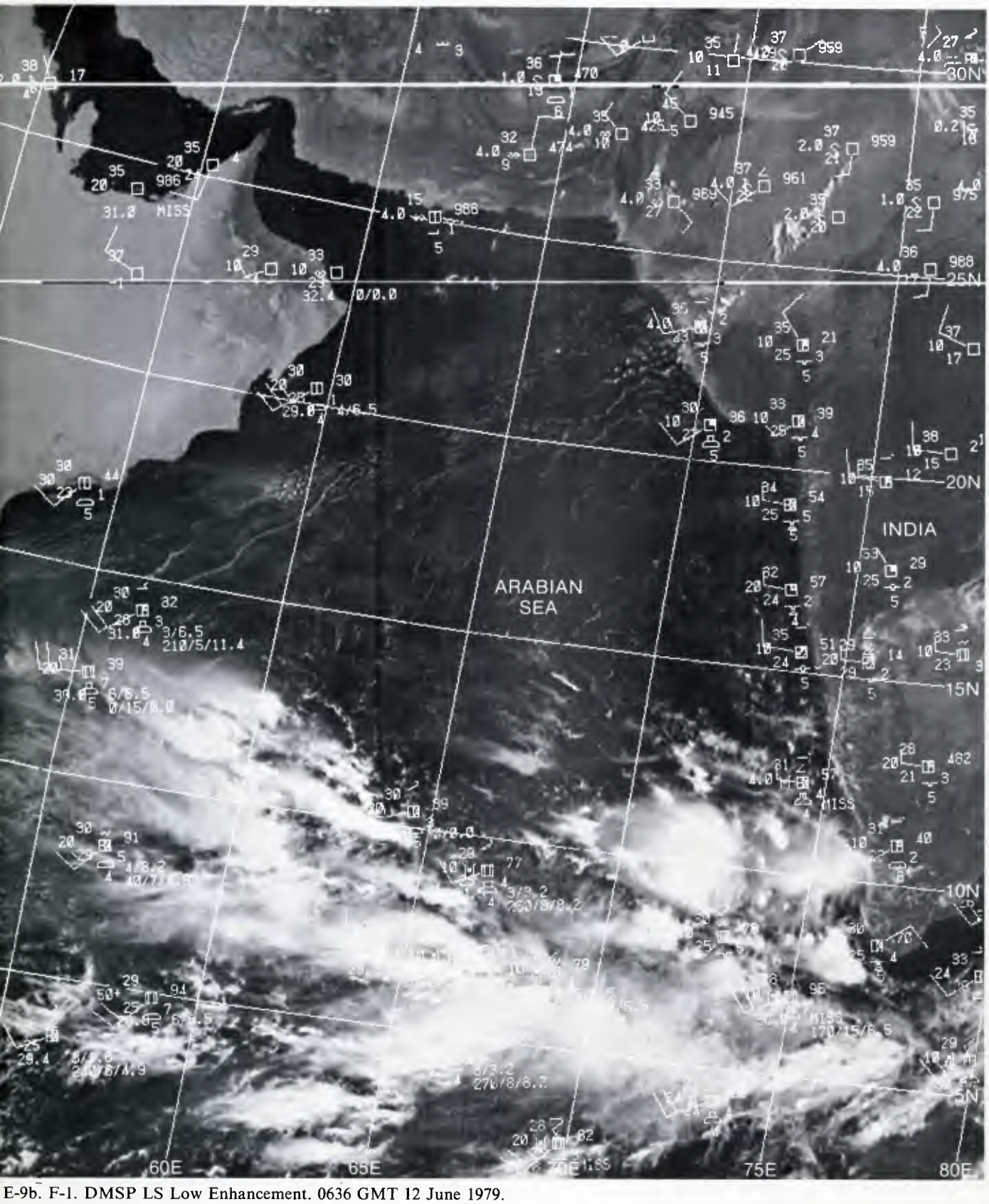

E-9b. F-1. DMSP LS Low Enhancement. 0636 GMT 12 June 1979.
Surface Wind Reports. 0600 GMT 12 June 1979.

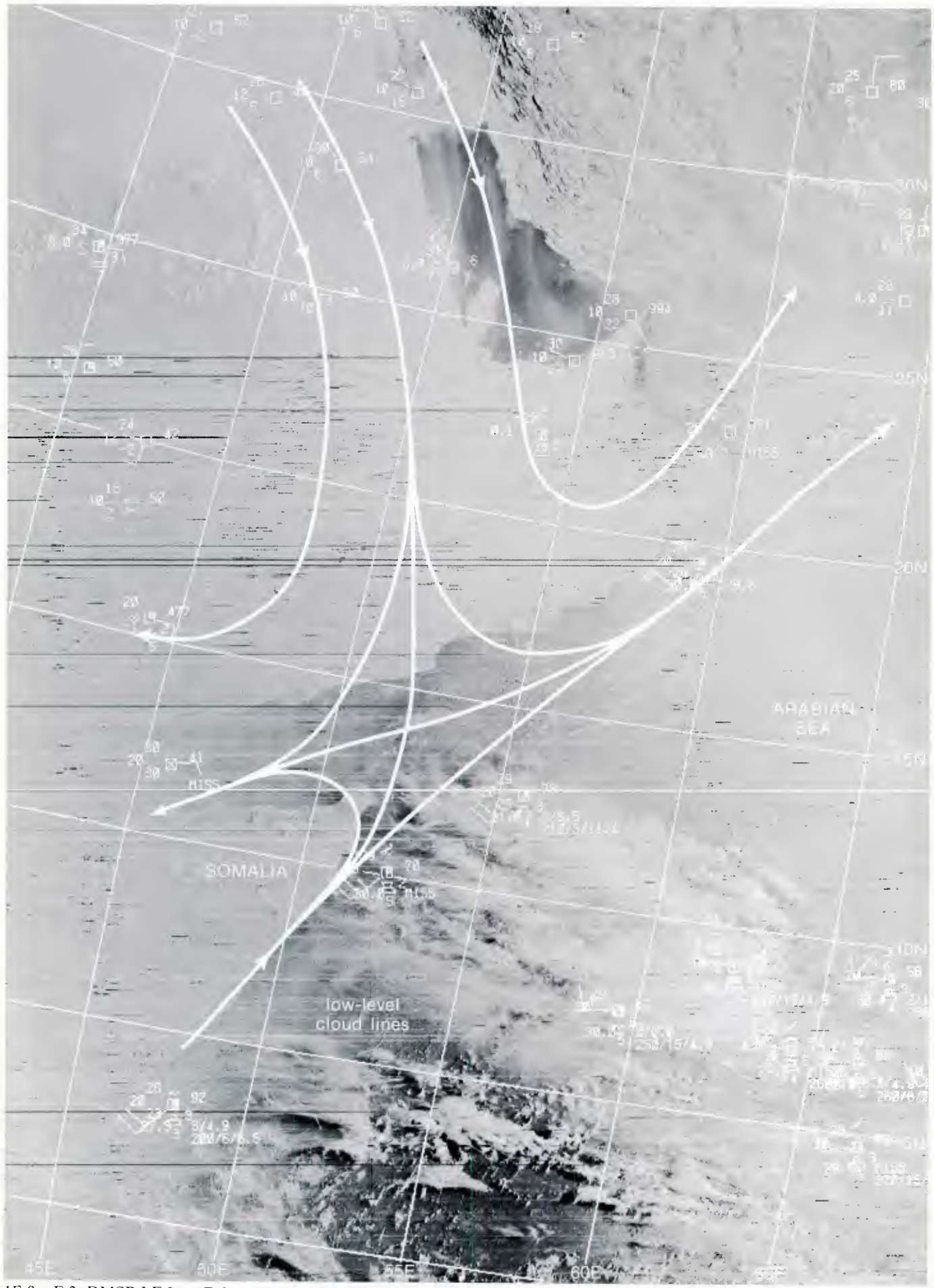

1E-9a. F-3. DMSP LF Low Enhancement. 0249 GMT 12 June 1979.
Surface Wind Reports and Streamline Analysis. 0000 GMT 12 June 1979.

Case 2 Arabian Sea/Bay of Bengal—Summer

Southwest Monsoon Onset

surface

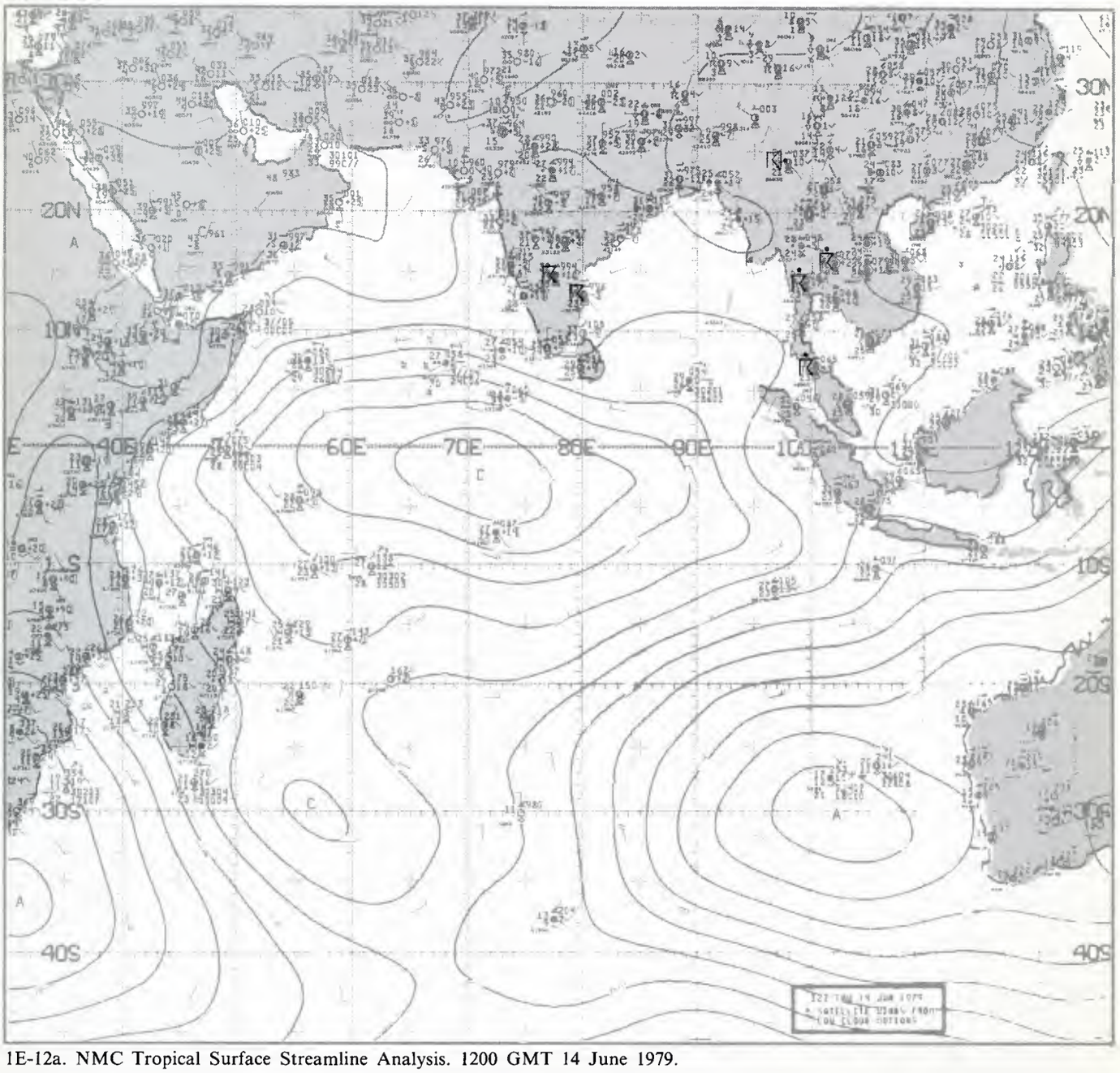

1E-12a. NMC Tropical Surface Streamline Analysis. 1200 GMT 14 June 1979.

14 June

On this date, the 1200 GMT surface streamline analysis (1E-12a) shows no evidence of a closed circulation indicating the presence of an onset vortex over the Arabian Sea. There are, however, indicators of deteriorating weather conditions. Reports of thunderstorms are noted over southern India where none existed earlier, and the weather reports from the land stations to the east of the Bay of Bengal indicate active southwest monsoon type weather.

The onset vortex **C1** is clearly indicated at 850 mb (1E-13a). A closed cyclonic cell is shown near 12° N, 70° E. A band of 35- to 45-kt westerly winds extends across the Arabian Sea to the south of the storm from the African coast to Sri Lanka. This is the initial development of the strong low-level westerly flow that will cover the majority of the Arabian Sea during the fully developed southwest monsoon. Comparing this date's conditions at 850 mb with those three days earlier (1E-13b) gives an indication of the increase in the 850-mb level westerly flow and also the increased strength of the cross-equatorial southerly flow. Speeds have generally doubled through the southern Arabian Sea except for near the axis of the near-equatorial clockwise gyre. A second cyclonic center **C2** (1E-13a) is located north of the Bay of Bengal; this system appears to be located in the southern limits of a migratory middle-latitude system.

The GOES-Indian Ocean visible picture at 0400 GMT (1E-13c) shows a large area of convective activity over the southeastern Arabian Sea that is associated with the developing vortex. This area of disturbed weather is about 600 n mi north of the convective activity noted on the 11th (1E-13d). Like the increase in 850-mb winds, this shift northward of the area of convective activity is characteristic of the onset period.

The flow pattern at 700 mb (1E-15b) has several characteristics that should be noted at this time. First, the vortex **C1** is closed at this level and may in fact be better developed than at 850 mb. An area of 50-kt winds is shown southwest of the vortex at this level. Second, easterly winds prevail north of the vortex with maximum speeds of over 40 kt. In the region of this easterly maximum, the 850-mb winds (1E-13a) are westerly at 15 kt. In fact, the 850-mb analysis has westerlies over the entire Arabian Sea north of the vortex circulation. The difference in wind at these two levels indicates strong shear between approximately 5,000 and 10,000 ft and likely turbulent flight conditions. Westerly flow will prevail over the Arabian Sea at 700 mb during the fully developed southwest monsoon regime. A third feature of the 700-mb flow at this time is the extension of the middle-latitude westerlies south of the Himalayas into the region north of the Bay of Bengal. This pattern will also show a marked change in the near future. Finally, note that the strong southerly cross-equatorial flow off Africa, noted at the surface and 850-mb levels, is not well developed at this level. While the areal extent of the cross-equatorial flow will expand some at this level during the full southwest monsoon, the strength of the flow will always be lighter than at the lower levels. This is in agreement with the climatological pattern of gradual deepening of the southwesterly flow as one progresses eastward across the Arabian Sea.

At 500 mb (1E-14b), the pattern of light and variable winds continues to prevail over the northern Indian Ocean region. The circulation about the onset vortex is not yet well developed at this level. As at the 700-mb level, the penetration of middle-latitude westerlies continues along the southern slopes of the Himalayas.

The most significant aspect of the 200-mb analysis (1E-14a) over the equatorial Indian Ocean at this time is the development of northerly cross-equatorial flow over the southern Arabian Sea. This pattern sets up rapidly from earlier days when the flow was nearly parallel to the Equator. The subtropical ridge near 20°–25° N is quite well developed at this time. Anticyclonic cells are located over the eastern Persian Gulf and northern Indo-China with connecting ridges. The development and northward shift of this system tends to move the westerlies northward. When the axis of the subtropical ridge moves north of the Himalayas, the southwest monsoon will spread over its normal full climatological area.

In the GOES-Indian Ocean infrared picture at 1330 GMT (1E-15a), the cirrus plumes over the equatorial region give a clear indication of the northerly cross-equatorial component of the upper flow. The cloud pattern associated with the vortex, as detected in the upper-air analyses, is seen as the dominant feature over the northern Indian Ocean. The upper-level easterly flow that exists over the equatorial northern Indian Ocean during the southwest monsoon normally drops off rapidly as it flows over eastern Africa and the southern Red Sea. The portion that reaches the Red Sea area curves anticyclonically and merges with the hemispheric-scale subtropical jet southwesterly flow. The convective cells in the vicinity of the southern Red Sea give clear evidence of reduced wind speeds over them. Note the near lack of cirrus plumes from the cells in the image and the corresponding reduction of speed shown at 200 mb (1E-14a). Infrared imagery taken throughout the southwest monsoon season will provide valuable insights to the upper-level flow pattern.

continued on page 1E-16

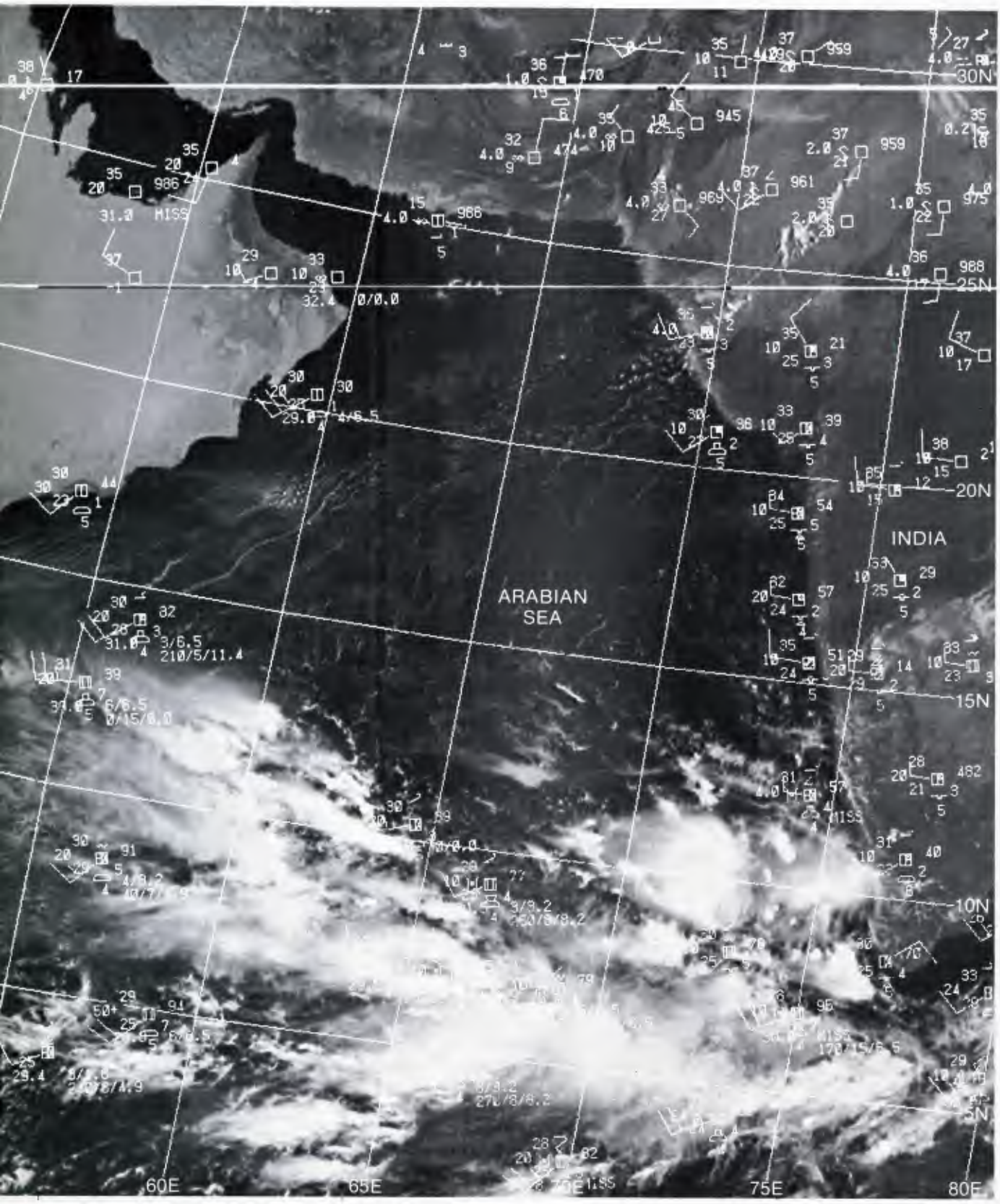

E-9b. F-1. DMSP LS Low Enhancement. 0636 GMT 12 June 1979.
urface Wind Reports. 0600 GMT 12 June 1979.

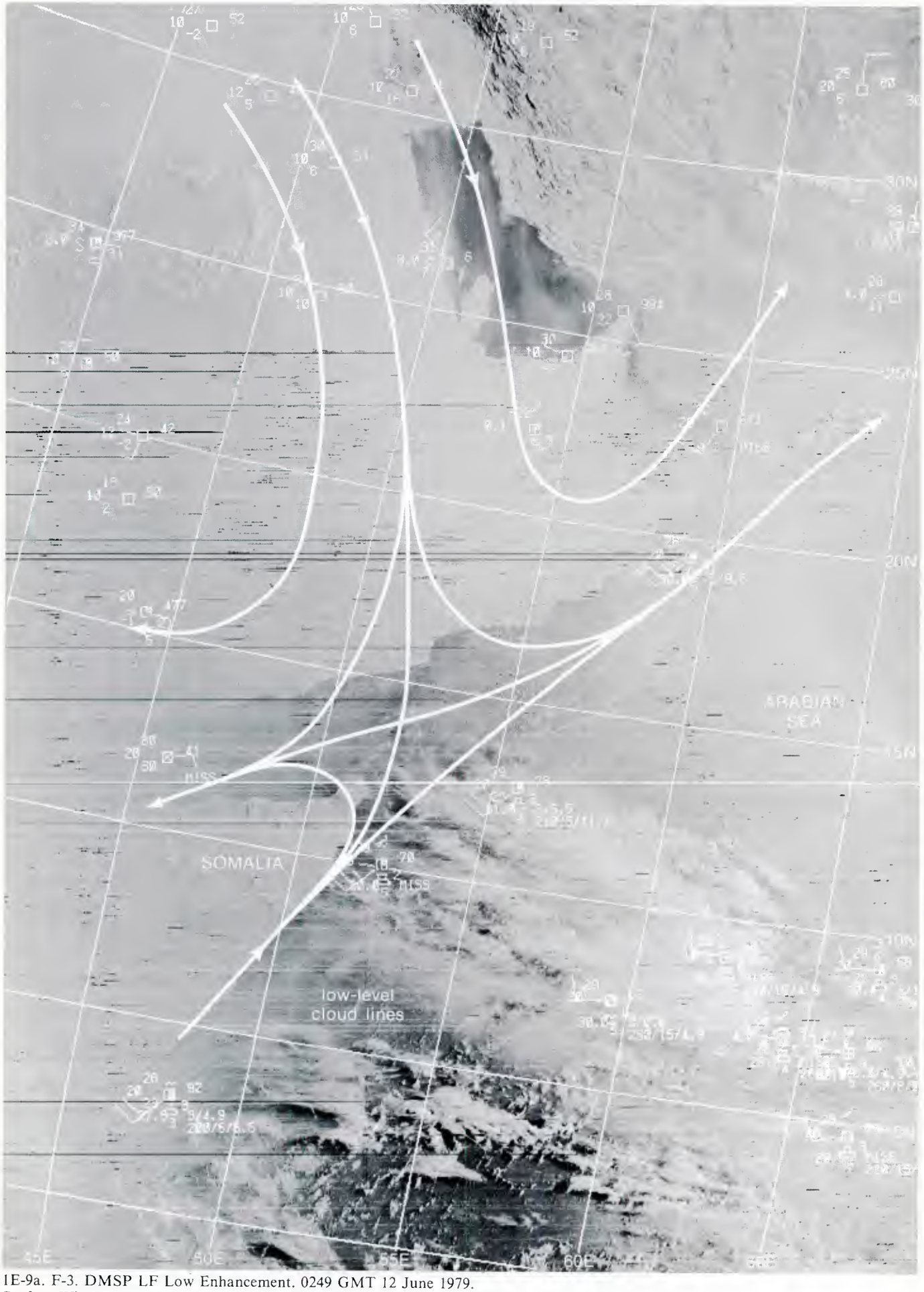

1E-9a. F-3. DMSP LF Low Enhancement. 0249 GMT 12 June 1979.
Surface Wind Reports and Streamline Analysis. 0000 GMT 12 June 1979.

Case 2 Arabian Sea/Bay of Bengal—Summer

Southwest Monsoon Onset

surface

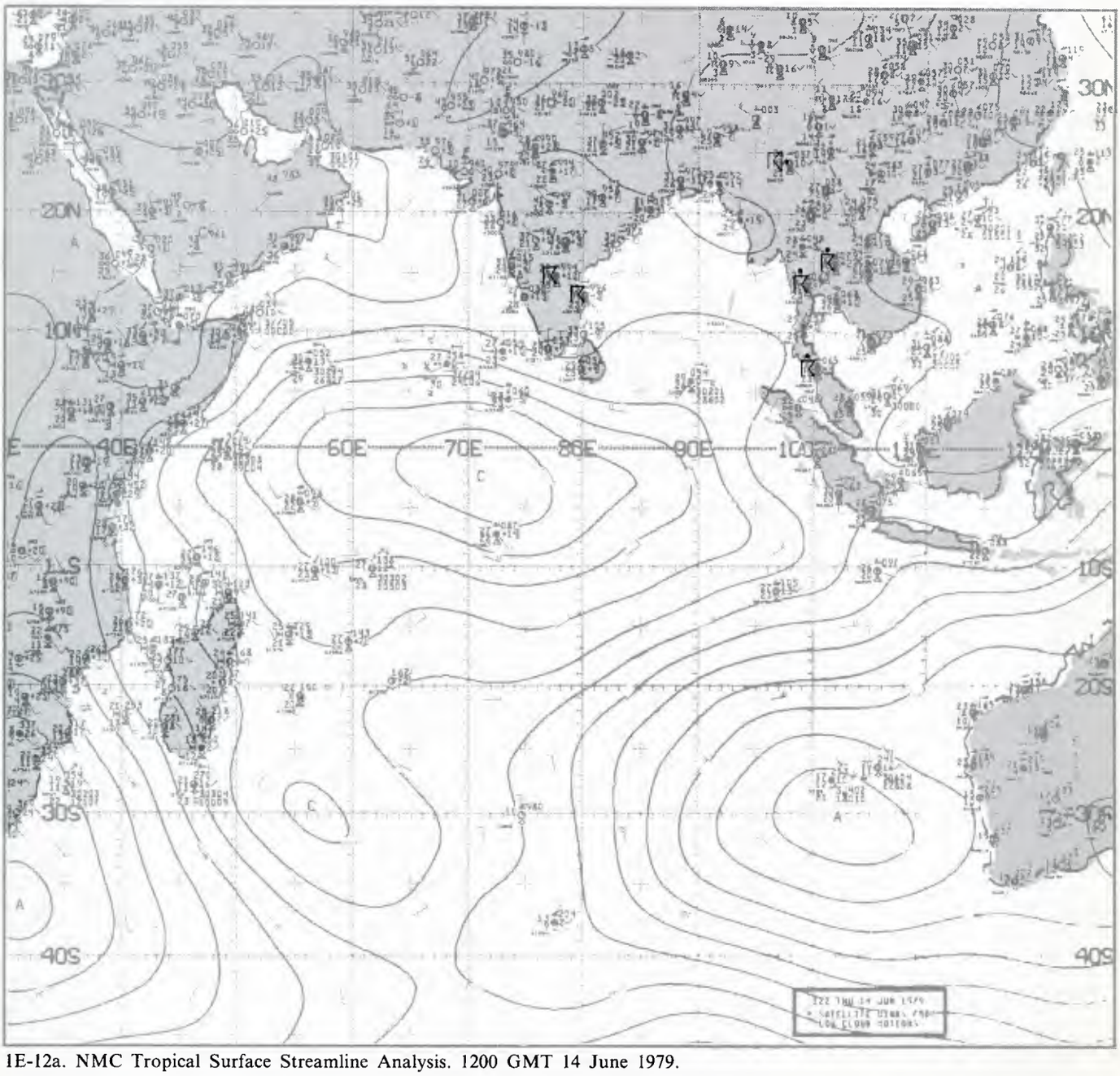

1E-12a. NMC Tropical Surface Streamline Analysis. 1200 GMT 14 June 1979.

14 June

On this date, the 1200 GMT surface streamline analysis (1E-12a) shows no evidence of a closed circulation indicating the presence of an onset vortex over the Arabian Sea. There are, however, indicators of deteriorating weather conditions. Reports of thunderstorms are noted over southern India where none existed earlier, and the weather reports from the land stations to the east of the Bay of Bengal indicate active southwest monsoon type weather.

The onset vortex **C1** is clearly indicated at 850 mb (1E-13a). A closed cyclonic cell is shown near 12° N, 70° E. A band of 35- to 45-kt westerly winds extends across the Arabian Sea to the south of the storm from the African coast to Sri Lanka. This is the initial development of the strong low-level westerly flow that will cover the majority of the Arabian Sea during the fully developed southwest monsoon. Comparing this date's conditions at 850 mb with those three days earlier (1E-13b) gives an indication of the increase in the 850-mb level westerly flow and also the increased strength of the cross-equatorial southerly flow. Speeds have generally doubled through the southern Arabian Sea except for near the axis of the near-equatorial clockwise gyre. A second cyclonic center **C2** (1E-13a) is located north of the Bay of Bengal; this system appears to be located in the southern limits of a migratory middle-latitude system.

The GOES-Indian Ocean visible picture at 0400 GMT (1E-13c) shows a large area of convective activity over the southeastern Arabian Sea that is associated with the developing vortex. This area of disturbed weather is about 600 n mi north of the convective activity noted on the 11th (1E-13d). Like the increase in 850-mb winds, this shift northward of the area of convective activity is characteristic of the onset period.

The flow pattern at 700 mb (1E-15b) has several characteristics that should be noted at this time. First, the vortex **C1** is closed at this level and may in fact be better developed than at 850 mb. An area of 50-kt winds is shown southwest of the vortex at this level. Second, easterly winds prevail north of the vortex with maximum speeds of over 40 kt. In the region of this easterly maximum, the 850-mb winds (1E-13a) are westerly at 15 kt. In fact, the 850-mb analysis has westerlies over the entire Arabian Sea north of the vortex circulation. The difference in wind at these two levels indicates strong shear between approximately 5,000 and 10,000 ft and likely turbulent flight conditions. Westerly flow will prevail over the Arabian Sea at 700 mb during the fully developed southwest monsoon regime. A third feature of the 700-mb flow at this time is the extension of the middle-latitude westerlies south of the Himalayas into the region north of the Bay of Bengal. This pattern will also show a marked change in the near future. Finally, note that the strong southerly cross-equatorial flow off Africa, noted at the surface and 850-mb levels, is not well developed at this level. While the areal extent of the cross-equatorial flow will expand some at this level during the full southwest monsoon, the strength of the flow will always be lighter than at the lower levels. This is in agreement with the climatological pattern of gradual deepening of the southwesterly flow as one progresses eastward across the Arabian Sea.

At 500 mb (1E-14b), the pattern of light and variable winds continues to prevail over the northern Indian Ocean region. The circulation about the onset vortex is not yet well developed at this level. As at the 700-mb level, the penetration of middle-latitude westerlies continues along the southern slopes of the Himalayas.

The most significant aspect of the 200-mb analysis (1E-14a) over the equatorial Indian Ocean at this time is the development of northerly cross-equatorial flow over the southern Arabian Sea. This pattern sets up rapidly from earlier days when the flow was nearly parallel to the Equator. The subtropical ridge near 20°–25° N is quite well developed at this time. Anticyclonic cells are located over the eastern Persian Gulf and northern Indo-China with connecting ridges. The development and northward shift of this system tends to move the westerlies northward. When the axis of the subtropical ridge moves north of the Himalayas, the southwest monsoon will spread over its normal full climatological area.

In the GOES-Indian Ocean infrared picture at 1330 GMT (1E-15a), the cirrus plumes over the equatorial region give a clear indication of the northerly cross-equatorial component of the upper flow. The cloud pattern associated with the vortex, as detected in the upper-air analyses, is seen as the dominant feature over the northern Indian Ocean. The upper-level easterly flow that exists over the equatorial northern Indian Ocean during the southwest monsoon normally drops off rapidly as it flows over eastern Africa and the southern Red Sea. The portion that reaches the Red Sea area curves anticyclonically and merges with the hemispheric-scale subtropical jet southwesterly flow. The convective cells in the vicinity of the southern Red Sea give clear evidence of reduced wind speeds over them. Note the near lack of cirrus plumes from the cells in the image and the corresponding reduction of speed shown at 200 mb (1E-14a). Infrared imagery taken throughout the southwest monsoon season will provide valuable insights to the upper-level flow pattern.

continued on page 1E-16

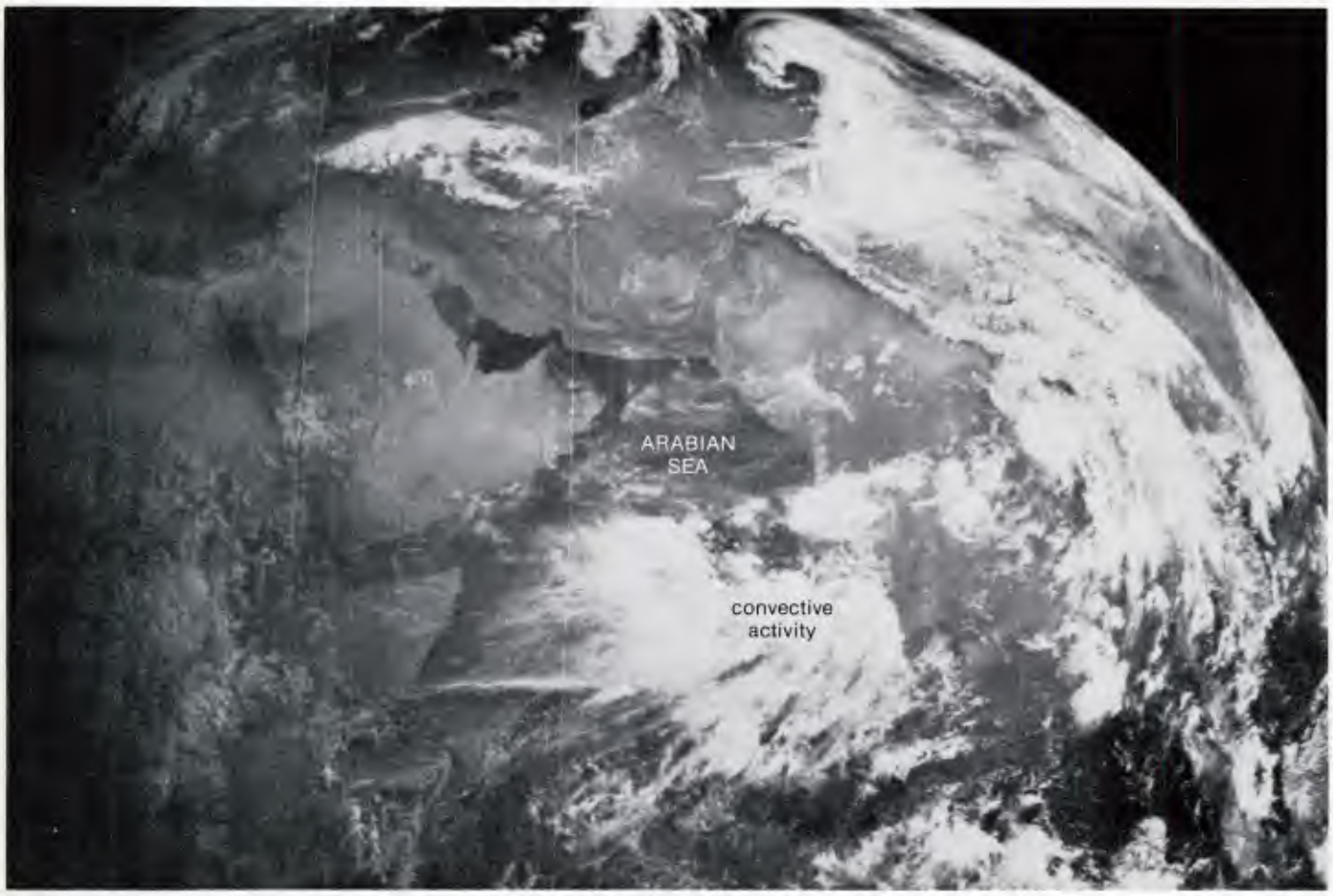

1E-13c. GOES-Indian Ocean. Enlarged View. Visible Picture. 0400 GMT 14 June 1979.

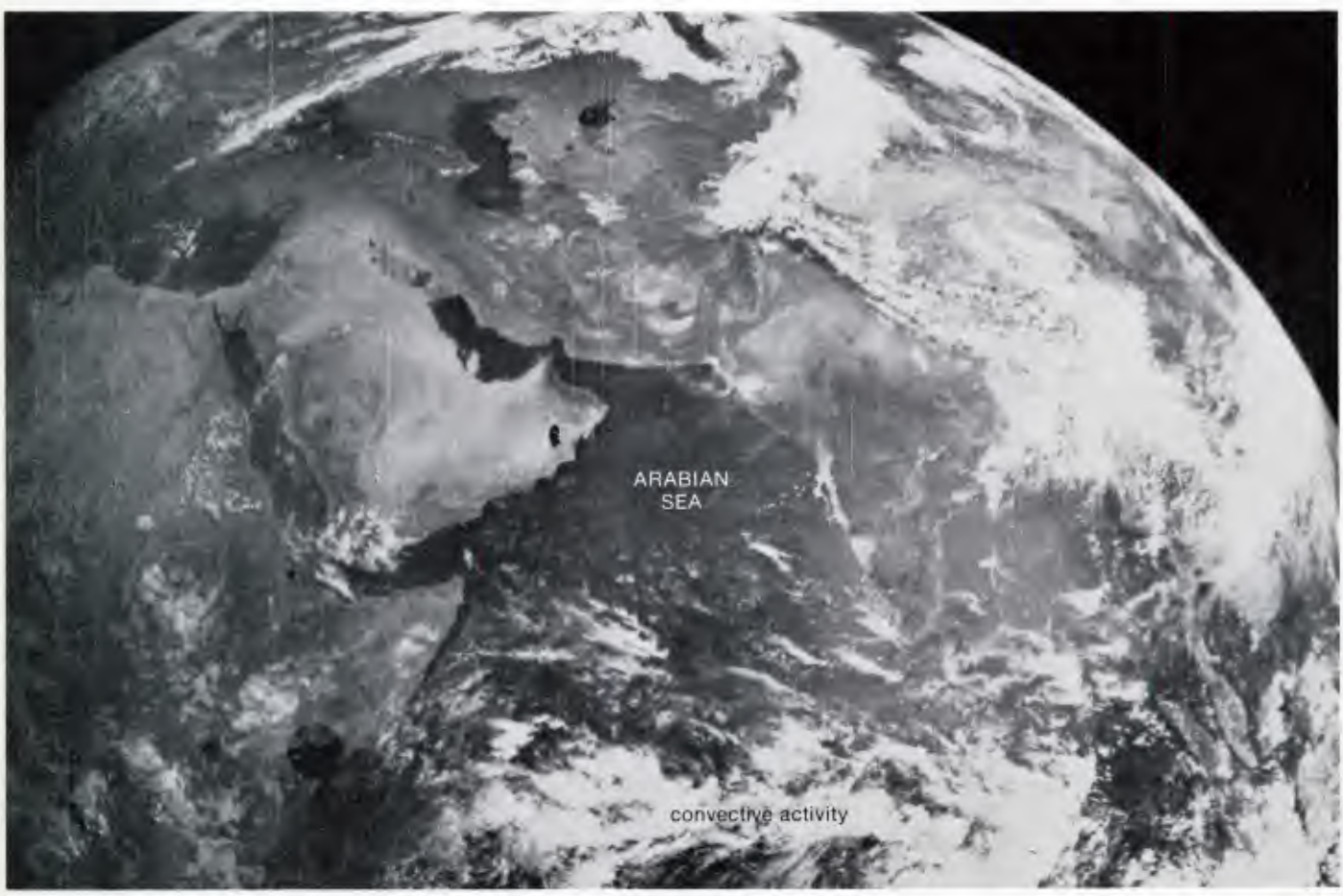

1E-13d. GOES-Indian Ocean. Enlarged View. Visible Picture. 0430 GMT 11 June 1979.

850 mb

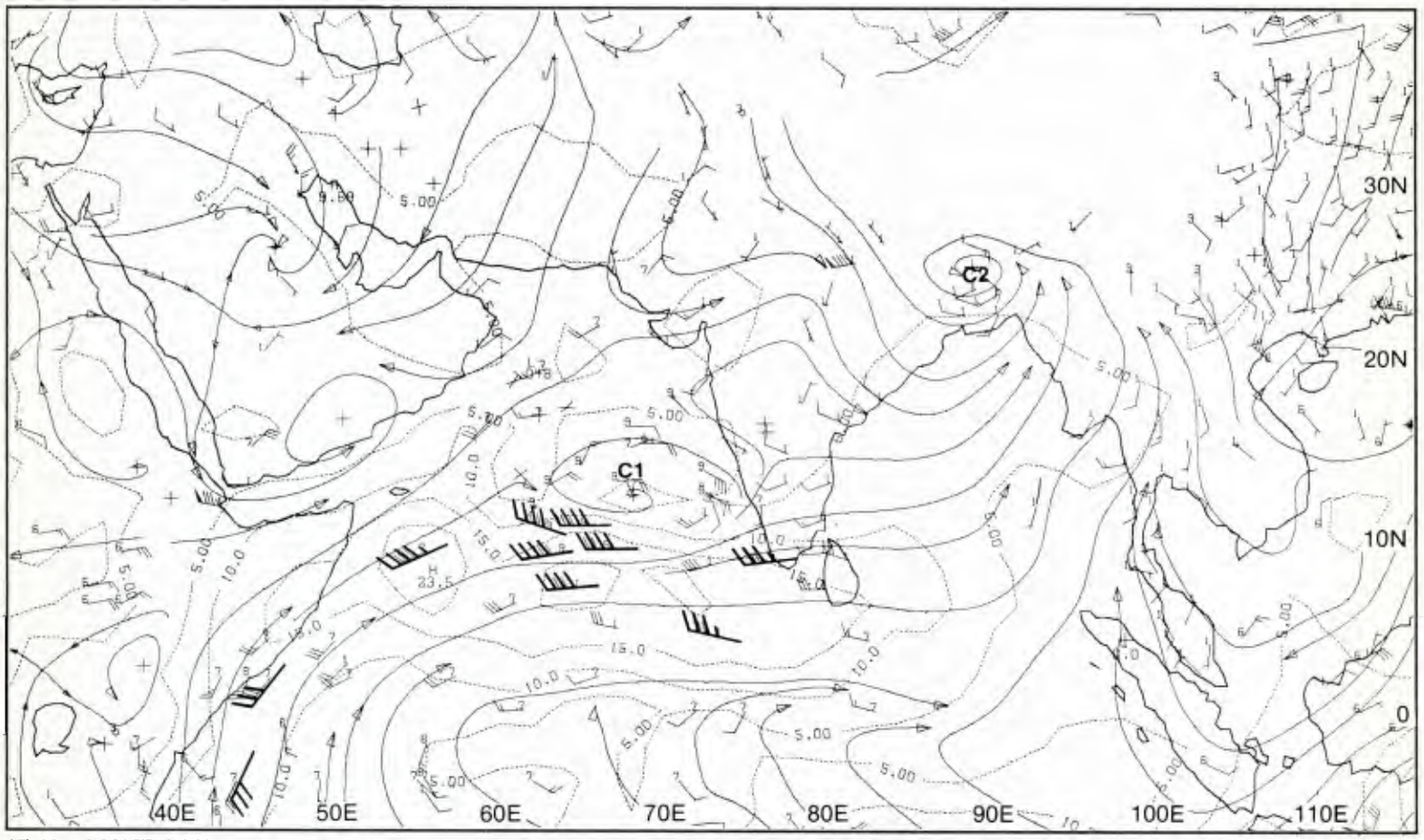

1E-13a. MONEX 850-mb Analysis. 1200 GMT 14 June 1979.

850 mb

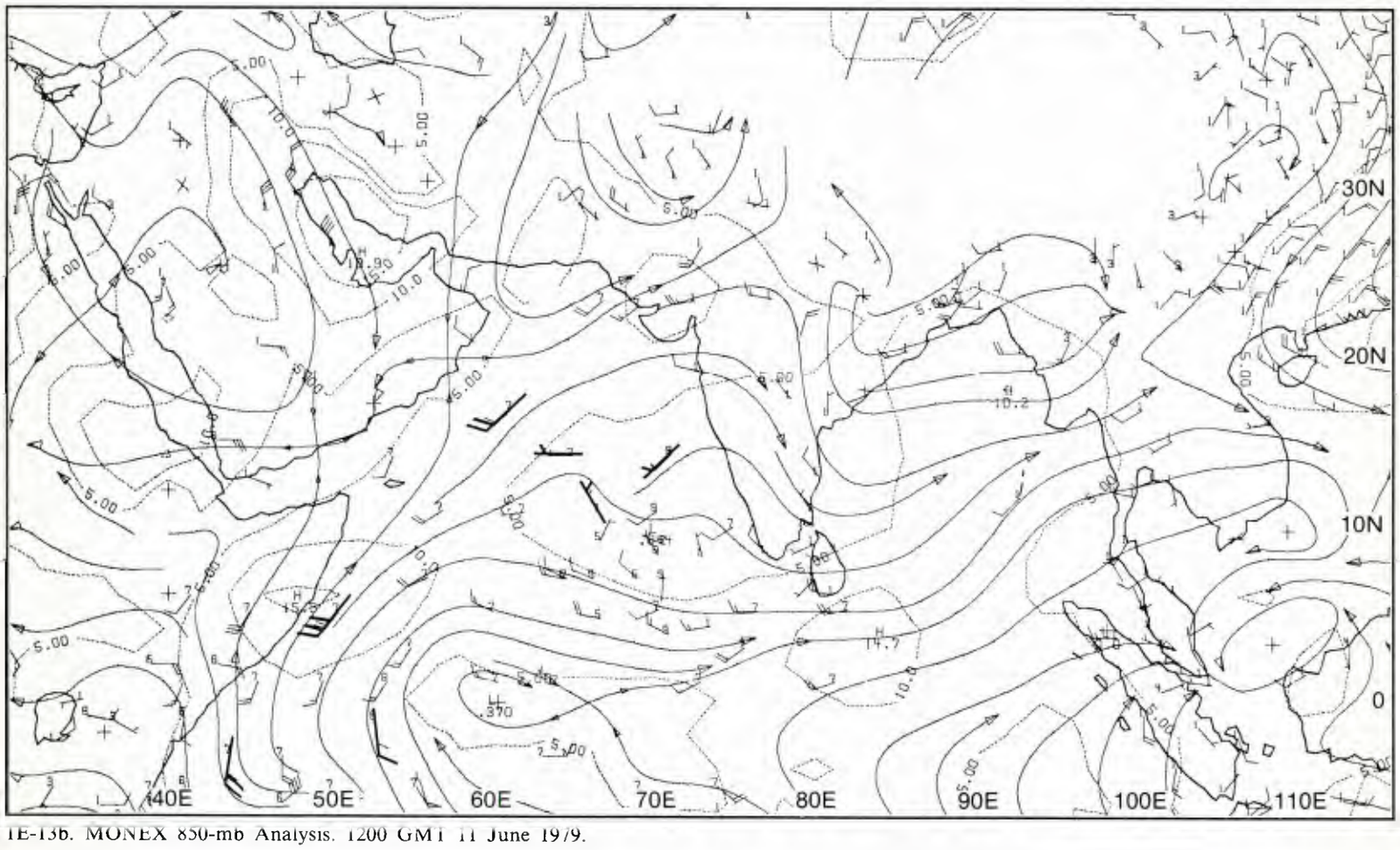

1E-13b. MONEX 850-mb Analysis. 1200 GMT 11 June 1979.

200 mb

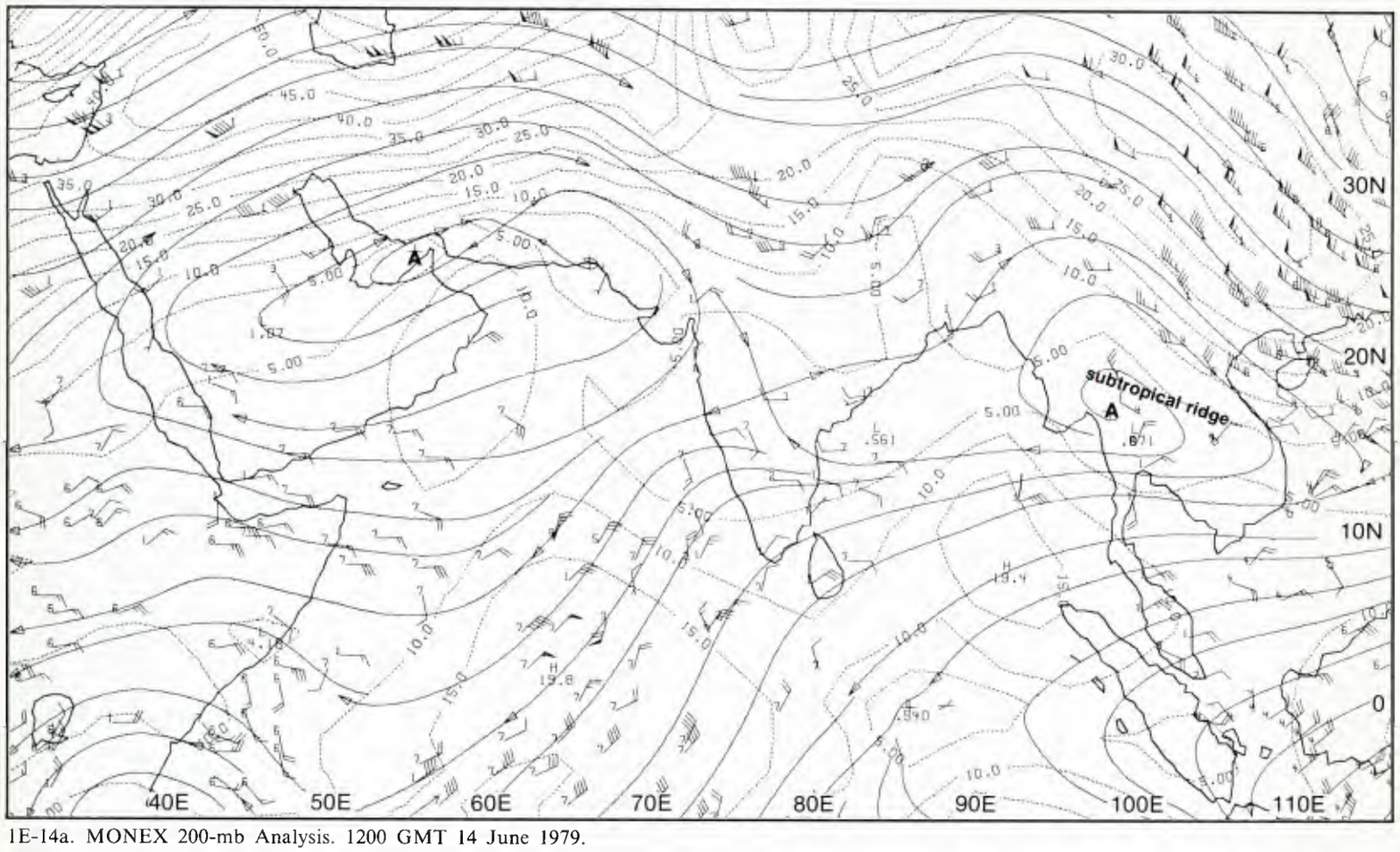

1E-14a. MONEX 200-mb Analysis. 1200 GMT 14 June 1979.

500 mb

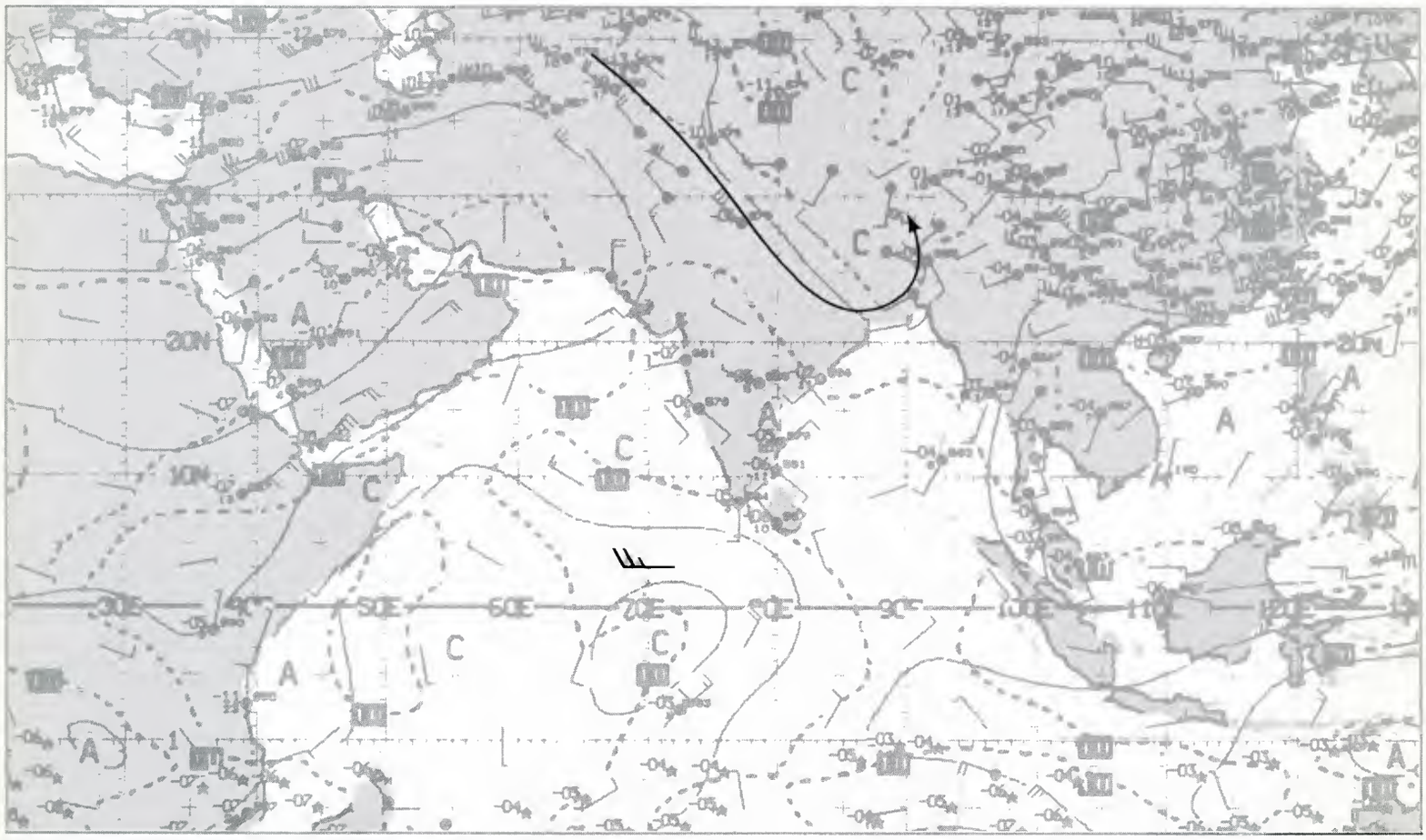

1E-14b. NMC Tropical 500-mb Streamline Analysis. 1200 GMT 14 June 1979.

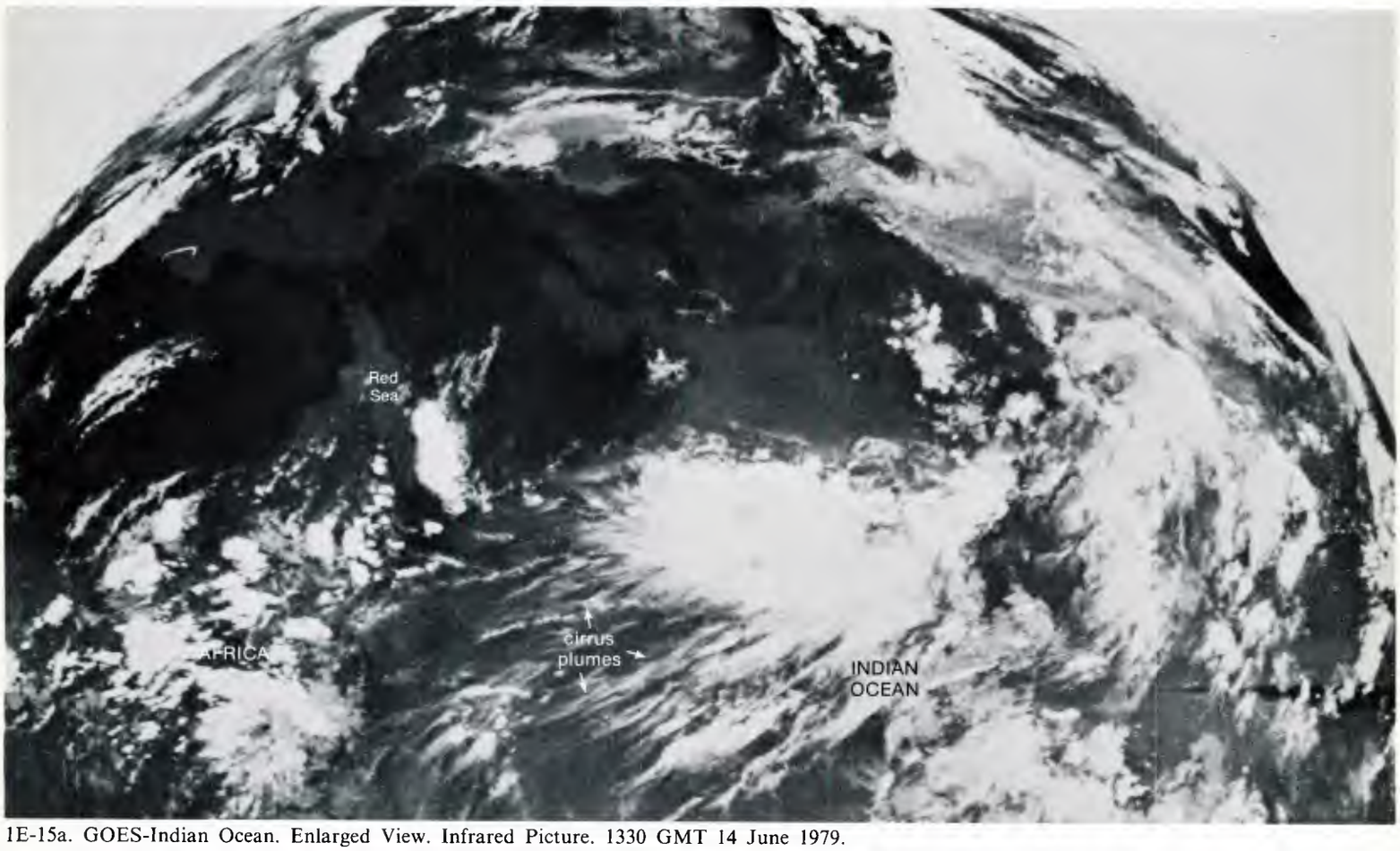

1E-15a. GOES-Indian Ocean. Enlarged View. Infrared Picture. 1330 GMT 14 June 1979.

700 mb

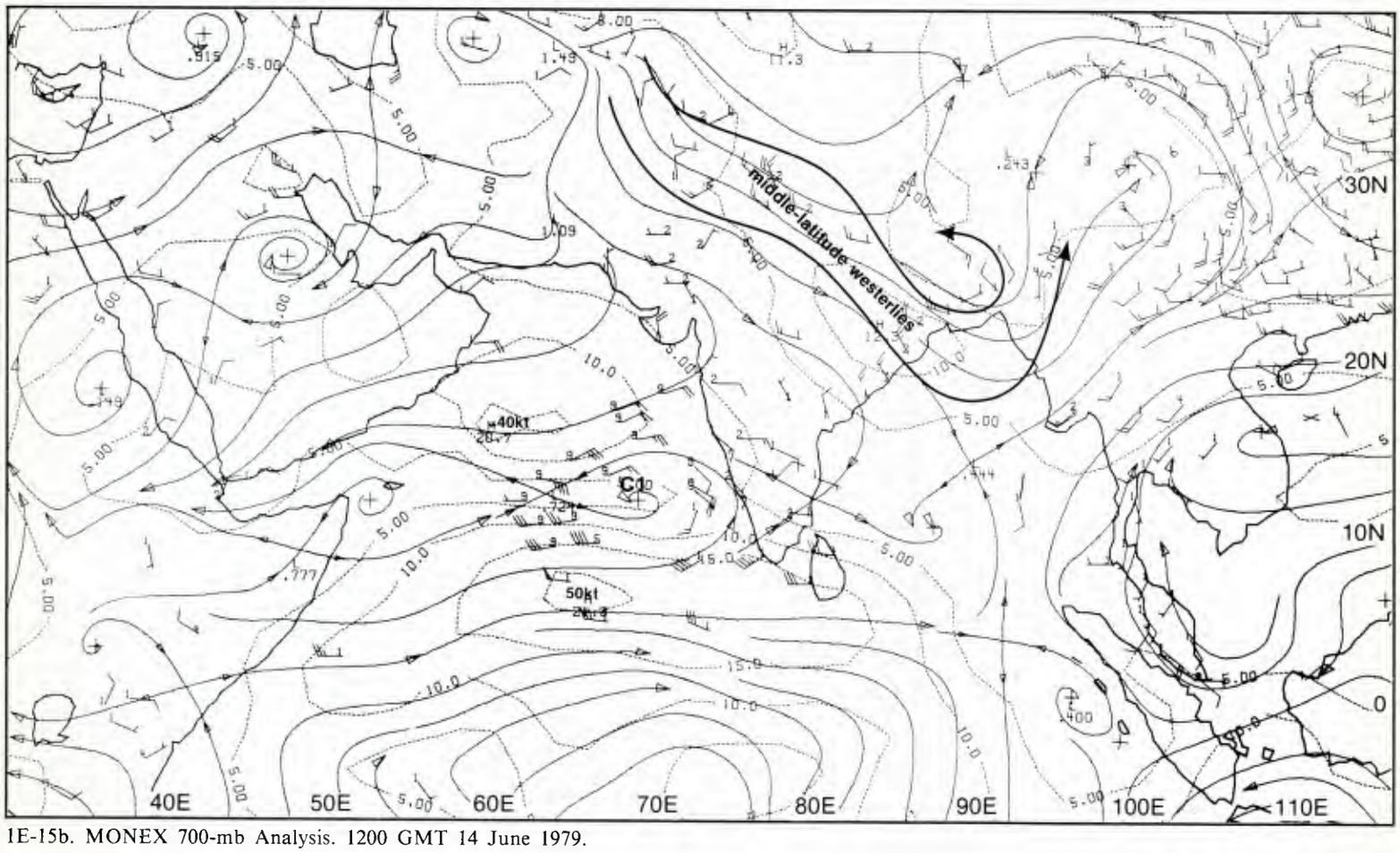

1E-15b. MONEX 700-mb Analysis. 1200 GMT 14 June 1979.

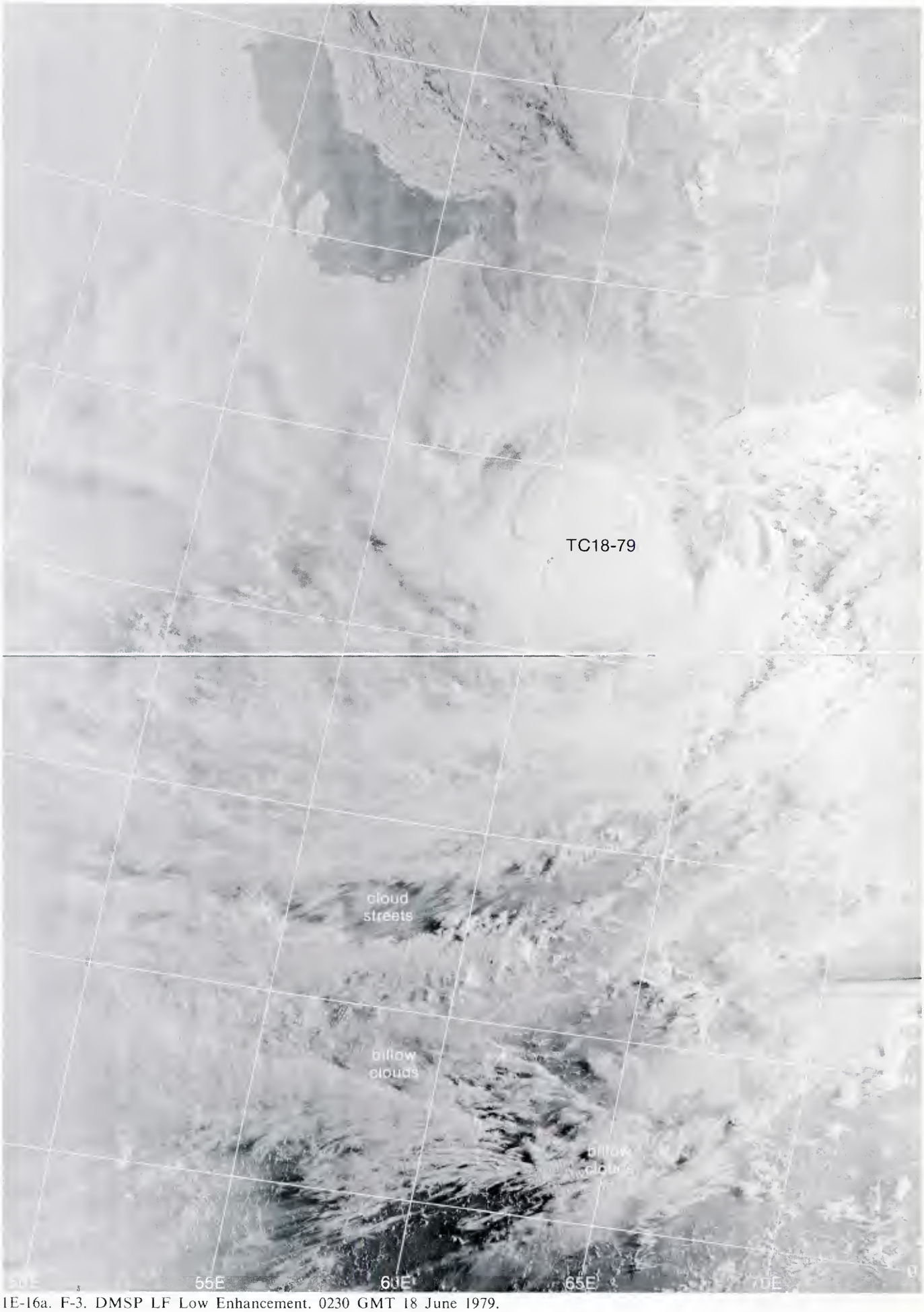

1E-16a. F-3. DMSP LF Low Enhancement. 0230 GMT 18 June 1979.

18 June

The DMSP visible picture at 0230 GMT (1E-16a) shows the complex cloud structure associated with the onset vortex shortly after the initial warning on the system as a tropical cyclone (TC 18-79, issued at 18/0000 GMT). The intense convective activity is clearly evident and a general sense of inward spiraling convective bands is apparent over the southern semicircle of the system. Lower-level cloud streets visible between breaks in upper-level cloud bands to the south (near 9° N, 62° E) have the tightly-spaced configuration indicative of strong low-level winds with speeds increasing with height. Note the numerous billow clouds south of this region indicative of strong vertical speed shear in a thin layer—probably at mid or high levels.

The anticyclonic nature of the outflow of this storm is apparent in the cirrus banding surrounding the central dense overcast cloud mass which obscures the center of circulation.

The surface streamline analysis at 1200 GMT (1E-17b) confirms the strong low-level winds south of the storm's center and reflects the continued rapid development of the southwest monsoon weather regime over the Arabian Sea and India. The vortex **C1** is now positioned near 18° N, 64° E with maximum sustained winds of 45 kt, and is forecast to move northwest at 5 kt. The position from the warning 24 hours later (19/1200 GMT) indicates an actual westerly movement of near 12 kt. At this later time the warning states that maximum sustained winds are 50 kt. The 19/1200 GMT position was very near landfall and subsequently the cyclone moved over Oman with winds decreasing rapidly. The residual convective activity continued over Oman until 22 June (not shown).

In the wake of the onset vortex, the southwest monsoon regime has been established to near 15° N over the Arabian Sea and India. Note that a trough **T1** (1E-17b) extends from the vortex **C1** southeastward past the southern tip of India to the Malay Peninsula. Surface wind reports over the central and western Arabian Sea range from 20 to 35 kt, and ships are reporting wind and swell heights to 16 feet. The southerly cross-equatorial flow continues to be well established from the African coast eastward to near 55° E. Precipitation and extensive cloud cover is becoming widespread in the wake of the onset vortex.

The GOES-Indian Ocean picture at 0500 GMT (1E-17a) shows the vortex TC 18-79 and the cloudiness that has formed in its wake. Heavy convective cloudiness can be seen extending from the vortex southeastward to Malaysia in association with the northern equatorial trough. Northward of the vortex clear conditions prevail. Neither the southwest monsoon flow nor middle-latitude systems are affecting the region immediately south of the Himalayas.

The 850-mb analysis (1E-19b) may best illustrate at this time the dramatic change in the low-level circulation that takes place during the southwest monsoon onset. A large area of the south central Arabian Sea is covered with 50- to 60-kt winds. Just seven days earlier (1E-13a) this area only had 5- to 15-kt winds. The strong westerly flow now extends eastward to southern India and then weakens over the Bay of Bengal. The cross-equatorial flow is now well established, with its areal extent nearly fully developed. The speeds tend to fluctuate by 10 to 20 kt in response to the Southern Hemisphere migrating system movements.

The 700-mb pattern (1E-19a) closely reflects that at the 850-mb level. The vortex **C1** is well developed with the center indicated to be slightly southeast of that at 850 mb. The wind field closely matches the 850-mb pattern with maximum winds greater than 50 kt located south of the vortex center. The strong vertical shear condition noted on the 14th no longer appears to exist, as the flow about the vortex now dominates and dictates the wind direction from the surface through the 700-mb level.

Likewise, the extension of the westerlies south of the Himalayas (1E-15b) no longer exists. The cross-equatorial southerly flow is weakly organized, but by 19/1200 GMT, 24 hours later (chart not shown), it becomes much better organized and approaches the areal extent of the 850-mb level. The speeds generally remain lighter at 700 mb than at 850 mb, reflecting the low-level nature of the Somali jet.

The onset vortex **C1** in its advanced development stage now extends through the 500-mb level (1E-18c). At this level the strongest winds are indicated to the north of the vortex. In the areas of the northern Indian Ocean, other than about the vortex and over the southern Arabian Sea, the winds remain light and variable at 500 mb. There is still no cross-equatorial flow at this level.

The upper-level northerly cross-equatorial flow remains strong and now extends over nearly the full width of the Indian Ocean. A divergent flow pattern is seen at 200 mb (1E-18a) over and to the west of the vortex center. The rapid drop off of the upper-level easterly flow in the region of the southern Red Sea is clearly indicated by the 250-mb analysis for 1200 GMT (1E-18b). The 200- and 250-mb flows indicate sharp anticyclonic curvature over the south central Red Sea. This is the climatological area where the upper-level easterly jet of the southwest monsoon regime feeds into the Northern Hemisphere southwesterly subtropical jet. The northern Arabian Peninsula is known as an area of maximum intensity of the subtropical jet. The influx of mass via the tropical easterly jet quite likely contributes to the enhanced poleward flow via the subtropical jet.

The GOES-Indian Ocean infrared picture at 1330 GMT (1E-21a) indicates the divergent nature of the winds by the plume patterns emanating from the cloud canopy of the tropical cyclone TC 18-79. Notice that the eastern edge of the vortex canopy is nearly smooth indicating little outflow while around the remainder of the canopy cirrus streamers emanate outward with anticyclonic curvature. Those to the west and northwest appear more anticyclonically curved indicating the divergent pattern.

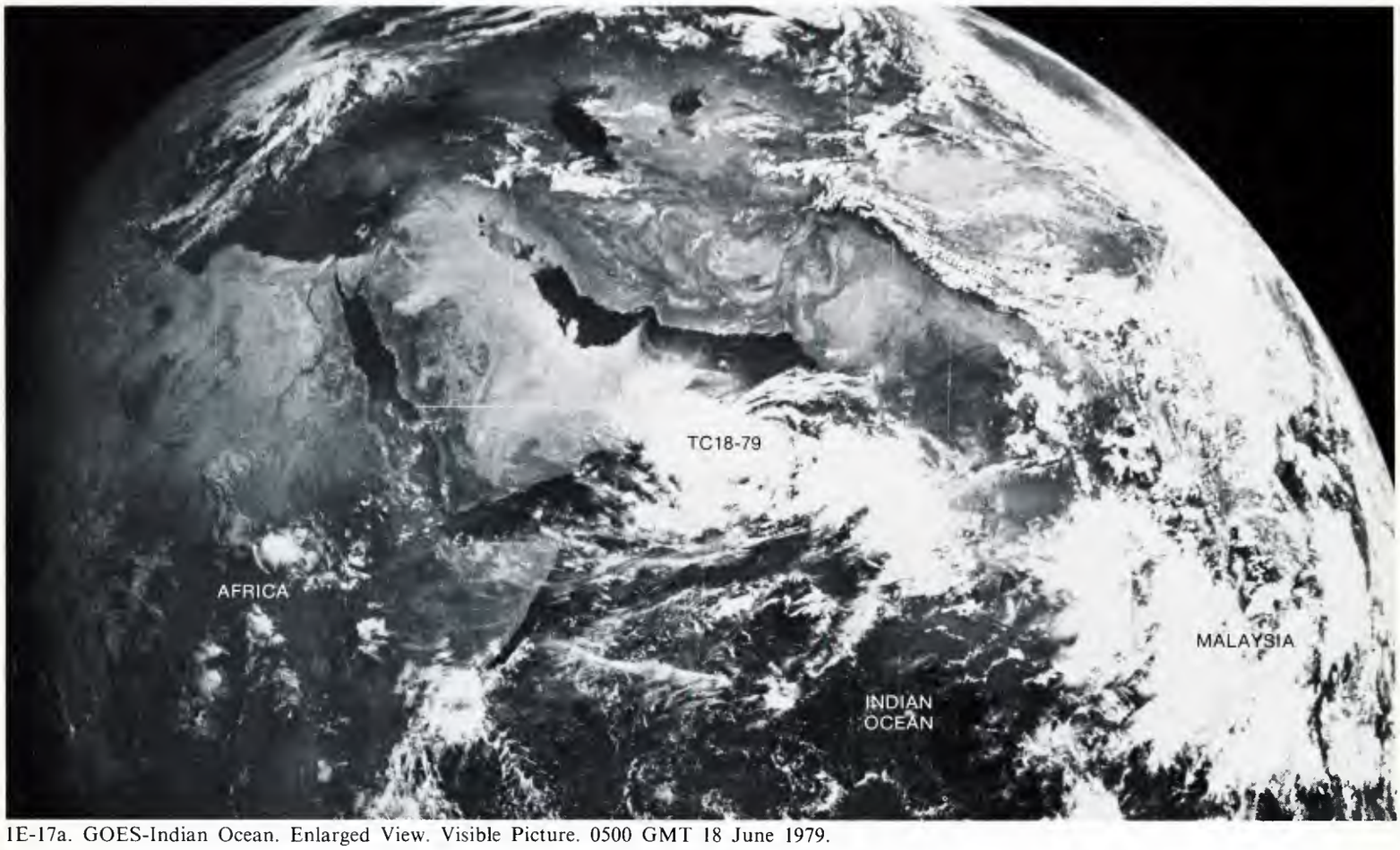

1E-17a. GOES-Indian Ocean. Enlarged View. Visible Picture. 0500 GMT 18 June 1979.

surface

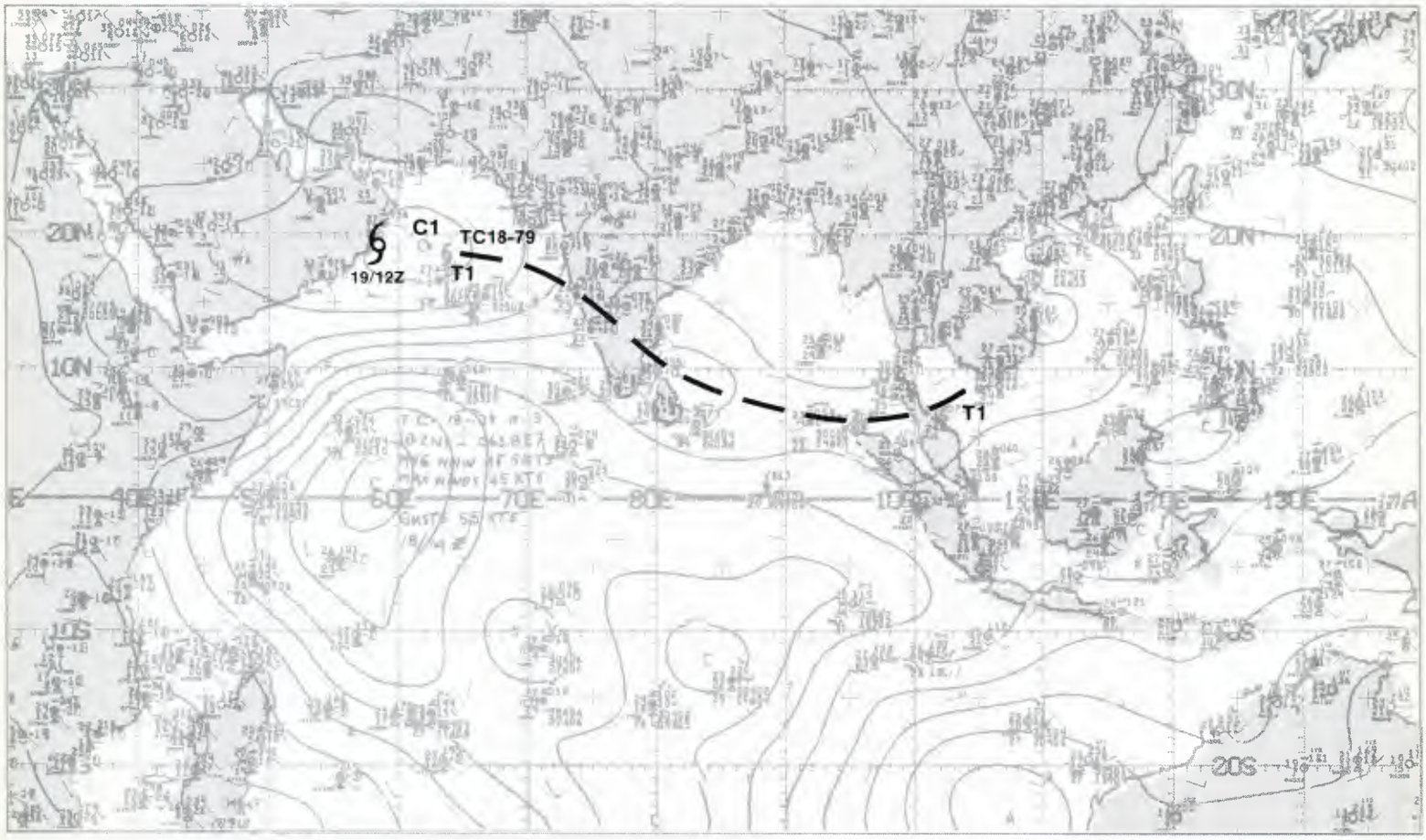

1E-17b. NMC Tropical Surface Streamline Analysis. 1200 GMT 18 June 1979.

200 mb

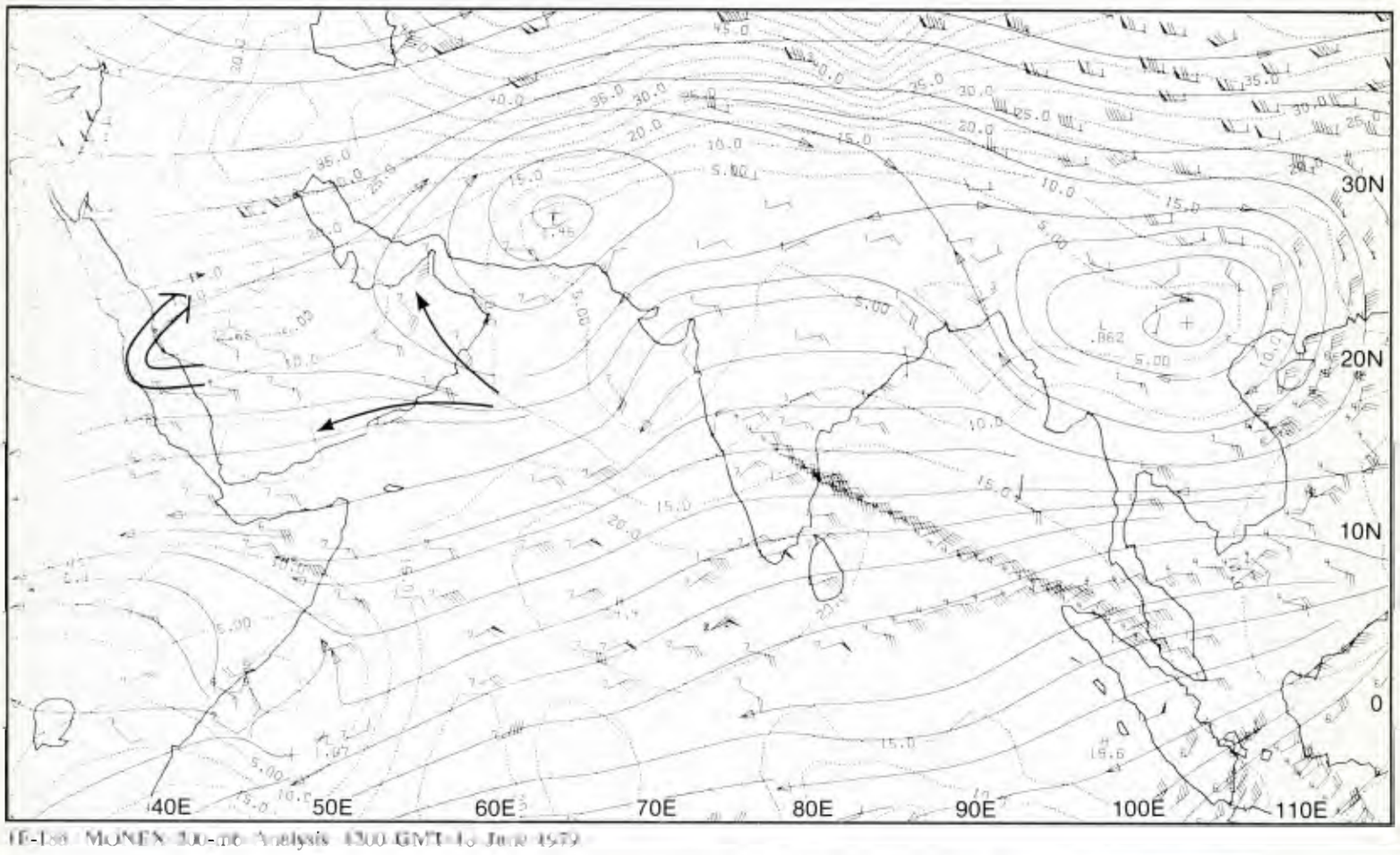

1E-18a. MONEX 200-mb Analysis. 1200 GMT 18 June 1979.

250 mb

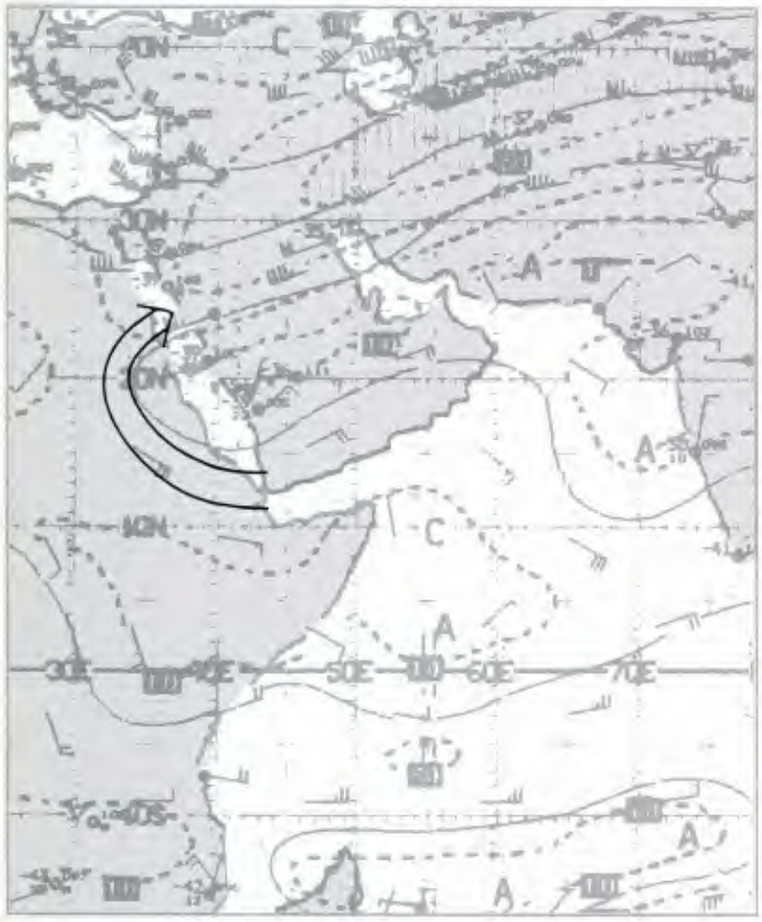

1E-18b. NMC Tropical 250-mb Streamline Analysis. 1200 GMT 18 June 1979.

500 mb

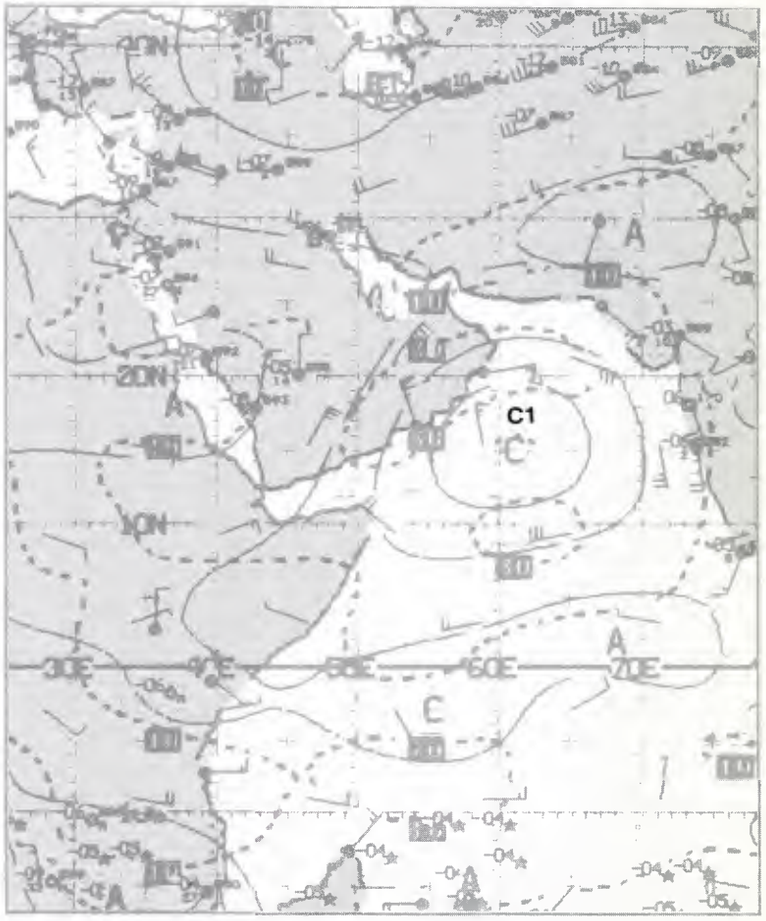

1E-18c. NMC Tropical 500-mb Streamline Analysis. 1200 GMT 18 June 1979.

700 mb

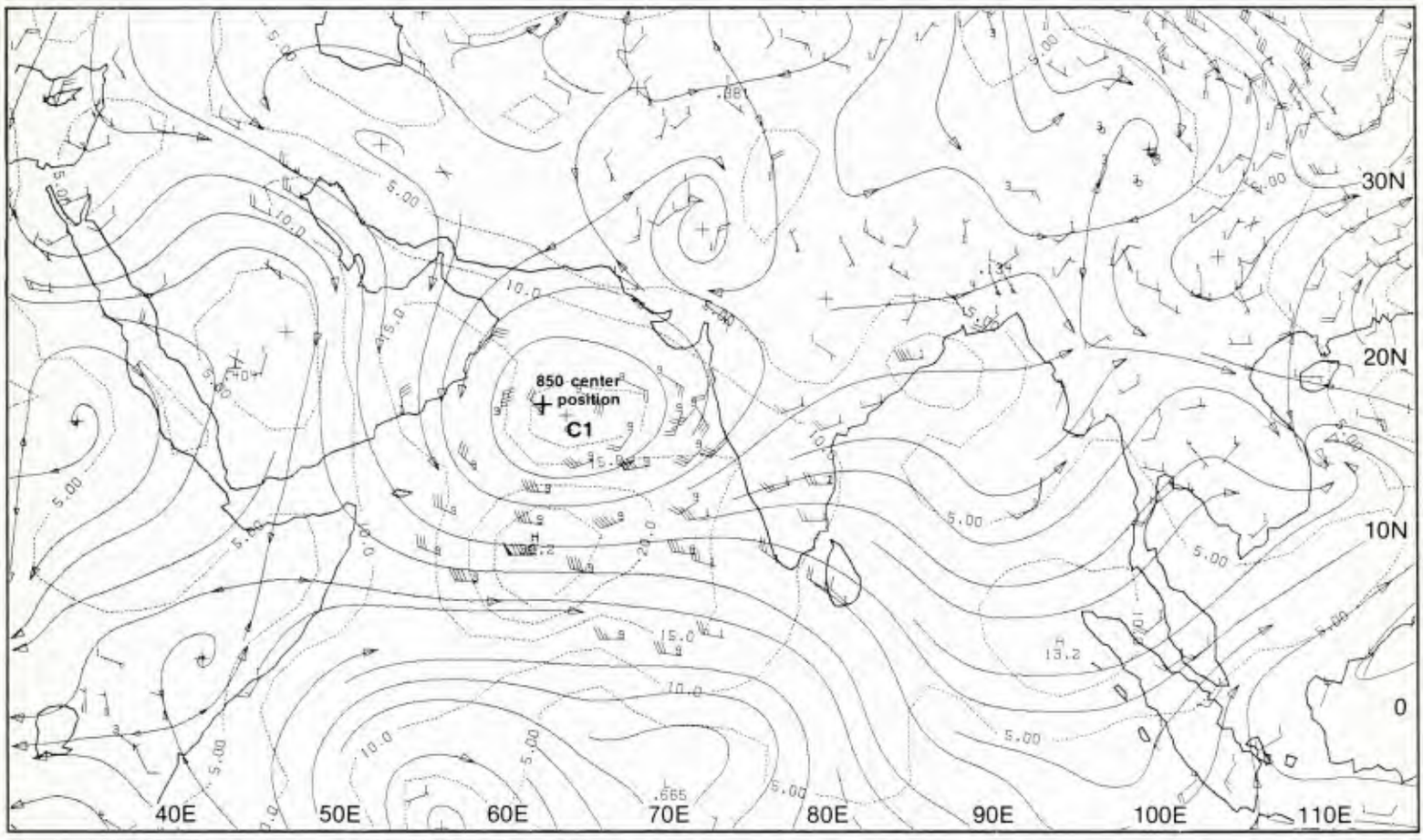

1E-19a. MONEX 700-mb Analysis. 1200 GMT 18 June 1979.

850 mb

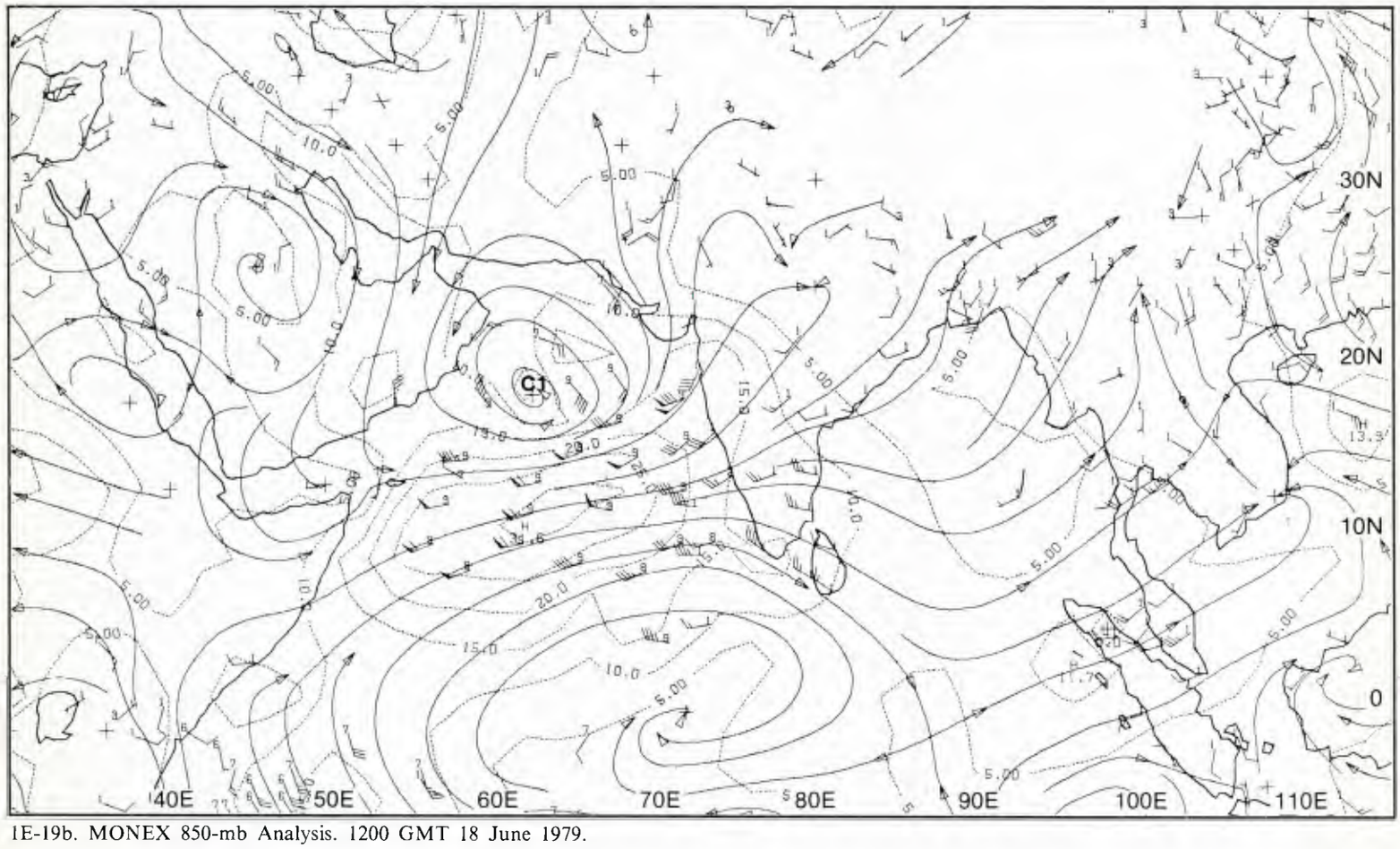

1E-19b. MONEX 850-mb Analysis. 1200 GMT 18 June 1979.

Important Conclusions

1. The southwest monsoon pattern and evolution have no direct correlation with classical middle-latitude circulation patterns and daily weather events. To understand the overall evolution of this regime, new conceptual ideas must be developed.

2. The southwest monsoon regime is of a scale larger than that typical in mid-latitudes and therefore responds primarily to other large-scale forcing functions such as the shifting solar insolation pattern and middle-latitude circulation blocking events. These large-scale forcing functions affect the basic development and maintenance of this regime.

3. Synoptic and smaller scale forcing functions such as middle-latitude migratory systems, internally developed vortices, and smaller convective systems relate to the diurnal changes in intensity in given locales.

4. The onset of the fully developed southwest monsoon occurs over large areas, such as the Arabian Sea and Indian Ocean from the Equator to near 15° N, within a few days. The changes in winds, weather and sky conditions take place nearly simultaneously over the entire region and are quite dramatic in nature.

5. The low-level pattern of generally westerly flow is established early in the evolution, but is significantly weaker than during the fully developed southwest monsoon.

6. The upper-level pattern, comprised of a dominant anticyclone over Tibet with an easterly jet on its equatorial side over the northern Indian Ocean, is the last part of the total southwest monsoon circulation pattern to develop.

7. The onset of the southwest monsoon over the Arabian Sea and subcontinent of India is frequently associated with an "onset vortex". This vortex forms from the combined effects of low-level convergence in a near-equatorial trough and the evolving upper-level divergence pattern associated with the Tibetan anticyclone.

8. The "onset vortex" typically forms over the southeastern Arabian Sea, tracks northward to near 20° N and then west-northwest across the Arabian Sea.

9. The "onset vortex" leaves in its wake low-level conditions favorable for southwest monsoon weather, and the developing upper-level easterly jet brings an upper-level divergent pattern suitable to sustain this weather.

10. Concurrent with the evolution of the "onset vortex" and following southwest monsoon weather is the intensification of low-level southerly cross-equatorial flow over the southwestern Arabian Sea. This flow provides the warm, moist air that feeds the convection and precipitation of the southwest monsoon.

11. The low-level southerly cross-equatorial convergent flow is counter balanced by upper-level northerly divergent cross-equatorial flow.

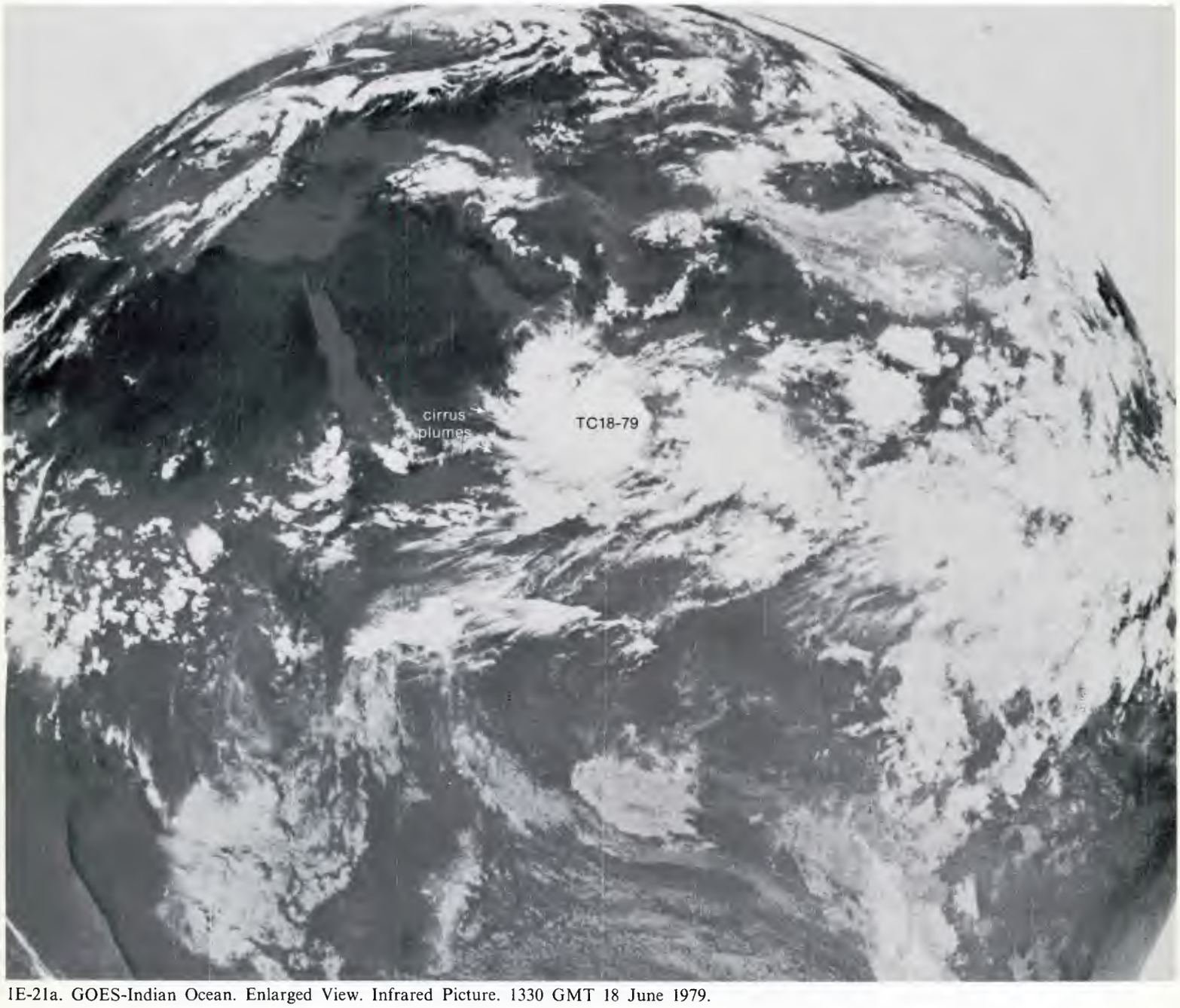

1E-21a. GOES-Indian Ocean. Enlarged View. Infrared Picture. 1330 GMT 18 June 1979.

Case 3 Arabian Sea/Bay of Bengal—Summer

The Southwest Monsoon

The 1979 southwest monsoon onset period started on 11 June when a dramatic increase in westerly flow was noted over the Arabian Sea (Krishnamurti, 1981). The flow continued to sharply increase for approximately four days, with the rains commencing over extreme southwest India about a week after the flow increase started.

Reference

Krishnamurti, T. N., 1981: The 10- and 20-day westward propagating mode and "breaks in the monsoons". *Tellus*, **32**, 15–26.

850 mb

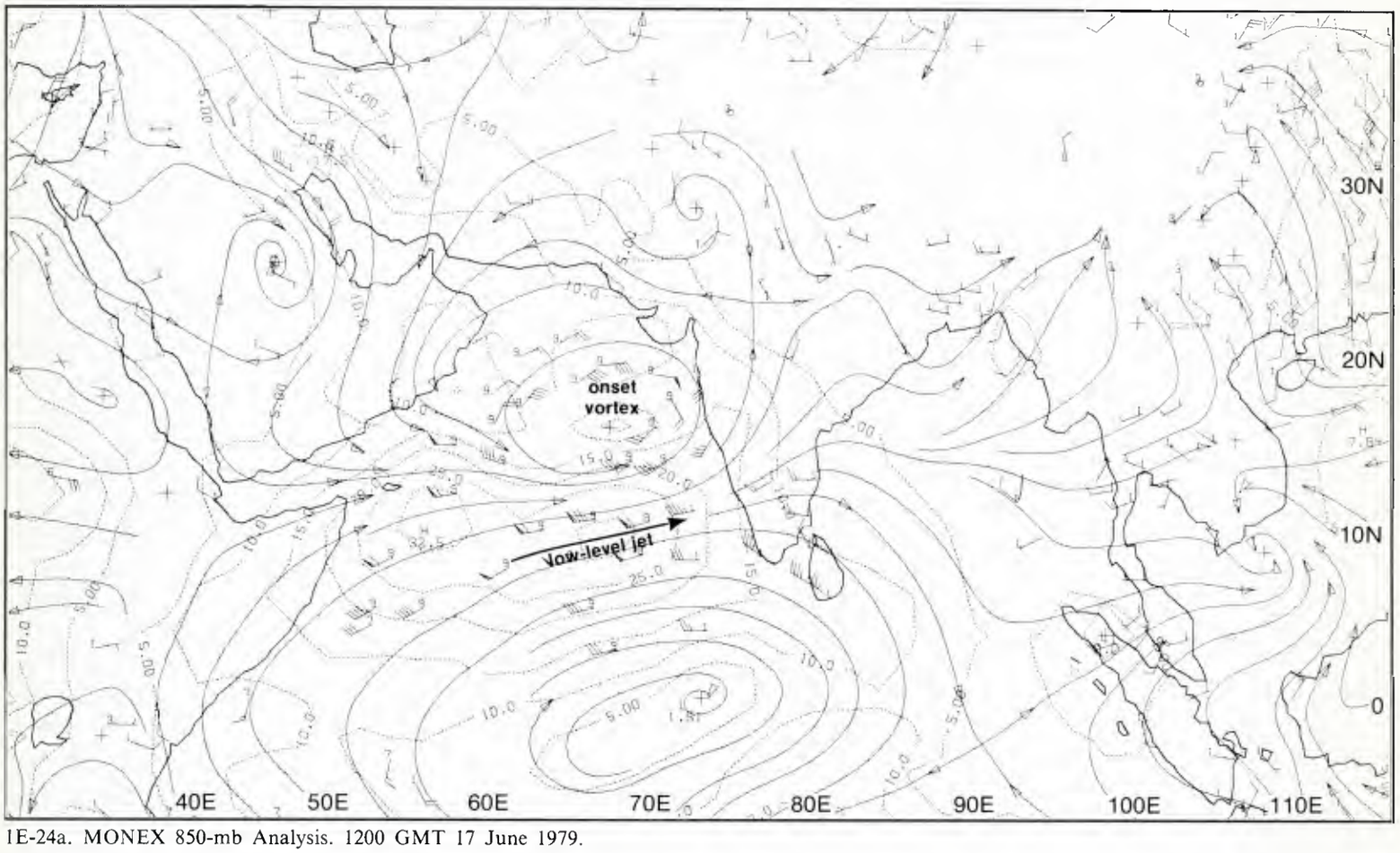

1E-24a. MONEX 850-mb Analysis. 1200 GMT 17 June 1979.

surface

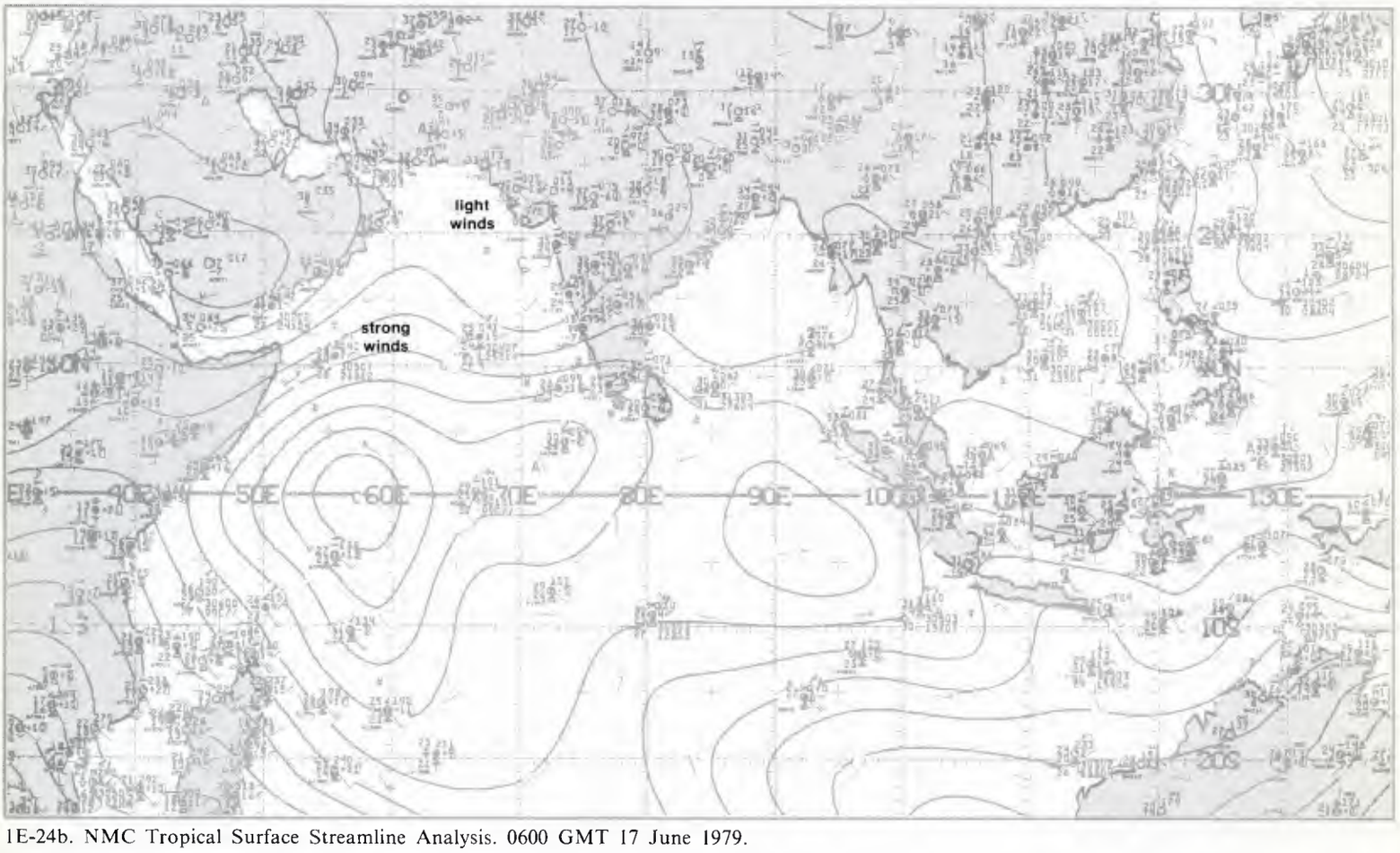

1E-24b. NMC Tropical Surface Streamline Analysis. 0600 GMT 17 June 1979.

17 June

The MONEX 850-mb analysis for 17 June (1E-24a) shows the low-level flow pattern during the onset period. A strong low-level jet is established over the Arabian Sea near 10° N. Also seen is the onset vortex that formed on 14 June. Strong westerly and southwesterly flow is occurring over India. The NMC surface streamline analysis for 0600 GMT (1E-24b) has the clockwise gyre centered near the Equator in the Indian Ocean region. The strong southwest flow over the southern Arabian Sea is depicted by an area of tightly-spaced streamlines from the coast of Somalia to southern India. Ships in this area of flow reported 30- to 40-kt winds. The northern Arabian Sea is an area of light winds. Reports in the area show 5- to 10-kt winds.

27 June

The MONEX 850-mb analysis (1E-25a) shows the established southwest monsoon circulation over the Arabian Sea. A strong low-level jet is now fully developed, with maximum winds of 60 kt. The west-southwest flow now extends completely across India, eastward to the eastern Bay of Bengal. The 0600 GMT surface streamline analysis (1E-25b) shows the monsoonal trough around 25° N over India, near the base of the Himalayas. Strong westerly wind reports prevail well to the south of the trough, becoming light and variable in the trough and to the north. Widespread haze and dust aloft (dust in suspension, not raised by the local wind) is reported over the central and southern Arabian Peninsula. The source region for this dust appears to be the eastern portion of Africa which is under the influence of strong southwesterly flow.

Cloudy conditions extend to 25° N over the Arabian Sea, India, and the Bay of Bengal, as shown in the DMSP visible picture at 0522 GMT (1E-26a). Cloud lines over the Arabian Sea also imply strong low-level westerly flow as indicated on the surface analysis (1E-25b). Extensive cloudiness over the Bay of Bengal is associated with the monsoonal trough and the development of a monsoonal depression over the bay (Krishnamurti, 1981). The mountain range in western India increases convective cloudiness and precipitation in that area. Wave clouds over India reflect the strong westerly flow occurring at this time.

The DMSP picture at 0704 GMT (1E-27a) shows the general reduced cloudiness of the western Arabian Sea during the established southwest monsoon. The long, parallel, closely-spaced low-level cloud lines clearly indicate the area of the well-developed low-level Somali jet. Dust and haze covers the Gulf of Aden, a common situation for that region during the southwest monsoon season. This picture was acquired at approximately 1000 LST, hence gray shades in the Gulf of Aden cannot be sunglint, which is confined to the eastern half of the image. The widespread dust and haze reports are concentrated in the col area on the 850-mb analysis (1E-25a). This suggests that cols are likely locations to concentrate dust suspensions and that the 850-mb analysis may be useful to pinpoint such locations of vastly decreased visibility. Forecasts for the movement of the col, or future col positions, could possibly be used to predict areas of decreased visibility.

Important Conclusions

1. The onset of the monsoon occurs with increased flow starting in the western Arabian Sea and progressing eastward to India in a few days.

2. Until the intrusion of maritime equatorial air into the monsoon flow, skies are generally cloud free over the Arabian Sea and India.

3. The western Arabian Sea remains largely cloud free during the established southwest monsoon.

4. The western Arabian Sea area loses the onset convection cloudiness and remains relatively cloud free during the established monsoon because the onset speed convergence is lost and general subsidence is established in the area by the ocean upwelling effects combining with the upper-level anticyclonic jet flow over the surface heat lows.

5. Low-level cloud lines that developed over the western Arabian Sea, as observed by satellite, are useful in depicting the low-level jet flow.

6. The 850-mb analysis is useful in predicting the areas where dust in suspension is likely to remain for one or two days after the surface storm has ended. The suspended dust is likely to remain in the light wind regions characteristic of cols.

Reference

Krishnamurti, T. N., 1981: The 10- and 20-day westward propagating mode and "breaks in the monsoons". *Tellus*, **32**, 15–26.

850 mb

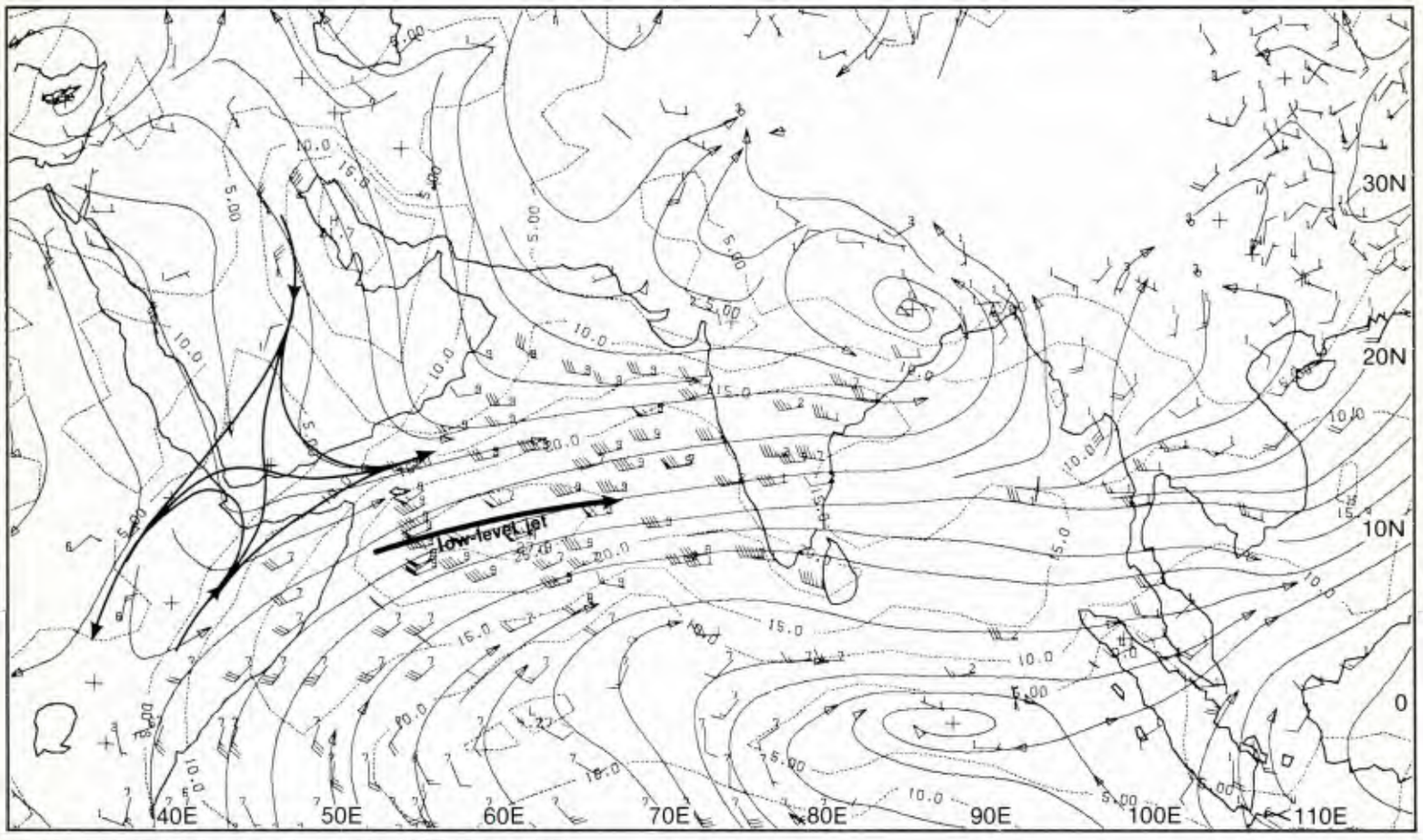

1E-25a. MONEX 850-mb Analysis. 1200 GMT 27 June 1979.

surface

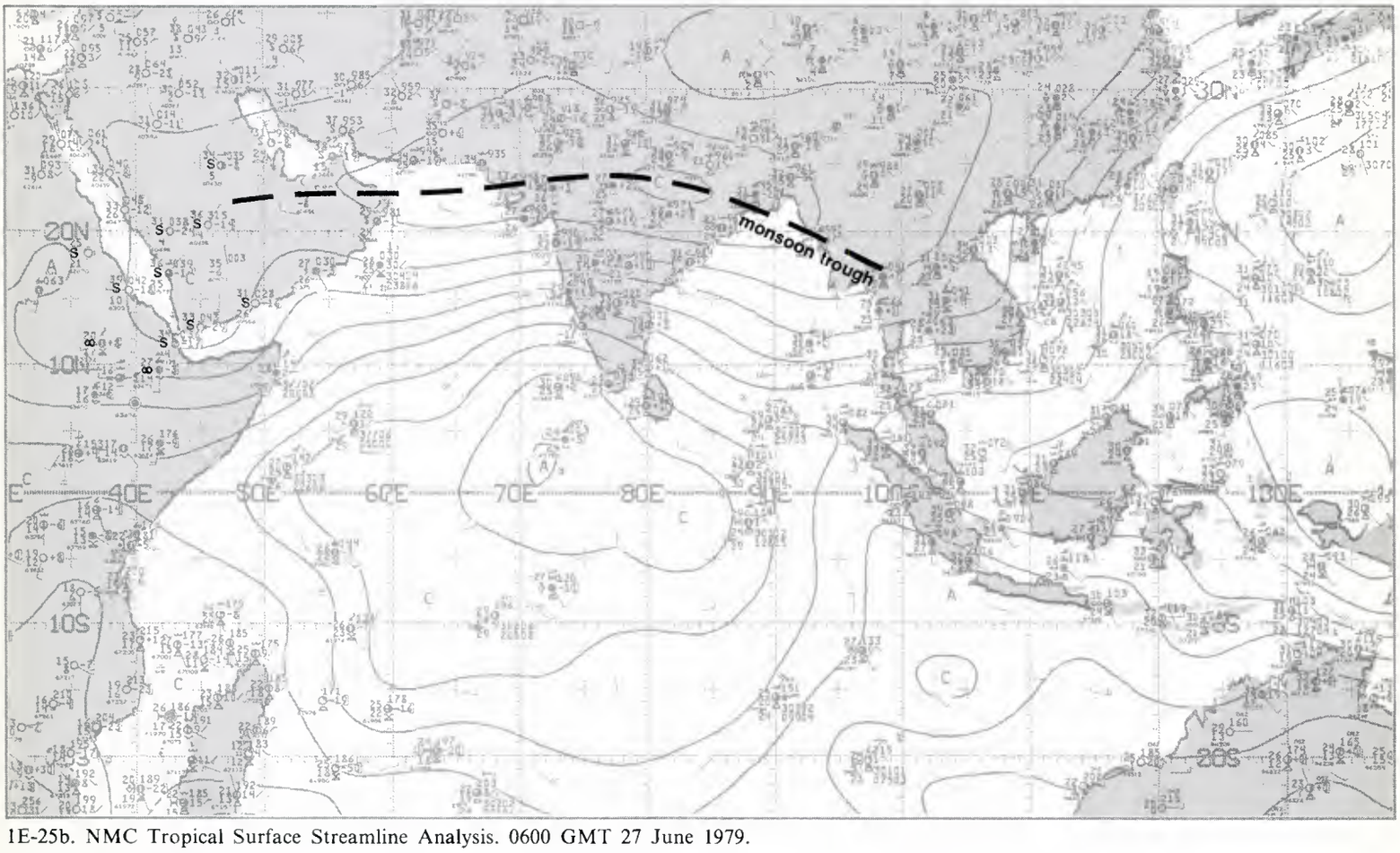

1E-25b. NMC Tropical Surface Streamline Analysis. 0600 GMT 27 June 1979.

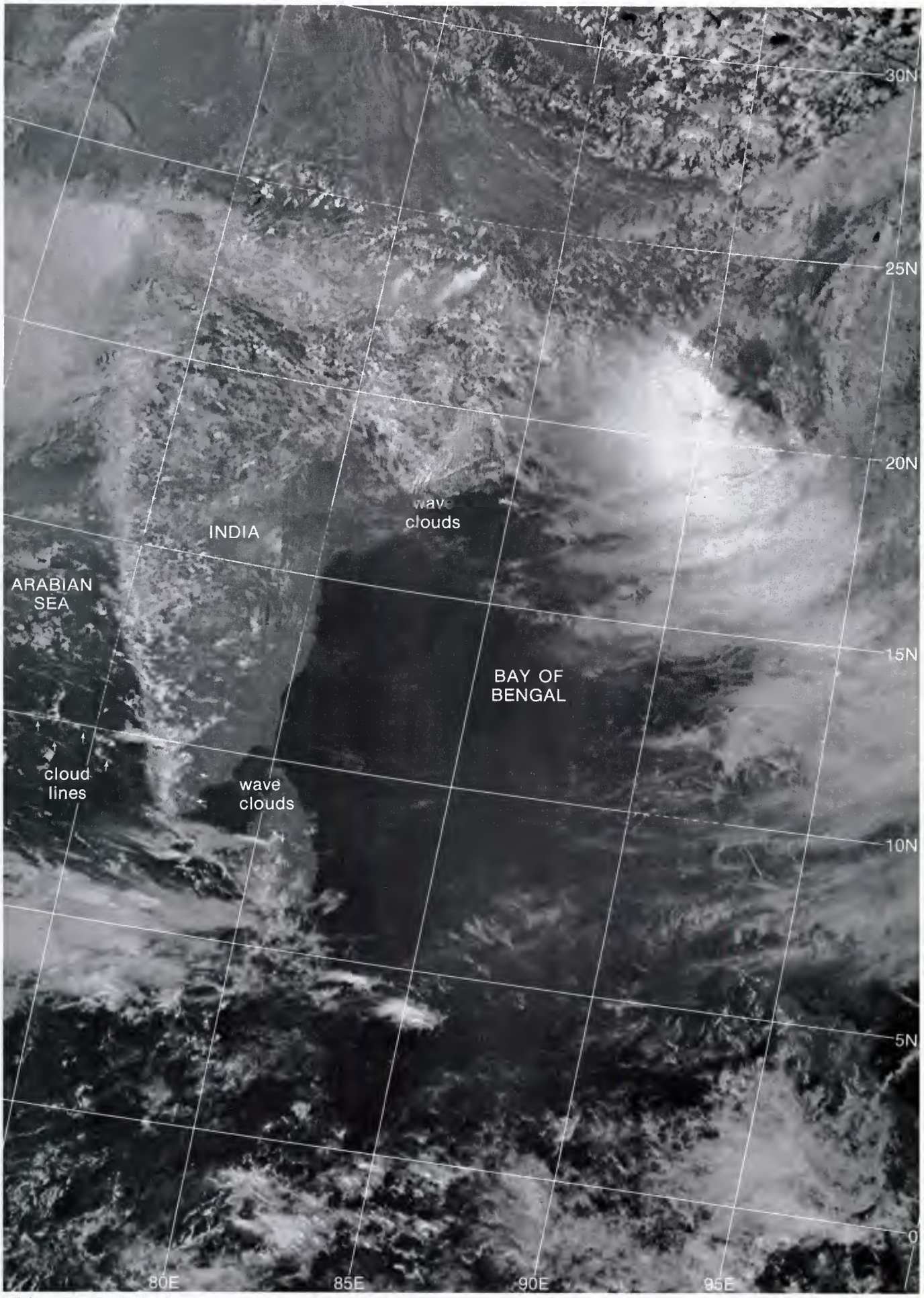

1E-26a. F-1. DMSP LS Low Enhancement. 0522 GMT 27 June 1979.

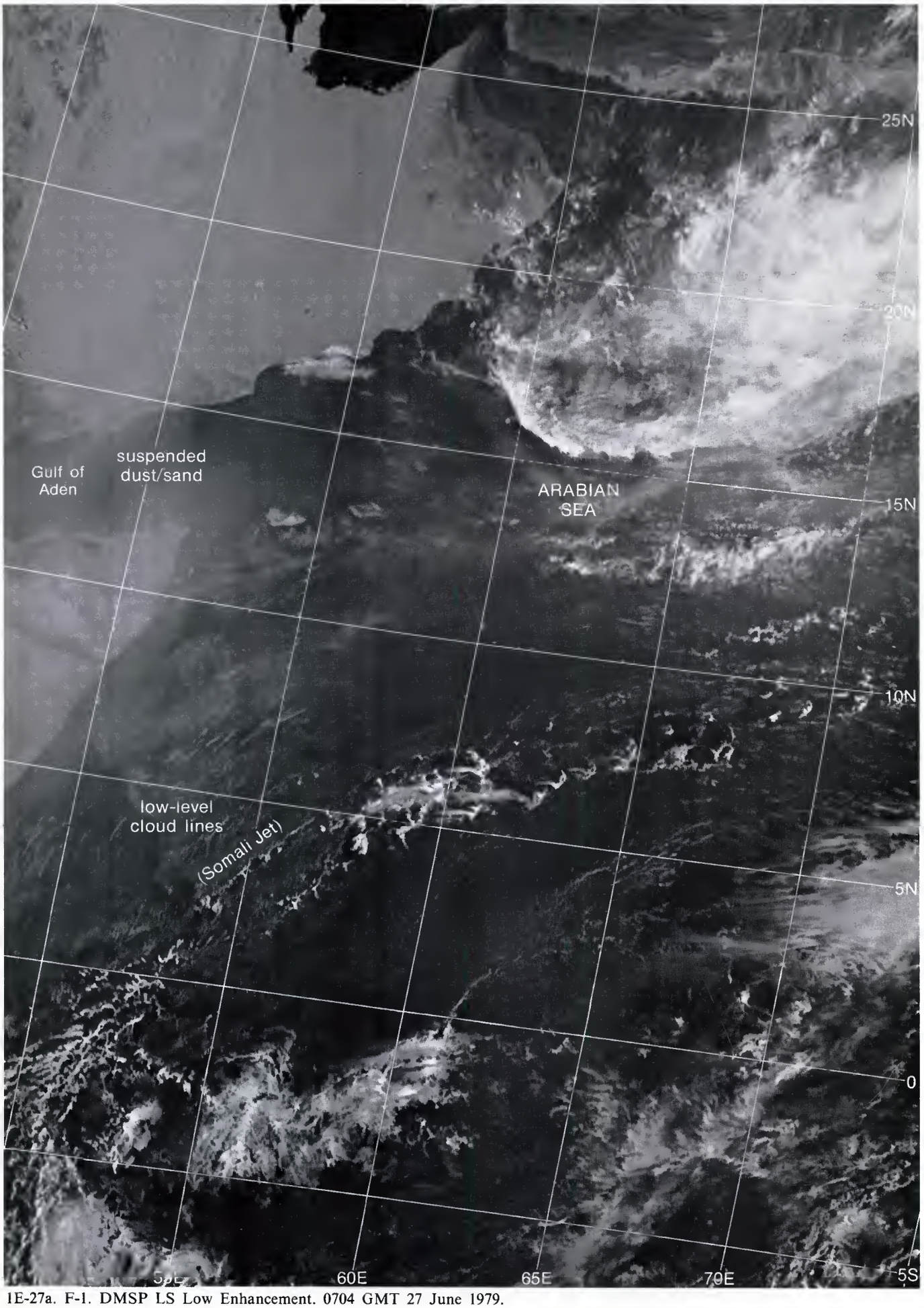

1E-27a. F-1. DMSP LS Low Enhancement. 0704 GMT 27 June 1979.

Case 4 Arabian Sea/Bay of Bengal—Summer

Monsoon Depressions

During the months of June through September, low pressure systems are observed to move and often intensify over the northern Bay of Bengal. When speeds reach 17–33 kt and the observed pressure gradient between the center and a point 250 km out is observed to be in the range of 5 to 13 mb, these storms are referred to as "monsoon depressions" (Ray, 1982). They rarely intensify beyond the depression stage and generally move in a northwestward direction across the Bay of Bengal until making landfall over northern India, where they merge with the monsoon trough. Heavy rains are experienced over India in conjunction with the movement of such systems.

Saha and Sanders (1981) examined a large sample of monsoon depressions and found that most of them were associated with predecessor disturbances originating far to the east in the region of the South China Sea. Through isallobaric analysis, they determined that the monsoon depressions "had a period of slightly less than five days, a westward phase speed slightly less than 6 m s^{-1}, and a wavelength of about 2,300 km". The storms were deep systems extending through the 300-mb level with little vertical tilt. Their horizontal dimension averaged 1,000 km.

The first indication of the formation of a monsoon depression is generally given by falling pressure over the Bay of Bengal, as the isallobaric center enters the region from Burma. Satellite indications of such movement are shown by the presence of abundant, but disorganized, convective cloud clusters.

References

Ray, S. P., 1982: Surface drag contribution to the depth of monsoon depression over the Indian region. *Arch. Met. Geohp. Biobl. Ser. A*, **31**, 237–241.

Saha, K., and F. Sanders, 1981: Westward propagating predecessors of monsoon depressions. *Mon. Wea. Rev.*, **109**, 330–343.

200 mb

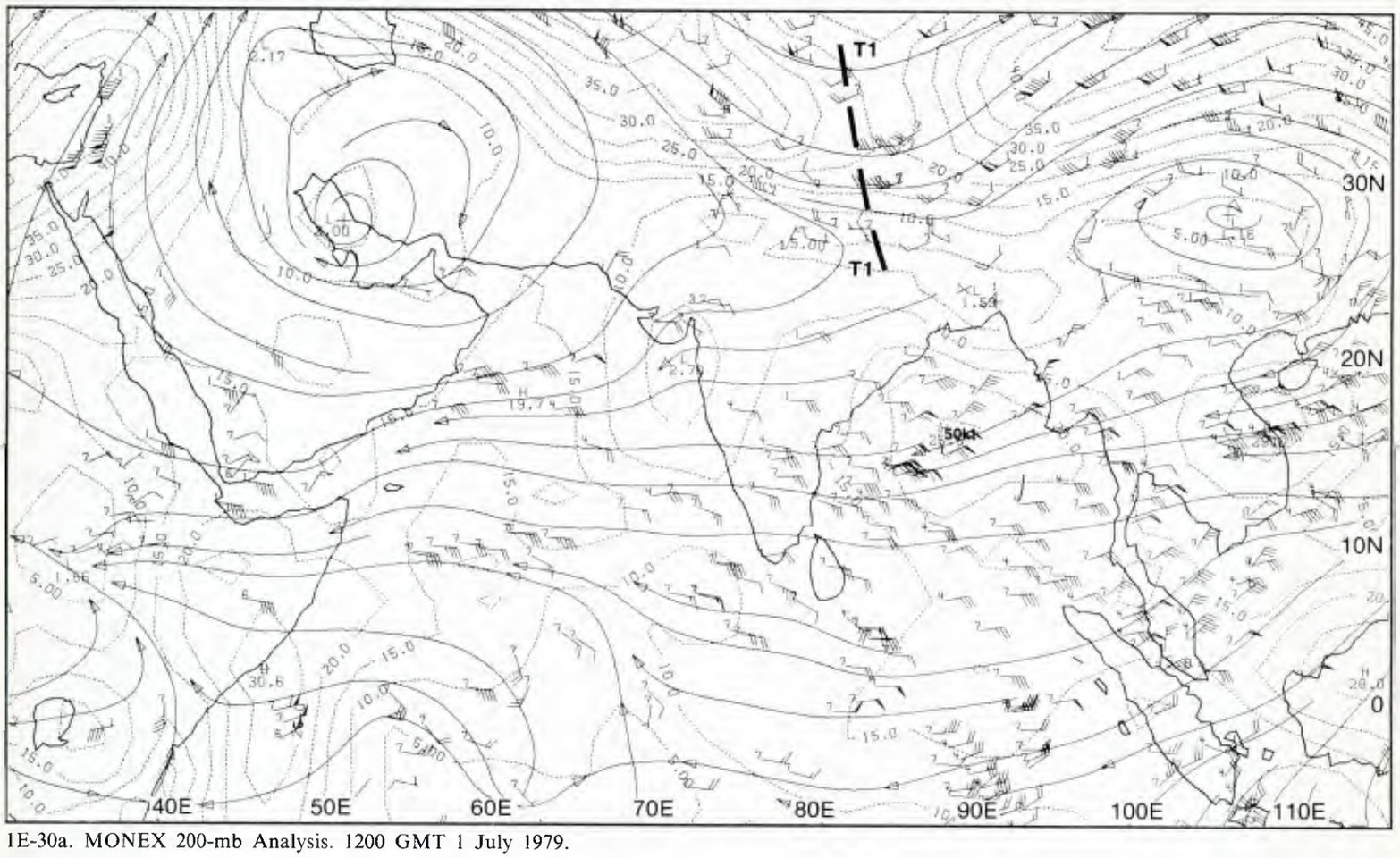

1E-30a. MONEX 200-mb Analysis. 1200 GMT 1 July 1979.

500 mb

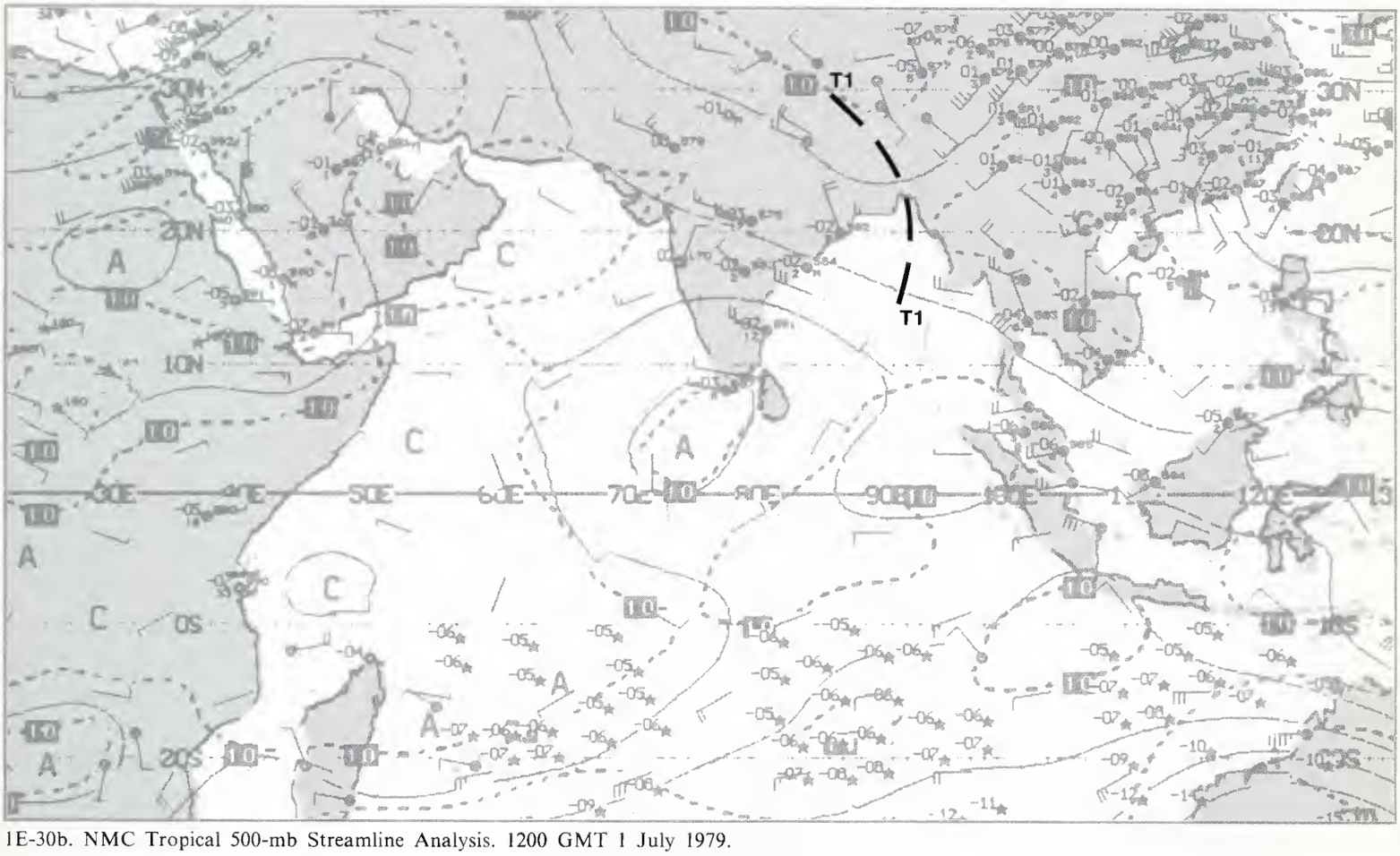

1E-30b. NMC Tropical 500-mb Streamline Analysis. 1200 GMT 1 July 1979.

Monsoon Depression
Bay of Bengal
July 1979

1 July

The NMC surface streamline analysis for 1200 GMT (1E-31b) reveals typical southwest monsoonal conditions, with southeasterly trades crossing the Equator off the coast of Africa, becoming southwesterly across the Arabian Sea, westerly across India, and then digging southward under the influence of the monsoonal trough which extends down into the northern Bay of Bengal.

The strength of this flow is well depicted on the MONEX 850-mb analysis (1E-31a) which reveals an isotach maximum of greater than 50 kt in the central Arabian Sea. The monsoonal trough in the Bay of Bengal is also well revealed on this analysis and shows pronounced cyclonic shear.

The trough is seen to extend up to the 500-mb level (1E-30b), where much lighter wind conditions prevail. The light and variable wind conditions at this level are typical since this level is near the transition from low-level westerlies to upper-level easterlies. At 200 mb (1E-30a), the trough is displaced well to the north and strong northeasterly flow, with speeds in excess of 50 kt, crosses over the Bay of Bengal.

The DMSP picture (1E-31c) reveals heavy convective cloudiness embedded in the monsoonal trough over the northern portion of the Bay of Bengal. Banding within the convection suggests a cyclonic circulation. South of this area, the bay is relatively clear except for cirrus plumes from scattered convective build-ups being blown by the strong easterlies aloft.

4 July

The southwest monsoon was quite inactive over most of the Arabian Sea, India, and the Bay of Bengal at this time. The reports on the surface streamline analysis (1E-33a) reflect a minimum of precipitation and convective clouds. The trough over the Bay of Bengal, however, appears to have deepened and shows increased amplitude. A closed vortex is shown on the 850-mb analysis (1E-32b), and wind reports about the vortex imply strong cyclonic shear favorable for intensification. At 200 mb (1E-32a), a weak trough in moderately strong easterly flow is shown.

The DMSP picture (1E-33b) reveals considerable convective cloudiness in the region of the 850-mb vortex. However, there is little or no indication of cyclonic banding to define the vortex center. Cirrus plumes reveal the strong easterly and northeasterly upper-level flow covering much of the area.

Orientation of low-level cloud lines southwest and southeast of Sri Lanka implies northwesterly flow in agreement with the surface analysis (1E-33a). This flow is seen to turn more westerly south of the cloudy area, thereby defining the low-level trough intersection in that region. The clear conditions on the east coasts of India and Sri Lanka exhibit the typical lee drying effects of the southwest monsoon.

6 July

The surface streamline analysis on this date (1E-34d) continues to suggest relatively weak southwest monsoonal conditions with no indication of vortex formation over the northern Bay of Bengal region. However, the 850-mb analysis (1E-34c) reveals a powerful low-level circulation in the Bay of Bengal, with 30-kt winds encircling the center.

The strength of the southwest monsoonal current over the Arabian Sea is also much more evident on this analysis than on the surface. The cyclonic circulation is also well defined at the 500-mb level (1E-34b), which shows a large diameter circulation centered over the lower-level position. The circulation does not extend up to the 200-mb level (1E-34a), however. This analysis reveals diffluent easterly flow over the vortex center which would encourage low-level convergence and convective development.

The DMSP picture (1E-35a) shows banded convection in the northern portion of the Bay of Bengal, in the region near and south of the 850-mb circulation center. The northernmost cloud mass nearest the center has weak low-level cloud lines spiraling into its northern edge, indicative of only weak near-surface flow conditions.

continued on page 1E-36

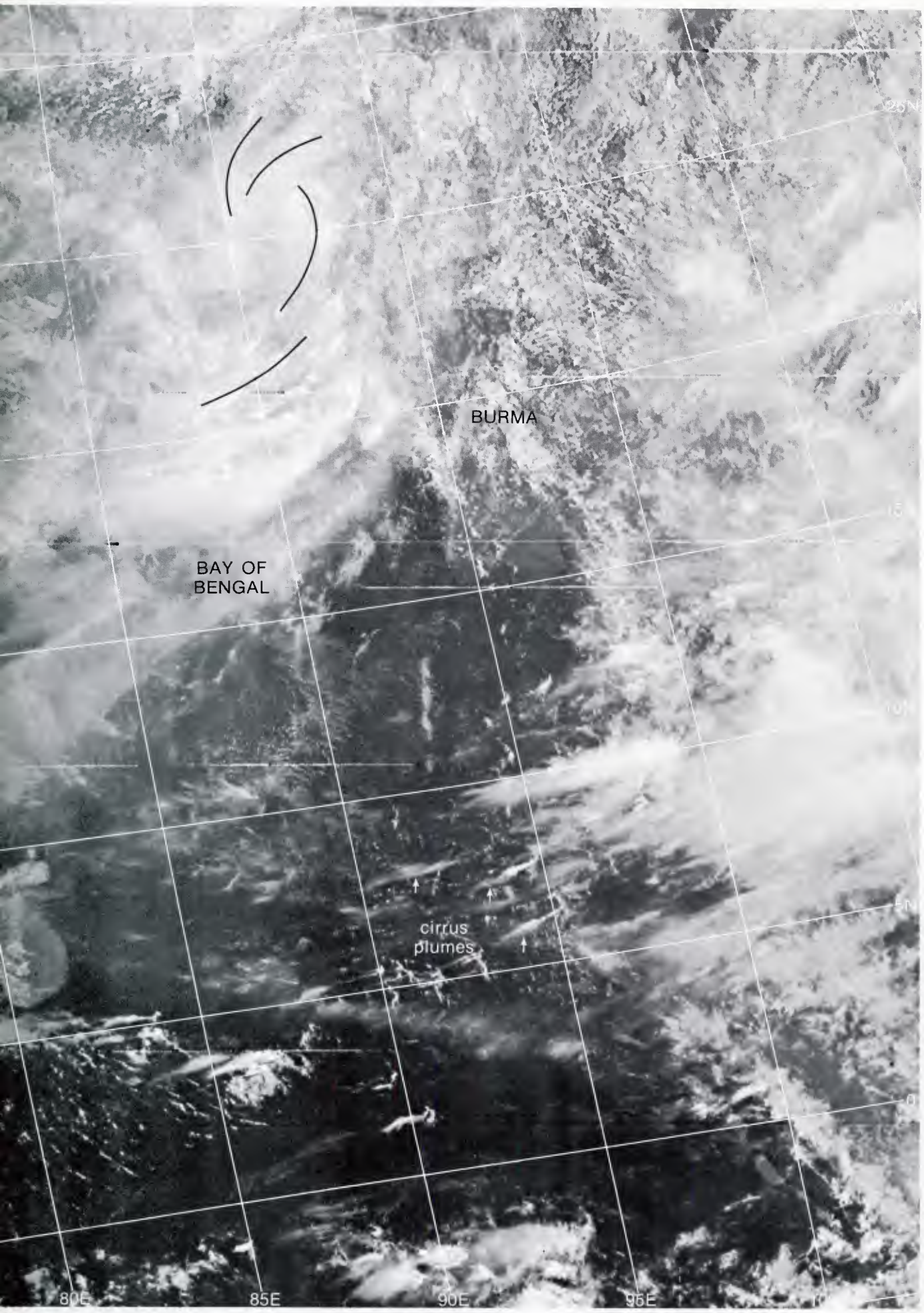

E-31c. F-4. DMSP LS Low Enhancement. 0356 GMT 1 July 1979.

850 mb

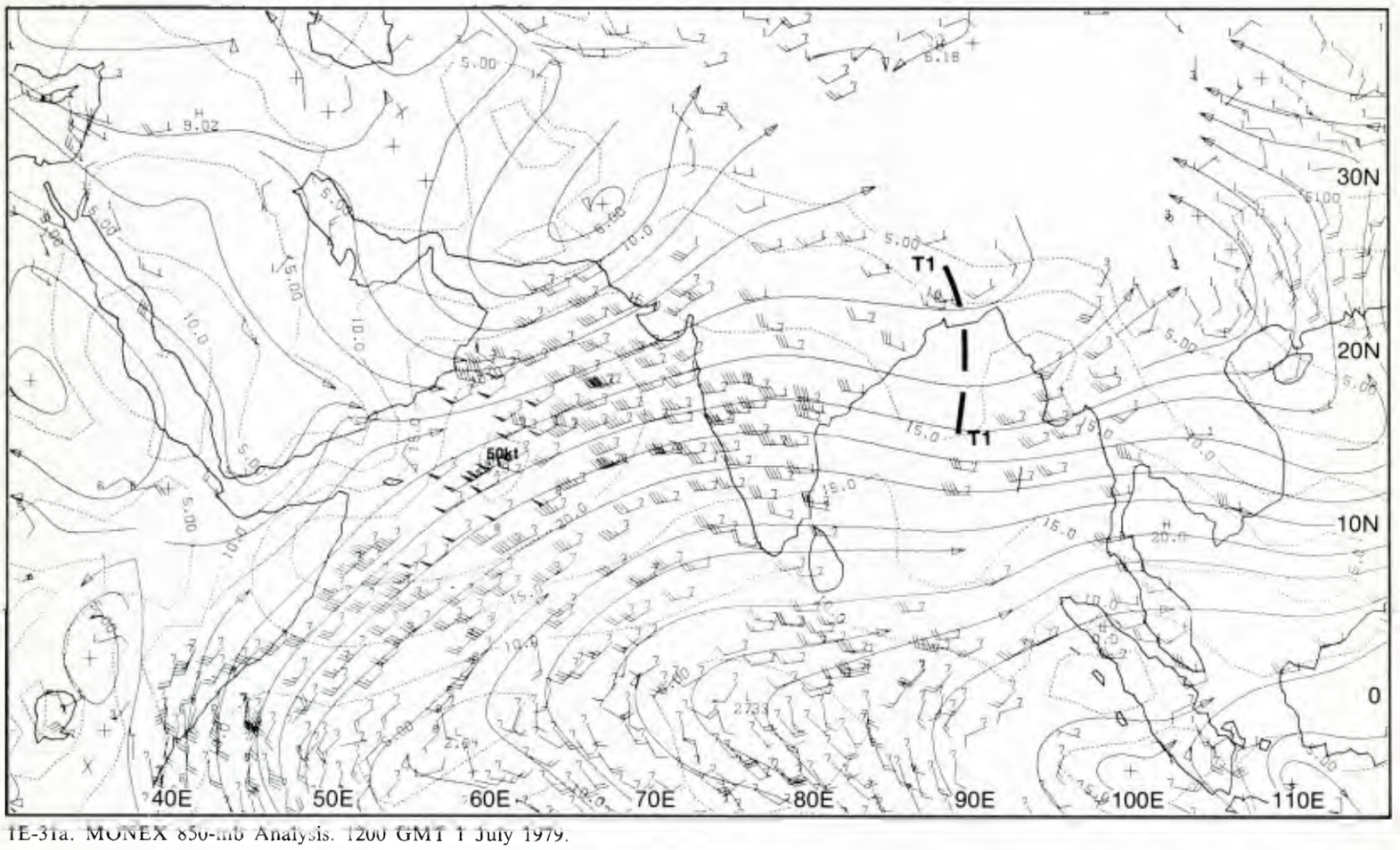

1E-31a. MONEX 850-mb Analysis. 1200 GMT 1 July 1979.

surface

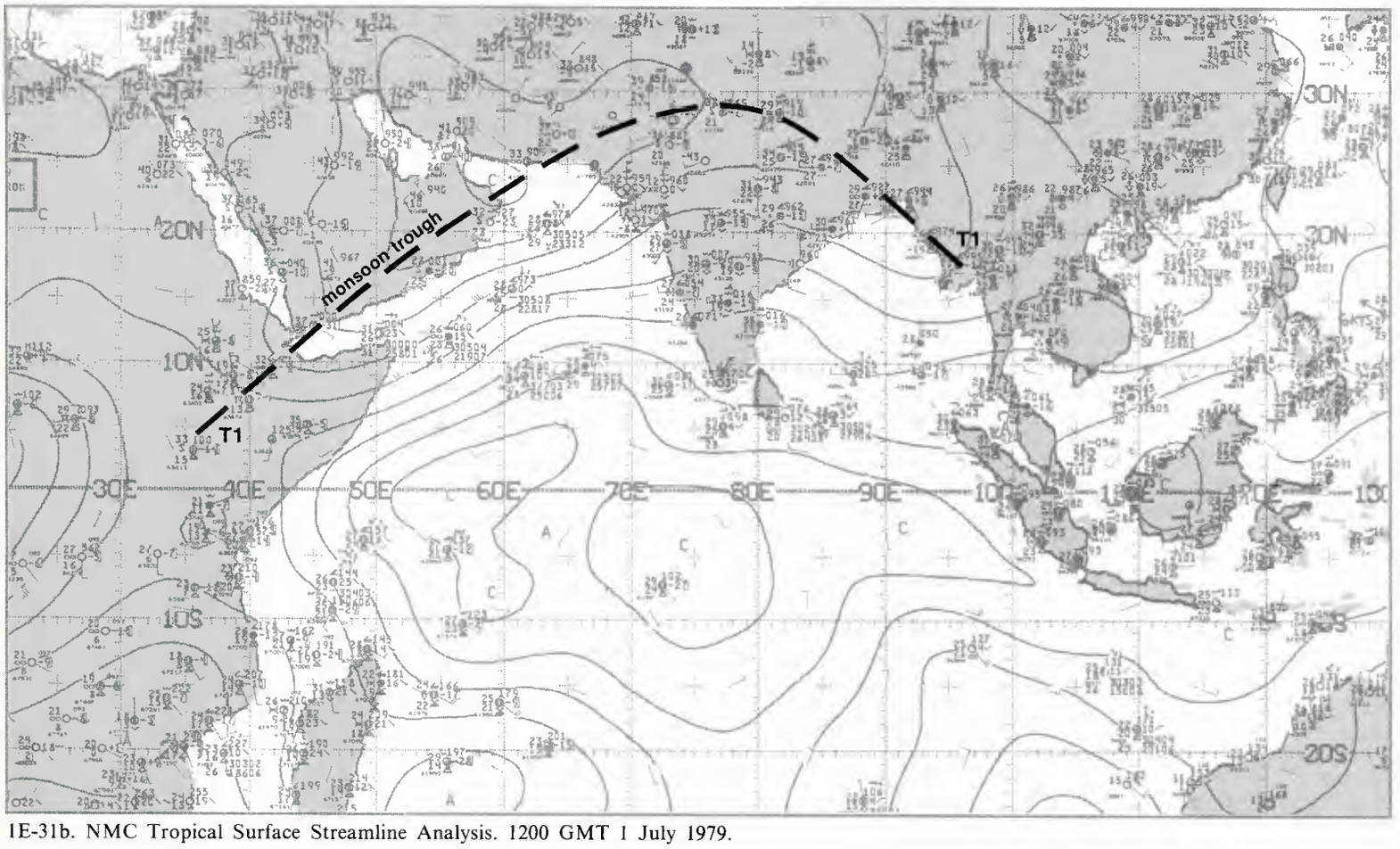

1E-31b. NMC Tropical Surface Streamline Analysis. 1200 GMT 1 July 1979.

200 mb

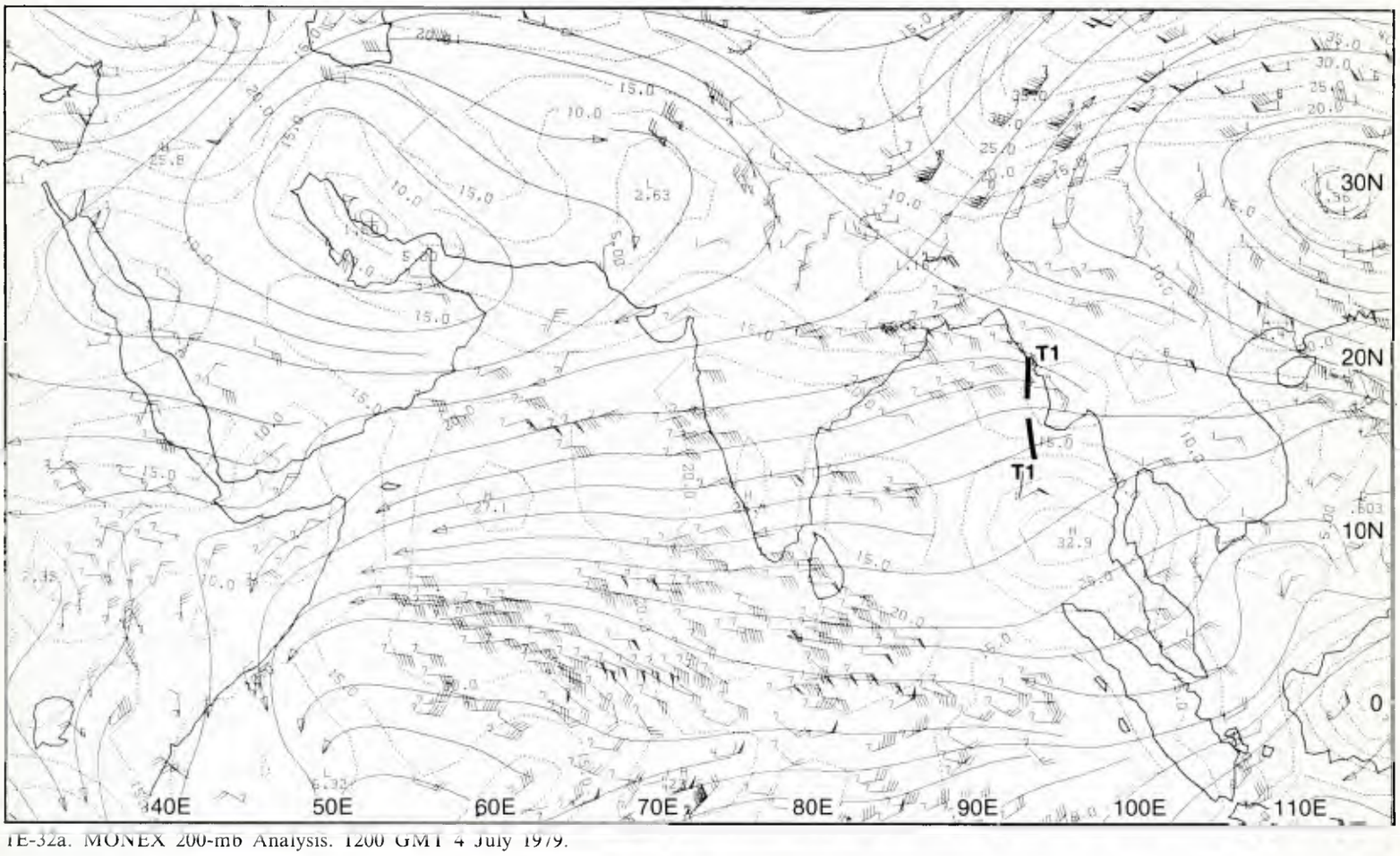

1E-32a. MONEX 200-mb Analysis. 1200 GMT 4 July 1979.

850 mb

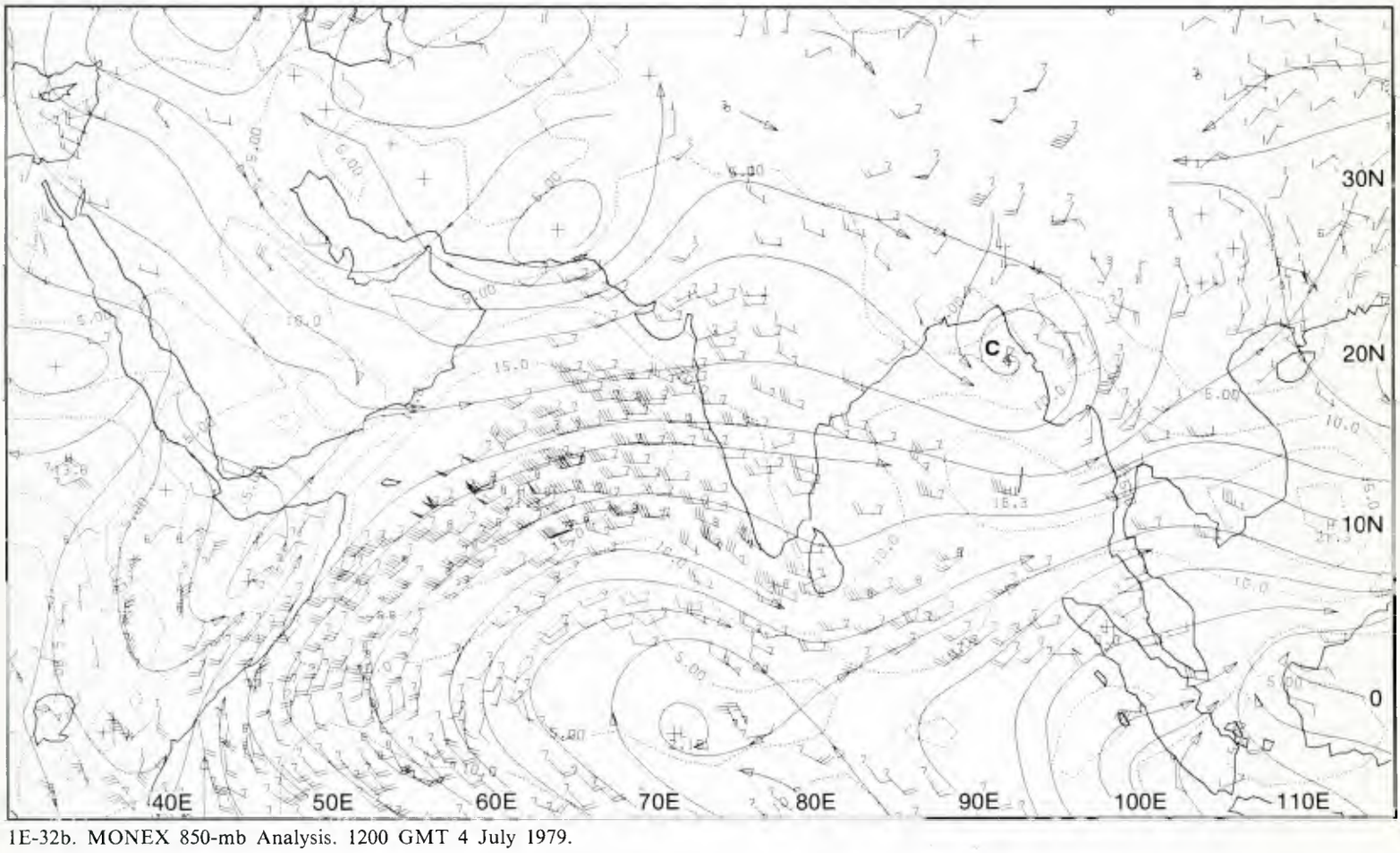

1E-32b. MONEX 850-mb Analysis. 1200 GMT 4 July 1979.

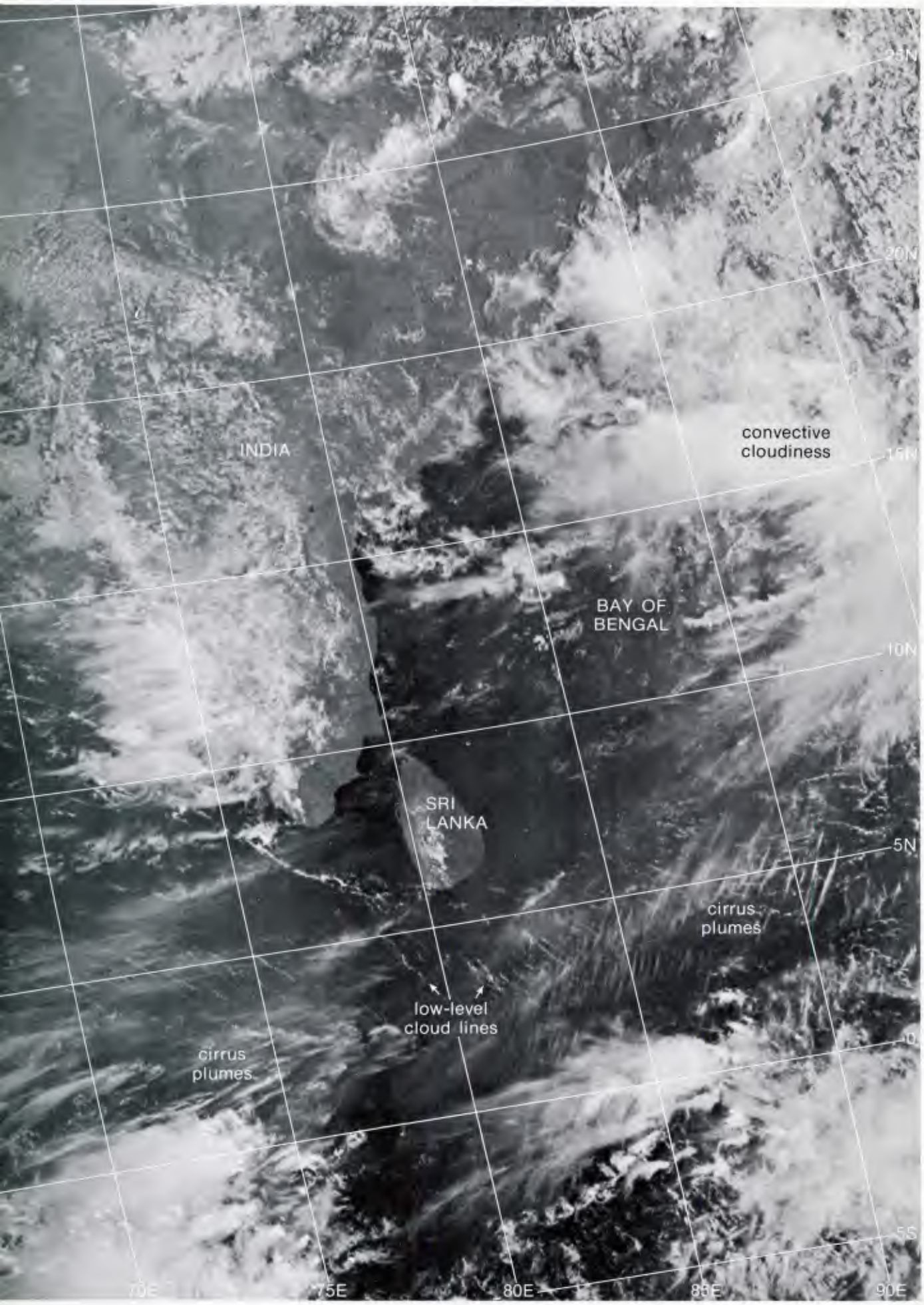

1E-33b. F-4. DMSP LS Normal Enhancement. 0441 GMT 4 July 1979.

surface

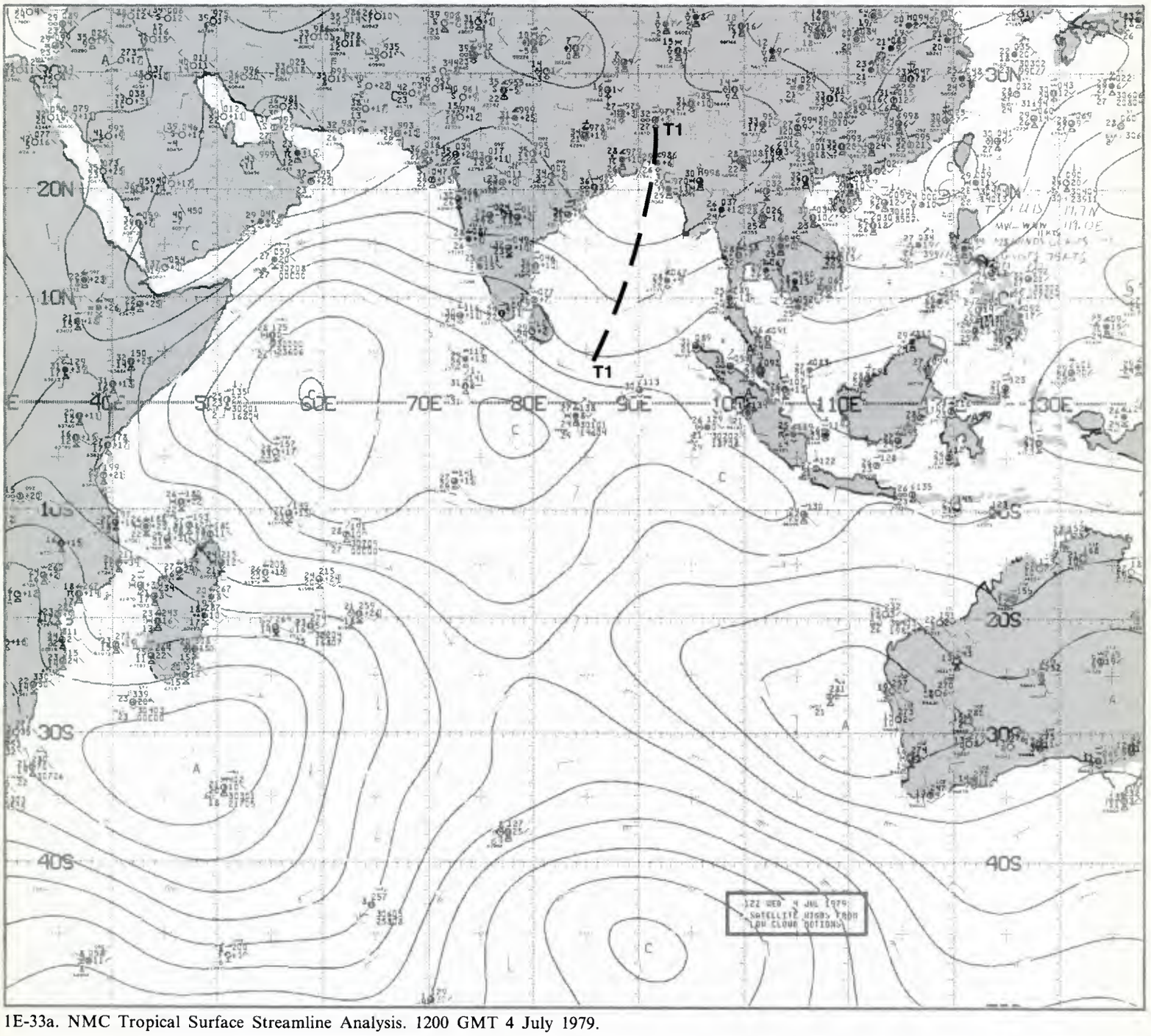

1E-33a. NMC Tropical Surface Streamline Analysis. 1200 GMT 4 July 1979.

200 mb

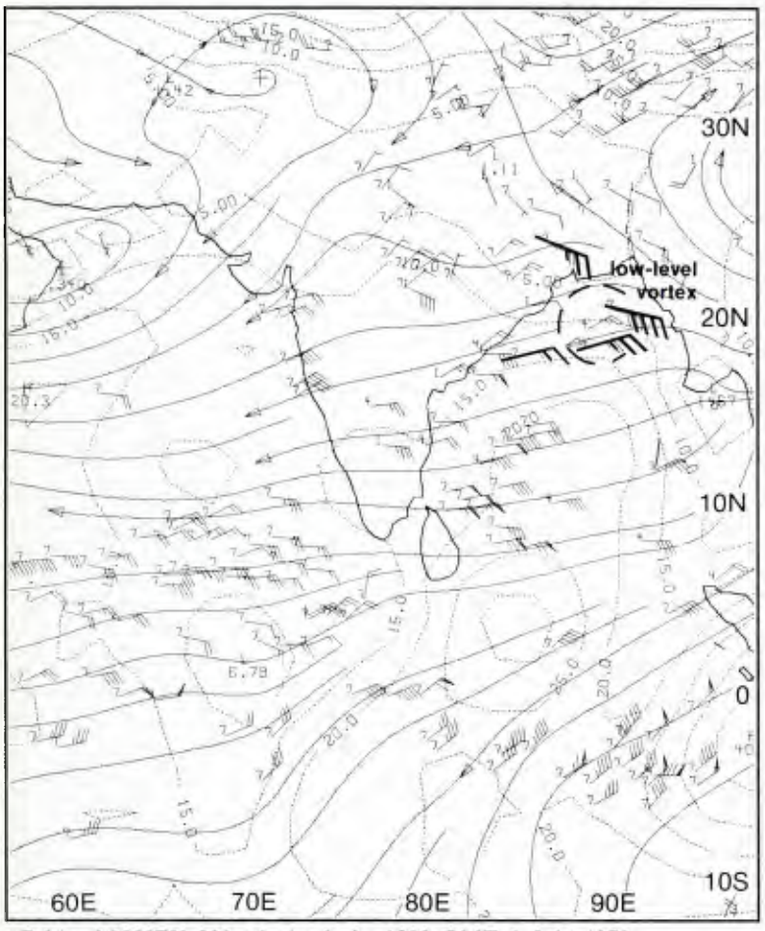

1E-34a. MONEX 200-mb Analysis. 1200 GMT 6 July 1979.

500 mb

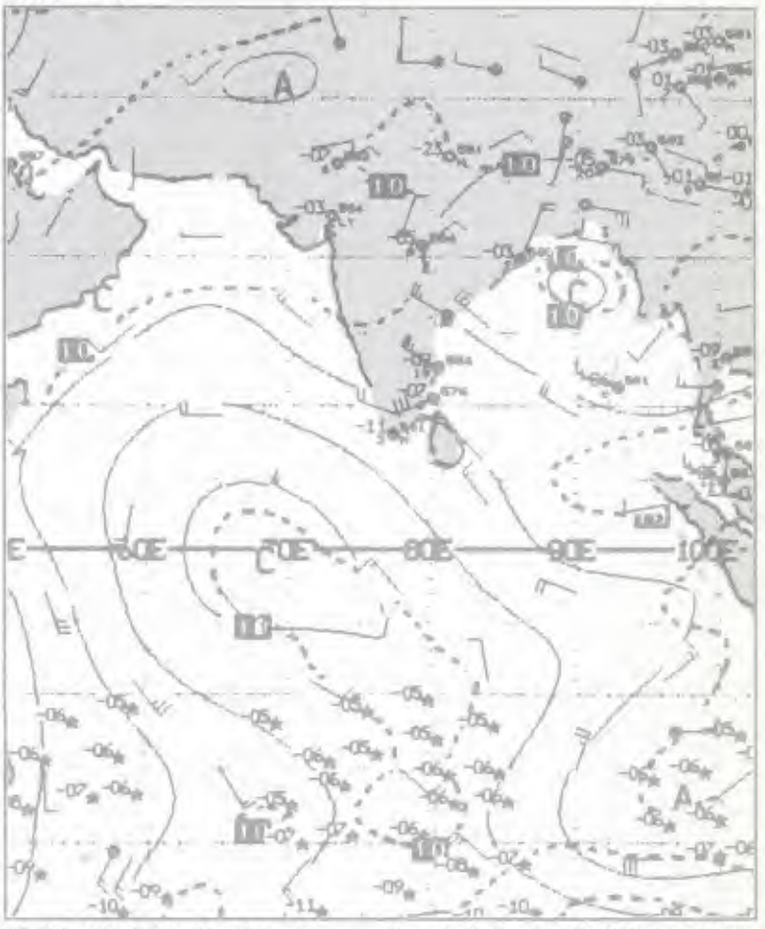

1E-34b. NMC Tropical 500-mb Streamline Analysis. 1200 GMT 6 July 1979.

850 mb

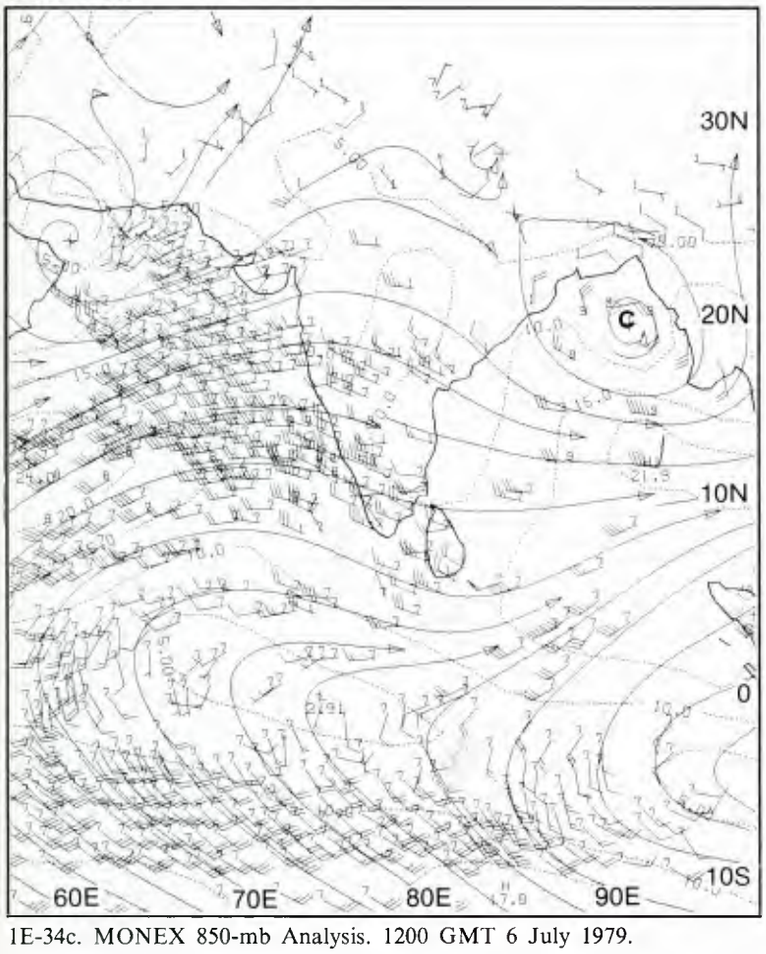

1E-34c. MONEX 850-mb Analysis. 1200 GMT 6 July 1979.

surface

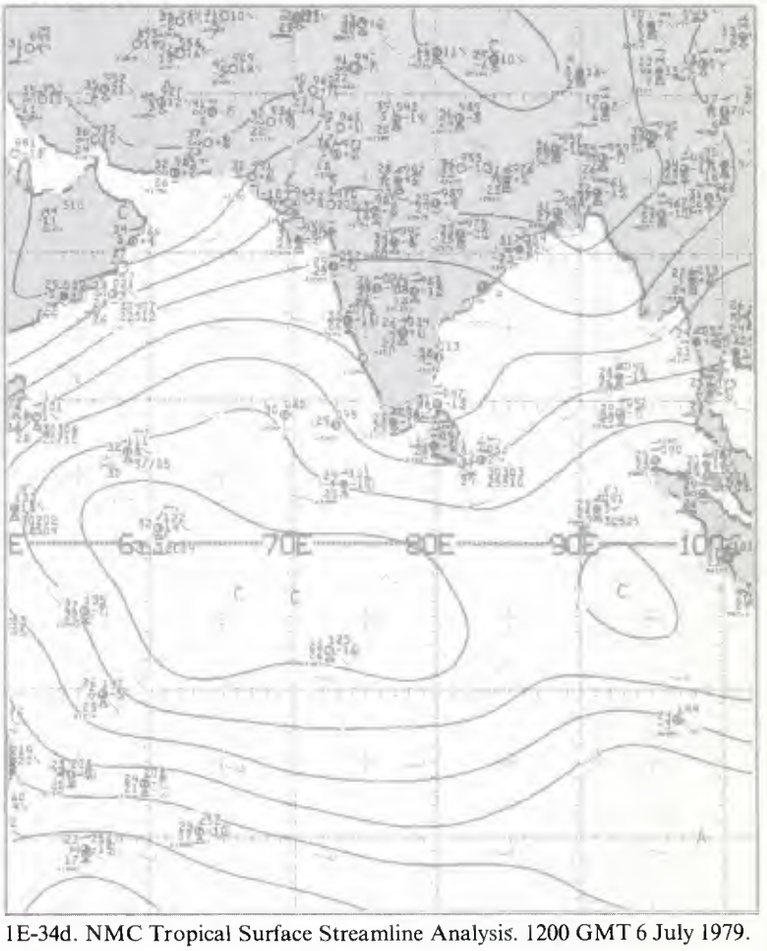

1E-34d. NMC Tropical Surface Streamline Analysis. 1200 GMT 6 July 1979.

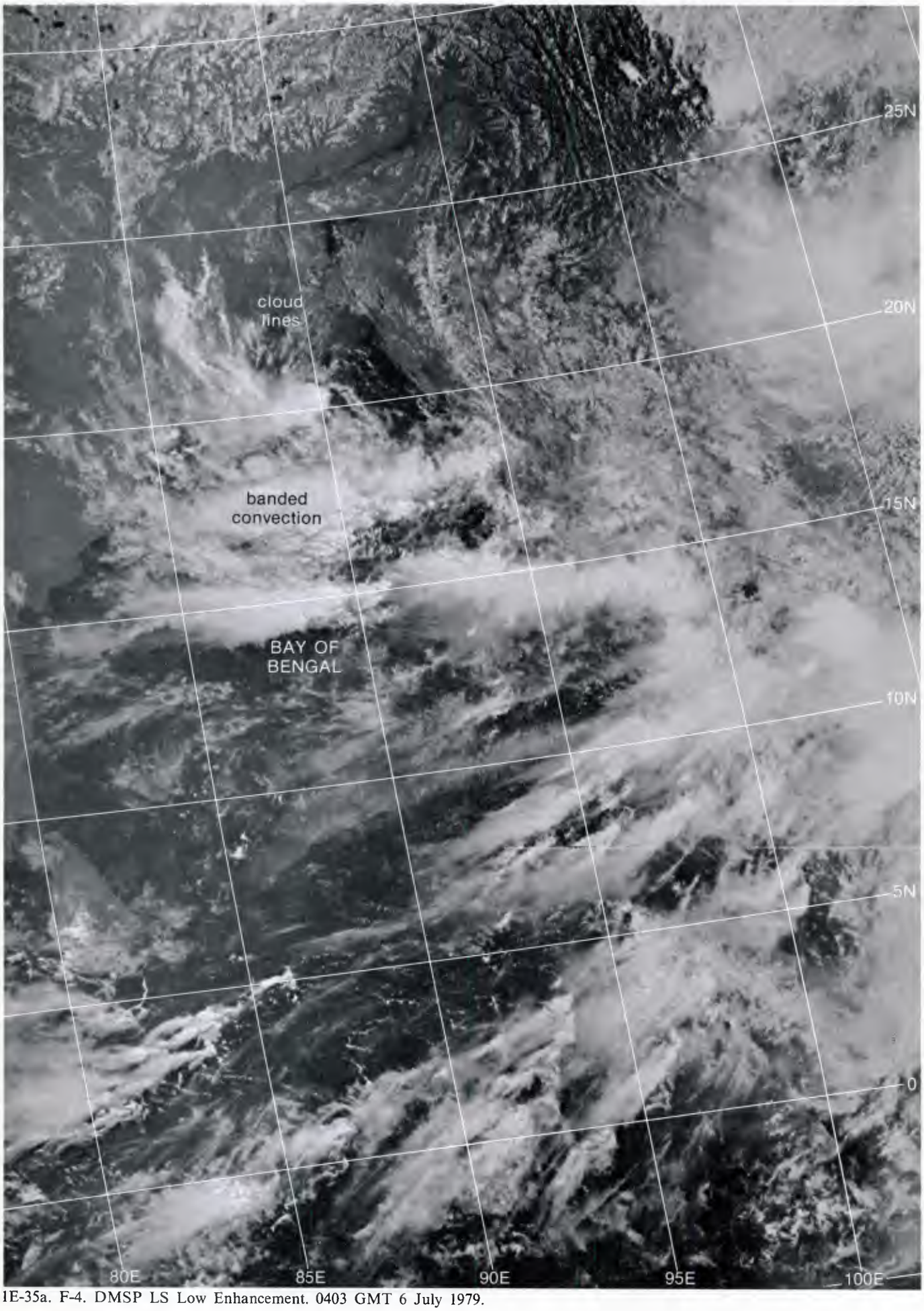

1E-35a. F-4. DMSP LS Low Enhancement. 0403 GMT 6 July 1979.

200 mb

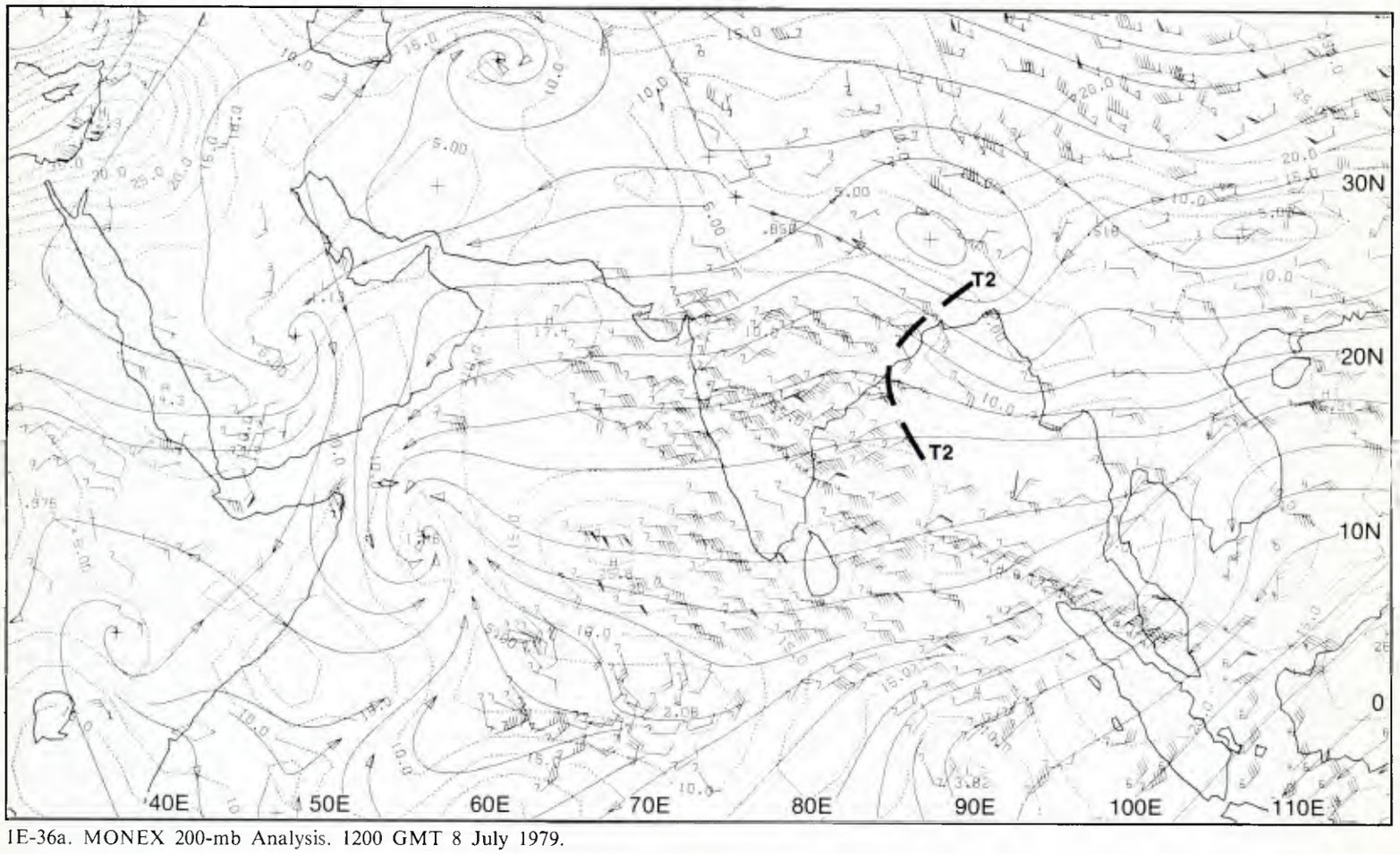

1E-36a. MONEX 200-mb Analysis. 1200 GMT 8 July 1979.

500 mb

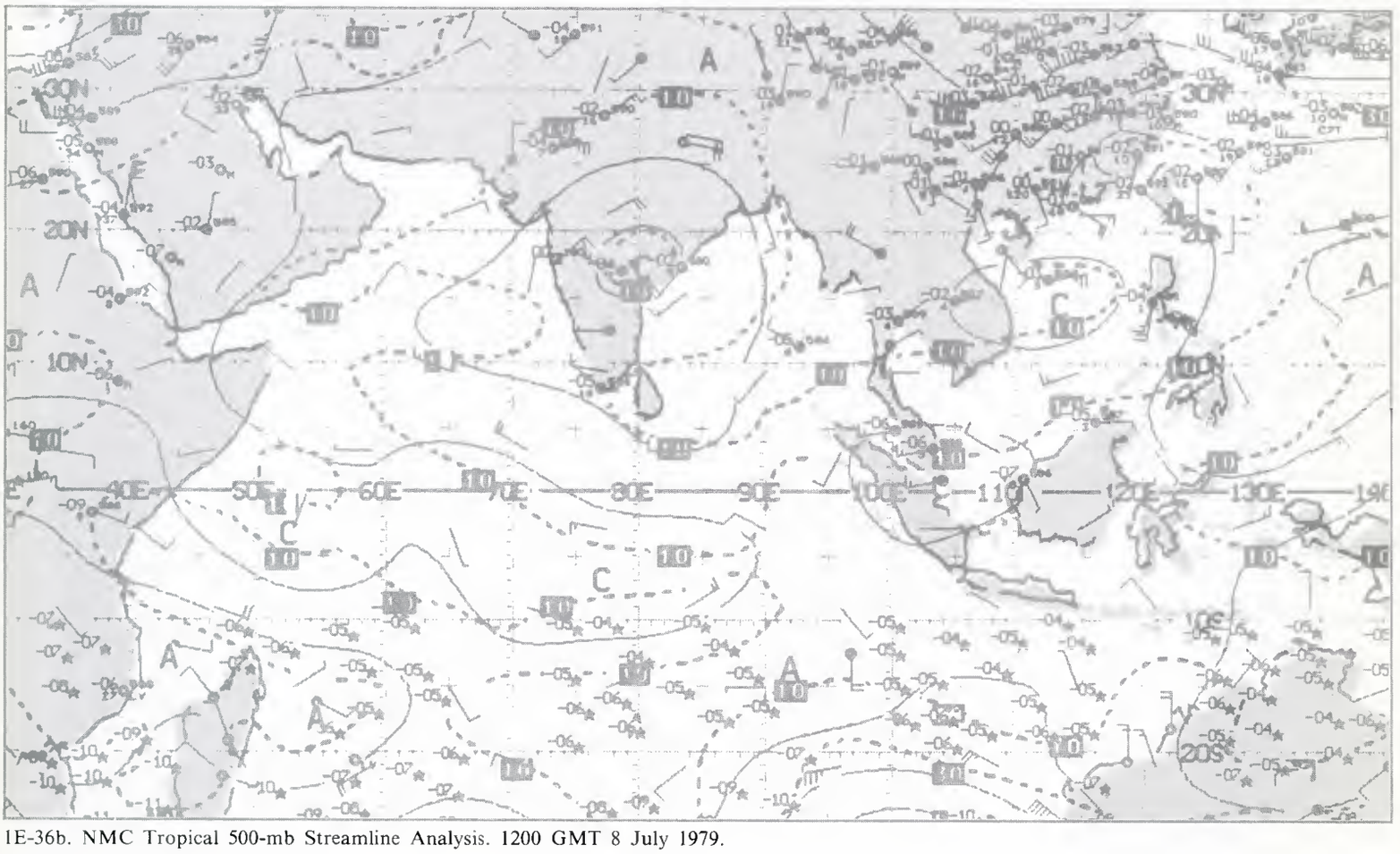

1E-36b. NMC Tropical 500-mb Streamline Analysis. 1200 GMT 8 July 1979.

8 July

A cyclonic circulation center first appears on the surface streamline analysis (1E-37b) on this date, as the storm moved onshore over India, with the center near 20° N, 84° W. The 850-mb analysis (1E-37a) illustrates the massive influence of this disturbance which exhibits a cyclonic circulation having a diameter of over 15 degrees of longitude. Strongest winds of up to 40 kt appear in the southeastern quadrant, with lighter speeds inward toward the center. This pronounced cyclonic shear contributes importantly to the vorticity of the system, favoring retention of strength even as the storm moves over land. The storm is equally apparent at the 500-mb level (1E-36b), with a diameter of 20 degrees of longitude while at 200 mb (1E-36a) a trough lies over the region.

The DMSP picture (1E-37c) shows heavy convection near the storm center, rather precisely defined by the series of curved low-level cloud lines spiraling into that region. Most of the remaining heavy convective cloudiness associated with this system lies in the southeast quadrant, where heavy rain would likewise be expected to occur. The fact that the rain is occurring in this quadrant is typical for storms moving northwest and west-northwest. After recurvature, the general observation is that heaviest rainfall occurs in the northeast quadrant generally in the same direction as the storm center motion (Rajamani and Rao, 1981).

10 July

The surface weather reports (1E-39a) indicate that the effects of the disturbance (clouds and precipitation) continue over northern India and a weak cyclonic center is shown near 21° N, 87° E. However, the weakened intensity of the system is clearly revealed by the 850-mb analysis (1E-38b) which shows only faint indications of a circulation center in that region. At 200 mb (1E-38a), a weak trough persists above the region of the possible low-level center.

The DMSP picture (1E-39b) suggests that the disturbance has essentially dissipated. No vortex is evident; however, a region of convective cloudiness debris is apparent over west-central India. This may be the remnant of the previous vigorous convection.

Important Conclusions

1. Monsoon depressions form over the Bay of Bengal from predecessor disturbances originating far to the east in the region of the South China Sea.

2. The strength of monsoon depression circulations is greatest near the 850-mb level.

3. Monsoon depressions generally track westward or northwestward until after landfall over India, where recurvature to the northeast may occur.

4. Heaviest rainfall for westerly or west-northwesterly moving monsoon depressions is chiefly in the southeast quadrant. After recurvature, heaviest rainfall is to the northeast in the direction of storm movement.

5. The depression circulation pattern tends to expand significantly when the center moves over land.

Reference

Rajamani, S., and K. V. Rao, 1981: On the occurrence of rainfall over the southwest section of a monsoon depression. *Mausam*, **32**, 215–220.

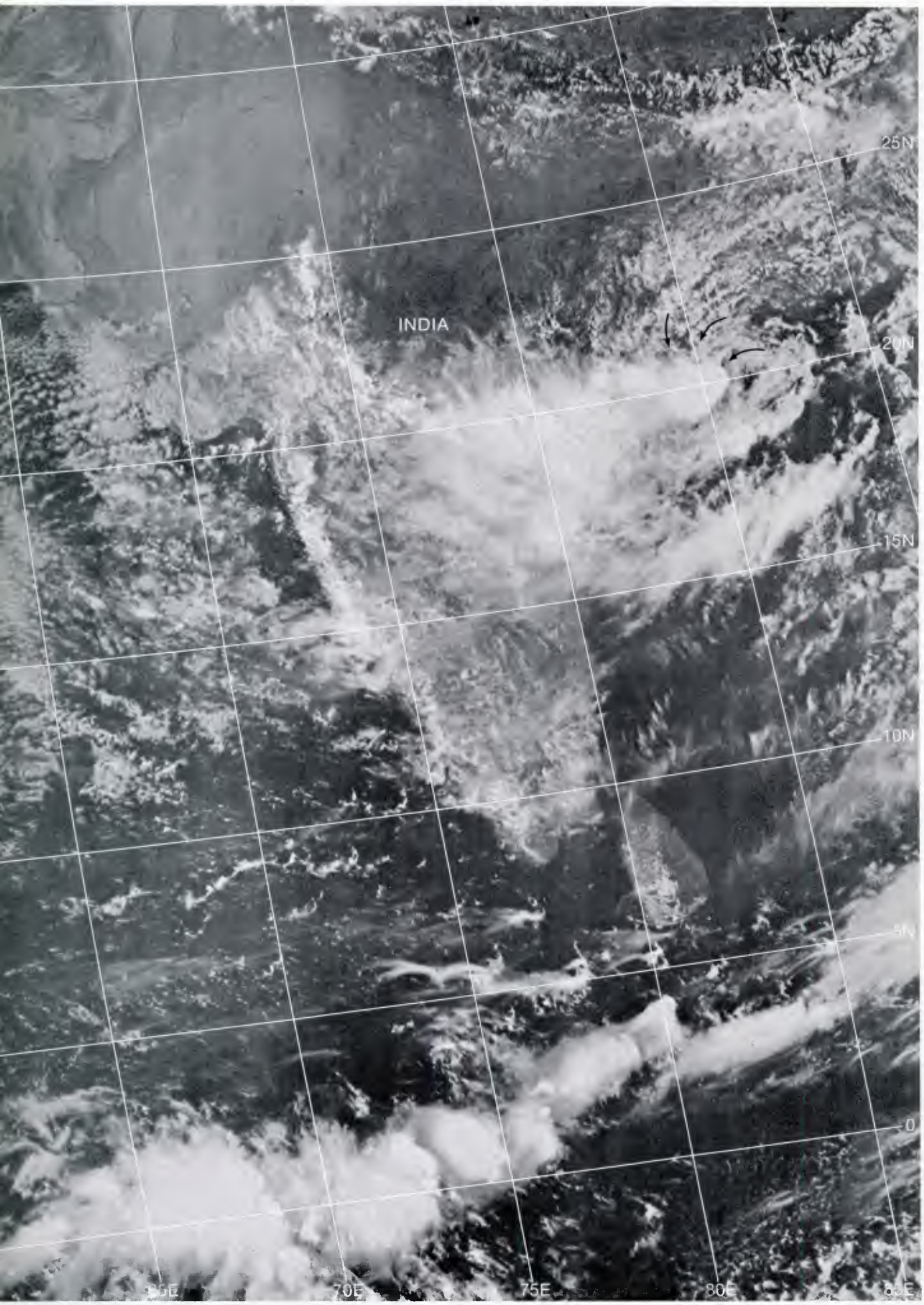

1E-37c. F-4. DMSP LS Low Enhancement. 0507 GMT 8 July 1979.

850 mb

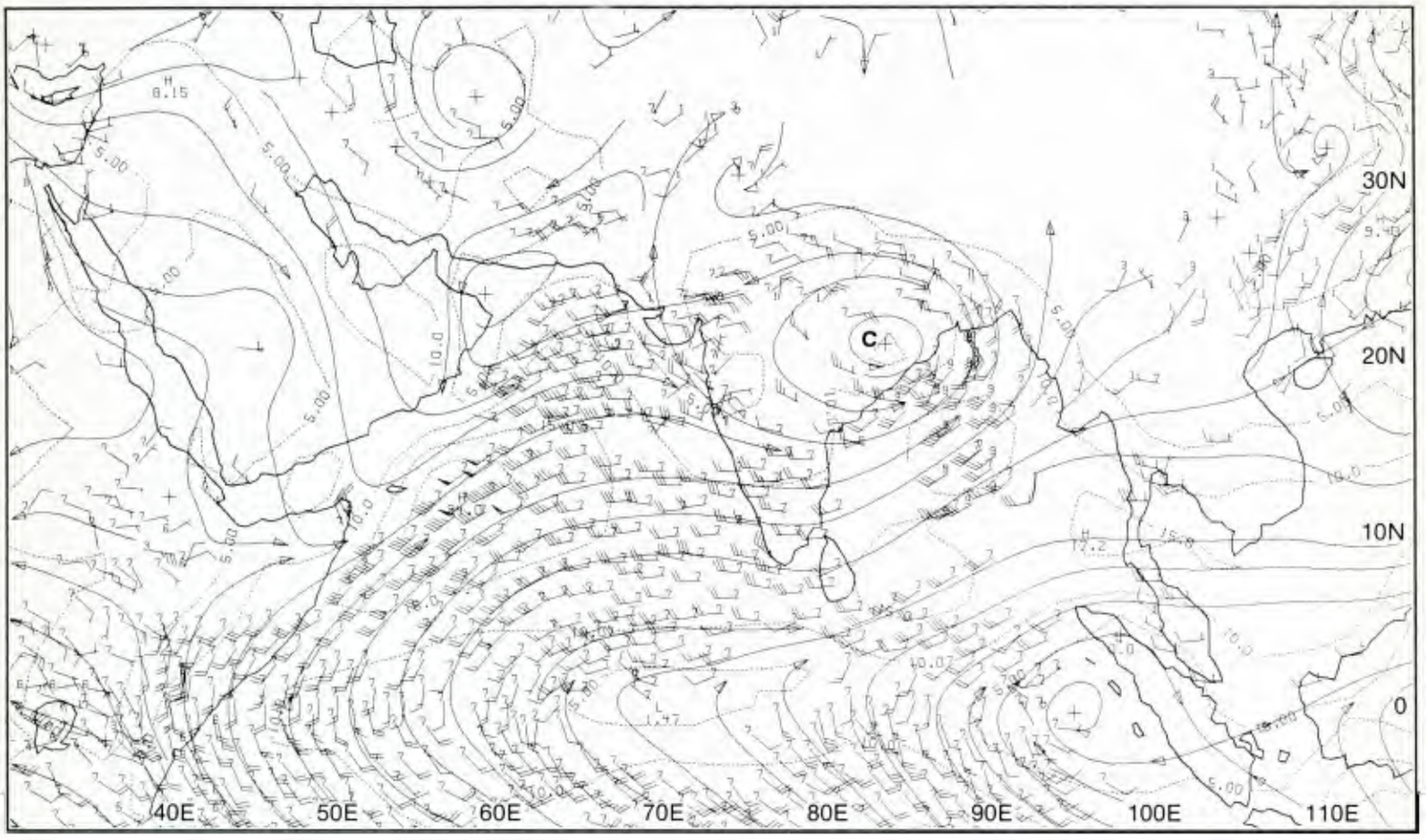

1E-37a. MONEX 850-mb Analysis. 1200 GMT 8 July 1979.

surface

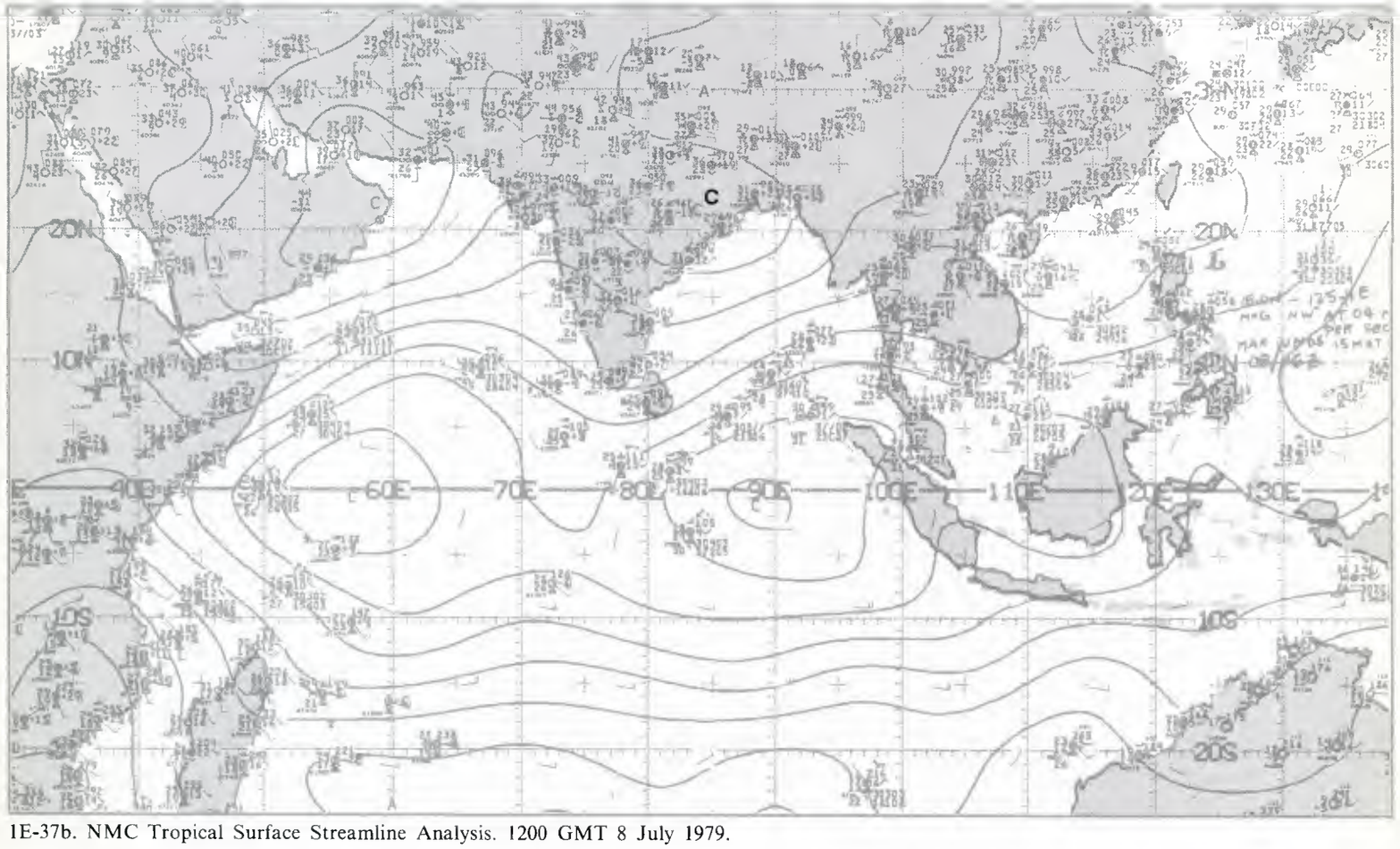

1E-37b. NMC Tropical Surface Streamline Analysis. 1200 GMT 8 July 1979.

200 mb

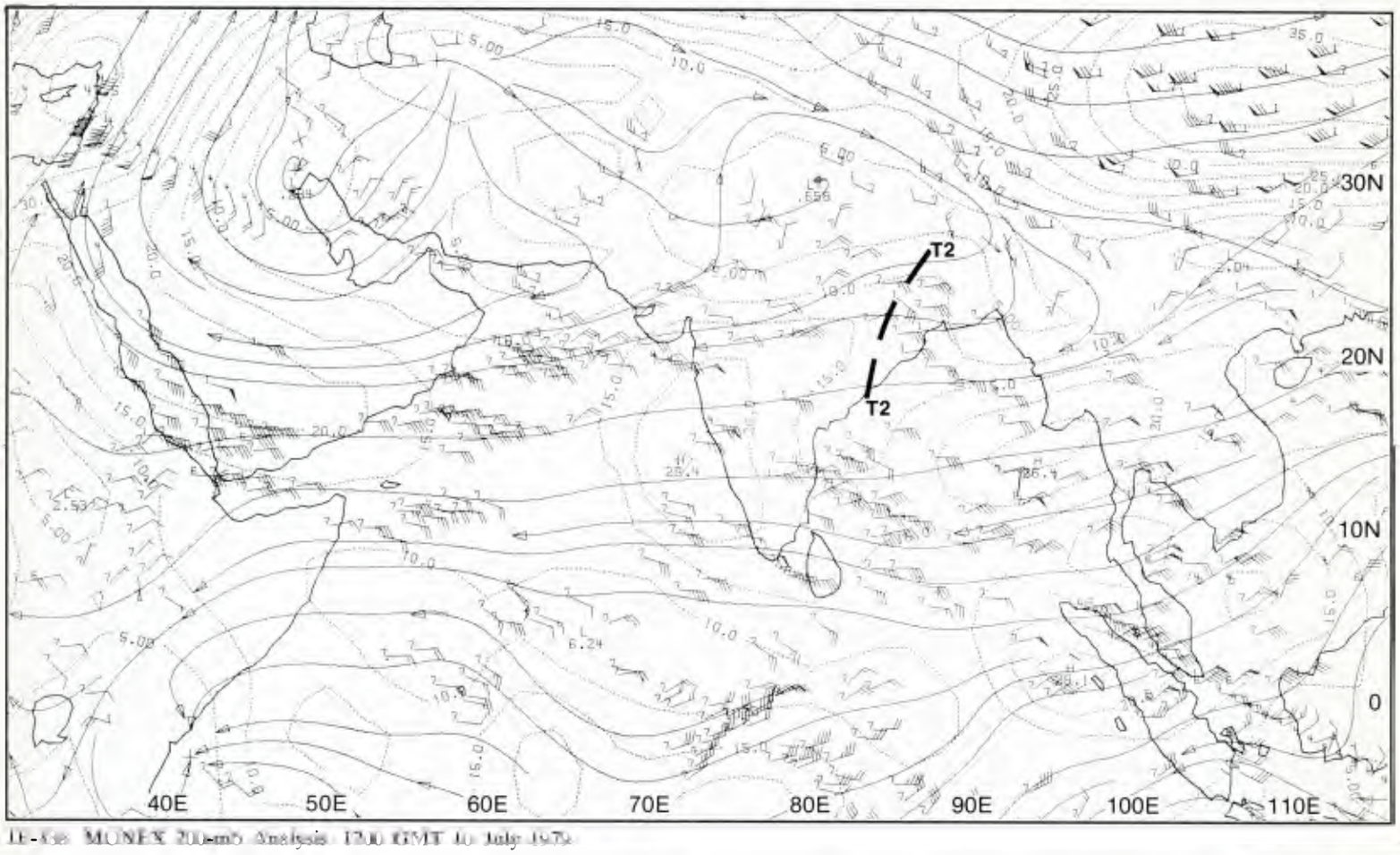

1E-38a. MONEX 200-mb Analysis. 1200 GMT 10 July 1979.

850 mb

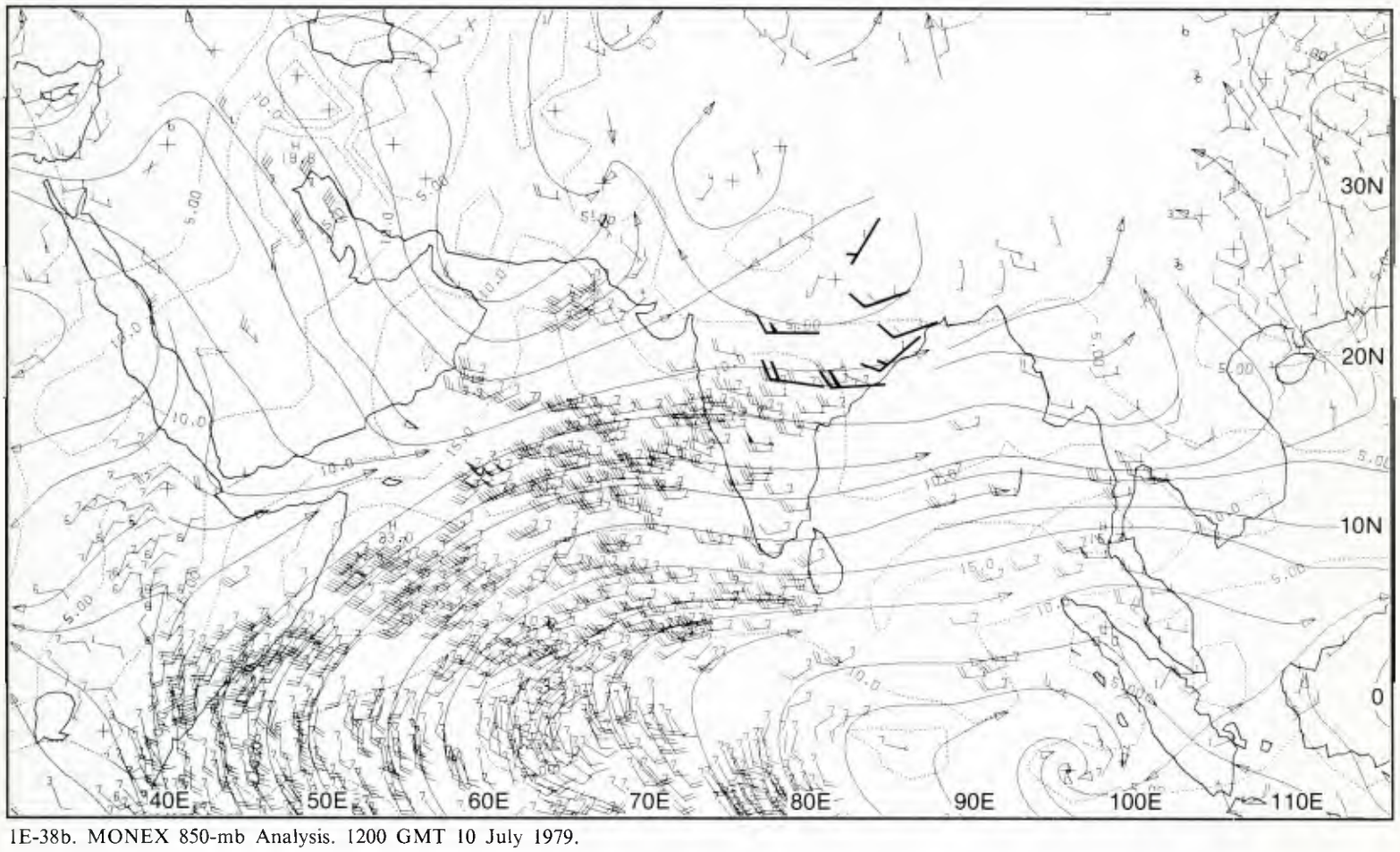

1E-38b. MONEX 850-mb Analysis. 1200 GMT 10 July 1979.

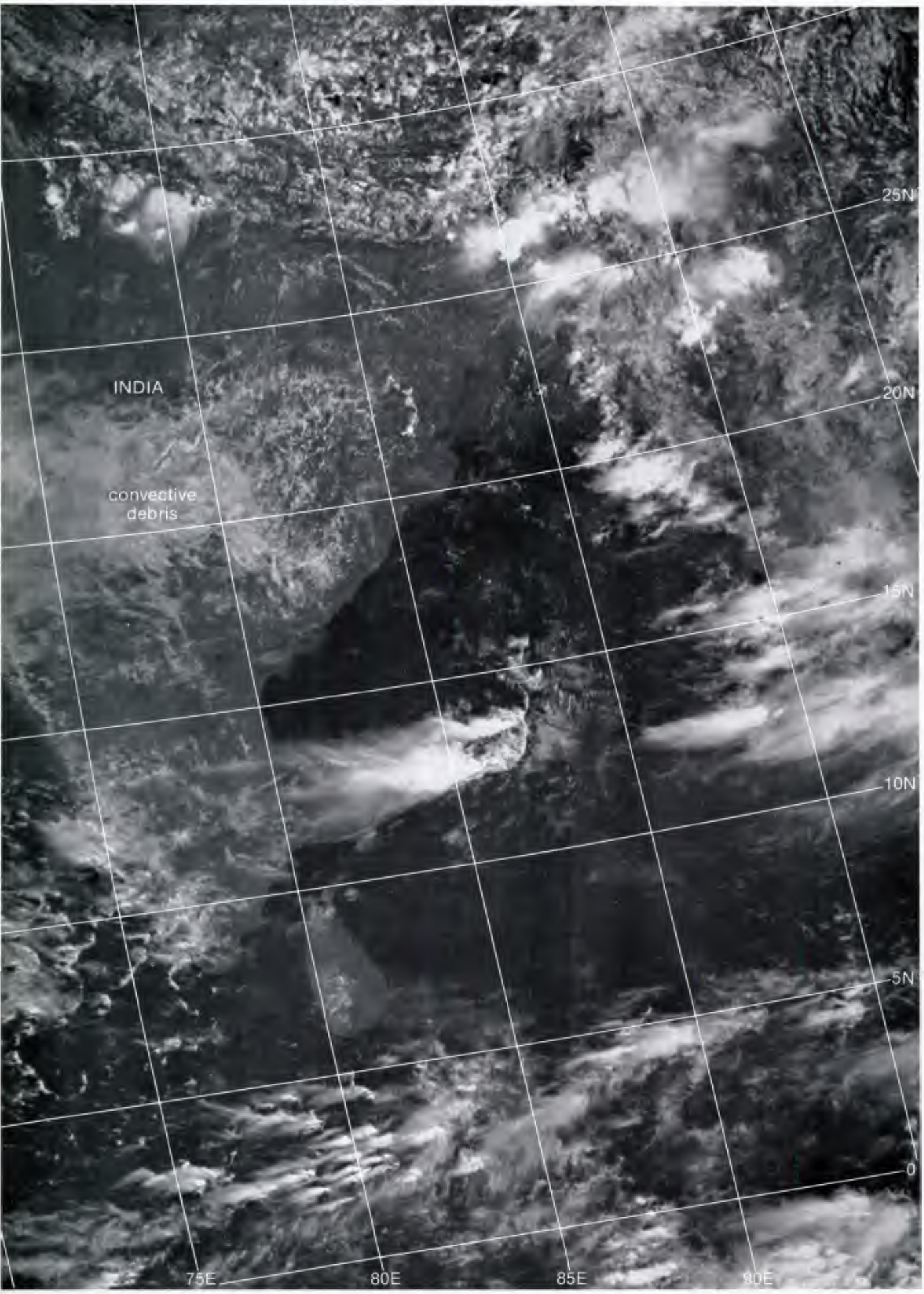

1E-39b. F-4. DMSP LS Low Enhancement. 0429 GMT 10 July 1979.

surface

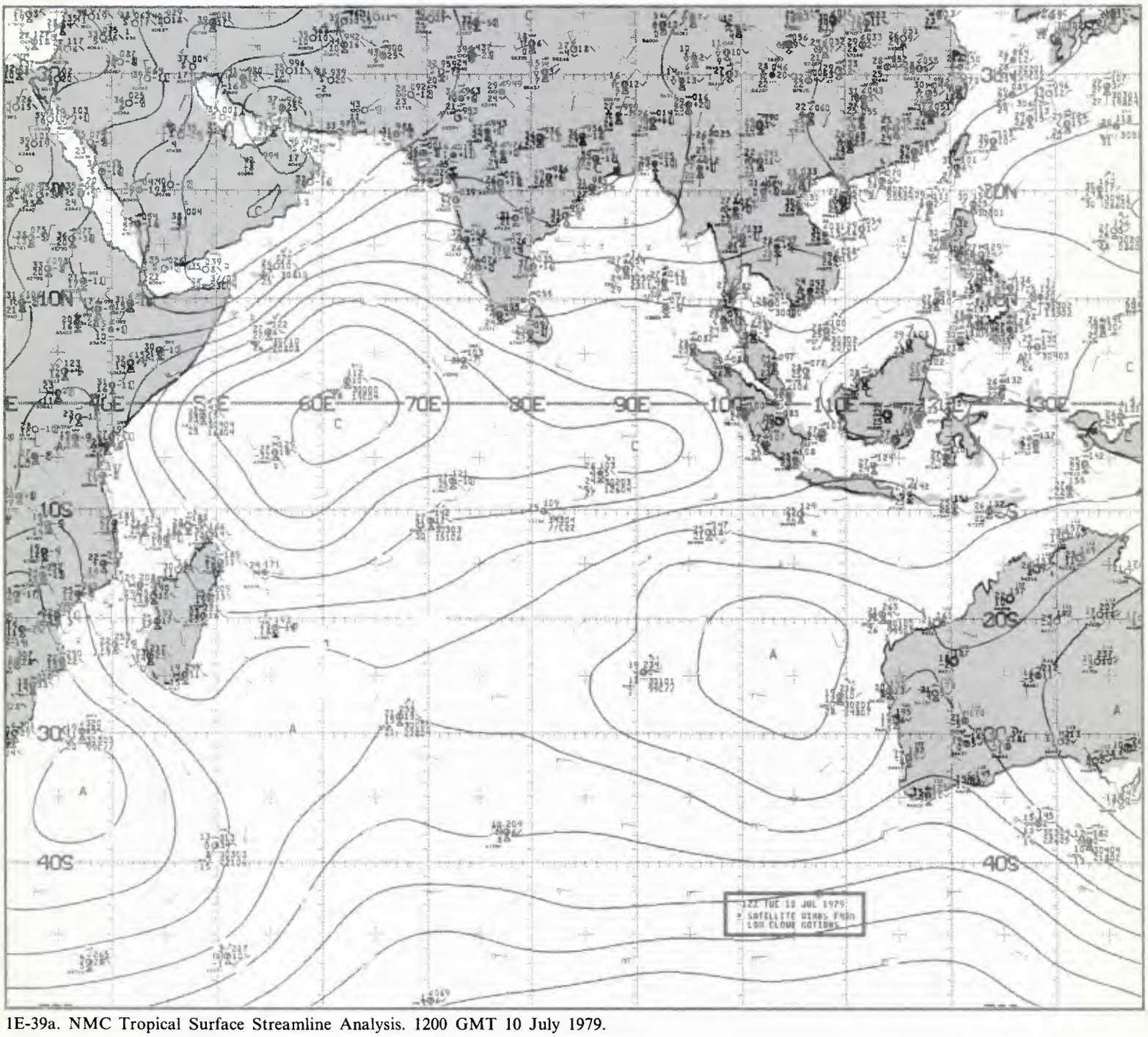

1E-39a. NMC Tropical Surface Streamline Analysis. 1200 GMT 10 July 1979.

Case 5 Arabian Sea/Bay of Bengal—Summer

Breaks in the Southwest Monsoon

The 1979 monsoon arrived about 10 days late, was generally weak during most of July and then after an active early August went into an extended break period near mid-August. The break extended from 15 August to the end of the southwest monsoon season, on about 20 September. This 37-day period is believed to be a record monsoon break period. The precipitation amounts over sections of India (1E-41a) show that the last half of July through mid-August was a period of appreciable rainfall.

Reference

Krishnamurti, T. N., P. Ardanuy, Y. Ramanathan, and R. Pasch, 1979: Quick look summer MONEX atlas. Part II: The onset phase. FSU Report No. 79-5, Florida State University, Tallahassee, FL, 205 pp.

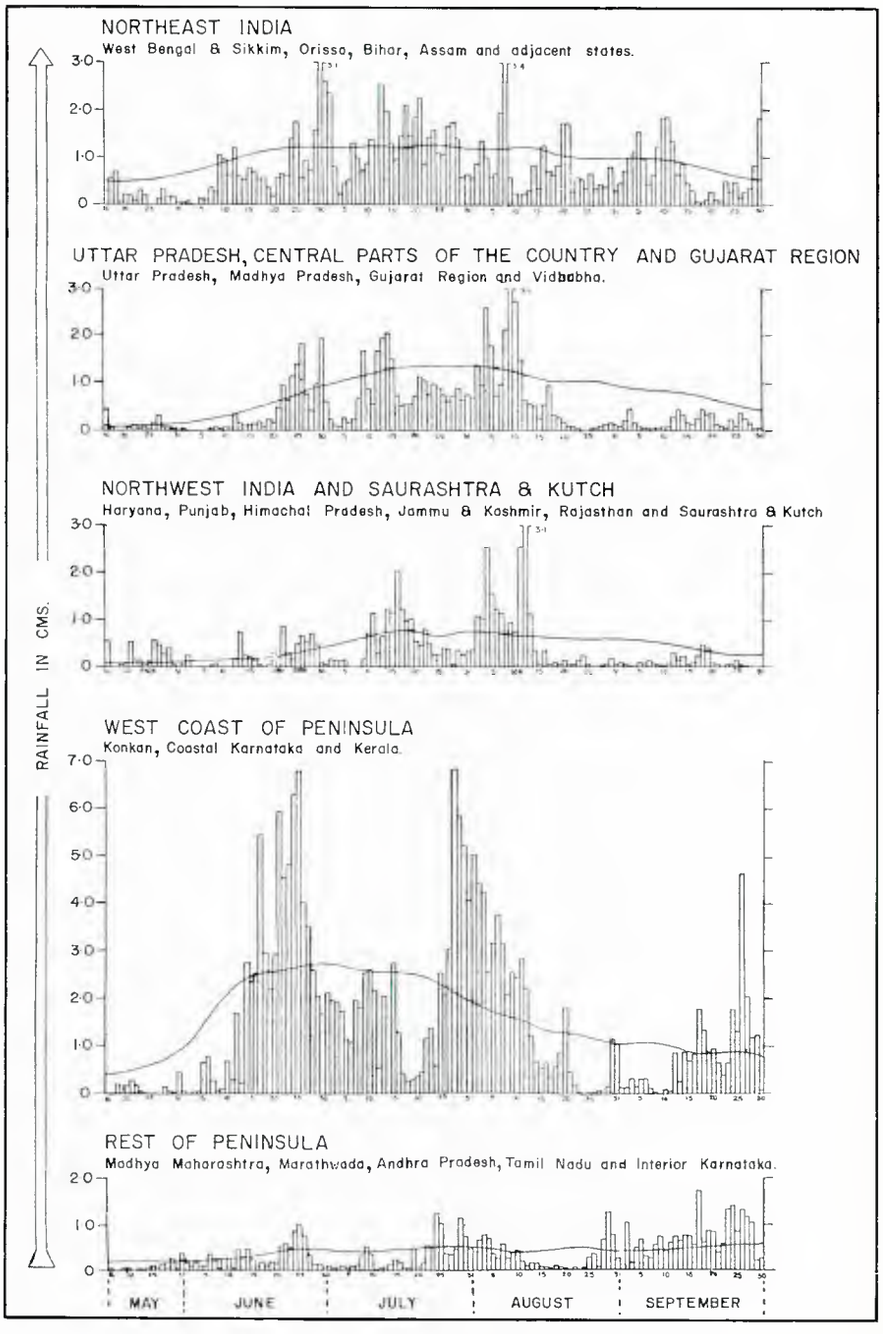

1E-41a. Progress of the monsoon day by day. 16 May–30 September 1979. Stepped curves represent actual rainfall and continuous curves represent normal rainfall. (Krishnamurti, 1979.)

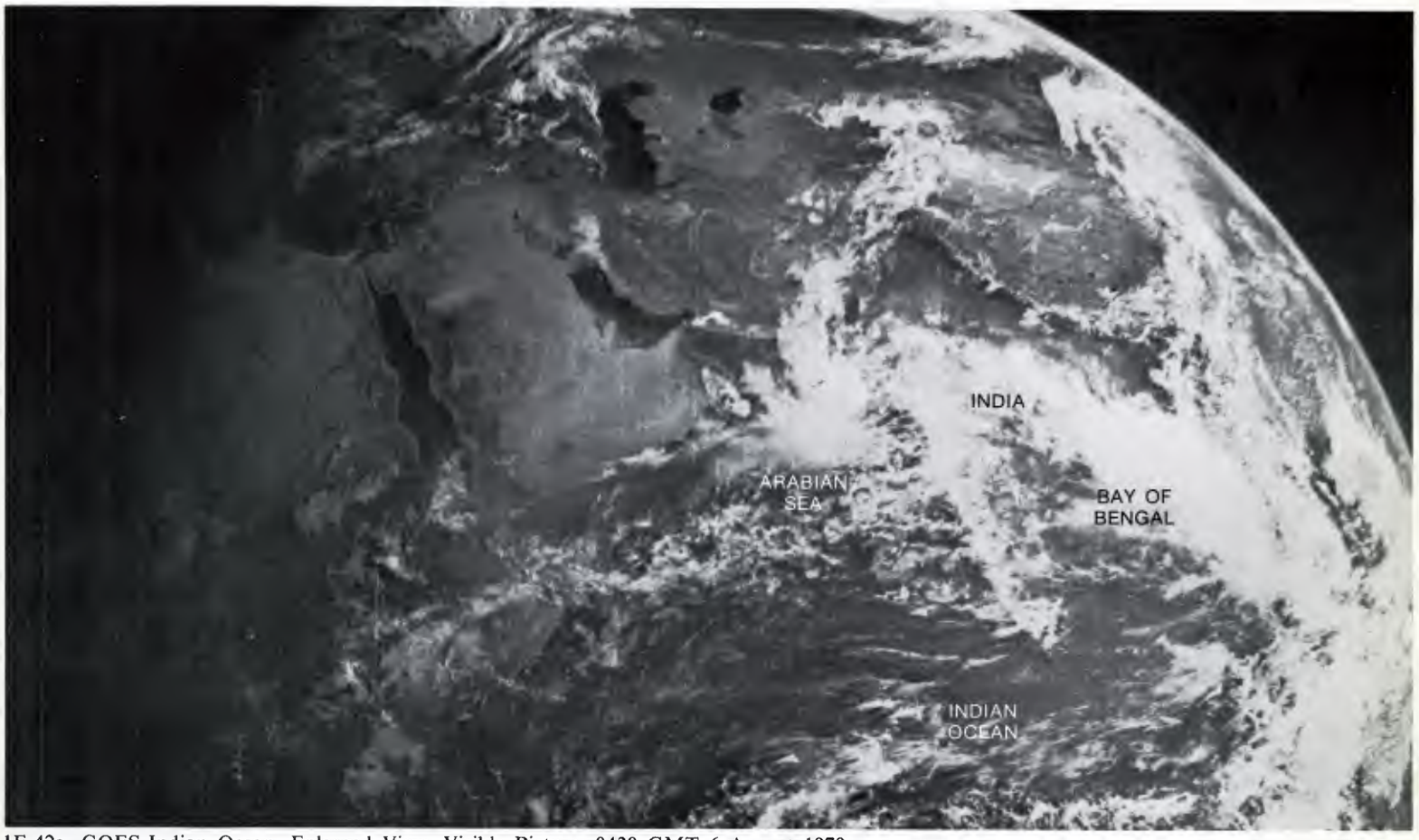

1E-42a. GOES-Indian Ocean. Enlarged View. Visible Picture. 0430 GMT 6 August 1979.

1E-42b. GOES-Indian Ocean. Enlarged View. Visible Picture. 0500 GMT 30 August 1979.

Break in the Southwest Monsoon of 1979
India
August 1979

5–30 August

The GOES-Indian Ocean picture acquired on 6 August at 0430 GMT (1E-42a) is representative of the period just before the break. It reveals extensive cloudiness over the Bay of Bengal, India (especially the western mountain range), and the northeast Arabian Sea. There is little activity over the Indian Ocean near the equatorial region, and there is evidence of a series of westerly disturbances (cloud patterns) in the Northern Hemisphere mid latitudes. These cloud conditions are indicative of a normal southwest monsoon.

A more detailed view of cloud conditions for 5 August is shown in the DMSP picture (1E-43a). While the most active convection is occurring over the northern Bay of Bengal and north-central India, the majority of India is covered by cloudy conditions. Little cloud activity exists north of about 25° N (foothills of the Himalayas) or in the tropical region south of India.

A contrasting view of the region during the period of the break is shown on the GOES-Indian Ocean picture for 30 August at 0500 GMT (1E-42b). In comparison to the previous GOES picture (1E-42a), convective activity over India is much reduced as is cloudiness over the Bay of Bengal and Arabian Sea. On the other hand, convective activity in the equatorial region south of India is enhanced over that of 5 August (1E-42a). Some cloud activity enhancement is also seen at this time over the southern slopes of the Himalayas, north of the Bay of Bengal.

A detailed view of India shown by a DMSP picture for 25 August (1E-45c) indicates vastly reduced convective cloudiness over India. Note the land breeze cloud line off southwest India, an indication of a very weak large-scale low-level southwesterly flow. This condition is further implied by the total lack of convective clouds over the western mountain range. These contrasting conditions are equally well depicted on the 700-mb analysis for 5 August (1E-45a) and 25 August (1E-45b). The analysis on 5 August shows the monsoonal trough near 20° N with moderate southwesterly monsoonal flow immediately to the south covering the land mass of India. On 25 August, the trough is nearer 30° N and more poorly defined. Speed of flow is extremely light to the south over India and more northerly directed.

Conditions at higher levels are also quite different. At 500 mb on 5 August (1E-44a), the Tibetan high is seen located near 38° N, 80° E. It is not a large cell and does not impede the movement of mobile troughs to the north. A cyclonic circulation off the west coast of India is associated with a disturbance that has developed within the monsoonal trough over the northern Arabian Sea (1E-42a).

On 25 August, the 500-mb analysis (1E-44b) reveals that a large blocking ridge has developed, extending from an anticyclone center near 11° N, 111° E. The amplitude of the ridge is large, reaching to almost 60° N. West of the ridge, a semi-permanent trough is anchored extending through the region previously occupied by the Tibetan anticyclone (1E-44a). Note that temperatures and height values have also dropped appreciably in this region in comparison to the earlier example.

Important Conclusions

1. Breaks in the southwest monsoon are clearly indicated in satellite imagery by a marked decrease in cloud cover over India and surrounding waters.

2. When a break period cloud pattern is detected in the imagery, a number of large- and small-scale circulation features can be deduced. Large-scale features associated with break periods include:
   a. A blocking ridge located between 90° E and 115° E that extends from near 35° N to 70° N.
   b. A near-stationary trough that lies to the west of the blocking ridge.
   c. The upper-level subtropical ridge, in particular, the Tibetan anticyclone is either completely displaced or significantly weakened.
   d. The upper-troposphere over northwest India is marked by cool temperatures and negative thickness anomalies.

3. Changes in synoptic-scale features within the southwest monsoon circulation pattern:
   a. The upper-level easterly jet is weakened and tends to shift northward.
   b. The low-level southwesterly flow is weakened and the northern branch of the low-level jet over the Arabian Sea becomes the stronger branch.
   c. Cloud cover and precipitation are at a minimum over India.
   d. The monsoon trough shifts northward to the Tibetan plateau and convective activity increases over the Himalayas.
   e. A zone of active convection develops in the equatorial region south of India.
   f. The rainfall belt normally near 20° N is replaced by one near 25° N and a second one near 7° N.
   g. With the weakened low-level southwesterly flow, land breeze cloud lines develop off southwest India.

4. Breaks in the monsoon are most likely to occur in August and average about 6 days in length.

References

Ramamurthy, K., 1969: Some aspects of the break in the Indian summer monsoons during July and August. Forecasting Manual No. IV. India Meteorological Department, Poona, India, 57 pp.

Rao, Y. P., 1976: Southwest monsoons. Meteorological Monograph No. 1. India Meteorological Department, New Delhi, India, 367 pp.

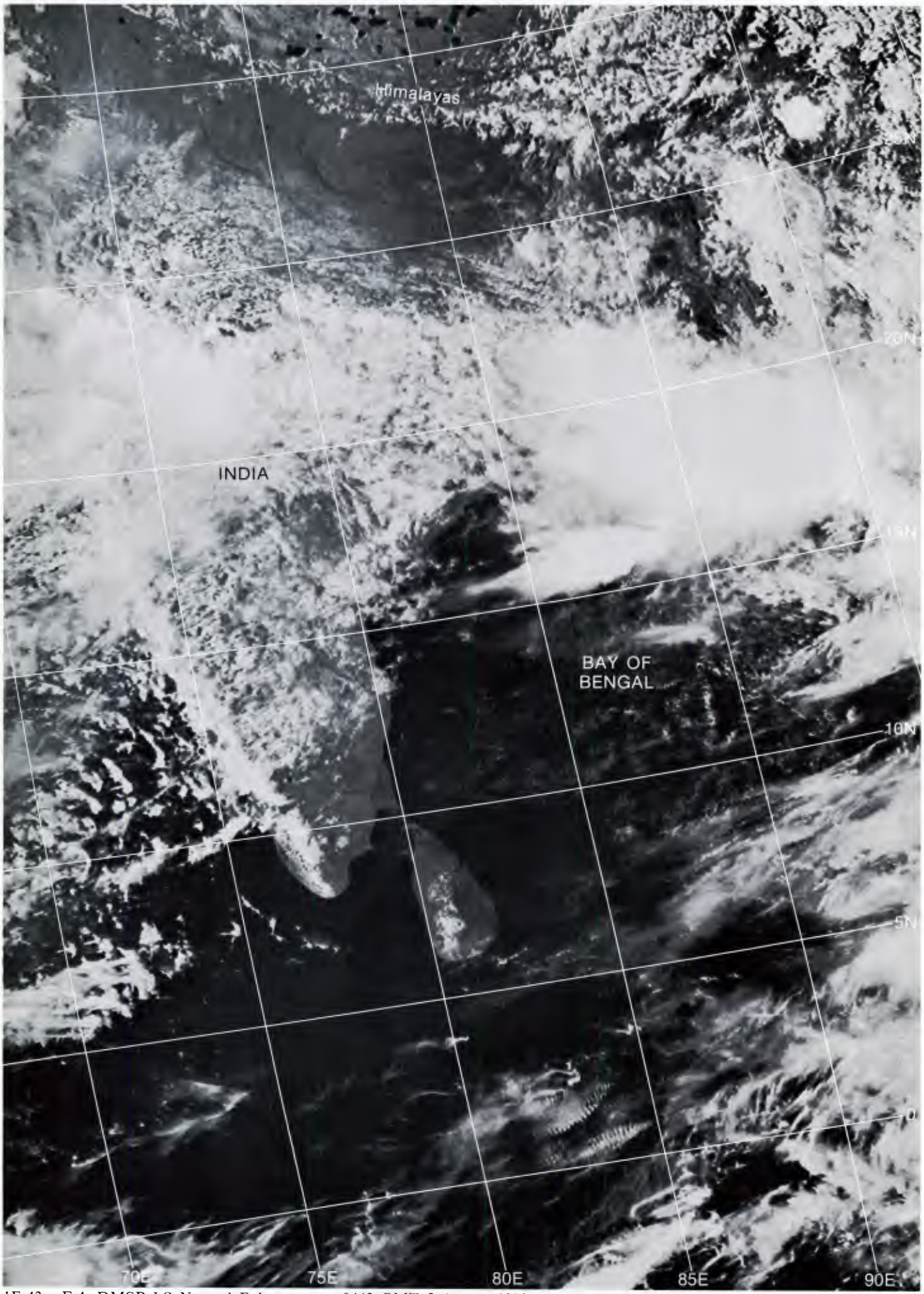

1E-43a. F-4. DMSP LS Normal Enhancement. 0443 GMT 5 August 1979.

500 mb

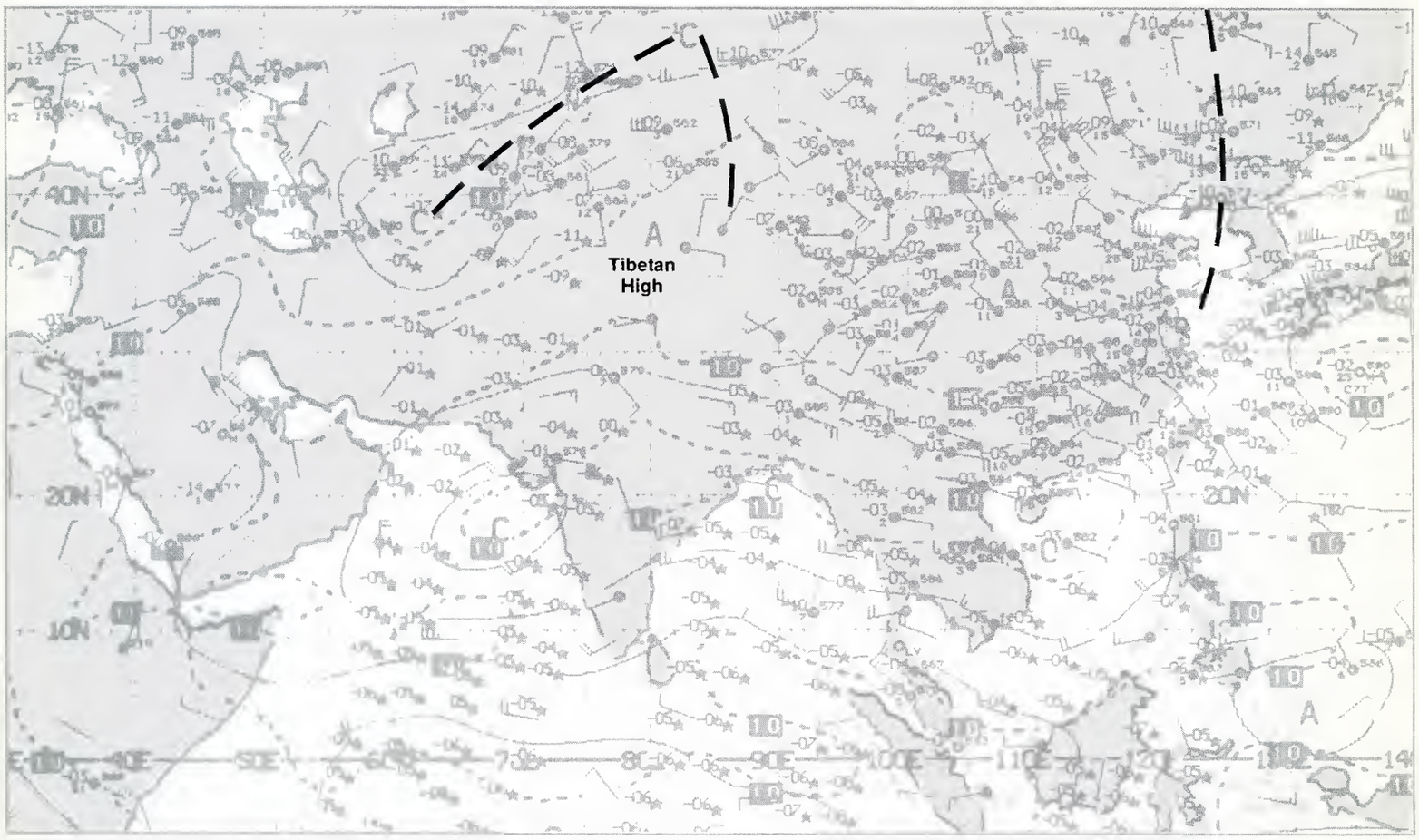

1E-44a. NMC Tropical 500-mb Streamline Analysis. 0000 GMT 5 August 1979.

500 mb

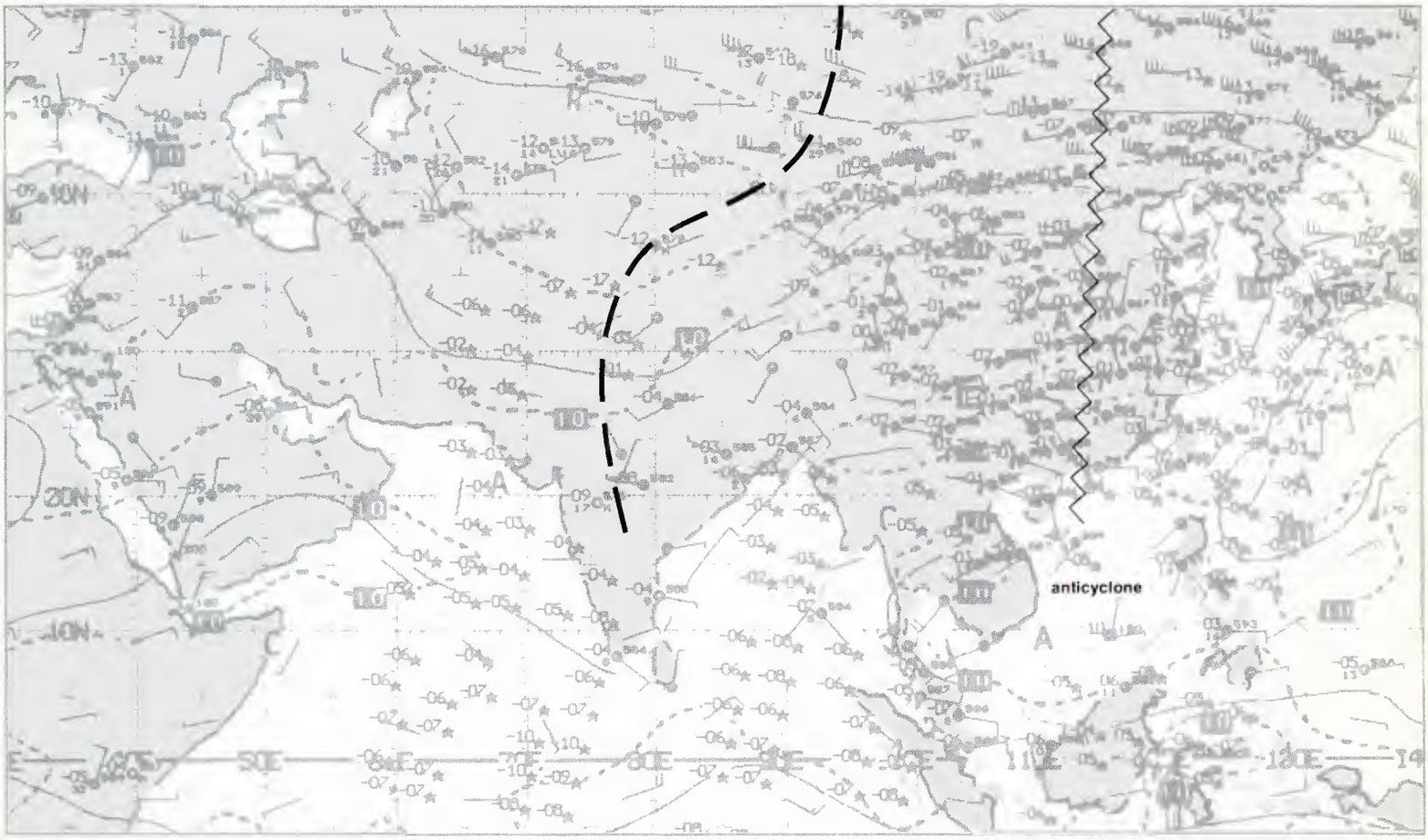

1E-44b. NMC Tropical 500-mb Streamline Analysis. 0000 GMT 25 August 1979.

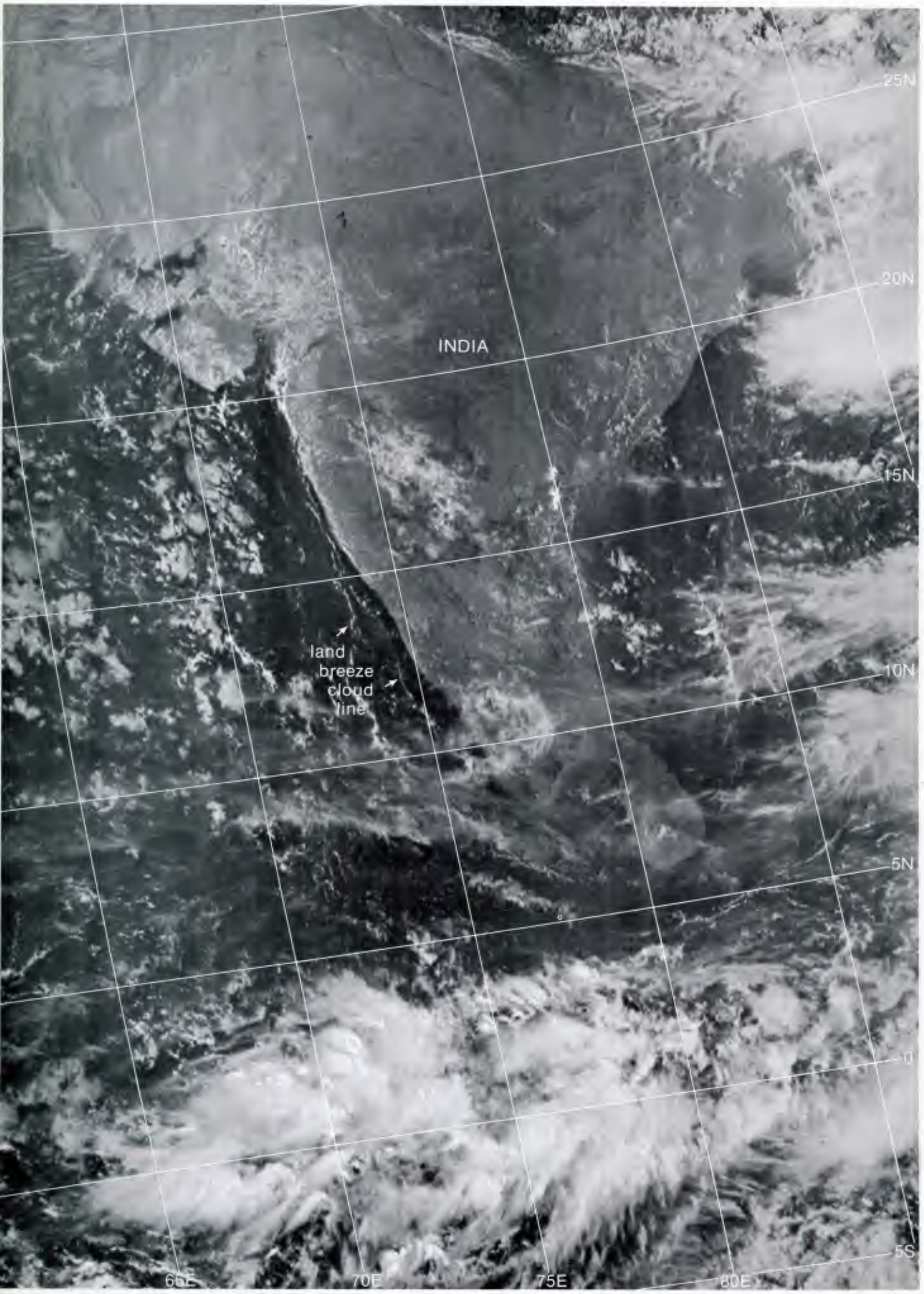

1E-45c. F-4. DMSP LS Low Enhancement. 0509 GMT 25 August 1979.

700 mb

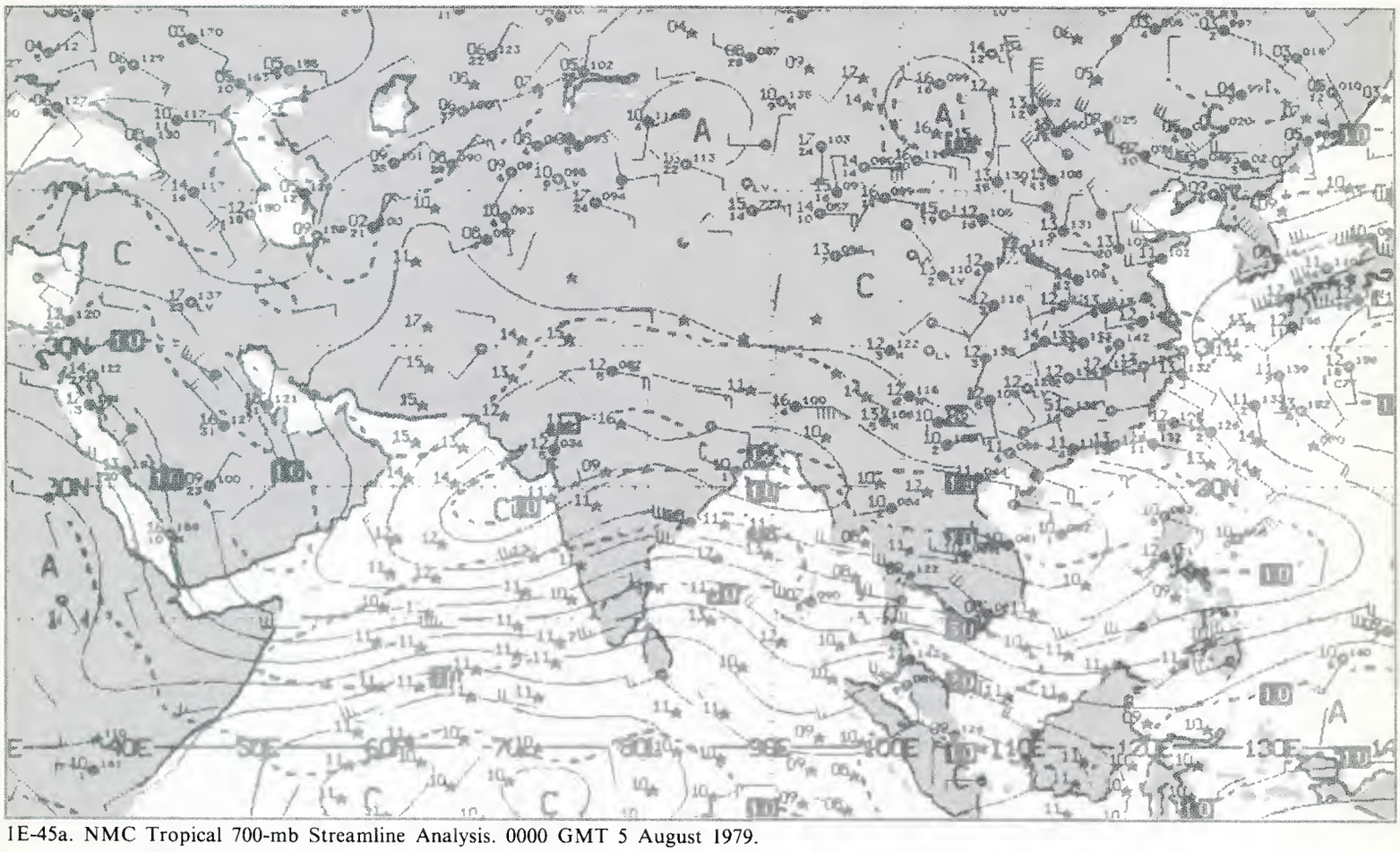

1E-45a. NMC Tropical 700-mb Streamline Analysis. 0000 GMT 5 August 1979.

700 mb

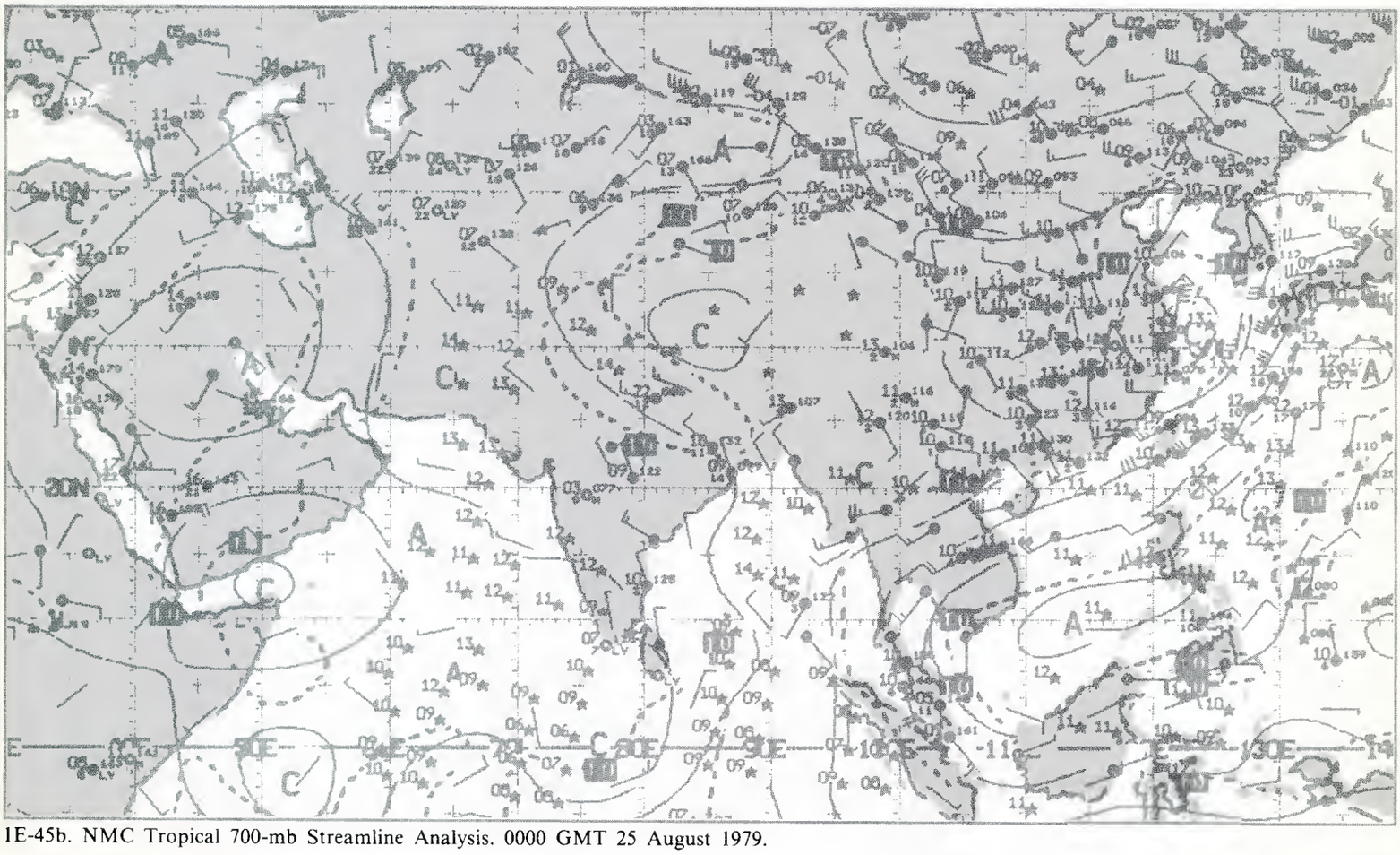

1E-45b. NMC Tropical 700-mb Streamline Analysis. 0000 GMT 25 August 1979.

Case 6 Arabian Sea/Bay of Bengal—Summer

The Somali Current Prime Eddy

The Somali current prime eddy is a warm, anticyclonic eddy which occurs each year during the southwest monsoon off of the northern tip of Somalia. Figure 1E-47a is a TIROS-N infrared depiction showing the eddy on 18 August 1979. Low cloud convection tends to be maximized over the warm waters of the prime eddy.

Upwelling occurs between the Somalia coast and the eddy. A ring of this upwelled cold water tends to encircle the eddy, facilitating identification of its outer boundaries. Cloud development is inhibited in the upwelled region, creating a crescent-shaped clear area as depicted in satellite visible imagery.

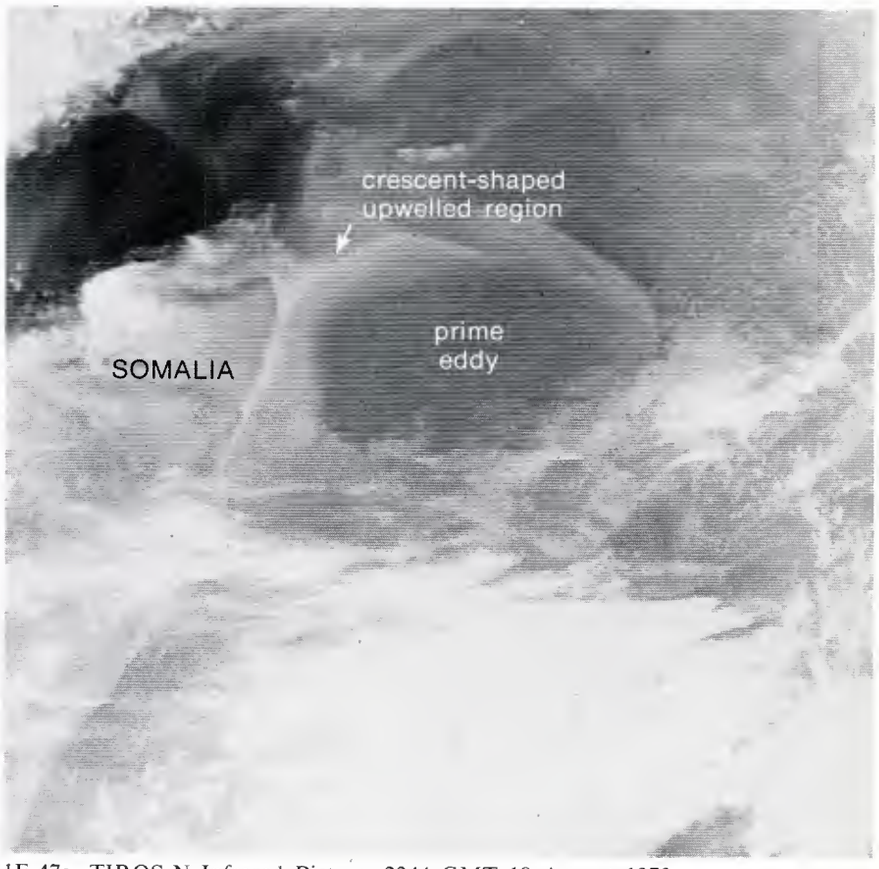

1E-47a. TIROS-N Infrared Picture. 2344 GMT 18 August 1979.
(Photo Courtesy of R. Whritner, Scripps Institution of Oceanography.)

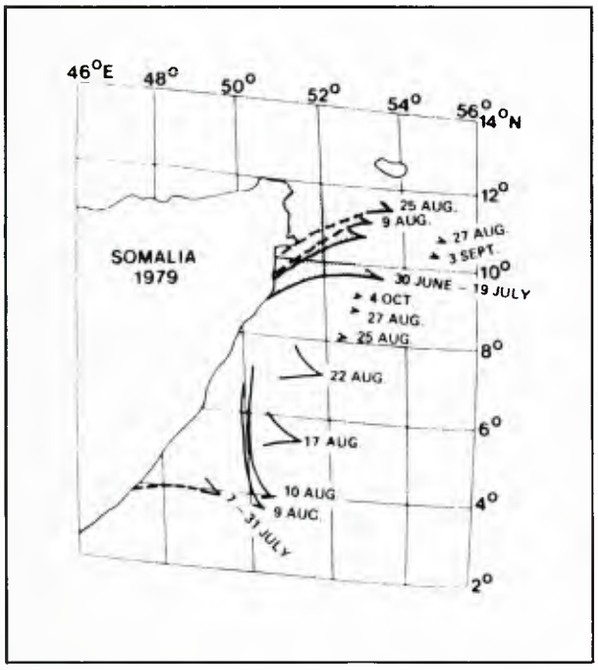

1E-48a. Time sequence of satellite-observed frontal locations for northern and southern frontal wedges for year 1979 (after Evans and Brown, 1981).

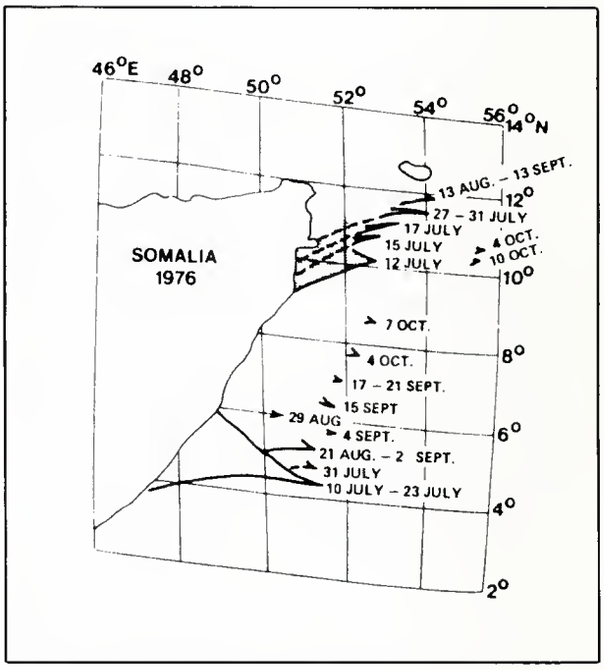

1E-48b. Time sequence of satellite-observed frontal locations for northern and southern frontal wedges for year 1976 (after Evans and Brown, 1981).

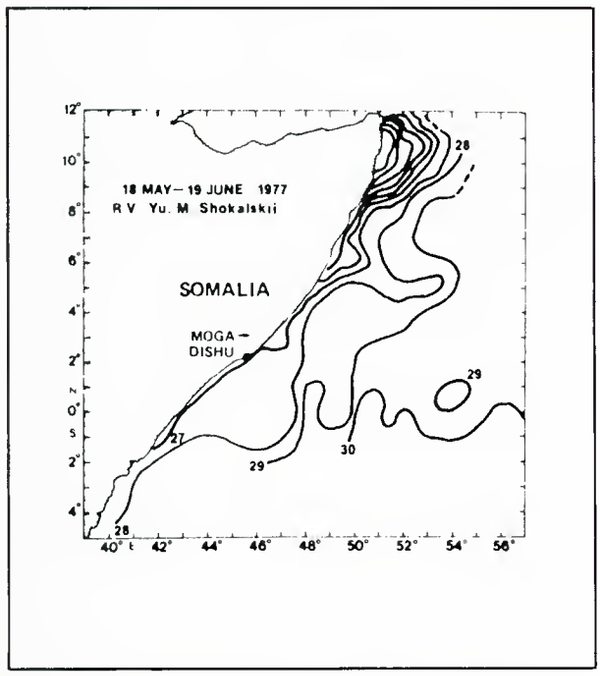

1E-48c. Surface temperature map derived from measurements made onboard the R. V. SHOKALSKII during May and June, 1977 off Somalia (after Evans and Brown, 1981).

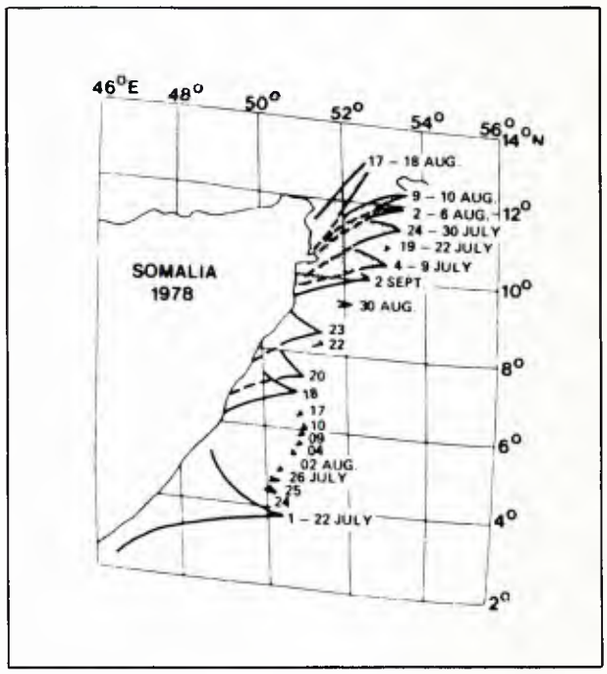

1E-48d. Time sequence of satellite-observed frontal locations for northern and southern frontal wedges for year 1978 (after Evans and Brown, 1981).

Cloudiness Patterns Associated with the Somali Current Prime Eddy
Arabian Sea
June–July 1979

Bruce, Quadfasel, and Swallow (1980) describe the evolution of the Somali current prime eddy SST pattern as follows: During the southwest monsoon regime the Somali current flows northeastward along the east Africa coast, commencing by late April south of the Equator, progressing northward during May and June and reaching full strength during July and August. In the vicinity of the Somalia coast at this time, large ocean anticyclonic (clockwise) circulation eddies are formed. The largest of these (diameter 400–600 km) is termed the prime eddy. It appears to occur each year between approximately 4° to 12° N, and between the Somalia coast and 58° E. During some years an eddy forms adjacent to and south (approximately 0° to 5° N, and from the Somalia coast to 53° E) of the prime eddy.

A study by Evans and Brown (1981) using surface ship-of-opportunity SST reports and satellite-sensed SST data for the years 1976–1979 indicates the prime eddy occurred each year, with some variation in the southern eddy (1E-48a, 48b, 48c, and 48d). The southern eddy may also be an annual event, but the lack of broad-scale routing observations by satellite and/or dense SST reports may have resulted in oversights of the feature during most years. The study also presents the evolution of the SST pattern from mid-April through early September of 1979. Prior to the onset of the southwest monsoon flow (1E-49a), water warmer than 30° C is indicated along the Somalia coast from the Gulf of Aden southward to 2° N. By mid-May (1E-49b), cool water (26°–28° C) is appearing from near the Equator to near 7° N. During late May and early June, the light to moderate southern winds off Somalia produce upwelling and resulting coastal cooling northward to near 11° N (1E-49c). During this period the thermal front north of about 4° N is generally within 50–100 km of the coast and the strongest gradients are reported to be about 0.025° C per kilometer. Minimum near-coastal temperatures are 25°–26° C. With the onset of the southwest monsoon and the development of strong southerly surface winds, the offshore transport of water increases, compensating upwelling increases, and significant SST drops occur off Somalia. During late June and all of July in 1979 (1E-49d) the configuration of wedge-shaped regions of cold upwelled water and general crescent shape of the ocean thermal front result from the advection pattern of the large oceanic anticyclonic eddies.

In the DMSP visible picture (1E-50a), from the early stage of the southwest monsoon (18 June 1979), the zone free of low clouds extends from near 2° N to about 9° N. The northern portion is somewhat obscured by cirrus. The zone extends from the coast seaward 60 n mi. The seaward boundary is marked by enhanced low clouds from about 2° to 5° N. On 14 July 1979, the DMSP picture (1E-51a) shows the cloud-free zone with a more pronounced crescent shape than in June. The visible picture leaves some uncertainty to the offshore extent of the ends of the crescent.

As a comparison, the DMSP picture (1E-51b) shows the cloud conditions that exist during the northeast monsoon (21 Jan 1980) in the area off Somalia. There is no reduction of clouds near the coast. Simultaneous DMSP visible (1E-52a) and infrared (1E-53a) pictures from 5 July 1979, illustrate the continuity of the cloud-free zone from mid-June to mid-July 1979 and provide insight to the air-sea interaction that produces the condition. The visible imagery once more gives an indication of a crescent-shaped area of inhibited low-cloud development. The infrared image, however, shows a well-defined crescent-shaped gray shade that corresponds with the cloud-free zone of the visible image.

The simultaneous infrared (1E-53a) and visible (1E-52a) DMSP pictures of 5 July 1979 give a clear view of the upwelling and thermal patterns off Somalia. In the infrared the crescent-shaped pattern with cold wedge-shaped areas projecting offshore correlates directly with the SST that was derived from ship reports (1E-48d). Note that the thermal pattern which depicts the upwelling and advection pattern in the infrared picture is largely free of clouds in the visible picture. In fact, there is an indication of a crescent-shaped cloud-free area in the visible image that closely agrees with the infrared crescent-shaped SST pattern. This indicates that the temperature pattern of the infrared image is in fact primarily that of the ocean surface and not cloud contamination. Further, there is the indication that the cold upwelled water tends to inhibit low cloud development. Therefore, the upwelling pattern will be discernible in visible imagery when high clouds do not obscure the area and low clouds bound the outer region of the pattern.

Investigation of the oceanic features off Somalia has shown that the SST pattern associated with the established southwest monsoon (late June, July, early August) is quite stable. The SST pattern (1E-49d) generally persists throughout July. During the late summer and early fall with the weakening of the southwest monsoon some dynamic changes occur in the current structure off Somalia (1E-49e). The southern gyre tends to move northward with the decrease in the speed of the low-level winds off Somalia. The prime gyre appears to shift first slightly northward and then southward and the two gyres coalesce. This single gyre and thermal pattern then slowly decays over a two to three month period as the southwest monsoon flow breaks down. The annual progression during 1979, 1976, and 1978 (1E-48a, 48b, 48c, and 48d) show that while the thermal pattern is a yearly feature, there are variations from year to year. This most likely relates to the annual variations in the intensity of the forcing southwest monsoon flow.

The imagery off Somalia, therefore, provides intelligence as to both cloud conditions and SST patterns. The fact that the area of extreme upwelling is free of low clouds, and more precisely fog and stratus, is surprising. Ramage (1971) provides a case study in the area and explanations of the fog and stratus-free conditions. The following material is summarized from Ramage.

continued on page 1E-53

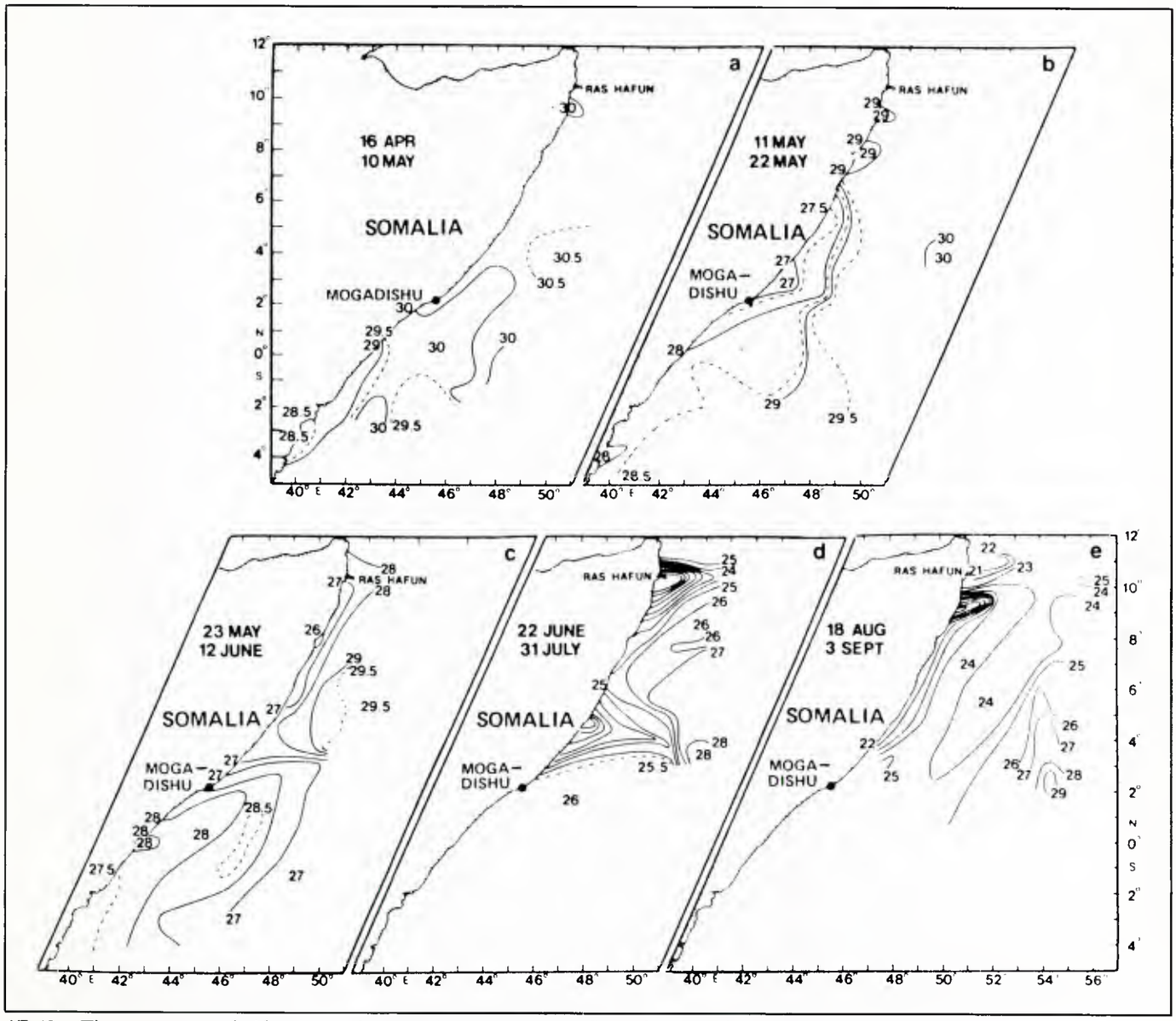

1E-49a. Time sequence of ship-observed sea-surface temperature fields for oceanic response to the southwest monsoon of 1979 (after Evans and Brown, 1981).

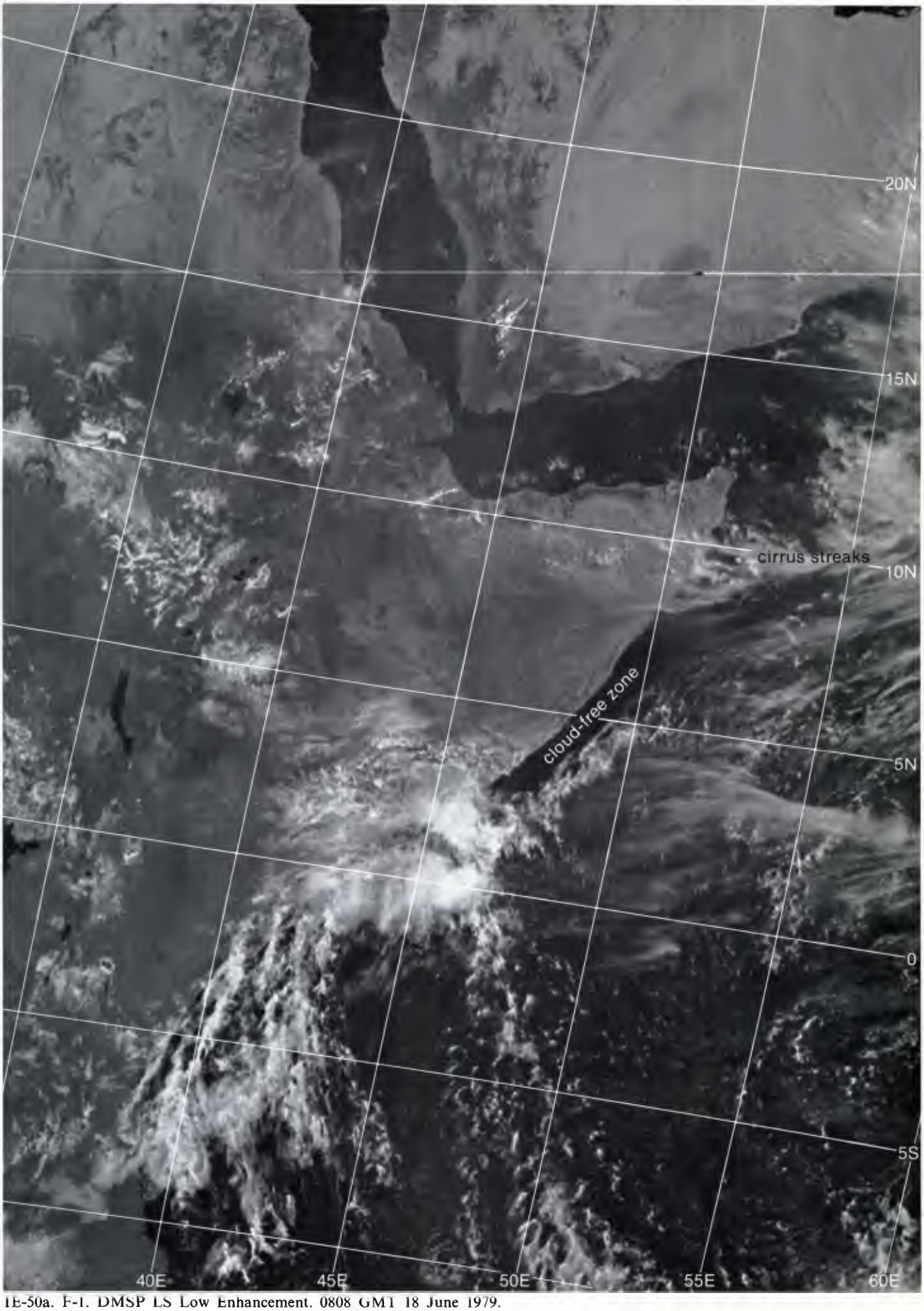

1E-50a. F-1. DMSP LS Low Enhancement. 0808 GMT 18 June 1979.

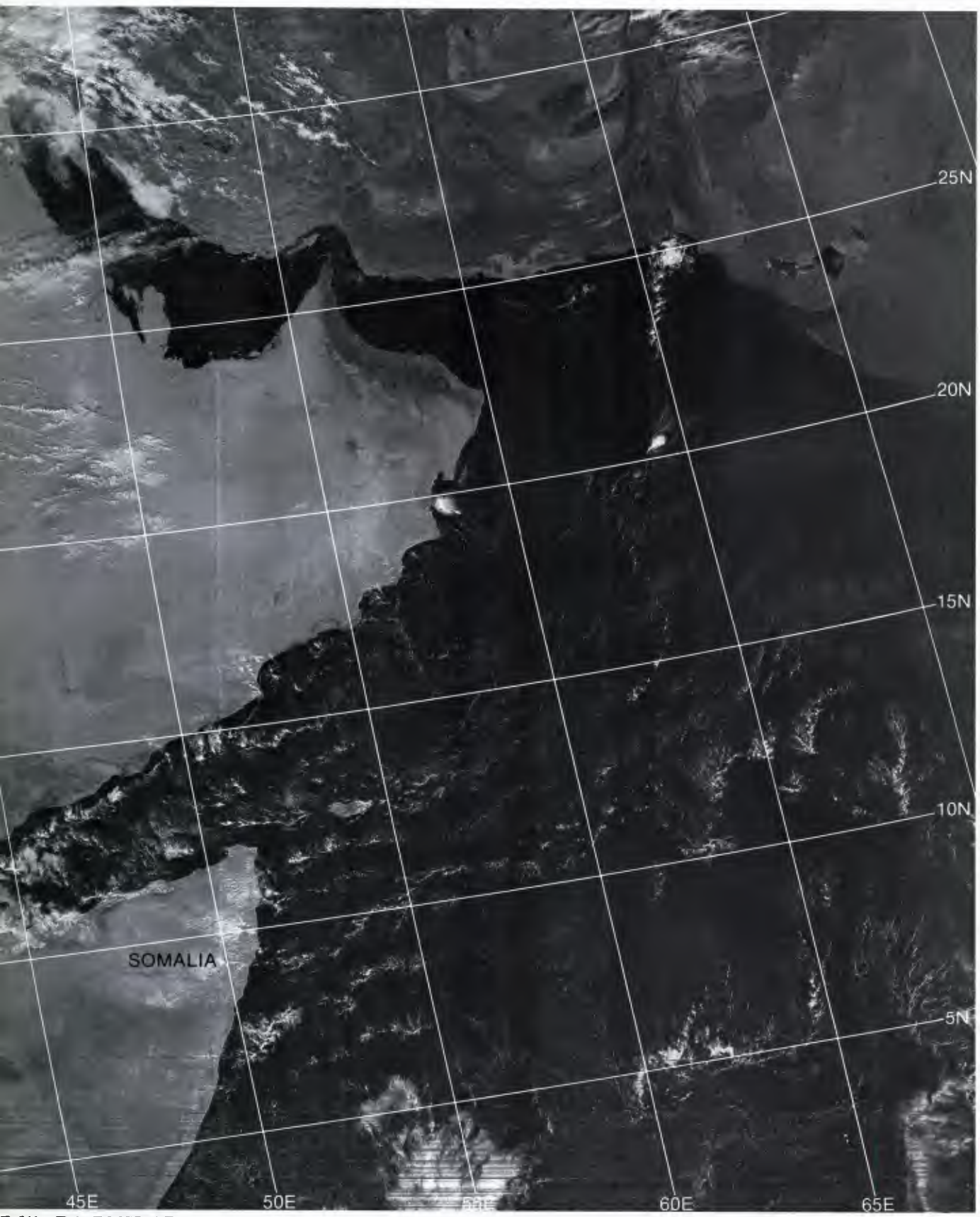

E-51b. F-4. DMSP LF Low Enhancement. 0623 GMT 21 January 1980.

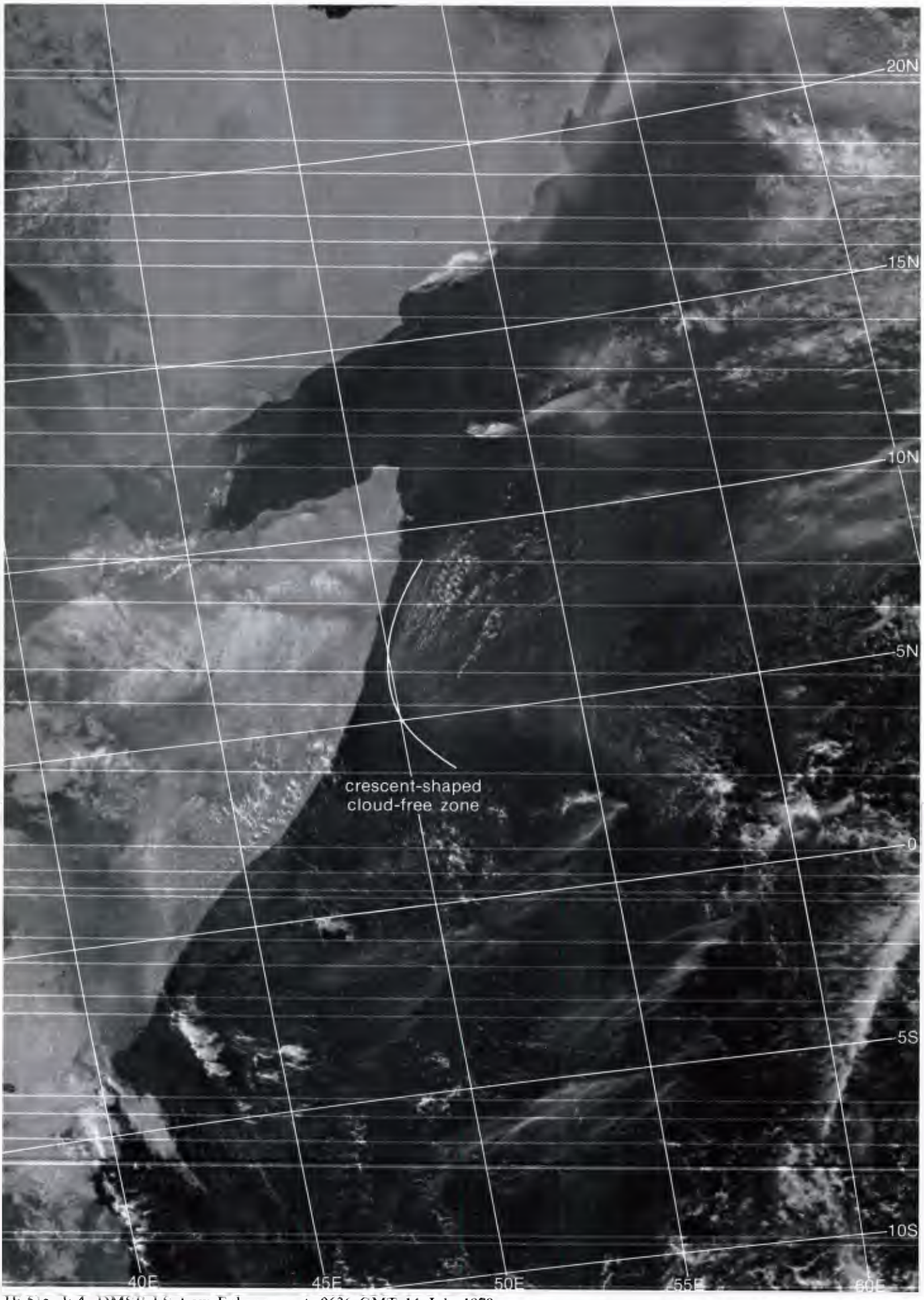

IE-51a. F-4. DMSP LS Low Enhancement. 0636 GMT 14 July 1979.

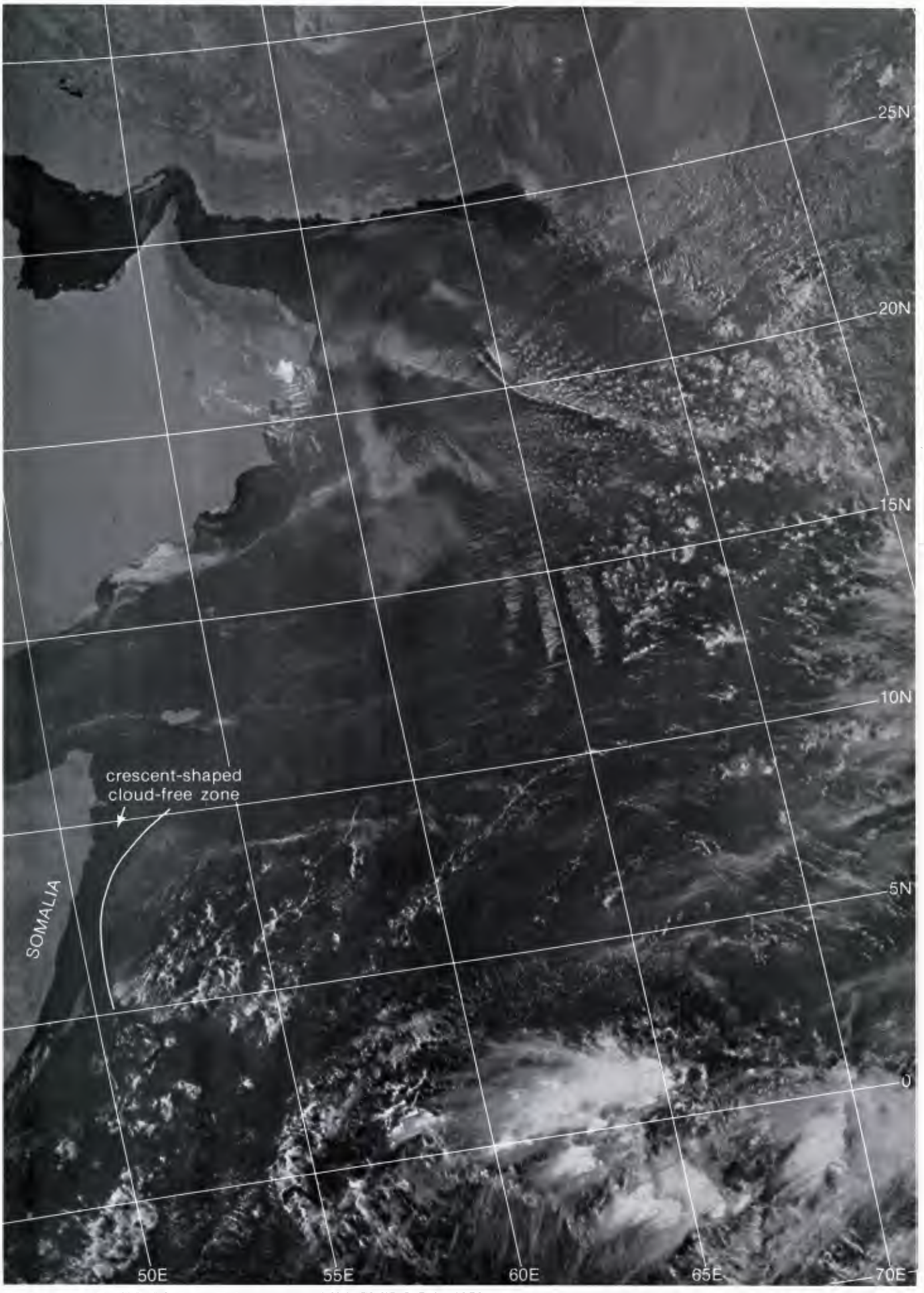

1E-52a. F-4. DMSP LS Low Enhancement. 0604 GMT 5 July 1979.

The research vessel Discovery was off the Somalia coast during the summer of 1964. From 16 to 21 August, Discovery never recorded more than 10% low cloud nor visibility below 10 km. Winds blew persistently from between south and southwest at from 10 to 15 m sec^{-1}. At the outset, air and sea temperatures were the same and a weak inversion extending from about 200 to 800 m inhibited low-cloud development. Then when the ship encountered cold water near 8.5° N, the inversion extended to the surface, being intensified both from below and above to greater than 10° C. Although the relative humidity of the surface air exceeded 90% no fog developed, despite the fact that the air moving over the cooling surface had possessed but 24 hours before, a dew point 9° C higher than the temperature of the upwelled water.

Discovery's soundings reveal a rapid decrease in relative humidity accompanied by a slight increase in mixing ratio with height in the inversion, thus confirming the existence of a downward moisture flux. The strong surface winds no doubt facilitated downward transport of heat and moisture despite the great stability of the air.

At the surface, the effect of upwelling cold water was to increase the downwind pressure gradient and so to accelerate the winds. The consequent divergence by bringing the subsidence inversion down to the surface ensured a supply of dry air adequate to prevent fog from forming. Since summer fog never develops off Somalia, a surface subsidence inversion must be a season-long phenomenon.

Important Conclusions

1. A persistent low cloud-free area with unrestricted visibility exists off the Somalia coast throughout the southwest monsoon season.

2. The area has a rather unique crescent shape and reflects a SST pattern resulting from oceanic upwelling that is driven by the low-level Somali jet.

3. A strong surface-based inversion persists over the low cloud-free area.

4. Air and sea temperatures are markedly lower in the cloud-free area.

5. The pattern repeats year after year with the development of the southwest monsoon.

References

Bruce, J. G., D. R. Quadfasel, and J. C. Swallow, 1980: Somali eddy formation during the commencement of the southwest monsoon, 1978. *J. Geophys. Res.*, **85**, 6654–6660.

Evans, R. H., and O. B. Brown, 1981: Propagation of thermal fronts in the Somali current system. *Deep-Sea Research*, **28A**, 521–527.

Ramage, C. S., 1968: Problems of a monsoon ocean. *Weather*, **23**, 28–37.

Ramage, C. S., 1971: Monsoon Meteorology. Academic Press, New York, 296 pp.

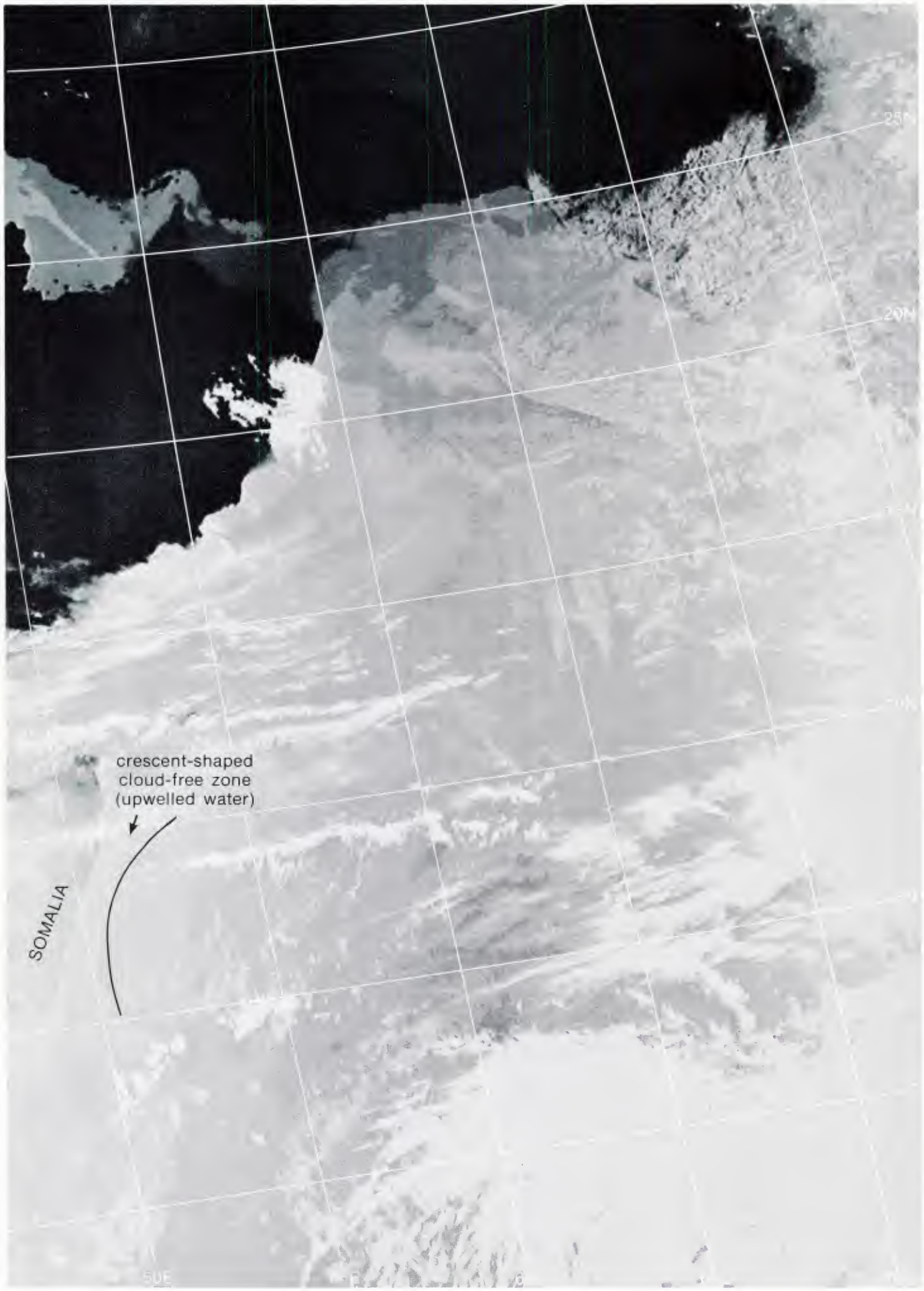

1E-53a. F-4. DMSP TS Low Enhancement. 0604 GMT 5 July 1979.